Appendix ACCHIONE01

```
leader  01899nas-a2200529-a-4500
001     991000000000392510
005     20221206174804.0
006     m-----o--d--------
007     cr-||||||||||
008     080422c20099999txubr-pso-----0---a0eng-c
010     ##$a  2008215260
015     ##$aGBB638084 $2bnb
016     7#$a2537838-7 $2DE-600
016     7#$a2537838-7 $2DE-600
022     ##$a1942-0870
035     ##$a(OCoLC)225933748
035     ##$a(CKB)1000000000392510
035     ##$a(CONSER)--2008215260
035     ##$a(DE-599)ZDB2537838-7
037     ##$bLandes Bioscience, 1002 West Avenue, Austin, TX 78701
042     ##$apcc $ansdp
050     00$aRM282.M65
082     10$a615 $214
130     0#$aMAbs (Online)
222     #0$aMAbs $b(Online)
245     10$aMAbs.
260     ##$aAustin, TX : $bLandes Bioscience, $c2009-
310     ##$aBimonthly
336     ##$atext $btxt $2rdacontent
337     ##$acomputer $bc $2rdamedia
338     ##$aonline resource $bcr $2rdacarrier
362     1#$aBegan with: Vol. 1, issue 1 (Jan./Feb. 2009).
588     ##$aDescription based on: Vol. 1, issue 1 (Jan./Feb. 2009); title from editor's page (Landes Bioscience website, viewed July 6, 2009).
588     ##$aLatest issue consulted: Vol. 10, issue 2 (2018), (Taylor & Francis Online viewed April 3, 2018).
500     ##$aRefereed/Peer-reviewed
506     0#$fUnrestricted online access $2star
650     #0$aMonoclonal antibodies $xTherapeutic use $vPeriodicals.
650     #0$aMonoclonal antibodies $vPeriodicals.
650     #7$aMonoclonal antibodies. $2fast $0(OCoLC)fst01025547
650     #7$aMonoclonal antibodies $xTherapeutic use. $2fast $0(OCoLC)fst01025554
650     12$aAntibodies, Monoclonal.
655     #2$aPeriodical.
655     #7$aPeriodicals. $2fast $0(OCoLC)fst01411641
710     2#$aTaylor & Francis, $eissuing body.
740     0#$aTaylor & Francis Online (Servicio en línea)
776     ##$x1942-0862
906     ##$aJOURNAL
```



JOURNAL

MAbs (Online)

Austin, TX : Landes Bioscience; Began with: Vol. 1, issue 1 (Jan./Feb. 2009).

2009-

PEER REVIEWED OPEN ACCESS

Available Online

View Journal Contents

TOP
SEND TO
SEARCH INSIDE
ONLINE ACCESS
LINKS
DETAILS

Send to

QR PERMALINK EMAIL CITATION EXPORT BIBTEX ENDNOTE BASIC

EXPORT TO EXCEL MENDELEY REFWORKS EXPORT RIS PRINT

Search inside

Search for articles within this journal

Article title or keyword

Online access

Full availability (Access issues? Try using the VPN)

DOAJ Directory of Open Access Journals SHOW LICENSE
Available from 2019.

PubMed Central
Available from 2009 volume: 1.

ROAD: Directory of Open Access Scholarly Resources
Available from 2009.
UC open access

Taylor & Francis Current Content Access SHOW LICENSE
Available from 01/01/2009 until 2023.

Taylor & Francis Open Access
Available from 01/01/2020 volume: 12 issue: 1.
UC open access

Links

MARC Record

Details

Author / Contributor	Taylor & Francis, issuing body.
Title	MAbs (Online)
Other Title	Taylor & Francis Online (Servicio en línea)
Uniform title	MAbs (Online)
Publication Information	Austin, TX : Landes Bioscience, 2009-
Type	Journal
Notes	Refereed/Peer-reviewed
Language	English
Subject	Monoclonal antibodies -- Therapeutic use -- Periodicals Monoclonal antibodies -- Periodicals Monoclonal antibodies

	Monoclonal antibodies -- Therapeutic use ›
Genre	Periodical. ›
	Periodicals. ›
MESH Subjects	Antibodies, Monoclonal ›
	Periodical ›
Frequency	Bimonthly
Identifier	LC : 2008215260
	ISSN : 1942-0870
	OCLC : (OCoLC)225933748
	ISSN : 1942-0862
MMS ID	9914807242906531
Access/Restrictions	Unrestricted online access star
Source	Library Catalog

We are committed to updating our catalog records and finding aids whenever feasible to revise problematic descriptions and subjects, including the addition of relevant context. **To report harmful language, please use** this form.



Appendix ACCHIONE02

mAbs 4:3, 362-372; May/June 2012; © 2012 Landes Bioscience

Impact of linker and conjugation chemistry on antigen binding, Fc receptor binding and thermal stability of model antibody-drug conjugates

Mauro Acchione,[1] Hyewon Kwon,[1] Claudia M. Jochheim[2] and William M. Atkins[1,*]

[1]Department of Medicinal Chemistry; University of Washington; Seattle, WA USA; [2]CMC Consulting; Seattle, WA USA

Keywords: conjugate, thermostability, Fc, linker, SPR, DSC, amine, thiol, carbohydrate, CD32b

Abbreviations: SPR, surface plasmon resonance; DSC, differential scanning calorimetry; FcγIIb, Fcgamma receptor IIb; T_m, melting temperature; ADC, antibody-drug conjugate; MSP, membrane scaffold protein; RU, response units; SD, standard deviation

Antibody-drug conjugates (ADCs) with biotin as a model cargo tethered to IgG1 mAbs via different linkers and conjugation methods were prepared and tested for thermostability and ability to bind target antigen and Fc receptor. Most conjugates demonstrated decreased thermostability relative to unconjugated antibody, based on DSC, with carbohydrate and amine coupled ADCs showing the least effect compared with thiol coupled conjugates. A strong correlation between biotin-load and loss of stability is observed with thiol conjugation to one IgG scaffold, but the stability of a second IgG scaffold is relatively insensitive to biotin load. The same correlation for amine coupling was less significant. Binding of antibody to antigen and Fc receptor was investigated using surface plasmon resonance. None of the conjugates exhibited altered antigen affinity. Fc receptor FcγIIb (CD32b) interactions were investigated using captured antibody conjugate. Protein G and Protein A, known inhibitors of Fc receptor (FcR) binding to IgG, were also used to extend the analysis of the impact of conjugation on Fc receptor binding. $H10_NPEG4$ was the only conjugate to show significant negative impact to FcR binding, which is likely due to higher biotin-load compared with the other ADCs. The ADC $aHIS_NLC$ and $aHIS_1PEG8$ demonstrated some loss in affinity for FcR, but to much lower extent. The general insensitivity of target binding and effector function of the IgG1 platform to conjugation highlight their utility. The observed changes in thermostability require consideration for the choice of conjugation chemistry, depending on the system being pursued and particular application of the conjugate.

The US Food and Drug Administration's approval of brentuximab vedotin (Adcetris™) in August 2011 demonstrates the therapeutic potential of antibody-drug conjugates (ADCs) to treat many cancers. The therapeutic effects of ADCs can result from a complex combination of mechanisms, including anti-proliferative or cell-killing potential through delivery of cytotoxic agents, apoptotic signaling, antibody-dependent cell-mediated cytotoxicity (ADCC) and complement dependent cytotoxicity (CDC). The inherent specificity of ADCs, coupled with their long serum half-life and low immunogenicity have generated substantial interest and investment toward improving these drug delivery platforms.

The choice of linker that connects the drug to the antibody scaffold is a critical factor in determining the effectiveness of ADC therapy. There has been notable progress recently in linker technology and the range of chemical reagents available for coupling the antibody to the drug of interest.[1] Several factors contribute to optimal linker function, including stability in vivo, immunogenicity and efficiency of drug release from ADC. The linker should be sufficiently stable to allow the antibody to carry the toxic payload to the cell of interest and subsequently into the cell, where it must then release the active cytotoxic drug. This last step may be of critical importance, and it depends on the method of cellular uptake and internalization of the ADC, which in turn may change with linker properties.[2,3] Furthermore, a linker should be chosen that induces no or minimal immunogenicity or off-target binding.

The site of conjugation must also be considered. Ideally, the site for conjugation must not interfere with any therapeutic function, nor significantly disrupt regions that may confer fold stability. The most common approach in preparing ADCs is to use heterobifunctional linkers. These consist of a spacer with chemically distinct reactive groups on either end that can couple to various functional groups on the respective antibody or drug molecule. This provides considerable control and flexibility in how one attaches the linker. There are several targets on the antibody available for conjugation. Three common strategies include thiol coupling to reduced cysteines, amine coupling to lysine

*Correspondence to: William M. Atkins; Email: winky@uw.edu
Submitted: 02/05/12; Accepted: 03/12/12
http://dx.doi.org/10.4161/mabs.4.3.19449

DAC EX. 2040 IPR2022-01531 Page 946 of 1299

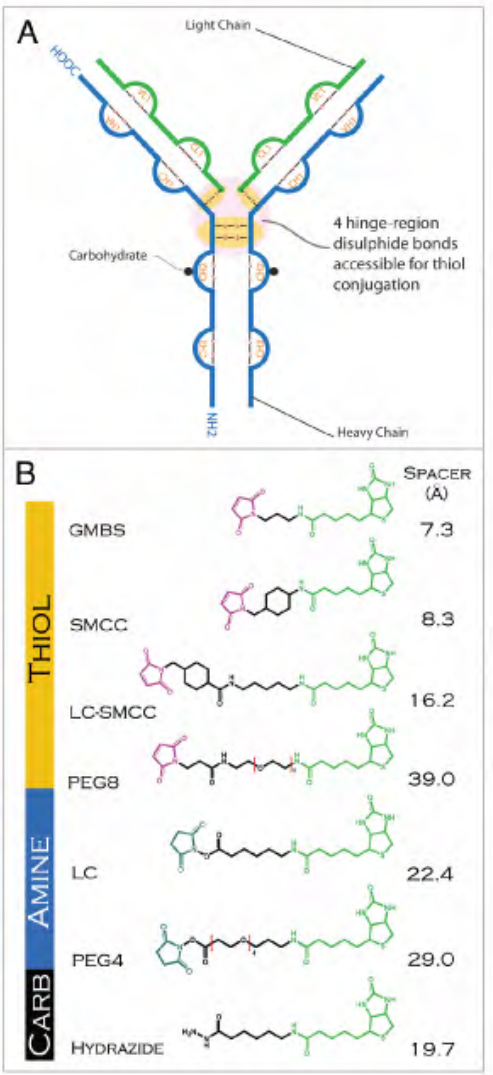


Figure 1. (A) Schematic representation of an IgG1 antibody showing sites of conjugation (thiol, amine and carbohydrate) used in generating the antibody-biotin conjugates. (B) Structure and length of linkers used in conjugating biotin (biocytin) to antibody. N-hydroxysuccinimide (blue), spacer arm (black), maleimide (violet), biotin (biocytin) (green).

residues and coupling to oxidized sugar residues on glycosylated mAbs. In principle, each method offers advantages and disadvantages with regard to product heterogeneity, stability and potential impact on effector function. Because in some cases modification of antibody residues spatially distant from the CDR domains can affect antigen binding, it is reasonable to expect that conjugation to the different functional groups may have different functional affects.[4]

Since different IgG1s can in principle have different sensitivities to conjugation with drugs, it is important to determine whether the trends observed in effects of conjugation for one IgG1 can be generalized to others. In addition to variable linkers and coupling strategies, we compared two distinct IgG1 scaffolds, to determine if different Fab domains would differentially be affected by the different linkers. The IgG1s used here include anti-6xHis (aHIS), which is directed against his-tags and therefore can be used with varying antigens that vary in size or other property, and HyHEL-10 (H10) anti-hen lysozyme, which provides a well-characterized scaffold with well-understood interactions with its antigen. In effect, we constructed a matrix of linker, IgG1 scaffold and conjugation chemistry to explore their effects on in vitro properties of ADCs.

Although the available literature suggests indirectly that the optimal choice of linker and conjugation site may vary with mAb idiotype, drug payload, conjugation site and antigen, no direct comparison of the effects of linker characteristics on functional properties for multiple mAbs and variable antigen has been reported in the public domain. General 'rules' about the advantages or disadvantages of specific linkers or conjugation methods are not well documented. Here we systematically evaluate the impact of linker and coupling chemistry on the properties of two model IgG1 antibodies (**Fig. 1A**). The results demonstrate some general trends concerning optimal linker strategies.

Results

Overall strategy. To explore the effects of IgG1 structure, conjugation chemistry and linker on ADC properties, we exploited two model IgG1 scaffolds, with multiple linkers of variable length and hydrophobicity. The linkers were used to attach the model 'drug' biotin to amines, reduced thiols, or oxidized carbohydrates on each IgG. In all cases, the form of biotin used for conjugation was biocytin, which allows for facile amine coupling of the biotin. Amine and carbohydrate linkers were purchased with this biocytin attached. For clarity, we refer to the group as biotin rather than biocytin in the remainder of this report. The structures of the linkers and biotin are shown in **Figure 1B**. For ADC identification, the subscripts 'N', 'T' and 'C' refer to coupling to amines, thiols or carbohydrates respectively. Biotin was chosen as a model drug for several reasons. Biotin, while hydrophobic, has a relatively low propensity to form aggregates or to bind non-specifically to protein surfaces. It also provides a rapid method to verify conjugation via SPR, quantify the level of biotin load on the ADC (**Table 1**) and verify that the recognition of biotin by streptavidin is not compromised in the conjugates. All IgG-linker-biotin conjugates synthesized showed positive capture by the Biacore streptavidin-linked CAP sensor chip surface (data not shown). IgG1 idiotype monoclonal antibodies (mAbs), such as the mouse H10 and aHIS, are the most abundant and commonly used mAb platform for ADCs, and the IgG1 idiotype contains a total of 16 disulfide bonds including four interchain (2 heavy-heavy, two heavy-light) and 12 intrachain disulfide bonds (**Fig. 1A**). The four interchain disulfide bonds are accessible to

DAC EX. 2040 IPR2022-01531 Page 947 of 1299

Table 1. Impact of linker and conjugation chemistry on ADC thermal stability as measured by DSC

ADC[a]	Transition Temperature T_m (°C)			
	Component 1	Component 2	Component 3	Component 4
H10	77.5	74.2		
H10/w TCEP	76.4	74.8		
$H10_NPEG4_L$	76.4	73.3		
$H10_NPEG4_H$	75.1	71.8		
$H10_TSMCC$	77.6	72.5	70.0	
$H10_TLC\text{-}SMCC$	78.2	72.4	69.0	
$H10_TGMBS$	77.4	72.9	66.8	
$H10_TPEG8$	77.5	72.9	67.3	
$H10_C$	76.8	74.8		
aHIS	78.9	71.2	67.5	61.7
aHIS/w TCEP	79.0	65.8	63.2	60.1
$aHIS_NPEG4$	78.3	70.7	67.1	61.3
$aHIS_NLC$	78.1	70.6	67.0	61.1
$aHIS_TSMCC$	78.0		60.8	58.3
$aHIS_TLC\text{-}SMCC$	78.1		60.7	58.0
$aHIS_TGMBS$	78.2		60.7	58.0
$aHIS_TPEG8$	77.7		60.5	57.9

[a]N, amine; T, thiol; C, Carbohydrate; L, low linker ratio; H, high linker ratio

reduction without unfolding the antibody. This gives a total of eight potential conjugation sites, assuming reduction of all four bonds. In practice, a mixture of thiol conjugates with different load (0, 2, 4, 6 and 8) is presumed. For amine coupling there are many surface accessible lysine residues distributed over a characteristic IgG1 structure. No attempt was made here to separate mixtures of antibodies loaded with different levels of biotin, and the average number of biotins per ADC were used as a measure of biotin load (**Table 2**).

Thermal stability. DSC was used to characterize each antibody and its corresponding ADCs to determine effects of linker and coupling strategy on thermal stability. Each DSC thermogram was fit to multiple components. A shift to lower T_m for a component is indicative of a loss in stability. Replicates for SD analysis are not available for each ADC. When evaluating significance of changes to T_m for a particular ADC from the naked antibody we used the conservative value of greater than 1°C as a minimum. In fact in the samples where a significant change in T_m is noted, the values reported are much greater than those characteristic for replicate samples with this instrument.[5] The naked H10 antibody unfolds in two distinct but overlapping irreversible transitions (**Fig. 2A**), whereas the naked aHIS antibody unfolds with four distinct but overlapping irreversible transitions (**Fig. 2C**). IgG1 mAbs often exhibit two or more transitions in DSC thermograms due to the vastly different stabilities[6] of the immunoglobin structural domains. The heterogeneity in drug-load with all ADC preparations is expected to cause some broadening of transitions seen in DSC thermograms. However, all DSC thermograms fit well to between two and four components using a non-two state model. In the absence of knowledge regarding the degree of heterogeneity in biotin load, a relative comparison of linkers and conjugation chemistries was pursued.

Table 2. Impact of linker and conjugation chemistry on ADC binding to antigen

ADC[a]	K_D (pM)		BTN:Ab[b]	
H10	397	±32.5		
$H10_NPEG4_L$	546	±80.4	6.4	±0.3
$H10_NPEG4_H$	825	±172.0	14.2	±0.4
$H10_TSMCC$	451	±52.4	4.9	±0.2
$H10_TLC\text{-}SMCC$	297	±38.6	4.9	±0.8
$H10_TGMBS$	376	±63.3	6.6	±0.3
$H10_TPEG8$	356	±1.1	6.5	±0.4
$H10_C$	371	±34.4	0.7	±0.1
aHIS	20.8	±1.8		
$aHIS_NPEG4$	24.1	±0.1	3.6	±1.1
$aHIS_NLC$	21.8	±0.3	3.7	±0.9
$aHIS_TSMCC$	22.6	±0.6	5.7	±1.4
$aHIS_TLC\text{-}SMCC$	22.5	±0.4	6.0	±2.3
$aHIS_TGMBS$	22.8	±2.4	4.9	±0.6
$aHIS_TPEG8$	23.3	±2.8	7.7	±0.04

[a]N, amine; T, thiol; C, Carbohydrate; L, low linker ratio; H, high linker ratio; [b]BTN, biotin; Ab, antibody

With H10 generated ADCs, the amine and carbohydrate conjugation chemistries did not alter the pattern of two component

DAC EX. 2040 IPR2022-01531 Page 948 of 1299

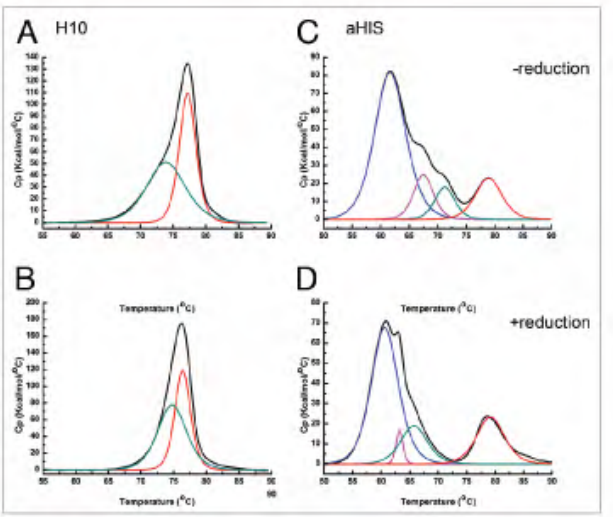


Figure 2. DSC thermograms and deconvoluted component transitions for the two unconjugated IgG1 antibodies in the presence and absence of TCEP. Left parts: (A) H10 without reducing agent (B) H10 with reducing agent; Right parts (C) aHIS without reducing agent (D) aHIS with reducing agent. Raw thermogram is shown in black. Individual transitions from non-two state fit are color coded as component 1 (red), component 2 (green), component 3 (magenta) and component 4 (blue).

transitions seen with the naked antibody (**Figs. 3A, C and D and Table 1**). Amine conjugation to accessible surface lysine residues presents an additional strategy for conjugation of drugs, with the potential to modify stability of the antibody fold. There was a clear difference in stability observed with the amine coupled ADCs with a drop in T_m for both components 1 and 2. The greater the biotin load (**Table 2**) the greater the change in T_m. For the corresponding thiol conjugates (**Fig. 3B and Table 1**), a new component is observed with a much lower thermostability than the other two components. While component 1 does not change significantly in T_m for the thiol generated ADCs, the presence of this new lower temp transition results in ADC that are significantly less stable than the naked antibody, with $H10_TGMBS$ beginning to partially unfold at a T_m 7.4°C below that of any component in the naked antibody. This ADC was also the one with the highest biotin load.

For the aHIS ADCs, the pattern of component transitions observed with DSC again differs depending on conjugation chemistry (**Fig. 3E–G and Table 1**). However, unlike H10 the number of visible components decreases from 4 with the naked antibody and amine-coupled ADCs to 3 for the thiol ADCs. It is unclear whether the lack of a component 2 for thiol-coupled ADCs reflects its superposition with another component in the thermogram that makes it indistinguishable. For amine aHIS ADCs, components 1–4 remain largely unaffected, even with higher biotin load (**Table 2**). For the thiol aHIS ADCs component 3 shows a large decline in T_m relative to the naked antibody of between 7.0-6.7°C which is comparable to the difference observed between components 2 and 3 for the thiol H10 ADCs. Component 4 showed a modest decline in T_m compared with the naked antibody, decreasing as much as 3.8°C for $aHIS_TPEG8$. So, in comparison to aHIS, the impact of thiol conjugation to thermostability was greater for H10 ADCs with comparable biotin load. The results for the shifts in low temperature DSC components with different model ADCs are summarized in **Figure 4**. In general, the results clearly demonstrate that different thiol-conjugates IgGs yield ADCs with significantly different sensitivity to drug load, even with the same linkers.

For this work, we were interested in changes in thermostability that may be important for the manufacture and use of these 'model' therapeutics. Therefore, we focused on notable changes in the relative components with the lowest temperature transition. For thiol conjugates, H10 showed a strong correlation ($R^2 = 0.87$) between higher biotin load and loss of stability. For aHIS, no correlation was observed for the corresponding thiol conjugates when comparing the lowest temperature transitions. However, among different DSC components there are similarities. This suggests that conjugation to free thiols located in the hinge region can differentially affect IgG1 scaffolds in ways that could have implications for their manufacture. With amine conjugates there were only two linkers used for each antibody. For amine H10 conjugates the correlation between biotin load and change in T_m for the low temperature component is less than that of thiol H10 conjugates. With amine aHIS conjugates the two T_m values are too close to confidently assess the correlation between biotin load and change in T_m. However, both values are below that observed with any of the thiol conjugates when those data sets are extrapolated to comparable biotin loads. What is clear from this data are that amine coupling has had less impact on thermostability compared with thiol conjugation for both antibodies. Also, for thiol conjugation the impact on thermostability with biotin load is very different among the two antibodies tested.

To determine the affect of reduction without chemical elaboration of the hinge region disulfides alone, both antibodies were unfolded in the presence of TCEP as the reducing agent. At the concentrations tested here (10 mM), TCEP had negligible impact on the DSC baseline. As stated previously, the H10 antibody has two characteristic component transitions (**Fig. 2A**) and the number of components, as well as the transition temperatures, did not change in the presence of this reducing agent (**Fig. 2B**). For the aHIS antibody, reduction of the hinge inter-chain disulfides with TCEP showed a slight negative affect on thermogram components 2, 3 and 4 with decreased thermostability (**Fig. 2D**). These data demonstrate that the effect of thiol reduction on stability can be IgG dependent, but the reduction of IgG by itself does not cause a significant decrease in thermal stability in either antibody used here.

In addition to thiol and amine conjugation strategies, we examined the effect of linking via carbohydrate. IgGs include N-linked oligosaccharides on two conserved asparagine residues (Asn297) in the CH_2 domain of the Fc region and approximately

DAC EX. 2040 IPR2022-01531 Page 949 of 1299

15–20% also have N-linked oligosaccharides in the variable region.[7] Oxidation of these N-linked sugars offers a convenient means of conjugation of a drug or small molecule at a defined location, with potentially less of a destabilizing effect than hinge-region thiol conjugation. Among the conjugation strategies we tested, the carbohydrate linked ADCs had the smallest changes in T_m for DSC profile compared with the unconjugated antibody (**Fig. 3D**). This may be in part due to the much lower level of conjugation (**Table 2**). However, even taking this into account, the affect of conjugation on T_m was much less than that for the thiol or amine conjugated antibodies.

Antigen binding. Because tight binding to its target is inherent in the strategy when using these drug delivery platforms, any effects on antigen binding due to conjugation are important. Such effects are possible, in principle, due to long range structural effects transmitted from conjugation sites to the antigen binding sites, or in the case of amine-conjugation potentially affecting hotspot lysine residues at the interface. Given the moderate role for disulfides in antibody stability (**Fig. 2**), we also studied whether conjugation to hinge-region disulfides affects antigen binding.[8] Each individual antibody and its respective ADCs were tested for binding to antigen. Representative sensorgrams are shown in **Figure 5**; comparisons of K_D were made by assessment of differences (>2-fold difference from unconjugated antibody) with conjugation chemistry or linker. None of ADCs for either antibody were different than the unconjugated antibody (**Table 2**). For the mAbs tested in this study, there was no clear disadvantage to antigen binding for any of the linkers or chemistries investigated here. The amine-conjugated $H10_NPEG4_H$ ADC was the one notable exception, and most likely reflects modification of a lysine residue at or near the paratope when the biotin load is sufficiently high.

Effector function and Fc binding. Effector functions mediated by binding of the Fc region of IgG1 antibodies to Fc receptors (FcR) can play an important role in the overall effectiveness of ADC therapies.[9-11] Modifciation of residues directly involved or near the Fc recdeptor binding site, such as regions of glycosylation on antibodies, may have an important role in FcR binding and in the structural integrity.[12,13] The potential therapeutic benefits of FcR activation or binding to other 'FcR-like' proteins make these interactions a target for optimization. All three conjugation strategies and linkers explored in this study could have direct or indirect effects on the structure and accessibility of the Fc region of the antibody. To test this, we captured the ADC to a SPR sensor surface on which native antigen was immobilized and then investigated binding of FcR to the captured ADC (**Figs. 6–8**). Effectively we began with a surface of ADC that was already bound to its corresponding antigen. This approach had several advantages over coupling of the antibody directly to the CM5 dextran surface of the chip or the Fc receptor. Because one of the approaches undertaken in conjugation involved amine coupling, the amine-sites available for coupling the ADCs to a CM5 sensor chip were much lower. Capturing the antibody on the SPR chip via its antigen also minimizes the possibility of interactions between the chip surface and the Fc region that could be confused with effects of N-linked biotin on the Fc region. The SPR data of FcR binding to ADC captured on the chip surface all fit very well to a one-site binding model. There was no statistically significant improvement of the fits to the data for a two-site binding model with non-equivalent binding sites, as observed by others.[14] As noted above, one important distinction to other work using SPR in this area is that in our experiments the antibody/ADC was captured to the chip surface via the antigen rather than using direct amine coupling.

Some conjugation strategies were found to have a significant affect on binding to certain FcR-binding partners. For $H10_NPEG4_H$ the affinity was reduced 17-fold for Protein G (**Table 3**). This may be due to coupling to lysine residues proximal to, or

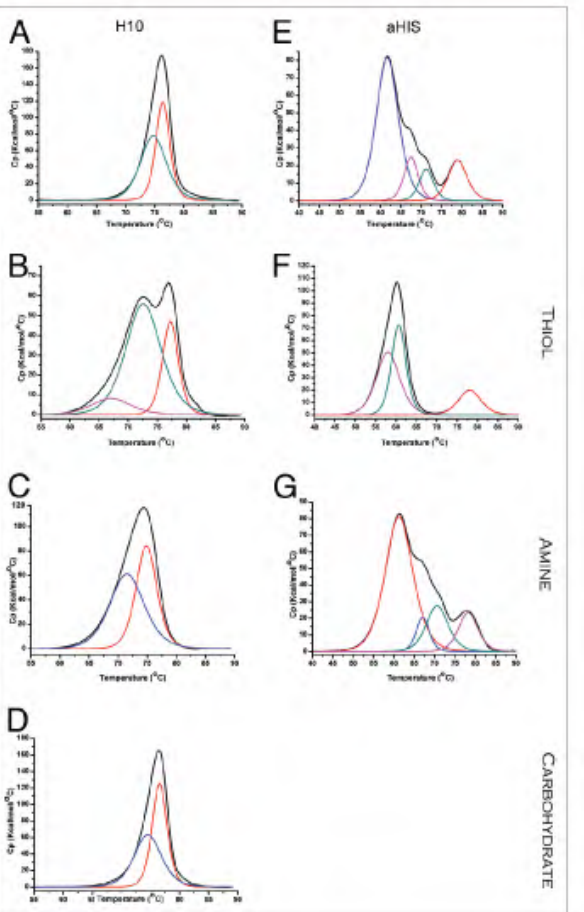


Figure 3. DSC thermograms comparing ADCs prepared with different conjugation chemistries. Raw thermograms are shown in black. Individual transitions are color coded as: component 1 (red), component 2 (green), component 3 (magenta) and component 4 (blue). (A) H10, (B) $H10_TSMCC$ (C) $H10_NPEG4_H$, (D) $H10_C$ (E) aHIS (F) $aHIS_TLC$-SMCC (G) $aHIS_NPEG4$.

DAC EX. 2040 IPR2022-01531 Page 950 of 1299

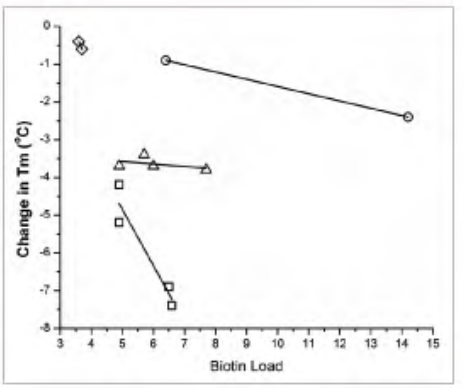


Figure 4. Correlation between biotin load and change in T_m for low-temperature components from DSC for ADC, grouped according to conjugation chemistry and/or antibody. (circle) amine-conjugated H10, (diamond) amine-conjugated aHIS, (triangle) thiol-conjugated aHIS and (square) thiol-conjugated H10.

in direct contact with, Protein G binding residues. There was also a decrease in binding to Protein G observed with amine coupled $aHIS_NLC$. The $aHIS_TPEG_8$ ADC was the only one to show some negative affect on binding with all FcR model proteins (CD32b, Protein A and Protein G). For this conjugate, the higher ratio of biotin load may be one reason for this (**Table 2**). CD32b is an inhibitor for Fcγ receptors that are often involved in effector functions such as ADCC and C1q mediated complement activation. A reduction in expression of CD32b has been associated with enhanced antitumor activity for antibodies.[15] These results suggest that amine coupling at high load-ratios can have a significant affect on binding to the Fc domain, and a similar evaluation would prove useful for any therapeutic ADC targeting effector function and using this conjugation chemistry. Other reports suggest a strong correlation with pegylation of antibodies and a reduction in FcR binding.[16,17] We observed a large reduction, but only with one ADC binding to one particular FcR.

Discussion

The lack of any significant change to antigen binding, or in most cases FcR binding, with any of the linkers or conjugation methods used, support the important role for antibodies as robust drug platforms for therapeutics. One attractive aspect to amine conjugation is the potential for increased drug load compared with using the fixed eight thiols presented by the IgG1 hinge disulfides. Because increased drug load on the ADC might be expected to improve therapeutic efficacy, the relatively mild perturbations to both Fc receptor binding and antigen binding observed in this work suggest that this advantage might be exploitable. However, in the case of thiol ADC, an increase in drug load does not necessarily correlate with improved therapeutic outcome.[18] With amine coupling, these results suggest that an analysis of FcR binding may prove useful when comparing leads that may present differences in serum half-life.

Table 3. Impact of linker and conjugation chemistry on ADC binding to Fc receptor

ADC[a]	K_D (nM)					
	CD32b		Protein G		Protein A	
H10	168.7	±13.1	134.3	±7.5	434.3	±3.2
$H10_NPEG4_L$	150.3	±10.8	324.3	±17.1	510.0	±5.2
$H10_NPEG4_H$	87.9	±12.1	2314.0	±175.0	334.0	±5.2
$H10_TSMCC$	134.0	±10.5	124.3	±18.9	495.3	±10.4
$H10_TLC$-SMCC	267.7	±14.0	99.2	±9.6	442.3	±56.7
$H10_TGMBS$	136.3	±20.4	110.0	±3.5	445.3	±59.5
$H10_TPEG8$	227.3	±10.6	132.3	±18.6	454.3	±55.4
$H10_C$	124.7	±6.4	90.5	±18.2	454.7	±34.5
aHIS	203.0	±9.5	119.6	±28.1	309.6	±28.6
$aHIS_NPEG4$	163.4	±20.5	137.0	±25.1	361.6	±73.4
$aHIS_NLC$	163.2	±16.3	197.9	±9.3	368.8	±50.2
$aHIS_TSMCC$	138.8	±27.9	157.3	±36.3	165.9	±39.4
$aHIS_TLC$-SMCC	139.2	±25.6	163.3	±8.4	164.8	±36.7
$aHIS_TGMBS$	206.5	±15.0	149.6	±5.5	232.0	±36.3
$aHIS_TPEG8$	448.7	±68.3	253.4	±9.1	523.0	±88.1

[a]N, amine; T, thiol; C, Carb

Increasing circulating half-life has often been associated with improved therapeutic efficacy for ADCs. Correlation between protein stability and in vivo half-life has been known for some time.[19,20] The more obvious correlation would be expected for changes in neonatal Fc receptor (FcRn) binding, which is a major factor in determining the rate of catabolism of IgGs not displaying target-mediated disposition, although there is some evidence that other factors may play a more significant role in serum half-life than affinity for FcRn.[21] We chose the bacterial receptors Protein G and Protein A as surrogates for natural FcR since they are both known to overlap with FcR binding sites and compete for their binding.[22,23] Our results suggest that binding to FcRn would not be expected to change with any of the conjugation chemistries or linkers investigated here. Therefore, the circulating half-life is not expected to change as a direct result of these modifications. However, catabolic mechanisms mediated by the cytosol are a possibility with any of these ADCs. Since terminal amine residues are a determining factor in that pathway, there is potential for influence on half-life in the case of amine coupling to the N-terminus of the antibody.

Biotin is small and somewhat water soluble whereas many chemotherapeutics are larger and more hydrophobic. Our results with biotinylating IgG1 antibodies demonstrate little or no impact on antigen/Fc receptor binding. With the exception of $H10_NPEG4_H$, these results are in contrast to several other reports which suggest that coupling of PEG molecules to an antibody can have a significant detrimental impact on antigen binding.[24] The results with the $H10_NPEG4_H$ ADC more likely reflect a difference in biotin load and location of conjugation on the antibody rather than the identity of the linker itself. The physiochemical characteristics and ultimate cellular disposition

DAC EX. 2040 IPR2022-01531 Page 951 of 1299

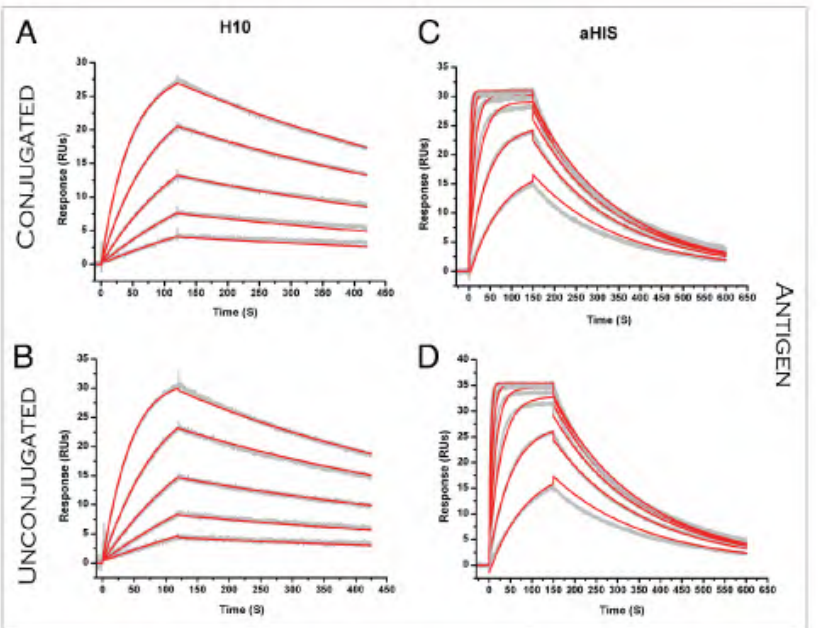


Figure 5. SPR sensorgrams comparing binding of ADC (analyte) to antigen (ligand). (A) H10 binding to JQL (B). $H10_1PEG8$ binding to JQL. (C) aHIS binding to 6xHis peptide (D). $aHIS_NPEG4$ binding to 6xHis peptide. Raw sensorgrams are shown in gray with results from fitting that data to a 1:1 binding model depicted in red.

of the drug should also be considered when interpreting these results. Consideration of unintended consequences to secondary roles mediated through Fc receptor mediated binding would seem to warrant a similar analysis for ADCs currently being developed. There remains the possibility that a different small molecule, peptide, protein or nucleic acid bound to a different antibody via these methods might have a significant impact on antigen/Fc receptor binding. However, we tested two distinct IgG1 antibodies with completely different targets, and our results suggest a more general relationship in the case of smaller molecules. Clearly, many of the current chemotherapeutic drugs employed or explored for therapy differ significantly in size, charge and hydrophobicity from biotin. With much larger drug payloads like bacterial exotoxins we would expect that steric hindrance could play a significant role in modulating antigen/Fc receptor binding. While not a drug, there is clear evidence that with much larger PEG moieties used in the linker, the negative impact on antigen binding can be dramatic;[17,25-27] In cases where the drug payload is highly hydrophobic and 'sticky', the chemical identity and length of the linker may influence the ability of those drug molecules to self-associate and promote aggregation.

While this report focuses on the relative thermal stability of conjugates, there has been much interest in investigating the stability of linkers in vivo. The work here demonstrates that linker identity has little or no impact on the inherent stability of the ADC construct, especially when compared with the relative impact of conjugation chemistry. Although outside the scope of this study, it would be interesting to compare conjugation chemistries known to impact thermal stability of an ADC with similar linkers and drugs to see if there is any correlation with the stability of a given linker to processing in vivo.

For all ADCs synthesized here, conjugation had some impact on thermostability of the molecule that could influence decisions for the manufacturing and storage for any particular ADC and may guide initial decisions on coupling strategies for therapeutic use based on possible correlations between thermal stability for the protein fold and serum half-life. Of the three functional groups investigated, thiol conjugation resulted in the greatest decreases in observed T_m as monitored by DSC. Furthermore, the degree of change in T_m is correlated with the number of biotin molecules linked to the antibody via thiols. The degree to which the T_m was independent of the length of the linker used or its hydrophobicity when the molecule being attached to the antibody is small and slightly hydrophobic. It remains to be seen if this relationship holds for much larger or more hydrophobic drugs such as exotoxins or auristatins. DSC showed clear differences in the number of components observed in thermograms for the two IgG1 antibodies and those differences also extended to how those component transitions were differentially impacted by conjugation chemistry. Perhaps most importantly, the results demonstrate the potential utility of DSC as a method to study comparability between ADC preparations.

DAC EX. 2040 IPR2022-01531 Page 952 of 1299

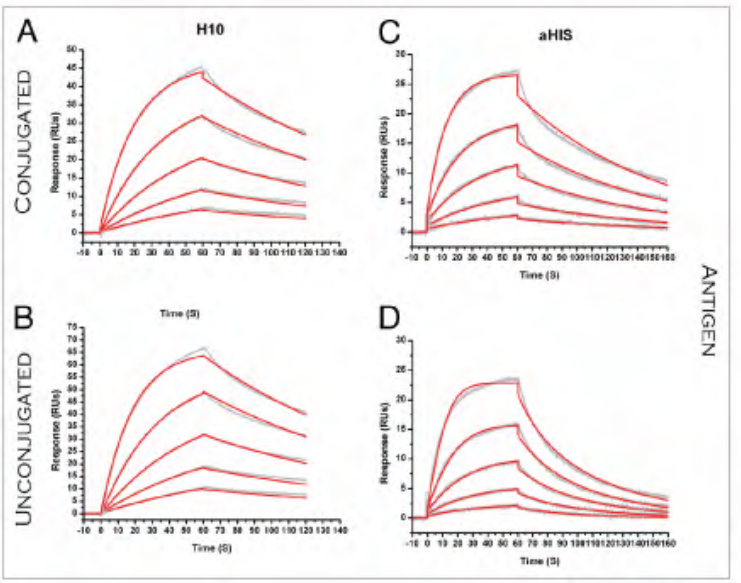


Figure 6. SPR sensorgrams comparing binding of ADC (ligand) to Protein G (analyte). (A) H10 (B). $H10_T$PEG8 (C) aHIS (D). $aHIS_N$PEG4. Raw sensorgrams are shown in gray with results from fitting that data to a 1:1 binding model depicted in red.

Materials and Methods

Materials. Buffer salts and biocytin for ADC synthesis and purification were purchased from Sigma. Heterobifuctional linkers, both with and without biotin attached, T-gel and Zeba columns were obtained from Thermo Scientific. Concentrated hybridoma supernatant containing mouse HyHEL-10 IgG1 (H10) whole antibody was provided by Dr. Sandi Smith-Gill, (National Cancer Institute, Frederick, MD). Japanese quail lysozyme was purified from egg white. Purified mouse monoclonal anti-6xHis IgG1 (aHIS) whole antibody was purchased from Invitrogen and dialyzed into PBS, pH 7.2. Hexa histidine peptides were obtained from AnaSpec. An engineered variant of apolipoprotein A1 (MSP1D1) was purified using the hepta-histidine tag via Ni-affinity chromatography as previously described in reference 28. Reagents and consumables for DSC and SPR analysis were obtained from GE Health Sciences.

Purification of H10 antibody. Concentrated fractions of H10 antibody from hybridoma cultures were clarified by centrifugation at 50,000x g for 20 min at 4°C. The supernatant was then applied to a T-gel column and purified according to the manufacturer's instructions. Antibody fractions were concentrated via Millipore Amicon-Ultra 0.5 spin-ultrafiltration columns and then passed through a GE Superose 10/300 GL gel filtration column pre-equilibrated with HBS buffer (10 mM HEPES, 150 mM NaCl, 3 mM EDTA, pH 7.4). Purified antibody was stored in HBS at 4°C until further use.

Preparation of thiol conjugated ADCs. Stock solutions containing 5 μM H10 and aHIS were reduced with 10 mM TCEP in nitrogen purged phosphate buffer (10 mM sodium phosphate, 150 mM NaCl, 5 mM EDTA, pH 7.2) for 2 h at 37°C. A fresh solution of 30 mM SMCC (**Fig. 1B**) in DMSO was prepared and mixed with biocytin at a ratio of 1:20 in Phosphate Buffer for 2 h at 37°C. Initial attempts to reduce disulfide bonds in these antibodies to form thiol-linked conjugate using low ratios of TCEP:Ab[29] proved unsuccessful. When using ratios below 5:1 no significant level of conjugate was observed. Considerably higher ratios of reducing agent:mAb were required (2,000:1) at elevated temperatures, which is more consistent with those reported for other IgG1s.[30] The reduced antibody was then buffer exchanged into HBS (PBS for aHIS) buffer using three Zeba desalting columns equilibrated with HBS buffer. Removal of TCEP reducing agent during this step prevented inhibition of the maleimide reaction.[31] The reduced antibody was then mixed with 1/10 volume equivalent of the SMCC-biocytin reaction mixture and allowed to equilibrate at room temperature for 2.5 h in the dark. An excess of L-cysteine was then added to cap unreacted thiol groups and the mixture was allowed to incubate for 30 min at room temperature.

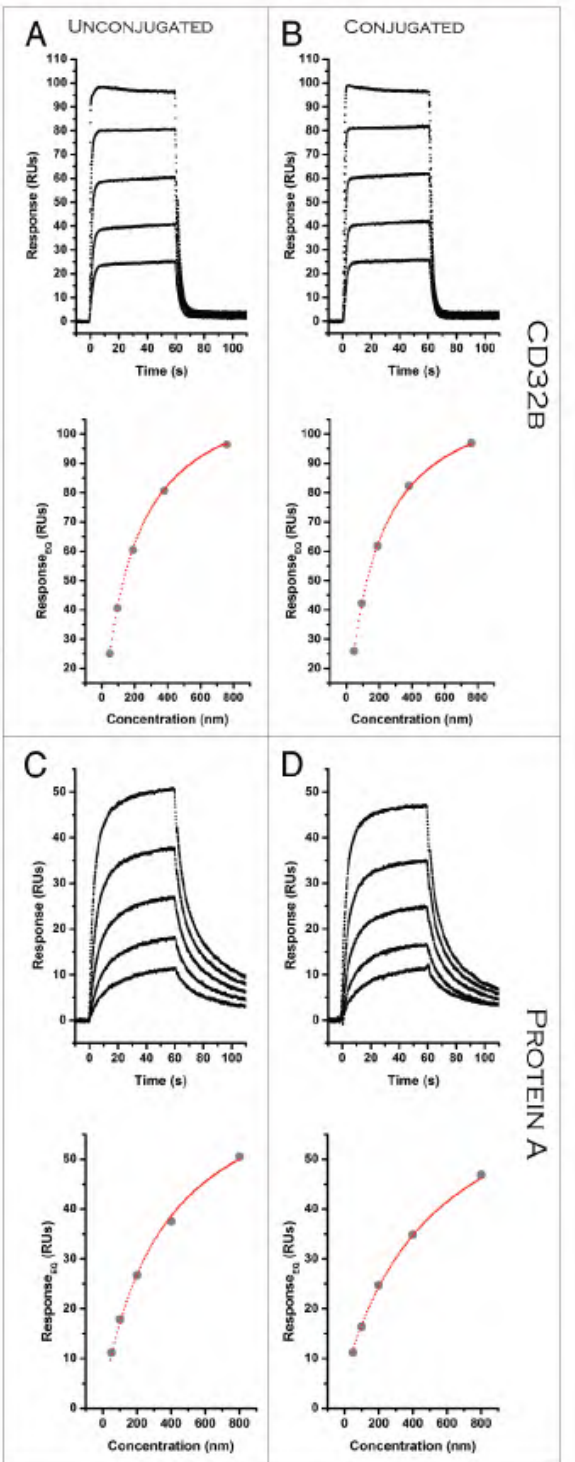
Preparation of amine conjugated ADCs. NHS-PEG4-Biotin (**Fig. 1B**) was re-suspended in PBS and mixed with HyHEL-10 IgG in a final molar ratio of 20:1 and 40:1 and both reactions were incubated at room temperature for 2 h. For aHIS IgG, NHS-LC-Biotin (**Fig. 1B**) prepared in DMSO and NHS-PEG4-Biotin (**Fig. 1B**) were re-suspended in PBS and mixed with aHIS IgG in final molar ratio of 25:1 and incubated at room temperature for 30 min. In both cases, excess linker was removed with Zeba desalting columns.

Preparation of carbohydrate conjugated ADCs. Stock solutions of 50 μM H10 were oxidized in freshly prepared sodium periodate in PBS at room temperature in the dark for 2 h.[32] Excess oxidizing agent was removed with Zeba desalting columns and the oxidized antibodies were immediately reacted with the hydrizide-biocytin linker (**Fig. 1B**) at a ratio of 1:20 for 2 h at room temperature.

Purification, determination of biotin-load and storage of ADCs. All ADC mixtures were further purified and buffer exchanged using a Superose 10/300 GL size exclusion column pre-equilibrated with HBS-E (10 mM HEPES, 150 mM NaCl, 3 mM EDTA) for H10 ADCs and PBS (10 mM sodium phosphate, 150 mM NaCl, pH 7.2) for aHIS ADCs at a flow rate of 0.55 mL/min, with UV detection at 280 nm. Protein fractions corresponding to the ADC peak (based on retention times of unconjugated antibody) were pooled and stored at 4°C

DAC EX. 2040 IPR2022-01531 Page 953 of 1299

Figure 7. SPR equilibrium data comparing ADC (ligand) binding to CD32b and Protein A (analyte). (A) H10 (B). $H10_NPEG4_L$ (C) H10 (D) $H10_NPEG4_L$. Raw sensorgrams are shown in black with corresponding results from fitting that data to a 1:1 binding model depicted in a binding isotherm below.



until further use. Typical reaction yields after purification were between 30–55%. Degree of biotin conjugation on ADC was determined using the fluorescence biotin quantification kit from Thermo Scientific.

Stability analysis of conjugates using DSC. Differential scanning calorimetry was used to determine the affect of ligand and conjugation chemistry on the stability of all antibodies and ADCs. Samples were prepared immediately prior to analysis and any aggregates formed during storage were removed by size-exclusion chromatography in HBS-E buffer (10 mM HEPES, 150 mM NaCl, 3 mM EDTA, pH 7.4) or PBS for aHIS ADCs. Concentrations of antibody and conjugate used were 4–6 μM. All samples were analyzed using a Microcal VP-Capillary DSC equipped with autosampler and temperature controlled sample storage accessories. Unfolding was monitored between 10°C and 90°C (20°C and 90°C for aHIS ADCs) with a ramp rate of 1°C/min and a filtering period of 16 sec with no gain. H10 antibody was analyzed by DSC using ramp rates of 0.5°C/min and 1.5°C/min and there was no siginificant change in T_m or component profiles in the thermograms. Thermograms were normalized for concentration and then baseline corrected prior to fitting to a non-two-state unfolding model to determine transition melting temperature T_m for each component.

Determination of binding affinity for HEL antigen using SPR. SPR was used to compare effects of conjugation on ADC binding to its antigen. All experiments were conducted on a Biacore T100 with CM5 sensor chips. The antibodies were amine coupled to the sensor surface using 10 mM sodium acetate, pH 5.0 at a level that resulted in a maximum analyte response no higher than 40 response units (RUs). This, together with a flow rate of 100 μL/min, negated any significant mass transport effects for this very tight association. Several different concentrations of analyte diluted in HBS-EP running buffer (10 mM HEPES, 150 mM NaCl, 3 mM EDTA, 0.005% v/v P20) were injected for 120 sec followed by monitoring dissociation for 10 min. Raw sensorgrams were double reference subtracted using a reference flow cell with no ADC immobilized and by injections of running buffer. Corrected sensorgrams were fit globally to a 1:1 interaction model using the Biacore evaluation software. The quality of the nonlinear fit to this model was evaluated using coefficient of variance (CV) values and residuals. Unless otherwise stated in the figure captions, all values reported for apparent affinity K_D are an average of three independent measurements made from separate dilutions of analyte stock. All experimental cycles were conducted at 25°C. Chip surfaces were regenerated after each cycle using 10 mM Glycine, pH 1.5.

DAC EX. 2040 IPR2022-01531 Page 954 of 1299

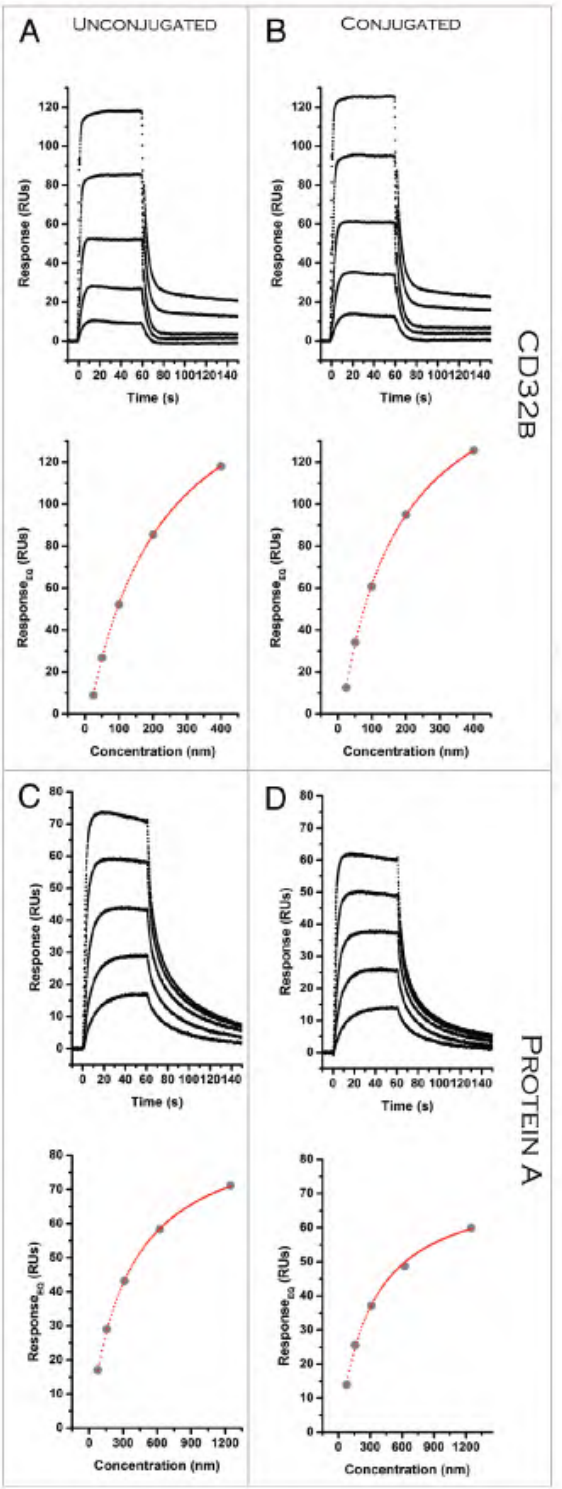


Figure 8. SPR equilibrium data comparing ADC (ligand) binding to CD32b and Protein A (analyte). (A) aHIS (B). aHIS$_N$LC (C) aHIS (D) aHIS$_N$-PEG4. Raw sensorgrams are shown in black with corresponding results from fitting that data to a 1:1 binding model depicted in a binding isotherm below.

Determination of binding affinity for 6xHis peptide antigen using SPR. ADCs were diluted into 10 mM sodium acetate buffer, pH 5.0 at a concentration of 10 μg/mL and immobilized on CM5 sensor surface chips using amine-coupling chemistry to give a maximum analyte response of approximately 40 response units (RUs). All binding analysis of antibodies with 6xHis peptides antigen were performed at 25°C in PBS (pH 7.2) as running buffer. Several concentrations of 6xHis peptides diluted in running buffer were injected for 150 sec at a flow rate of 50 μL/min followed by monitoring dissociation for 450 sec. Raw sensorgrams were double referenced by both subtracting a flow cell with no antibodies immobilized and subtracting a run of buffer only injection. The surface was regenerated with 10 mM glycine, pH 2.0 at a flow rate of 20 μL/min.

Determination of binding affinity for Fc receptor using SPR. Assessing the effect of conjugation on effector role function was done by first immobilizing the antigenic HEL ligand (a His-tagged apolipoprotein A1 variant for aHIS) onto a CM5 sensor surface onto which a high level of conjugate was captured. This configuration allows us to assess whether antigen bound ADC can still effectively bind Fc receptor. Between 3,500–4,000 RUs of capture ligand (antigen) was immobilized on each flow cell including the reference flow cell. To this was then captured approximately 500–1,000 RUs of ADC diluted in SPR running buffer HBS-EP (PBS for aHIS). The level of captured ADC was chosen to give sufficient signal to provide good signal to noise for fitting while at the same time minimizing (for Protein G) the potential for mass transport limitations. Several concentrations of Fc receptor analyte were freshly prepared and injected over the antigen-captured ADC surface.

For Protein G, the protocol used was for kinetic measurements with a flow rate of 10 μL/min, an association time of 60 sec and a dissociation time of 60 sec (120 sec for aHIS). To assess potential mass-transport limitations tests with higher flow rates of 20 μL/min and 40 μL/min were conducted. No significantly change in on-rate was observed. Chip surfaces were regenerated after each cycle using 10 mM Glycine, pH 2.5. Analyte binding level was consistent among replicates, decreasing less than 5% after repeated regeneration cycles, and calculated rate used in determination of K_D were highly reproducible from cycle to cycle. Raw sensorgrams were double referenced using a flow cell with no ligand immobilized and by injections of running buffer. Corrected sensorgrams were fit globally to a 1:1 interaction model using the Biacore evaluation software. Quality of the nonlinear fitting to this model was evaluated using CV values and the residuals. Values reported for apparent affinity K_D are an average of three independent measurements made from separate dilutions of analyte stock.

Determination of binding affinity for CD32b and protein A by equilibrium binding. For both CD32b binding and Protein A binding, the on rates and off rates were too fast

DAC EX. 2040 IPR2022-01531 Page 955 of 1299

to be measured with confidence using the T100. Therefore the apparent affinity was determined by measuring equilibrium binding levels at several different analyte concentrations in HBS-EP buffer. After correcting raw sensorgrams for the reference flow cell and buffer injections, equilibrium responses were plotted against analyte concentration using Biacore evaluation software and fit to a 1:1 association model using nonlinear Scatchard analysis. Each concentration was measured in triplicate and both methods were conducted using a sensor surface temperature of 25°C.

Disclosure of Potential Conflicts of Interest Statement

No potential conflicts of interest were disclosed.

Acknowledgements

We wish to thank Sandi Smith-Gill from the National Cancer Institute for the kind gift of the mouse H10 IgG1 antibody. We would also like the thank John Sumida from the Bioanalytical Pharmacy Core, the Center for Intracellular Delivery Biologics and the Washington State Life Sciences Discovery Fund.

References

1. Ojima I, Geng X, Wu X, Qu C, Borella CP, Xie H, et al. Tumor-specific novel taxoid-monoclonal antibody conjugates. J Med Chem 2002; 45:5620-3; PMID:12477344; http://dx.doi.org/10.1021/jm025540g.
2. Smith LM, Nesterova A, Alley SC, Torgov MY, Carter PJ. Potent cytotoxicity of an auristatin-containing antibody-drug conjugate targeting melanoma cells expressing melanotransferrin/p97. Mol Cancer Ther 2006; 5:1474-82; PMID:16818506; http://dx.doi.org/10.1158/1535-7163.MCT-06-0026.
3. Razani B, Woodman SE, Lisanti MP. Caveolae: from cell biology to animal physiology. Pharmacol Rev 2002; 54:431-67; PMID:12223531; http://dx.doi.org/10.1124/pr.54.3.431.
4. Torres M, Casadevall A. The immunoglobulin constant region contributes to affinity and specificity. Trends Immunol 2008; 29:91-7; PMID:18191616; http://dx.doi.org/10.1016/j.it.2007.11.004.
5. Wen J, Arthur K, Chemmalil L, Muzammil S, Gabrielson J, Jiang Y. Applications of differential scanning calorimetry for thermal stability analysis of proteins: qualification of DSC. J Pharm Sci 2012; 101:955-64; PMID:22147423; http://dx.doi.org/10.1002/jps.22820.
6. Vermeer AW, Norde W. The thermal stability of immunoglobulin: unfolding and aggregation of a multi-domain protein. Biophys J 2000; 78:394-404; PMID:10620303; http://dx.doi.org/10.1016/S0006-3495(00)76602-1.
7. Holland M, Yagi H, Takahashi N, Kato K, Savage CO, Goodall DM, et al. Differential glycosylation of polyclonal IgG, IgG-Fc and IgG-Fab isolated from the sera of patients with ANCA-associated systemic vasculitis. Biochim Biophys Acta 2006; 1760:669-77.
8. Harris RJ. Heterogeneity of recombinant antibodies: linking structure to function. Dev Biol (Basel) 2005; 122:117-27; PMID:16375256.
9. Sibéril S, Dutertre CA, Fridman WH, Teillaud JL. FcgammaR: The key to optimize therapeutic antibodies? Crit Rev Oncol Hematol 2007; 62:26-33; PMID:17240158; http://dx.doi.org/10.1016/j.critrevonc.2006.12.003.
10. Natsume A, Niwa R, Satoh M. Improving effector functions of antibodies for cancer treatment: Enhancing ADCC and CDC. Drug Des Devel Ther 2009; 3:7-16; PMID:19920917.
11. Moore GL, Chen H, Katki S, Lazar GA. Engineered Fc variant antibodies with enhanced ability to recruit complement and mediate effector functions. MAbs 2010; 2:181-9; PMID:20150767; http://dx.doi.org/10.4161/mabs.2.2.11158.
12. Radaev S, Sun PD. Recognition of IgG by Fcgamma receptor. The role of Fc glycosylation and the binding of peptide inhibitors. J Biol Chem 2001; 276:16478-83; PMID:11297533; http://dx.doi.org/10.1074/jbc.M100351200.
13. Krapp S, Mimura Y, Jefferis R, Huber R, Sondermann P. Structural analysis of human IgG-Fc glycoforms reveals a correlation between glycosylation and structural integrity. J Mol Biol 2003; 325:979-89; PMID:12527303; http://dx.doi.org/10.1016/S0022-2836(02)01250-0.
14. Vaccaro C, Zhou J, Ober RJ, Ward ES. Engineering the Fc region of immunoglobulin G to modulate in vivo antibody levels. Nat Biotechnol 2005; 23:1283-8; PMID:16186811; http://dx.doi.org/10.1038/nbt1143.
15. Clynes RA, Towers TL, Presta LG, Ravetch JV. Inhibitory Fc receptors modulate in vivo cytotoxicity against tumor targets. Nat Med 2000; 6:443-6; PMID:10742152; http://dx.doi.org/10.1038/74704.
16. Cunningham-Rundles C, Zhuo Z, Griffith B, Keenan J. Biological activities of polyethylene-glycol immunoglobulin conjugates. Resistance to enzymatic degradation. J Immunol Methods 1992; 152:177-90; PMID:1500728; http://dx.doi.org/10.1016/0022-1759(92)90139-K.
17. Anderson WL, Tomasi TB. Polymer modification of antibody to eliminate immune complex and Fc binding. J Immunol Methods 1988; 109:37-42; PMID:3128614; http://dx.doi.org/10.1016/0022-1759(88)90439-5.
18. Hamblett KJ, Senter PD, Chace DF, Sun MM, Lenox J, Cerveny CG, et al. Effects of drug loading on the antitumor activity of a monoclonal antibody drug conjugate. Clin Cancer Res 2004; 10:7063-70; PMID:15501986; http://dx.doi.org/10.1158/1078-0432.CCR-04-0789.
19. McLendon G, Radany E. Is protein turnover thermodynamically controlled? J Biol Chem 1978; 253:6335-7; PMID:687388.
20. Fontana A, Zambonin M, Polverino de Laureto P, De Filippis V, Clementi A, Scaramella E. Probing the conformational state of apomyoglobin by limited proteolysis. J Mol Biol 1997; 266:223-30; PMID:9047359; http://dx.doi.org/10.1006/jmbi.1996.0787.
21. Gurbaxani B, Dela Cruz LL, Chintalacharuvu K, Morrison SL. Analysis of a family of antibodies with different half-lives in mice fails to find a correlation between affinity for FcRn and serum half-life. Mol Immunol 2006; 43:1462-73; PMID:16139891; http://dx.doi.org/10.1016/j.molimm.2005.07.032.
22. Sulica A, Medesan C, Laky M, Onica D, Sjöquist J, Ghetie V. Effect of protein A of Staphylococcus aureus on the binding of monomeric and polymeric IgG to Fc receptor-bearing cells. Immunology 1979; 38:173-9; PMID:511216.
23. Stone GC, Sjöbring U, Björck L, Sjöquist J, Barber CV, Nardella FA. The Fc binding site for streptococcal protein G is in the Cgamma2–Cgamma3 interface region of IgG and is related to the sites that bind staphylococcal protein A and human rheumatoid factors. J Immunol 1989; 143:565-70; PMID:2738404.
24. Chapman AP. PEGylated antibodies and antibody fragments for improved therapy: a review. Adv Drug Deliv Rev 2002; 54:531-45; PMID:12052713; http://dx.doi.org/10.1016/S0169-409X(02)00026-1.
25. Kitamura K, Takahashi T, Yamaguchi T, Noguchi A, Noguchi A, Takashina K, et al. Chemical engineering of the monoclonal antibody A7 by polyethylene glycol for targeting cancer chemotherapy. Cancer Res 1991; 51:4310-5; PMID:1868453.
26. Suzuki T, Kanbara N, Tomono T, Hayashi N, Shinohara I. Physicochemical and biological properties of poly(ethylene glycol)-coupled immunoglobulin G. Biochim Biophys Acta 1984; 788:248-55; PMID:6743669; http://dx.doi.org/10.1016/0167-4838(84)90268-1.
27. Takashina K, Kitamura K, Yamaguchi T, Noguchi A, Noguchi A, Tsurumi H, et al. Comparative pharmacokinetic properties of murine monoclonal antibody A7 modified with neocarzinostatin, dextran and polyethylene glycol. Jpn J Cancer Res 1991; 82:1145-50; PMID:1720116; http://dx.doi.org/10.1111/j.1349-7006.1991.tb01769.x.
28. Ritchie TK, Grinkova YV, Bayburt TH, Denisov IG, Zolnerciks JK, Atkins WM, et al. Chapter 11—Reconstitution of membrane proteins in phospholipid bilayer nanodiscs. Methods Enzymol 2009; 464:211-31; PMID:19903557; http://dx.doi.org/10.1016/S0076-6879(09)64011-8.
29. Sun MM, Beam KS, Cerveny CG, Hamblett KJ, Blackmore RS, Torgov MY, et al. Reduction-alkylation strategies for the modification of specific monoclonal antibody disulfides. Bioconjug Chem 2005; 16:1282-90; PMID:16173809; http://dx.doi.org/10.1021/bc050201y.
30. Liu H, Chumsae C, Gaza-Bulseco G, Hurkmans K, Radziejewski CH. Ranking the susceptibility of disulfide bonds in human IgG1 antibodies by reduction, differential alkylation, and LC-MS analysis. Anal Chem 2010; 82:5219-26; PMID:20491447; http://dx.doi.org/10.1021/ac100575n.
31. Getz EB, Xiao M, Chakrabarty T, Cooke R, Selvin PR. A comparison between the sulfhydryl reductants tris(2-carboxyethyl)phosphine and dithiothreitol for use in protein biochemistry. Anal Biochem 1999; 273:73-80; PMID:10452801; http://dx.doi.org/10.1006/abio.1999.4203.
32. Hermanson GT. Bioconjugate techniques. Amsterdam; Boston: Elsevier Academic Press 2008.

DAC EX. 2040 IPR2022-01531 Page 956 of 1299

Appendix HAMBLETT01

MARC View

LEADER 20328nas a2202329 a 4500			
001 1811522			
003 SIRSI			
005 20160707134635.0			
008 950308c19959999njusr p 0 a0eng d			
010			a| sn 94002948
019			a| MARS
022		0	a| 1078-0432
035			a| LIAS1829343
035			a| (CStRLIN)NJPG95-S381
035			a| (OCoLC)30960261
040			c| PSt d| WaOLN d| UtOrBLW
245	0	0	a| Clinical cancer research.
264		1	a| Philadelphia, PA : b| American Association for Cancer Research, c| [1995-]
264		4	c| ©1995-
300			a| volumes : b| illustrations (some color) ; c| 28 cm
310			a| Semimonthly, b| Aug. 15, 2003-
321			a| Monthly, b| 1995-Aug. 2003
336			a| text b| txt 2| rdacontent
337			a| unmediated b| n 2| rdamedia
338			a| volume b| nc 2| rdacarrier
362	0		a| Vol. 1, no. 1 (Jan. 1995)-
500			a| Title from cover.
515			a| Some nos. issued in pts.
550			a| "An official journal of the American Association for Cancer Research".
650		0	a| Cancer x| Research v| Periodicals.
650		2	a| Neoplasms.
650		0	a| Cancer v| Periodicals.
655		2	a| Periodicals.
710	2		a| American Association for Cancer Research.
949			a| RC261.C546 v.1 no.1-4 1995 w| LCPER c| 1 i| 000073969693 d| 4/20/1995 l| PATERNO-4 m| UP-PAT r| Y s| Y t| PERIODICAL u| 4/13/2001
949			a| RC261.C546 v.7 no.1-2 2001 w| LCPER c| 1 i| 000048241809 l| PATERNO-4 m| UP-PAT r| Y s| Y t| PERIODICAL u| 10/25/2001
949			a| RC261.C546 v.7 no.3-4 2001 w| LCPER c| 1 i| 000048240345 l| PATERNO-4 m| UP-PAT r| Y s| Y t| PERIODICAL u| 10/25/2001
949			a| RC261.C546 v.7 no.5-6 2001 w| LCPER c| 1 i| 000048240352 l| PATERNO-4 m| UP-PAT r| Y s| Y t| PERIODICAL u| 10/25/2001
949			a| RC261.C546 v.6 no.11-12 2000 & suppl. w| LCPER c| 1 i| 000047188730 l| PATERNO-4 m| UP-PAT r| Y s| Y t| PERIODICAL u| 11/27/2001
949			a| RC261.C546 v.7 no.9-10 2001 w| LCPER c| 1 i| 000048293143 l| PATERNO-4 m| UP-PAT r| Y s| Y t| PERIODICAL u| 3/27/2002
949			a| RC261.C546 v.7 no.11 2001 & suppl. w| LCPER c| 1 i| 000048389501 l| PATERNO-4 m| UP-PAT r| Y s| Y t| PERIODICAL u| 6/26/2002
949			a| RC261.C546 v.7 no.8 2001 w| LCPER c| 1 i| 000048389495 l| PATERNO-4 m| UP-PAT r| Y s| Y t| PERIODICAL u| 6/26/2002
949			a| RC261.C546 v.7 no.12 2001 & suppl. w| LCPER c| 1 i| 000048389488 l| PATERNO-4 m| UP-PAT r| Y s| Y t| PERIODICAL u| 6/26/2002
949			a| RC261.C546 v.8 no.5-6 2002 w| LCPER c| 1 i| 000048454193 l| PATERNO-4 m| UP-PAT r| Y s| Y t| PERIODICAL u| 8/20/2002
949			a| RC261.C546 v.8 no.3-4 2002 w| LCPER c| 1 i| 000048454179 l| PATERNO-4 m| UP-PAT r| Y s| Y t| PERIODICAL u| 8/20/2002
949			a| RC261.C546 v.8 no.1-2 2002 w| LCPER c| 1 i| 000048454186 l| PATERNO-4 m| UP-PAT r| Y s| Y t| PERIODICAL u| 8/20/2002
949			a| RC261.C546 v.8 no.7-8 2002 w| LCPER c| 1 i| 000051757885 l| PATERNO-4 m| UP-PAT r| Y s| Y t| PERIODICAL u| 1/22/2003
949			a| RC261.C546 v.8 no.11-12 2002 w| LCPER c| 1 i| 000051843601 l| PATERNO-4 m| UP-PAT r| Y s| Y t| PERIODICAL u| 3/21/2003
949			a| RC261.C546 v.8 no.9-10 2002 w| LCPER c| 1 i| 000051843618 l| PATERNO-4 m| UP-PAT r| Y s| Y t| PERIODICAL u| 3/21/2003
949			a| RC261.C546 v.9 no.1 2003 & suppl. w| LCPER c| 1 i| 000051880798 l| PATERNO-4 m| UP-PAT r| Y s| Y t| PERIODICAL u| 5/19/2003
949			a| RC261.C546 v.9 no.2-3 2003 w| LCPER c| 1 i| 000051822781 l| PATERNO-4 m| UP-PAT r| Y s| Y t| PERIODICAL u| 7/25/2003
949			a| RC261.C546 v.9 no.4-5 2003 w| LCPER c| 1 i| 000052542480 d| 3/3/2017 l| PATERNO-4 m| UP-PAT q| 1 r| Y s| Y t| PERIODICAL u| 8/28/2003
949			a| RC261.C546 v.9 no.6-7 2003 w| LCPER c| 1 i| 000052542619 l| PATERNO-4 m| UP-PAT r| Y s| Y t| PERIODICAL u| 8/28/2003

ASK A LIBRARIAN

949 a| RC261.C546 v.9 no.8-9 2003 w| LCPER c| 1 i| 000052578847 l| PATERNO-4 m| UP-PAT r| Y s| Y t| PERIODICAL u| 10/30/2003

949 a| RC261.C546 v.9 no.10-11 2003 & suppl. w| LCPER c| 1 i| 000052588495 l| PATERNO-4 m| UP-PAT r| Y s| Y t| PERIODICAL u| 11/13/2003

949 a| RC261.C546 v.9 no.12-13 2003 w| LCPER c| 1 i| 000052778223 l| PATERNO-4 m| UP-PAT r| Y s| Y t| PERIODICAL u| 1/16/2004

949 a| RC261.C546 v.9 no.16-17 2003 & suppl. w| LCPER c| 1 i| 000052800009 l| PATERNO-4 m| UP-PAT r| Y s| Y t| PERIODICAL u| 2/26/2004

949 a| RC261.C546 v.9 no.14-15 2003 w| LCPER c| 1 i| 000052799853 l| PATERNO-4 m| UP-PAT r| Y s| Y t| PERIODICAL u| 2/26/2004

949 a| RC261.C546 v.10 no.1-2 2004 & suppl. w| LCPER c| 1 i| 000052807794 l| PATERNO-4 m| UP-PAT r| Y s| Y t| PERIODICAL u| 3/5/2004

949 a| RC261.C546 v.10 no.3-4 2004 w| LCPER c| 1 i| 000052833519 l| PATERNO-4 m| UP-PAT r| Y s| Y t| PERIODICAL u| 6/3/2004

949 a| RC261.C546 v.10 no.5-6 2004 w| LCPER c| 1 i| 000052833502 l| PATERNO-4 m| UP-PAT r| Y s| Y t| PERIODICAL u| 6/3/2004

949 a| RC261.C546 v.10 no.7-8 2004 w| LCPER c| 1 i| 000052833526 l| PATERNO-4 m| UP-PAT r| Y s| Y t| PERIODICAL u| 6/3/2004

949 a| RC261.C546 v.10 no.9-10 2004 w| LCPER c| 1 i| 000054777781 l| PATERNO-4 m| UP-PAT r| Y s| Y t| PERIODICAL u| 8/19/2004

949 a| RC261.C546 v.10 no.11-12 2004 & suppl. w| LCPER c| 1 i| 000054777798 l| PATERNO-4 m| UP-PAT r| Y s| Y t| PERIODICAL u| 8/19/2004

949 a| RC261.C546 v.10 no.13-14 2004 w| LCPER c| 1 i| 000054867154 l| PATERNO-4 m| UP-PAT r| Y s| Y t| PERIODICAL u| 10/7/2004

949 a| RC261.C546 v.10 no.15-16 2004 w| LCPER c| 1 i| 000054870796 l| PATERNO-4 m| UP-PAT r| Y s| Y t| PERIODICAL u| 11/2/2004

949 a| RC261.C546 v.10 no.17-18 2004 & suppl. w| LCPER c| 1 i| 000054826366 l| PATERNO-4 m| UP-PAT r| Y s| Y t| PERIODICAL u| 2/21/2005

949 a| RC261.C546 v.10 no.19-20 2004 w| LCPER c| 1 i| 000054826359 l| PATERNO-4 m| UP-PAT r| Y s| Y t| PERIODICAL u| 2/21/2005

949 a| RC261.C546 v.10 no.21-22 2004 w| LCPER c| 1 i| 000054846906 l| PATERNO-4 m| UP-PAT r| Y s| Y t| PERIODICAL u| 3/31/2005

949 a| RC261.C546 v.10 no.23-24 2004 w| LCPER c| 1 i| 000054854529 l| PATERNO-4 m| UP-PAT r| Y s| Y t| PERIODICAL u| 4/8/2005

949 a| RC261.C546 v.11 no.3-4 2005 w| LCPER c| 1 i| 000054986558 l| PATERNO-4 m| UP-PAT r| Y s| Y t| PERIODICAL u| 5/13/2005

949 a| RC261.C546 v.11 no.1-2 2005 & suppl. w| LCPER c| 1 i| 000054986541 l| PATERNO-4 m| UP-PAT r| Y s| Y t| PERIODICAL u| 5/13/2005

949 a| RC261.C546 v.11 no.7-8 2005 w| LCPER c| 1 i| 000055014755 l| PATERNO-4 m| UP-PAT r| Y s| Y t| PERIODICAL u| 7/21/2005

949 a| RC261.C546 v.11 no.5-6 2005 w| LCPER c| 1 i| 000055014601 l| PATERNO-4 m| UP-PAT r| Y s| Y t| PERIODICAL u| 7/21/2005

949 a| RC261.C546 v.11 no.9-10 2005 w| LCPER c| 1 i| 000055018395 l| PATERNO-4 m| UP-PAT r| Y s| Y t| PERIODICAL u| 7/28/2005

949 a| RC261.C546 v.11 no.11-12 2005 w| LCPER c| 1 i| 000055047906 l| PATERNO-4 m| UP-PAT r| Y s| Y t| PERIODICAL u| 10/27/2005

949 a| RC261.C546 v.11 no.13-14 2005 & suppl. w| LCPER c| 1 i| 000054940802 l| PATERNO-4 m| UP-PAT r| Y s| Y t| PERIODICAL u| 12/12/2005

949 a| RC261.C546 v.11 no.15-16 2005 w| LCPER c| 1 i| 000054944923 l| PATERNO-4 m| UP-PAT r| Y s| Y t| PERIODICAL u| 1/13/2006

949 a| RC261.C546 v.11 no.17-18 2005 w| LCPER c| 1 i| 000054947924 l| PATERNO-4 m| UP-PAT r| Y s| Y t| PERIODICAL u| 1/23/2006

949 a| RC261.C546 v.11 no.19-20 2005 & suppl. w| LCPER c| 1 i| 000054962132 l| PATERNO-4 m| UP-PAT r| Y s| Y t| PERIODICAL u| 3/3/2006

949 a| RC261.C546 v.11 no.21-22 2005 w| LCPER c| 1 i| 000054970533 l| PATERNO-4 m| UP-PAT r| Y s| Y t| PERIODICAL u| 3/23/2006

949 a| RC261.C546 v.12 no.1-2 2006 w| LCPER c| 1 i| 000055115513 l| PATERNO-4 m| UP-PAT r| Y s| Y t| PERIODICAL u| 6/2/2006

949 a| RC261.C546 v.11 no.23-24 2005 & suppl. w| LCPER c| 1 i| 000055116879 l| PATERNO-4 m| UP-PAT r| Y s| Y t| PERIODICAL u| 6/12/2006

949 a| RC261.C546 v.12 no.3-4 2006 & suppl. w| LCPER c| 1 i| 000055122276 l| PATERNO-4 m| UP-PAT r| Y s| Y t| PERIODICAL u| 6/26/2006

949 a| RC261.C546 v.12 no.7-8 2006 & suppl. w| LCPER c| 1 i| 000055131940 l| PATERNO-4 m| UP-PAT r| Y s| Y t| PERIODICAL u| 7/20/2006

949 a| RC261.C546 v.12 no.5-6 2006 w| LCPER c| 1 i| 000055131674 l| PATERNO-4 m| UP-PAT r| Y s| Y t| PERIODICAL u| 7/20/2006

949 a| RC261.C546 v.12 no.9-10 2006 w| LCPER c| 1 i| 000055070690 l| PATERNO-4 m| UP-PAT r| Y s| Y t| PERIODICAL u| 9/22/2006

949 a| RC261.C546 v.12 no.11-12 2006 & suppl. w| LCPER c| 1 i| 000055075282 l| PATERNO-4 m| UP-PAT r| Y s| Y t| PERIODICAL u| 10/11/2006

949 a| RC261.C546 v.12 no.13-14 2006 & suppl. w| LCPER c| 1 i| 000055193986 l| PATERNO-4 m| UP-PAT r| Y s| Y t| PERIODICAL u| 2/26/2007

949 a| RC261.C546 v.12 no.17-18 2006 w| LCPER c| 1 i| 000055195447 l| PATERNO-4 m| UP-PAT r| Y s| Y t| PERIODICAL u| 3/2/2007

949 a| RC261.C546 v.12 no.15-16 2006 w| LCPER c| 1 i| 000055195430 l| PATERNO-4 m| UP-PAT r| Y s| Y t| PERIODICAL u| 3/2/2007

949 a| RC261.C546 v.12 no.21-22 2006 w| LCPER c| 1 i| 000055219525 l| PATERNO-4 m| UP-PAT r| Y s| Y t| PERIODICAL u| 7/10/2007

949 a| RC261.C546 v.12 no.19-20 2006 w| LCPER c| 1 i| 000055219372 l| PATERNO-4 m| UP-PAT r| Y s| Y t| PERIODICAL u| 7/10/2007

949 a| RC261.C546 v.12 no.23-24 2006 w| LCPER c| 1 i| 000061725911 l| PATERNO-4 m| UP-PAT r| Y s| Y t| PERIODICAL u| 8/21/2007

949 a| RC261.C546 v.13 no.3-4 2007 w| LCPER c| 1 i| 000061743335 l| PATERNO-4 m| UP-PAT r| Y s| Y t| PERIODICAL u| 11/15/2007

949 a| RC261.C546 v.13 no.1-2 2007 w| LCPER c| 1 i| 000061743328 l| PATERNO-4 m| UP-PAT r| Y s| Y t| PERIODICAL u| 11/15/2007

949 a| RC261.C546 v.13 no.5-6 2007 w| LCPER c| 1 i| 000061744813 l| PATERNO-4 m| UP-PAT r| Y s| Y t| PERIODICAL u| 11/19/2007

949 a| RC261.C546 v.13 no.7-8 2007 w| LCPER c| 1 i| 000055146067 l| PATERNO-4 m| UP-PAT r| Y s| Y t| PERIODICAL u| 2/8/2008

949 a| RC261.C546 v.13 no.9-10 2007 w| LCPER c| 1 i| 000059618010 l| PATERNO-4 m| UP-PAT r| Y s| Y t| PERIODICAL u| 3/7/2008

949 a| RC261.C546 v.13 no.11-12 2007 w| LCPER c| 1 i| 000059628712 l| PATERNO-4 m| UP-PAT r| Y s| Y t| PERIODICAL u| 3/21/2008

949 a| RC261.C546 v.13 no.13-14 2007 w| LCPER c| 1 i| 000059628705 l| PATERNO-4 m| UP-PAT r| Y s| Y t| PERIODICAL u| 3/21/2008

949 a| RC261.C546 v.13 no.17-18 2007 & suppl. w| LCPER c| 1 i| 000059633136 l| PATERNO-4 m| UP-PAT r| Y s| Y t| PERIODICAL u| 4/18/2008

949 a| RC261.C546 v.13 no.15-16 2007 w| LCPER c| 1 i| 000059633143 l| PATERNO-4 m| UP-PAT r| Y s| Y t| PERIODICAL u| 4/21/2008

949 a| RC261.C546 v.13 no.19-20 2007 w| LCPER c| 1 i| 000059656814 l| PATERNO-4 m| UP-PAT r| Y s| Y t| PERIODICAL u| 7/2/2008

949 a| RC261.C546 v.13 no.21-22 2007 w| LCPER c| 1 i| 000059673002 l| PATERNO-4 m| UP-PAT r| Y s| Y t| PERIODICAL u| 9/19/2008

949 a| RC261.C546 v.13 no.23-24 2007 w| LCPER c| 1 i| 000059677574 l| PATERNO-4 m| UP-PAT r| Y s| Y t| PERIODICAL u| 9/29/2008

949 a| RC261.C546 v.14 no.1-2 2008 w| LCPER c| 1 i| 000055226226 l| PATERNO-4 m| UP-PAT r| Y s| Y t| PERIODICAL u| 10/24/2008
949 a| RC261.C546 v.14 no.3-4 2008 w| LCPER c| 1 i| 000055229487 l| PATERNO-4 m| UP-PAT r| Y s| Y t| PERIODICAL u| 11/19/2008
949 a| RC261.C546 v.14 no.5-6 2008 w| LCPER c| 1 i| 000055239585 l| PATERNO-4 m| UP-PAT r| Y s| Y t| PERIODICAL u| 1/23/2009
949 a| RC261.C546 v.14 no.7-8 2008 w| LCPER c| 1 i| 000059735434 l| PATERNO-4 m| UP-PAT r| Y s| Y t| PERIODICAL u| 2/26/2009
949 a| RC261.C546 v.14 no.9-10 2008 w| LCPER c| 1 i| 000059742807 l| PATERNO-4 m| UP-PAT r| Y s| Y t| PERIODICAL u| 3/24/2009
949 a| RC261.C546 v.14 no.11-12 2008 w| LCPER c| 1 i| 000059749233 l| PATERNO-4 m| UP-PAT r| Y s| Y t| PERIODICAL u| 4/23/2009
949 a| RC261.C546 v.14 no.13-14 2008 w| LCPER c| 1 i| 000059758723 l| PATERNO-4 m| UP-PAT r| Y s| Y t| PERIODICAL u| 5/18/2009
949 a| RC261.C546 v.14 no.15-16 2008 w| LCPER c| 1 i| 000059806769 l| PATERNO-4 m| UP-PAT r| Y s| Y t| PERIODICAL u| 5/29/2009
949 a| RC261.C546 v.14 no.21-22 2008 w| LCPER c| 1 i| 000059808572 l| PATERNO-4 m| UP-PAT r| Y s| Y t| PERIODICAL u| 6/3/2009
949 a| RC261.C546 v.14 no.19-20 2008 w| LCPER c| 1 i| 000059808565 l| PATERNO-4 m| UP-PAT r| Y s| Y t| PERIODICAL u| 6/5/2009
949 a| RC261.C546 v.14 no.17-18 2008 w| LCPER c| 1 i| 000059806493 l| PATERNO-4 m| UP-PAT r| Y s| Y t| PERIODICAL u| 6/11/2009
949 a| RC261.C546 v.15 no.3-4 2009 w| LCPER c| 1 i| 000059816447 l| PATERNO-4 m| UP-PAT r| Y s| Y t| PERIODICAL u| 7/1/2009
949 a| RC261.C546 v.14 no.23-24 2008 w| LCPER c| 1 i| 000059812173 l| PATERNO-4 m| UP-PAT r| Y s| Y t| PERIODICAL u| 7/2/2009
949 a| RC261.C546 v.15 no.1-2 2009 w| LCPER c| 1 i| 000059816614 l| PATERNO-4 m| UP-PAT r| Y s| Y t| PERIODICAL u| 7/2/2009
949 a| RC261.C546 v.15 no.5-6 Mar 2009 w| LCPER c| 1 i| 000059772439 l| PATERNO-4 m| UP-PAT r| Y s| Y t| PERIODICAL u| 8/24/2009
949 a| RC261.C546 v.15 no.7-8 2009 w| LCPER c| 1 i| 000059786153 l| PATERNO-4 m| UP-PAT r| Y s| Y t| PERIODICAL u| 10/20/2009
949 a| RC261.C546 v.15 no.9-10 2009 w| LCPER c| 1 i| 000059785811 l| PATERNO-4 m| UP-PAT r| Y s| Y t| PERIODICAL u| 10/28/2009
949 a| RC261.C546 v.15 no.11-12 2009 w| LCPER c| 1 i| 000059799504 l| PATERNO-4 m| UP-PAT r| Y s| Y t| PERIODICAL u| 12/23/2009
949 a| RC261.C546 v.15 no.13-14 2009 w| LCPER c| 1 i| 000061850255 l| PATERNO-4 m| UP-PAT r| Y s| Y t| PERIODICAL u| 3/1/2010
949 a| RC261.C546 v.15 no.15-16 2009 w| LCPER c| 1 i| 000061872509 l| PATERNO-4 m| UP-PAT r| Y s| Y t| PERIODICAL u| 5/10/2010
949 a| RC261.C546 v.15 no.17-18 2009 w| LCPER c| 1 i| 000061877504 l| PATERNO-4 m| UP-PAT r| Y s| Y t| PERIODICAL u| 6/1/2010
949 a| RC261.C546 v.15 no.19-20 2009 w| LCPER c| 1 i| 000061889064 l| PATERNO-4 m| UP-PAT r| Y s| Y t| PERIODICAL u| 7/14/2010
949 a| RC261.C546 v.15 no.21-22 2009 w| LCPER c| 1 i| 000061892446 l| PATERNO-4 m| UP-PAT r| Y s| Y t| PERIODICAL u| 8/4/2010
949 a| RC261.C546 v.15 no.23-24 2009 w| LCPER c| 1 i| 000061896840 l| PATERNO-4 m| UP-PAT r| Y s| Y t| PERIODICAL u| 8/16/2010
949 a| RC261.C546 v.16 no.4 2010 w| LCPER c| 1 i| 000061834248 l| PATERNO-4 m| UP-PAT r| Y s| Y t| PERIODICAL u| 3/31/2011
949 a| RC261.C546 v.16 no.5 2010 w| LCPER c| 1 i| 000061834156 l| PATERNO-4 m| UP-PAT r| Y s| Y t| PERIODICAL u| 3/31/2011
949 a| RC261.C546 v.16 no.6 2010 w| LCPER c| 1 i| 000061834231 l| PATERNO-4 m| UP-PAT r| Y s| Y t| PERIODICAL u| 3/31/2011
949 a| RC261.C546 v.16 no.7 2010 w| LCPER c| 1 i| 000059401094 l| PATERNO-4 m| UP-PAT r| Y s| Y t| PERIODICAL u| 4/11/2011
949 a| RC261.C546 v.16 no.8 2010 w| LCPER c| 1 i| 000059401100 l| PATERNO-4 m| UP-PAT r| Y s| Y t| PERIODICAL u| 4/11/2011
949 a| RC261.C546 v.16 no.10 2010 w| LCPER c| 1 i| 000059407423 l| PATERNO-4 m| UP-PAT r| Y s| Y t| PERIODICAL u| 5/5/2011
949 a| RC261.C546 v.16 no.9 2010 w| LCPER c| 1 i| 000059407430 l| PATERNO-4 m| UP-PAT r| Y s| Y t| PERIODICAL u| 5/5/2011
949 a| RC261.C546 v.16 no.11 2010 w| LCPER c| 1 i| 000059325055 l| PATERNO-4 m| UP-PAT r| Y s| Y t| PERIODICAL u| 5/26/2011
949 a| RC261.C546 v.16 no.12 2010 w| LCPER c| 1 i| 000059410881 l| PATERNO-4 m| UP-PAT r| Y s| Y t| PERIODICAL u| 5/26/2011
949 a| RC261.C546 v.16 no.14 2010 w| LCPER c| 1 i| 000059418689 l| PATERNO-4 m| UP-PAT r| Y s| Y t| PERIODICAL u| 6/16/2011
949 a| RC261.C546 v.16 no.13 2010 w| LCPER c| 1 i| 000059418696 l| PATERNO-4 m| UP-PAT r| Y s| Y t| PERIODICAL u| 6/16/2011
949 a| RC261.C546 v.16 no.15 2010 w| LCPER c| 1 i| 000059420927 l| PATERNO-4 m| UP-PAT r| Y s| Y t| PERIODICAL u| 7/8/2011
949 a| RC261.C546 v.16 no.16 2010 w| LCPER c| 1 i| 000059420934 l| PATERNO-4 m| UP-PAT r| Y s| Y t| PERIODICAL u| 7/8/2011
949 a| RC261.C546 v.16 no.17-18 2010 w| LCPER c| 1 i| 000059425939 l| PATERNO-4 m| UP-PAT r| Y s| Y t| PERIODICAL u| 7/26/2011
949 a| RC261.C546 v.16 no.19-20 2010 w| LCPER c| 1 i| 000059424949 l| PATERNO-4 m| UP-PAT r| Y s| Y t| PERIODICAL u| 8/5/2011
949 a| RC261.C546 v.16 no.21-22 2010 w| LCPER c| 1 i| 000059429180 l| PATERNO-4 m| UP-PAT r| Y s| Y t| PERIODICAL u| 8/24/2011
949 a| RC261.C546 v.16 no.23-24 2010 w| LCPER c| 1 i| 000059429173 l| PATERNO-4 m| UP-PAT r| Y s| Y t| PERIODICAL u| 8/24/2011
949 a| RC261.C546 v.17 no.1-2 2011 w| LCPER c| 1 i| 000059429166 l| PATERNO-4 m| UP-PAT r| Y s| Y t| PERIODICAL u| 9/1/2011
949 a| RC261.C546 v.17 no.3-4 2011 w| LCPER c| 1 i| 000059429159 l| PATERNO-4 m| UP-PAT r| Y s| Y t| PERIODICAL u| 9/1/2011
949 a| RC261.C546 v.17 no.5-6 2011 w| LCPER c| 1 i| 000059432982 l| PATERNO-4 m| UP-PAT r| Y s| Y t| PERIODICAL u| 9/22/2011
949 a| RC261.C546 v.17 no.7 2011 w| LCPER c| 1 i| 000059436300 l| PATERNO-4 m| UP-PAT r| Y s| Y t| PERIODICAL u| 10/21/2011
949 a| RC261.C546 v.17 no.8 2011 w| LCPER c| 1 i| 000059436331 l| PATERNO-4 m| UP-PAT r| Y s| Y t| PERIODICAL u| 10/21/2011
949 a| RC261.C546 v.17 no.10 2011 w| LCPER c| 1 i| 000059439684 l| PATERNO-4 m| UP-PAT r| Y s| Y t| PERIODICAL u| 11/10/2011
949 a| RC261.C546 v.17 no.9 2011 w| LCPER c| 1 i| 000059439677 l| PATERNO-4 m| UP-PAT r| Y s| Y t| PERIODICAL u| 11/10/2011
949 a| RC261.C546 v.17 no.11 2011 w| LCPER c| 1 i| 000059364221 d| 1/12/2012 l| PATERNO-4 m| UP-PAT q| 1 r| Y s| Y t| PERIODICAL u| 12/13/2011
949 a| RC261.C546 v.17 no.12 2011 w| LCPER c| 1 i| 000059365242 d| 1/12/2012 l| PATERNO-4 m| UP-PAT q| 1 r| Y s| Y t| PERIODICAL u| 12/13/2011
949 a| RC261.C546 v.17 no.13 2011 w| LCPER c| 1 i| 000059368458 l| PATERNO-4 m| UP-PAT r| Y s| Y t| PERIODICAL u| 1/24/2012
949 a| RC261.C546 v.17 no.14 2011 w| LCPER c| 1 i| 000059368441 l| PATERNO-4 m| UP-PAT r| Y s| Y t| PERIODICAL u| 1/24/2012
949 a| RC261.C546 v.17 no.16 2011 w| LCPER c| 1 i| 000059368250 l| PATERNO-4 m| UP-PAT r| Y s| Y t| PERIODICAL u| 1/24/2012
949 a| RC261.C546 v.17 no.15 2011 w| LCPER c| 1 i| 000059368267 l| PATERNO-4 m| UP-PAT r| Y s| Y t| PERIODICAL u| 1/24/2012
949 a| RC261.C546 v.17 no.17 2011 w| LCPER c| 1 i| 000059373100 l| PATERNO-4 m| UP-PAT r| Y s| Y t| PERIODICAL u| 2/2/2012
949 a| RC261.C546 v.17 no.18 2011 w| LCPER c| 1 i| 000059373025 l| PATERNO-4 m| UP-PAT r| Y s| Y t| PERIODICAL u| 2/2/2012
949 a| RC261.C546 v.17 no.19 2011 w| LCPER c| 1 i| 000059373018 l| PATERNO-4 m| UP-PAT r| Y s| Y t| PERIODICAL u| 2/2/2012
949 a| RC261.C546 v.17 no.20 2011 w| LCPER c| 1 i| 000059373117 l| PATERNO-4 m| UP-PAT r| Y s| Y t| PERIODICAL u| 2/2/2012
949 a| RC261.C546 v.17 no.21 2011 w| LCPER c| 1 i| 000059373094 l| PATERNO-4 m| UP-PAT r| Y s| Y t| PERIODICAL u| 2/2/2012
949 a| RC261.C546 v.17 no.22 2011 w| LCPER c| 1 i| 000059372974 l| PATERNO-4 m| UP-PAT r| Y s| Y t| PERIODICAL u| 2/2/2012
949 a| RC261.C546 v.17 no.23 2011 w| LCPER c| 1 i| 000059373193 l| PATERNO-4 m| UP-PAT r| Y s| Y t| PERIODICAL u| 2/2/2012
949 a| RC261.C546 v.17 no.24 2011 w| LCPER c| 1 i| 000059373124 l| PATERNO-4 m| UP-PAT r| Y s| Y t| PERIODICAL u| 2/2/2012
949 a| RC261.C546 v.2 no.1-2 1996 w| LCPER c| 1 i| 000073969655 l| PATERNO-4 m| UP-PAT r| Y s| Y t| PERIODICAL u| 6/17/2013
949 a| RC261.C546 v.3 no.1-3 1997 w| LCPER c| 1 i| 000073970507 l| PATERNO-4 m| UP-PAT r| Y s| Y t| PERIODICAL u| 6/17/2013
949 a| RC261.C546 v.1 no.5-8 1995 w| LCPER c| 1 i| 000073969686 l| PATERNO-4 m| UP-PAT r| Y s| Y t| PERIODICAL u| 6/17/2013

949		a| RC261.C546 v.1 no.9-10 1995 w| LCPER c| 1 i| 000073969679 l| PATERNO-4 m| UP-PAT r| Y s| Y t| PERIODICAL u| 6/17/2013
949		a| RC261.C546 v.1 no.11-12 1995 w| LCPER c| 1 i| 000073969662 l| PATERNO-4 m| UP-PAT r| Y s| Y t| PERIODICAL u| 6/17/2013
949		a| RC261.C546 v.2 no.3-4 1996 w| LCPER c| 1 i| 000073969648 l| PATERNO-4 m| UP-PAT r| Y s| Y t| PERIODICAL u| 6/17/2013
949		a| RC261.C546 v.2 no.5-8 1996 w| LCPER c| 1 i| 000073969631 l| PATERNO-4 m| UP-PAT r| Y s| Y t| PERIODICAL u| 6/17/2013
949		a| RC261.C546 v.2 no.9-10 1996 w| LCPER c| 1 i| 000073969624 l| PATERNO-4 m| UP-PAT r| Y s| Y t| PERIODICAL u| 6/17/2013
949		a| RC261.C546 v.2 no.11-12 1996 w| LCPER c| 1 i| 000073969617 l| PATERNO-4 m| UP-PAT r| Y s| Y t| PERIODICAL u| 6/17/2013
949		a| RC261.C546 v.3 no.4-6 1997 w| LCPER c| 1 i| 000073970491 l| PATERNO-4 m| UP-PAT r| Y s| Y t| PERIODICAL u| 6/17/2013
949		a| RC261.C546 v.3 no.7-9 1997 w| LCPER c| 1 i| 000073970484 l| PATERNO-4 m| UP-PAT r| Y s| Y t| PERIODICAL u| 6/17/2013
949		a| RC261.C546 v.3 no.10-11 1997 w| LCPER c| 1 i| 000073970477 l| PATERNO-4 m| UP-PAT r| Y s| Y t| PERIODICAL u| 6/17/2013
949		a| RC261.C546 v.3 no.12 1997 w| LCPER c| 1 i| 000073970460 l| PATERNO-4 m| UP-PAT r| Y s| Y t| PERIODICAL u| 6/17/2013
949		a| RC261.C546 v.4 no.1-3 1998 w| LCPER c| 1 i| 000073970453 l| PATERNO-4 m| UP-PAT r| Y s| Y t| PERIODICAL u| 6/17/2013
949		a| RC261.C546 v.5 no.1-3 1999 w| LCPER c| 1 i| 000073970415 l| PATERNO-4 m| UP-PAT r| Y s| Y t| PERIODICAL u| 6/17/2013
949		a| RC261.C546 v.6 no.1-2 2000 w| LCPER c| 1 i| 000073970347 l| PATERNO-4 m| UP-PAT r| Y s| Y t| PERIODICAL u| 6/17/2013
949		a| RC261.C546 v.4 no.4-6 1998 w| LCPER c| 1 i| 000073970446 l| PATERNO-4 m| UP-PAT r| Y s| Y t| PERIODICAL u| 6/17/2013
949		a| RC261.C546 v.4 no.7-9 1998 w| LCPER c| 1 i| 000073970439 l| PATERNO-4 m| UP-PAT r| Y s| Y t| PERIODICAL u| 6/17/2013
949		a| RC261.C546 v.4 no.10-12 1998 w| LCPER c| 1 i| 000073970422 l| PATERNO-4 m| UP-PAT r| Y s| Y t| PERIODICAL u| 6/17/2013
949		a| RC261.C546 v.5 no.4-6 1999 w| LCPER c| 1 i| 000073970408 l| PATERNO-4 m| UP-PAT r| Y s| Y t| PERIODICAL u| 6/17/2013
949		a| RC261.C546 v.5 no.7-8 1999 w| LCPER c| 1 i| 000073970392 l| PATERNO-4 m| UP-PAT r| Y s| Y t| PERIODICAL u| 6/17/2013
949		a| RC261.C546 v.5 no.9 1999 w| LCPER c| 1 i| 000073970385 l| PATERNO-4 m| UP PAT r| Y s| Y t| PERIODICAL u| 6/17/2013
949		a| RC261.C546 v.5 no.10 1999 & suppl. w| LCPER c| 1 i| 000073970378 l| PATERNO-4 m| UP-PAT r| Y s| Y t| PERIODICAL u| 6/17/2013
949		a| RC261.C546 v.5 no.11 1999 & suppl. w| LCPER c| 1 i| 000073970361 l| PATERNO-4 m| UP-PAT r| Y s| Y t| PERIODICAL u| 6/17/2013
949		a| RC261.C546 v.5 no.12 1999 w| LCPER c| 1 i| 000073970354 l| PATERNO-4 m| UP-PAT r| Y s| Y t| PERIODICAL u| 6/17/2013
949		a| RC261.C546 v.6 no.3-4 2000 w| LCPER c| 1 i| 000073970330 l| PATERNO-4 m| UP-PAT r| Y s| Y t| PERIODICAL u| 6/17/2013
949		a| RC261.C546 v.6 no.5-6 2000 w| LCPER c| 1 i| 000073970323 l| PATERNO-4 m| UP-PAT r| Y s| Y t| PERIODICAL u| 6/17/2013
949		a| RC261.C546 v.6 no.7-8 2000 w| LCPER c| 1 i| 000073970316 l| PATERNO-4 m| UP-PAT r| Y s| Y t| PERIODICAL u| 6/17/2013
949		a| RC261.C546 v.6 no.9-10 2000 w| LCPER c| 1 i| 000073970309 l| PATERNO-4 m| UP-PAT r| Y s| Y t| PERIODICAL u| 6/17/2013
852	0	a| PSt b| UP-PAT c| PATERNO-4 h| RC261 i| .C546
866	0 8	0 a| v.1(1995)-v.7:no.6(2001), v.7:no.8(2001)-v.17(2011)

PennState

Copyright @2019 The Pennsylvania State University. All rights reserved. Except where otherwise noted, this work is subject to a Creative Commons Attribution 4.0 license. Details and exceptions.

Legal Statements | PSU Hotlines

PENN STATE UNIVERSITY LIBRARIES

Libraries Home
Libraries Intranet (Staff Only)
Accessibility Help
Website Feedback
Policies and Guidelines
Staff Directory

(814) 865-6368

CONNECT WITH PENN STATE UNIVERSITY LIBRARIES

Facebook
Twitter
Instagram

Clinical cancer research

Published	Philadelphia, PA : American Association for Cancer Research, [1995-]
Copyright Date	©1995-
Physical Description	volumes : illustrations (some color) ; 28 cm
Additional Creators	American Association for Cancer Research

ASK A LIBRARIAN

Availability

Browse Nearby on Shelf | I Want It

Pattee Library and Paterno Library Stacks (163 items)

Call number	Material	Location
Paterno - 4th Floor: Holdings Summary v.1(1995)-v.7:no.6(2001), v.7:no.8(2001)-v.17(2011)		
RC261.C546 v.17 no.24 2011	Bound Journal	Paterno - 4th Floor
RC261.C546 v.17 no.23 2011	Bound Journal	Paterno - 4th Floor
RC261.C546 v.17 no.22 2011	Bound Journal	Paterno - 4th Floor
RC261.C546 v.17 no.21 2011	Bound Journal	Paterno - 4th Floor
RC261.C546 v.17 no.20 2011	Bound Journal	Paterno - 4th Floor
RC261.C546 v.17 no.19 2011	Bound Journal	Paterno - 4th Floor
RC261.C546 v.17 no.18 2011	Bound Journal	Paterno - 4th Floor
RC261.C546 v.17 no.17 2011	Bound Journal	Paterno - 4th Floor
RC261.C546 v.17 no.16 2011	Bound Journal	Paterno - 4th Floor
RC261.C546 v.17 no.15 2011	Bound Journal	Paterno - 4th Floor
RC261.C546 v.17 no.14 2011	Bound Journal	Paterno - 4th Floor
RC261.C546 v.17 no.13 2011	Bound Journal	Paterno - 4th Floor
RC261.C546 v.17 no.12 2011	Bound Journal	Paterno - 4th Floor
RC261.C546 v.17 no.11 2011	Bound Journal	Paterno - 4th Floor
RC261.C546 v.17 no.10 2011	Bound Journal	Paterno - 4th Floor
RC261.C546 v.17 no.9 2011	Bound Journal	Paterno - 4th Floor
RC261.C546 v.17 no.8 2011	Bound Journal	Paterno - 4th Floor
RC261.C546 v.17 no.7 2011	Bound Journal	Paterno - 4th Floor
RC261.C546 v.17 no.5-6 2011	Bound Journal	Paterno - 4th Floor
RC261.C546 v.17 no.3-4 2011	Bound Journal	Paterno - 4th Floor
RC261.C546 v.17 no.1-2 2011	Bound Journal	Paterno - 4th Floor
RC261.C546 v.16 no.23-24 2010	Bound Journal	Paterno - 4th Floor
RC261.C546 v.16 no.21-22 2010	Bound Journal	Paterno - 4th Floor
RC261.C546 v.16 no.19-20 2010	Bound Journal	Paterno - 4th Floor
RC261.C546 v.16 no.17-18 2010	Bound Journal	Paterno - 4th Floor
RC261.C546 v.16 no.16 2010	Bound Journal	Paterno - 4th Floor
RC261.C546 v.16 no.15 2010	Bound Journal	Paterno - 4th Floor
RC261.C546 v.16 no.14 2010	Bound Journal	Paterno - 4th Floor

RC261.C546 v.16 no.13 2010	Bound Journal	Paterno - 4th Floor
RC261.C546 v.16 no.12 2010	Bound Journal	Paterno - 4th Floor
RC261.C546 v.16 no.11 2010	Bound Journal	Paterno - 4th Floor
RC261.C546 v.16 no.10 2010	Bound Journal	Paterno - 4th Floor
RC261.C546 v.16 no.9 2010	Bound Journal	Paterno - 4th Floor
RC261.C546 v.16 no.8 2010	Bound Journal	Paterno - 4th Floor
RC261.C546 v.16 no.7 2010	Bound Journal	Paterno - 4th Floor
RC261.C546 v.16 no.6 2010	Bound Journal	Paterno - 4th Floor
RC261.C546 v.16 no.5 2010	Bound Journal	Paterno - 4th Floor
RC261.C546 v.16 no.4 2010	Bound Journal	Paterno - 4th Floor
RC261.C546 v.15 no.23-24 2009	Bound Journal	Paterno - 4th Floor
RC261.C546 v.15 no.21-22 2009	Bound Journal	Paterno - 4th Floor
RC261.C546 v.15 no.19-20 2009	Bound Journal	Paterno - 4th Floor
RC261.C546 v.15 no.17-18 2009	Bound Journal	Paterno - 4th Floor
RC261.C546 v.15 no.15-16 2009	Bound Journal	Paterno - 4th Floor
RC261.C546 v.15 no.13-14 2009	Bound Journal	Paterno - 4th Floor
RC261.C546 v.15 no.11-12 2009	Bound Journal	Paterno - 4th Floor
RC261.C546 v.15 no.9-10 2009	Bound Journal	Paterno - 4th Floor
RC261.C546 v.15 no.7-8 2009	Bound Journal	Paterno - 4th Floor
RC261.C546 v.15 no.5-6 Mar 2009	Bound Journal	Paterno - 4th Floor
RC261.C546 v.15 no.3-4 2009	Bound Journal	Paterno - 4th Floor
RC261.C546 v.15 no.1-2 2009	Bound Journal	Paterno - 4th Floor
RC261.C546 v.14 no.23-24 2008	Bound Journal	Paterno - 4th Floor
RC261.C546 v.14 no.21-22 2008	Bound Journal	Paterno - 4th Floor
RC261.C546 v.14 no.19-20 2008	Bound Journal	Paterno - 4th Floor
RC261.C546 v.14 no.17-18 2008	Bound Journal	Paterno - 4th Floor
RC261.C546 v.14 no.15-16 2008	Bound Journal	Paterno - 4th Floor
RC261.C546 v.14 no.13-14 2008	Bound Journal	Paterno - 4th Floor
RC261.C546 v.14 no.11-12 2008	Bound Journal	Paterno - 4th Floor
RC261.C546 v.14 no.9-10 2008	Bound Journal	Paterno - 4th Floor
RC261.C546 v.14 no.7-8 2008	Bound Journal	Paterno - 4th Floor
RC261.C546 v.14 no.5-6 2008	Bound Journal	Paterno - 4th Floor
RC261.C546 v.14 no.3-4 2008	Bound Journal	Paterno - 4th Floor
RC261.C546 v.14 no.1-2 2008	Bound Journal	Paterno - 4th Floor
RC261.C546 v.13 no.23-24 2007	Bound Journal	Paterno - 4th Floor
RC261.C546 v.13 no.21-22 2007	Bound Journal	Paterno - 4th Floor
RC261.C546 v.13 no.19-20 2007	Bound Journal	Paterno - 4th Floor
RC261.C546 v.13 no.17-18 2007 & suppl.	Bound Journal	Paterno - 4th Floor
RC261.C546 v.13 no.15-16 2007	Bound Journal	Paterno - 4th Floor
RC261.C546 v.13 no.13-14 2007	Bound Journal	Paterno - 4th Floor
RC261.C546 v.13 no.11-12 2007	Bound Journal	Paterno - 4th Floor
RC261.C546 v.13 no.9-10 2007	Bound Journal	Paterno - 4th Floor
RC261.C546 v.13 no.7-8 2007	Bound Journal	Paterno - 4th Floor
RC261.C546 v.13 no.5-6 2007	Bound Journal	Paterno - 4th Floor
RC261.C546 v.13 no.3-4 2007	Bound Journal	Paterno - 4th Floor
RC261.C546 v.13 no.1-2 2007	Bound Journal	Paterno - 4th Floor
RC261.C546 v.12 no.23-24 2006	Bound Journal	Paterno - 4th Floor
RC261.C546 v.12 no.21-22 2006	Bound Journal	Paterno - 4th Floor
RC261.C546 v.12 no.19-20 2006	Bound Journal	Paterno - 4th Floor

RC261.C546 v.12 no.17-18 2006	Bound Journal	Paterno - 4th Floor
RC261.C546 v.12 no.15-16 2006	Bound Journal	Paterno - 4th Floor
RC261.C546 v.12 no.13-14 2006 & suppl.	Bound Journal	Paterno - 4th Floor
RC261.C546 v.12 no.11-12 2006 & suppl.	Bound Journal	Paterno - 4th Floor
RC261.C546 v.12 no.9-10 2006	Bound Journal	Paterno - 4th Floor
RC261.C546 v.12 no.7-8 2006 & suppl.	Bound Journal	Paterno - 4th Floor
RC261.C546 v.12 no.5-6 2006	Bound Journal	Paterno - 4th Floor
RC261.C546 v.12 no.3-4 2006 & suppl.	Bound Journal	Paterno - 4th Floor
RC261.C546 v.12 no.1-2 2006	Bound Journal	Paterno - 4th Floor
RC261.C546 v.11 no.23-24 2005 & suppl.	Bound Journal	Paterno - 4th Floor
RC261.C546 v.11 no.21-22 2005	Bound Journal	Paterno - 4th Floor
RC261.C546 v.11 no.19-20 2005 & suppl.	Bound Journal	Paterno - 4th Floor
RC261.C546 v.11 no.17-18 2005	Bound Journal	Paterno - 4th Floor
RC261.C546 v.11 no.15-16 2005	Bound Journal	Paterno - 4th Floor
RC261.C546 v.11 no.13-14 2005 & suppl.	Bound Journal	Paterno - 4th Floor
RC261.C546 v.11 no.11-12 2005	Bound Journal	Paterno - 4th Floor
RC261.C546 v.11 no.9-10 2005	Bound Journal	Paterno - 4th Floor
RC261.C546 v.11 no.7-8 2005	Bound Journal	Paterno - 4th Floor
RC261.C546 v.11 no.5-6 2005	Bound Journal	Paterno - 4th Floor
RC261.C546 v.11 no.3-4 2005	Bound Journal	Paterno - 4th Floor
RC261.C546 v.11 no.1-2 2005 & suppl.	Bound Journal	Paterno - 4th Floor
RC261.C546 v.10 no.23-24 2004	Bound Journal	Paterno - 4th Floor
RC261.C546 v.10 no.21-22 2004	Bound Journal	Paterno - 4th Floor
RC261.C546 v.10 no.19-20 2004	Bound Journal	Paterno - 4th Floor
RC261.C546 v.10 no.17-18 2004 & suppl.	Bound Journal	Paterno - 4th Floor
RC261.C546 v.10 no.15-16 2004	Bound Journal	Paterno - 4th Floor
RC261.C546 v.10 no.13-14 2004	Bound Journal	Paterno - 4th Floor
RC261.C546 v.10 no.11-12 2004 & suppl.	Bound Journal	Paterno - 4th Floor
RC261.C546 v.10 no.9-10 2004	Bound Journal	Paterno - 4th Floor
RC261.C546 v.10 no.7-8 2004	Bound Journal	Paterno - 4th Floor
RC261.C546 v.10 no.5-6 2004	Bound Journal	Paterno - 4th Floor
RC261.C546 v.10 no.3-4 2004	Bound Journal	Paterno - 4th Floor
RC261.C546 v.10 no.1-2 2004 & suppl.	Bound Journal	Paterno - 4th Floor
RC261.C546 v.9 no.16-17 2003 & suppl.	Bound Journal	Paterno - 4th Floor
RC261.C546 v.9 no.14-15 2003	Bound Journal	Paterno - 4th Floor
RC261.C546 v.9 no.12-13 2003	Bound Journal	Paterno - 4th Floor
RC261.C546 v.9 no.10-11 2003 & suppl.	Bound Journal	Paterno - 4th Floor
RC261.C546 v.9 no.8-9 2003	Bound Journal	Paterno - 4th Floor
RC261.C546 v.9 no.6-7 2003	Bound Journal	Paterno - 4th Floor
RC261.C546 v.9 no.4-5 2003	Bound Journal	Paterno - 4th Floor
RC261.C546 v.9 no.2-3 2003	Bound Journal	Paterno - 4th Floor
RC261.C546 v.9 no.1 2003 & suppl.	Bound Journal	Paterno - 4th Floor
RC261.C546 v.8 no.11-12 2002	Bound Journal	Paterno - 4th Floor
RC261.C546 v.8 no.9-10 2002	Bound Journal	Paterno - 4th Floor
RC261.C546 v.8 no.7-8 2002	Bound Journal	Paterno - 4th Floor
RC261.C546 v.8 no.5-6 2002	Bound Journal	Paterno - 4th Floor
RC261.C546 v.8 no.3-4 2002	Bound Journal	Paterno - 4th Floor
RC261.C546 v.8 no.1-2 2002	Bound Journal	Paterno - 4th Floor

RC261.C546 v.7 no.12 2001 & suppl.	Bound Journal	Paterno - 4th Floor
RC261.C546 v.7 no.11 2001 & suppl.	Bound Journal	Paterno - 4th Floor
RC261.C546 v.7 no.9-10 2001	Bound Journal	Paterno - 4th Floor
RC261.C546 v.7 no.8 2001	Bound Journal	Paterno - 4th Floor
RC261.C546 v.7 no.5-6 2001	Bound Journal	Paterno - 4th Floor
RC261.C546 v.7 no.3-4 2001	Bound Journal	Paterno - 4th Floor
RC261.C546 v.7 no.1-2 2001	Bound Journal	Paterno - 4th Floor
RC261.C546 v.6 no.11-12 2000 & suppl.	Bound Journal	Paterno - 4th Floor
RC261.C546 v.6 no.9-10 2000	Bound Journal	Paterno - 4th Floor
RC261.C546 v.6 no.7-8 2000	Bound Journal	Paterno - 4th Floor
RC261.C546 v.6 no.5-6 2000	Bound Journal	Paterno - 4th Floor
RC261.C546 v.6 no.3-4 2000	Bound Journal	Paterno - 4th Floor
RC261.C546 v.6 no.1-2 2000	Bound Journal	Paterno - 4th Floor
RC261.C546 v.5 no.12 1999	Bound Journal	Paterno - 4th Floor
RC261.C546 v.5 no.11 1999 & suppl.	Bound Journal	Paterno - 4th Floor
RC261.C546 v.5 no.10 1999 & suppl.	Bound Journal	Paterno - 4th Floor
RC261.C546 v.5 no.9 1999	Bound Journal	Paterno - 4th Floor
RC261.C546 v.5 no.7-8 1999	Bound Journal	Paterno - 4th Floor
RC261.C546 v.5 no.4-6 1999	Bound Journal	Paterno - 4th Floor
RC261.C546 v.5 no.1-3 1999	Bound Journal	Paterno - 4th Floor
RC261.C546 v.4 no.10-12 1998	Bound Journal	Paterno - 4th Floor
RC261.C546 v.4 no.7-9 1998	Bound Journal	Paterno - 4th Floor
RC261.C546 v.4 no.4-6 1998	Bound Journal	Paterno - 4th Floor
RC261.C546 v.4 no.1-3 1998	Bound Journal	Paterno - 4th Floor
RC261.C546 v.3 no.12 1997	Bound Journal	Paterno - 4th Floor
RC261.C546 v.3 no.10-11 1997	Bound Journal	Paterno - 4th Floor
RC261.C546 v.3 no.7-9 1997	Bound Journal	Paterno - 4th Floor
RC261.C546 v.3 no.4-6 1997	Bound Journal	Paterno - 4th Floor
RC261.C546 v.3 no.1-3 1997	Bound Journal	Paterno - 4th Floor
RC261.C546 v.2 no.11-12 1996	Bound Journal	Paterno - 4th Floor
RC261.C546 v.2 no.9-10 1996	Bound Journal	Paterno - 4th Floor
RC261.C546 v.2 no.5-8 1996	Bound Journal	Paterno - 4th Floor
RC261.C546 v.2 no.3-4 1996	Bound Journal	Paterno - 4th Floor
RC261.C546 v.2 no.1-2 1996	Bound Journal	Paterno - 4th Floor
RC261.C546 v.1 no.11-12 1995	Bound Journal	Paterno - 4th Floor
RC261.C546 v.1 no.9-10 1995	Bound Journal	Paterno - 4th Floor
RC261.C546 v.1 no.5-8 1995	Bound Journal	Paterno - 4th Floor
RC261.C546 v.1 no.1-4 1995	Bound Journal	Paterno - 4th Floor

Dates of Publication and/or Sequential Designation

Vol. 1, no. 1 (Jan. 1995)-

Subject(s)

Cancer—Research—Periodicals
Neoplasms
Cancer—Periodicals

ISSN

1078-0432

Publication Frequency

Semimonthly, Aug. 15, 2003-
Monthly, 1995-Aug. 2003

Note
Title from cover.

Special Numbering
Some nos. issued in pts.

Issuing Body
"An official journal of the American Association for Cancer Research".

View MARC record | catkey: 1811522

PennState

Copyright @2019 The Pennsylvania State University. All rights reserved. Except where otherwise noted, this work is subject to a Creative Commons Attribution 4.0 license. Details and exceptions.

Legal Statements | PSU Hotlines

PENN STATE UNIVERSITY LIBRARIES

Libraries Home (814) 865-6368
Libraries Intranet (Staff Only)
Accessibility Help
Website Feedback
Policies and Guidelines
Staff Directory

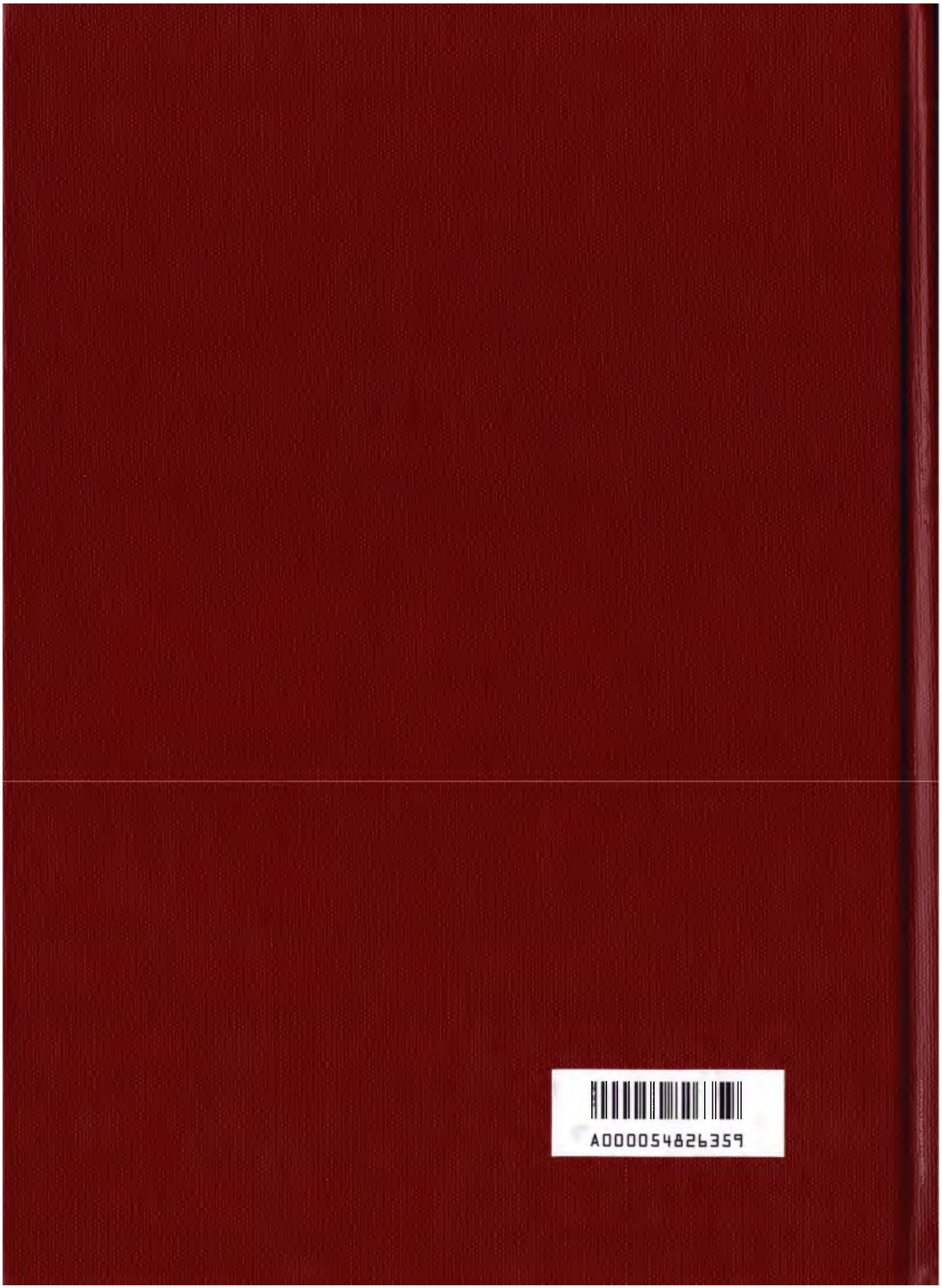
CONNECT WITH PENN STATE UNIVERSITY LIBRARIES

Facebook
Twitter
Instagram

Appendix HAMBLETT02




CLINICAL CANCER RESEARCH 10 OCT 2004 RC261 .C546


A00005482635?

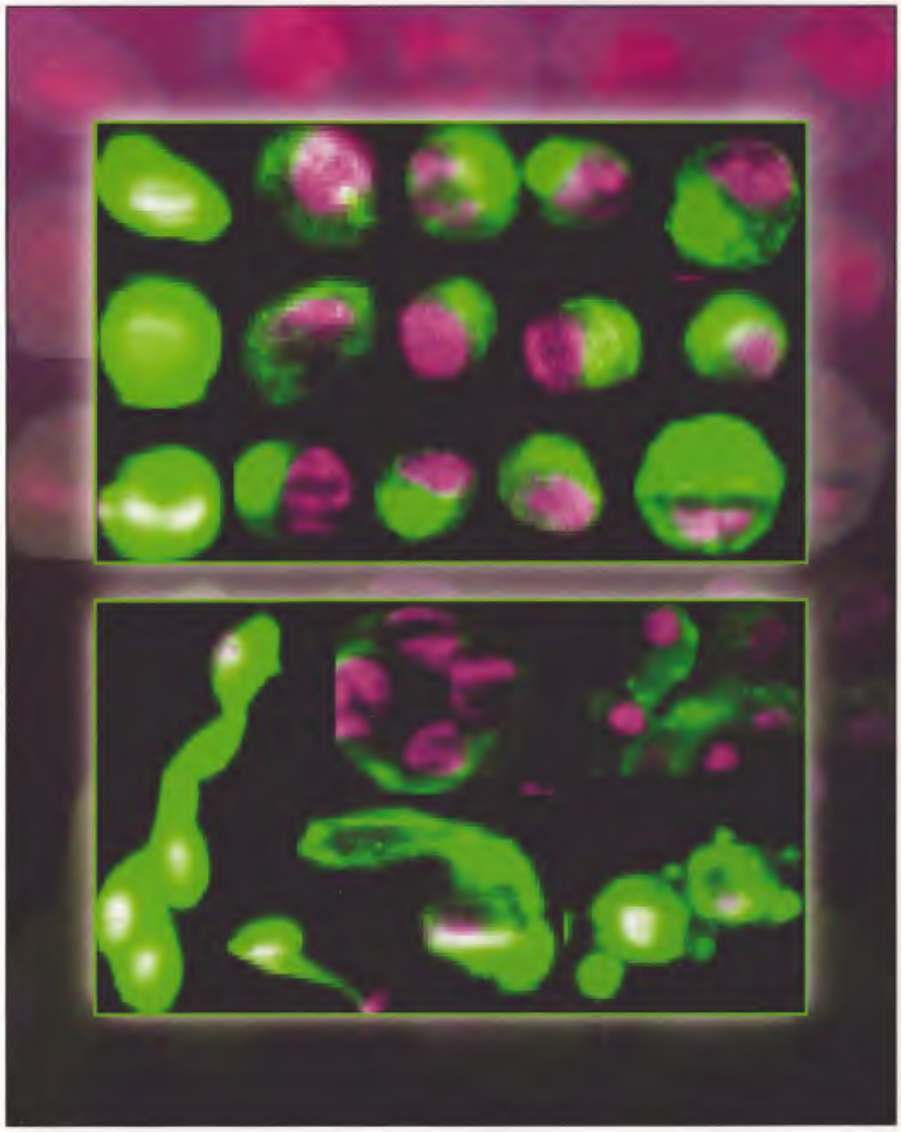
www.aacrjournals.org
American Association for Cancer Research

Life Sci

October 15, 2004
Volume 10
Number 20
Pages 6759–7108

Clinical Cancer Research

RECEIVED
OCT 26 2004
PENNSYLVANIA STATE UNIVERSITY LIBRARIES



Neoadjuvant Docetaxel and Capecitabine for Breast Cancer
Page 6764

Activation of Akt/mTOR/4E-BP1 by ErbB2 Predicts Tumor Progression
Page 6779

Molecular Profiling of Inflammatory Breast Cancer Predicts Prognosis
Page 6789

Carcinoma Cells Isolated From Blood
Page 6897

A Journal of Clinical and Translational Research

Clinical Cancer Research

A Journal of the American Association for Cancer Research

Editor-in-Chief
John Mendelsohn
Growth Factors, Hormones, Cell Growth, Surgery, Subspecialty Investigation

Deputy Editor – Waun Ki Hong
Clinical Trials Targeted at Specific Malignancies, Chemoprevention

Co-Deputy Editor – William N. Hait
Special Features, Molecular Pharmacology, Clinical Trials

Senior Editors

Bruce A. Chabner
Clinical Pharmacology and Pharmacokinetics, Drug Metabolism, Drug Sensitivity and Resistance, Drug Interactions

Allen M. Gown
Immunohistochemical Markers

Stanley R. Hamilton
Pathology, Metastasis

W. Gillies McKenna
Radiation Oncology

Jerome Ritz
Immunotherapy and Cytokines—Preclinical, Clinical Trials, and Hematologic Malignancies

Edward A. Sausville
Cell Cycle Regulation, Cell Death, Pharmacology

David Sidransky
Molecular Pathogenesis, Molecular Correlates

Beverly A. Teicher
Experimental Therapeutics, Preclinical Pharmacology, Combined Modality Regimens, Animal Therapy Models

Barbara L. Weber
Genetics, Cytogenetics

Editorial Board

Andrea Abati
James L. Abbruzzese
Bharat B. Aggarwal
Steven A. Ahrendt
Joseph Aisner
Carmen J. Allegra
Francis Ali-Osman
Enrique Alvarez
Kenneth Anderson
Jean-Pierre Armand
Carlos L. Arteaga
Avi Ashkenazi
Yehuda G. Assaraf
Frank M. Balis
Barthel Barlogie
Jiri Bartek
Jose´ Baselga
Robert C. Bast, Jr.
Susan E. Bates
Hector Battifora
David G. Beer
Colin B. Begg
Michael E. Berens
P. Leif Bergsagel
Irwin D. Bernstein
Donald A. Berry
Joseph R. Bertino
Jay A. Berzofsky
Kapil N. Bhalla
Ernest C. Borden
George J. Bosl
Ruud H. Brakenhoff
Lawrence C. Brody
Powel Brown
Ronald M. Bukowski
Paul A. Bunn, Jr.
Angelika M. Burger
Arnan U. Buzdar
Michael A. Caligiuri
A. Hilary Calvert
Stephen A. Cannistra
David Paul Carbone
Michael A. Carducci
Richard E. Champlin
Paul B. Chapman
Nai-Kong V. Cheung
Paul J. Chiao
Kathleen R. Cho
Michaele C. Christian
Edward Chu
Fortunato Ciardiello
Gary Clayman
Michael B. Cohen
Robert L. Comis
Barbara A. Conley
Kathleen A. Cooney
Jorge E. Cortes
Carlo M. Croce
David T. Curiel
Peter V. Danenberg
Andrew J. Dannenberg
Nancy E. Davidson
Yves A. DeClerck
Albert B. Deisseroth
George D. Demetri
Sally J. DeNardo
Mark W. Dewhirst
Robert B. Diasio
Colin P. Dinney
Ethan Dmitrovsky
Ross C. Donehower
James H. Doroshow
Glenn Dranoff
Louis Dubeau
Raymond N. DuBois
Alan R. Eastman
S. Gail Eckhardt
Merrill J. Egorin
Wafik S. El-Deiry
Lee M. Ellis
Adel K. El-Naggar
Paul F. Engstrom
Francisco J. Esteva
Eric R. Fearon
Soldano Ferrone
Isaiah J. Fidler
William D. Figg
Olivera J. Finn
Antonio T. Fojo
Kenneth A. Foon
Arlene A. Forastiere
David A. Frank
Arthur E. Frankel
Ralph S. Freedman
Henry S. Friedman
Herbert A. Fritsche
Gary E. Gallick
Varsha V. Gandhi
Judy E. Garber
Spiridione Garbisa
Shiva Gautam
Adi F. Gazdar
Stephen L. George
Stanton L. Gerson
Giuseppe Giaccone
Luca Gianni
Eli J. Glatstein
Bonnie S. Glisson
I. David Goldman
Jennifer Rubin Grandis
Steven Grant
Joe W. Gray
Jean L. Grem
William Grizzle
Louise Barnett Grochow
Stephen B. Gruber
Bruce G. Haffty
Anne W. Hamburger
Paul M. Harari
Adrian L. Harris
Curtis C. Harris
Daniel F. Hayes
Nicholas Hayward
Lee J. Helman
Mary J. C. Hendrix
Roy S. Herbst
James G. Herman
John A. Hickman
Manuel Hidalgo
Walter N. Hittelman
Samuel B. Ho
Robert M. Hoffman
Monica Hollstein
Shawn E. Holt
Sandra Horning
Gabriel N. Hortobagyi
Janet A. Houghton
Peter J. Houghton
Stephen B. Howell
Ralph H. Hruban
Clifford Hudis
John T. Isaacs
Mark A. Israel
Jean-Pierre Issa
Elizabeth M. Jaffee
Rakesh K. Jain
C. David James
Jin Jen
Bruce E. Johnson
David H. Johnson
Patrick Johnston
Monica Brown Jones
V. Craig Jordan
William G. Kaelin, Jr.
Barton A. Kamen
Hagop Kantarjian
Judith E. Karp
Scott H. Kaufmann
John J. Kavanagh
S. B. Kaye
Robert S. Kerbel
Michael Kerin
Khandan Keyomarsi
David Khayat
Fadlo R. Khuri
Timothy J. Kinsella
Thomas J. Kipps
John M. Kirkwood
Hynda K. Kleinman
Elise C. Kohn
Donald W. Kufe
Rakesh Kumar
Razelle Kurzrock
Steven M. Larson
John S. Lazo
Fredrick Leach
Jin S. Lee
Stanley Lipkowitz
Scott M. Lipprnan
Alan Lipton
Paul Liu
Philip O. Livingston
Albert F. LoBuglio
Christopher J. Logothetis
Reuben Lotan
H. Kim Lyerly
Li Mao
Francesco Marincola
Maurie Markman
Sanford Markowitz
David J. McConkey
Howard L. McLeod
Paul S. Meltzer
Raymond E. Meyn, Jr.
Frank L. Meyskens, Jr.
Luka Milas
Randall E. Millikan
Gordon B. Mills
John D. Minna
Bruce Minsky
Malcolm S. Mitchell
Richard A. Morgan
Michael A. Morse
Hasan Mukhtar
Carolyn Y. Muller
Robert J. Mullin
James L. Mulshine
William G. Nelson
Larry Norton
Steven O'Day
Michael O'Reilly
Joyce A. O'Shaughnessy
Robert F. Ozols
Rodney L. Page
Klaus Pantel
Drew M. Pardoll
Jae-Gahb Park
Harvey Pass
Ira Pastan
Richard Pazdur
George E. Peoples
Roman Perez-Soler
David G. Pfister
Kenneth J. Pienta
Herbert M. Pinedo
William K. Plunkett
Donald A. Podoloff
Kornelia Polyak
Yves G. Pommier
Jerome B. Posner
Garth Powis
Arnold B. Rabson
Derek Raghavan
Mark J. Ratain
Eddie Reed
John C. Reed
Ralph A. Reisfeld
Michael Reiss
C. Patrick Reynolds
Paul Richardson
Michael J. Robertson
Miriam P. Rosin
Jack A. Roth
Mace Rothenberg
Eric K. Rowinsky
Eric H. Rubin
Lawrence Rubinstein
Youcef M. Rustum
David P. Ryan
Guido Sauter
Charles L. Sawyers
David A. Scheinberg
Howard I. Scher
Joan H. Schiller
Richard L. Schilsky
Steven B. Scholnick
Richard M. Schultz
Gary K. Schwartz
Michael V. Seiden
Adrian M. Senderowicz
Geoffrey I. Shapiro
Laura K. Shawver
Jerry W. Shay
Weichung Joe Shih
Dong Moon Shin
Edward B. Silberstein
Richard M. Simon
George W. Sledge
Matthew Smith
John F. Smyth
Robert Soiffer
Jeffrey A. Sosman
Michael B. Spom
Cy Stein
William G. Stetler-Stevenson
Jeffrey G. Supko
Sandra M. Swain
Trevor W. Sweatman
Chris H. Takimoto
Moshe Talpaz
David Tarin
Margaret A. Tempero
Joel E. Tepper
Masaaki Terada
Mary B. Todd
William D. Travis
Donald L. Trump
David Vail
Carter Van Waes
Ellen S. Vitetta
Everett E. Vokes
Daniel D. Von Hoff
Robert Vonderheide
Jeffrey S. Weber
Louis M. Weiner
I. Bernard Weinstein
Winfried Wels
William Westra
Theresa L. Whiteside
Max S. Wicha
Robert E. Wittes
Keping Xie
Chung S. Yang
Wei Zhang

American Association for Cancer Research

615 Chestnut Street, 17th Floor
Philadelphia, PA 19106-4404

www.aacr.org
E-mail: ccr@aacr.org

Chief Executive Officer ..... Margaret Foti
Publisher ..... Kathleen Case
Editorial Staff
Assistant Director, Publications ..... Michael J. Beveridge
Production Manager ..... June Eberharter
Production Editors ..... Mark Miklosovich, Victoria Salvucci
Special Issues Editor ..... Diane M. Marinelli
Editorial Office Manager ..... Kelly Hadsell
Editorial Assistants ..... William J. Siegmann, Brianna Gallagher, Jonathan F. McCabe
M.D. Anderson Editorial Staff
Administrative Editor ..... Beth Notzon
Editorial Secretary ..... Sue L. Davis

DAC EX. 2040 IPR2022-01531 Page 972 of 1299

Clinical Cancer Research (ISSN 1078-0432) is published twice monthly, one volume per year, by the American Association for Cancer Research, Inc., 615 Chestnut Street, 17th Floor, Philadelphia, PA 19106-4404. Periodicals postage paid at Philadelphia, PA, and additional mailing offices. POSTMASTER: Send address changes to AACR Subscription Office, P.O. Box 11806, Birmingham, AL 35202. Copyright © 2004 by the American Association for Cancer Research, Inc. Printed on acid-free paper in the United States of America.

Submission of Manuscripts

Clinical Cancer Research publishes original articles describing clinical research on the cellular and molecular characterization, prevention, diagnosis, and therapy of human cancer. Its focus is on innovative clinical research and translational research that bridges the laboratory and the clinic. *Clinical Cancer Research* is especially interested in clinical trials evaluating new treatments for cancer; research on molecular abnormalities that predict incidence, response to therapy, and outcome; and laboratory studies of new drugs and biological agents that will lead to clinical trials in patients. All submissions undergo peer review. Papers can now be submitted online at http://www.rapidreview.com/AACR2/author.html. Authors are strongly encouraged to submit online to expedite the review process. Authors who are unable to submit online should address hard-copy submissions to Dr. John Mendelsohn, Editor-in-Chief, *Clinical Cancer Research,* AACR Publications Department, 615 Chestnut Street, 17th Floor, Philadelphia, PA 19106-4404. Please refer to the Information for Authors before submitting a manuscript.

Subscription Information

Subscriptions to *Clinical Cancer Research* are available for $100 annually for members and $225 for individual nonmembers. *Clinical Cancer Research* is only available to institutions as a combined subscription with *Cancer Research.* The combined 2004 institutional subscription price of $1550 includes $550 for a subscription to *Clinical Cancer Research.* Print subscription includes online access. The standard institutional subscription allows access to authorized users at machines located in the subscribing library. For networked or remote institutional access, a site license is required, Institutional site license customers, contact AACR Publications Department at the above address. Phone: (215) 440-9300; fax: (215) 440-9455; E-mail: pubs@aacr.org.

Claims for missing issues made within six months of the issue date will be honored while supplies last. Institutions and nonmember individuals, contact AACR Subscription Office. Phone: (800) 633-4931 or (205) 995-1567; fax: (205) 995-1588; E-mail: aacrsubs@ebsco.com. AACR members, contact AACR Member Services Department. Phone: (215) 440-9300; fax: (215) 440-9412; E-mail: membership@aacr.org.

Single issue copies and copies of back stock of the journal may be ordered from AACR Subscription Office, P.O. Box 11806, Birmingham, AL 35202 [Phone: (800) 633-4931 or (205) 995-1567; FAX: (205) 995-1588; E-mail: aacrsubs@ebsco.com]. As long as supplies permit, single copies will be sold by this company at $25.00/copy. Orders outside the U.S. add $3.00/copy to offset postage costs.

Advertisements

Advertisement insertion orders and copy must be received one month prior to the date of issue in which the advertisement is to be published. The journal is mailed on approximately the 1st day of the month of issue. Inquiries about advertising should be directed to M. J. Mrvica Associates, Inc., 2 West Taunton Ave., Berlin, NJ 08009 [Telephone: (856) 768-9360; FAX: (856) 753-0064].

Copyright and Permissions

Authors who wish to publish in *Clinical Cancer Research* must formally transfer copyright to the proprietor of the journal, the American Association for Cancer Research, Inc. It is understood by this transfer that the authors relinquish all exclusive rights of copyright ownership, including the rights of reproduction, derivation, distribution, sale, and display.

Authors who prepared their articles as part of their official duties as employees of the U.S. Federal Government are not required to transfer copyright to the American Association for Cancer Research, Inc., since these articles are considered to be in the public domain. In the case of articles supported by federal grants or contracts, copyright transfer to the American Association for Cancer Research, Inc., is required. The federal government may retain a nonexclusive license to publish or republish such material.

The Journal will routinely allow authors (or others with the permission of the authors) to include select parts of a copyrighted article in reviews, books, or subsequent papers, upon written request to the AACR Director of Publications. All permission requests must include a brief description of intended use and a stamped, self-addressed envelope. Third parties should obtain the approval of the authors *before* corresponding with the AACR.

Address requests to AACR Publications Department [Phone: (215) 440-9300; FAX: (215) 440-9354; E-mail: permissions@aacr.org].

Copies of the articles in *Clinical Cancer Research* may be made for personal or internal use, provided that the copier pay a per-copy fee of $11.00 through the Copyright Clearance Center, Inc. This Center is a nonprofit organization through which individuals and institutions may reimburse a copyright owner for photocopying of journal articles beyond what is defined as fair use in Sections 107 and 108 of the Copyright Revision Act of 1978. Those who wish to photocopy articles for which the AACR holds the copyright should report the title of the Journal, the month and year of publication, the initial page number of the article, the number of copies made, and the appropriate fee code to: Copyright Clearance Center, Inc., 222 Rosewood Drive, Danvers, MA 01923; Phone: (508) 750-8400. Fax: (508) 750-4744. Remittances may be sent to the Center at the time of reporting or the Center will bill the user on a monthly basis. Deposit accounts and prepayment plans may also be used.

Clinical Cancer Research is abstracted and/or indexed in *Cancer Lit, Chemical Abstracts, Current Contents/Clinical Medicine,* and *Index Medicus*/MEDLINE.

Clinical Cancer Research

Volume 10, Number 20
October 15, 2004

CONTENTS

Perspective

6759 **Evaluating the Efficiency of Targeted Designs for Randomized Clinical Trials.** Richard Simon and Aboubakar Maitournam.

Featured Articles

Clinical Trials

6764 **A Phase II Trial of Neoadjuvant Docetaxel and Capecitabine for Locally Advanced Breast Cancer.** Peter F. Lebowitz, Jennifer Eng-Wong, Sandra M. Swain, Arlene Berman, Maria J. Merino, Catherine K. Chow, David Venzon, Farah Zia, David Danforth, Edison Liu, and JoAnne Zujewski.

Molecular Oncology, Markers, Clinical Correlates

6770 **Clinical and Biomarker Correlates of Androgen-Independent, Locally Aggressive Prostate Cancer With Limited Metastatic Potential.** Vasily J. Assikis, Kim-Anh Do, Sijin Wen, Xuemei Wang, Jeong Hee Cho-Vega, Shawn Brisbay, Remigio Lopez, Christopher J. Logothetis, Patricia Troncoso, Christos N. Papandreou, and Timothy J. McDonnell.

6779 **Activation of the Akt/Mammalian Target of Rapamycin/4E-BP1 Pathway by ErbB2 Overexpression Predicts Tumor Progression in Breast Cancers.** Xiaoyan Zhou, Ming Tan, Valerie Stone Hawthorne, Kristine S. Klos, Keng-Hsueh Lan, Ying Yang, Wentao Yang, Terry L. Smith, Daren Shi, and Dihua Yu.

6789 **Molecular Profiling of Inflammatory Breast Cancer: Identification of a Poor-Prognosis Gene Expression Signature.** Ivan Bièche, Florence Lerebours, Sengül Tozlu, Marc Espie, Michel Marty, and Rosette Lidereau.

6796 **Variability in the Degree of Expression of Phosphorylated IκBα in Chronic Lymphocytic Leukemia Cases With Nodal Involvement.** Antonia Rodríguez, Nerea Martínez, Francisca I. Camacho, Elena Ruíz-Ballesteros, Patrocinio Algara, Juan-Fernando García, Javier Menárguez, Tomás Alvaro, Manuel F. Fresno, Fernando Solano, Manuela Mollejo, Carmen Martin, and Miguel A. Piris.

Experimental Therapeutics, Preclinical Pharmacology

6807 **Components of the Cell Death Machine and Drug Sensitivity of the National Cancer Institute Cell Line Panel.** Phyllis A. Svingen, David Loegering, Joe Rodriquez, Xue Wei Meng, Peter W. Mesner, Jr., Susan Holbeck, Anne Monks, Stan Krajewski, Dominic A. Scudiero, Edward A. Sausville, John C. Reed, Yuri A. Lazebnik, and Scott H. Kaufmann.

6821 **Induction of Thyroid Cancer Cell Apoptosis by a Novel Nuclear Factor κB Inhibitor, Dehydroxymethylepoxyquinomicin.** Dmitriy V. Starenki, Hiroyuki Namba, Vladimir A. Saenko, Akira Ohtsuru, Shigeto Maeda, Kazuo Umezawa, and Shunichi Yamashita.

Regular Articles

Clinical Trials

6830 **A Phase I and Pharmacodynamic Study of Fludarabine, Carboplatin, and Topotecan in Patients With Relapsed, Refractory, or High-Risk Acute Leukemia.** Brenda W. Cooper, Gareth J. Veal, Tomas Radivoyevitch, Michael J. Tilby, Howard J. Meyerson, Hillard M. Lazarus, Omer N. Koc, Richard J. Creger, Graham Pearson, Geoff M. Nowell, David Gosky, Stephen T. Ingalls, Charles L. Hoppel, and Stanton L. Gerson.

6840 **Effects of α_1-Acid Glycoprotein on the Clinical Pharmacokinetics of 7-Hydroxystaurosporine.** Alex Sparreboom, Huachen Chen, Milin R. Acharya, Adrian M. Senderowicz, Richard A. Messmann, Takashi Kuwabara, David J. Venzon, Anthony J. Murgo, Donna Headlee, Edward A. Sausville, and William D. Figg.

6847 **Phase I Clinical Trial of Oral Curcumin: Biomarkers of Systemic Activity and Compliance.** Ricky A. Sharma, Stephanie A. Euden, Sharon L. Platton, Darren N. Cooke, Aisha Shafayat, Heather R. Hewitt, Timothy H. Marczylo, Bruno Morgan, David Hemingway, Simon M. Plummer, Munir Pirmohamed, Andreas J. Gescher, and William P. Steward.

6855 **Effects of Recombinant Erythropoietin in Palliative Treatment of Unselected Cancer Patients.** Elisabet Lindholm, Peter Daneryd, Ulla Körner, Anders Hyltander, Marita Fouladiun, and Kent Lundholm.

Molecular Oncology, Markers, Clinical Correlates

6865 **Phospho-Akt Overexpression in Non–Small Cell Lung Cancer Confers Significant Stage-Independent Survival Disadvantage.** Odile David, James Jett, Helena LeBeau, Grace Dy, Janet Hughes, Mitchell Friedman, and Arnold R. Brody.

6872 **Modulation of Pulmonary Leukotriene B_4 Production by Cyclooxygenase-2 Inhibitors and Lipopolysaccharide.** Jenny T. Mao, I-Hsien Tsu, Steven M. Dubinett, Bradley Adams, Theodore Sarafian, Felicita Baratelli, Michael D. Roth, and Kenneth J. Serio.

DAC EX. 2040 IPR2022-01531 Page 974 of 1299

6879 **Induction of Endothelial Nitric Oxide Synthase Expression by Melanoma Sensitizes Endothelial Cells to Tumor Necrosis Factor-Driven Cytotoxicity.** Simone Mocellin, Maurizio Provenzano, Carlo Riccardo Rossi, Pierluigi Pilati, Romano Scalerta, Mario Lise, and Donato Nitti.

6887 **Proteomic Analysis of Human Acute Leukemia Cells: Insight into Their Classification.** Jiu-Wei Cui, Jie Wang, Kun He, Bao-Feng Jin, Hong-Xia Wang, Wei Li, Li-Hua Kang, Mei-Ru Hu, Hui-Yan Li, Ming Yu, Bei-fen Shen, Guan-Jun Wang, and Xue-Min Zhang.

6897 **Tumor Cells Circulate in the Peripheral Blood of All Major Carcinomas but not in Healthy Subjects or Patients With Nonmalignant Diseases.** W. Jeffrey Allard, Jeri Matera, M. Craig Miller, Madeline Repollet, Mark C. Connelly, Chandra Rao, Arjan G. J. Tibbe, Jonathan W. Uhr, and Leon W. M. M. Terstappen.

6905 **Expression of ΔNp73 Predicts Poor Prognosis in Lung Cancer.** Hidetaka Uramoto, Kenji Sugio, Tsunehiro Oyama, Shoji Nakata, Kenji Ono, Masaru Morita, Keiko Funa, and Kosei Yasumoto.

6912 **Is a Lymph Node Detected by the Dye-Guided Method a True Sentinel Node in Gastric Cancer?** Hirohisa Osaka, Masakazu Yashiro, Tetsuji Sawada, Kei Katsuragi, and Kosei Hirakawa.

6919 **Lymphatic Vessel Density and Vascular Endothelial Growth Factor-C Expression Correlate with Malignant Behavior in Human Pancreatic Endocrine Tumors.** Laura Rubbia-Brandt, Benoit Terris, Emile Giostra, Bertrand Dousset, Philippe Morel, and Michael S. Pepper.

6929 **Effect of Human Papillomavirus-16 Infection on CD8+ T-Cell Recognition of a Wild-Type Sequence $p53_{264-272}$ Peptide in Patients with Squamous Cell Carcinoma of the Head and Neck.** Nicky Sirianni, Patrick K. Ha, Mattias Oelke, Joseph Califano, William Gooding, William Westra, Theresa L. Whiteside, Wayne M. Koch, Jonathan P. Schneck, Albert DeLeo, and Robert L. Ferris.

6938 **Concomitant Overexpression of Cyclooxygenase-2 in HER-2–Positive on Smad4-Reduced Human Gastric Carcinomas Is Associated with a Poor Patient Outcome.** Hirokazu Okano, Hisashi Shinohara, Akiko Miyamoto, Kyoichi Takaori, and Nobuhiko Tanigawa.

6946 **The Spontaneous $CD8^+$ T-Cell Response to HLA-A2–Restricted NY-ESO-1b Peptide in Hepatocellular Carcinoma Patients.** Xiao-Ying Shang, Hong-Song Chen, Hua-Gang Zhang, Xue-Wen Pang, Huan Qiao, Ji-Run Peng, Li-Ling Qin, Ran Fei, Ming-Hui Mei, Xi-Sheng Leng, Sacha Gnjatic, Gerd Ritter, Andrew J. G. Simpson, Lloyd J. Old, and Wei-Feng Chen.

6956 **The Absence of Human Equilibrative Nucleoside Transporter 1 Is Associated with Reduced Survival in Patients With Gemcitabine-Treated Pancreas Adenocarcinoma.** Jennifer Spratlin, Randeep Sangha, Darryl Glubrecht, Laith Dabbagh, James D. Young, Charles Dumontet, Carol Cass, Raymond Lai, and John R. Mackey.

6962 **HDAC6 Expression Is Correlated with Better Survival in Breast Cancer.** Zhenhuan Zhang, Hiroko Yamashita, Tatsuya Toyama, Hiroshi Sugiura, Yoko Omoto, Yoshiaki Ando, Keiko Mita, Maho Hamaguchi, Shin-ichi Hayashi, and Hirotaka Iwase.

6969 **Rat Sodium Iodide Symporter for Radioiodide Therapy of Cancer.** Elena Mitrofanova, Robert Unfer, Nick Vahanian, Wayne Daniels, Erica Roberson, Tatiana Seregina, Prem Seth, and Charles Link, Jr.

Experimental Therapeutics, Preclinical Pharmacology

6977 **Monitoring the Response of Orthotopic Bladder Tumors to Granulocyte Macrophage Colony-Stimulating Factor Therapy Using the *Prostate-Specific Antigen* Gene as a Reporter.** Qinghui Wu, Kesavan Esuvaranathan, and Ratha Mahendran.

6985 **Treatment of Neuroblastoma Meningeal Carcinomatosis with Intrathecal Application of α-Emitting Atomic Nanogenerators Targeting Disialo-Ganglioside GD2.** Matthias Miederer, Michael R. McDevitt, Paul Borchardt, Ira Bergman, Kim Kramer, Nai-Kong V. Cheung, and David A. Scheinberg.

6993 **Effect of Rapamycin Alone and in Combination with Antiangiogenesis Therapy in an Orthotopic Model of Human Pancreatic Cancer.** Susann Stephan, Kaustubh Datta, Enfeng Wang, Jinping Li, Rolf A. Brekken, Sareh Parangi, Philip E. Thorpe, and Debabrata Mukhopadhyay.

7001 **Fibrinogen-Coated Droplets of Olive Oil for Delivery of Docetaxel to a Fibrin(ogen)-Rich Ascites Form of a Murine Mammary Tumor.** Charity M. Einhaus, Andrew C. Retzinger, Andre O. Perrotta, Michael D. Dentler, Abhijeet S. Jakate, Pankaj B. Desai, and Gregory S. Retzinger.

7011 **The *In vitro* and *In vivo* Effects of Re-Expressing Methylated *von Hippel-Lindau* Tumor Suppressor Gene in Clear Cell Renal Carcinoma with 5-Aza-2′-deoxycytidine.** Wade G. Alleman, Ray L. Tabios, Gadisetti V. R. Chandramouli, Olga N. Aprelikova, Carlos Torres-Cabala, Arnulfo Mendoza, Craig Rodgers, Nikolai A. Sopko, W. Marston Linehan, and James R. Vasselli.

7022 **Troglitazone Acts on Cellular pH and DNA Synthesis through a Peroxisome Proliferator-Activated Receptor γ-Independent Mechanism in Breast Cancer-Derived Cell Lines.** Francesco Turturro, Ellen Friday, Rocky Fowler, Diya Surie, and Tomas Welbourne.

7031 **Targeting Mammalian Target of Rapamycin Synergistically Enhances Chemotherapy-Induced Cytotoxicity in Breast Cancer Cells.** Wallace H. Mondesire, Weiguo Jian, Haixia Zhang, Joe Ensor, Mien-Chie Hung, Gordon B. Mills, and Funda Meric-Bernstam.

7043 **Heteroclitic CD33 Peptide With Enhanced Anti-Acute Myeloid Leukemic Immunogenicity.** Jooeun Bae, Jeffrey A. Martinson, and Hans G. Klingemann.

7053 **Recognition of Adult T-Cell Leukemia/Lymphoma Cells by $CD4^+$ Helper T Lymphocytes Specific for Human T-Cell Leukemia Virus Type I Envelope Protein.** Hiroya Kobayashi, Toshihiro Nagato, Mitsuru Yanai, Kensuke Oikawa, Keisuke Sato, Shoji Kimura, Masatoshi Tateno, Ryusuke Omiya, and Esteban Celis.

7063 **Effects of Drug Loading on the Antitumor Activity of a Monoclonal Antibody Drug Conjugate.** Kevin J. Hamblett, Peter D. Senter, Dana F. Chace, Michael M. C. Sun, Joel Lenox, Charles G. Cerveny, Kim M. Kissler, Starr X. Bernhardt, Anastasia K. Kopcha, Roger F. Zabinski, Damon L. Meyer, and Joseph A. Francisco.

7071 **HMMC-1: A Humanized Monoclonal Antibody With Therapeutic Potential Against Müllerian Duct-Related Carcinomas.** Shiro Nozawa, Daisuke Aoki, Katsumi Tsukazaki, Nobuyuki Susumu, Motoko Sakayori, Nao Suzuki, Atsushi Suzuki, Rie Wakita, Makio Mukai, Yuko Egami, Kyoko Kojima-Aikawa, Isao Ishida, Frederic Belot, Ole Hindsgaul, Minoru Fukuda, and Michiko N. Fukuda.

7079 **Abrogation of Head and Neck Squamous Cell Carcinoma Growth by Epidermal Growth Factor Receptor Ligand Fused to *Pseudomonas* Exotoxin Transforming Growth Factor α-PE38.** Sufi M. Thomas, Qing Zeng, Michael W. Epperly, William E. Gooding, Ira Pastan, Qing Cheng Wang, Joel Greenberger, and Jennifer Rubin Grandis.

7088 **Bioactive Suture: A Novel Immunotherapy for Head and Neck Cancer.** Terry Y. Shibuya, Sanghun Kim, Kevin Nguyen, Johnny Do, Christine E. McLaren, Kuo-Tung Li, Wen-Pin Chen, Parag Parikh, Ashish Wadhwa, Xiaolin Zi, Vincent Y. Chen, Hau-Sin Wong, William B. Armstrong, and George H. Yoo.

7100 **Aberrant Methylation of *DPYD* Promoter, *DPYD* Expression, and Cellular Sensitivity to 5-Fluorouracil in Cancer Cells.** Takuya Noguchi, Keiji Tanimoto, Tatsushi Shimokuni, Kei Ukon, Hiroaki Tsujimoto, Masakazu Fukushima, Tsuyoshi Noguchi, Katsunobu Kawahara, Keiko Hiyama, and Masahiko Nishiyama.

i **Instructions for Authors** CCR-109841-05:2-

The Cover

Cover photograph: Gallery of circulating tumor cell (CTC) images showing examples of intact CTCs, CTC clusters, and irregularly shaped CTCs. Tumor cells were isolated from 7.5 mL of blood from patients with a variety of metastatic carcinomas by using the CellSearch Circulating Tumor Cell Kit (Veridex LLC, Raritan, NJ) and displayed on the CellSpotter Analyzer (Veridex). Nuclei were stained with DAPI (depicted in magenta) and the cytoplasm was stained with a cocktail of antibodies to cytokeratins 8, 18, and 19 (depicted in green). Some of the nuclear images are depicted in white because of the intensity of the cytokeratin staining. See Allard *et al.* in this issue.

Effects of Drug Loading on the Antitumor Activity of a Monoclonal Antibody Drug Conjugate

Kevin J. Hamblett, Peter D. Senter, Dana F. Chace, Michael M. C. Sun, Joel Lenox, Charles G. Cerveny, Kim M. Kissler, Starr X. Bernhardt, Anastasia K. Kopcha, Roger F. Zabinski, Damon L. Meyer, and Joseph A. Francisco

Seattle Genetics, Inc., Bothell, Washington

ABSTRACT

Purpose: **An antibody-drug conjugate consisting of monomethyl auristatin E (MMAE) conjugated to the anti-CD30 monoclonal antibody (mAb) cAC10, with eight drug moieties per mAb, was previously shown to have potent cytotoxic activity against $CD30^+$ malignant cells. To determine the effect of drug loading on antibody-drug conjugate therapeutic potential, we assessed cAC10 antibody-drug conjugates containing different drug-mAb ratios *in vitro* and *in vivo*.**

Experimental Design: **Coupling MMAE to the cysteines that comprise the interchain disulfides of cAC10 created an antibody-drug conjugate population, which was purified using hydrophobic interaction chromatography to yield antibody-drug conjugates with two, four, and eight drugs per antibody (E2, E4, and E8, respectively). Antibody-drug conjugate potency was tested *in vitro* against $CD30^+$ lines followed by *in vivo* xenograft models. The maximum-tolerated dose and pharmacokinetic profiles of the antibody-drug conjugates were investigated in mice.**

Results: **Although antibody-drug conjugate potency *in vitro* was directly dependent on drug loading (IC_{50} values E8<E4<E2), the *in vivo* antitumor activity of E4 was comparable with E8 at equal mAb doses, although the E4 contained half the amount of MMAE per mAb. E2 was also an active antitumor agent but required higher doses. The maximum-tolerated dose of E2 in mice was at least double that of E4, which in turn was twice that of E8. MMAE loading affected plasma clearance, as E8 cleared 3-fold faster than E4 and 5-fold faster than E2.**

Conclusions: **By decreasing drug loading per antibody, the therapeutic index was increased demonstrating that drug loading is a key design parameter for antibody-drug conjugates.**

INTRODUCTION

Recent success in the development of monoclonal antibodies (mAbs) for the treatment of cancer, such as rituximab for the treatment of non-Hodgkin's B-cell lymphoma and trastuzumab for breast cancer (1), have proven that mAbs can be a valuable weapon in the battle against cancer. To further advance the use of mAb-based therapies for cancer, a number of novel approaches have been explored. For example several approaches have been shown to enhance the ability of an antibody to mediate antibody-dependent cell-mediated cytotoxicity by optimizing the structure of the Fc-associated N-linked oligosaccharide (2, 3). Alternatively, cell-killing payloads such as protein toxins (4), radionuclides (5, 6), and anticancer drugs (7–9) have been conjugated to mAbs to generate immunotoxins, radioimmunoconjugates, and antibody-drug conjugates, respectively.

Gemtuzumab ozogamicin, an antibody-drug conjugate that is composed of the potent DNA minor groove binder calicheamicin linked covalently to an anti-CD33 mAb (8), was approved in 2000 by the United States Food and Drug Administration for the treatment of patients with relapsed acute myeloid leukemia (10). Other antibody-drug conjugates currently in development use a number of different cytotoxic drugs and linkage systems. For example, the maytansine-derivative DM1, a potent antimicrotubule agent, is used in huN901-DM1 for small-cell lung cancer and huC242-DM1, which targets the CanAg antigen present on various tumors (9). SGN-15 is an anti-Lewis Y antibody conjugated to doxorubicin and is currently in a phase II trial for non–small-cell lung cancer (7). Several other antibody-drug conjugates have shown pronounced activities in preclinical models and are advancing toward or have entered clinical trials (11–15).

Development of antibody-drug conjugates with therapeutic potential involves the optimization of several critical parameters. These include the use of highly potent drugs that are attenuated and stable while attached to the mAbs (12–14, 16) and the use of drug-mAb linkers that allow for the release of active drug only when the mAb has reached the target site (12, 17–20). Another key factor is the choice of target antigen. The target antigen should internalize upon mAb binding, have high expression on tumor cells, and little to no expression on normal cells.

The antigen CD30 is highly expressed on the surface of cancer cells such as Hodgkin's disease (21) and anaplastic large cell lymphomas (22). This expression, coupled with limited expression on normal cells (21, 23, 24), makes CD30 an attractive target for antibody-drug conjugate therapy. We recently demonstrated that the chimeric mAb cAC10 has antitumor activity against Hodgkin's disease both *in vitro* and in s.c. and disseminated SCID mouse xenograft models (25). We subse-

Received 4/21/04; revised 7/12/04; accepted 7/13/04.
The costs of publication of this article were defrayed in part by the payment of page charges. This article must therefore be hereby marked *advertisement* in accordance with 18 U.S.C. Section 1734 solely to indicate this fact.

Requests for reprints: Joseph A. Francisco, Seattle Genetics, Inc., 21823 30th Drive Southeast, Bothell, WA 98021. Phone: (425) 527-4910; Fax: (425) 527-4609; E-mail: jfrancisco@seagen.com.

©2004 American Association for Cancer Research.

DAC EX. 2040 IPR2022-01531 Page 977 of 1299

quently reported that the antitumor activity of cAC10 could be dramatically enhanced by generating antibody-drug conjugates with derivatives of the cytotoxic agent auristatin E as the drug component (12, 13). These antibody-drug conjugates were highly effective in murine xenograft models at well-tolerated doses.

In developing the cAC10 antibody-drug conjugate, emphasis was placed on the stability of the linker, the method by which the drug was covalently attached to the mAb, and optimizing the potency of the drug component. Historically, augmenting the potency of an antibody-drug conjugate involved increasing the number of drugs on an antibody (20) or conjugating more potent drugs (12). Although previous reports describe how drug loading influences *in vitro* characteristics (16, 20, 26), the effects of drug multiplicity on *in vivo* parameters of antibody-drug conjugates has not been described. In the present work, we have evaluated the effect of drug loading on the *in vitro* and *in vivo* properties of cAC10 antibody-drug conjugates. The characteristics of cAC10 loaded with different ratios of MMAE demonstrate how drug loading affects pharmacokinetics and the therapeutic index parameters of efficacy and toxicity, which reveals drug loading as an important design parameter of antibody-drug conjugates.

MATERIALS AND METHODS

Cells and Reagents. CD30-positive anaplastic large-cell lymphoma line Karpas-299 and CD30-negative WSU-NHL were obtained from the Deutsche Sammlung von Mikroorganism und Zellkulturen GmbH (Braunschweig, Germany). L540cy, a derivative of the Hodgkin's disease line L540 adapted to xenograft growth, was developed by Dr. Harald Stein (Institüt für Pathologie, University of Veinikum Benjamin Franklin, Berlin, Germany). Cell lines were grown in RPMI 1640 (Life Technologies, Inc., Gaithersburg, MD) supplemented with 10% fetal bovine serum.

Construction and Purification of cAC10-Val-Cit-MMAE Antibody-Drug Conjugates. The E8 antibody-drug conjugate was generated as described previously (12, 13). Briefly, cAC10 was mixed with DTT at 37°C for 30 minutes, and the buffer was exchanged by elution through Sephadex G-25 resin with PBS containing 1 mmol/L diethylenetriaminepentaacetic acid. PBS containing 1 mmol/L diethylenetriaminepentaacetic acid (PBS/D) was added to the reduced mAb (final concentration, 2.5 mg/mL). The thiol concentration was ~8.4 thiols/mAb as measured by Ellman's reagent, 5,5′-dithiobis(2-nitrobenzoic acid) [DTNB]. A 9.5-fold molar excess of maleimidocaproyl-Val-Cit-MMAE, subsequently referred to as Val-Cit-MMAE, was added to the reduced antibody at 4°C for 1 hour, and the conjugation reaction was quenched by adding a 20-fold excess of cysteine. The reaction mixture was concentrated by centrifugal ultrafiltration and buffer-exchanged through Sephadex G-25 equilibrated in PBS at 4°C. The conjugate was then sterile filtered through a 0.2-μm filter.

The generation of cAC10 antibody-drug conjugates with two and four MMAE molecules per antibody, E2 and E4, respectively, involved a partial reduction of the mAb followed by reaction with Val-Cit-MMAE. The antibody cAC10 (10 mg/mL) was partially reduced by addition of DTT to a final DTT:mAb molar ratio of 3.0 followed by incubation at 37°C for ~2 hours. The reduction reaction was then chilled to ~10°C and the reduced cAC10 purified away from excess DTT via diafiltration. After diafiltration, the thiol concentration in the partially reduced cAC10 was determined by DTNB; in this manner, an average of approximately two disulfide bonds were reduced, thus exposing approximately four reduced Cys:mAb. To conjugate all of the reduced Cys, Val-Cit-MMAE was added to a final Val-Cit-MMAE:reduced Cys molar ratio of ~1.15. The conjugation reaction was carried out in the presence of 15% v/v of DMSO and allowed to proceed at ~10°C for ~30 minutes. After the conjugation reaction, excess free Cys (2 mol/L Cys per mol/L Val-Cit-MMAE) was added to quench unreacted Val-Cit-MMAE to produce the Cys-Val-Cit-MMAE adduct. The Cys quenching reaction was allowed to proceed at ~10°C for ~30 minutes. The Cys-quenched reaction mixture was purified and buffer-exchanged into PBS by diafiltration to obtain the partially loaded cAC10-Val-Cit-MMAE referred to as E4-Mixture.

Preparative Hydrophobic Interaction Chromatography Fractionation. All chromatographic steps were performed at room temperature. A 1.6 × 25-cm column (~50 mL) was packed with Toyopearl Phenyl-650M HIC resin (Tosoh Bioscience, Montgomeryville, PA) and equilibrated with >5 column volumes of buffer A [50 mmol/L sodium phosphate, 2 mol/L NaCl (pH 7.0)]. To prepare the sample for loading onto the column, 39 mL of E4-Mixture (12.9 mg/mL) were mixed with an equivalent volume of buffer A′ [50 mmol/L sodium phosphate, 4 mol/L NaCl (pH 7.0)]. After sample loading, the column was washed with buffer A until an $A_{280\ nm}$ baseline was achieved. E2 was eluted and collected with a step gradient consisting of 65% buffer A/35% buffer B [80% v/v 50 mmol/L sodium phosphate (pH 7.0), 20% v/v acetonitrile]. After baseline was again achieved, E4 was eluted and collected with a step gradient consisting of 30% buffer A/70% buffer B. Both E2 and E4 peaks were collected to ~20% of their respective peak heights. The fractions of interest were buffer exchanged into PBS using Ultrafree-15 centrifugal filter devices with a molecular weight cutoff of M_r 30,000 (Millipore, Billerica, MA).

Analysis of Conjugates. Analysis of the conjugates was accomplished by hydrophobic interaction chromatography–high-performance liquid chromatography using an Ether-5PW column (Tosoh Bioscience, Montgomeryville, PA). The method consisted of a linear gradient from 100% buffer A to 100% buffer C [80% v/v 50 mmol/L sodium phosphate (pH 7.0), 10% v/v acetonitrile, 10% v/v isopropanol] in 50 minutes. The flow rate was set at 1 mL/min, the temperature was set at 30°C, and detection was followed at both 248 and 280 nm. The identity of unmodified cAC10 and E8 peaks was confirmed by injection of cAC10 and E8 standards. Because the antibody and drug have distinct absorbance maxima (λ_{max} = 280 and 248 nm, respectively), it was possible to identify peaks corresponding to cAC10 conjugates with two, four, and six drugs per antibody by overlaying peak spectra.

Additional confirmation of the identity of purified E2 and E4 was accomplished by UV-VIS analysis. The absorbance at 280 nm of the drug and the antibody contribute to the total absorbance ($A_{280\ nm}$):

$$A_{280} = \epsilon_D^{280} C_D l + \epsilon_{Ab}^{280} C_{Ab} l \quad (1)$$

DAC EX. 2040 IPR2022-01531 Page 978 of 1299

where

ϵ_D^{280} = extinction coefficient of the drug at 280 nm,

ϵ_{Ab}^{280} = extinction coefficient of the mAb at 280 nm,

C_D = concentration of the drug,

C_{Ab} = concentration of the mAb, and

l = detector path length; and an analogous equation for the total absorbance at 248 nm:

$$A_{248} = \epsilon_D^{248} C_D l + \epsilon_{Ab}^{248} C_{Ab} l \quad (2)$$

Dividing equation 2 by equation 1 and rearranging:

$$MR = \frac{\epsilon_{Ab}^{248} - R\epsilon_{Ab}^{280}}{R\epsilon_D^{280} - \epsilon_D^{248}} \quad (3)$$

where

$MR = C_D/C_{Ab}$ = Drug:mAb molar ratio

$R = A_{248}/A_{280}$ = Absorbance ratio.

The drug:mAb molar ratio was then calculated using equation 3 and extinction coefficients of the drug ($\epsilon_D^{248} = 1.5 \times 10^3$ L/mol · cm and $\epsilon_D^{280} = 1.59 \times 10^4$ L/mol · cm) and mAb ($\epsilon_{Ab}^{248} = 9.413 \times 10^4$ L/mol · cm and $\epsilon_{Ab}^{280} = 2.3415 \times 10^5$ L/mol · cm).

***In vitro* Characterization of cAC10-Val-Cit-MMAE Antibody-Drug Conjugates.** Competition binding was performed on the antibody-drug conjugates to determine whether the conjugation process or presence of drug impaired the antigen binding. To compare saturation binding of mAb and antibody-drug conjugate, 5×10^5 Karpas-299 cells were combined with serial dilutions of cAC10, E2, E4, or E8 in the presence of 1 μg/mL cAC10 labeled with Alexa Fluor 488 (Molecular Probes, Eugene, OR) in staining medium for 30 minutes on ice then washed twice with ice-cold staining medium. Labeled cells were measured using a Fusion microplate reader (Perkin-Elmer, Boston, MA). Sample data were baseline corrected and reported as the percentage of maximum fluorescence as calculated by the sample fluorescence divided by the fluorescence of cells stained with 1 μg/mL cAC10-Alexa Fluor 488 alone.

The growth inhibitory activities of cAC10 conjugates were determined by measuring DNA synthesis. Conjugates were incubated with $CD30^+$ Karpas-299 or L540cy cells or $CD30^-$ WSU-NHL cells. After a 92-hour incubation with cAC10 or cAC10 antibody-drug conjugates, cells were labeled with [^{3}H]thymidine, 0.5 μCi/well, for 4 hours at 37°C. Cells were harvested onto filters using a harvester, mixed with scintillation fluid, and the radioactivity was measured with a Topcount scintillation counter (Packard Instruments, Meriden, CT). The percent radioactivity incorporation relative to untreated controls was plotted *versus* concentration for each molecule. The data were fit to a sigmoidal dose-response curve (variable slope) with Prism 4.01 software (GraphPad Software, Inc., San Diego, CA) to determine the IC_{50} (defined as the mAb concentration that gave 50% inhibition of DNA synthesis).

Xenograft Models of Human Anaplastic Large-Cell Lymphoma. To establish a s.c. disease model of anaplastic large-cell lymphoma, 5×10^6 Karpas-299 cells were implanted into the right flank of C.B-17 SCID mice (Harlan, Indianapolis, IN). Therapy with antibody-drug conjugates was initiated when the tumor size in each group of 6 to 10 animals averaged 90 and 100 mm^3 for the single-dose and multidose experiments, respectively. Treatment consisted of either a single injection or multiple i.v. injections using the schedule of one injection every 4 days for 4 injections (q4d×4). Tumor volume was calculated using the formula (length × width ^{2})/2. A tumor that decreased in size such that it was impalpable was defined as a complete regression. A complete regression that lasted >100 days after tumor implant was defined as a cure. Animals were euthanized when tumor volumes reached ~1000 mm^3. Pairwise treatment groups were compared using Kaplan-Meier analysis for survival with Prism 4.01 software.

Maximum-Tolerated Dose (MTD). Groups of three BALB/c mice (Harlan) received injections of 30 to 60 mg/kg E8, 60 to 120 mg/kg E4, or 200 to 250 mg/kg E2 via the tail vein to determine the single-dose MTD. Mice were monitored daily for 14 days, and both weight and clinical observations were recorded. Mice that developed significant signs of distress were sacrificed in accordance with Institutional Animal Care and Use Committee guidelines. The MTD was defined as the highest dose that did not cause serious overt toxicities or >20% weight loss in any of the animals.

Pharmacokinetics. The pharmacokinetics of cAC10, E2, E4, and E8 were evaluated in SCID mice. SCID mice (n = 3) were administered 10 mg/kg test material (based on the antibody component) by tail vein injection. Blood samples were collected from each mouse via the saphenous vein at 1 hour, 4 hours, 1 day, 2 days, 4 days, 7 days, 14 days, 21 days, 28 days, 35 days, 42 days, and 49 days after injection. Blood was collected into heparin coated tubes followed by centrifugation (14,000 × g, 3 minutes) to isolate plasma. Plasma concentrations of cAC10 and antibody-drug conjugates were measured by ELISA.

Briefly, the ELISA consisted of the following steps: plate coat, block, sample binding, secondary mAb, 3,3′,5,5′-tetramethylbenzidine dihydrochloride, and acid quench. After each step, the wells were washed with wash buffer [PBS, 0.05% Tween 20 (pH 7.4)] three times. In the plate coat step, anti-cAC10 mAb was coated onto 96-well plates at 2 μg/mL in carbonate buffer [0.1 mol/L carbonate/bicarbonate (pH 9.6)] at 4°C overnight. After the plate coat, blocking buffer (PBS, 1% BSA, 0.05% Tween 20) was added and incubated at room temperature for 1 hour. Next, 100 μL of standard or diluted plasma sample were added to triplicate wells for 1 hour at room temperature. The secondary step consisted of a mouse antihuman IgG-horseradish peroxidase conjugate (Southern Biotech, Birmingham, AL) incubated for 1 hour. Subsequently, 100 μL of 3,3′,5,5′-tetramethylbenzidine (Sigma, St. Louis, MO) were added to each well, and upon color development, the reaction was stopped with 100 μL of 1 N sulfuric acid. Absorbance was measured using a VMax Kinetic Microplate reader (Molecular Devices, Sunnyvale, CA) at 450 nm and a blank at 630 nm. Noncompartmental pharmacokinetic parameters were calculated with WinNonlin (Pharsight, Mountain View, CA).

RESULTS

Generation of Antibody-Drug Conjugate with Reduced Drug Loading. Our previous studies demonstrated that an anti-CD30 antibody-drug conjugate containing eight MMAE drug molecules per mAb (referred to here as E8) had potent and

DAC EX. 2040 IPR2022-01531 Page 979 of 1299

specific cytotoxic activity against CD30 expressing cells both *in vitro* and *in vivo* (12, 13). This antibody-drug conjugate was constructed by reducing the four interchain disulfide bonds of cAC10 and conjugating Val-Cit-MMAE to the eight exposed sulfhydryls. To evaluate the effect of drug loading on the activity of cAC10 antibody-drug conjugates, conjugates with two and four MMAE molecules per mAb, E2 and E4, respectively, were constructed. cAC10 was partially reduced with DTT to yield an average of four reactive sulfhydryls per mAb. The partially reduced mAb was then mixed with reactive Val-Cit-MMAE to generate cAC10-Val-Cit-MMAE with an average molar ratio of 4.0 to 4.2 MMAE molecules per antibody, referred to as E4-Mixture. As determined by hydrophobic interaction chromatography–high-performance liquid chromatography (Fig. 1*A*), the resulting product was a mixture of species that were identified as cAC10, cAC10 conjugated with two molecules of MMAE (E2), four molecules of MMAE (E4), six molecules of MMAE (E6), and eight molecules of MMAE (E8). The five major peaks can be positively identified because attachment of drug results in greater absorbance at ~248 nm (λ_{max} for drug) relative to 280 nm (λ_{max} for cAC10; Fig. 1*A*, insert). This partially loaded antibody-drug conjugate mixture contained ~9% unconjugated cAC10, 22% E2, 30% E4, 23% E6, and 9% E8. Upon preparative hydrophobic interaction chromatography fractionation, E2 (Fig. 1*B*) and E4 (Fig. 1*C*) were found to be >95% pure by analytical hydrophobic interaction chromatography–high-performance liquid chromatography. Additional confirmation of the identity of E2 and E4 was obtained by UV-VIS analysis using extinction coefficients of the drug and antibody (see Materials and Methods), resulting in drug to mAb molar ratios of 2.0 and 4.0 for E2 and E4, respectively. Production of E8 was described previously and the molar ratio was determined to be 8.0 (13). For studies described herein the concentrations of antibody-drug conjugates are reported based on the mAb component.

***In vitro* Characterization.** Competition binding experiments were performed to determine whether conjugation of MMAE to cAC10 interferes with the CD30 binding capability of the antibody-drug conjugates. $CD30^+$ Karpas-299 cells were incubated with 1 μg/mL fluorescently labeled cAC10 combined with serial dilutions of unlabeled antibody, E2, E4, or E8. Each of the antibody-drug conjugate variants effectively competed with fluorescently labeled cAC10 equivalent to unlabeled cAC10 as shown in Fig. 2. Thus, conjugation with MMAE did not reduce the CD30 binding capabilities of the cAC10 antibody-drug conjugates.

The *in vitro* cytotoxic activities of the antibody-drug conjugates were evaluated by a [^{3}H]thymidine incorporation assay with $CD30^+$ Karpas-299 and L540cy cells and $CD30^-$ WSU-NHL cells. E8 demonstrated significant activity against the Karpas-299 cells with an IC_{50} of 1.0 ng/mL (Fig. 3*A*). Decreasing the amount of drug in half to four MMAE molecules per mAb (E4) increased the IC_{50} to 2.9 ng/mL. Halving the drug loading again additionally increased the IC_{50} to 6.2 ng/mL with E2. Against the Hodgkin's disease line L540cy, the antibody-drug conjugates had a similar trend with IC_{50} values of 1.4, 4.5, and 9.2 ng/mL for E8, E4, and E2, respectively (Fig. 3*B*). Selectivity of the antibody-drug conjugates was evaluated with $CD30^-$ WSU-NHL cell line, which was insensitive to all cAC10-antibody-drug conjugates with IC_{50} values > 1000 ng/mL (data not shown).

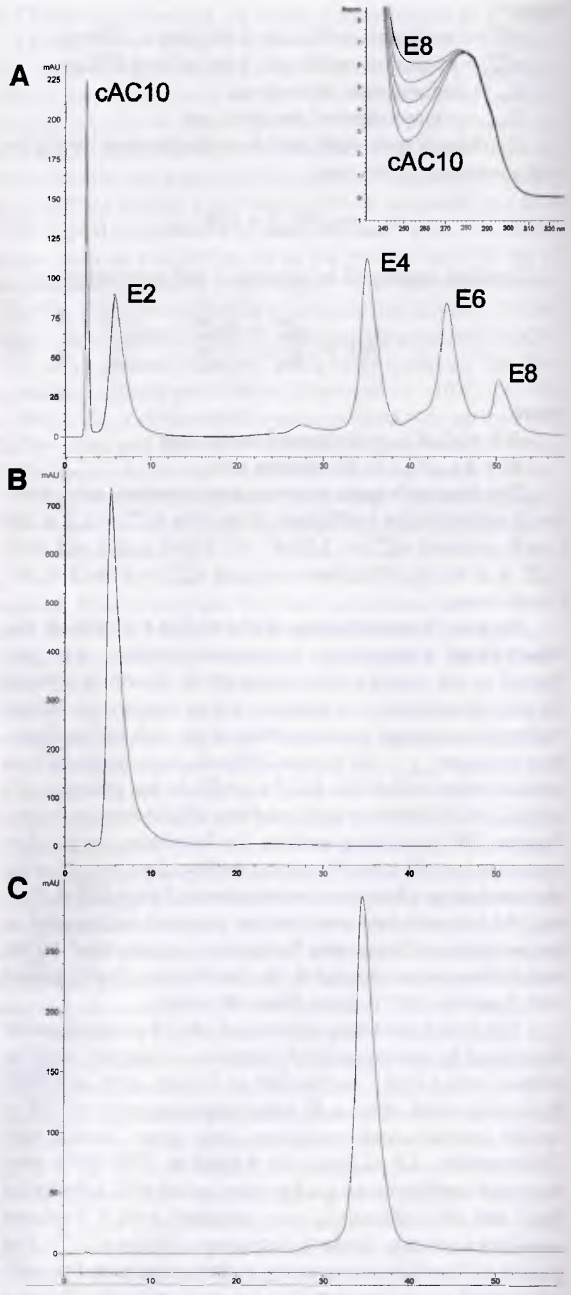


Fig. 1 Hydrophobic interaction chromatography–high-performance liquid chromatography chromatograms of partially loaded E4-Mixture (*A*), E2 (*B*), and E4 (*C*). The insert in *A* shows an overlay of UV spectra corresponding to peaks cAC10, E2, E4, E6, and E8.

Xenograft Models of Human Anaplastic Large-Cell Lymphoma. The effect of drug loading on *in vivo* antitumor activity was evaluated in SCID mice with human Karpas-299

DAC EX. 2040 IPR2022-01531 Page 980 of 1299

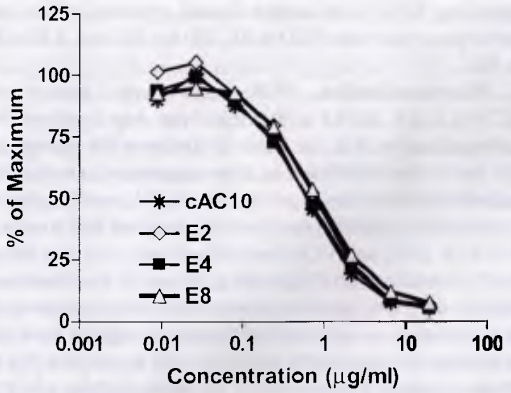


Fig. 2 CD30$^+$ Karpas-299 cells were combined with 1 μg/mL fluorescently labeled cAC10 and serial dilutions of either cAC10, E2, E4, or E8 from 20 μg/mL to 9 ng/mL. The labeled cells were washed with staining media and the fluorescence was measured. The normalized fluorescence intensities were plotted *versus* mAb concentration as described in Materials and Methods.

s.c. xenografts. Therapy was administered every fourth day for a total of four injections (q4d×4), starting when tumor volumes reached 50 to 100 mm^3. Using this schedule, we previously found that E8 at 1 mg/kg produced 100% complete regressions (13). At the same dose level, E4 also led to 100% complete regressions (data not shown). With the goal of comparing the activity of the antibody-drug conjugates, lower doses were used for E4 and E8. Cohorts of mice bearing s.c. Karpas-299 xenografts were treated with multiple doses of E4 or E8 at 0.25 or 0.5 mg/kg/dose. Although E8 had twice the amount of MMAE as E4 at the same mAb dose, they were equally effective at 0.5 mg/kg (P = 0.36; Table 1 and Fig. 4*A*). At a 0.5 mg/kg/dose, 5 of the 10 animals treated with E4 achieved complete regressions, and E8 induced 6 of 10 complete regressions. At 0.25 mg/kg/dose, both of these antibody-drug conjugates induced a similar delay in tumor growth compared with untreated control animals but no complete regressions. Unexpectedly, E2 at 1.0 mg/kg/dose, which contained the same amount of MMAE as E4 at 0.5 mg/kg/dose and E8 at 0.25 mg/kg, gave the best therapeutic response with 10 of 10 cures. A physical mixture of the drug MMAE with cAC10, equivalent to E8 at the 0.5 mg/kg dose, produced only a slight delay in tumor growth compared with untreated (P = 0.1), highlighting that the linkage of drug to antibody is critical for achieving antitumor activity.

To additionally compare antibody-drug conjugate with different drug loading, single-dose treatments with E2, E4, and E8 in this same model were then compared at 0.5 and 1.0 mg/kg (Table 1 and Fig. 4*B*). At the low dose of 0.5 mg/kg, there was a marginal delay in tumor growth in animals dosed with the antibody-drug conjugates compared with untreated. Any difference between E2, E4, and E8 was minimal at 0.5 mg/kg, with zero, one, and two cures, respectively. Treatment at the 1 mg/kg dose produced significant responses with cures in all treatment groups. Cures were obtained in five of six animals treated with 1 mg/kg E8. Of the six animals treated with 1 mg/kg E4 all achieved complete regressions with five cures out to 108 days, the end of the study (one animal was found dead on day 72 with no sign of tumor mass). Although E2 at 1.0 mg/kg contained half as much MMAE as E4, four of six mice achieved complete regressions. A physical mixture consisting of 1 mg/kg cAC10

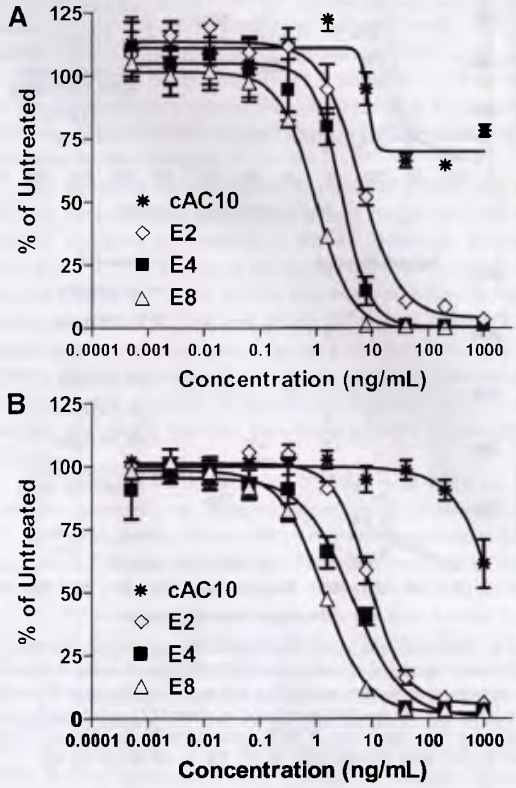


Fig. 3 Karpas-299 (*A*) and L540cy (*B*) cells were incubated with serial dilutions of cAC10 and cAC10 antibody-drug conjugates. After a 96 h incubation with the samples, [^{3}H]thymidine was added, and its incorporation was measured. The radioactivity of the treated samples were normalized to the untreated controls and plotted *versus* concentration.

Table 1 Antitumor activity of E2, E4, and E8 in a s.c. Karpas-299 xenograft model

Schedule	Antibody-drug conjugate	Dose (mg/kg)	Complete regressions	Cures
q4d×4	E2	0.5	0/10	0/10
		1.0	10/10	10/10
	E4	0.25	1/10	1/10
		0.50	5/10	3/10
	E8	0.25	0/10	0/10
		0.50	6/10	6/10
×1	E2	0.5	0/6	0/6
		1.0	4/6	4/6
	E4	0.5	1/6	1/6
		1.0	6/6	5/6*
	E8	0.5	2/6	2/6
		1.0	5/6	5/6

* One mouse with a cure was found dead on day 72 with no sign of tumor mass.

DAC EX. 2040 IPR2022-01531 Page 981 of 1299

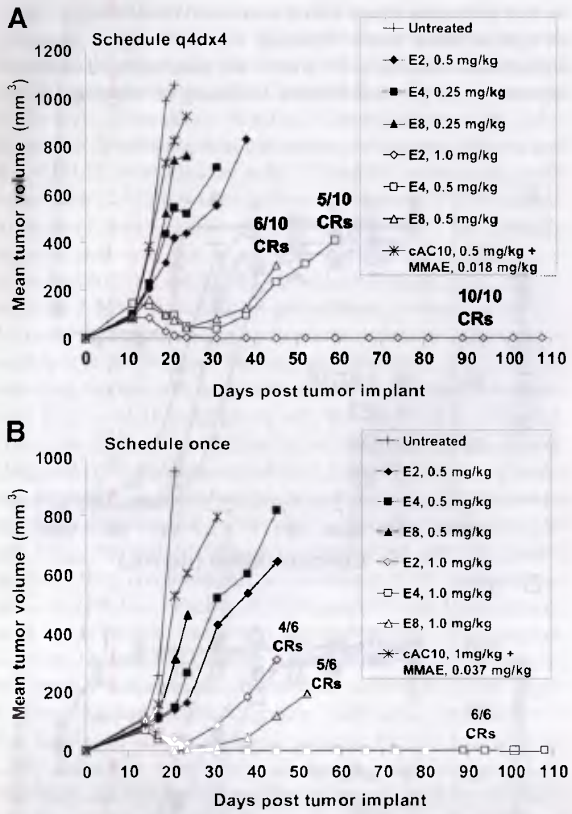


Fig. 4 Multidose and single-dose antibody-drug conjugate efficacy of SCID mice bearing s.c. xenografts. *A*. SCID mice bearing Karpas-299 s.c. tumors were injected with E2 at 0.5 or 1.0 mg/kg every 4 days for four injections. E4 and E8 were dosed at either 0.25 or 0.5 mg/kg every 4 days for four injections. *B*. SCID mice with Karpas-299 s.c. tumors were treated with a single dose of E2, E4, or E8 at 1.0 mg/kg.

plus 0.037 mg/kg free MMAE, equivalent to the amount of drug contained in 1 mg/kg E8, had little effect on tumor growth compared with untreated mice.

MTD and Therapeutic Index. The single-dose tolerability of E2, E4, and E8 was evaluated in BALB/c mice, the immunocompetent parent strain of SCID mice. The MTD was defined as the highest dose that did not induce >20% weight loss, severe signs of distress, or overt toxicities in any of the animals. For E8, mice were dosed at 10 mg/kg intervals from 30 to 60 mg/kg. At a dose of 50 mg/kg, mice had a maximum weight loss of 14% 6 days after injection, after which the weight loss was recovered. A dose of 60 mg/kg induced 23% weight loss 6 days postinjection in one animal. With E4 at 100 mg/kg animals had minimal weight loss, whereas at 120 mg/kg E4, one animal displayed signs of significant distress and 17% weight loss, and the animal was euthanized. Mice treated with E2 at doses up to 250 mg/kg, the highest dose tested, experienced a maximum weight loss of 10.5% 6 days postinjection, with no signs of distress. On the basis of these results, the MTD of E8 was 50 mg/kg, for E4 it was 100 mg/kg, and for E2 was at least 250 mg/kg. Therapeutic index, as defined by the ratio of the single-dose MTD to the multidose dose achieving >50% complete regressions, were 100 for E8, 200 for E4, and at least 250 for E2.

Pharmacokinetics. SCID mice were treated with cAC10, E2, E4, and E8 to determine how drug loading effects pharmacokinetics (Fig. 5). Table 2 illustrates the pharmacokinetic parameters established by noncompartmental analysis. The time-concentration curves of cAC10, E2, E4, and E8 appeared to follow bi-exponential declines. The terminal half-lives were 16.7, 16.9, 14.0, and 14.7 days, respectively, and thus did not directly correlate with drug loading. However, the exposure of antibody-drug conjugates as determined by the area under the curve increased as drug loading decreased, ranging from 2638 μg-day/mL for unmodified cAC10 to 520 μg-day/mL for E8. Clearance values increased from 3.8 mL/day/kg for cAC10 to 4.4, 6.0, and 19.2 mL/day/kg as drug loading increased for E2, E4, and E8, respectively. Similarly, the volume of distribution was found to correlate with drug loading.

DISCUSSION

The effects of drug multiplicity on the *in vitro* activities of a few other antibody-drug conjugates have been reported. For example, doxorubicin-antibody-drug conjugates displayed a correlation between drug loading and cell cytotoxicity *in vitro* (20, 26). The use of branched linkers increased molar ratios as high as 16 doxorubicin molecules per mAb, which additionally

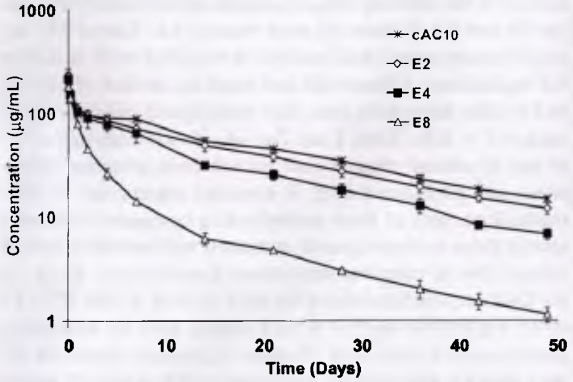


Fig. 5 Pharmacokinetics of cAC10 and cAC10–antibody-drug conjugates. SCID mice were injected via the tail vein with 10 mg/kg cAC10, E2, E4, and E8. Plasma samples were analyzed by ELISA to determine the antibody or antibody-drug conjugate concentration.

Table 2 Pharmacokinetic parameters of cAC10 and cAC10 antibody-drug conjugates in SCID mice at a dose of 10 mg/kg (± SD)

Name	Half-time (days)	Area under the curve (μg-day/mL)	Clearance (mL/day/kg)	Volume of distribution (mL/kg)
cAC10	16.7 (0.2)	2638 (64)	3.8 (0.1)	91 (3.2)
E2	16.9 (1.7)	2313 (282)	4.4 (0.6)	107 (14)
E4	14.0 (2.5)	1689 (187)	6.0 (0.6)	122 (30)
E8	14.9 (1.8)	520 (21)	19.2 (0.8)	414 (66)

DAC EX. 2040 IPR2022-01531 Page 982 of 1299

improved the *in vitro* potency without affecting antigen binding (20). The activities of TA.1-maytansinoid conjugates with an average ranging from one to six drugs per mAb were compared *in vitro*, and optimal cytotoxicity was achieved with an average of four drugs per mAb (16). Here, we described how drug multiplicity affects both the *in vitro* and *in vivo* characteristics of antibody-drug conjugates produced with MMAE.

Attaching a drug to a mAb can be accomplished through a variety of approaches, including lysine, aldehyde, or, as we have used here, cysteine chemistries. IgG1 molecules contain 12 intrachain and 4 interchain disulfide bonds. However, it has been shown that the latter are significantly more susceptible to reduction by agents such as DTT than are the intrachain bonds (27, 28). In fact, Willner *et al.* (27) reported that reduction of a chimeric antibody with up to 100 molar equivalents of DTT could only generate eight sulfhydryls per antibody corresponding to reduction of the four interchain disulfide bonds. Using lower concentrations of DTT, the reducing conditions that we used here in preparation of the fully and partially loaded antibody-drug conjugate yielded 8 and 4 thiols/mAb, respectively. Fully loaded E8 thus has one MMAE molecule attached to each cysteine that comprises the interchain disulfides of a mAb. Partially loaded E2 and E4 can theoretically occupy any two or four of these locations, respectively. It is not known if there is preferential localization of the drugs to the heavy/light chain or hinge disulfide bonds. Given that the partial reduction process described here results in production of antibody-drug conjugates with only even numbers of MMAE per antibody as shown in Fig. 1*A* and subsequent characterization (data not shown), it is likely that localization of drugs occurs simultaneously at both cysteine residues of a disulfide bond.

Competition binding experiments revealed that loading cAC10 with two, four, or eight drugs per antibody had no measurable effect on the binding to the target antigen CD30 (Fig. 2). On the basis of the IC_{50} values, E4 was 3-fold less potent than E8, and the E2 was 2-fold less potent than E4 for both $CD30^+$ cell lines tested. Similar to doxorubicin–antibody-drug conjugates (20, 26), the *in vitro* potency of the cAC10–antibody-drug conjugates was directly dependent on drug loading and thus the total MMAE exposure.

E4 demonstrated antitumor activity comparable with E8 in a Karpas-299 xenograft model at the same antibody dose, half the MMAE dose. On the basis of the *in vitro* finding that potency was directly related to drug loading, an equivalent *in vivo* antitumor activity of E4 and E8 was unanticipated. Investigation of the pharmacokinetics of the antibody-drug conjugates revealed that clearance was dependent on drug loading of the antibody-drug conjugates and exposure (area under the curve) was inversely related to drug loading. The 3-fold larger area under the curve, and thus increased tumor exposure, of E4 compared with E8 was apparently sufficient to compensate for reduced potency, leading to equivalent efficacy. Attempts to improve efficacy by decelerating the plasma elimination half-life to augment area under the curves have been accomplished by methods including the construction of albumin fusion proteins for IFN α (29) and liposomal delivery of the anticancer drug lurtotecan (30). Unlike these examples where the objective was to lengthen the plasma half-life, the enhanced exposure of E4 was a valuable unexpected consequence of reducing MMAE loading. Although the concentrations reported here are based on the antibody component it has been observed that MMAE is released from the antibody-drug conjugate over time *in vivo*.[1]

Dosing E2 with 1.0 mg/kg/dose q4d×4 yielded 10 of 10 cures, an improved antitumor effect compared with E4 and E8 at 0.5 mg/kg/dose ($P = 0.0012$ and $P = 0.0289$, respectively). Although E2 did not demonstrate equivalent antitumor activity compared with E4 ($P < 0.0001$) at the same mAb dose (0.5 mg/kg, q4d×4), the dose of E2 needed to achieve equivalent antitumor activity compared with E4 is probably <2-fold based on the *in vivo* efficacy experiments. Similar to E4, the improved exposure of E2 may play a significant part in compensating for the lower *in vitro* potency.

To maximize the therapeutic potential of cAC10-Val-Cit-MMAE antibody-drug conjugates, a high therapeutic index is needed. Reducing the amount of MMAE molecules per mAb from eight to four enhanced the therapeutic index 2-fold. Additional studies are under way to determine whether the target organ toxicities of E2, E4, and E8 are different or if the MTD is simply due to the presence of the total amount of drug in the system. Given the steep dose-response curves of chemotherapeutic reagents, a 2-fold difference in therapeutic index is significant and should translate into improvements in therapeutic efficacy.

By reducing the quantity of MMAE from eight to four molecules per mAb, we reported a decrease of *in vitro* activity, yet more importantly, demonstrated equivalent antitumor activity *in vivo*. Although an additional reduction in drug loading to two MMAE molecules per antibody further reduced the *in vitro* activity, E2 had equivalent or better efficacy than E4 and E8 at double the dose in a multidose setting. The therapeutic index was increased 2-fold by reducing drug loading from eight MMAE molecules to four and, at the very least, maintained with a further reduction to two drugs per antibody. In summary, there is considerable value in optimizing drug substitution of antibody-drug conjugates that may lead to enhanced product candidates such as the anti-CD30 antibody-drug conjugate described here.

REFERENCES

1. Carter P. Improving the efficacy of antibody-based cancer therapies. Nat Rev Cancer 2001;1(2):118–29.

2. Shields RL, Lai J, Keck R, et al. Lack of fucose on human IgG1 N-linked oligosaccharide improves binding to human Fcgamma RIII and antibody-dependent cellular toxicity. J Biol Chem 2002;277(30): 26733–40.

3. Shinkawa T, Nakamura K, Yamane N et al. The absence of fucose but not the presence of galactose or bisecting *N*-acetylglucosamine of human IgG1 complex-type oligosaccharides shows the critical role of enhancing antibody-dependent cellular cytotoxicity. J Biol Chem 2003; 278(5):3466–73.

4. Pastan I, Kreitman RJ. Immunotoxins in cancer therapy. Curr Opin Investig Drugs 2002;3(7):1089–91.

[1] R. J. Sanderson, M. A. Hering, M. M. C. Sun, A. W. Siadak, P. D. Senter, and A. F. Wahl. *In vivo* drug-linker stability of cAC10-vcMMAE, an anti-CD30 dipeptide-linked monomethyl auristatin E immunoconjugate, submitted for publication.

DAC EX. 2040 IPR2022-01531 Page 983 of 1299

5. Juweid ME. Radioimmunotherapy of B-cell non-Hodgkin's lymphoma: from clinical trials to clinical practice. J Nucl Med 2002;43(11): 1507–29.

6. Cheson BD. Radioimmunotherapy of non-Hodgkin lymphomas. Blood 2003;101(2):391–8.

7. Saleh MN, Sugarman S, Murray J, et al. Phase I trial of the anti-Lewis Y drug immunoconjugate BR96-doxorubicin in patients with Lewis Y-expressing epithelial tumors. J Clin Oncol 2000;18(11):2282–92.

8. Sievers EL, Larson RA, Stadtmauer EA, et al. Efficacy and safety of gemtuzumab ozogamicin in patients with CD33-positive acute myeloid leukemia in first relapse. J Clin Oncol 2001;19(13):3244–54.

9. Tolcher AW, Ochoa L, Hammond LA, et al. Cantuzumab mertansine, a maytansinoid immunoconjugate directed to the CanAg antigen: a phase I, pharmacokinetic, and biologic correlative study. J Clin Oncol 2003;21(2):211–22.

10. Bross PF, Beitz J, Chen G, et al. Approval summary: gemtuzumab ozogamicin in relapsed acute myeloid leukemia. Clin Cancer Res 2001; 7(6):1490–6.

11. Chan SY, Gordon AN, Coleman RE, et al. A phase 2 study of the cytotoxic immunoconjugate CMB-401 (hCTM01-calicheamicin) in patients with platinum-sensitive recurrent epithelial ovarian carcinoma. Cancer Immunol Immunother 2003;52(4):243–8.

12. Doronina SO, Toki BE, Torgov MY, et al. Development of potent and highly efficacious monoclonal antibody auristatin conjugates for cancer therapy. Nat Biotechnol 2003;21(7):778–84.

13. Francisco JA, Cerveny CG, Meyer DL, et al. cAC10-vcMMAE, an anti-CD30-monomethyl auristatin E conjugate with potent and selective antitumor activity. Blood 2003;102:1458–65.

14. Chari RV, Jackel KA, Bourret LA, et al. Enhancement of the selectivity and antitumor efficacy of a CC-1065 analogue through immunoconjugate formation. Cancer Res 1995;55(18):4079–84.

15. Meyer DL, Senter PD. Recent advances in antibody drug conjugates for cancer therapy, Chp 23. Annu Rep Med Chem 2003;38:229–37.

16. Chari RV, Martell BA, Gross JL, et al. Immunoconjugates containing novel maytansinoids: promising anticancer drugs. Cancer Res 1992; 52(1):127–31.

17. Dubowchik GM, Firestone RA, Padilla L, et al. Cathepsin B-labile dipeptide linkers for lysosomal release of doxorubicin from internalizing immunoconjugates: model studies of enzymatic drug release and antigen-specific in vitro anticancer activity. Bioconjug Chem 2002;13(4): 855–69.

18. Hamann PR, Hinman LM, Hollander I, et al. Gemtuzumab ozogamicin, a potent and selective anti-CD33 antibody-calicheamicin conjugate for treatment of acute myeloid leukemia. Bioconjug Chem 2002; 13(1):47–58.

19. Hamann PR, Hinman LM, Beyer CF, et al. An anti-CD33 antibody-calicheamicin conjugate for treatment of acute myeloid leukemia. Choice of linker. Bioconjug Chem 2002;13(1):40–6.

20. King HD, Yurgaitis D, Willner D, et al. Monoclonal antibody conjugates of doxorubicin prepared with branched linkers: a novel method for increasing the potency of doxorubicin immunoconjugates. Bioconjug Chem 1999;10(2):279–88.

21. Schwab U, Stein H, Gerdes J, et al. Production of a monoclonal antibody specific for Hodgkin and Sternberg-Reed cells of Hodgkin's disease and a subset of normal lymphoid cells. Nature (Lond.) 1982; 299(5878):65–7.

22. Stein H, Mason DY, Gerdes J, et al. The expression of the Hodgkin's disease associated antigen Ki-1 in reactive and neoplastic lymphoid tissue: evidence that Reed-Sternberg cells and histiocytic malignancies are derived from activated lymphoid cells. Blood 1985; 66(4):848–58.

23. Gerdes J, Schwarting R, Stein H. High proliferative activity of Reed Sternberg associated antigen Ki-1 positive cells in normal lymphoid tissue. J Clin Pathol (Lond.) 1986;39(9):993–7.

24. Horie R, Watanabe T. CD30: expression and function in health and disease. Semin Immunol 1998;10(6):457–70.

25. Wahl AF, Klussman K, Thompson JD, et al. The anti-CD30 monoclonal antibody SGN-30 promotes growth arrest and DNA fragmentation in vitro and affects antitumor activity in models of Hodgkin's disease. Cancer Res 2002;62(13):3736–42.

26. Firestone RA, Willner D, Hofstead SJ, et al. Synthesis and antitumor activity of the immunoconjugate BR96-Dox. J Control Release 1996;39:251–9.

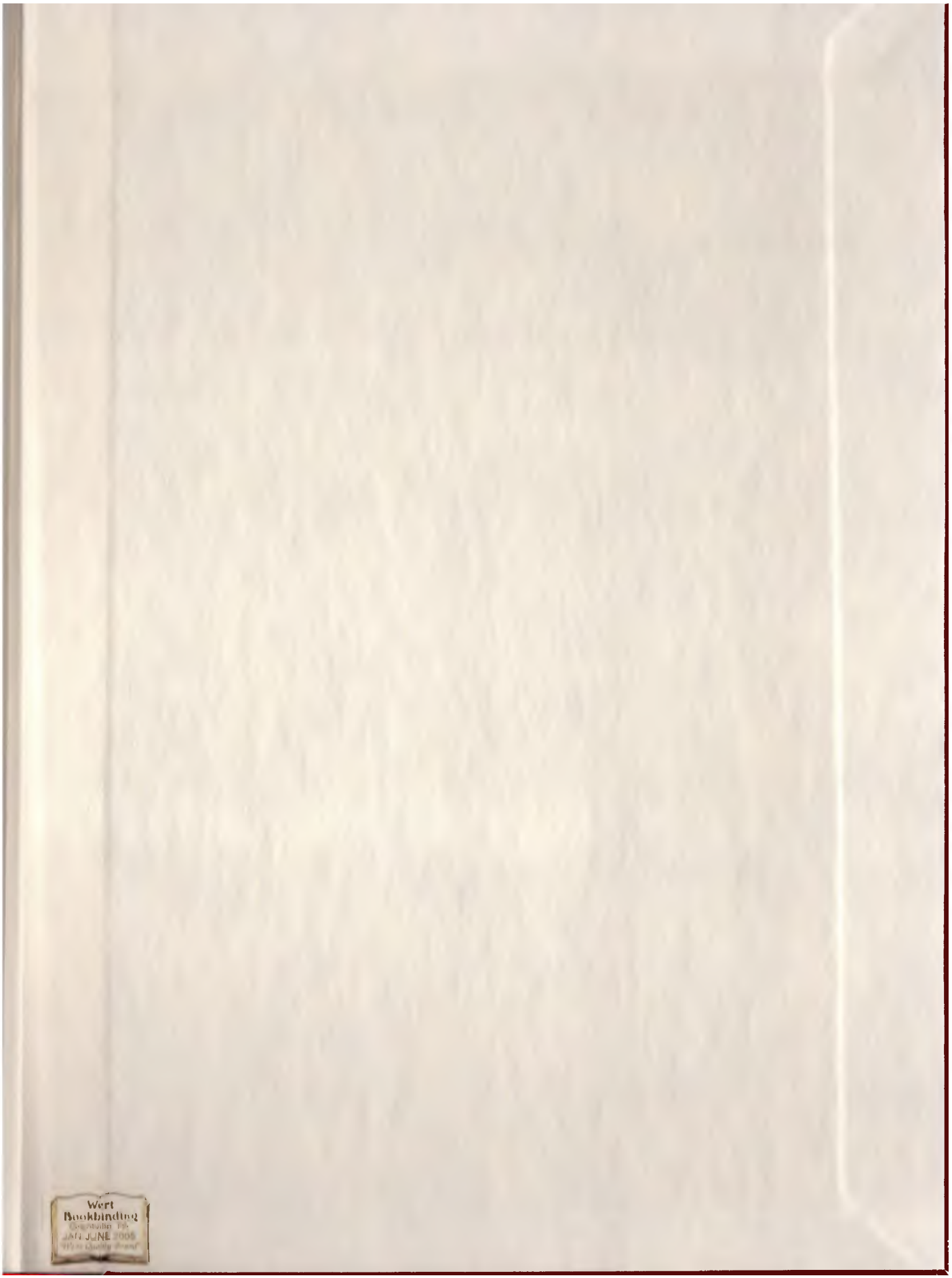
27. Willner D, Trail PA, Hofstead SJ, et al. (6-Maleimidocaproyl)hydrazone of doxorubicin: a new derivative for the preparation of immunoconjugates of doxorubicin. Bioconjug Chem 1993;4(6):521–7.

28. Schroeder DD, Tankersley DL, Lundblad JL. A new preparation of modified immune serum globulin (human) suitable for intravenous administration. I. Standardization of the reduction and alkylation reaction. Vox Sang 1981;40(6):373–82.

29. Osborn BL, Olsen HS, Nardelli, B et al. Pharmacokinetic and pharmacodynamic studies of a human serum albumin-interferon-alpha fusion protein in cynomolgus monkeys. J Pharmacol Exp Ther 2002; 303(2):540–8.

30. Emerson DL, Bendele R, Brown E, et al. Antitumor efficacy, pharmacokinetics, and biodistribution of NX 211: a low-clearance liposomal formulation of lurtotecan. Clin Cancer Res 2000;6(7):2903–12.

DAC EX. 2040 IPR2022-01531 Page 984 of 1299


Wert
Bookbinding
JAN JUNE 2005

Appendix JUNUTULA01

MARC View

LEADER 02696nas a2200541 a 4500				
001 46037767				
003 SIRSI				
005 20241114090046.0				
006 m o d				
007 cr n				
008 990805c19969999nyumr pss 0 a0eng c				
010				a| 2003215582
016	7			a| 012434484 2| Uk
019				a| DO NOT EDIT this 360 MARC RECORD
022				a| 1546-1696 l| 1087-0156 y| 1087-0156
035				a| (WaSeSS)ssj0006466
037				b| Nature Biotechnology Subscription Dept., P.O. Box 5054, Brentwood, TN 37024-5054 c| $119.00
040				a| OHS b| eng e| pn c| OHS d| MXC d| EYM d| OCLCQ d| NSD d| OCLCQ d| SBH d| NSD d| OCLCQ d| OCLCO d| OCLCQ d| DLC d| OCLCF d| OCLCO d| EUW d| OCLCO d| OCLCQ d| WT2 d| OCLCO d| UEJ d| OCLCO d| BUF d| U3W d| UUM d| MOW d| OCLCQ d| TOF d| OCLCO d| LHU d| AU@ d| OCLCO d| WYU d| OCLCO d| UKMGB d| OCLCA d| VT2 d| LEAUB d| DLC d| OCLCQ d| OCLCO d| OCLCA d| SFB d| QGK d| UBY d| OCLCO d| OCLCQ d| WaSeSS
042				a| nsdp a| pcc
050	0	0	a| TP248.3	
082	1	0	a| 660 2| 13	
130	0		a| Nature biotechnology (Online)	
210	0		a| Nat. biotechnol. b| (Online)	
222		0	a| Nature biotechnology b| (Online)	
245	1	0	a| Nature biotechnology h| [electronic resource].	
260			a| New York : b| Nature America, Inc., c| ©1996-	
310			a| Monthly	
362	0		a| Vol. 14, issue 3 (Mar. 1996)-	
500			a| "Some content from issues published prior to the November 1998 re-launch of Nature Biotechnology Online may not be available in full-text or PDF format."	
500			a| Title from title screen (viewed Aug. 5, 1999).	
525			a| Supplements accompany some volumes; issues for <Vol. 21 (2003)> have occasional supplement: Bioentrepreneur. Beginning in 2003? Bioentrepreneur published as a separate 'portal."	
530			a| Also issued in print.	
538			a| Mode of access: World Wide Web.	
580			a| Complements the journal: Nature.	
588	1		a| Vol. 38, no. 1 (Jan. 2020) (Nature website, viewed Jan. 27, 2020).	
650		0	a| Biochemical engineering v| Periodicals.	
650		0	a| Biotechnology v| Periodicals.	
650		2	a| Biotechnology	
655		2	a| Periodical	
710	2		a| Nature Publishing Group.	
776	1		t| Nature biotechnology x| 1087-0156 w| (DLC) 96647227 w| (OCoLC)34160925	
780	0	0	t| Bio/technology (Nature Publishing Company : Online) x| 2331-3684 w| (DLC) 2005264500 w| (OCoLC)58834187	
787	1		t| Nature (Online) x| 1476-4687 w| (DLC) 2005233250 w| (OCoLC)47076528	
787	1		t| Bioentrepreneur (Online) x| 1542-6572 w| (DLC) 2002211753 w| (OCoLC)51094383	
856	4	0	u| http://SK8ES4MC2L.search.serialssolutions.com/?V=1.0&L=SK8ES4MC2L&S=JCs&C=NATUBIO&T=marc	
910			a| CONSER online	
850			a| DLC	
949			a| Electronic resource w| ASIS c| 1 i| 46037767-1001 l| ONLINE m| ONLINE r| Y s| Y t| ONLINE u| 11/16/2024 o| .STAFF. 360 MARC	

ASK A LIBRARIAN

PennState

Copyright ©2019 The Pennsylvania State University. All rights reserved. Except where otherwise noted, this work is subject to a Creative Commons Attribution 4.0 license. Details and exce tions.

PENN STATE UNIVERSITY LIBRARIES
Libraries Home (814) 865-6368
Libraries Intranet (Staff

CONNECT WITH PENN STATE UNIVERSITY LIBRARIES
Facebook

Nature biotechnology [electronic resource].

Uniform Title	Nature biotechnology (Online)
Additional Titles	Nat. biotechnol. (Online)
Published	New York : Nature America, Inc., ©1996-
Additional Creators	Nature Publishing Group

Access Online

serialssolutions.com

ASK A LIBRARIAN

Continues

Bio/technology (Nature Publishing Company : Online)

Dates of Publication and/or Sequential Designation

Vol. 14, issue 3 (Mar. 1996)-

Subject(s)

Biochemical engineering—Periodicals
Biotechnology—Periodicals
Biotechnology

ISSN

1546-1696

Publication Frequency

Monthly

Note

"Some content from issues published prior to the November 1998 re-launch of Nature Biotechnology Online may not be available in full-text or PDF format."
Title from title screen (viewed Aug. 5, 1999).

Supplement Note

Supplements accompany some volumes; issues for have occasional supplement: Bioentrepreneur. Beginning in 2003? Bioentrepreneur published as a separate "portal."

Other Forms

Also issued in print.

Technical Details

Mode of access: World Wide Web.

Complexity Note

Complements the journal: Nature.

View MARC record | catkey: 46037767

PennState

Copyright ©2019 The Pennsylvania State University. All rights reserved. Except where otherwise noted, this work is subject to a Creative Commons Attribution 4.0 license. Details and exceptions.

Legal Statements | PSU Hotlines

PENN STATE UNIVERSITY LIBRARIES

Libraries Home (814) 865-6368
Libraries Intranet (Staff Only)
Accessibility Help
Website Feedback
Policies and Guidelines
Staff Directory

CONNECT WITH PENN STATE UNIVERSITY LIBRARIES

Facebook
Twitter
Instagram

All Journals Only Books Only Videos Only

Title begins with Search

Show more search options ▼

Showing results 1 through 1 of 1

for the search: "NATUBIO"

Refine Results: All | Journals Only | Books Only | Videos Only

Limit by: Peer Reviewed | Open Access

Nature biotechnology

ISSN: 1087-0156

Peer Reviewed

11/01/1998 to 08/31/2003 in Academic Search Complete (Ebsco)
11/01/1998 to Present in Nature Journals Online
01/01/2000 to 12/31/2021 in Opposing Viewpoints
06/28/2023 to Present in Nexis Uni

Search inside this journal Search

Back to Top

Last Updated on 12-02-2024 © Ex Libris, a ProQuest Company, 2000-2024
Privacy Policy

nature biotechnology

nature › nature biotechnology › articles › article

Article | Published: 20 July 2008

Site-specific conjugation of a cytotoxic drug to an antibody improves the therapeutic index

Jagath R Junutula, Helga Raab, Suzanna Clark, Sunil Bhakta, Douglas D Leipold, Sylvia Weir, Yvonne Chen, Michelle Simpson, Siao Ping Tsai, Mark S Dennis, Yanmei Lu, Y Gloria Meng, Carl Ng, Jihong Yang, Chien C Lee, Eileen Duenas, Jeffrey Gorrell, Viswanatham Katta, Amy Kim, Kevin McDorman, Kelly Flagella, Rayna Venook, Sarajane Ross, Susan D Spencer, ... William Mallet

+ Show authors

Nature Biotechnology **26**, 925–932 (2008)

28k Accesses | **1018** Citations | **31** Altmetric | Metrics

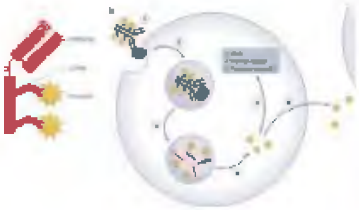
Abstract

Antibody-drug conjugates enhance the antitumor effects of antibodies and reduce adverse systemic effects of potent cytotoxic drugs. However, conventional drug conjugation strategies yield heterogenous conjugates with relatively narrow therapeutic index (maximum tolerated dose/curative dose). Using leads from our previously described phage display–based method to predict suitable conjugation sites, we engineered cysteine substitutions at positions on light and heavy chains that provide reactive thiol groups and do not perturb immunoglobulin folding and assembly, or alter antigen binding. When conjugated to monomethyl auristatin E, an antibody against the ovarian cancer antigen MUC16 is as efficacious as a conventional conjugate in mouse xenograft models. Moreover, it is tolerated at higher doses in rats and cynomolgus monkeys than the same conjugate prepared by conventional approaches. The favorable *in vivo* properties of the near-homogenous composition of this conjugate suggest that

DAC EX. 2040 IPR2022-01531 Page 991 of 1299

our strategy offers a general approach to retaining the antitumor efficacy of antibody-drug conjugates, while minimizing their systemic toxicity.

Similar content being viewed by others



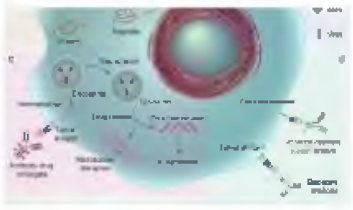
Antibody–drug conjugates come of age in oncology

Article | 12 June 2023



Unlocking the potential of antibody–drug conjugates for cancer therapy

Article | 08 February 2021



Emerging new therapeutic antibody derivatives for cancer treatment

Article | Open access
07 February 2022

Main

Targeted therapy using monoclonal antibodies (mAbs) has revolutionized cancer treatment, with several mAbs recognizing antigens expressed on the surfaces of tumor cells already having demonstrated their clinical potential[1,2]. As antibodies against tumor-specific antigens often lack therapeutic activity, they alternatively can be covalently linked to cytotoxic drugs. In principle, selective delivery of cytotoxic agents should reduce the systemic toxicity associated with traditional small-molecule chemotherapeutics[3,4].

Antibodies have been conjugated to a variety of cytotoxic drugs, including small molecules that alkylate DNA (e.g., duocarmycin and calicheamicin), disrupt microtubules (e.g., maytansinoids and auristatins) or bind DNA (e.g., anthracyclins)[5]. These antibody-drug conjugates (ADC) have displayed potent and selective killing of target tumor cells *in vitro* and in mouse tumor xenograft studies. Humanized anti-CD33 conjugated to calicheamicin (gemtuzumab ozogamicin; Mylotarg) was approved by the US Food and Drug Administration in 2000 for the treatment of acute myeloid leukemia,

DAC EX. 2040 IPR2022-01531 Page 992 of 1299

and several ADCs are being actively pursued to combat diverse forms of cancer[6,7,8,9,10,11,12,13,14,15,16,17,18,19]. An adequate safety margin will be required to make ADCs a common therapeutic option for cancer.

Cytotoxic drugs are generally conjugated to antibodies either through lysine side-chain amines or through cysteine sulfhydryl groups activated by reducing interchain disulfide bonds. Both of these procedures yield heterogenous products, containing a mixture of species with different molar ratios of drug to antibody, linked at different sites, each with distinct *in vivo* pharmacokinetic, efficacy and safety profiles[8,20]. In a study that underscored the consequences of this heterogeneity, researchers purified ADC fractions with exactly two, four or eight drugs attached to each antibody and compared these fractions for *in vivo* efficacy, tolerability in mice and pharmacokinetics[8]. The most heavily conjugated species had the lowest maximum tolerated IgG dose and most rapid clearance but did not confer a proportional increase in efficacy. This suggests that it would be desirable to selectively generate only conjugates with a moderate drug stoichiometry, perhaps two drugs per antibody. However, the purification process used in that study is not practical on the scale required for clinical testing, as a large amount of ADC would yield a relatively small amount of the desired stoichiometric fraction. Additionally, this approach still yields antibodies with disrupted interchain disulfide bonds, potentially affecting antibody stability and/or distribution *in vivo*. Finally, even a purified ADC with a uniform stoichiometry would still carry drugs conjugated to multiple sites and therefore be a complex mixture of unique entities. Each species could potentially have a distinct set of properties, and consistent batch-to-batch production would be difficult to control.

To limit the potential liabilities associated with such conjugation methods, we have engineered reactive cysteine residues at specific sites in antibodies to allow drugs to be conjugated with defined stoichiometry without disruption of interchain disulfide bonds. The excellent yields of these antibodies, named THIOMABs, and their derivatives conjugated with a drug of interest suggest the potential for scale-up to allow clinical

DAC EX. 2040 IPR2022-01531 Page 993 of 1299

evaluation. One such THIOMAB-drug conjugate (TDC) retains the *in vivo* efficacy of a conventional ADC and exhibits superior safety in preclinical models.

Results

Engineering cysteine residues for site-specific conjugation

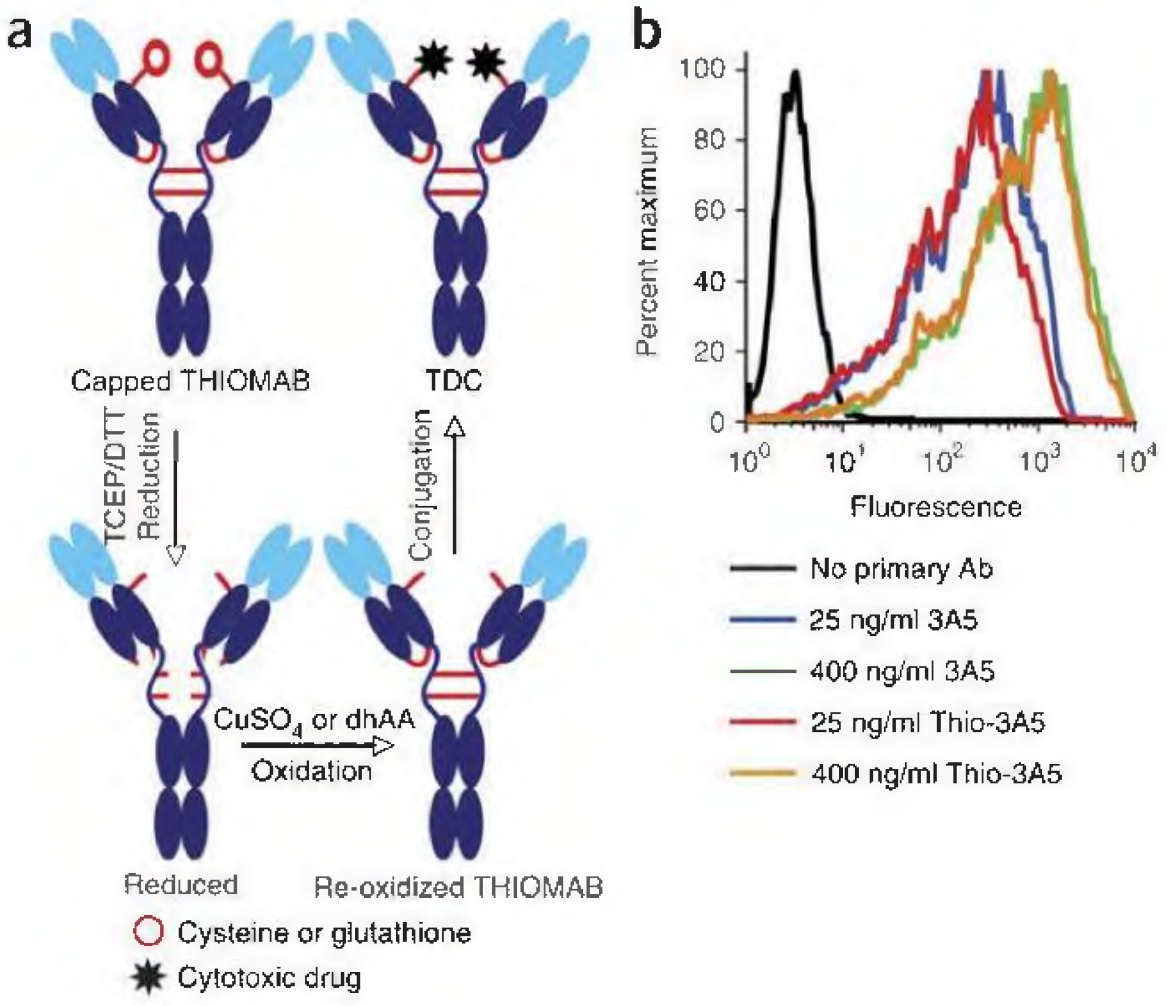
In seeking sites that might be substituted with cysteine residues, we focused on those not involved with antibody effector functions, such as the light and heavy chains of the constant domains of the antibody Fab region, which has no apparent role in antigen binding or in Fc-mediated effector functions[21]. We recently reported a phage display–based method (PHESELECTOR) to screen reactive cysteines on the Fab surface of the antibodies[22]. As applying this approach to the anti-Her2 antibody trastuzumab (Herceptin) suggested the suitability of the variants LC-V110C and HC-A114C (Kabat numbering) for site-specific labeling of Fabs[22], we selected these two sites to develop a conjugation process in the context of full-length antibodies. After expression in Chinese hamster ovary (CHO) cells, our initial attempts to conjugate THIOMABs in a single step with cysteine-reactive probes, *N*-ethyl maleimide or biotinyl-3-maleimidopropionamidyl-3,6-dioxaoctainediamine (biotin-PEO-maleimide) were unsuccessful. Liquid chromatography (LC)/mass spectroscopy (MS) analysis confirmed that the engineered cysteine residues were in mixed disulfides with cysteine or glutathione, presumably formed during the fermentation process (Supplementary Fig. 1 online).

Figure 1a illustrates the conjugation scheme that was subsequently developed to covalently attach thiol-reactive probes to the engineered cysteines. First, the cysteine and glutathione adducts were removed from the THIOMABs by partial reduction followed by diafiltration. This partial reduction also disrupts interchain disulfide bonds but not intrachain disulfide bonds. The interchain disulfide bonds were allowed to reform by air oxidation or by accelerated oxidation using $CuSO_4$ or dehydro-ascorbic acid (dhAA), as demonstrated by nonreducing SDS-PAGE analysis (Supplementary Fig. 2a online) or by LC/MS analysis (Supplementary Fig. 3 online). After this treatment, THIOMAB variants LC-V110C and HC-A114C (in the context of two different mAbs) were

DAC EX. 2040 IPR2022-01531 Page 994 of 1299

then conjugated with biotin-PEO-maleimide. Biotinylation of the appropriate antibody subunit was demonstrated by probing western blots with streptavidin-horseradish peroxidase (Supplementary Fig. 2b online). Whereas 100% biotin conjugation (two moles of biotin per mAb) was observed for the HC-A114C variant, only 25–50% was seen with the LC-V110C variant (Supplementary Fig. 2b online). Papain digestion and LC/MS analysis showed that during reoxidation, some of the LC-V110 cysteines had formed an unexpected disulfide bond between the two Fab portions of the antibody and thus were unavailable for drug conjugation (Supplementary Fig. 4 online). The HC-A114C variant of various antibodies did not show this property and so was selected for further studies (Supplementary Table 1 and Supplementary Fig. 2c online).

Figure 1: Characterization of THIOMABs.



DAC EX. 2040 IPR2022-01531 Page 995 of 1299

(**a**) Conjugation of cytotoxic drugs to engineered THIOMABs. Schematic representation of the reduction and oxidation process used to generate reactive THIOMABs and their conjugation to biotin or cytotoxic drugs. (**b**) The THIOMAB variant of anti-MUC16 3A5 retains high-affinity binding to cell-surface antigen. Humanized anti-MUC16 Thio-3A5 or conventional 3A5 antibody was incubated with OVCAR-3 cells expressing endogenous MUC16 and bound antibody detected using a fluorescent anti-human Fc secondary antibody. Flow cytometry histograms illustrate binding at saturating (400 ng/ml) and subsaturating (25 ng/ml) concentrations. At all antibody concentrations analyzed, the two anti-MUC16 variants gave equivalent binding, suggesting equivalent affinities for the antigen. Ab, antibody; TCEP, tris(2-carboxyethyl)phosphine; dhAA, dehydro-ascorbic acid; DTT, dithiothreitol; TDC, THIOMAB-drug conjugate.

Table 1 Analytical characterization of anti-MUC16 drug conjugates

The efficient conjugation at HC-A114C but not at LC-V110C prompted us to seek further sites for cysteine engineering. We substituted most of the available serine, alanine and valine residues (24 variants) in the light chain domain of the trastuzumab-Fab. Thio-Fab phage were isolated, biotinylated and tested for binding to the Her2 extracellular domain (ECD) and streptavidin, as described earlier[22]. LC-V205C, LC-S114C, LC-V110C and LC-S127C showed the highest thiol reactivity values (0.8–1.0) (Supplementary Fig. 5 online). The discrepancy between the results with the LC-V110C Fab versus the LC-V110C full-length antibody prompted us to evaluate the most promising sites in the context of the full-length antibody. Based on current and previous PHESELECTOR assay results[22], we have selected eight sites on the light chain (LC-V15C, LC-V110C, LC-S114C, LC-S121C, LC-S127C, LC-A153C, LC-S168C and LC-V205C) and four sites on the heavy chain (HC-S112C, HC-S113C, HC-S115C and HC-T116C). All of these THIOMABs were expressed and purified along with the HC-A114C variant and unmodified trastuzumab. The purified proteins were conjugated to biotin-maleimide, and the extent of conjugation was quantified by LC/MS analysis. As 9 of the 13 THIOMABs showed >90% conjugation efficiency, they should be as suitable for site-specific conjugation of thiol reactive

DAC EX. 2040 IPR2022-01531 Page 996 of 1299

probes as the HC-A114C variant described below (Supplementary Table 1 online). In this report, we focus on the properties of one THIOMAB (anti-MUC16) and its conjugates. Studies with multiple antibody-antigen combinations have established the general utility of this strategy (data not shown).

Anti-MUC16 THIOMAB retains antigen binding and specificity

The successful biotinylation of HC-A114C variants prompted us to test TDCs *in vitro* and *in vivo*. MUC16 is a cell-surface protein that is overexpressed in many ovarian malignancies. As we previously reported encouraging findings with conventional anti-MUC16 (monoclonal antibody 3A5) drug conjugates[6], which were efficacious at tolerated doses *in vivo*, we chose to focus on anti-MUC16 to evaluate the potential of the THIOMAB strategy for expanding the therapeutic index. Chimeric (ch3A5) and fully humanized (hu3A5) anti-MUC16 antibodies were engineered to have the HC-A114C mutation (Kabat numbering; equivalent to A118C in Eu numbering and A117C in sequential numbering). Generation of the chimeric immunoglobulin was described previously[6]. To produce a humanized anti-MUC16 antibody, the complementarity-determining regions (CDR) of mu3A5 were grafted into human consensus $V_{L_{kI}}$ and $V_{H_{subgroupIII}}$ frameworks (Supplementary Methods and Supplementary Figs. 6a,b online). Relative to chimeric 3A5, the binding affinity of the 3A5 CDR-graft for MUC16 was markedly reduced (Supplementary Table 2 online). To restore binding, we introduced mutations into the CDR regions of the 3A5 graft to reconstitute appropriate CDR-framework interactions or to select more favorable CDR-antigen interactions. A library of CDR variants were displayed as Fab on phage and panned for improved interactions with the antigen. Enhanced binding was observed only in variants with substitutions in CDR-H3 (Supplementary Fig. 6c online). Four representative clones, reformatted and expressed as IgG and assessed for MUC16 binding relative to chimeric 3A5, demonstrated that changes in CDR-H3 fully restore antigen binding (Supplementary Table 2 online). One clone was taken forward as humanized anti-MUC16.

DAC EX. 2040 IPR2022-01531 Page 997 of 1299

To be useful for therapeutic development, the THIOMAB strategy must yield an antibody with comparable or higher binding affinity and specificity for the target antigen as compared with the conventional antibody. Affinities of humanized anti-MUC16 HC-A114C THIOMAB and conventional 3A5 IgG were compared by flow cytometry on OVCAR-3 cells (ovarian cancer cells that express endogenous MUC16), serially diluting the antibodies until a reduced shift was observed (Fig. 1b). Antibodies were in excess of cellular binding sites throughout the titration. At each concentration tested, thio-anti-MUC16 bound to OVCAR-3 cells as efficiently as conventional anti-MUC16. Surface plasmon resonance–based analyses using portions of the human MUC16 ECD also confirmed the high affinity of this THIOMAB for this antigen (K_D = 116 pM). Comparison of cells with high and low or absent MUC16 expression based on RT-PCR studies revealed that this THIOMAB binds to cells that express MUC16 but not to MUC16-negative cell lines (Supplementary Fig. 7 online). Thus, substitution at HC-A114 does not affect antigen binding.

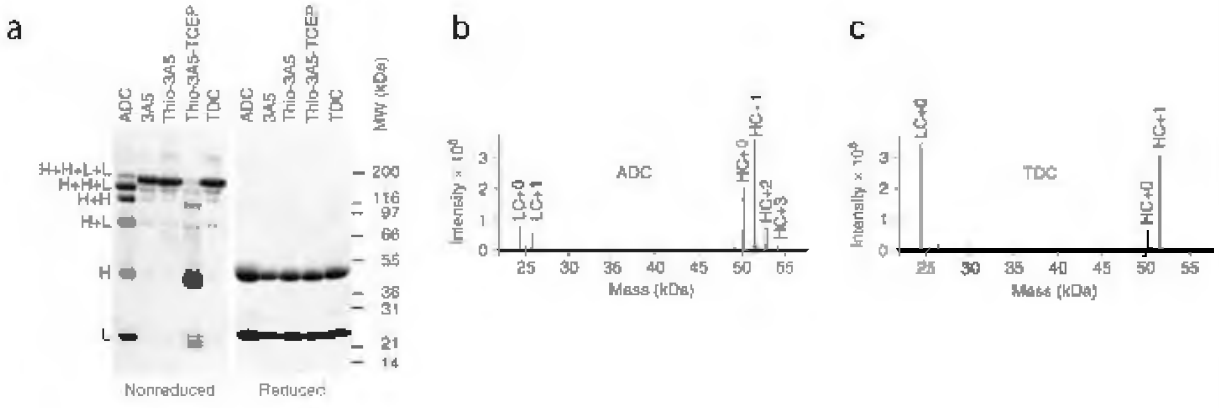
Anti-MUC16 THIOMAB yields nearly homogeneous conjugates

THIOMAB 3A5 antibodies were partially reduced and reoxidized to yield two free thiol groups per antibody, then conjugated to the cytotoxic drug monomethyl auristatin E (MMAE) via the protease-labile maleimido-caproyl-valine-citrulline-para-amino-benzyloxy carbonyl (MC-vc-PAB) linker (Supplementary Fig. 8a online)[23,24]. For simplicity, the conventional conjugate (anti-MUC16-MC-vc-PAB-MMAE) will subsequently be referred to as anti-MUC16 ADC and the THIOMAB conjugate (thio-anti-MUC16-MC-vc-PAB-MMAE) will be referred to as anti-MUC16 TDC. Anti-MUC16 ADC contained an average drug-antibody ratio (DAR) of 3.1 (Table 1) and migrated as multiple species on nonreducing SDS-PAGE, consistent with the loss of interchain disulfide bonds through drug conjugation (Fig. 2a). In contrast, the interchain disulfides were retained in anti-MUC16 TDC, which migrated as a single major band. Hydrophobic interaction chromatography was used to resolve antibodies with different stoichiometries of drug conjugation. Anti-MUC16 TDC was modified with zero, one or two drugs (average DAR = 1.6; Table 1 and Supplementary Fig. 8b online). The absence of higher stoichiometric

DAC EX. 2040 IPR2022-01531 Page 998 of 1299

ratios indicates that only the engineered A114C cysteines were conjugated, as confirmed by LC/MS analysis and peptide mapping (Supplementary Figs. 9 and 10 and Supplementary Tables 3 and 4 online). In line with previous reports[8,14], standard 3A5 ADCs are a mixture of seven different drug stoichiometries (zero, one, two, three, four, six and eight drugs per antibody; Table 1 and Supplementary Fig. 8b online) with the possibility of conjugating to any of eight cysteines, potentially generating >100 different ADC species. LC/MS analysis showed that the linker drug was distributed to both the light (one drug) and heavy chain (one, two or three drugs) of anti-MUC16 ADC but only to the heavy chain (one drug) of the cognate TDC (Fig. 2b,c). Finally, anti-MUC16 TDC retains high affinity for the human MUC16 ECD (K_D = 117 pM).

Figure 2: THIOMAB drug conjugates retain interchain disulfide bonds with site-specific drug attachment.



(**a**) SDS-PAGE analysis of antibody-drug conjugates under nonreducing and reducing conditions. The appearance of multiple species in the standard ADCs is due to loss of interchain disulfide bonds. (**b,c**) Deconvoluted mass spectra of ADC (**b**) and TDC (**c**) variants of an antibody against MUC16. Drug conjugates are deglycosylated and reduced before LC/MS analysis. ADC mass spectra displayed zero or one drug species on the light chain and zero, one, two or three drug species on the heavy chain. TDC displayed only one drug species on the heavy chain. ADC, anti-MUC16-MC-vc-PAB-MMAE; TDC, thio-anti-MUC16-MC-vc-PAB-MMAE; THIOMAB-TCEP, THIOMAB reduced with tris(2-carboxyethyl)phosphine (TCEP); H, heavy chain; L, light chain.

DAC EX. 2040 IPR2022-01531 Page 999 of 1299

Along with reduced heterogeneity, the anti-MUC16 TDC preparation lacks species that have the higher drug loads reported to not be tolerated as well in rodents[8]. Subsequent process development has yielded conjugates with almost exactly two drugs per antibody. The species carrying the two drugs on the engineered cysteines and nowhere else is by far the predominant species in the preparation (Table 1 and Supplementary Fig. 8d online).

Anti-MUC16 TDC displays comparable efficacy to ADC

We previously have reported that the conventional anti-MUC16 drug conjugates are highly efficacious in mouse OVCAR-3 xenograft models[6]. To determine if the thio-anti-MUC16 retains this property, the ADC and TDC variants of anti-MUC16 were subjected to *in vitro* cell proliferation and *in vivo* xenograft studies. *In vitro*, the ADC and TDC formats of chimeric anti-MUC16 had similar cytotoxicities, with median inhibitory concentration (IC_{50}) < 50 ng antibody/ml against OVCAR-3 cells and PC3 cells transfected with a recombinant form of MUC16 (Supplementary Fig. 11 online). The IC_{50} values of the anti-MUC16 TDC were approximately twofold higher than those of the ADC, possibly due to the twofold lower drug load of the TDC. Parental PC3 cells lacking MUC16 expression were not affected by either conjugate up to 3 μg/ml, demonstrating the specificity of the antiproliferative effect. The rates of internalization into OVCAR-3 cells *in vitro* were comparable, as expected, given that neither method of drug conjugation detectably influences antigen binding (data not shown).

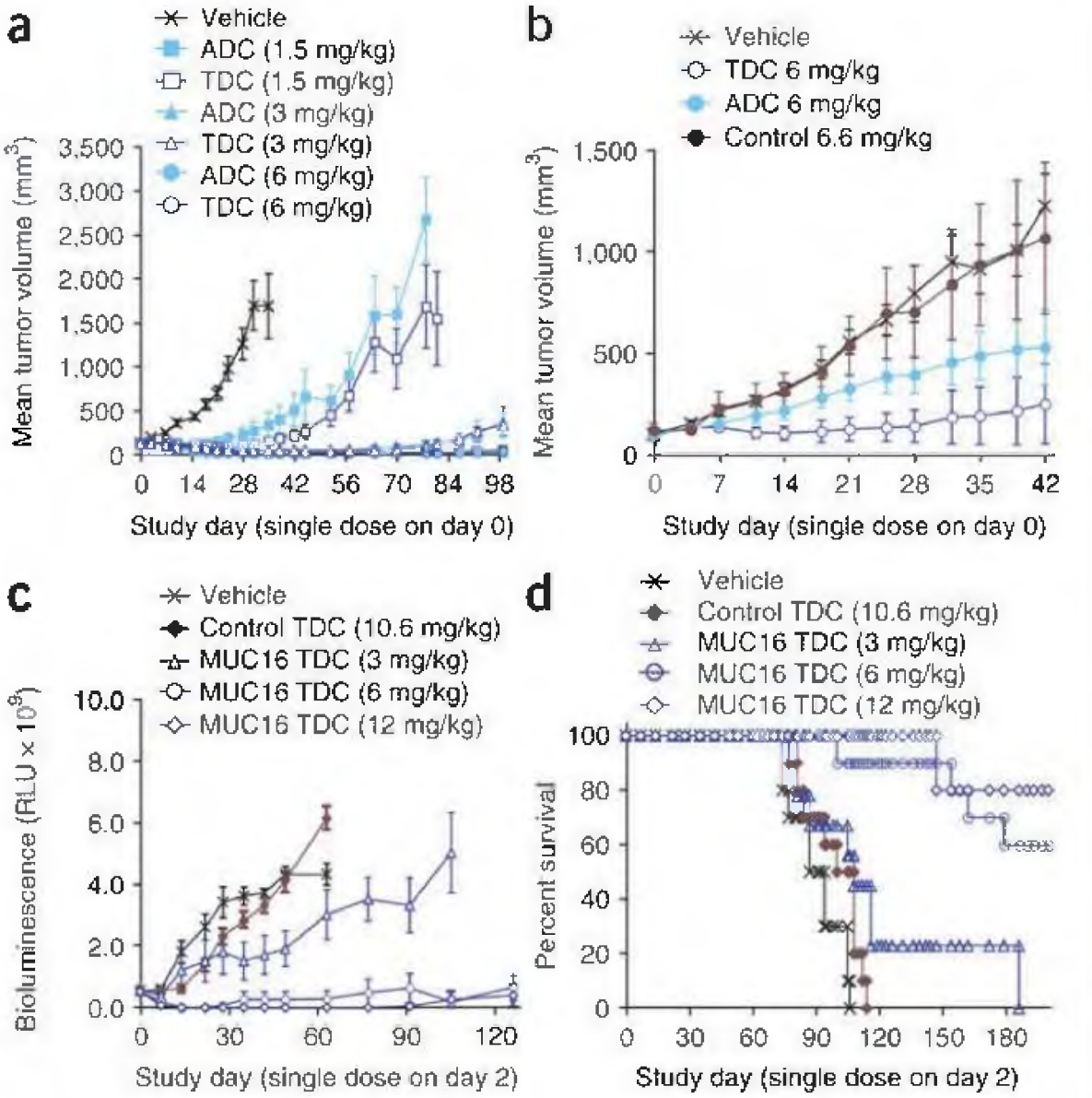
Anti-MUC16 ADC and anti-MUC16 TDC were also compared *in vivo* using chimeric antibody conjugates and an OVCAR-3 xenograft model (Fig. 3a). Mice bearing established tumors (~150 mm^3) were dosed once with either anti-MUC16 ADC or anti-MUC16 TDC over a range of dose levels. The anti-MUC16 TDC was at least as active as the ADC at each IgG dose level, providing partial efficacy at 1.5 mg/kg (MMAE doses are 35 μg/m^2 for the TDC and 71 μg/m^2 for the ADC) and near-complete elimination of tumors at 3 mg/kg (69 versus 141 μg/m^2 MMAE) and 6 mg/kg (139 versus 283 μg/m^2 MMAE). When stated in terms of MMAE dose, anti-MUC16 TDC was approximately twice as

DAC EX. 2040 IPR2022-01531 Page 1000 of 1299

efficacious as anti-MUC16 ADC. No adverse effects of either conjugate were observed at any dose level. Anti-MUC16 TDC was also at least as active as anti-MUC16 ADC against a transplant xenograft model of ovarian cancer (Fig. 3b), and subsequent studies have demonstrated potent activity of the TDC against several tumor models (Figs. 3c,d and Supplementary Figs. 12, 13 online). The study using the intraperitoneal OVCAR-3/luciferase xenograft model (Figs. 3c,d) demonstrated single-dose activity of the anti-MUC16 TDC at 3 mg/kg against a tumor growing at a more relevant anatomic site, with improved activity at higher dose levels. Our previous studies using the ADC also achieved significant efficacy but with multiple weekly dosing[6].

Figure 3: *In vivo* efficacy is retained with the TDC format.

DAC EX. 2040 IPR2022-01531 Page 1001 of 1299



(**a**) Tumors derived from OVCAR-3 cells were serially transplanted into the mammary fat pads of female SCID mice, as previously reported[6], and anti-MUC16 ADC and TDC were compared. When palpable tumors were established, mice were randomized to a mean tumor volume of ~150 mm^3 in each group (ten/group; range = 100–200 mm^3) and then treated intravenously once (day 0) with chimeric anti-MUC16 ADC (3.1 drugs per antibody) or TDC (1.6 drugs per antibody) at the indicated doses. Mean tumor volumes (± s.e.m.) are plotted over time, with the ADC and TDC curves superimposed for the 3 mg/kg and 6 mg/kg groups. (**b**) Female nu/nu mice were inoculated with OVXF 1023 primary ovarian cancer tumors and anti-MUC16 ADC and TDC were compared. Chimeric anti-MUC16 ADC (3.1 drugs per antibody) or TDC (1.6 drugs per antibody) or a control ADC were dosed once as indicated. Mean tumor volumes (± s.e.m.) are

DAC EX. 2040 IPR2022-01531 Page 1002 of 1299

plotted over time. (**c,d**) Female SCID mice were inoculated in the peritoneal cavity with OVCAR-3/luciferase cells, as previously reported[6]. Tumor burden was assessed by bioluminescence measurement after injection of luciferin. Once bioluminescence was stable (~3 weeks after inoculation), mice were grouped on the basis of luminescence and dosed once with humanized anti-MUC16 TDC (1.6 drugs per antibody) or an irrelevant TDC (1.9 drugs per antibody) as indicated. Changes in mean bioluminescence intensities (± s.e.m.) over time. Bioluminescence intensities plotted in terms of relative light units (RLU) (**c**). Changes in the percentages of surviving mice over time (**d**).

Improved therapeutic index with anti-MUC16 TDCs

As noted above, the different conjugation procedures yielded anti-MUC16 ADC and TDC with different drug stoichiometries. Therefore, equivalent efficacy using the anti-MUC16 TDC is achieved with approximately one-half the dose of cytotoxic MMAE. Our preliminary studies have indicated that the toxicity of ADCs in animals is closely associated with the cytotoxic drug dose, and the adverse events are largely consistent with the safety profile of the drug itself. This suggests that the anti-MUC16 TDC may be better tolerated in animals than the ADC at equivalent mg/kg dose levels.

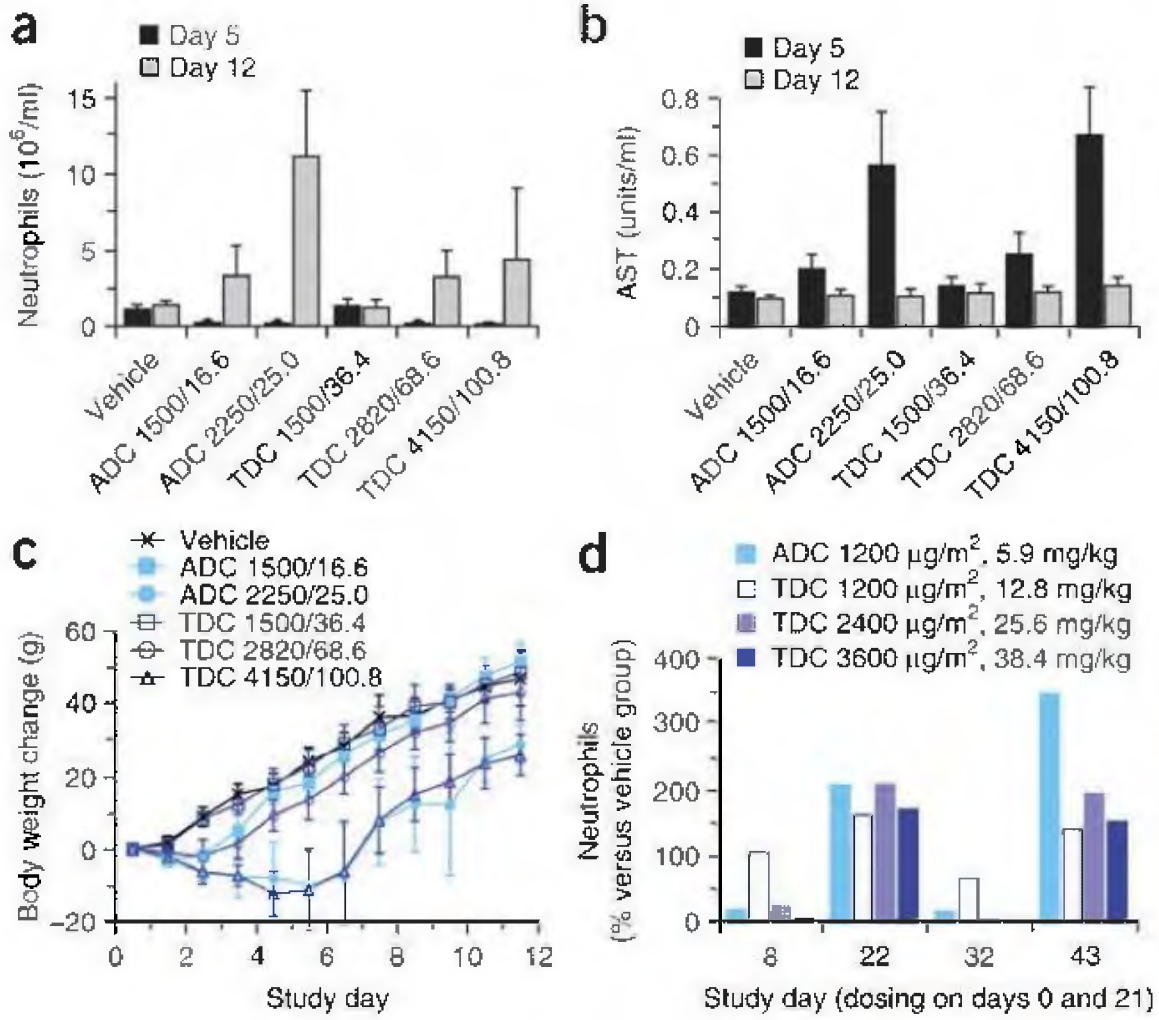
We evaluated the safety of the anti-MUC16 ADC and TDC in Sprague-Dawley rats and cynomolgus monkeys. Both species express MUC16, although the primary sequence of the cynomolgus monkey antigen is more similar to the human counterpart than the rat antigen is. In a competitive binding assay, mAb 3A5 binding to CA125 was inhibited with similar concentrations of human and monkey MUC16 ECD proteins (IC_{50} = 0.76 nM and 1.88 nM, respectively), but competition by the rat MUC16 ECD was much less efficient (IC_{50} = 13.5 nM). Both rats and cynomolgus monkeys are sensitive to antibody-MMAE conjugates. As safety studies using a related cytotoxic compound, dolastatin-10, showed mice to be relatively insensitive to this class of drug, the mouse models used in the efficacy studies were not considered useful for safety assessment[25]. In rats, a single dose of 16.6 mg/kg anti-MUC16 ADC (1,500 μg/m^2 MMAE) produced a marked depletion of circulating neutrophils and other white blood cells at day 5 (4 d post-dose; Fig. 4a and

DAC EX. 2040 IPR2022-01531 Page 1003 of 1299

data not shown), followed by a compensatory rebound at day 12. This anti-MUC16 ADC dose also led to a mild elevation in serum levels of the liver enzyme aspartate aminotransferase (AST; Fig. 4b) and transient weight loss (Fig. 4c). The AST levels were more profoundly affected by a 50% increase in dose (24.5 mg/kg ADC; 2,250 μg/m^2 MMAE); at that dose, three of six rats did not survive to the end of the study (day 12). In contrast, 36.4 mg/kg of anti-MUC16 TDC (equivalent to 1,500 μg/m^2 MMAE exposure) yielded no adverse effects, with all parameters essentially identical to vehicle-treated animals. A dose of 68.6 mg/kg anti-MUC16 TDC (2,820 μg/m^2 drug) produced toxicities that were nearly equivalent to those observed using the anti-MUC16 ADC at one-fourth that dose. Although the highest anti-MUC16 TDC dose (100.8 mg/kg; 4,150 μg/m^2 MMAE) led to pronounced effects (and two of six rats were killed due to excessive weight loss), the overall profile of adverse effects was quite similar to that observed at the higher anti-MUC16 ADC dose (24.5 mg/kg ADC; 2,250 μg/m^2 MMAE). The same trends were observed in a preliminary study using chimeric conjugates (Supplementary Fig. 14 online).

Figure 4: The TDC format is better tolerated *in vivo*.

DAC EX. 2040 IPR2022-01531 Page 1004 of 1299



(**a–c**) Normal Sprague-Dawley rats were dosed once (day 1) with humanized anti-MUC16 ADC or TDC at the indicated dose levels. Dose levels are given in terms of µg/m^2 MMAE (the cytotoxic drug dose per body surface area, derived from the stoichiometry of conjugation) and mg/kg IgG; for example, "TDC 1500/36.4" indicates TDC dosed at 36.4 mg/kg IgG, which at 1.6 drugs per IgG corresponds to 1,500 µg/m^2 MMAE. Blood was drawn from rats at study day 5 (4 d after dosing) and day 12 (immediately before they were killed) for hematology (neutrophil counts in **a**) and serum chemistry (serum AST levels in **b**). *X*-axis labels for **b** apply also to **a** (treatment groups are graphed in the same order). (**c**) Rats were weighed daily after dosing and changes in body weight over time relative to day 1 plotted. (**d**) Higher doses of the TDC format are required to reduce neutrophil counts in cynomolgus monkeys. In two separate studies, female Chinese cynomolgus monkeys were dosed on days 1 and 22 with: humanized anti-MUC16 ADC (5.9 mg/kg IgG = 1,200 µg/m^2 MMAE; white bars); TDC at 12.8 mg/kg IgG (1,200 µg/m^2 MMAE; light gray bars); TDC at 25.6 mg/kg IgG (2,400 µg/m^2 MMAE; dark gray bars); or

DAC EX. 2040 IPR2022-01531 Page 1005 of 1299

TDC at 38.4 mg/kg IgG (3,600 μg/m^2 MMAE; black bars). Blood was drawn for hematology and serum chemistry at the indicated intervals (day 22 values are from before the second dose). Average circulating neutrophil counts were normalized to the average counts from vehicle-treated monkeys at the given time point of the same study. Note the nadir in neutrophil levels ~1 week after dosing, followed by a recovery to normal levels within 3 weeks.

The most prominent adverse event in cynomolgus monkeys dosed with anti-MUC16 ADC or TDC is a reversible decrease in neutrophils. Whereas a marked decrease was induced by anti-MUC16 ADC at a drug exposure of 1,200 μg/m^2 drug (5.9 mg/kg antibody), anti-MUC16 TDC at 1,200 μg/m^2 drug (12.8 mg/kg antibody) yielded no notable adverse events, with neutrophil counts tracking closely with sham-treated animals (Fig. 4d). Doubling the dose resulted in decreased neutrophil counts, which were completely reversible. An even higher dose of anti-MUC16 TDC (38.4 mg/kg; 3,600 μg/m^2 drug) gave no marked effects beyond the neutrophil decrease, which was more pronounced than at the middle-dose level but remained reversible. Importantly, no toxicities were observed in cornea, lung, oviduct and uterus—all organs known to express MUC16. The only notable histopathologic findings were minimal-to-mild increases in bone marrow myelopoiesis and minimal-to-mild thymic lymphoid depletion, consistent with the decreases in neutrophil count and indicative of a regenerative response.

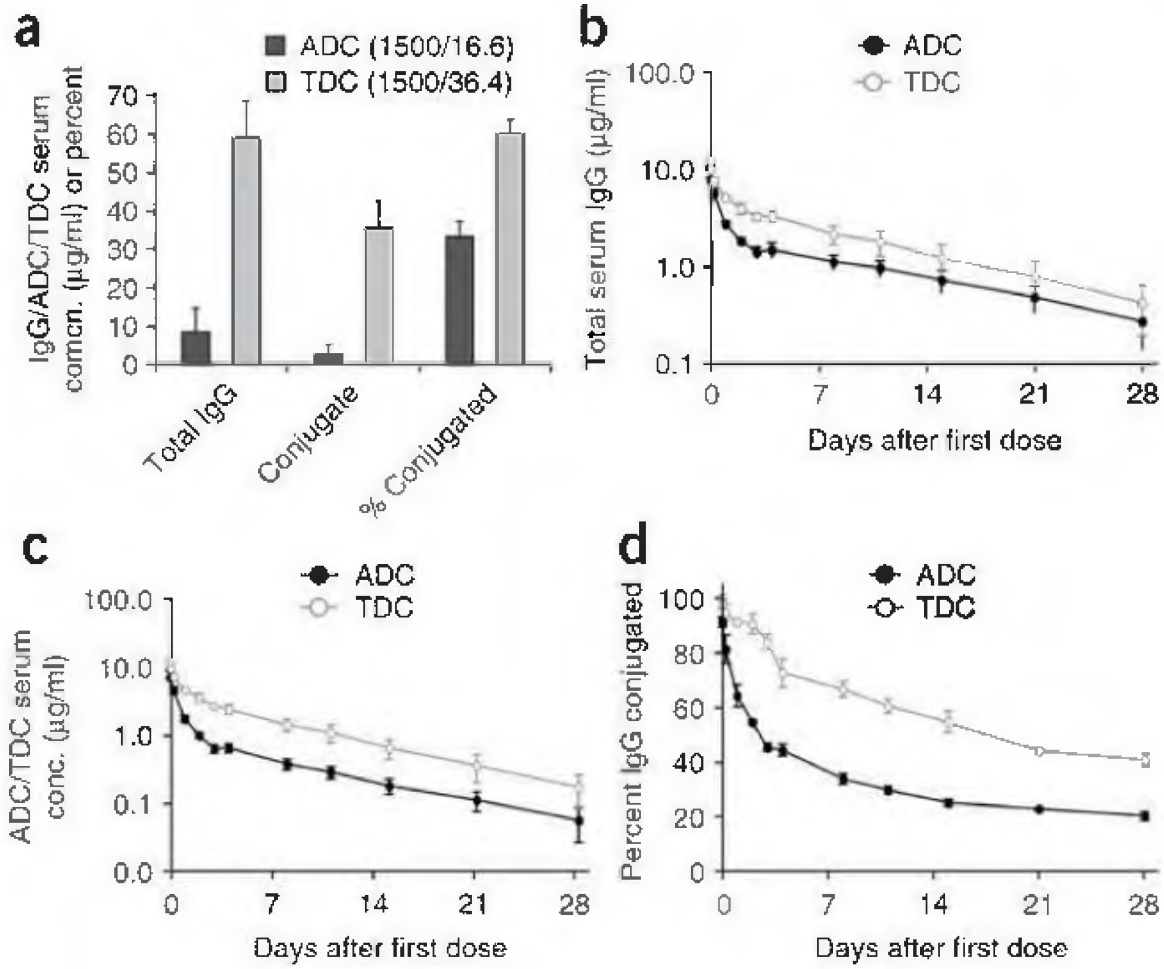
These results demonstrate that the anti-MUC16 TDC is safer than anti-MUC16 ADC in preclinical models, even when compared on the basis of cytotoxic drug dose (that is, equivalent μg/m^2). To begin to understand this, we have analyzed the kinetics of clearance of each type of conjugate in rats. At a dose of 36.4 mg/kg IgG (1,500 μg/m^2 MMAE), anti-MUC16 TDC remained in circulation at much higher levels than anti-MUC16 ADC dosed at 16.6 mg/kg IgG (1,500 μg/m^2 MMAE), even after accounting for the differences in dose levels (Fig. 5a). Nonetheless, anti-MUC16 TDC at that dose yielded no adverse effects. We observed the same results when dosing rats with chimeric ADC and TDC at a matched mg/kg dose (Supplementary Fig. 14d online). A more thorough kinetic analysis using chimeric antibodies (Fig. 5b–d) showed that the total TDC is cleared

DAC EX. 2040 IPR2022-01531 Page 1006 of 1299

somewhat more slowly than the ADC (9.5 ± 2.9 versus 16.1 ± 3.5 ml/day/kg), and the proportion of TDC still bearing at least one drug decreased substantially more slowly than the corresponding proportion of ADC (14.1 ± 3.0 versus 41.6 ± 4.8 ml/day/kg). Interestingly, the ADC and TDC kinetics are comparable in tumor-bearing mice (Supplementary Fig. 15 online). Slower clearance of the TDC variant has consistently been observed using different antibodies, suggesting that the kinetics of the anti-MUC16 conjugates in the mouse may be an anomaly. The drug conjugate assay generates a lower signal from a TDC with exactly one drug than from a TDC with two drugs. However, the discrepancy is minor and cannot explain the different behaviors of the ADC and TDC variants. Therefore, we conclude that despite bearing fewer drugs per antibody on average, the TDC variants retain the conjugated drugs more effectively in rats than their ADC counterparts.

Figure 5: In rats, a higher proportion of TDC is retained in circulation, compared with its ADC counterpart.

DAC EX. 2040 IPR2022-01531 Page 1007 of 1299



(**a**) Serum levels of total anti-MUC16 IgG ('Total antibody') and antibody carrying at least one cytotoxic drug (Conjugate) were measured at day 12 of the rat safety study described in Figure 4a–c. The percentage of antibody with at least one drug still attached (% Conjugated) was calculated from the ratio of Conjugate and Total IgG and is plotted next to the absolute values for ease of interpretation. Data for the 1,500 µg/m^2 MMAE groups are shown. (**b–d**) In a separate study, normal Sprague-Dawley rats were dosed once with 0.5 mg/kg chimeric ADC or TDC at study day 0. At the indicated intervals, blood was drawn for determination of total anti-MUC16 IgG (**b**) and anti-MUC16 carrying at least one MMAE (**c**). The fraction of drug-conjugated to total IgG was determined as the ratio of conjugated to total IgG and is plotted over time (**d**). Similar data were observed at higher dose levels.

Discussion

The unfavorable *in vivo* effects associated with heterogeneity in the drug load and sites of attachment in antibody-drug conjugates could compromise their promise as cancer

DAC EX. 2040 IPR2022-01531 Page 1008 of 1299

therapeutics. Conjugation through lysine residues was shown to distribute to ~40 different sites, potentially resulting in >10^6 ADC species[20]. Conjugates generated through cysteines by partial reduction of interchain-disulfide bonds also have variable stoichiometry (zero to eight drugs per antibody) and potentially yield >100 species[8]. Solvent-accessible interchain-disulfide bond cysteines have been replaced with serine to allow directed conjugation to the remaining cysteines[26]. However, elimination of these disulfide bonds could disrupt quaternary structure of the antibody, thereby perturbing the behavior of the antibody *in vivo*, including changes in antibody effector functions[27,28,29]. Our THIOMAB technology resolves the issue of conjugate heterogeneity by directing the attachment of drugs at defined sites and with near-uniform stoichiometry. Additionally, the conjugation chemistry retains all of the native immunoglobulin disulfide bonds. Cysteine engineering into antibodies for site-specific conjugation has been achieved previously but with poor yield and no potential for large-scale processing[30,31]. Notably, site-specific conjugation to antibody-Fabs has been reported using cysteine engineering[22,32]. However, the engineered cysteines were shown to be blocked by cysteinylation or glutathionylation in the context of full-length antibodies (Supplementary Fig. 1 online). Our novel conjugation method reactivates the engineered cysteines for conjugation, thus achieving site-specific antibody-drug conjugates at high yield and purity. We have observed no challenges with this conjugation strategy even up to a multi-gram scale. Also, our methodology should be amenable to a wide range of cytotoxic drugs, requiring only that the drugs be compatible with sulfhydryl-directed conjugation chemistries.

These properties alone represent a substantial advancement for product development. In addition, we have found that the anti-MUC16 TDC exhibits a markedly improved therapeutic index in preclinical animal models. When comparing matched IgG (mg/kg) dose levels, our data show equivalent efficacy of the anti-MUC16 TDC and ADC in mouse xenografts, whereas in rats the 68.6 mg/kg (2,820 μg/m^2 MMAE) dose of the TDC exerts similar toxicities as the 16.6 mg/kg (1,500 μg/m^2 MMAE) dose of the ADC. When compared in terms of MMAE exposure, the TDC is both safer and more efficacious than the ADC. Although the success of the approach has yet to be tested in humans, even a

DAC EX. 2040 IPR2022-01531 Page 1009 of 1299

modest increase in the range of safe and efficacious doses could dramatically enhance the clinical value of the conjugate. The efficacy and toxicity of an antibody-drug conjugate could be influenced substantially by a host immune response against the conjugate. In cynomolgus monkeys, we have observed little if any immune response against the anti-MUC16 TDC and only sporadic responses against the ADC. Improved safety without loss of efficacy has been observed for several different antibodies targeting multiple tumor antigens (our unpublished results), indicating that the THIOMAB technology is a general path to an expanded therapeutic window.

We do not yet know what accounts for the improved safety of the TDC in rats and primates. The *in vivo* kinetics of the total TDC in rats are quite comparable to those of native (nonconjugated) antibodies, whereas the total ADC clears somewhat faster. When considering the kinetics of conjugated antibodies, the difference between the TDC and the ADC is more pronounced, and over time a far greater proportion of circulating TDC retains at least one drug (Fig. 5b–d). This could point to a mechanism of clearance used by a fraction of the ADC but not the TDC and leading to ADC metabolism and toxicity. For example, the relatively more highly conjugated species within the ADC preparation may clear more rapidly, thereby enriching for the unconjugated antibody that is 12% of the original preparation (Table 1). Consistent with our findings, a correlation has been shown between total antibody clearance and toxicity in mice dosed with a DAR8 ADC[8]. Therefore, it is possible that the relative safety of the TDC can be attributed at least partly to the absence of high-drug-load species. Although the ADC preparations used in the present studies did not contain high levels of antibodies with greater than four drugs attached, rats may be more sensitive than mice to more moderate drug loading. The previous work[8] suggests that a similarly favorable profile of safety and activity might be observed with a hypothetical homogenous ADC preparation having a preponderance of a single species bearing two drugs conjugated at two sites only. ADC conjugation chemistry does not presently allow such a preparation at the scale necessary for preclinical evaluation, not to mention the scale required for clinical testing.

DAC EX. 2040 IPR2022-01531 Page 1010 of 1299

An alternative explanation for the pharmacokinetic data is that the MMAE may be more readily released from the ADC than from the TDC in circulation. Several mechanisms might lead to greater stability of the TDC. The engineered cysteines may be relatively 'protected' sites that resist proteolytic attack in circulation. We have observed that the accessibility of a cysteine residue varies depending where it is located in the antibody-Fab[22]. An ADC is produced by conjugating a drug at reduced hinge disulfides, one of the most accessible regions of the antibody[33]. Therefore, the ADC may be more readily processed than the TDC and release more active MMAE in circulation, thus increasing ADC toxicity in rats. Also, although the TDC and the ADC variants have equivalent affinity for FcRn (Supplementary Figs. 16, 17 and Supplementary Table 5 online), it is possible that the ADC is less stable while traversing the FcRn-mediated intracellular recycling pathway.

Either mechanism (differences in antibody clearance or rate of MMAE release) could affect safety. Indeed, relatively higher levels of ADC-derived free MMAE in circulation could readily account for the adverse effects that we have observed in our preclinical safety studies. Specifically, the myelotoxicity manifested by marked neutrophil decline was also the dose-limiting toxicity in animals treated with dolastatin-10, the parent molecule of MMAE. Also, elevated serum AST results from dosing rats with dolastatin-10, ADC and TDC. The rapid clearance of highly conjugated ADC could also directly lead to toxicity within the organ of clearance and systemic release of MMAE. At present, we cannot distinguish between these two mechanisms, and both may operate.

Our preclinical safety data suggest that MMAE exposure will determine the tolerability of the anti-MUC16 TDC in the clinic. If so, one clear benefit to the TDC over the ADC would be to reduce the MMAE exposure at an efficacious dose of conjugate. In turn, the improved tolerability of the TDC could permit higher dose levels on a mg/kg antibody basis. This could be critical to producing a therapeutic benefit for patients with more challenging malignancies, such as reduced sensitivity to MMAE or relatively lower levels of MUC16 expression. Overall, the TDC conjugation strategy confers improved *in vivo*

DAC EX. 2040 IPR2022-01531 Page 1011 of 1299

properties and may represent a decisive advancement in the development of therapeutic antibody-drug conjugates.

Methods

Site directed mutagenesis, THIOMAB expression and purification.

Cysteine mutations were introduced in antibody light or heavy chain constructs (in pRK expression vectors) using double-stranded DNA as a template by PCR-based site-directed mutagenesis as described earlier[22]. THIOMAB light and heavy chain constructs were transiently transfected into CHO cells, and the antibodies were purified over Protein A columns followed by ion exchange chromatography.

Conjugation.

THIOMAB conjugation was performed at Genentech, Seattle Genetics or NPIL Pharma UK using methods developed at Genentech. Before conjugation of the THIOMAB to biotin or MMAE derivatized with a maleimide-containing linker, the blocking cysteine or glutathione that was present on the introduced cysteine was removed by mild reduction in PBS at 25 °C by the addition of tenfold molar excess reducing agent, TCEP or dithiothreitol (DTT) followed by diafiltration. To re-form the interchain disulfide bonds, the THIOMAB was incubated for three hours at 25 °C with $CuSO_4$ or with dhAA (Sigma-Aldrich) at a twofold molar excess over the reducing agent concentration. The formation of interchain disulfide bonds was monitored either by nonreducing SDS-PAGE or by denaturing reversed phase high-performance liquid chromatography (HPLC) PLRP column chromatography. The maleimide-linked labeling reagent, either biotin-PEO-maleimide (tenfold molar excess over protein) or MC-vc-PAB-MMAE (threefold molar excess over protein), was incubated with the activated THIOMAB for 1 h at 25 °C. The antibody conjugate was purified on HiTrap S column (GE Healthcare Bio-Sciences) to remove excess reagents. The number of conjugated biotin or MC-vc-PAB-MMAE molecules per mAb was quantified by LC/MS analysis. Initial biotin conjugation experiments were carried out with $CuSO_4$; all the cytotoxic drug conjugation experiments described in this paper were carried out with dhAA.

DAC EX. 2040 IPR2022-01531 Page 1012 of 1299

Mass spectrometric analysis.

LC/MS analysis was performed on a TSQ Quantum Triple quadrupole mass spectrometer with extended mass range (Thermo Electron). Samples were chromatographed on a PRLP-S, 1000 A, microbore column (50 mm × 2.1 mm, Polymer Laboratories) heated to 75 °C. A linear gradient from 30–40% B (solvent A, 0.05% TFA in water; solvent B, 0.04% TFA in acetonitrile) was used and the eluant was directly ionized using the electrospray source. Data were collected by the Xcalibur data system and deconvolution was performed using ProMass (Novatia). Before LC/MS analysis, antibodies or drug conjugates (50 µg) were treated with PNGase F (2 units/ml; PROzyme) for 2 h at 37 °C to remove N-linked carbohydrates.

Hydrophobic interaction chromatography (HIC).

Samples were injected onto a Butyl HIC NPR column (2.5 µm, 4.6 mm × 3.5 cm) (Tosoh Bioscience) and eluted with a linear gradient from 0 to 70% B at 0.8 ml/min (A, 1.5 M ammonium sulfate in 50 mM potassium phosphate, pH 7; B, 50 mM potassium phosphate pH 7, 20% isopropanol). An Agilent 1100 series HPLC system equipped with a multi-wavelength detector and Chemstation software was used to resolve and quantify antibody species with different ratios of drugs per antibody.

Flow cytometry and *in vitro* studies.

OVCAR-3 cells (30,000 cells per sample) were incubated on ice with humanized conventional or thio anti-MUC16 mAb for 75 min in 1 ml total volume. Antibodies were applied at 25, 50, 100, 200 and 400 ng/ml in PBS + 1% FBS + 2 mM EDTA. After this incubation, cells were washed and then incubated with phycoerythrin-labeled goat anti-human Fc secondary antibody (1 h on ice). Cells were then washed and analyzed by flow cytometry as described previously[6]. Based on our published data, 3×10^4 OVCAR-3 cells express ~1×10^{10} binding sites for anti-MUC16 antibody 3A5. Even the lowest antibody concentration tested (25 ng or ~1×10^{11} antibodies) provides a molar excess of

DAC EX. 2040 IPR2022-01531 Page 1013 of 1299

antibodies over binding sites. Therefore, the concentration at which binding is reduced (as detected by flow cytometry) will reflect the affinity of the antibody for MUC16.

Cell proliferation in the presence of antibody-drug conjugates was assessed in PC3/neo (MUC16-negative), PC3/MUC16 and OVCAR-3 cells in a 96-well format essentially as described previously[6]. Binding affinities of anti-MUC16 variants were determined by surface plasmon resonance and by enzyme-linked immunosorbent assays (ELISA) using conventional procedures (described in Supplementary Methods online).

In vivo efficacy.

Efficacy studies were performed using female C.B-17 severe combined immunodeficient (SCID) beige mice (Charles River Laboratories). All studies were conducted in accordance with the Guide for the Care and Use of Laboratory Animals. The OVCAR-3 mammary fat pad transplant efficacy model was employed as described previously[6], evaluating tumor volume after a single intravenous dose. The OVCAR-3/luciferase model has also been described previously[6].

Safety assessment.

The toxicities of anti-MUC16 ADC and TDC were compared in female adolescent Sprague-Dawley rats (100–125 g) receiving a single intravenous bolus dose (day 1). Body weight was measured daily. Analyses of serum chemistry and hematology (including quantification of separate lymphocytic populations) were conducted using sera collected on days 5 and 12. A thorough histopathological assessment followed euthanasia and necropsies on day 12.

The toxicities of anti-MUC16 ADC and TDC also were evaluated in two separate studies using female cynomolgus monkeys of Chinese origin (2.6–3.0 kg) receiving two bolus doses on days 1 and 22. Animals were dosed such that each animal in a given group received the same MMAE drug dose (in $\mu g/m^2$), allowing the antibody dose (in mg/kg) to vary slightly according to body weight. Each animal was observed twice daily for

DAC EX. 2040 IPR2022-01531 Page 1014 of 1299

mortality, abnormalities, and signs of pain or distress. Body weights were measured on unfasted animals twice during the predose phase, before dosing on day 1 and weekly thereafter. Analyses of clinical chemistry, hematology and coagulation were made with blood collected twice during the predose phase and on days 4, 8, 15, 22 (predose), 25, 32 and 43. Animals were euthanized on day 43 by anesthesia with sodium pentobarbital and exsanguination, and tissues were subjected to a thorough gross pathological and histopathological evaluation.

In vivo kinetic analyses.

The disposition of the anti-MUC16 antibody-drug conjugates *in vivo* was analyzed by measuring the serum concentrations of antibody and of drug conjugate. For kinetic analyses in rats (Figs. 5b–d), serum was collected at 5 min, 1 h, 6 h, 24 h, and 2, 3, 4, 8, 11, 15, 21 and 28 d after a single intravenous dose. For kinetic analyses in mice (Supplementary Fig. 15 online), serum was collected at 3 min, 1 h, 6 h, 24 h, and 2, 3, 4, 7, 11, 14 and 21 d after a single intravenous dose. Concentrations of antibody-drug conjugates bearing at least one cytotoxic drug were measured with an ELISA that used the MUC16 ECD protein for capture and anti-MMAE mouse monoclonal antibody SG2.15 (generously provided by Seattle Genetics) plus anti-mouse-Fc-horseradish peroxidase (HRP) for detection. We have observed a decreased signal in this assay for TDC with one versus two conjugated drugs. Therefore, the levels of conjugates may be greater than what we have measured. Total ch3A5 and ch3A5 THIOMAB concentrations in serum were measured with an ELISA that used the MUC16 ECD protein for capture and anti-human-Fc HRP as the secondary antibody. This assay measures any anti-MUC16 antibody, both with and without conjugated MMAE. The assays have lower limits of quantification of 0.78 ng/ml with a minimum dilution of 1:10. The serum concentration-time data from each animal was analyzed using a two-compartment model with IV bolus input, first-order elimination and macro-rate constants (Model 8, WinNonlin Pro v.5.0.1, Pharsight Corporation). Serum from the day 12 bleeds of the rat safety study were assayed using the same formats to generate the total and conjugated antibody data shown in Figure 5a.

DAC EX. 2040 IPR2022-01531 Page 1015 of 1299

Note: Supplementary information is available on the Nature Biotechnology website.

References

1 Adams, G.P. & Weiner, L.M. Monoclonal antibody therapy of cancer. *Nat. Biotechnol.* **23**, 1147–1157 (2005).

2 Baker, M. Upping the ante on antibodies. *Nat. Biotechnol.* **23**, 1065–1072 (2005).

3 Polakis, P. Arming antibodies for cancer therapy. *Curr. Opin. Pharmacol.* **5**, 382–387 (2005).

4 Wu, A.M. & Senter, P.D. Arming antibodies: prospects and challenges for immunoconjugates. *Nat. Biotechnol.* **23**, 1137–1146 (2005).

5 Lambert, J.M. Drug-conjugated monoclonal antibodies for the treatment of cancer. *Curr. Opin. Pharmacol.* **5**, 543–549 (2005).

6 Chen, Y. et al. Armed antibodies targeting the mucin repeats of the ovarian cancer antigen, MUC16, are highly efficacious in animal tumor models. *Cancer Res.* **67**, 4924–4932 (2007).

7 Doronina, S.O. et al. Development of potent monoclonal antibody auristatin conjugates for cancer therapy. *Nat. Biotechnol.* **21**, 778–784 (2003).

8 Hamblett, K.J. et al. Effects of drug loading on the antitumor activity of a monoclonal antibody drug conjugate. *Clin. Cancer Res.* **10**, 7063–7070 (2004).

DAC EX. 2040 IPR2022-01531 Page 1016 of 1299

9 Henry, M.D. et al. A prostate-specific membrane antigen-targeted monoclonal antibody-chemotherapeutic conjugate designed for the treatment of prostate cancer. *Cancer Res.* **64**, 7995–8001 (2004).

10 Kovtun, Y.V. et al. Antibody-drug conjugates designed to eradicate tumors with homogeneous and heterogeneous expression of the target antigen. *Cancer Res.* **66**, 3214–3221 (2006).

11 Liu, C. & Chari, R.V. The development of antibody delivery systems to target cancer with highly potent maytansinoids. *Expert Opin. Investig. Drugs* **6**, 169–172 (1997).

12 Ross, S. et al. Prostate stem cell antigen as therapy target: tissue expression and in vivo efficacy of an immunoconjugate. *Cancer Res.* **62**, 2546–2553 (2002).

13 Sanderson, R.J. et al. In vivo drug-linker stability of an anti-CD30 dipeptide-linked auristatin immunoconjugate. *Clin. Cancer Res.* **11**, 843–852 (2005).

14 Sun, M.M. et al. Reduction-alkylation strategies for the modification of specific monoclonal antibody disulfides. *Bioconjug. Chem.* **16**, 1282–1290 (2005).

15 Tassone, P. et al. In vitro and in vivo activity of the maytansinoid immunoconjugate huN901–N2′-deacetyl-N2′-(3-mercapto-1-oxopropyl)-maytansine against CD56+ multiple myeloma cells. *Cancer Res.* **64**, 4629–4636 (2004).

DAC EX. 2040 IPR2022-01531 Page 1017 of 1299

16 Tolcher, A.W. et al. Cantuzumab mertansine, a maytansinoid immunoconjugate directed to the CanAg antigen: a phase I, pharmacokinetic, and biologic correlative study. *J. Clin. Oncol.* **21**, 211–222 (2003).

17 Doronina, S.O. et al. Enhanced activity of monomethylauristatin F through monoclonal antibody delivery: effects of linker technology on efficacy and toxicity. *Bioconjug. Chem.* **17**, 114–124 (2006).

18 Ma, D. et al. Potent antitumor activity of an auristatin-conjugated, fully human monoclonal antibody to prostate-specific membrane antigen. *Clin. Cancer Res.* **12**, 2591–2596 (2006).

19 Tse, K.F. et al. CR011, a fully human monoclonal antibody-auristatin E conjugate, for the treatment of melanoma. *Clin. Cancer Res.* **12**, 1373–1382 (2006).

20 Wang, L., Amphlett, G., Blattler, W.A., Lambert, J.M. & Zhang, W. Structural characterization of the maytansinoid-monoclonal antibody immunoconjugate, huN901–DM1, by mass spectrometry. *Protein Sci.* **14**, 2436–2446 (2005).

21 Jefferis, R. Structure-function relationships of the IgG subclasses. in *The Human IgG Subclasses: Molecular Analysis of Structure, Function and Regulation* (ed. Shakib, F.) 93–108 (Pergamon Press, Oxford, 1990).

22 Junutula, J.R. et al. Rapid identification of reactive cysteine residues for site-specific labeling of antibody-Fabs. *J. Immunol. Methods* **332**, 41–52 (2008).

DAC EX. 2040 IPR2022-01531 Page 1018 of 1299

23 Dubowchik, G.M. et al. Cathepsin B-labile dipeptide linkers for lysosomal release of doxorubicin from internalizing immunoconjugates: model studies of enzymatic drug release and antigen-specific in vitro anticancer activity. *Bioconjug. Chem.* **13**, 855–869 (2002).

24 Francisco, J.A. et al. cAC10-vcMMAE, an anti-CD30-monomethyl auristatin E conjugate with potent and selective antitumor activity. *Blood* **102**, 1458–1465 (2003).

25 Mirsalis, J.C. et al. Toxicity of dolastatin 10 in mice, rats and dogs and its clinical relevance. *Cancer Chemother. Pharmacol.* **44**, 395–402 (1999).

26 McDonagh, C.F. et al. Engineered antibody-drug conjugates with defined sites and stoichiometries of drug attachment. *Protein Eng. Des. Sel.* **19**, 299–307 (2006).

27 Michaelsen, T.E. et al. One disulfide bond in front of the second heavy chain constant region is necessary and sufficient for effector functions of human IgG3 without a genetic hinge. *Proc. Natl. Acad. Sci. USA* **91**, 9243–9247 (1994).

28 Romans, D.G., Tilley, C.A., Crookston, M.C., Falk, R.E. & Dorrington, K.J. Conversion of incomplete antibodies to direct agglutinins by mild reduction: evidence for segmental flexibility within the Fc fragment of immunoglobulin G. *Proc. Natl. Acad. Sci. USA* **74**, 2531–2535 (1977).

DAC EX. 2040 IPR2022-01531 Page 1019 of 1299

29 Seegan, G.W., Smith, C.A. & Schumaker, V.N. Changes in quaternary structure of IgG upon reduction of the interheavy-chain disulfide bond. *Proc. Natl. Acad. Sci. USA* **76**, 907–911 (1979).

30 Lyons, A. et al. Site-specific attachment to recombinant antibodies via introduced surface cysteine residues. *Protein Eng.* **3**, 703–708 (1990).

31 Stimmel, J.B. et al. Site-specific conjugation on serine right-arrow cysteine variant monoclonal antibodies. *J. Biol. Chem.* **275**, 30445–30450 (2000).

32 Chapman, A.P. et al. Therapeutic antibody fragments with prolonged in vivo half-lives. *Nat. Biotechnol.* **17**, 780–783 (1999).

33 Xiang, T., Lundell, E., Sun, Z. & Liu, H. Structural effect of a recombinant monoclonal antibody on hinge region peptide bond hydrolysis. *J. Chromatogr. B Analyt. Technol. Biomed. Life Sci.* **858**, 254–262 (2007).

Acknowledgements

The authors wish to thank our Genentech colleagues: Jennifer Speer for preparing trastuzumab THIOMAB DNA constructs; Mary Cole for insights into the OVCAR-3 intraperitoneal efficacy model; Elmer Wu, Darshana Patel, Mark Rowen and Anthony Delucchi for providing critical reagents; Natalia Gomez and George Dutina for large-scale transient transfection/fermentation; Fred Jacobson and Charity Bechtel for their help with analytical characterization of TDCs; and Allen Ebens for critical review of the manuscript. We thank Damon Meyer and his colleagues at Seattle Genetics for preparation of the early lots of anti-MUC16 ADC and TDC and for many helpful comments and suggestions. We thank employees of NPIL Pharma UK for their assistance with large-scale conjugations. We also thank the staff of Oncotest for conducting some

DAC EX. 2040 IPR2022-01531 Page 1020 of 1299

of the efficacy studies described in this manuscript. Anti-MMAE mouse monoclonal antibody SG2.15 was generously provided by Seattle Genetics, Inc.

Author information

Kevin McDorman

Present address: Present address: Division of Pathology, Charles River Preclinical Services, Nevada, 6995 Longley Lane, Reno, Nevada 89511, USA.,

Authors and Affiliations

Genentech Inc., 1 DNA Way, South San Francisco, 94080, California, USA

Jagath R Junutula, Helga Raab, Suzanna Clark, Sunil Bhakta, Douglas D Leipold, Sylvia Weir, Yvonne Chen, Michelle Simpson, Siao Ping Tsai, Mark S Dennis, Yanmei Lu, Y Gloria Meng, Carl Ng, Jihong Yang, Chien C Lee, Eileen Duenas, Jeffrey Gorrell, Viswanatham Katta, Amy Kim, Kevin McDorman, Kelly Flagella, Rayna Venook, Sarajane Ross, Susan D Spencer, Wai Lee Wong, Henry B Lowman, Richard Vandlen, Mark X Sliwkowski, Richard H Scheller, Paul Polakis & William Mallet

Contributions

J.R.J. and W.M. led the overall program, designed experiments, performed *in vitro* studies, analyzed the data and wrote the manuscript. Y.C. and M.S.D. humanized the anti-MUC16 antibody. S.B. generated the anti-MUC16 THIOMAB DNA constructs and performed pilot expression studies. M.S., E.D. and J.G. performed larger-scale antibody production. H.R. established procedures for TDC conjugation and analytical characterization. C.C.L. carried out analytical characterization of TDCs. S.W., S.P.T., Y.L., Y.G.M., C.N. and J.Y. performed *in vitro* binding studies. S.C., R. Venook and S.R. performed *in vivo* efficacy studies. D.D.L. designed and analyzed pharmacokinetic studies. A.K., K.M. and K.F. designed and executed safety assessment studies. V.K., S.D.S., W.L.W., H.B.L., R. Vandlen, M.X.S., R.H.S. and P.P. provided direction and guidance for the various functional areas and assisted in writing the manuscript.

Corresponding authors

Correspondence to Jagath R Junutula or William Mallet.

DAC EX. 2040 IPR2022-01531 Page 1021 of 1299

Ethics declarations

Competing interests

All authors are full-time employees of Genentech. Inc.

Supplementary information

Supplementary Text and Figures

Supplementary Figures 1–17, Tables 1–5, Methods (PDF 3037 kb)

Rights and permissions

Reprints and permissions

About this article

Cite this article

Junutula, J., Raab, H., Clark, S. *et al.* Site-specific conjugation of a cytotoxic drug to an antibody improves the therapeutic index. *Nat Biotechnol* **26**, 925–932 (2008). https://doi.org/10.1038/nbt.1480

Received
17 April 2008

Accepted
19 June 2008

Published
20 July 2008

Issue Date
August 2008

DOI
https://doi.org/10.1038/nbt.1480

Share this article

Anyone you share the following link with will be able to read this content:

DAC EX. 2040 IPR2022-01531 Page 1022 of 1299

Get shareable link

Provided by the Springer Nature SharedIt content-sharing initiative

Nature Biotechnology (*Nat Biotechnol*) ISSN 1546-1696 (online) ISSN 1087-0156 (print)

DAC EX. 2040 IPR2022-01531 Page 1023 of 1299

Appendix JUNUTULA02

nature biotechnology

© 2008 Nature Publishing Group http://www.nature.com/naturebiotechnology

Site-specific conjugation of a cytotoxic drug to an antibody improves the therapeutic index

Jagath R Junutula[1], Helga Raab[1], Suzanna Clark[1], Sunil Bhakta[1], Douglas D Leipold[1], Sylvia Weir[1], Yvonne Chen[1], Michelle Simpson[1], Siao Ping Tsai[1], Mark S Dennis[1], Yanmei Lu[1], Y Gloria Meng[1], Carl Ng[1], Jihong Yang[1], Chien C Lee[1], Eileen Duenas[1], Jeffrey Gorrell[1], Viswanatham Katta[1], Amy Kim[1], Kevin McDorman[1,2], Kelly Flagella[1], Rayna Venook[1], Sarajane Ross[1], Susan D Spencer[1], Wai Lee Wong[1], Henry B Lowman[1], Richard Vandlen[1], Mark X Sliwkowski[1], Richard H Scheller[1], Paul Polakis[1] & William Mallet[1]

Antibody-drug conjugates enhance the antitumor effects of antibodies and reduce adverse systemic effects of potent cytotoxic drugs. However, conventional drug conjugation strategies yield heterogenous conjugates with relatively narrow therapeutic index (maximum tolerated dose/curative dose). Using leads from our previously described phage display–based method to predict suitable conjugation sites, we engineered cysteine substitutions at positions on light and heavy chains that provide reactive thiol groups and do not perturb immunoglobulin folding and assembly, or alter antigen binding. When conjugated to monomethyl auristatin E, an antibody against the ovarian cancer antigen MUC16 is as efficacious as a conventional conjugate in mouse xenograft models. Moreover, it is tolerated at higher doses in rats and cynomolgus monkeys than the same conjugate prepared by conventional approaches. The favorable *in vivo* properties of the near-homogenous composition of this conjugate suggest that our strategy offers a general approach to retaining the antitumor efficacy of antibody-drug conjugates, while minimizing their systemic toxicity.

Targeted therapy using monoclonal antibodies (mAbs) has revolutionized cancer treatment, with several mAbs recognizing antigens expressed on the surfaces of tumor cells already having demonstrated their clinical potential[1,2]. As antibodies against tumor-specific antigens often lack therapeutic activity, they alternatively can be covalently linked to cytotoxic drugs. In principle, selective delivery of cytotoxic agents should reduce the systemic toxicity associated with traditional small-molecule chemotherapeutics[3,4].

Antibodies have been conjugated to a variety of cytotoxic drugs, including small molecules that alkylate DNA (e.g., duocarmycin and calicheamicin), disrupt microtubules (e.g., maytansinoids and auristatins) or bind DNA (e.g., anthracyclins)[5]. These antibody-drug conjugates (ADC) have displayed potent and selective killing of target tumor cells *in vitro* and in mouse tumor xenograft studies. Humanized anti-CD33 conjugated to calicheamicin (gemtuzumab ozogamicin; Mylotarg) was approved by the US Food and Drug Administration in 2000 for the treatment of acute myeloid leukemia, and several ADCs are being actively pursued to combat diverse forms of cancer[6–19]. An adequate safety margin will be required to make ADCs a common therapeutic option for cancer.

Cytotoxic drugs are generally conjugated to antibodies either through lysine side-chain amines or through cysteine sulfhydryl groups activated by reducing interchain disulfide bonds. Both of these procedures yield heterogenous products, containing a mixture of species with different molar ratios of drug to antibody, linked at different sites, each with distinct *in vivo* pharmacokinetic, efficacy and safety profiles[8,20]. In a study that underscored the consequences of this heterogeneity, researchers purified ADC fractions with exactly two, four or eight drugs attached to each antibody and compared these fractions for *in vivo* efficacy, tolerability in mice and pharmacokinetics[8]. The most heavily conjugated species had the lowest maximum tolerated IgG dose and most rapid clearance but did not confer a proportional increase in efficacy. This suggests that it would be desirable to selectively generate only conjugates with a moderate drug stoichiometry, perhaps two drugs per antibody. However, the purification process used in that study is not practical on the scale required for clinical testing, as a large amount of ADC would yield a relatively small amount of the desired stoichiometric fraction. Additionally, this approach still yields antibodies with disrupted interchain disulfide bonds, potentially affecting antibody stability and/or distribution *in vivo*. Finally, even a purified ADC with a uniform stoichiometry would still carry drugs conjugated to multiple sites and therefore be a complex mixture of unique entities. Each species could potentially have a distinct set of properties, and consistent batch-to-batch production would be difficult to control.

To limit the potential liabilities associated with such conjugation methods, we have engineered reactive cysteine residues at specific sites in antibodies to allow drugs to be conjugated with defined stoichiometry without disruption of interchain disulfide bonds. The excellent yields of these antibodies, named THIOMABs, and their

[1]Genentech Inc., 1 DNA Way, South San Francisco, California 94080, USA. [2]Present address: Division of Pathology, Charles River Preclinical Services, Nevada, 6995 Longley Lane, Reno, Nevada 89511, USA. Correspondence should be addressed to W.M. (wmallet@gene.com) or J.R.J. (jagath@gene.com).

Received 17 April; accepted 19 June; published online 20 July 2008; doi:10.1038/nbt.1480

DAC EX. 2040 IPR2022-01531 Page 1025 of 1299

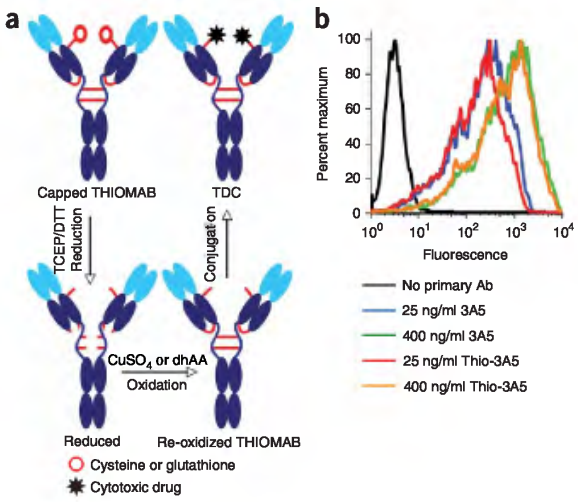


Figure 1 Characterization of THIOMABs. (**a**) Conjugation of cytotoxic drugs to engineered THIOMABs. Schematic representation of the reduction and oxidation process used to generate reactive THIOMABs and their conjugation to biotin or cytotoxic drugs. (**b**) The THIOMAB variant of anti-MUC16 3A5 retains high-affinity binding to cell-surface antigen. Humanized anti-MUC16 Thio-3A5 or conventional 3A5 antibody was incubated with OVCAR-3 cells expressing endogenous MUC16 and bound antibody detected using a fluorescent anti-human Fc secondary antibody. Flow cytometry histograms illustrate binding at saturating (400 ng/ml) and subsaturating (25 ng/ml) concentrations. At all antibody concentrations analyzed, the two anti-MUC16 variants gave equivalent binding, suggesting equivalent affinities for the antigen. Ab, antibody; TCEP, tris(2-carboxyethyl)phosphine; dhAA, dehydro-ascorbic acid; DTT, dithiothreitol; TDC, THIOMAB-drug conjugate.

derivatives conjugated with a drug of interest suggest the potential for scale-up to allow clinical evaluation. One such THIOMAB-drug conjugate (TDC) retains the *in vivo* efficacy of a conventional ADC and exhibits superior safety in preclinical models.

RESULTS

Engineering cysteine residues for site-specific conjugation

In seeking sites that might be substituted with cysteine residues, we focused on those not involved with antibody effector functions, such as the light and heavy chains of the constant domains of the antibody Fab region, which has no apparent role in antigen binding or in Fc-mediated effector functions[21]. We recently reported a phage display–based method (PHESELECTOR) to screen reactive cysteines on the Fab surface of the antibodies[22]. As applying this approach to the anti-Her2 antibody trastuzumab (Herceptin) suggested the suitability of the variants LC-V110C and HC-A114C (Kabat numbering) for site-specific labeling of Fabs[22], we selected these two sites to develop a conjugation process in the context of full-length antibodies. After expression in Chinese hamster ovary (CHO) cells, our initial attempts to conjugate THIOMABs in a single step with cysteine-reactive probes, *N*-ethyl maleimide or biotinyl-3-maleimido-propionamidyl-3,6-dioxaoctanediamine (biotin-PEO-maleimide) were unsuccessful. Liquid chromatography (LC)/mass spectroscopy (MS) analysis confirmed that the engineered cysteine residues were in mixed disulfides with cysteine or glutathione, presumably formed during the fermentation process (**Supplementary Fig. 1** online).

Figure 1a illustrates the conjugation scheme that was subsequently developed to covalently attach thiol-reactive probes to the engineered cysteines. First, the cysteine and glutathione adducts were removed from the THIOMABs by partial reduction followed by diafiltration. This partial reduction also disrupts interchain disulfide bonds but not intrachain disulfide bonds. The interchain disulfide bonds were allowed to reform by air oxidation or by accelerated oxidation using $CuSO_4$ or dehydro-ascorbic acid (dhAA), as demonstrated by non-reducing SDS-PAGE analysis (**Supplementary Fig. 2a** online) or by LC/MS analysis (**Supplementary Fig. 3** online). After this treatment, THIOMAB variants LC-V110C and HC-A114C (in the context of two different mAbs) were then conjugated with biotin-PEO-maleimide. Biotinylation of the appropriate antibody subunit was demonstrated by probing western blots with streptavidin-horseradish peroxidase (**Supplementary Fig. 2b** online). Whereas 100% biotin conjugation (two moles of biotin per mAb) was observed for the HC-A114C variant, only 25–50% was seen with the LC-V110C variant (**Supplementary Fig. 2b** online). Papain digestion and LC/MS analysis showed that during reoxidation, some of the LC-V110 cysteines had formed an unexpected disulfide bond between the two Fab portions of the antibody and thus were unavailable for drug conjugation (**Supplementary Fig. 4** online). The HC-A114C variant of various antibodies did not show this property and so was selected for further studies (**Supplementary Table 1** and **Supplementary Fig. 2c** online).

The efficient conjugation at HC-A114C but not at LC-V110C prompted us to seek further sites for cysteine engineering. We substituted most of the available serine, alanine and valine residues (24 variants) in the light chain domain of the trastuzumab-Fab. Thio-Fab phage were isolated, biotinylated and tested for binding to the Her2 extracellular domain (ECD) and streptavidin, as described earlier[22]. LC-V205C, LC-S114C, LC-V110C and LC-S127C showed the highest thiol reactivity values (0.8–1.0) (**Supplementary Fig. 5** online). The discrepancy between the results with the LC-V110C Fab versus the LC-V110C full-length antibody prompted us to evaluate the most promising sites in the context of the full-length

Table 1 Analytical characterization of anti-MUC16 drug conjugates

				Drug conjugate species distribution (%)						
Antibody-drug conjugate	Scale	DAR	Monomer (%)	0	1	2	3	4	6	8
ADC	1 mg–1 gm	3.10	98	12	3	42	3	32	7	1
ch3A5 TDC initial process	~50 mg	1.60	95	5	35	60	–	–	–	–
hu3A5 TDC initial process	~50 mg	1.60	98	6.4	29	64.5	–	–	–	–
hu3A5 TDC improved process	<10 g	1.97	>98	0.6	6.7	88.4	4.3	–	–	–
TDC improved process	>100 g	2.00	>98	0.3	3.3	92.1	4.3	–	–	–

Drug conjugate species distribution and drugs/antibody were quantified based on hydrophobic interaction chromatographic analysis as described in Methods. Percent of monomer was determined by size-exclusion chromatography.

© 2008 Nature Publishing Group http://www.nature.com/naturebiotechnology

DAC EX. 2040 IPR2022-01531 Page 1026 of 1299

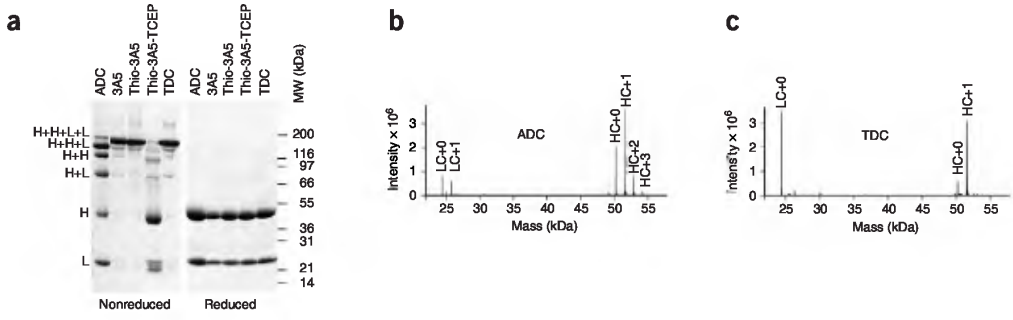


Figure 2 THIOMAB drug conjugates retain interchain disulfide bonds with site-specific drug attachment. (**a**) SDS-PAGE analysis of antibody-drug conjugates under nonreducing and reducing conditions. The appearance of multiple species in the standard ADCs is due to loss of interchain disulfide bonds. (**b**,**c**) Deconvoluted mass spectra of ADC (**b**) and TDC (**c**) variants of an antibody against MUC16. Drug conjugates are deglycosylated and reduced before LC/MS analysis. ADC mass spectra displayed zero or one drug species on the light chain and zero, one, two or three drug species on the heavy chain. TDC displayed only one drug species on the heavy chain. ADC, anti-MUC16-MC-vc-PAB-MMAE; TDC, thio-anti-MUC16-MC-vc-PAB-MMAE; THIOMAB-TCEP, THIOMAB reduced with tris(2-carboxyethyl)phosphine (TCEP); H, heavy chain; L, light chain.

© 2008 Nature Publishing Group http://www.nature.com/naturebiotechnology

antibody. Based on current and previous PHESELECTOR assay results[22], we have selected eight sites on the light chain (LC-V15C, LC-V110C, LC-S114C, LC-S121C, LC-S127C, LC-A153C, LC-S168C and LC-V205C) and four sites on the heavy chain (HC-S112C, HC-S113C, HC-S115C and HC-T116C). All of these THIOMABs were expressed and purified along with the HC-A114C variant and unmodified trastuzumab. The purified proteins were conjugated to biotin-maleimide, and the extent of conjugation was quantified by LC/MS analysis. As 9 of the 13 THIOMABs showed >90% conjugation efficiency, they should be as suitable for site-specific conjugation of thiol reactive probes as the HC-A114C variant described below (**Supplementary Table** 1 online). In this report, we focus on the properties of one THIOMAB (anti-MUC16) and its conjugates. Studies with multiple antibody-antigen combinations have established the general utility of this strategy (data not shown).

Anti-MUC16 THIOMAB retains antigen binding and specificity

The successful biotinylation of HC-A114C variants prompted us to test TDCs *in vitro* and *in vivo*. MUC16 is a cell-surface protein that is overexpressed in many ovarian malignancies. As we previously reported encouraging findings with conventional anti-MUC16 (monoclonal antibody 3A5) drug conjugates[6], which were efficacious at tolerated doses *in vivo*, we chose to focus on anti-MUC16 to evaluate the potential of the THIOMAB strategy for expanding the therapeutic index. Chimeric (ch3A5) and fully humanized (hu3A5) anti-MUC16 antibodies were engineered to have the HC-A114C mutation (Kabat numbering; equivalent to A118C in Eu numbering and A117C in sequential numbering). Generation of the chimeric immunoglobulin was described previously[6]. To produce a humanized anti-MUC16 antibody, the complementarity-determining regions (CDR) of mu3A5 were grafted into human consensus $V_{L\kappa I}$ and $V_{H_{subgroupIII}}$ frameworks (**Supplementary Methods** and **Supplementary Figs. 6a**,**b** online). Relative to chimeric 3A5, the binding affinity of the 3A5 CDR-graft for MUC16 was markedly reduced (**Supplementary Table 2** online). To restore binding, we introduced mutations into the CDR regions of the 3A5 graft to reconstitute appropriate CDR-framework interactions or to select more favorable CDR-antigen interactions. A library of CDR variants were displayed as Fab on phage and panned for improved interactions with the antigen. Enhanced binding was observed only in variants with substitutions in CDR-H3 (**Supplementary Fig. 6c** online). Four representative clones, reformatted and expressed as IgG and assessed for MUC16 binding relative to chimeric 3A5, demonstrated that changes in CDR-H3 fully restore antigen binding (**Supplementary Table 2** online). One clone was taken forward as humanized anti-MUC16.

To be useful for therapeutic development, the THIOMAB strategy must yield an antibody with comparable or higher binding affinity and specificity for the target antigen as compared with the conventional antibody. Affinities of humanized anti-MUC16 HC-A114C THIOMAB and conventional 3A5 IgG were compared by flow cytometry on OVCAR-3 cells (ovarian cancer cells that express endogenous MUC16), serially diluting the antibodies until a reduced shift was observed (**Fig. 1b**). Antibodies were in excess of cellular binding sites throughout the titration. At each concentration tested, thio-anti-MUC16 bound to OVCAR-3 cells as efficiently as conventional anti-MUC16. Surface plasmon resonance–based analyses using portions of the human MUC16 ECD also confirmed the high affinity of this THIOMAB for this antigen (K_D = 116 pM). Comparison of cells with high and low or absent MUC16 expression based on RT-PCR studies revealed that this THIOMAB binds to cells that express MUC16 but not to MUC16-negative cell lines (**Supplementary Fig. 7** online). Thus, substitution at HC-A114 does not affect antigen binding.

Anti-MUC16 THIOMAB yields nearly homogeneous conjugates

THIOMAB 3A5 antibodies were partially reduced and reoxidized to yield two free thiol groups per antibody, then conjugated to the cytotoxic drug monomethyl auristatin E (MMAE) via the protease-labile maleimido-caproyl-valine-citrulline-para-amino-benzyloxy carbonyl (MC-vc-PAB) linker (**Supplementary Fig. 8a** online)[23,24]. For simplicity, the conventional conjugate (anti-MUC16-MC-vc-PAB-MMAE) will subsequently be referred to as anti-MUC16 ADC and the THIOMAB conjugate (thio-anti-MUC16-MC-vc-PAB-MMAE) will be referred to as anti-MUC16 TDC. Anti-MUC16 ADC contained an average drug-antibody ratio (DAR) of 3.1 (**Table 1**) and migrated as multiple species on nonreducing SDS-PAGE, consistent with the loss of interchain disulfide bonds through drug conjugation (**Fig. 2a**). In contrast, the interchain disulfides were retained in anti-MUC16 TDC, which migrated as a single major band. Hydrophobic interaction chromatography was used to resolve antibodies with different stoichiometries of drug conjugation. Anti-MUC16 TDC was modified with zero, one or two drugs (average DAR = 1.6; **Table 1** and

DAC EX. 2040 IPR2022-01531 Page 1027 of 1299

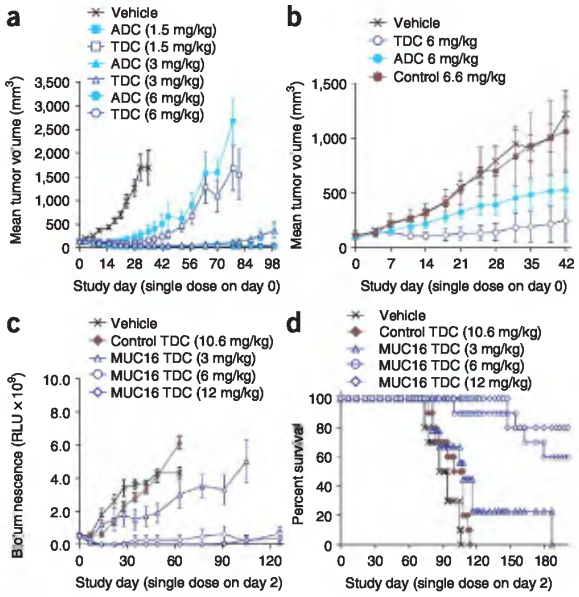


Figure 3 *In vivo* efficacy is retained with the TDC format. (**a**) Tumors derived from OVCAR-3 cells were serially transplanted into the mammary fat pads of female SCID mice, as previously reported[6], and anti-MUC16 ADC and TDC were compared. When palpable tumors were established, mice were randomized to a mean tumor volume of ~150 mm^3 in each group (ten/group; range = 100–200 mm^3) and then treated intravenously once (day 0) with chimeric anti-MUC16 ADC (3.1 drugs per antibody) or TDC (1.6 drugs per antibody) at the indicated doses. Mean tumor volumes (± s.e.m.) are plotted over time, with the ADC and TDC curves superimposed for the 3 mg/kg and 6 mg/kg groups. (**b**) Female nu/nu mice were inoculated with OVXF 1023 primary ovarian cancer tumors and anti-MUC16 ADC and TDC were compared. Chimeric anti-MUC16 ADC (3.1 drugs per antibody) or TDC (1.6 drugs per antibody) or a control ADC were dosed once as indicated. Mean tumor volumes (± s.e.m.) are plotted over time. (**c,d**) Female SCID mice were inoculated in the peritoneal cavity with OVCAR-3/luciferase cells, as previously reported[6]. Tumor burden was assessed by bioluminescence measurement after injection of luciferin. Once bioluminescence was stable (~3 weeks after inoculation), mice were grouped on the basis of luminescence and dosed once with humanized anti-MUC16 TDC (1.6 drugs per antibody) or an irrelevant TDC (1.9 drugs per antibody) as indicated. Changes in mean bioluminescence intensities (± s.e.m.) over time. Bioluminescence intensities plotted in terms of relative light units (RLU) (**c**). Changes in the percentages of surviving mice over time (**d**).

Supplementary Fig. 8b online). The absence of higher stoichiometric ratios indicates that only the engineered A114C cysteines were conjugated, as confirmed by LC/MS analysis and peptide mapping (**Supplementary Figs. 9** and **10** and **Supplementary Tables 3** and **4** online). In line with previous reports[8,14], standard 3A5 ADCs are a mixture of seven different drug stoichiometries (zero, one, two, three, four, six and eight drugs per antibody; **Table 1** and **Supplementary Fig. 8b** online) with the possibility of conjugating to any of eight cysteines, potentially generating >100 different ADC species. LC/MS analysis showed that the linker drug was distributed to both the light (one drug) and heavy chain (one, two or three drugs) of anti-MUC16 ADC but only to the heavy chain (one drug) of the cognate TDC (**Fig. 2b,c**). Finally, anti-MUC16 TDC retains high affinity for the human MUC16 ECD (K_D = 117 pM).

Along with reduced heterogeneity, the anti-MUC16 TDC preparation lacks species that have the higher drug loads reported to not be tolerated as well in rodents[8]. Subsequent process development has yielded conjugates with almost exactly two drugs per antibody. The species carrying the two drugs on the engineered cysteines and nowhere else is by far the predominant species in the preparation (**Table 1** and **Supplementary Fig. 8d** online).

Anti-MUC16 TDC displays comparable efficacy to ADC

We previously have reported that the conventional anti-MUC16 drug conjugates are highly efficacious in mouse OVCAR-3 xenograft models[6]. To determine if the thio-anti-MUC16 retains this property, the ADC and TDC variants of anti-MUC16 were subjected to *in vitro* cell proliferation and *in vivo* xenograft studies. *In vitro*, the ADC and TDC formats of chimeric anti-MUC16 had similar cytotoxicities, with median inhibitory concentration (IC_{50}) < 50 ng antibody/ml against OVCAR-3 cells and PC3 cells transfected with a recombinant form of MUC16 (**Supplementary Fig. 11** online). The IC_{50} values of the anti-MUC16 TDC were approximately twofold higher than those of the ADC, possibly due to the twofold lower drug load of the TDC. Parental PC3 cells lacking MUC16 expression were not affected by either conjugate up to 3 μg/ml, demonstrating the specificity of the antiproliferative effect. The rates of internalization into OVCAR-3 cells *in vitro* were comparable, as expected, given that neither method of drug conjugation detectably influences antigen binding (data not shown).

Anti-MUC16 ADC and anti-MUC16 TDC were also compared *in vivo* using chimeric antibody conjugates and an OVCAR-3 xenograft model (**Fig. 3a**). Mice bearing established tumors (~150 mm^3) were dosed once with either anti-MUC16 ADC or anti-MUC16 TDC over a range of dose levels. The anti-MUC16 TDC was at least as active as the ADC at each IgG dose level, providing partial efficacy at 1.5 mg/kg (MMAE doses are 35 μg/m^2 for the TDC and 71 μg/m^2 for the ADC) and near-complete elimination of tumors at 3 mg/kg (69 versus 141 μg/m^2 MMAE) and 6 mg/kg (139 versus 283 μg/m^2 MMAE). When stated in terms of MMAE dose, anti-MUC16 TDC was approximately twice as efficacious as anti-MUC16 ADC. No adverse effects of either conjugate were observed at any dose level. Anti-MUC16 TDC was also at least as active as anti-MUC16 ADC against a transplant xenograft model of ovarian cancer (**Fig. 3b**), and subsequent studies have demonstrated potent activity of the TDC against several tumor models (**Figs. 3c,d** and **Supplementary Figs. 12,13** online). The study using the intraperitoneal OVCAR-3/luciferase xenograft model (**Figs. 3c,d**) demonstrated single-dose activity of the anti-MUC16 TDC at 3 mg/kg against a tumor growing at a more relevant anatomic site, with improved activity at higher dose levels. Our previous studies using the ADC also achieved significant efficacy but with multiple weekly dosing[6].

Improved therapeutic index with anti-MUC16 TDCs

As noted above, the different conjugation procedures yielded anti-MUC16 ADC and TDC with different drug stoichiometries. Therefore, equivalent efficacy using the anti-MUC16 TDC is achieved with approximately one-half the dose of cytotoxic MMAE. Our preliminary studies have indicated that the toxicity of ADCs in animals is closely associated with the cytotoxic drug dose, and the adverse events are largely consistent with the safety profile of the drug itself. This suggests that the anti-MUC16 TDC may be better tolerated in animals than the ADC at equivalent mg/kg dose levels.

We evaluated the safety of the anti-MUC16 ADC and TDC in Sprague-Dawley rats and cynomolgus monkeys. Both species express

© 2008 Nature Publishing Group http://www.nature.com/naturebiotechnology

DAC EX. 2040 IPR2022-01531 Page 1028 of 1299

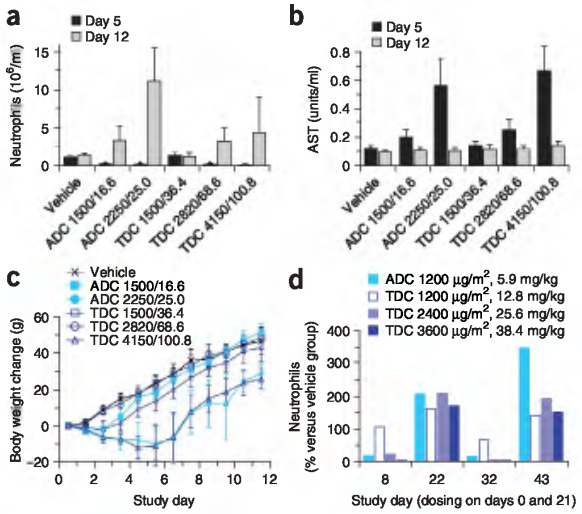


Figure 4 The TDC format is better tolerated *in vivo*. (**a**–**c**) Normal Sprague-Dawley rats were dosed once (day 1) with humanized anti-MUC16 ADC or TDC at the indicated dose levels. Dose levels are given in terms of μg/m^2 MMAE (the cytotoxic drug dose per body surface area, derived from the stoichiometry of conjugation) and mg/kg IgG; for example, "TDC 1500/36.4" indicates TDC dosed at 36.4 mg/kg IgG, which at 1.6 drugs per IgG corresponds to 1,500 μg/m^2 MMAE. Blood was drawn from rats at study day 5 (4 d after dosing) and day 12 (immediately before they were killed) for hematology (neutrophil counts in **a**) and serum chemistry (serum AST levels in **b**). *X*-axis labels for **b** apply also to **a** (treatment groups are graphed in the same order). (**c**) Rats were weighed daily after dosing and changes in body weight over time relative to day 1 plotted. (**d**) Higher doses of the TDC format are required to reduce neutrophil counts in cynomolgus monkeys. In two separate studies, female Chinese cynomolgus monkeys were dosed on days 1 and 22 with: humanized anti-MUC16 ADC (5.9 mg/kg IgG = 1,200 μg/m^2 MMAE; white bars); TDC at 12.8 mg/kg IgG (1,200 μg/m^2 MMAE; light gray bars); TDC at 25.6 mg/kg IgG (2,400 μg/m^2 MMAE; dark gray bars); or TDC at 38.4 mg/kg IgG (3,600 μg/m^2 MMAE; black bars). Blood was drawn for hematology and serum chemistry at the indicated intervals (day 22 values are from before the second dose). Average circulating neutrophil counts were normalized to the average counts from vehicle-treated monkeys at the given time point of the same study. Note the nadir in neutrophil levels ~1 week after dosing, followed by a recovery to normal levels within 3 weeks.

MUC16, although the primary sequence of the cynomolgus monkey antigen is more similar to the human counterpart than the rat antigen is. In a competitive binding assay, mAb 3A5 binding to CA125 was inhibited with similar concentrations of human and monkey MUC16 ECD proteins (IC_{50} = 0.76 nM and 1.88 nM, respectively), but competition by the rat MUC16 ECD was much less efficient (IC_{50} = 13.5 nM). Both rats and cynomolgus monkeys are sensitive to antibody-MMAE conjugates. As safety studies using a related cytotoxic compound, dolastatin-10, showed mice to be relatively insensitive to this class of drug, the mouse models used in the efficacy studies were not considered useful for safety assessment[25]. In rats, a single dose of 16.6 mg/kg anti-MUC16 ADC (1,500 μg/m^2 MMAE) produced a marked depletion of circulating neutrophils and other white blood cells at day 5 (4 d post-dose; **Fig. 4a** and data not shown), followed by a compensatory rebound at day 12. This anti-MUC16 ADC dose also led to a mild elevation in serum levels of the liver enzyme aspartate aminotransferase (AST; **Fig. 4b**) and transient weight loss (**Fig. 4c**). The AST levels were more profoundly affected by a 50% increase in dose (24.5 mg/kg ADC; 2,250 μg/m^2 MMAE); at that dose, three of six rats did not survive to the end of the study (day 12). In contrast, 36.4 mg/kg of anti-MUC16 TDC (equivalent to 1,500 μg/m^2 MMAE exposure) yielded no adverse effects, with all parameters essentially identical to vehicle-treated animals. A dose of 68.6 mg/kg anti-MUC16 TDC (2,820 μg/m^2 drug) produced toxicities that were nearly equivalent to those observed using the anti-MUC16 ADC at one-fourth that dose. Although the highest anti-MUC16 TDC dose (100.8 mg/kg; 4,150 μg/m^2 MMAE) led to pronounced effects (and two of six rats were killed due to excessive weight loss), the overall profile of adverse effects was quite similar to that observed at the higher anti-MUC16 ADC dose (24.5 mg/kg ADC; 2,250 μg/m^2 MMAE). The same trends were observed in a preliminary study using chimeric conjugates (**Supplementary Fig. 14** online).

The most prominent adverse event in cynomolgus monkeys dosed with anti-MUC16 ADC or TDC is a reversible decrease in neutrophils. Whereas a marked decrease was induced by anti-MUC16 ADC at a drug exposure of 1,200 μg/m^2 drug (5.9 mg/kg antibody), anti-MUC16 TDC at 1,200 μg/m^2 drug (12.8 mg/kg antibody) yielded no notable adverse events, with neutrophil counts tracking closely with sham-treated animals (**Fig. 4d**). Doubling the dose resulted in decreased neutrophil counts, which were completely reversible. An even higher dose of anti-MUC16 TDC (38.4 mg/kg; 3,600 μg/m^2

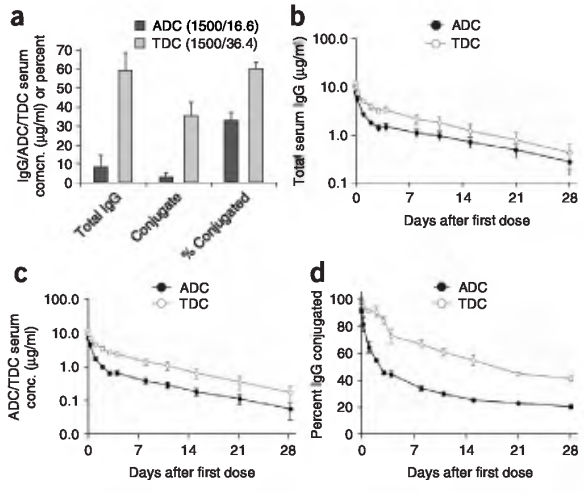


Figure 5 In rats, a higher proportion of TDC is retained in circulation, compared with its ADC counterpart. (**a**) Serum levels of total anti-MUC16 IgG ('Total antibody') and antibody carrying at least one cytotoxic drug (Conjugate) were measured at day 12 of the rat safety study described in **Figure 4a**–**c**. The percentage of antibody with at least one drug still attached (% Conjugated) was calculated from the ratio of Conjugate and Total IgG and is plotted next to the absolute values for ease of interpretation. Data for the 1,500 μg/m^2 MMAE groups are shown. (**b**–**d**) In a separate study, normal Sprague-Dawley rats were dosed once with 0.5 mg/kg chimeric ADC or TDC at study day 0. At the indicated intervals, blood was drawn for determination of total anti-MUC16 IgG (**b**) and anti-MUC16 carrying at least one MMAE (**c**). The fraction of drug-conjugated to total IgG was determined as the ratio of conjugated to total IgG and is plotted over time (**d**). Similar data were observed at higher dose levels.

© 2008 Nature Publishing Group http://www.nature.com/naturebiotechnology

DAC EX. 2040 IPR2022-01531 Page 1029 of 1299

drug) gave no marked effects beyond the neutrophil decrease, which was more pronounced than at the middle-dose level but remained reversible. Importantly, no toxicities were observed in cornea, lung, oviduct and uterus—all organs known to express MUC16. The only notable histopathologic findings were minimal-to-mild increases in bone marrow myelopoiesis and minimal-to-mild thymic lymphoid depletion, consistent with the decreases in neutrophil count and indicative of a regenerative response.

These results demonstrate that the anti-MUC16 TDC is safer than anti-MUC16 ADC in preclinical models, even when compared on the basis of cytotoxic drug dose (that is, equivalent $\mu g/m^2$). To begin to understand this, we have analyzed the kinetics of clearance of each type of conjugate in rats. At a dose of 36.4 mg/kg IgG (1,500 $\mu g/m^2$ MMAE), anti-MUC16 TDC remained in circulation at much higher levels than anti-MUC16 ADC dosed at 16.6 mg/kg IgG (1,500 $\mu g/m^2$ MMAE), even after accounting for the differences in dose levels (**Fig. 5a**). Nonetheless, anti-MUC16 TDC at that dose yielded no adverse effects. We observed the same results when dosing rats with chimeric ADC and TDC at a matched mg/kg dose (**Supplementary Fig. 14d** online). A more thorough kinetic analysis using chimeric antibodies (**Fig. 5b–d**) showed that the total TDC is cleared somewhat more slowly than the ADC (9.5 ± 2.9 versus 16.1 ± 3.5 ml/day/kg), and the proportion of TDC still bearing at least one drug decreased substantially more slowly than the corresponding proportion of ADC (14.1 ± 3.0 versus 41.6 ± 4.8 ml/day/kg). Interestingly, the ADC and TDC kinetics are comparable in tumor-bearing mice (**Supplementary Fig. 15** online). Slower clearance of the TDC variant has consistently been observed using different antibodies, suggesting that the kinetics of the anti-MUC16 conjugates in the mouse may be an anomaly. The drug conjugate assay generates a lower signal from a TDC with exactly one drug than from a TDC with two drugs. However, the discrepancy is minor and cannot explain the different behaviors of the ADC and TDC variants. Therefore, we conclude that despite bearing fewer drugs per antibody on average, the TDC variants retain the conjugated drugs more effectively in rats than their ADC counterparts.

DISCUSSION

The unfavorable *in vivo* effects associated with heterogeneity in the drug load and sites of attachment in antibody-drug conjugates could compromise their promise as cancer therapeutics. Conjugation through lysine residues was shown to distribute to ~40 different sites, potentially resulting in $>10^6$ ADC species[20]. Conjugates generated through cysteines by partial reduction of interchain-disulfide bonds also have variable stoichiometry (zero to eight drugs per antibody) and potentially yield >100 species[8]. Solvent-accessible interchain-disulfide bond cysteines have been replaced with serine to allow directed conjugation to the remaining cysteines[26]. However, elimination of these disulfide bonds could disrupt quaternary structure of the antibody, thereby perturbing the behavior of the antibody *in vivo*, including changes in antibody effector functions[27–29]. Our THIOMAB technology resolves the issue of conjugate heterogeneity by directing the attachment of drugs at defined sites and with near-uniform stoichiometry. Additionally, the conjugation chemistry retains all of the native immunoglobulin disulfide bonds. Cysteine engineering into antibodies for site-specific conjugation has been achieved previously but with poor yield and no potential for large-scale processing[30,31]. Notably, site-specific conjugation to antibody-Fabs has been reported using cysteine engineering[22,32]. However, the engineered cysteines were shown to be blocked by cysteinylation or glutathionylation in the context of full-length antibodies (**Supplementary Fig. 1** online). Our novel conjugation method reactivates the engineered cysteines for conjugation, thus achieving site-specific antibody-drug conjugates at high yield and purity. We have observed no challenges with this conjugation strategy even up to a multi-gram scale. Also, our methodology should be amenable to a wide range of cytotoxic drugs, requiring only that the drugs be compatible with sulfhydryl-directed conjugation chemistries.

These properties alone represent a substantial advancement for product development. In addition, we have found that the anti-MUC16 TDC exhibits a markedly improved therapeutic index in preclinical animal models. When comparing matched IgG (mg/kg) dose levels, our data show equivalent efficacy of the anti-MUC16 TDC and ADC in mouse xenografts, whereas in rats the 68.6 mg/kg (2,820 $\mu g/m^2$ MMAE) dose of the TDC exerts similar toxicities as the 16.6 mg/kg (1,500 $\mu g/m^2$ MMAE) dose of the ADC. When compared in terms of MMAE exposure, the TDC is both safer and more efficacious than the ADC. Although the success of the approach has yet to be tested in humans, even a modest increase in the range of safe and efficacious doses could dramatically enhance the clinical value of the conjugate. The efficacy and toxicity of an antibody-drug conjugate could be influenced substantially by a host immune response against the conjugate. In cynomolgus monkeys, we have observed little if any immune response against the anti-MUC16 TDC and only sporadic responses against the ADC. Improved safety without loss of efficacy has been observed for several different antibodies targeting multiple tumor antigens (our unpublished results), indicating that the THIOMAB technology is a general path to an expanded therapeutic window.

We do not yet know what accounts for the improved safety of the TDC in rats and primates. The *in vivo* kinetics of the total TDC in rats are quite comparable to those of native (nonconjugated) antibodies, whereas the total ADC clears somewhat faster. When considering the kinetics of conjugated antibodies, the difference between the TDC and the ADC is more pronounced, and over time a far greater proportion of circulating TDC retains at least one drug (**Fig. 5b–d**). This could point to a mechanism of clearance used by a fraction of the ADC but not the TDC and leading to ADC metabolism and toxicity. For example, the relatively more highly conjugated species within the ADC preparation may clear more rapidly, thereby enriching for the unconjugated antibody that is 12% of the original preparation (**Table 1**). Consistent with our findings, a correlation has been shown between total antibody clearance and toxicity in mice dosed with a DAR8 ADC[8]. Therefore, it is possible that the relative safety of the TDC can be attributed at least partly to the absence of high-drug-load species. Although the ADC preparations used in the present studies did not contain high levels of antibodies with greater than four drugs attached, rats may be more sensitive than mice to more moderate drug loading. The previous work[8] suggests that a similarly favorable profile of safety and activity might be observed with a hypothetical homogenous ADC preparation having a preponderance of a single species bearing two drugs conjugated at two sites only. ADC conjugation chemistry does not presently allow such a preparation at the scale necessary for preclinical evaluation, not to mention the scale required for clinical testing.

An alternative explanation for the pharmacokinetic data is that the MMAE may be more readily released from the ADC than from the TDC in circulation. Several mechanisms might lead to greater stability of the TDC. The engineered cysteines may be relatively 'protected' sites that resist proteolytic attack in circulation. We have observed that the accessibility of a cysteine residue varies depending where it is located in the antibody-Fab[22]. An ADC is produced by conjugating a drug at reduced hinge disulfides, one of the most accessible regions

© 2008 Nature Publishing Group http://www.nature.com/naturebiotechnology

DAC EX. 2040 IPR2022-01531 Page 1030 of 1299

of the antibody[33]. Therefore, the ADC may be more readily processed than the TDC and release more active MMAE in circulation, thus increasing ADC toxicity in rats. Also, although the TDC and the ADC variants have equivalent affinity for FcRn (**Supplementary Figs. 16,17** and **Supplementary Table 5** online), it is possible that the ADC is less stable while traversing the FcRn-mediated intracellular recycling pathway.

Either mechanism (differences in antibody clearance or rate of MMAE release) could affect safety. Indeed, relatively higher levels of ADC-derived free MMAE in circulation could readily account for the adverse effects that we have observed in our preclinical safety studies. Specifically, the myelotoxicity manifested by marked neutrophil decline was also the dose-limiting toxicity in animals treated with dolastatin-10, the parent molecule of MMAE. Also, elevated serum AST results from dosing rats with dolastatin-10, ADC and TDC. The rapid clearance of highly conjugated ADC could also directly lead to toxicity within the organ of clearance and systemic release of MMAE. At present, we cannot distinguish between these two mechanisms, and both may operate.

Our preclinical safety data suggest that MMAE exposure will determine the tolerability of the anti-MUC16 TDC in the clinic. If so, one clear benefit to the TDC over the ADC would be to reduce the MMAE exposure at an efficacious dose of conjugate. In turn, the improved tolerability of the TDC could permit higher dose levels on a mg/kg antibody basis. This could be critical to producing a therapeutic benefit for patients with more challenging malignancies, such as reduced sensitivity to MMAE or relatively lower levels of MUC16 expression. Overall, the TDC conjugation strategy confers improved *in vivo* properties and may represent a decisive advancement in the development of therapeutic antibody-drug conjugates.

METHODS

Site directed mutagenesis, THIOMAB expression and purification. Cysteine mutations were introduced in antibody light or heavy chain constructs (in pRK expression vectors) using double-stranded DNA as a template by PCR-based site-directed mutagenesis as described earlier[22]. THIOMAB light and heavy chain constructs were transiently transfected into CHO cells, and the antibodies were purified over Protein A columns followed by ion exchange chromatography.

Conjugation. THIOMAB conjugation was performed at Genentech, Seattle Genetics or NPIL Pharma UK using methods developed at Genentech. Before conjugation of the THIOMAB to biotin or MMAE derivatized with a maleimide-containing linker, the blocking cysteine or glutathione that was present on the introduced cysteine was removed by mild reduction in PBS at 25 °C by the addition of tenfold molar excess reducing agent, TCEP or dithiothreitol (DTT) followed by diafiltration. To re-form the interchain disulfide bonds, the THIOMAB was incubated for three hours at 25 °C with $CuSO_4$ or with dhAA (Sigma-Aldrich) at a twofold molar excess over the reducing agent concentration. The formation of interchain disulfide bonds was monitored either by nonreducing SDS-PAGE or by denaturing reversed phase high-performance liquid chromatography (HPLC) PLRP column chromatography. The maleimide-linked labeling reagent, either biotin-PEO-maleimide (tenfold molar excess over protein) or MC-vc-PAB-MMAE (threefold molar excess over protein), was incubated with the activated THIOMAB for 1 h at 25 °C. The antibody conjugate was purified on HiTrap S column (GE Healthcare Bio-Sciences) to remove excess reagents. The number of conjugated biotin or MC-vc-PAB-MMAE molecules per mAb was quantified by LC/MS analysis. Initial biotin conjugation experiments were carried out with $CuSO_4$; all the cytotoxic drug conjugation experiments described in this paper were carried out with dhAA.

Mass spectrometric analysis. LC/MS analysis was performed on a TSQ Quantum Triple quadrupole mass spectrometer with extended mass range (Thermo Electron). Samples were chromatographed on a PRLP-S, 1000 A, microbore column (50 mm × 2.1 mm, Polymer Laboratories) heated to 75 °C. A linear gradient from 30–40% B (solvent A, 0.05% TFA in water; solvent B, 0.04% TFA in acetonitrile) was used and the eluant was directly ionized using the electrospray source. Data were collected by the Xcalibur data system and deconvolution was performed using ProMass (Novatia). Before LC/MS analysis, antibodies or drug conjugates (50 μg) were treated with PNGase F (2 units/ml; PROzyme) for 2 h at 37 °C to remove N-linked carbohydrates.

Hydrophobic interaction chromatography (HIC). Samples were injected onto a Butyl HIC NPR column (2.5 μm, 4.6 mm × 3.5 cm) (Tosoh Bioscience) and eluted with a linear gradient from 0 to 70% B at 0.8 ml/min (A, 1.5 M ammonium sulfate in 50 mM potassium phosphate, pH 7; B, 50 mM potassium phosphate pH 7, 20% isopropanol). An Agilent 1100 series HPLC system equipped with a multi-wavelength detector and Chemstation software was used to resolve and quantify antibody species with different ratios of drugs per antibody.

Flow cytometry and *in vitro* studies. OVCAR-3 cells (30,000 cells per sample) were incubated on ice with humanized conventional or thio anti-MUC16 mAb for 75 min in 1 ml total volume. Antibodies were applied at 25, 50, 100, 200 and 400 ng/ml in PBS + 1% FBS + 2 mM EDTA. After this incubation, cells were washed and then incubated with phycoerythrin-labeled goat anti-human Fc secondary antibody (1 h on ice). Cells were then washed and analyzed by flow cytometry as described previously[6]. Based on our published data, 3×10^4 OVCAR-3 cells express $\sim 1 \times 10^{10}$ binding sites for anti-MUC16 antibody 3A5. Even the lowest antibody concentration tested (25 ng or $\sim 1 \times 10^{11}$ antibodies) provides a molar excess of antibodies over binding sites. Therefore, the concentration at which binding is reduced (as detected by flow cytometry) will reflect the affinity of the antibody for MUC16.

Cell proliferation in the presence of antibody-drug conjugates was assessed in PC3/neo (MUC16-negative), PC3/MUC16 and OVCAR-3 cells in a 96-well format essentially as described previously[6]. Binding affinities of anti-MUC16 variants were determined by surface plasmon resonance and by enzyme-linked immunosorbent assays (ELISA) using conventional procedures (described in **Supplementary Methods** online).

***In vivo* efficacy.** Efficacy studies were performed using female C.B-17 severe combined immunodeficient (SCID) beige mice (Charles River Laboratories). All studies were conducted in accordance with the Guide for the Care and Use of Laboratory Animals. The OVCAR-3 mammary fat pad transplant efficacy model was employed as described previously[6], evaluating tumor volume after a single intravenous dose. The OVCAR-3/luciferase model has also been described previously[6].

Safety assessment. The toxicities of anti-MUC16 ADC and TDC were compared in female adolescent Sprague-Dawley rats (100–125 g) receiving a single intravenous bolus dose (day 1). Body weight was measured daily. Analyses of serum chemistry and hematology (including quantification of separate lymphocytic populations) were conducted using sera collected on days 5 and 12. A thorough histopathological assessment followed euthanasia and necropsies on day 12.

The toxicities of anti-MUC16 ADC and TDC also were evaluated in two separate studies using female cynomolgus monkeys of Chinese origin (2.6–3.0 kg) receiving two bolus doses on days 1 and 22. Animals were dosed such that each animal in a given group received the same MMAE drug dose (in $\mu g/m^2$), allowing the antibody dose (in mg/kg) to vary slightly according to body weight. Each animal was observed twice daily for mortality, abnormalities, and signs of pain or distress. Body weights were measured on unfasted animals twice during the predose phase, before dosing on day 1 and weekly thereafter. Analyses of clinical chemistry, hematology and coagulation were made with blood collected twice during the predose phase and on days 4, 8, 15, 22 (predose), 25, 32 and 43. Animals were euthanized on day 43 by anesthesia with sodium pentobarbital and exsanguination, and tissues were subjected to a thorough gross pathological and histopathological evaluation.

***In vivo* kinetic analyses.** The disposition of the anti-MUC16 antibody-drug conjugates *in vivo* was analyzed by measuring the serum concentrations of

© 2008 Nature Publishing Group http://www.nature.com/naturebiotechnology

DAC EX. 2040 IPR2022-01531 Page 1031 of 1299

antibody and of drug conjugate. For kinetic analyses in rats (**Figs. 5b–d**), serum was collected at 5 min, 1 h, 6 h, 24 h, and 2, 3, 4, 8, 11, 15, 21 and 28 d after a single intravenous dose. For kinetic analyses in mice (**Supplementary Fig. 15** online), serum was collected at 3 min, 1 h, 6 h, 24 h, and 2, 3, 4, 7, 11, 14 and 21 d after a single intravenous dose. Concentrations of antibody-drug conjugates bearing at least one cytotoxic drug were measured with an ELISA that used the MUC16 ECD protein for capture and anti-MMAE mouse monoclonal antibody SG2.15 (generously provided by Seattle Genetics) plus anti-mouse-Fc-horseradish peroxidase (HRP) for detection. We have observed a decreased signal in this assay for TDC with one versus two conjugated drugs. Therefore, the levels of conjugates may be greater than what we have measured. Total ch3A5 and ch3A5 THIOMAB concentrations in serum were measured with an ELISA that used the MUC16 ECD protein for capture and anti-human-Fc HRP as the secondary antibody. This assay measures any anti-MUC16 antibody, both with and without conjugated MMAE. The assays have lower limits of quantification of 0.78 ng/ml with a minimum dilution of 1:10. The serum concentration-time data from each animal was analyzed using a two-compartment model with IV bolus input, first-order elimination and macro-rate constants (Model 8, WinNonlin Pro v.5.0.1, Pharsight Corporation). Serum from the day 12 bleeds of the rat safety study were assayed using the same formats to generate the total and conjugated antibody data shown in **Figure 5a.**

Note: Supplementary information is available on the Nature Biotechnology website.

ACKNOWLEDGMENTS

The authors wish to thank our Genentech colleagues: Jennifer Speer for preparing trastuzumab THIOMAB DNA constructs; Mary Cole for insights into the OVCAR-3 intraperitoneal efficacy model; Elmer Wu, Darshana Patel, Mark Rowen and Anthony Delucchi for providing critical reagents; Natalia Gomez and George Dutina for large-scale transient transfection/fermentation; Fred Jacobson and Charity Bechtel for their help with analytical characterization of TDCs; and Allen Ebens for critical review of the manuscript. We thank Damon Meyer and his colleagues at Seattle Genetics for preparation of the early lots of anti-MUC16 ADC and TDC and for many helpful comments and suggestions. We thank employees of NPIL Pharma UK for their assistance with large-scale conjugations. We also thank the staff of Oncotest for conducting some of the efficacy studies described in this manuscript. Anti-MMAE mouse monoclonal antibody SG2.15 was generously provided by Seattle Genetics, Inc.

AUTHOR CONTRIBUTIONS

J.R.J. and W.M. led the overall program, designed experiments, performed *in vitro* studies, analyzed the data and wrote the manuscript. Y.C. and M.S.D. humanized the anti-MUC16 antibody. S.B. generated the anti-MUC16 THIOMAB DNA constructs and performed pilot expression studies. M.S., E.D. and J.G. performed larger-scale antibody production. H.R. established procedures for TDC conjugation and analytical characterization. C.C.L. carried out analytical characterization of TDCs. S.W., S.P.T., Y.L., Y.G.M., C.N. and J.Y. performed *in vitro* binding studies. S.C., R. Venook and S.R. performed *in vivo* efficacy studies. D.D.L. designed and analyzed pharmacokinetic studies. A.K., K.M. and K.F. designed and executed safety assessment studies. V.K., S.D.S., W.L.W., H.B.L., R. Vandlen, M.X.S., R.H.S. and P.P. provided direction and guidance for the various functional areas and assisted in writing the manuscript.

COMPETING INTERESTS STATEMENT

The authors declare competing financial interests: details accompany the full-text HTML version of the paper at http://www.nature.com/naturebiotechnology/

Published online at http://www.nature.com/naturebiotechnology/
Reprints and permissions information is available online at http://npg.nature.com/reprintsandpermissions/

1. Adams, G.P. & Weiner, L.M. Monoclonal antibody therapy of cancer. *Nat. Biotechnol.* **23**, 1147–1157 (2005).
2. Baker, M. Upping the ante on antibodies. *Nat. Biotechnol.* **23**, 1065–1072 (2005).
3. Polakis, P. Arming antibodies for cancer therapy. *Curr. Opin. Pharmacol.* **5**, 382–387 (2005).
4. Wu, A.M. & Senter, P.D. Arming antibodies: prospects and challenges for immunoconjugates. *Nat. Biotechnol.* **23**, 1137–1146 (2005).
5. Lambert, J.M. Drug-conjugated monoclonal antibodies for the treatment of cancer. *Curr. Opin. Pharmacol.* **5**, 543–549 (2005).
6. Chen, Y. *et al.* Armed antibodies targeting the mucin repeats of the ovarian cancer antigen, MUC16, are highly efficacious in animal tumor models. *Cancer Res.* **67**, 4924–4932 (2007).
7. Doronina, S.O. *et al.* Development of potent monoclonal antibody auristatin conjugates for cancer therapy. *Nat. Biotechnol.* **21**, 778–784 (2003).
8. Hamblett, K.J. *et al.* Effects of drug loading on the antitumor activity of a monoclonal antibody drug conjugate. *Clin. Cancer Res.* **10**, 7063–7070 (2004).
9. Henry, M.D. *et al.* A prostate-specific membrane antigen-targeted monoclonal antibody-chemotherapeutic conjugate designed for the treatment of prostate cancer. *Cancer Res.* **64**, 7995–8001 (2004).
10. Kovtun, Y.V. *et al.* Antibody-drug conjugates designed to eradicate tumors with homogeneous and heterogeneous expression of the target antigen. *Cancer Res.* **66**, 3214–3221 (2006).
11. Liu, C. & Chari, R.V. The development of antibody delivery systems to target cancer with highly potent maytansinoids. *Expert Opin. Investig. Drugs* **6**, 169–172 (1997).
12. Ross, S. *et al.* Prostate stem cell antigen as therapy target: tissue expression and in vivo efficacy of an immunoconjugate. *Cancer Res.* **62**, 2546–2553 (2002).
13. Sanderson, R.J. *et al.* In vivo drug-linker stability of an anti-CD30 dipeptide-linked auristatin immunoconjugate. *Clin. Cancer Res.* **11**, 843–852 (2005).
14. Sun, M.M. *et al.* Reduction-alkylation strategies for the modification of specific monoclonal antibody disulfides. *Bioconjug. Chem.* **16**, 1282–1290 (2005).
15. Tassone, P. *et al.* In vitro and in vivo activity of the maytansinoid immunoconjugate huN901–N2′-deacetyl-N2′-(3-mercapto-1-oxopropyl)-maytansine against CD56+ multiple myeloma cells. *Cancer Res.* **64**, 4629–4636 (2004).
16. Tolcher, A.W. *et al.* Cantuzumab mertansine, a maytansinoid immunoconjugate directed to the CanAg antigen: a phase I, pharmacokinetic, and biologic correlative study. *J. Clin. Oncol.* **21**, 211–222 (2003).
17. Doronina, S.O. *et al.* Enhanced activity of monomethylauristatin F through monoclonal antibody delivery: effects of linker technology on efficacy and toxicity. *Bioconjug. Chem.* **17**, 114–124 (2006).
18. Ma, D. *et al.* Potent antitumor activity of an auristatin-conjugated, fully human monoclonal antibody to prostate-specific membrane antigen. *Clin. Cancer Res.* **12**, 2591–2596 (2006).
19. Tse, K.F. *et al.* CR011, a fully human monoclonal antibody-auristatin E conjugate, for the treatment of melanoma. *Clin. Cancer Res.* **12**, 1373–1382 (2006).
20. Wang, L., Amphlett, G., Blattler, W.A., Lambert, J.M. & Zhang, W. Structural characterization of the maytansinoid-monoclonal antibody immunoconjugate, huN901–DM1, by mass spectrometry. *Protein Sci.* **14**, 2436–2446 (2005).
21. Jefferis, R. Structure-function relationships of the IgG subclasses. in *The Human IgG Subclasses: Molecular Analysis of Structure, Function and Regulation* (ed. Shakib, F.) 93–108 (Pergamon Press, Oxford, 1990).
22. Junutula, J.R. *et al.* Rapid identification of reactive cysteine residues for site-specific labeling of antibody-Fabs. *J. Immunol. Methods* **332**, 41–52 (2008).
23. Dubowchik, G.M. *et al.* Cathepsin B-labile dipeptide linkers for lysosomal release of doxorubicin from internalizing immunoconjugates: model studies of enzymatic drug release and antigen-specific in vitro anticancer activity. *Bioconjug. Chem.* **13**, 855–869 (2002).
24. Francisco, J.A. *et al.* cAC10-vcMMAE, an anti-CD30-monomethyl auristatin E conjugate with potent and selective antitumor activity. *Blood* **102**, 1458–1465 (2003).
25. Mirsalis, J.C. *et al.* Toxicity of dolastatin 10 in mice, rats and dogs and its clinical relevance. *Cancer Chemother. Pharmacol.* **44**, 395–402 (1999).
26. McDonagh, C.F. *et al.* Engineered antibody-drug conjugates with defined sites and stoichiometries of drug attachment. *Protein Eng. Des. Sel.* **19**, 299–307 (2006).
27. Michaelsen, T.E. *et al.* One disulfide bond in front of the second heavy chain constant region is necessary and sufficient for effector functions of human IgG3 without a genetic hinge. *Proc. Natl. Acad. Sci. USA* **91**, 9243–9247 (1994).
28. Romans, D.G., Tilley, C.A., Crookston, M.C., Falk, R.E. & Dorrington, K.J. Conversion of incomplete antibodies to direct agglutinins by mild reduction: evidence for segmental flexibility within the Fc fragment of immunoglobulin G. *Proc. Natl. Acad. Sci. USA* **74**, 2531–2535 (1977).
29. Seegan, G.W., Smith, C.A. & Schumaker, V.N. Changes in quaternary structure of IgG upon reduction of the interheavy-chain disulfide bond. *Proc. Natl. Acad. Sci. USA* **76**, 907–911 (1979).
30. Lyons, A. *et al.* Site-specific attachment to recombinant antibodies via introduced surface cysteine residues. *Protein Eng.* **3**, 703–708 (1990).
31. Stimmel, J.B. *et al.* Site-specific conjugation on serine right-arrow cysteine variant monoclonal antibodies. *J. Biol. Chem.* **275**, 30445–30450 (2000).
32. Chapman, A.P. *et al.* Therapeutic antibody fragments with prolonged in vivo half-lives. *Nat. Biotechnol.* **17**, 780–783 (1999).
33. Xiang, T., Lundell, E., Sun, Z. & Liu, H. Structural effect of a recombinant monoclonal antibody on hinge region peptide bond hydrolysis. *J. Chromatogr. B Analyt. Technol. Biomed. Life Sci.* **858**, 254–262 (2007).

© 2008 Nature Publishing Group http://www.nature.com/naturebiotechnology

DAC EX. 2040 IPR2022-01531 Page 1032 of 1299

Appendix CASI01

PennState University Libraries | Catalog

Bookmarks 0 Course Reserves My Account

Keyword Search... Search Advanced search Start Over

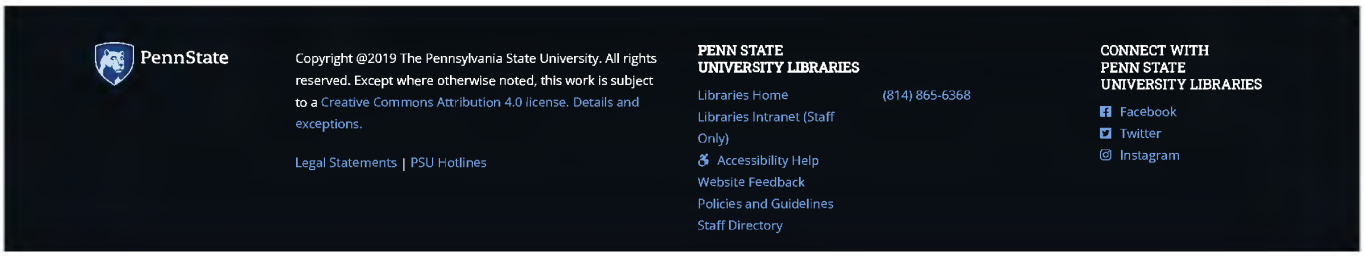
Share Bookmark Report an Issue

MARC View

LEADER 03049nas a2200661 a 4500				
001 46006139				
003 SIRSI				
005 20241114090046.0				
006 m o d				
007 cr n				
008 980410c19849999ne sn pss 0 a0eng c				
010				a| 2003233270
016	7			a| 012433775 2| Uk
016				a| 012433775
019				a| DO NOT EDIT this 360 MARC RECORD
022				a| 1873-4995 l| 0168-3659 y| 0168-3659
035				a| (WaSeSS)ssj0005347
040				a| OH1 b| eng c| OH1 d| OCL d| OCLCQ d| GUA d| OCLCQ d| EEM d| CLU d| U9S d| OCLCQ d| UKMGB d| OCLCQ d| OCLCF d| OCLCQ d| DEFHM d| OCLCO d| OCLCA d| BUF d| EZC d| OCLCO d| U3W d| OCLCA d| AU@ d| OCLCO d| WYU d| OCLCO d| TKN d| VT2 d| OCLCO d| OCLCA d| OCLCO d| QGK d| OCLCO d| OCL d| OCLCQ d| UAB d| WaSeSS
042				a| pcc
050	1	4		a| RS201.C64
130	0			a| Journal of controlled release (Online)
222			0	a| Journal of controlled release b| (Online)
245	1		0	a| Journal of controlled release h| [electronic resource].
246	1	3		a| CR f| <12 Nov. 2008->
260				a| Amsterdam ; a| New York : b| Elsevier
310				a| Twenty-four no. a year, b| <2001->
321				a| Fifteen no. a year, b| <1995->
362	1			a| Began with vol. 1, no. 1 (Sept. 1984).
500				a| Some issues also have distinctive titles.
515				a| Some nos. issued in combined form.
521	8			a| "Investigators involved in pharmacy, biomaterials, chemistry, polymer chemistry, several specializations in medicine, agricultural sciences, pharmacutics, chemical technology, and mechanical engineering."
530				a| Also issued in print.
538				a| Mode of access: World Wide Web.
550				a| Official journal of the Controlled Release Society, and of the Japanese Society of Drug Delivery Systems.
588				a| Description based on: Vol. 33, issue 1 (Jan. 1995); title from title screen (ScienceDirect, viewed Oct. 20, 2003).
588				a| Latest issue consulted: Vol. 133, issue 2 (19 Jan. 2009) (viewed Jan. 19, 2009).
650			0	a| Drugs x| Dosage forms v| Periodicals.
650			0	a| Drugs x| Controlled release v| Periodicals.
650			0	a| Controlled release preparations v| Periodicals.
650			0	a| Drugs x| Dosage forms.
650			0	a| Drugs.
650			2	a| Delayed-Action Preparations v| periodicals.
650			2	a| Dosage Forms v| periodicals.
650			2	a| Drugs v| periodicals.
650			2	a| Delayed-Action Preparations v| Periodicals.
650			2	a| Dosage Forms v| Periodicals.
650			2	a| Pharmaceutical Preparations v| Periodicals.
650			2	a| Delayed-Action Preparations
650			2	a| Dosage Forms
650			2	a| Pharmaceutical Preparations
655			0	a| Electronic journals.
655			2	a| Periodical
710	2			a| Controlled Release Society.
710	2			a| Nihon DDS Gakkai.
776	0	8		i| Print version: t| Journal of controlled release x| 0168-3659 w| (DLC)sn 85024003 w| (OCoLC)11301964
856	4		0	u| http://SK8ES4MC2L.search.serialssolutions.com/?V=1.0&L=SK8ES4MC2L&S=JCs&C=JOURNOFCONTREL&T=marc

ASK A LIBRARIAN

910	a| CONSER online
949	a| Electronic resource w| ASIS c| 1 i| 46006139-1001 l| ONLINE m| ONLINE r| Y s| Y t| ONLINE u| 11/16/2024 o| .STAFF. 360 MARC



PennState University Libraries | Catalog

Bookmarks 0 Course Reserves My Account

Keyword Search... Search Advanced search Start Over

Share Bookmark Report an Issue

Journal of controlled release [electronic resource].

Uniform Title	Journal of controlled release (Online)
Additional Titles	CR <12 Nov. 2008->
Published	Amsterdam ; New York : Elsevier
Additional Creators	Controlled Release Society and Nihon DDS Gakkai

Access Online
serialssolutions.com

ASK A LIBRARIAN

Dates of Publication and/or Sequential Designation
Began with vol. 1, no. 1 (Sept. 1984).

Subject(s)
Drugs—Dosage forms—Periodicals
Drugs—Controlled release—Periodicals
Controlled release preparations—Periodicals
Drugs—Dosage forms
Drugs
Delayed-Action Preparations—periodicals
Dosage Forms—periodicals
Drugs—periodicals
Delayed-Action Preparations—Periodicals
Dosage Forms—Periodicals
Pharmaceutical Preparations—Periodicals
Delayed-Action Preparations
Dosage Forms
Pharmaceutical Preparations

Genre(s)
Electronic journals

ISSN
1873-4995

Publication Frequency
Twenty-four no. a year, <2001->
Fifteen no. a year, <1995->

Audience Notes
"Investigators involved in pharmacy, biomaterials, chemistry, polymer chemistry, several specializations in medicine, agricultural sciences, pharmacutics, chemical technology, and mechanical engineering."

Note
Some issues also have distinctive titles.

Special Numbering
Some nos. issued in combined form.

Other Forms
Also issued in print.

Technical Details
Mode of access: World Wide Web.

Issuing Body
Official journal of the Controlled Release Society, and of the Japanese Society of Drug Delivery Systems.

View MARC record | catkey: 46006139

PennState

Copyright ©2019 The Pennsylvania State University. All rights reserved. Except where otherwise noted, this work is subject to a Creative Commons Attribution 4.0 license. Details and exceptions.

Legal Statements | PSU Hotlines

PENN STATE UNIVERSITY LIBRARIES

Libraries Home (814) 865-6368
Libraries Intranet (Staff Only)
Accessibility Help
Website Feedback
Policies and Guidelines
Staff Directory

CONNECT WITH PENN STATE UNIVERSITY LIBRARIES

Facebook
Twitter
Instagram

All Journals Only Books Only Videos Only

Title begins with Search

Show more search options ▼

Showing results 1 through 1 of 1

for the search: "JOURNOFCONTREL"

Refine Results: All | Journals Only | Books Only | Videos Only

Limit by: Peer Reviewed | Open Access



Journal of controlled release

ISSN: 0168-3659

Peer Reviewed

1984 to 1994 in Backfile Package - Pharmacology, Toxicology and Pharmaceutics (Legacy) [YPH]
Backfile Package - Pharmacology, Toxicology and Pharmaceutics including Supplement 1 [YUZ]

09/01/1984 to Present in ScienceDirect Journals

Search inside this journal Search

Back to Top

Last Updated on 12-02-2024 © Ex Libris, a ProQuest Company, 2000-2024
Privacy Policy

ScienceDirect

Journal of Controlled Release
Volume 161, Issue 2, 20 July 2012, Pages 422-428

Review

Antibody–drug conjugates: Basic concepts, examples and future perspectives

Giulio Casi [a], Dario Neri [b]

Show more

Outline | Share | Cite

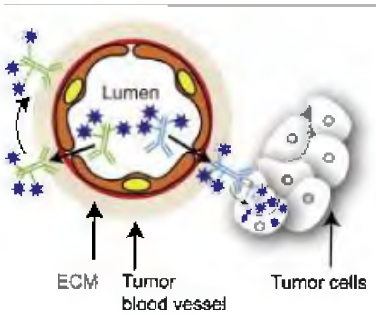
https://doi.org/10.1016/j.jconrel.2012.01.026
Get rights and content

Abstract

Conventional anticancer therapeutics often suffer from lack of specificity, resulting in poor therapeutic indexes and substantial toxicities to normal healthy tissues. Monoclonal antibodies have demonstrated considerable utility in cancer medicine, but their curative potential is often limited. Antibody–drug conjugates represent an innovative therapeutic approach that combines the desirable properties of monoclonal antibodies, with the cell killing activity of cytotoxic drugs, reducing systemic toxicity and increasing the therapeutic benefit for patients.

In this review, we outline prominent examples of early and recent antibody–drug conjugates, discussing drugs, linker chemistries and classes of targets for product development.

Graphical abstract



Download: Download high-res image (186KB)
Download: Download full-size image

DAC EX. 2040 IPR2022-01531 Page 1039 of 1299

Previous Next

Keywords

Antibody–drug conjugates; Non-internalizing monoclonal antibodies; Traceless linkers

1. Antibody–drug conjugates (ADCs): general considerations and historical perspectives

Monoclonal antibodies (mAbs) have led to the development of approved biopharmaceutical products in many therapeutic areas, including cardiovascular diseases, infection, immune disorders and cancer [1]. At present, the last two therapeutic fields dominate both in terms of sales and number of antibody products in industrial development. However, with few exceptions, the curative potential of "naked" immunoglobulins is limited and it is not surprising that large research efforts are being devoted to the "arming" of monoclonal antibodies with bioactive payloads (e.g., drugs, cytokines, radionuclides) [2].

Cytotoxic agents often display little selectivity and substantial toxicity to normal tissues. Considerable efforts have been invested for combining the desirable properties of monoclonal antibodies with the cell killing activity of cytotoxic drugs, reducing systemic toxicity and increasing the therapeutic benefit for patients [2], [3], [4], [5].

Although the concept of antibody–drug conjugates (ADCs) appears simple, the development of efficacious products often represents a considerable challenge. Many parameters have to be optimized for a successful ADC product, some of which are specific to individual tumor types. These include ADC stability (the drug should not be released before the ADC reaches its target *in vivo*), pharmacokinetics (the drug should not confer an undesired accumulation in a non-target organ), retention of immunoreactivity, and efficient release of the active form of the drug at site of disease.

Early work on ADCs relied on clinically approved chemotherapeutic drugs with the aim to increase tumor specificity. Initially this strategy took advantage of readily available drugs with known toxicity profiles. However, many other parameters related to ADC development, such as the choice of mAb, drug loading and potency, as well as release mechanisms were not immediately considered as crucial determinants, for the success of ADC strategies.

A prominent example of this first-generation ADCs is represented by BR96-doxorubicin [6]. This immunoconjugate consists of a chimeric mAb directed against the Lewis^Y tetra-saccharide commonly expressed on human carcinomas, modified with eight molecules of doxorubicin conjugated to the hinge cysteines. Doxorubicin is a DNA intercalator approved for the treatment of a broad range of tumors [7]. Drug release was engineered through an acid-labile hydrazone linker. Upon binding of the ADC to the cell surface antigens, the conjugate would be internalized inside cells, and doxorubicin released within the acidic endosomal and lysosomal vesicles. Treatment of tumor-bearing mice and rats with BR96-doxorubicin led to cures in tumors, which displayed the cognate antigen. Doses in excess of 100mg/kg were used, reflecting the

DAC EX. 2040 IPR2022-01531 Page 1040 of 1299

low potency of the targeted drug [6]. A phase I clinical trial confirmed the ability of the immunoconjugate to deliver doxorubicin to the tumor cells. The maximum tolerated dose (MTD) of BR96-doxorubicin was found to be approximately 700 mg/m^2. Despite higher total serum levels of doxorubicin (i.e. free doxorubicin plus doxorubicin bound to the antibody) were achieved compared to an intravenous administration of the unmodified drug, dose-limiting toxicities were not the same as conventional doxorubicin-related adverse events. Indeed, serum levels of free doxorubicin were below the detection limit in all patients assessed [8]. A subsequent randomized phase II trial on a population with confirmed sensitivity to doxorubicin revealed that the toxicities might have been of gastrointestinal origin, due to normal gut expression of Lewis^Y [9]. In both trials little antitumor activity was observed. Therefore, the normal tissue cross-reactivity of BR96 and the low molar potency of doxorubicin represented clear limitations for the industrial development of BR96-doxorubicin. In addition, the discrepancy between hydrazone stability ($t_{1/2} \approx 43$h) and pharmacokinetic terminal half-life of the BR96 antibody (12 days, roughly 7 fold longer than the hydrazone half-life) represented a cause of concern. The development of doxorubicin-based ADC may still continue in the future, since a second ADC loaded with the same drug successfully cured SCID mice at single low doses of immunoconjugate in non-Hodgkin lymphoma tumor model [10]. Moreover novel classes of ADCs produced with hydrazone technology are currently in advanced stages of clinical trials for non-Hodgkin lymphoma [11], confirming that the combination antibody–drug-linker has to be properly investigated on a case-to-case basis.

Today ADCs are developed starting from mAbs that selectively bind to tumors and display little cross-reactivity with healthy tissues. Moreover, the appropriate mAb format may have to be selected in order to tune ADC tumor uptake and blood clearance properties with linker stability and drug release, thus minimizing the exposure of healthy organs to toxic agents [12]. Since the total amount of ADC which can be realistically administered to patients is limited by cost-of-goods, and since coupling of too many drug molecules may lead to a loss of potency [13], (i.e., compromised binding ability and pharmacokinetic properties) more effective drugs became necessary for the industrial development of next-generation ADC. The requirement for potent bioactive molecules is also a consequence of the inefficient localization of mAbs at the tumor site. Typically, a maximum of 0.08% injected dose per gram of tumor accumulates in human malignancies. This is due to the increased interstitial fluid pressure (IFP) in the tumor environment, which represents a barrier to the extravasation and diffusion of antibodies [14]. The use of different signal transduction antagonists (e.g. PGE_1, VEGF and PGDF, TGFß) or of pro-inflammatory cytokines that lower tumor IFP has, in some cases led to an improved anticancer activity [15].

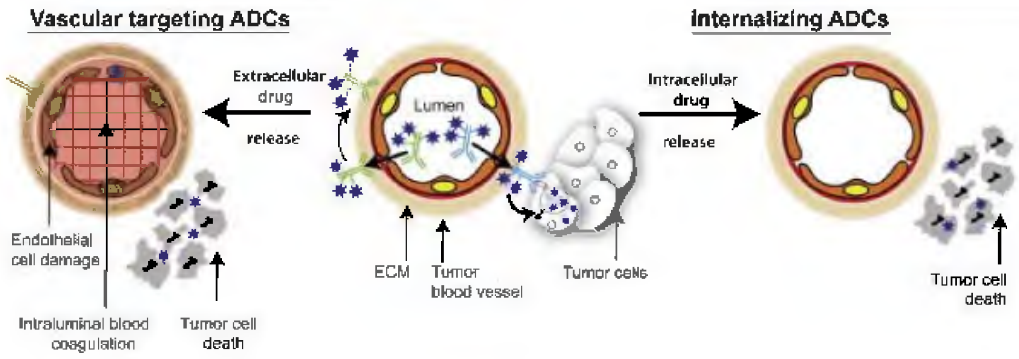
Recognizing the value of drug choice in ADC development, several programs were started in parallel in the late 1990s, with the aim to identify more potent drugs for ADC application. Here it is worth mentioning calicheamicins, [16] maytansinoids, [3] auristatins, [2] and CC1065 analogs [17], since these classes of potent cytotoxics represent the “backbone” of current industrial development programs.

Finally, the choice of cleavable linkers is crucial for the performance of ADC strategies. Depending on the drug delivery mechanism selected, the active form of the cytotoxic agent may be released more or less efficiently inside the target cell.

2. Internalizing vs. non-internalizing ADCs

DAC EX. 2040 IPR2022-01531 Page 1041 of 1299

Targeted antitumor therapy takes advantage of specific molecular differences between healthy and diseased tissues. So far, most efforts have been devoted to the targeting of tumor-associated antigens expressed on the surface of cancer cells [4] (Fig. 1, right) (Table 1) This class of ADC products typically requires mAbs that are internalized inside cells by receptor-mediated endocytosis. Different chemical mechanisms may allow the subsequent drug release, as described in the next section. The use of internalizing ADC is at the basis of products that are either approved or in advanced stages of clinical trials. However, targeting antigens on tumor cells is a complex task, due to a number of physical and kinetic barriers associated with large solid tumors, and to the potential down-regulation of tumor-associated antigens targeted by the immunoconjugate, as each cell has to express the target antigen in order to be reached by the cytotoxic agent.



Download: Download high-res image (379KB)

Download: Download full-size image

Fig. 1. Antibody–drug conjugates (ADC) and their effect. (*Right*) Tumor cell death induced by internalizing ADCs (blue). Upon ADC internalization inside tumor cells, the active drug is released and leads to tumor cell death. (*Left*) Effect of tumor targeting ADCs specific to markers of angiogenesis expressed on the endothelial extracellular matrix (green). The long residence time of vascular targeting ADCs allows the localized drug release, leading to intravascular blood coagulation, and to an avalanche of tumor cell death.

Table 1. Selected examples of intracellular, ECM and vascular targets used in ADC development.

	Antigen	Reference
Tumor cells	CD30	[24]
	Can Ag	[3]
	HER2	[25]
	CD22	[26]
ECM	Fibronectin(EDA:EDB)	[27], [28]
	Tenascin-C(A1)	[29]
	Periostin	[30]
EC	Integrins	[19]
	PSMA	[19]

DAC EX. 2040 IPR2022-01531 Page 1042 of 1299

Antigen	Reference
VEGFR-2	[19]

An alternative approach has been developed that targets markers expressed on tumor neo-vasculature (Fig. 1, left). This strategy is compatible with the use of non-internalizing antibodies [18], [19]. Vascular targets are more easily accessible from the blood stream compared to systemically administered agents. Tumors require blood supply for their growth and neoplastic capillaries are significantly different at the molecular level from normal healthy vasculature. Remarkably, since angiogenesis is a common feature of all malignancies and tumors express common markers of angiogenesis, a single agent should in principle be applicable to a wide range of tumor entities [18], [19]. In particular, markers of angiogenesis, found in the subendothelial extracellular matrix (ECM), are more stable compared to cellular antigens and facilitate an antibody residence time of days/weeks. The potential of targeting antigens expressed on tumor neo-vasculature has been confirmed in pre-clinical and clinical applications [20].

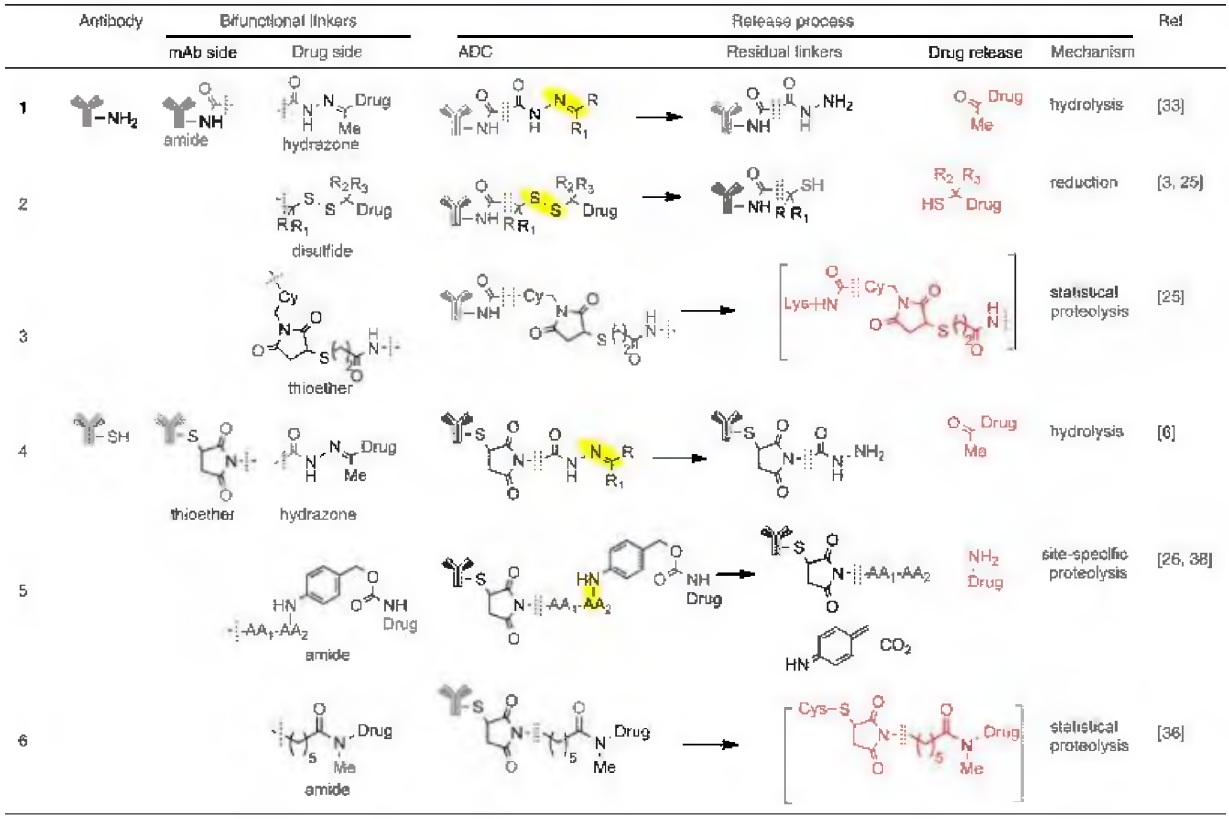
Endothelial cells (EC) are readily accessible from the blood stream. Anti-VEGF mAbs have been shown to have the potential to localize at tumor sites *in vivo* [21]. However, this strategy is hardly compatible with non-internalizing antibodies, as the released drug would enter the bloodstream. Alternatively, subendothelial modified ECM components may serve as target for ADCs, which do not require internalization for their activity. Upon extravasation, a specific mAb product comes into contact with more abundant and stable antigens, thus ensuring a long residence time of ADC at the tumor site. Work in this area has been performed with the human mAb (L19), specific to the extra-domain B (EDB) of fibronectin, a marker of angiogenesis. EDB is normally not present in the healthy protein, but is inserted during active tissue remodeling by alternative splicing, and is highly abundant in many aggressive solid tumors. L19 fused to different effector molecules is currently in multiple stages of clinical development [22]. In addition, we have recently started the use of oncofetal fibronectin as a target for ADC development [23].

3. Drug release strategies for ADCs

Specific linkers are designed to append toxic payloads to mAbs and to allow a selective drug release at the tumor site. Linkers differ in terms of plasma stability and in the mechanism of release. Acid-labile hydrazone linkers have been employed in the first class of ADCs developed (Table 2, entries 1, 4) [6], [31], [32], [33]. Hydrazones are preferentially cleaved within intracellular lysosomes and endosomes, as a consequence of the lower pH found in these environments (pH ≈ 5).

Table 2. Representative examples of ADC chemistries. Current ADC assembly strategies rely on bifunctional linkers. Specific release processes are responsible for active drug release. Selective scissile bonds are highlighted in yellow. The postulated active form of the released drug is depicted in red. R_i=H, Me.

DAC EX. 2040 IPR2022-01531 Page 1043 of 1299



Disulfides (Table2, entry 2) have been extensively exploited as ADC linkers since they are stable at physiological pH and release their payload upon internalization inside cells, where the cytosol provides a significantly more reducing environment compared to the extracellular milieu [34]. Several *in vitro* and *in vivo* studies have been performed to establish the effect of increasing substitution at disulfides in the pharmacokinetic and toxicity profiles of different ADCs [3], [25]. Two classes of calicheamicin–antibody conjugates containing both disulfide linkers were tested in different tumor models. An additional hydrolyzable hydrazone group was present in a subgroup of the ADCs, and allowed direct comparison between the two linkers.

In an ADC based on the CTM01 antibody (where CTM01 is a murine IgG1 that recognizes MUC1 antigen present on a broad spectrum of solid tumors), the additional hydrazone was not necessary for activity [35]. Surprisingly, when the Anti-CD33 P67.6 antibody was used for ADC development, the disulfide moiety in the linker was insufficient for the proper release of calicheamicin, while the hydrazone moiety was essential [33].

Alternative linker strategies rely on “non-cleavable” linkers and take advantage of the catabolic degradation of internalized antibodies in the lysosomal and endosomal compartments. ADCs that consist of either peptide bonds, or of chemical bonds normally stable under physiologic conditions, rely in the statistical proteolytic degradation of the conjugate [25], [36] (Table2, entries 3, 6). In a series of disulfide-linked ADCs for the intracellular release of cytotoxic drugs, it was surprisingly found that a Trastuzumab-DM1 control conjugate in which the disulfide was replaced with a non-cleavable thioether bond, was the most effective ADC variant in *in vivo* therapy tests [25]. Thus, while cleavable disulfide linkers are often associated with

DAC EX. 2040 IPR2022-01531 Page 1044 of 1299

ADC activity, the precise choice of the most active linker chemistry requires the screening of several candidates, including non-cleavable linkers which may release drug only after a proteolytic digestion of the antibody molecule [37].

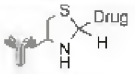
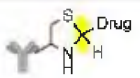
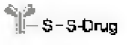
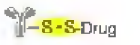
Alternatively protease-specific sequences introduced in the linker control the hydrolytic process, as reported for the lysosome abundant protease cathepsin B [24], [38] (Table2, entry 5). This approach was confirmed to be superior to the hydrolytically labile hydrazone linker both in terms of specificity and toxicity in a series of monomethyl-auristatins (MMAE) conjugated to cBR96 mAb [24].

Most ADC manufacturing processes exploit the chemical modification of the primary amino group of lysine residues or of the thiol group of cysteines. The different abundance of the two residues is reflected also in the complexity of the heterogeneous mixture generated [39]. When the release technology relies on statistical proteolysis, traces of the modified amino acids might be found in the active released form of the drug (Table2, entries 3, 6).

In the examples described so far, bifunctional linkers feature one moiety for conjugation of the drug to the mAb, and one moiety for drug release.

Traceless linkers eliminate this distinction since coupling and release chemistry are identical (Table2) We have recently described an innovative linker technology that relies on the site-specific coupling and release of cytotoxic drugs from thiazolidines. The linker, generated upon reaction of aldehydes with 1,2-aminothiol moieties on the antibody, is stable for synthesis, and allows the hydrolytic drug release under physiological conditions. The release process is traceless as it restores the free drug, and the intact antibody (Table3, entry 1) [40]. Alternatively cysteines introduced in mAb sequences by site directed mutagenesis afford site-specific disulfide linkages with thiol–drugs (Table3, entry 2) [23].

Table3. Recent examples of linkerless ADC assembly. The cleavage process restores the unmodified antibody and the drug used for ADC development. Scissile bonds are highlighted in yellow. The postulated active form of the released drug is depicted in red.

	Antibody	Traceless linkers	Release process				Ref
			ADC	Residual linkers	Drug release	Mechanism	
1		 thiazolidine				hydrolysis	[32]
2		 disulfide			HS-Drug	reduction	[22]

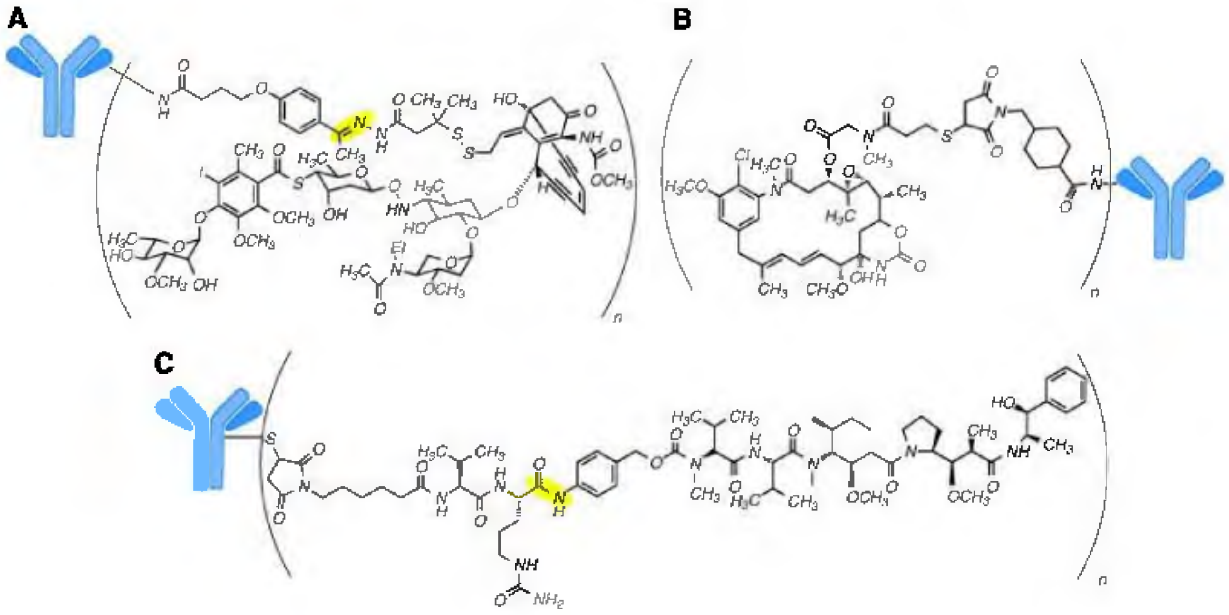
Disulfides based linkers may find ADC applications also with non-internalizing antibodies. Indeed, the localization of these ADCs at the tumor ECM could expose the disulfide linkage to reducing agents (cysteine, glutathione) initially released by dying cells and progressively amplified by drug-mediated cell killing.

Remarkably, in these two last examples, the release process restores the original antibody and the active drug, which simplifies drug manufacturing and should diminish ADC immunogenicity.

4. Representative ADCs at different stages of clinical development

DAC EX. 2040 IPR2022-01531 Page 1045 of 1299

Mylotarg was the first ADC ever approved in the US. The product had an indication for the treatment of acute myeloid leukemia (AML) in patients older than 60 not eligible for other chemotherapies. The ADC consisted of a humanized anti-CD33 mAb (hP67.6) attached to the calicheamicin drug through an acid labile hydrazone linker [41], [42] (Fig.2A).



Download: Download high-res image (486KB)

Download: Download full-size image

Fig.2. Structures of selected ADCs used in cancer therapy. Mylotarg (A), T-DM1 (B), ADCETRIS™ (C). Scissile bonds are highlighted in yellow.

Calicheamicin derives from the family of enediyne antibiotics extracted from the soil microorganism *Micromonospora echinospora*, and binds in the minor groove of DNA. The highly reactive 1,4-benzenoyl diradical generated by intracellular reduction, caused extensive DNA damage and subsequent cell apoptosis [43], [16]. The acid labile hydrazone linker [33] held the two components together and supposedly was cleaved before the sterically hindered disulfide, and thioester moieties. Mylotarg was administered as a 1:1 mixture of unconjugated and conjugated mAb to 4–6 equivalents of drug, with an average drug loading of 2–3 moles of drug to mAb. The drug was approved under FDA's accelerated approval program based on a response rate of about 30% [44]. However, it failed to confirm therapeutic benefits (i.e., higher response rates) to AML patients in clinical trials, when administered in combination with chemotherapy. Indeed a greater number of deaths occurred in the group of patients receiving Mylotarg, compared to those receiving chemotherapy. Potentially, the veno-occlusive disease observed at initial approval, worsened in the post marketing setting, causing fatalities to increase. The product was voluntarily withdrawn in June 2010 (http://www.fda.gov/NewsEvents/Newsroom/PressAnnouncements/ucm216448.htm ↗)

Trastuzumab-DM1 (T-DM1) is an ADC currently in advanced stage clinical trials designed for the treatment of Her2-positive metastatic breast cancer. T-DM1 consists of the approved anti-Her2-mAb Trastuzumab (Herceptin) directly conjugated to DM1, via a non-cleavable thioether linker present in an N-maleimido cyclohexane-1-carboxylate group (also named MCC) (Fig.2B). Herceptin has been introduced in the market

DAC EX. 2040 IPR2022-01531 Page 1046 of 1299

in 1998 for Her2+ breast cancer, and showed clinical benefits in combination with chemotherapy as first line or adjuvant therapy [45], [46]. Despite these objective results, part of the patients treated either did not respond initially, or relapsed [47]. DM1 is a maytansinoid derivative, binds directly to microtubules and inhibits their assembly with consequent apoptosis, similar to what was observed for the *Vinca* alkaloids [48], [49]. T-DM1 undergoes cell internalization and complete lysosomal proteolysis [25] and, in analogy to what has been reported for huC242-MCC-DM1 [50], (huC242 is a humanized antibody with high affinity for the carbohydrate antigen CanAg) the major active drug metabolite is believed to be the weakly membrane permeable Lys-MCC-DM1 (Table2, entry 3).

T-DM1 carries an average of 3.5 molecules of DM1/mAb and is now used in clinical trials on heavily pre-treated patients, including Trastuzumab. A phase I dose escalation study showed partial responses in 25% of the patients when treated with doses starting from 0.3 mg/kg and going up to 4.8 mg/kg [51]. More remarkably in a phase II trial, third-line metastatic breast cancer showed a 33% objective response rate in 110 patients treated with 3.6 mg/kg T-DM1 every 3 weeks [52]. Moreover T-DM1 was well tolerated by patients with no cardiovascular toxicities. For these impressive results, approval of T-DM1 is expected in 2012, even though the FDA has refused a Biologics License Application submitted in July 2010 for accelerated approval.

In July 2011 brentuximab vedotin (SGN-35, Adcetris) was approved by the FDA for the treatment of patients with Hodgkin lymphoma after failure of autologous stem cell transplant, and for patients with systemic anaplastic large cell lymphoma after failure of at least one prior multi-agent chemotherapy regimen (http://www.fda.gov/NewsEvents/Newsroom/PressAnnouncements/ucm268781.htm ↗) In SGN-35 an anti-CD30 monoclonal antibody is attached through a cathepsin-B cleavable valine-citrulline dipeptide (Val-Cit) to an average of 4 monomethyl auristatin E (MMAE) molecules (Fig.2C). MMAE drugs are structurally related to dolastatin 10 and afford a potent antitumor activity by inhibiting tubulin polymerization [2], [53]. The conjugation occurs between reduced anti-CD30 mAb and maleimido containing MMAE to form 4 thioether linkers. The ADC generated is highly homogenous and stable (half life 6 and 9.6 days in mice and monkeys) [24]. Upon binding to CD30 on the cell surface, SGN-35 is internalized, and digested inside lysosomes. Drug release begins with the selective proteolysis of the Val-Cit linker catalyzed by cathepsin-B. Following proteolytic cleavage, 1,6-elimination of the p-aminobenzyl ester group affords the unmodified drug (Table2, entry 5) [38], [54], [55]. A phase I clinical trial showed tumor regressions in about 93% of treated patients, and 56% objective response rates [56], [57]. A single arm phase II study for Hodgkin lymphoma on 102 patients treated with SGN-35 showed 75% objective responses and 34% complete responses [58], [59]. The drug was approved under FDA's accelerated approval program, based on objective response rates (http://www.fda.gov/NewsEvents/Newsroom/PressAnnouncements/ucm268781.htm ↗)

5. Concluding remarks

The area of ADC development is in rapid expansion, with large investments being made by pharmaceutical companies [60]. At present, maytansinoids and auristatins are the most frequently used drugs for ADC developments. Since ADC, at some stage, are cleared from circulation (either via the renal route or the hepatobiliary route) it is probable that future research efforts will closely evaluate therapeutic candidates not only on the basis of their tumor toxicity, but also in terms of the side-effects associated to the ADC excretion process. The complex pharmacokinetic profiles and the high cost of goods for ADC will be justified if the therapeutic performance is sufficiently good and if the disease is a severe one. In principle, advantages

DAC EX. 2040 IPR2022-01531 Page 1047 of 1299

such as the drug release at site of disease should lead to a reduced systemic toxicity and to higher therapeutic indexes, compared to non-targeted drugs.

In the future, we envisage that novel linkers chemistry (including traceless linkers) and non-internalizing antibodies will expand the repertoire of tools for ADC development.

Competing interests statement

Giulio Casi is employed at Philochem AG.

Dario Neri is a co-founder and shareholder of Philogen SpA.

Special issue articles Recommended articles

References

[1] A.L. Nelson, E. Dhimolea, J.M. Reichert
Development trends for human monoclonal antibody therapeutics
Nat. Rev. Drug Discov., 9 (2010), pp. 767-774
Crossref ↗ View in Scopus ↗ Google Scholar ↗

[2] A.M. Wu, P.D. Senter
Arming antibodies: prospects and challenges for immunoconjugates
Nat. Biotechnol., 23 (2005), pp. 1137-1146
Crossref ↗ View in Scopus ↗ Google Scholar ↗

[3] R.V.J. Chari
Targeted cancer therapy: Conferring specificity to cytotoxic drugs
Acc. Chem. Res., 41 (2008), pp. 98-107
Crossref ↗ View in Scopus ↗ Google Scholar ↗

[4] P.D. Senter
Potent antibody drug conjugates for cancer therapy
Curr. Opin. Chem. Biol., 13 (2009), pp. 235-244
View PDF View article View in Scopus ↗ Google Scholar ↗

[5] S.C. Alley, N.M. Okeley, P.D. Senter
Antibody–drug conjugates: targeted drug delivery for cancer
Curr. Opin. Chem. Biol., 14 (2010), pp. 529-537
View PDF View article View in Scopus ↗ Google Scholar ↗

[6] P.A. Trail, D. Willner, S.J. Lasch, A.J. Henderson, S. Hofstead, A.M. Casazza, R.A. Firestone, I. Hellström, K.E. Hellström
Cure of xenografted human carcinomas by BR96-doxorubicin immunoconjugates
Science, 261 (1993), pp. 212-215
Crossref ↗ View in Scopus ↗ Google Scholar ↗

DAC EX. 2040 IPR2022-01531 Page 1048 of 1299

[7] G.M. Dubowchik, M.A. Walker
Receptor-mediated and enzyme-dependent targeting of cytotoxic anticancer drugs
Pharmacol. Ther., 83 (1999), pp. 67-123
View PDF View article View in Scopus ↗ Google Scholar ↗

[8] M.N. Saleh, S. Sugarman, J. Murray, J.B. Ostroff, D. Healey, D. Jones, C.R. Daniel, D. LeBherz, H. Brewer, N. Onetto, A.F. LoBuglio
Phase I trial of the anti-Lewis Y drug immunoconjugate BR96-doxorubicin in patients with Lewis Y-expressing epithelial tumors
J. Clin. Oncol., 18 (2000), pp. 2282-2292
View in Scopus ↗ Google Scholar ↗

[9] A.W. Tolcher, S. Sugarman, K.A. Gelmon, R. Cohen, M. Saleh, C. Isaacs, L. Young, D. Healey, N. Onetto, W. Slichenmyer
Randomized phase II study of BR96-doxorubicin conjugate in patients with metastatic breast cancer
J. Clin. Oncol., 17 (1999), pp. 478-484
View in Scopus ↗ Google Scholar ↗

[10] G.L. Griffiths, M.J. Mattes, R. Stein, S.V. Govindan, I.D. Horak, H.J. Hansen, D.M. Goldenberg
Cure of SCID mice bearing human B-lymphoma xenografts by an Anti-CD74 antibody–anthracycline drug conjugate
Clin. Cancer Res., 9 (2003), pp. 6567-6571
View in Scopus ↗ Google Scholar ↗

[11] A.G. Polson, W.Y. Ho, V. Ramakrishnan
Investigational antibody–drug conjugates for hematological malignancies
Expert Opin. Investig. Drugs, 20 (2011), pp. 75-85
Crossref ↗ View in Scopus ↗ Google Scholar ↗

[12] P.J. Carter
Potent antibody therapeutics by design
Nat. Rev. Immunol., 6 (2006), pp. 343-357
Crossref ↗ View in Scopus ↗ Google Scholar ↗

[13] K.J. Hamblett, P.D. Senter, D.F. Chace, M.M.C. Sun, J. Lenox, C.G. Cerveny, K.M. Kissler, S.X. Bernhardt, A.K. Kopcha, R.F. Zabinski, D.L. Meyer, J.A. Francisco
Effects of drug loading on the antitumor activity of a monoclonal antibody drug conjugate
Clin. Cancer Res., 10 (2004), pp. 7063-7070
View in Scopus ↗ Google Scholar ↗

[14] C.H. Heldin, K. Rubin, K. Pietras, A. Östman
High interstitial fluid pressure—an obstacle in cancer therapy
Nat. Rev. Cancer, 4 (2004), pp. 806-813
Crossref ↗ View in Scopus ↗ Google Scholar ↗

[15] H.H. Sedlacek, G. Seemann, D. Hoffmann, J. Czech, P. Lorenz, C. Kolar, K. Bosslet

DAC EX. 2040 IPR2022-01531 Page 1049 of 1299

Antibodies as carriers of cytotoxicity, vol. 43, Karger AG, Munich, Germany (1992)

[16] N.K. Damle, P. Frost
Antibody-targeted chemotherapy with immunoconjugates of calicheamicin
Curr. Opin. Pharmacol., 3 (2003), pp. 386-390
View PDF View article View in Scopus ↗ Google Scholar ↗

[17] R.V.J. Chari, K.A. Jackel, L.A. Bourret, S.M. Derr, B.M. Tadayoni, K.M. Mattocks, S.A. Shah, C.N. Liu, W.A. Blättler, V.S. Goldmacher
Enhancement of the selectivity and antitumor efficacy of a CC-1065 analogue through immunoconjugate formation
Cancer Res., 55 (1995), pp. 4079-4084
View in Scopus ↗ Google Scholar ↗

[18] C. Schliemann, D. Neri
Antibody-based targeting of the tumor vasculature
BBA: Rev. Cancer, 1776 (2007), pp. 175-192
View PDF View article View in Scopus ↗ Google Scholar ↗

[19] H.-P. Gerber, P.D. Senter, I.S. Grewal
Antibody drug-conjugates targeting the tumor vasculature. Current and future developments
MAbs, 1 (2009), pp. 247-253
Crossref ↗ View in Scopus ↗ Google Scholar ↗

[20] A. Palumbo, F. Hauler, P. Dziunycz, K. Schwager, A. Soltermann, F. Pretto, C. Alonso, G.F. Hofbauer, R.W. Boyle, D. Neri
A chemically modified antibody mediates complete eradication of tumours by selective disruption of tumour blood vessels
Br. J. Cancer, 104 (2011), pp. 1106-1115
Crossref ↗ View in Scopus ↗ Google Scholar ↗

[21] T.H. Stollman, M.G.W. Scheer, W.P.J. Leenders, K.C.N. Verrijp, A.C. Soede, W.J.G. Oyen, T.J.M. Ruers, O.C. Boerman
Specific imaging of VEGF-A expression with radiolabeled anti-VEGF monoclonal antibody
Int. J. Cancer, 122 (2008), pp. 2310-2314
Crossref ↗ View in Scopus ↗ Google Scholar ↗

[22] A. Menrad, H.D. Menssen
ED-B fibronectin as a target for antibody-based cancer treatments
Expert Opin. Ther. Targets, 9 (2005), pp. 491-500
Crossref ↗ View in Scopus ↗ Google Scholar ↗

[23] G.J.L. Bernardes, G. Casi, I. Hartmann, S. Trüssel, K. Schwager, J. Scheuermann, D. Neri
A traceless vascular-targeting antibody–drug conjugate for cancer therapy
Angew. Chem. Int. Ed., 51 (2012), pp. 941-944
Crossref ↗ View in Scopus ↗ Google Scholar ↗

DAC EX. 2040 IPR2022-01531 Page 1050 of 1299

[24] S.O. Doronina, B.E. Toki, M.Y. Torgov, B.A. Mendelsohn, C.G. Cerveny, D.F. Chace, R.L. DeBlanc, R.P. Gearing, T.D. Bovee, C.B. Siegall, J.A. Francisco, A.F. Wahl, D.L. Meyer, P.D. Senter
Development of potent monoclonal antibody auristatin conjugates for cancer therapy
Nat. Biotechnol., 21 (2003), pp. 778-784
View in Scopus ↗ Google Scholar ↗

[25] G.D.L. Phillips, G. Li, D.L. Dugger, L.M. Crocker, K.L. Parsons, E. Mai, W.A. Blättler, J.M. Lambert, R.V.J. Chari, R.J. Lutz, W.L.T. Wong, F.S. Jacobson, H. Koeppen, R.H. Schwall, S.R. Kenkare-Mitra, S.D. Spencer, M.X. Sliwkowski
Targeting HER2-positive breast cancer with trastuzumab-DM1, an antibody–cytotoxic drug conjugate
Cancer Res., 68 (2008), pp. 9280-9290
Google Scholar ↗

[26] J.F. DiJoseph, M.M. Dougher, D.Y. Evans, B.-B. Zhou, N.K. Damle
Preclinical anti-tumor activity of antibody-targeted chemotherapy with CMC-544 (inotuzumab ozogamicin), a CD22-specific immunoconjugate of calicheamicin, compared with non-targeted combination chemotherapy with CVP or CHOP
Cancer Chemother. Pharmacol., 67 (2011), pp. 741-749
Crossref ↗ View in Scopus ↗ Google Scholar ↗

[27] A. Villa, E. Trachsel, M. Kaspar, C. Schliemann, R. Sommavilla, J.-N. Rybak, C. Rösli, L. Borsi, D. Neri
A high-affinity human monoclonal antibody specific to the alternatively spliced EDA domain of fibronectin efficiently targets tumor neo-vasculature in vivo
Int. J. Cancer, 122 (2008), pp. 2405-2413
Crossref ↗ View in Scopus ↗ Google Scholar ↗

[28] A. Pini, F. Viti, A. Santucci, B. Carnemolla, L. Zardi, P. Neri, D. Neri
Design and use of a phage display library—human antibodies with subnanomolar affinity against a marker of angiogenesis eluted from a two-dimensional gel
J. Biol. Chem., 273 (1998), pp. 21769-21776
View PDF View article View in Scopus ↗ Google Scholar ↗

[29] S.S. Brack, M. Silacci, M. Birchler, D. Neri
Tumor-targeting properties of novel antibodies specific to the large isoform of tenascin-C
Clin. Cancer Res., 12 (2006), pp. 3200-3208
View in Scopus ↗ Google Scholar ↗

[30] V. Castronovo, D. Waltregny, P. Kischel, C. Roesli, G. Elia, J.N. Rybak, D. Neri
A chemical proteomics approach for the identification of accessible antigens expressed in human kidney cancer
Mol. Cell. Proteomics, 5 (2006), pp. 2083-2091
View PDF View article View in Scopus ↗ Google Scholar ↗

[31] R.L. Reeves
Condensations Leading to Double Bonds
S. Patai (Ed.), The chemistry of the carbonyl group, Interscience Publisher, New York (1966), pp. 567-619

DAC EX. 2040 IPR2022-01531 Page 1051 of 1299

Crossref ↗ View in Scopus ↗ Google Scholar ↗

[32] G.R. Braslawsky, M.A. Edson, W. Pearce, T. Kaneko, R.S. Greenfield
Antitumor activity of adriamycin (hydrazone-linked) immunoconjugates compared with free adriamycin and specificity of tumor cell killing
Cancer Res., 50 (1990), pp. 6608-6614
View in Scopus ↗ Google Scholar ↗

[33] P.R. Hamann, L.M. Hinman, C.F. Beyer, D. Lindh, J. Upeslacis, D.A. Flowers, I. Bernstein
An anti-CD33 antibody-calicheamicin conjugate for treatment of acute myeloid leukemia. Choice of linker
Bioconjug. Chem., 13 (2002), pp. 40-46
View in Scopus ↗ Google Scholar ↗

[34] A. Meister, M.E. Anderson
Glutathione
Annu. Rev. Biochem., 52 (1983), pp. 711-760
Crossref ↗ View in Scopus ↗ Google Scholar ↗

[35] P.R. Hamann, L.M. Hinman, C.F. Beyer, D. Lindh, J. Upeslacis, D. Shochat, A. Mountain
A calicheamicin conjugate with a fully humanized anti-MUC1 antibody shows potent antitumor effects in breast and ovarian tumor xenografts
Bioconjug. Chem., 16 (2005), pp. 354-360
Crossref ↗ View in Scopus ↗ Google Scholar ↗

[36] S.O. Doronina, B.A. Mendelsohn, T.D. Bovee, C.G. Cerveny, S.C. Alley, D.L. Meyer, E. Oflazoglu, B.E. Toki, R.J. Sanderson, R.F. Zabinski, A.F. Wahl, P.D. Senter
Enhanced activity of monomethylauristatin F through monoclonal antibody delivery: effects of linker technology on efficacy and toxicity
Bioconjug. Chem., 17 (2006), pp. 114-124
Crossref ↗ View in Scopus ↗ Google Scholar ↗

[37] A.G. Polson, J. Calemine-Fenaux, P. Chan, W. Chang, E. Christensen, S. Clark, F.J. de Sauvage, D. Eaton, K. Elkins, J.M. Elliott, G. Frantz, R.N. Fuji, A. Gray, K. Harden, G.S. Ingle, N.M. Kljavin, H. Koeppen, C. Nelson, S. Prabhu, H. Raab, S. Ross, D.S. Slaga, J.-P. Stephan, S.J. Scales, S.D. Spencer, R. Vandlen, B. Wranik, S.-F. Yu, B. Zheng, A. Ebens
Antibody–drug conjugates for the treatment of non-Hodgkin's lymphoma: target and linker-drug selection
Cancer Res., 69 (2009), pp. 2358-2364
Google Scholar ↗

[38] G.M. Dubowchik, K. Mosure, J.O. Knipe, R.A. Firestone
Cathepsin B-sensitive dipeptide prodrugs. 2. Models of anticancer drugs paclitaxel (Taxol ®), mitomycin C and doxorubicin
Bioorg. Med. Chem. Lett., 8 (1998), pp. 3347-3352
View PDF View article View in Scopus ↗ Google Scholar ↗

DAC EX. 2040 IPR2022-01531 Page 1052 of 1299

[39] J.R. Junutula, H. Raab, S. Clark, S. Bhakta, D.D. Leipold, S. Weir, Y. Chen, M. Simpson, S.P. Tsai, M.S. Dennis, Y. Lu, Y.G. Meng, C. Ng, J. Yang, C.C. Lee, E. Duenas, J. Gorrell, V. Katta, A. Kim, K. McDorman, K. Flagella, R. Venook, S. Ross, S.D. Spencer, W.L. Wong, H.B. Lowman, R. Vandlen, M.X. Sliwkowski, R.H. Scheller, P. Polakis, W. Mallet
Site-specific conjugation of a cytotoxic drug to an antibody improves the therapeutic index
Nat. Biotechnol., 26 (2008), pp. 925-932
Crossref ↗ View in Scopus ↗ Google Scholar ↗

[40] G. Casi
Protein–drug conjugates, PCT/EP2011/004664
(2010)
(pending)
Google Scholar ↗

[41] P.F. Bross, J. Beitz, G. Chen, X.H. Chen, E. Duffy, L. Kieffer, S. Roy, R. Sridhara, A. Rahman, G. Williams, R. Pazdur
Approval summary: gemtuzumab ozogamicin in relapsed acute myeloid leukemia
Clin. Cancer Res., 7 (2001), pp. 1490-1496
View in Scopus ↗ Google Scholar ↗

[42] P.R. Hamann, L.M. Hinman, I. Hollander, C.F. Beyer, D. Lindh, R. Holcomb, W. Hallett, H.R. Tsou, J. Upeslacis, D. Shochat, A. Mountain, D.A. Flowers, I. Bernstein
Gemtuzumab ozogamicin, a potent and selective anti-CD33 antibody–calicheamicin conjugate for treatment of acute myeloid leukemia
Bioconjug. Chem., 13 (2002), pp. 47-58
View in Scopus ↗ Google Scholar ↗

[43] N. Zein, A.M. Sinha, W.J. McGahren, G.A. Ellestad
Calicheamicin γ_1^I—an antitumor antibiotic that cleaves double-stranded DNA site specifically
Science, 240 (1988), pp. 1198-1201
Crossref ↗ View in Scopus ↗ Google Scholar ↗

[44] R.A. Larson, M. Boogaerts, E. Estey, C. Karanes, E.A. Stadtmauer, E.L. Sievers, P. Mineur, J.M. Bennett, M.S. Berger, C.B. Eten, M. Munteanu, M.R. Loken, J.J.M. van Dongen, I.D. Bernstein, F.R. Appelbaum
Antibody-targeted chemotherapy of older patients with acute myeloid leukemia in first relapse using Mylotarg (gemtuzumab ozogamicin)
Leukemia, 16 (2002), pp. 1627-1636
Crossref ↗ View in Scopus ↗ Google Scholar ↗

[45] D.J. Slamon, B. Leyland-Jones, S. Shak, H. Fuchs, V. Paton, A. Bajamonde, T. Fleming, W. Eiermann, J. Wolter, M. Pegram, J. Baselga, L. Norton
Use of chemotherapy plus a monoclonal antibody against HER2 for metastatic breast cancer that overexpresses HER2
N. Engl. J. Med., 344 (2001), pp. 783-792
View in Scopus ↗ Google Scholar ↗

DAC EX. 2040 IPR2022-01531 Page 1053 of 1299

[46] I. Smith, M. Procter, R.D. Gelber, S. Guillaume, A. Feyereislova, M. Dowsett, A. Goldhirsch, M. Untch, G. Mariani, J. Baselga, M. Kaufmann, D. Cameron, R. Bell, J. Bergh, R. Coleman, A. Wardley, N. Harbeck, R.I. Lopez, P. Mallmann, K. Gelmon, N. Wilcken, E. Wist, P. Sànchez Rovira, M. Piccart-Gebhart
2-year follow-up of trastuzumab after adjuvant chemotherapy in HER2-positive breast cancer: a randomised controlled trial
Lancet, 369 (2007), pp. 29-36
View PDF View article View in Scopus ↗ Google Scholar ↗

[47] R. Nahta, D.H. Yu, M.C. Hung, G.N. Hortobagyi, F.J. Esteva
Mechanisms of disease: understanding resistance to HER2-targeted therapy in human breast cancer
Nat. Clin. Pract. Oncol., 3 (2006), pp. 269-280
Crossref ↗ View in Scopus ↗ Google Scholar ↗

[48] J.M. Cassady, K.K. Chan, H.G. Floss, E. Leistner
Recent developments in the maytansinoid antitumor agents
Chem. Pharm. Bull., 52 (2004), pp. 1-26
View in Scopus ↗ Google Scholar ↗

[49] S. Remillard, L.I. Rebhun, G.A. Howie, S.M. Kupchan
Antimitotic activity of potent tumor inhibitor maytansine
Science, 189 (1975), pp. 1002-1005
Crossref ↗ View in Scopus ↗ Google Scholar ↗

[50] H.K. Erickson, P.U. Park, W.C. Widdison, Y.V. Kovtun, L.M. Garrett, K. Hoffman, R.J. Lutz, V.S. Goldmacher, W.A. Blättler
Antibody-maytansinoid conjugates are activated in targeted cancer cells by lysosomal degradation and linker-dependent intracellular processing
Cancer Res., 66 (2006), pp. 4426-4433
View in Scopus ↗ Google Scholar ↗

[51] I.E. Krop, M. Beeram, S. Modi, N. Rabbee, S. Girish, J. Tibbitts, S.N. Holden, S.G. Lutzker, H.A. Burris
A phase I study of trastuzumab-DM1, a first-in-class HER2 antibody-drug conjugate, in patients with advanced HER2+ breast cancer
Breast Cancer Res. Treat., 106 (Suppl. 1) (2007), p. S33
Google Scholar ↗

[52] I. Krop, P. LoRusso, K.D. Miller, S. Modi, D. Yardley, G. Rodriguez, S. Agresta, M. Zheng, L. Amler, H. Rugo
A Phase II Study of trastuzumab-DM1 (T-DM1), a novel HER2 antibody–drug conjugate, in patients previously treated with lapatinib, trastuzumab, and chemotherapy
Cancer Res., 69 (Suppl. 3) (2009)
Abstract 710
Google Scholar ↗

[53] M. Otani, T. Natsume, J. Watanabe, M. Kobayashi, M. Murakoshi, T. Mikami, T. Nakayama

DAC EX. 2040 IPR2022-01531 Page 1054 of 1299

TZT-1027, an antimicrotubule agent, attacks tumor vasculature and induces tumor cell death

Jpn. J. Cancer Res., 91 (2000), pp. 837-844

Crossref ↗ View in Scopus ↗ Google Scholar ↗

[54] G.M. Dubowchik, R.A. Firestone

Cathepsin B-sensitive dipeptide prodrugs. 1. A model study of structural requirements for efficient release of doxorubicin

Bioorg. Med. Chem. Lett., 8 (1998), pp. 3341-3346

View PDF View article View in Scopus ↗ Google Scholar ↗

[55] B.E. Toki, C.G. Cerveny, A.F. Wahl, P.D. Senter

Protease-mediated fragmentation of p-amidobenzyl ethers: a new strategy for the activation of anticancer prodrugs

J. Org. Chem., 67 (2002), pp. 1866-1872

View in Scopus ↗ Google Scholar ↗

[56] A. Younes, A. Forero-Torres, N.L. Bartlett, J.P. Leonard, D.A. Kennedy, E.L. Sievers

Robust antitumor activity of the antibody-drug conjugate SGN-35 when administered every 3 weeks to patients with relapsed or refractory CD30 positive hematologic malignancies in a phase 1 study

Haematologica, 94 (Suppl. 2) (2009), p. 205

Crossref ↗ View in Scopus ↗ Google Scholar ↗

[57] M. Fanale, N.L. Bartlett, A. Forero-Torres, J. Rosenblatt, S.J. Horning, A.R. Franklin, C.M. Lynch, E.L. Sievers, D.A. Kennedy

The antibody–drug conjugate brentuximab vedotin (SGN-35) induced multiple objective responses in patients with relapsed or refractory CD30-positive lymphomas in a phase 1 weekly dosing study

Blood, 114 (2009)

Abstract 2731

Google Scholar ↗

[58] R. Chen, A.K. Gopal, S.E. Smith, S.M. Ansell, J.D. Rosenblatt, R. Klasa, J.M. Connors, A. Engert, E.K. Larsen, D.A. Kennedy, E.L. Sievers, A. Younes

Results of a pivotal phase 2 study of brentuximab vedotin (SGN-35) in patients with relapsed or refractory Hodgkin lymphoma

Blood, 116 (2010)

Abstract 283

Google Scholar ↗

[59] R.W. Chen, A.K. Gopal, S.E. Smith, S.M. Ansell, J.D. Rosenblatt, K.J. Savage, J.M. Connors, A. Engert, E.K. Larsen, D.A. Kennedy, E.L. Sievers, A. Younes

Results from a pivotal phase II study of brentuximab vedotin (SGN-35) in patients with relapsed or refractory Hodgkin lymphoma (HL)

J. Clin. Oncol., 29 (Suppl. 1) (2011)

DAC EX. 2040 IPR2022-01531 Page 1055 of 1299

Abstract 8031

Google Scholar ↗

[60] S. Webb

Pharma interest surges in antibody drug conjugates

Nat. Biotechnol., 29 (2011), pp. 297-298

Crossref ↗ View in Scopus ↗ Google Scholar ↗

Cited by (0)

View Abstract

Copyright © 2012 Elsevier B.V. All rights reserved.

ELSEVIER

All content on this site: Copyright © 2024 Elsevier B.V., its licensors, and contributors. All rights are reserved, including those for text and data mining, AI training, and similar technologies. For all open access content, the Creative Commons licensing terms apply.

RELX™

Appendix CASI02

Journal of Controlled Release 161 (2012) 422–428

Contents lists available at SciVerse ScienceDirect

Journal of Controlled Release

journal homepage: www.elsevier.com/locate/jconrel

Review

Antibody–drug conjugates: Basic concepts, examples and future perspectives

Giulio Casi [a], Dario Neri [b,*]

[a] Philochem AG, Libernstrasse 3, CH-8112 Otelfingen, Switzerland
[b] Department of Chemistry and Applied Biosciences, Swiss Federal Institute of Technology (ETH Zürich), Wolfgang-Pauli-Strasse 10, CH-8093 Zürich, Switzerland

ARTICLE INFO

Article history:
Received 30 October 2011
Accepted 19 January 2012
Available online 28 January 2012

Keywords:
Antibody–drug conjugates
Non-internalizing monoclonal antibodies
Traceless linkers

ABSTRACT

Conventional anticancer therapeutics often suffer from lack of specificity, resulting in poor therapeutic indexes and substantial toxicities to normal healthy tissues. Monoclonal antibodies have demonstrated considerable utility in cancer medicine, but their curative potential is often limited. Antibody–drug conjugates represent an innovative therapeutic approach that combines the desirable properties of monoclonal antibodies, with the cell killing activity of cytotoxic drugs, reducing systemic toxicity and increasing the therapeutic benefit for patients.

In this review, we outline prominent examples of early and recent antibody–drug conjugates, discussing drugs, linker chemistries and classes of targets for product development.

© 2012 Elsevier B.V. All rights reserved.

Contents

1. Antibody–drug conjugates (ADCs): general considerations and historical perspectives . . . 422
2. Internalizing vs. non-internalizing ADCs . . . 423
3. Drug release strategies for ADCs . . . 423
4. Representative ADCs at different stages of clinical development . . . 424
5. Concluding remarks . . . 426
Competing interests statement . . . 426
References . . . 426

1. Antibody–drug conjugates (ADCs): general considerations and historical perspectives

Monoclonal antibodies (mAbs) have led to the development of approved biopharmaceutical products in many therapeutic areas, including cardiovascular diseases, infection, immune disorders and cancer [1]. At present, the last two therapeutic fields dominate both in terms of sales and number of antibody products in industrial development. However, with few exceptions, the curative potential of "naked" immunoglobulins is limited and it is not surprising that large research efforts are being devoted to the "arming" of monoclonal antibodies with bioactive payloads (e.g., drugs, cytokines, radionuclides) [2].

Cytotoxic agents often display little selectivity and substantial toxicity to normal tissues. Considerable efforts have been invested for combining the desirable properties of monoclonal antibodies with the cell killing activity of cytotoxic drugs, reducing systemic toxicity and increasing the therapeutic benefit for patients [2–5].

Although the concept of antibody–drug conjugates (ADCs) appears simple, the development of efficacious products often represents a considerable challenge. Many parameters have to be optimized for a successful ADC product, some of which are specific to individual tumor types. These include ADC stability (the drug should not be released before the ADC reaches its target *in vivo*), pharmacokinetics (the drug should not confer an undesired accumulation in a non-target organ), retention of immunoreactivity, and efficient release of the active form of the drug at site of disease.

Early work on ADCs relied on clinically approved chemotherapeutic drugs with the aim to increase tumor specificity. Initially this strategy took advantage of readily available drugs with known toxicity profiles. However, many other parameters related to ADC development, such as the choice of mAb, drug loading and potency, as well as release mechanisms were not immediately considered as crucial determinants, for the success of ADC strategies.

A prominent example of this first-generation ADCs is represented by BR96-doxorubicin [6]. This immunoconjugate consists of a chimeric mAb directed against the Lewis^Y tetra-saccharide commonly expressed on human carcinomas, modified with eight molecules of doxorubicin conjugated to the hinge cysteines. Doxorubicin is a DNA intercalator

* Corresponding author.
E-mail address: Dario.Neri@pharma.ethz.ch (D. Neri).

0168-3659/$ – see front matter © 2012 Elsevier B.V. All rights reserved.
doi:10.1016/j.jconrel.2012.01.026

approved for the treatment of a broad range of tumors [7]. Drug release was engineered through an acid-labile hydrazone linker. Upon binding of the ADC to the cell surface antigens, the conjugate would be internalized inside cells, and doxorubicin released within the acidic endosomal and lysosomal vesicles. Treatment of tumor-bearing mice and rats with BR96-doxorubicin led to cures in tumors, which displayed the cognate antigen. Doses in excess of 100 mg/kg were used, reflecting the low potency of the targeted drug [6]. A phase I clinical trial confirmed the ability of the immunoconjugate to deliver doxorubicin to the tumor cells. The maximum tolerated dose (MTD) of BR96-doxorubicin was found to be approximately 700 mg/m^2. Despite higher total serum levels of doxorubicin (i.e. free doxorubicin plus doxorubicin bound to the antibody) were achieved compared to an intravenous administration of the unmodified drug, dose-limiting toxicities were not the same as conventional doxorubicin-related adverse events. Indeed, serum levels of free doxorubicin were below the detection limit in all patients assessed [8]. A subsequent randomized phase II trial on a population with confirmed sensitivity to doxorubicin revealed that the toxicities might have been of gastrointestinal origin, due to normal gut expression of Lewis^Y [9]. In both trials little antitumor activity was observed. Therefore, the normal tissue cross-reactivity of BR96 and the low molar potency of doxorubicin represented clear limitations for the industrial development of BR96-doxorubicin. In addition, the discrepancy between hydrazone stability ($t_{1/2} \approx$ 43h) and pharmacokinetic terminal half-life of the BR96 antibody (12 days, roughly 7 fold longer than the hydrazone half-life) represented a cause of concern. The development of doxorubicin-based ADC may still continue in the future, since a second ADC loaded with the same drug successfully cured SCID mice at single low doses of immunoconjugate in non-Hodgkin lymphoma tumor model [10]. Moreover novel classes of ADCs produced with hydrazone technology are currently in advanced stages of clinical trials for non-Hodgkin lymphoma [11], confirming that the combination antibody–drug-linker has to be properly investigated on a case-to-case basis.

Today ADCs are developed starting from mAbs that selectively bind to tumors and display little cross-reactivity with healthy tissues. Moreover, the appropriate mAb format may have to be selected in order to tune ADC tumor uptake and blood clearance properties with linker stability and drug release, thus minimizing the exposure of healthy organs to toxic agents [12]. Since the total amount of ADC which can be realistically administered to patients is limited by cost-of-goods, and since coupling of too many drug molecules may lead to a loss of potency [13], (i.e., compromised binding ability and pharmacokinetic properties) more effective drugs became necessary for the industrial development of next-generation ADC. The requirement for potent bioactive molecules is also a consequence of the inefficient localization of mAbs at the tumor site. Typically, a maximum of 0.08% injected dose per gram of tumor accumulates in human malignancies. This is due to the increased interstitial fluid pressure (IFP) in the tumor environment, which represents a barrier to the extravasation and diffusion of antibodies [14]. The use of different signal transduction antagonists (e.g. PGE_1, VEGF and PGDF, TGFß) or of pro-inflammatory cytokines that lower tumor IFP has, in some cases led to an improved anticancer activity [15].

Recognizing the value of drug choice in ADC development, several programs were started in parallel in the late 1990s, with the aim to identify more potent drugs for ADC application. Here it is worth mentioning calicheamicins, [16] maytansinoids, [3] auristatins, [2] and CC1065 analogs [17], since these classes of potent cytotoxics represent the "backbone" of current industrial development programs.

Finally, the choice of cleavable linkers is crucial for the performance of ADC strategies. Depending on the drug delivery mechanism selected, the active form of the cytotoxic agent may be released more or less efficiently inside the target cell.

2. Internalizing vs. non-internalizing ADCs

Targeted antitumor therapy takes advantage of specific molecular differences between healthy and diseased tissues. So far, most efforts have been devoted to the targeting of tumor-associated antigens expressed on the surface of cancer cells [4] (Fig. 1, right) (Table 1) This class of ADC products typically requires mAbs that are internalized inside cells by receptor-mediated endocytosis. Different chemical mechanisms may allow the subsequent drug release, as described in the next section. The use of internalizing ADC is at the basis of products that are either approved or in advanced stages of clinical trials. However, targeting antigens on tumor cells is a complex task, due to a number of physical and kinetic barriers associated with large solid tumors, and to the potential down-regulation of tumor-associated antigens targeted by the immunoconjugate, as each cell has to express the target antigen in order to be reached by the cytotoxic agent.

An alternative approach has been developed that targets markers expressed on tumor neo-vasculature (Fig. 1, left). This strategy is compatible with the use of non-internalizing antibodies [18,19]. Vascular targets are more easily accessible from the blood stream compared to systemically administered agents. Tumors require blood supply for their growth and neoplastic capillaries are significantly different at the molecular level from normal healthy vasculature. Remarkably, since angiogenesis is a common feature of all malignancies and tumors express common markers of angiogenesis, a single agent should in principle be applicable to a wide range of tumor entities [18,19]. In particular, markers of angiogenesis, found in the subendothelial extracellular matrix (ECM), are more stable compared to cellular antigens and facilitate an antibody residence time of days/weeks. The potential of targeting antigens expressed on tumor neo-vasculature has been confirmed in pre-clinical and clinical applications [20].

Endothelial cells (EC) are readily accessible from the blood stream. Anti-VEGF mAbs have been shown to have the potential to localize at tumor sites *in vivo* [21]. However, this strategy is hardly compatible with non-internalizing antibodies, as the released drug would enter the bloodstream. Alternatively, subendothelial modified ECM components may serve as target for ADCs, which do not require internalization for their activity. Upon extravasation, a specific mAb product comes into contact with more abundant and stable antigens, thus ensuring a long residence time of ADC at the tumor site. Work in this area has been performed with the human mAb (L19), specific to the extra-domain B (EDB) of fibronectin, a marker of angiogenesis. EDB is normally not present in the healthy protein, but is inserted during active tissue remodeling by alternative splicing, and is highly abundant in many aggressive solid tumors. L19 fused to different effector molecules is currently in multiple stages of clinical development [22]. In addition, we have recently started the use of oncofetal fibronectin as a target for ADC development [23].

3. Drug release strategies for ADCs

Specific linkers are designed to append toxic payloads to mAbs and to allow a selective drug release at the tumor site. Linkers differ in terms of plasma stability and in the mechanism of release. Acid-labile hydrazone linkers have been employed in the first class of ADCs developed (Table 2, entries 1, 4) [6,31–33]. Hydrazones are preferentially cleaved within intracellular lysosomes and endosomes, as a consequence of the lower pH found in these environments (pH $\approx$ 5).

Disulfides (Table 2, entry 2) have been extensively exploited as ADC linkers since they are stable at physiological pH and release their payload upon internalization inside cells, where the cytosol provides a significantly more reducing environment compared to the extracellular milieu [34]. Several *in vitro* and *in vivo* studies have been performed to establish the effect of increasing substitution at disulfides in the pharmacokinetic and toxicity profiles of different ADCs [3,25]. Two classes of calicheamicin–antibody conjugates containing

DAC EX. 2040 IPR2022-01531 Page 1059 of 1299

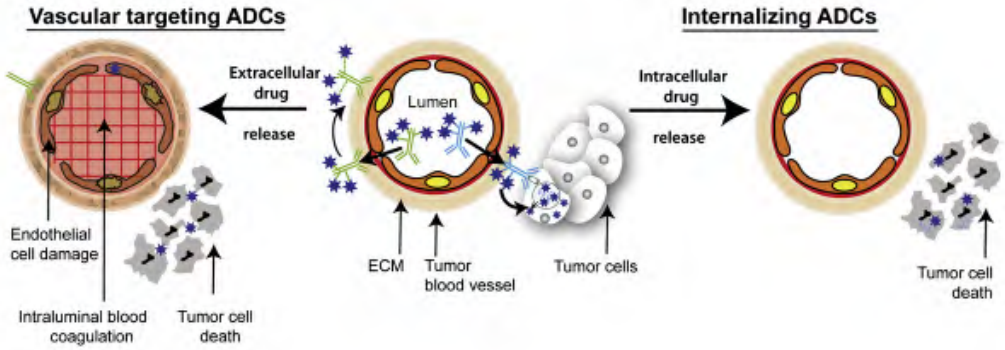


Fig. 1. Antibody–drug conjugates (ADC) and their effect. (*Right*) Tumor cell death induced by internalizing ADCs (blue). Upon ADC internalization inside tumor cells, the active drug is released and leads to tumor cell death. (*Left*) Effect of tumor targeting ADCs specific to markers of angiogenesis expressed on the endothelial extracellular matrix (green). The long residence time of vascular targeting ADCs allows the localized drug release, leading to intravascular blood coagulation, and to an avalanche of tumor cell death.

both disulfide linkers were tested in different tumor models. An additional hydrolyzable hydrazone group was present in a subgroup of the ADCs, and allowed direct comparison between the two linkers.

In an ADC based on the CTM01 antibody (where CTM01 is a murine IgG1 that recognizes MUC1 antigen present on a broad spectrum of solid tumors), the additional hydrazone was not necessary for activity [35]. Surprisingly, when the Anti-CD33 P67.6 antibody was used for ADC development, the disulfide moiety in the linker was insufficient for the proper release of calicheamicin, while the hydrazone moiety was essential [33].

Alternative linker strategies rely on "non-cleavable" linkers and take advantage of the catabolic degradation of internalized antibodies in the lysosomal and endosomal compartments. ADCs that consist of either peptide bonds, or of chemical bonds normally stable under physiologic conditions, rely in the statistical proteolytic degradation of the conjugate [25,36] (Table 2, entries 3, 6). In a series of disulfide-linked ADCs for the intracellular release of cytotoxic drugs, it was surprisingly found that a Trastuzumab-DM1 control conjugate in which the disulfide was replaced with a non-cleavable thioether bond, was the most effective ADC variant in *in vivo* therapy tests [25]. Thus, while cleavable disulfide linkers are often associated with ADC activity, the precise choice of the most active linker chemistry requires the screening of several candidates, including non-cleavable linkers which may release drug only after a proteolytic digestion of the antibody molecule [37].

Alternatively protease-specific sequences introduced in the linker control the hydrolytic process, as reported for the lysosome abundant protease cathepsin B [24,38] (Table 2, entry 5). This approach was confirmed to be superior to the hydrolytically labile hydrazone linker both in terms of specificity and toxicity in a series of monomethyl-auristatins (MMAE) conjugated to cBR96 mAb [24].

Most ADC manufacturing processes exploit the chemical modification of the primary amino group of lysine residues or of the thiol group of cysteines. The different abundance of the two residues is reflected also in the complexity of the heterogeneous mixture generated [39]. When the release technology relies on statistical proteolysis, traces of the modified amino acids might be found in the active released form of the drug (Table 2, entries 3, 6).

In the examples described so far, bifunctional linkers feature one moiety for conjugation of the drug to the mAb, and one moiety for drug release.

Traceless linkers eliminate this distinction since coupling and release chemistry are identical (Table 2) We have recently described an innovative linker technology that relies on the site-specific coupling and release of cytotoxic drugs from thiazolidines. The linker, generated upon reaction of aldehydes with 1,2-aminothiol moieties on the antibody, is stable for synthesis, and allows the hydrolytic drug release under physiological conditions. The release process is traceless as it restores the free drug, and the intact antibody (Table 3, entry 1) [40]. Alternatively cysteines introduced in mAb sequences by site directed mutagenesis afford site-specific disulfide linkages with thiol–drugs (Table 3, entry 2) [23].

Disulfides based linkers may find ADC applications also with non-internalizing antibodies. Indeed, the localization of these ADCs at the tumor ECM could expose the disulfide linkage to reducing agents (cysteine, glutathione) initially released by dying cells and progressively amplified by drug-mediated cell killing.

Remarkably, in these two last examples, the release process restores the original antibody and the active drug, which simplifies drug manufacturing and should diminish ADC immunogenicity.

Table 1
Selected examples of intracellular, ECM and vascular targets used in ADC development.

	Antigen	Reference
Tumor cells	CD30	[24]
	Can Ag	[3]
	HER2	[25]
	CD22	[26]
ECM	Fibronectin(EDA:EDB)	[27,28]
	Tenascin-C(A1)	[29]
	Periostin	[30]
EC	Integrins	[19]
	PSMA	[19]
	VEGFR-2	[19]

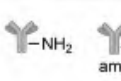
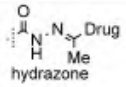
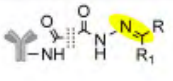
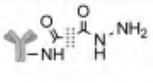
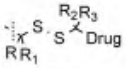
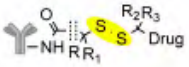
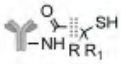
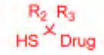
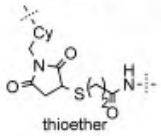
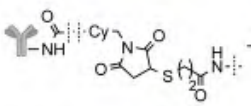
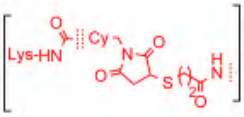
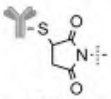
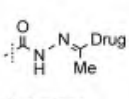
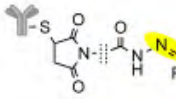
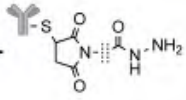
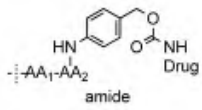
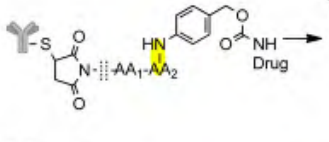
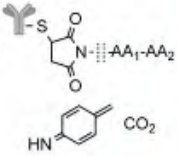
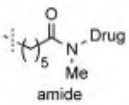
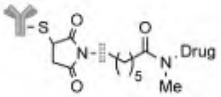
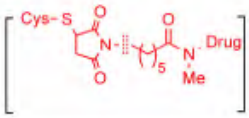
4. Representative ADCs at different stages of clinical development

Mylotarg was the first ADC ever approved in the US. The product had an indication for the treatment of acute myeloid leukemia (AML) in patients older than 60 not eligible for other chemotherapies. The ADC consisted of a humanized anti-CD33 mAb (hP67.6) attached to the calicheamicin drug through an acid labile hydrazone linker [41,42] (Fig. 2A).

Calicheamicin derives from the family of enediyne antibiotics extracted from the soil microorganism *Micromonospora echinospora*, and binds in the minor groove of DNA. The highly reactive 1,4-benzenoyl diradical generated by intracellular reduction, caused extensive DNA damage and subsequent cell apoptosis [43,16]. The acid labile hydrazone linker [33] held the two components together and supposedly was cleaved before the sterically hindered disulfide, and thioester moieties. Mylotarg was administered as a 1:1 mixture of unconjugated and conjugated mAb to 4–6 equivalents of drug, with an average drug loading of 2–3 moles of drug to mAb. The drug was approved under FDA's accelerated approval program based on a response rate

DAC EX. 2040 IPR2022-01531 Page 1060 of 1299

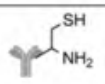
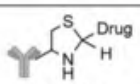
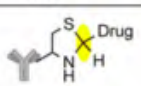
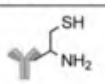
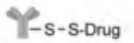
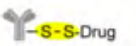
Table 2
Representative examples of ADC chemistries. Current ADC assembly strategies rely on bifunctional linkers. Specific release processes are responsible for active drug release. Selective scissile bonds are highlighted in yellow. The postulated active form of the released drug is depicted in red. R_i = H, Me.

	Antibody	Bifunctional linkers		Release process				Ref
		mAb side	Drug side	ADC	Residual linkers	Drug release	Mechanism	
1		amide	 hydrazone				hydrolysis	[33]
2			 disulfide				reduction	[3, 25]
3			 thioether				statistical proteolysis	[25]
4		 thioether	 hydrazone				hydrolysis	[6]
5			 amide				site-specific proteolysis	[26, 38]
6			 amide				statistical proteolysis	[36]

of about 30% [44]. However, it failed to confirm therapeutic benefits (i.e., higher response rates) to AML patients in clinical trials, when administered in combination with chemotherapy. Indeed a greater number of deaths occurred in the group of patients receiving Mylotarg, compared to those receiving chemotherapy. Potentially, the veno-occlusive disease observed at initial approval, worsened in the post marketing setting, causing fatalities to increase. The product was voluntarily withdrawn in June 2010 (http://www.fda.gov/NewsEvents/Newsroom/PressAnnouncements/ucm216448.htm)

Trastuzumab-DM1 (T-DM1) is an ADC currently in advanced stage clinical trials designed for the treatment of Her2-positive metastatic breast cancer. T-DM1 consists of the approved anti-Her2-mAb Trastuzumab (Herceptin) directly conjugated to DM1, via a non-cleavable thioether linker present in an N-maleimido cyclohexane-1-carboxylate group (also named MCC) (Fig. 2B). Herceptin has been introduced in the market in 1998 for Her2+ breast cancer, and showed clinical benefits in combination with chemotherapy as first line or adjuvant therapy [45,46]. Despite these objective results, part of the patients treated either did not respond initially, or relapsed [47]. DM1 is a maytansinoid derivative, binds directly to microtubules and inhibits their assembly with consequent apoptosis, similar to what was observed for the *Vinca* alkaloids [48,49]. T-DM1

Table 3
Recent examples of linkerless ADC assembly. The cleavage process restores the unmodified antibody and the drug used for ADC development. Scissile bonds are highlighted in yellow. The postulated active form of the released drug is depicted in red.

	Antibody	Traceless linkers	Release process				Ref
			ADC	Residual linkers	Drug release	Mechanism	
1		 thiazolidine				hydrolysis	[32]
2		 disulfide			HS-Drug	reduction	[22]

DAC EX. 2040 IPR2022-01531 Page 1061 of 1299

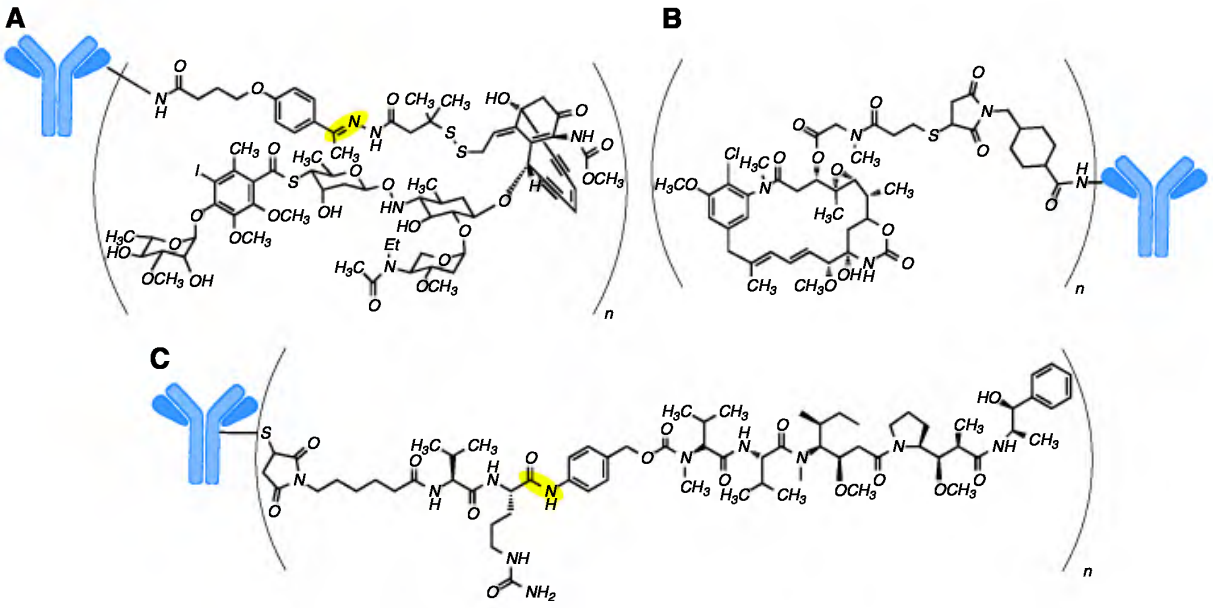


Fig. 2. Structures of selected ADCs used in cancer therapy. Mylotarg (A), T-DM1 (B), ADCETRIS™ (C). Scissile bonds are highlighted in yellow.

undergoes cell internalization and complete lysosomal proteolysis [25] and, in analogy to what has been reported for huC242-MCC-DM1 [50], (huC242 is a humanized antibody with high affinity for the carbohydrate antigen CanAg) the major active drug metabolite is believed to be the weakly membrane permeable Lys-MCC-DM1 (Table 2, entry 3).

T-DM1 carries an average of 3.5 molecules of DM1/mAb and is now used in clinical trials on heavily pre-treated patients, including Trastuzumab. A phase I dose escalation study showed partial responses in 25% of the patients when treated with doses starting from 0.3 mg/kg and going up to 4.8 mg/kg [51]. More remarkably in a phase II trial, third-line metastatic breast cancer showed a 33% objective response rate in 110 patients treated with 3.6 mg/kg T-DM1 every 3 weeks [52]. Moreover T-DM1 was well tolerated by patients with no cardiovascular toxicities. For these impressive results, approval of T-DM1 is expected in 2012, even though the FDA has refused a Biologics License Application submitted in July 2010 for accelerated approval.

In July 2011 brentuximab vedotin (SGN-35, Adcetris) was approved by the FDA for the treatment of patients with Hodgkin lymphoma after failure of autologous stem cell transplant, and for patients with systemic anaplastic large cell lymphoma after failure of at least one prior multi-agent chemotherapy regimen (http://www.fda.gov/NewsEvents/Newsroom/PressAnnouncements/ucm268781.htm) In SGN-35 an anti-CD30 monoclonal antibody is attached through a cathepsin-B cleavable valine-citrulline dipeptide (Val-Cit) to an average of 4 monomethyl auristatin E (MMAE) molecules (Fig. 2C). MMAE drugs are structurally related to dolastatin 10 and afford a potent antitumor activity by inhibiting tubulin polymerization [2,53]. The conjugation occurs between reduced anti-CD30 mAb and maleimido containing MMAE to form 4 thioether linkers. The ADC generated is highly homogenous and stable (half life 6 and 9.6 days in mice and monkeys) [24]. Upon binding to CD30 on the cell surface, SGN-35 is internalized, and digested inside lysosomes. Drug release begins with the selective proteolysis of the Val-Cit linker catalyzed by cathepsin-B. Following proteolytic cleavage, 1,6-elimination of the p-aminobenzyl ester group affords the unmodified drug (Table 2, entry 5) [38,54,55]. A phase I clinical trial showed tumor regressions in about 93% of treated patients, and 56% objective response rates [56,57]. A single arm phase II study for Hodgkin lymphoma on 102 patients treated with SGN-35 showed 75% objective responses and 34% complete responses [58,59]. The drug was approved under FDA's accelerated approval program, based on objective response rates (http://www.fda.gov/NewsEvents/Newsroom/PressAnnouncements/ucm268781.htm)

5. Concluding remarks

The area of ADC development is in rapid expansion, with large investments being made by pharmaceutical companies [60]. At present, maytansinoids and auristatins are the most frequently used drugs for ADC developments. Since ADC, at some stage, are cleared from circulation (either via the renal route or the hepatobiliary route) it is probable that future research efforts will closely evaluate therapeutic candidates not only on the basis of their tumor toxicity, but also in terms of the side-effects associated to the ADC excretion process. The complex pharmacokinetic profiles and the high cost of goods for ADC will be justified if the therapeutic performance is sufficiently good and if the disease is a severe one. In principle, advantages such as the drug release at site of disease should lead to a reduced systemic toxicity and to higher therapeutic indexes, compared to non-targeted drugs.

In the future, we envisage that novel linkers chemistry (including traceless linkers) and non-internalizing antibodies will expand the repertoire of tools for ADC development.

Competing interests statement

Giulio Casi is employed at Philochem AG.
Dario Neri is a co-founder and shareholder of Philogen SpA.

References

[1] A.L. Nelson, E. Dhimolea, J.M. Reichert, Development trends for human monoclonal antibody therapeutics, Nat. Rev. Drug Discov. 9 (2010) 767–774.
[2] A.M. Wu, P.D. Senter, Arming antibodies: prospects and challenges for immunoconjugates, Nat. Biotechnol. 23 (2005) 1137–1146.
[3] R.V.J. Chari, Targeted cancer therapy: Conferring specificity to cytotoxic drugs, Acc. Chem. Res. 41 (2008) 98–107.
[4] P.D. Senter, Potent antibody drug conjugates for cancer therapy, Curr. Opin. Chem. Biol. 13 (2009) 235–244.

DAC EX. 2040 IPR2022-01531 Page 1062 of 1299

[5] S.C. Alley, N.M. Okeley, P.D. Senter, Antibody–drug conjugates: targeted drug delivery for cancer, Curr. Opin. Chem. Biol. 14 (2010) 529–537.
[6] P.A. Trail, D. Willner, S.J. Lasch, A.J. Henderson, S. Hofstead, A.M. Casazza, R.A. Firestone, I. Hellström, K.E. Hellström, Cure of xenografted human carcinomas by BR96-doxorubicin immunoconjugates, Science 261 (1993) 212–215.
[7] G.M. Dubowchik, M.A. Walker, Receptor-mediated and enzyme-dependent targeting of cytotoxic anticancer drugs, Pharmacol. Ther. 83 (1999) 67–123.
[8] M.N. Saleh, S. Sugarman, J. Murray, J.B. Ostroff, D. Healey, D. Jones, C.R. Daniel, D. LeBherz, H. Brewer, N. Onetto, A.F. LoBuglio, Phase I trial of the anti-Lewis Y drug immunoconjugate BR96-doxorubicin in patients with Lewis Y-expressing epithelial tumors, J. Clin. Oncol. 18 (2000) 2282–2292.
[9] A.W. Tolcher, S. Sugarman, K.A. Gelmon, R. Cohen, M. Saleh, C. Isaacs, L. Young, D. Healey, N. Onetto, W. Slichenmyer, Randomized phase II study of BR96-doxorubicin conjugate in patients with metastatic breast cancer, J. Clin. Oncol. 17 (1999) 478–484.
[10] G.L. Griffiths, M.J. Mattes, R. Stein, S.V. Govindan, I.D. Horak, H.J. Hansen, D.M. Goldenberg, Cure of SCID mice bearing human B-lymphoma xenografts by an Anti-CD74 antibody–anthracycline drug conjugate, Clin. Cancer Res. 9 (2003) 6567–6571.
[11] A.G. Polson, W.Y. Ho, V. Ramakrishnan, Investigational antibody–drug conjugates for hematological malignancies, Expert Opin. Investig. Drugs 20 (2011) 75–85.
[12] P.J. Carter, Potent antibody therapeutics by design, Nat. Rev. Immunol. 6 (2006) 343–357.
[13] K.J. Hamblett, P.D. Senter, D.F. Chace, M.M.C. Sun, J. Lenox, C.G. Cerveny, K.M. Kissler, S.X. Bernhardt, A.K. Kopcha, R.F. Zabinski, D.L. Meyer, J.A. Francisco, Effects of drug loading on the antitumor activity of a monoclonal antibody drug conjugate, Clin. Cancer Res. 10 (2004) 7063–7070.
[14] C.H. Heldin, K. Rubin, K. Pietras, A. Östman, High interstitial fluid pressure—an obstacle in cancer therapy, Nat. Rev. Cancer 4 (2004) 806–813.
[15] H.H. Sedlacek, G. Seemann, D. Hoffmann, J. Czech, P. Lorenz, C. Kolar, K. Bosslet, Antibodies as carriers of cytotoxicity, vol. 43, Karger AG, Munich, Germany, 1992.
[16] N.K. Damle, P. Frost, Antibody-targeted chemotherapy with immunoconjugates of calicheamicin, Curr. Opin. Pharmacol. 3 (2003) 386–390.
[17] R.V.J. Chari, K.A. Jackel, L.A. Bourret, S.M. Derr, B.M. Tadayoni, K.M. Mattocks, S.A. Shah, C.N. Liu, W.A. Blättler, V.S. Goldmacher, Enhancement of the selectivity and antitumor efficacy of a CC-1065 analogue through immunoconjugate formation, Cancer Res. 55 (1995) 4079–4084.
[18] C. Schliemann, D. Neri, Antibody-based targeting of the tumor vasculature, BBA: Rev. Cancer 1776 (2007) 175–192.
[19] H.-P. Gerber, P.D. Senter, I.S. Grewal, Antibody drug-conjugates targeting the tumor vasculature. Current and future developments, MAbs 1 (2009) 247–253.
[20] A. Palumbo, F. Hauler, P. Dziunycz, K. Schwager, A. Soltermann, F. Pretto, C. Alonso, G.F. Hofbauer, R.W. Boyle, D. Neri, A chemically modified antibody mediates complete eradication of tumours by selective disruption of tumour blood vessels, Br. J. Cancer 104 (2011) 1106–1115.
[21] T.H. Stollman, M.G.W. Scheer, W.P.J. Leenders, K.C.N. Verrijp, A.C. Soede, W.J.G. Oyen, T.J.M. Ruers, O.C. Boerman, Specific imaging of VEGF-A expression with radiolabeled anti-VEGF monoclonal antibody, Int. J. Cancer 122 (2008) 2310–2314.
[22] A. Menrad, H.D. Menssen, ED-B fibronectin as a target for antibody-based cancer treatments, Expert Opin. Ther. Targets 9 (2005) 491–500.
[23] G.J.L. Bernardes, G. Casi, I. Hartmann, S. Trüssel, K. Schwager, J. Scheuermann, D. Neri, A traceless vascular-targeting antibody–drug conjugate for cancer therapy, Angew. Chem. Int. Ed. 51 (2012) 941–944.
[24] S.O. Doronina, B.E. Toki, M.Y. Torgov, B.A. Mendelsohn, C.G. Cerveny, D.F. Chace, R.L. DeBlanc, R.P. Gearing, T.D. Bovee, C.B. Siegall, J.A. Francisco, A.F. Wahl, D.L. Meyer, P.D. Senter, Development of potent monoclonal antibody auristatin conjugates for cancer therapy, Nat. Biotechnol. 21 (2003) 778–784.
[25] G.D.L. Phillips, G. Li, D.L. Dugger, L.M. Crocker, K.L. Parsons, E. Mai, W.A. Blättler, J.M. Lambert, R.V.J. Chari, R.J. Lutz, W.L.T. Wong, F.S. Jacobson, H. Koeppen, R.H. Schwall, S.R. Kenkare-Mitra, S.D. Spencer, M.X. Sliwkowski, Targeting HER2-positive breast cancer with trastuzumab-DM1, an antibody–cytotoxic drug conjugate, Cancer Res. 68 (2008) 9280–9290.
[26] J.F. DiJoseph, M.M. Dougher, D.Y. Evans, B.-B. Zhou, N.K. Damle, Preclinical anti-tumor activity of antibody-targeted chemotherapy with CMC-544 (inotuzumab ozogamicin), a CD22-specific immunoconjugate of calicheamicin, compared with non-targeted combination chemotherapy with CVP or CHOP, Cancer Chemother. Pharmacol. 67 (2011) 741–749.
[27] A. Villa, E. Trachsel, M. Kaspar, C. Schliemann, R. Sommavilla, J.-N. Rybak, C. Rösli, L. Borsi, D. Neri, A high-affinity human monoclonal antibody specific to the alternatively spliced EDA domain of fibronectin efficiently targets tumor neovasculature in vivo, Int. J. Cancer 122 (2008) 2405–2413.
[28] A. Pini, F. Viti, A. Santucci, B. Carnemolla, L. Zardi, P. Neri, D. Neri, Design and use of a phage display library—human antibodies with subnanomolar affinity against a marker of angiogenesis eluted from a two-dimensional gel, J. Biol. Chem. 273 (1998) 21769–21776.
[29] S.S. Brack, M. Silacci, M. Birchler, D. Neri, Tumor-targeting properties of novel antibodies specific to the large isoform of tenascin-C, Clin. Cancer Res. 12 (2006) 3200–3208.
[30] V. Castronovo, D. Waltregny, P. Kischel, C. Roesli, G. Elia, J.N. Rybak, D. Neri, A chemical proteomics approach for the identification of accessible antigens expressed in human kidney cancer, Mol. Cell. Proteomics 5 (2006) 2083–2091.
[31] R.L. Reeves, Condensations Leading to Double Bonds, in: S. Patai (Ed.), The chemistry of the carbonyl group, Interscience Publisher, New York, 1966, pp. 567–619.
[32] . G.R. Braslawsky, M.A. Edson, W. Pearce, T. Kaneko, R.S. Greenfield, Antitumor activity of adriamycin (hydrazone-linked) immunoconjugates compared with free adriamycin and specificity of tumor cell killing, Cancer Res. 50 (1990) 6608–6614.
[33] P.R. Hamann, L.M. Hinman, C.F. Beyer, D. Lindh, J. Upeslacis, D.A. Flowers, I. Bernstein, An anti-CD33 antibody-calicheamicin conjugate for treatment of acute myeloid leukemia. Choice of linker, Bioconjug. Chem. 13 (2002) 40–46.
[34] A. Meister, M.E. Anderson, Glutathione, Annu. Rev. Biochem. 52 (1983) 711–760.
[35] P.R. Hamann, L.M. Hinman, C.F. Beyer, D. Lindh, J. Upeslacis, D. Shochat, A. Mountain, A calicheamicin conjugate with a fully humanized anti-MUC1 antibody shows potent antitumor effects in breast and ovarian tumor xenografts, Bioconjug. Chem. 16 (2005) 354–360.
[36] S.O. Doronina, B.A. Mendelsohn, T.D. Bovee, C.G. Cerveny, S.C. Alley, D.L. Meyer, E. Oflazoglu, B.E. Toki, R.J. Sanderson, R.F. Zabinski, A.F. Wahl, P.D. Senter, Enhanced activity of monomethylauristatin F through monoclonal antibody delivery: effects of linker technology on efficacy and toxicity, Bioconjug. Chem. 17 (2006) 114–124.
[37] A.G. Polson, J. Calemine-Fenaux, P. Chan, W. Chang, E. Christensen, S. Clark, F.J. de Sauvage, D. Eaton, K. Elkins, J.M. Elliott, G. Frantz, R.N. Fuji, A. Gray, K. Harden, G.S. Ingle, N.M. Kljavin, H. Koeppen, C. Nelson, S. Prabhu, H. Raab, S. Ross, D.S. Slaga, J.-P. Stephan, S.J. Scales, S.D. Spencer, R. Vandlen, B. Wranik, S.-F. Yu, B. Zheng, A. Ebens, Antibody–drug conjugates for the treatment of non-Hodgkin's lymphoma: target and linker-drug selection, Cancer Res. 69 (2009) 2358–2364.
[38] G.M. Dubowchik, K. Mosure, J.O. Knipe, R.A. Firestone, Cathepsin B-sensitive dipeptide prodrugs. 2. Models of anticancer drugs paclitaxel (Taxol ®), mitomycin C and doxorubicin, Bioorg. Med. Chem. Lett. 8 (1998) 3347–3352.
[39] J.R. Junutula, H. Raab, S. Clark, S. Bhakta, D.D. Leipold, S. Weir, Y. Chen, M. Simpson, S.P. Tsai, M.S. Dennis, Y. Lu, Y.G. Meng, C. Ng, J. Yang, C.C. Lee, E. Duenas, J. Gorrell, V. Katta, A. Kim, K. McDorman, K. Flagella, R. Venook, S. Ross, S.D. Spencer, W.L. Wong, H.B. Lowman, R. Vandlen, M.X. Sliwkowski, R.H. Scheller, P. Polakis, W. Mallet, Site-specific conjugation of a cytotoxic drug to an antibody improves the therapeutic index, Nat. Biotechnol. 26 (2008) 925–932.
[40] G. Casi, Protein–drug conjugates, PCT/EP2011/004664, , 2010 (pending).
[41] P.F. Bross, J. Beitz, G. Chen, X.H. Chen, E. Duffy, L. Kieffer, S. Roy, R. Sridhara, A. Rahman, G. Williams, R. Pazdur, Approval summary: gemtuzumab ozogamicin in relapsed acute myeloid leukemia, Clin. Cancer Res. 7 (2001) 1490–1496.
[42] P.R. Hamann, L.M. Hinman, I. Hollander, C.F. Beyer, D. Lindh, R. Holcomb, W. Hallett, H.R. Tsou, J. Upeslacis, D. Shochat, A. Mountain, D.A. Flowers, I. Bernstein, Gemtuzumab ozogamicin, a potent and selective anti-CD33 antibody–calicheamicin conjugate for treatment of acute myeloid leukemia, Bioconjug. Chem. 13 (2002) 47–58.
[43] N. Zein, A.M. Sinha, W.J. McGahren, G.A. Ellestad, Calicheamicin γ_1^I—an antitumor antibiotic that cleaves double-stranded DNA site specifically, Science 240 (1988) 1198–1201.
[44] R.A. Larson, M. Boogaerts, E. Estey, C. Karanes, E.A. Stadtmauer, E.L. Sievers, P. Mineur, J.M. Bennett, M.S. Berger, C.B. Eten, M. Munteanu, M.R. Loken, J.J.M. van Dongen, I.D. Bernstein, F.R. Appelbaum, Antibody-targeted chemotherapy of older patients with acute myeloid leukemia in first relapse using Mylotarg (gemtuzumab ozogamicin), Leukemia 16 (2002) 1627–1636.
[45] D.J. Slamon, B. Leyland-Jones, S. Shak, H. Fuchs, V. Paton, A. Bajamonde, T. Fleming, W. Eiermann, J. Wolter, M. Pegram, J. Baselga, L. Norton, Use of chemotherapy plus a monoclonal antibody against HER2 for metastatic breast cancer that overexpresses HER2, N. Engl. J. Med. 344 (2001) 783–792.
[46] I. Smith, M. Procter, R.D. Gelber, S. Guillaume, A. Feyereislova, M. Dowsett, A. Goldhirsch, M. Untch, G. Mariani, J. Baselga, M. Kaufmann, D. Cameron, R. Bell, J. Bergh, R. Coleman, A. Wardley, N. Harbeck, R.I. Lopez, P. Mallmann, K. Gelmon, N. Wilcken, E. Wist, P. Sànchez Rovira, M. Piccart-Gebhart, 2-year follow-up of trastuzumab after adjuvant chemotherapy in HER2-positive breast cancer: a randomised controlled trial, Lancet 369 (2007) 29–36.
[47] R. Nahta, D.H. Yu, M.C. Hung, G.N. Hortobagyi, F.J. Esteva, Mechanisms of disease: understanding resistance to HER2-targeted therapy in human breast cancer, Nat. Clin. Pract. Oncol. 3 (2006) 269–280.
[48] J.M. Cassady, K.K. Chan, H.G. Floss, E. Leistner, Recent developments in the maytansinoid antitumor agents, Chem. Pharm. Bull. 52 (2004) 1–26.
[49] S. Remillard, L.I. Rebhun, G.A. Howie, S.M. Kupchan, Antimitotic activity of potent tumor inhibitor maytansine, Science 189 (1975) 1002–1005.
[50] H.K. Erickson, P.U. Park, W.C. Widdison, Y.V. Kovtun, L.M. Garrett, K. Hoffman, R.J. Lutz, V.S. Goldmacher, W.A. Blättler, Antibody-maytansinoid conjugates are activated in targeted cancer cells by lysosomal degradation and linker-dependent intracellular processing, Cancer Res. 66 (2006) 4426–4433.
[51] I.E. Krop, M. Beeram, S. Modi, N. Rabbee, S. Girish, J. Tibbitts, S.N. Holden, S.G. Lutzker, H.A. Burris, A phase I study of trastuzumab-DM1, a first-in-class HER2 antibody-drug conjugate, in patients with advanced HER2+ breast cancer, Breast Cancer Res. Treat. 106 (Suppl. 1) (2007) S33.
[52] I. Krop, P. LoRusso, K.D. Miller, S. Modi, D. Yardley, G. Rodriguez, S. Agresta, M. Zheng, L. Amler, H. Rugo, A Phase II Study of trastuzumab-DM1 (T-DM1), a novel HER2 antibody–drug conjugate, in patients previously treated with lapatinib, trastuzumab, and chemotherapy, Cancer Res. 69 (Suppl. 3) (2009) Abstract 710.
[53] M. Otani, T. Natsume, J. Watanabe, M. Kobayashi, M. Murakoshi, T. Mikami, T. Nakayama, TZT-1027, an antimicrotubule agent, attacks tumor vasculature and induces tumor cell death, Jpn. J. Cancer Res. 91 (2000) 837–844.
[54] G.M. Dubowchik, R.A. Firestone, Cathepsin B-sensitive dipeptide prodrugs. 1. A model study of structural requirements for efficient release of doxorubicin, Bioorg. Med. Chem. Lett. 8 (1998) 3341–3346.
[55] B.E. Toki, C.G. Cerveny, A.F. Wahl, P.D. Senter, Protease-mediated fragmentation of p-amidobenzyl ethers: a new strategy for the activation of anticancer prodrugs, J. Org. Chem. 67 (2002) 1866–1872.
[56] A. Younes, A. Forero-Torres, N.L. Bartlett, J.P. Leonard, D.A. Kennedy, E.L. Sievers, Robust antitumor activity of the antibody-drug conjugate SGN-35 when administered every 3 weeks to patients with relapsed or refractory CD30 positive hematologic malignancies in a phase 1 study, Haematologica 94 (Suppl. 2) (2009) 205.

DAC EX. 2040 IPR2022-01531 Page 1063 of 1299

[57] M. Fanale, N.L. Bartlett, A. Forero-Torres, J. Rosenblatt, S.J. Horning, A.R. Franklin, C.M. Lynch, E.L. Sievers, D.A. Kennedy, The antibody–drug conjugate brentuximab vedotin (SGN-35) induced multiple objective responses in patients with relapsed or refractory CD30-positive lymphomas in a phase 1 weekly dosing study, Blood 114 (2009) Abstract 2731.

[58] R. Chen, A.K. Gopal, S.E. Smith, S.M. Ansell, J.D. Rosenblatt, R. Klasa, J.M. Connors, A. Engert, E.K. Larsen, D.A. Kennedy, E.L. Sievers, A. Younes, Results of a pivotal phase 2 study of brentuximab vedotin (SGN-35) in patients with relapsed or refractory Hodgkin lymphoma, Blood 116 (2010) Abstract 283.

[59] R.W. Chen, A.K. Gopal, S.E. Smith, S.M. Ansell, J.D. Rosenblatt, K.J. Savage, J.M. Connors, A. Engert, E.K. Larsen, D.A. Kennedy, E.L. Sievers, A. Younes, Results from a pivotal phase II study of brentuximab vedotin (SGN-35) in patients with relapsed or refractory Hodgkin lymphoma (HL), J. Clin. Oncol. 29 (Suppl. 1) (2011) Abstract 8031.

[60] S. Webb, Pharma interest surges in antibody drug conjugates, Nat. Biotechnol. 29 (2011) 297–298.

DAC EX. 2040 IPR2022-01531 Page 1064 of 1299

Appendix LI01

MARC View

LEADER 01935nas a2200481 a 4500				
001 45924569				
003 SIRSI				
005 20241114090046.0				
006 m o d				
007 cr n				
008 970730c19909999dcumr pss 0 a0eng c				
010				a| sn 98004586
016	7			a| 1500067 9 2| DE-600
019				a| DO NOT EDIT this 360 MARC RECORD
022				a| 1520-4812 l| 1043-1802 y| 1043-1802
035				a| (WaSeSS)ssj0009182
040				a| DLM b| eng e| pn c| DLM d| OCL d| NSD d| IUL d| OCLCQ d| MUQ d| OCLCQ d| GUA d| XBM d| OCLCQ d| NUI d| OCLCQ d| OCLCF d| VT2 d| EUW d| OCLCQ d| GILDS d| AU@ d| AUD d| BWN d| DLC d| OCLCQ d| UAB d| WaSeSS
042				a| nsdp a| pcc
050	0	0		a| QP517.B49
050	1	4		a| QP517
060	0	0		a| W1 b| BI66L
082	1	0		a| 574 2| 13
130	0			a| Bioconjugate chemistry (Online)
210	0			a| Bioconjug. chem. b| (Online)
222			0	a| Bioconjugate chemistry b| (Online)
245	1	0		a| Bioconjugate chemistry h| [electronic resource].
246	1			a| BC bioconjugate chemistry
246	1			a| Bioconjugate chem.
260				a| Washington, D.C. : b| American Chemical Society, c| ©1990-
310				a| Monthly, b| 2008-
321				a| Bimonthly, b| 1990-2007
362	1			a| Print began with: Vol. 1, no. 1 (Jan./Feb. 1990).
500				a| Title from contents page (ACS Publications, viewed Sept. 15, 2006).
538				a| Mode of access: World Wide Web.
588				a| Latest issue consulted: Vol. 32, Issue 12 (December 15, 2021),(ACS Publications, viewed December 22, 2021)
650			0	a| Bioconjugates v| Periodicals.
655			0	a| Electronic journals.
710	2			a| American Chemical Society.
776	0	8		i| Print version: t| Bioconjugate chemistry x| 1043-1802 w| (DLC) 90649356 w| (OCoLC)19336743
856	4	0		u| http://SK8ES4MC2L.search.serialssolutions.com/?V=1.0&L=SK8ES4MC2L&S=JCs&C=BIOCCHE&T=marc
910				a| CONSER online
850				a| DLC
949				a| Electronic resource w| ASIS c| 1 i| 45924569-1001 l| ONLINE m| ONLINE r| Y s| Y t| ONLINE u| 11/16/2024 o| .STAFF. 360 MARC

ASK A LIBRARIAN

PennState

Copyright ©2019 The Pennsylvania State University. All rights reserved. Except where otherwise noted, this work is subject to a Creative Commons Attribution 4.0 license. Details and exceptions.

Legal Statements | PSU Hotlines

PENN STATE UNIVERSITY LIBRARIES

Libraries Home (814) 865-6368
Libraries Intranet (Staff Only)
Accessibility Help
Website Feedback
Policies and Guidelines
Staff Directory

CONNECT WITH PENN STATE UNIVERSITY LIBRARIES

Facebook
Twitter
Instagram

Bioconjugate chemistry [electronic resource].

Uniform Title	Bioconjugate chemistry (Online)
Additional Titles	Bioconjug. chem. (Online), BC bioconjugate chemistry, and Bioconjugate chem
Published	Washington, D.C. : American Chemical Society, ©1990-
Additional Creators	American Chemical Society

Access Online

serialssolutions.com

ASK A LIBRARIAN

Dates of Publication and/or Sequential Designation
Print began with: Vol. 1, no. 1 (Jan./Feb. 1990).

Subject(s)
Bioconjugates—Periodicals

Genre(s)
Electronic journals

ISSN
1520-4812

Publication Frequency
Monthly, 2008-
Bimonthly, 1990-2007

Note
Title from contents page (ACS Publications, viewed Sept. 15, 2006).

Technical Details
Mode of access: World Wide Web.

View MARC record | catkey: 45924569

PennState

Copyright ©2019 The Pennsylvania State University. All rights reserved. Except where otherwise noted, this work is subject to a Creative Commons Attribution 4.0 license. Details and exceptions.

Legal Statements | PSU Hotlines

PENN STATE UNIVERSITY LIBRARIES
Libraries Home
Libraries Intranet (Staff Only)
Accessibility Help
Website Feedback
Policies and Guidelines
Staff Directory
(814) 865-6368

CONNECT WITH PENN STATE UNIVERSITY LIBRARIES
Facebook
Twitter
Instagram

○ All ● Journals Only ○ Books Only ○ Videos Only

Title begins with | Search

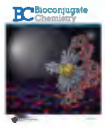
Show more search options ▼

Showing results 1 through 1 of 1

for the search: "BIOCCHE"

Refine Results: All | Journals Only | Books Only | Videos Only

Limit by: Peer Reviewed | Open Access



Bioconjugate chemistry

ISSN: 1043-1802

Peer Reviewed

01/01/1990 to 11/30/1995 in American Chemical Society Legacy Archives

01/01/1990 to Present in American Chemical Society Publications

Search inside this journal | Search

Back to Top

Last Updated on 12-02-2024 © Ex Libris, a ProQuest Company, 2000-2024

Privacy Policy

Bioconjugate Chemistry

Cite Share Jump to

ADVERTISEMENT

Get e-Alerts

Subscribed

Cite Share Jump to

ARTICLE | December 14, 2001

Vinyl Sulfone Bifunctional Derivatives of DOTA Allow Sulfhydryl- or Amino-Directed Coupling to Antibodies. Conjugates Retain Immunoreactivity and Have Similar Biodistributions

Lin Li, Shih-Wa Tsai, Anne-Line Anderson, David A. Keire, Andrew A. Raubitschek, and John E. Shively

View Author Information

Open PDF

Bioconjugate Chemistry

Cite this: *Bioconjugate Chem.* 2002, 13, 1, 110–115

https://doi.org/10.1021/bc015535b

Published December 14, 2001

Copyright © 2002 American Chemical Society

Request reuse permissions

Bioconjugate Chemistry

reduced recombinant antibody (chimeric anti-CEA antibody cT84.66) at pH 7 or to the amino groups of lysine residues at pH 9. The conjugation is sulfhydryl specific at pH 7 (case 1), and amino specific at pH 9 (case 2) as long as the antibody has no free sulhydryl groups. At a molar ratio of 50 BCA (bifunctional chelating agent) to mAb, the number of chelates conjugated is 0.8 for case 1, and 4.6 for case 2. The resulting conjugates can be radiolabeled with ^{111}In to high specific activity (5 mCi/mg) with high efficiency (>95%) at 43 °C in 60 min. The radiolabeled conjugates retained >95% immunoreactivity and are stable in serum containing 1mM DTPA over 3 d. When the radiolabeled conjugates were injected into nude mice bearing LS174T human colon tumor xenografts, over 40% ID/g accumulated in tumors during the period 24−72h. Tumor-to-blood ratios were 4.5, 3.5, and 2.5 for the sulfhydryl coupled conjugate at 24, 48, and 72 h, respectively, and 2.7, 2.5, and 2.3 for the amino-coupled conjugate at the same time points. For other organs the biodistributions were nearly identical whether the conjugates were attached via sulfhydryl or amino groups. These novel BCAs are easy to synthesize, offer versatile conjugation options, and give equivalent biodistributions that result in high tumor uptake and good tumor-to-blood ratios.

This publication is licensed under the terms of your institutional subscription. Request reuse permissions.

Copyright © 2002 American Chemical Society

Subjects

Anatomy Biopolymers Conjugate Acid-Base Pairs Immunology Peptides And Proteins

† Beckman Research Institute of the City of Hope.

‡ City of Hope Medical Center.

§ UCLA School of Medicine.

* To whom correspondence should be addressed. e-mail: jshively@coh.org.

Introduction

Bifunctional chelating agents (BCAs [1]) are routinely conjugated to recombinant antibodies for radiolabeling with radiometals such as ^{111}In for radioimmunoimaging and ^{90}Y for radioimmunotherapy (*1−4*). The main advantages of this approach is the ability to radiolabel the conjugate just prior to use and the exceptional stability of the chelated metal, preventing the release of the radionuclide from the conjugate. Starting with BCAs derived from EDTA (*5, 6*), and then DTPA (*7−11*), and more recently DOTA (*12−16*), increasingly more stable radiometal−chelate−antibody conjugates have been crafted. Nonetheless, the approach has certain drawbacks inherent in the biodistribution of the antibody which in the case of intact antibody can be deposited in the liver (

DAC EX. 2040 IPR2022-01531 Page 1070 of 1299

Bioconjugate Chemistry

excretion of these end-products from the lysosomal compartment. While it is assumed that the antibodies are completely degraded in the lysosome, releasing radiometal−chelate, it has only been proven in a few cases (*27*−*31*). In addition, the site of BCA conjugation to the antibody may play a key role in the fate of the radiolabel in both the tumor and normal organs. Furthermore, it is essential that the BCA be conjugated to the antibody without impairment of immunoreactivity. Since a major goal of the field is to reduce normal tissue uptake without decreasing the tumor uptake, we have investigated new BCA derivatives of DOTA that include the possibility of site-specific conjugation and linker specific cleavage. In previous work we showed that a maleimidocysteineamido derivative of DOTA coupled to sulfhydryl groups of mildly reduced intact antibody underwent pH dependent cleavage at the resulting succinimido groups (*32*), lowering blood levels while preserving high tumor uptake (*33*). However, the results were only a marginal improvement over our use of DOTA-active ester conjugated antibody (*34*, *35*). Oxidation of the thioether linker to a sulfone linker further increased the rate of linker bond cleavage, but the rate of blood clearance was too high, preventing good tumor uptake (*33*). Similar approaches utilizing ester linkers for reducing blood levels have been reported, but also suffer from lower blood levels to the point of reducing tumor uptake (*21*, *36*−*38*) . A similar problem is found in using antibody fragments, which clear the blood rapidly, but also give low tumor uptake (*25*). Thus, it is clear that the price of lowering blood levels is the concomitant lowering of tumor uptake, an unacceptable consequence in either radioimmunoimaging or radioimmunotherapy. A possible solution to the problem is the synthesis of BCAs with organ-specific cleavable linkers. Arano and co-workers (*26*, *39*−*41*) have synthesized C-terminal Lys linkers for a radioiodinated hippuric acid−Fab conjugatethat lowered kidney uptake by 50%. Meares and co-workers (*42*−*44*) have synthesized DOTA with cathepsin cleavable linkers for use in lowering liver levels. In the work reported here, we have made new derivatives of DOTA that incorporate a vinyl sulfone-based linker that shows versatility in terms of conjugation to either sulfhydryl or amino groups of antibodies. The BCA is easy to synthesize from readily available chemicals and gives high radiolabeling yields when conjugated to either sulfhydryl or amino groups. The biodistributions in tumor-bearing animals is nearly equivalent, suggesting that the site of conjugation has not affected either the tumor or normal organ uptake. The new BCA may be useful in preventing the impairment of immunoreactivity in cases where coupling through amino groups is problematic.

Experimental Procedures

General. DOTA trisodium salt and the free acid were purchased from Parish Chemical Co. (Orem, UT) and Macrocyclics, Inc. (Richardson, TX), respectively. DTPA was obtained from Fluka (Milwaukee, WI), vinyl sulfone from Aldrich (Milwaukee, WI), Chelex 100 from BioRad (Hercules, CA), and L-cysteine from Sigma (St. Louis, MO). Ultrapure water (18 MΩ-cm) was used to make all buffers that were passed over Chelex 100 and pH adjusted if necessary. $^{111}InCl_3$ was obtained from NEN Life Science products, Inc. (Boston, MA). The anti-CEA chT84.66 has been previously described (*35*, *45*). HPLC and TLC were performed as previously described (*32*). Mass spectra were recorded

DAC EX. 2040 IPR2022-01531 Page 1071 of 1299

Bioconjugate Chemistry

Melting points were recorded on a Thomas-Hoover uni-melt apparatus and are uncorrected. SDS and IEF gel electrophoresis was performed on a Pharmacia PhastGel apparatus according to the manufacturer's instructions.

Vinyl Sulfone−Cysteineamido−DOTA (VSC-DOTA; 2). Cysteineamido-DOTA (**1**) was synthesized as previously reported (*46*). To a solution of 3.24 mg (6.1 μmol) of **1** in 0.6 mL of 50 mM, pH 7.5 potassium phosphate was added 0.06 mL of 0.1 M DTT (6 mmol) and stirred for 0.5 h at RT under Ar. Vinyl sulfone (6.6 μL (64 μmol) in 0.6 mL of DMF was added with continuous stirring for 5 h at RT. A second aliquot was added and the reaction continued for another 22 h (final vol = 1.2 mL, 5.3 mM **1**, 107 mM vinyl sulfone). The excess vinyl sulfone was extracted with ethyl acetate (2 mL, ×3). The aqueous layer was adjusted to pH 8.4, applied to a BioRad Ag1-X4 column (HCO_2^- form, 1 × 10 cm), washed with 30 mL of water, and eluted stepwise with 0.05−2 M HCO_2H (5 mL per step). The product (**2**) was found in fractions 8−13 by ESI/MS. The product was repeatedly lyophilyzed from water to remove excess HCO_2H (yield 3.4 mg). The product had the expected protonated mass by ESI/MS (626.71, expected; 626.73, observed), gave a single spot on TLC, and had a melting point of 140−142 °C. Proton NMR (H_2O): δ 2.92 (m, 2H, $SCH_2CH_2SO_2$), δ 3.10 (m, 2H, $SCH_2CH_2SO_2$), δ 3.10−3.45 [br, 16H, (CH_2NCH_2) × 4], δ 3.53 (dd, 2H, CH_2SO_2), δ 3.45, 3.70, 3.84 (s, 6H, NCH_2CO_2H), δ 4.39 (m, 1H, $NHCHCO_2H$), δ 6.42 (dd, 2H, SO_2CHCH_2), δ 6.88 (dd, 1H, SO_2CHCH_2), δ 8.20 (d, 1H, CONH−CH).

Preparation of Amino-Conjnugated BCA Antibody (VSC-DOTA-NH-chT84.66). chT84.66 (FW= 150000, 1.0 mg, 6 nmol, at 10 mg/mL, 60 μM) was dialyzed vs 20 mM, pH 7.0 sodium phosphate buffer (three changes, × 1 L, 4 °C) and adjusted to pH 9.0 with 200 mM, pH 10 sodium phosphate (final volume, 0.1 mL). VSC-DOTA (0.1 mL of **2**, FW= 625, 0.7 mg, 1.12 μmol at 1.88 mg/mL, 3.1 mM in 50 mM, pH 9.0 sodium phosphate) was added and the solution rotated at 10 rpm for 4 h at 25 °C. The conjugate was dialyzed vs 250 mM NH_4 acetate (three changes, × 1 L, 4 °C).

Preparation of Sulfhydryl-Conjnugated BCA Antibody (VSC-DOTA-SH-chT84.66). chT84.66 was dialyzed as above and reduced with TCEP (20 μL of 10 mM in 50 mM sodium phosphate, pH 7.0) under argon for 2.5 h at 25 °C. TCEP was removed on a spin column (1 mL of Sephadex G25−50, 1200 rpm, 2 min) under argon. To 1.0 mg (60 nmol) of reduced chT84.66 in 0.1 mL of 50 mM sodium phosphate, pH 7, was added 0.1 mL of 3 mM (300 nmol) of VSC-DOTA (**2**) in the same buffer. The solution was rotated under argon overnight at 25 °C and dialyzed vs NH_4 acetate as described above. In parallel, 1 mg of TCEP reduced chT84.66 in 0.15 mL was reacted with 0.1 mL of 3 mM MC-DOTA and run as a control.

Radiolabeling of VSC-DOTA-chT84.66. The conjugates were radiolabeled with $^{111}InCl_3$ as previously described (*47*). For the animal studies, the conjugates (0.3 mL of 1 mg/mL in 250 mM NH_4 acetate, pH 5.7) were incubated with 0.3 mCi of ^{111}In (0.15 mL of 0.04 M HCl plus 0.03 mL of 250 mM NH_4 acetate, pH 5.7) for 60 min at 43 °C. Excess ^{111}In was chelated with 1 mM DTPA and the radiolabeled product purified on a TosoHaas TSK−Gel G2000SW column (0.75 × 30 cm in saline,

DAC EX. 2040 IPR2022-01531 Page 1072 of 1299

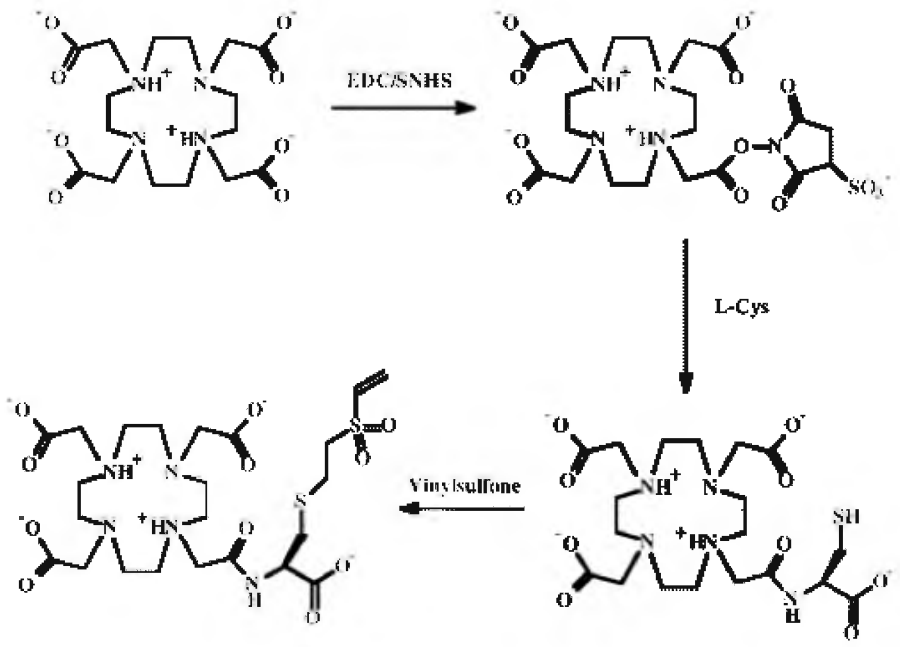
Bioconjugate Chemistry

Stability Studies. Aliquots (0.5 mL) of the radiolabeled conjugates in 1% HSA were mixed with 0.05 mL of 10 mM DTPA, stored at 37 °C and injected at various time points onto a Pharmacia Superose 12HR column (as above) to determine the amount of radiolabel in the conjugate and DTPA.

Animal Biodistributions. Groups of five nude mice (Charles River) bearing LS174T human colon tumor xenografts (ave size = 1.5 mg ± 0.5 at t = 0 h) were injected with 2 μCi (2 μg) of radiolabeled conjugate via tail vein. Animals were sacrificed at 0, 12, 24, 48, 72, and 96 h after injection. Major organs, tumor, and blood were weighed, radioactivity was measured, and the results were expressed as mean %ID/g ± SD.

Results

Synthesis and Antibody Conjugation. The synthesis of VSC-DOTA (**2**) is shown in Scheme 1. The product gave the expected proton NMR spectrum and protonated mass by ESI/MS and was free of DOTA and the bis-derivative. The reactivity of **2** to free L-cysteine was confirmed by ESI/MS (data not shown). At pH 7, only the mono-derivative was formed, suggesting that the thiol and not the α-amino group of L-cysteine was reactive under these conditions. When VSC-DOTA was incubated for 1−7 d in pH 7 PBS and analyzed by RP-HPLC, there was no evidence of chemical instability (data not shown).



Scheme 1

DAC EX. 2040 IPR2022-01531 Page 1073 of 1299

Bioconjugate Chemistry

conjugation reaction at pH 7, 8, and 9 shown in Figure 1A, lanes 3–5, demonstrate that little or no reaction occurs at pH 7, while substantial amounts of conjugate are formed at pH 9. The results at pH 8 are intermediate, with <20% product formed. The results at 37 °C, pH 9 demonstrate the expected effect of temperature on the extent of reaction (Figure 1A, lane 6). The products show no change in mobility when run on SDS gel electrophoresis under nonreducing conditions (data not shown). On the basis of these results, we reasoned that sulfhydryl specific conjugation could be performed at pH 7 with little or no conjugation at amino groups, while amino group specific conjugation could be performed at pH 9, as long as no free sulfhydryl groups are present. Since the cysteine residues in most antibodies are engaged in disulfide bonds, this criterion is easily met. In addition, under mild reducing conditions (no denaturing agents), only the hinge disulfides of antibodies are reduced, allowing site-specific conjugation at just these sulfhydryl groups (*48*, *49*) The conjugation of VSC-DOTA to mildly reduced chT84.66 at pH 7 shown in Figure 1B, lane 4, demonstrates that >90% of the antibody is conjugated under these conditions. It should be noted that either DTT or TCEP were successfully used as reducing agents. We prefer TCEP because a lower molar excess is required and since removal of the reducing agent by spin columns is not quantitative, better conjugation yields are routinely obtained.

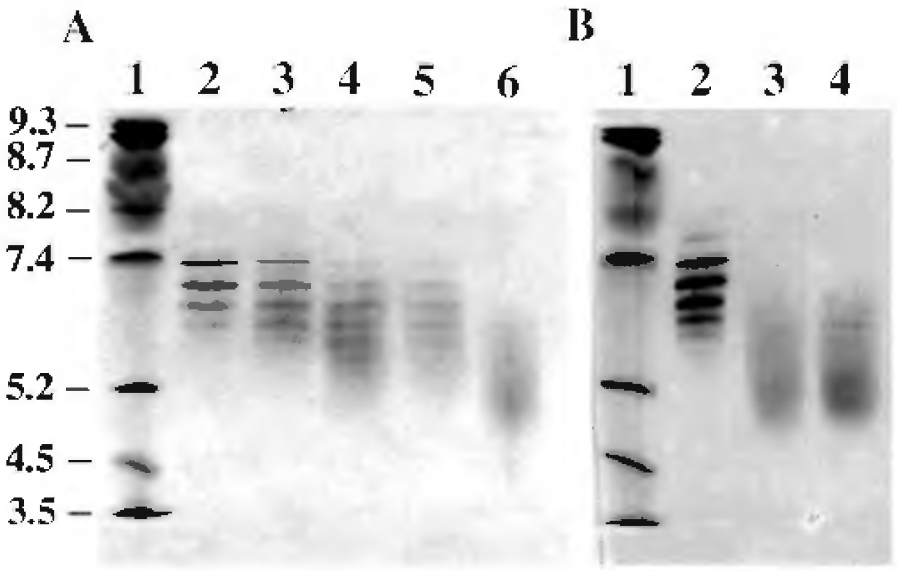


Figure 1 Analysis of VSC-DOTA-mAb conjugates by IEF gel electrophoresis. A: Lane 1: IEF standards; Lane 2: chT84.66 control; Lane 3: 30 μM chT84.66, 1.5 mM VSC-DOTA, pH 7.0, RT, 4h; Lane 4: 30 μM chT84.66, 1.5 mM VSC-DOTA, pH 8.0, RT, 4 h; Lane 5: 30 μM chT84.66, 1.5 mM VSC-DOTA, pH 9.0, RT, 4 h; Lane 6: 30 μM chT84.66, 1.5 mM VSC-DOTA, pH 9.0, 37 °C, 4 h. B: Lane 1: IEF standards; Lane 2: chT84.66 control; Lane 3: 30 μM chT84.66 reduced with 0.5 mM TCEP, the TCEP removed by spin column, and reacted with 1.5 mM MC-DOTA, pH 7.0, RT, 4 h; Lane 4: 30 μM chT84.66, reduced with 0.5 mM TCEP, the TCEP removed by spin column, and reacted with 1.5 mM VSC-DOTA, pH 7.0, RT, 4 h.

DAC EX. 2040 IPR2022-01531 Page 1074 of 1299

Bioconjugate Chemistry

Radiolabeling of these two conjugates with $^{111}InCl_3$ gave similar percent radiolabeling efficiencies, specific activities, and immunoreactivities (Table 1). When the radiolabeled conjugates were incubated in 1% HSA and 1 mM DTPA for 1–7d, negligible loss of radioactivity was seen to DTPA (Table 1). In addition, their immunoreactivities were >95% when radiolabeled, bound to excess CEA, and analyzed by gel filtration chromatography. Since their immunoreactivities were similar, we used these conjugates for a direct comparison in animal biodistribution studies.

Table 1. Radiometal Labeling and Immunoreactivity of VSC-DOTA-mAb[a]

sample	chelates/ mAb	labeling ratio (mCi/mg)	% efficiency	% immuno- reactivity
SH-mAb	0.8	1.0–5.0	>98	>98
NH-mAb	4.5	1.0–5.0	>98	>98

[a] VSC-DOTA was coupled to either SH or NH groups in the mAb as described in the text. The number of chelates per mAb was determined by trace labeling with ^{111}In in a standard solution of $InCl_3$. The labeling ratio was performed with 0.3 mCi of ^{111}In and 0.3 mg of conjugate in 0.3 mL of 0.25 mM ammonium acetate (pH 5.7), or 1.0 mCi of ^{111}In and 0.2 mg of conjugate in 0.2 mL of ammonium actetate (pH 5.7). Immunoreactivity was performed as described in Methods.

Comparative Animal Biodistributions of [^{111}In]VSC-DOTA-SH-chT84.66 and [^{111}In]VSC-DOTA-NH-chT84.66. The two ^{111}In-radiolabeled conjugates were injected into nude mice bearing human colon tumor xenografts and their biodistributions compared (Tables 2 and 3). The overall biodistributions are quite similar, resulting in maximal and sustained tumor uptake of 35–45% ID/g from 24 to 96 h. During the same time period the blood activity drops from about 45% ID/g to 2–3% ID/g. A comparison of tumor to blood curves over the time course suggests that the SH conjugate may be superior to the NH conjugate. Paradoxically, this difference may be due to a slightly slower blood clearance curve for the SH conjugate, resulting in higher uptake. A close analysis of the normal organs reveals nearly identical uptake levels and time courses for the spleen, kidney, and lung, but there are some interesting differences in the liver. The SH conjugate shows lower liver uptake at the earlier time points, suggesting that the NH conjugate accumulates more rapidly in the liver. This result would also account for their observed differences in blood clearance curves.

Table 2. Biodistribution of ^{111}In-Labeled VSC-DOTA-SH mAb in Nude Mice Bearing LS174T Xenografts[a]

	0 h	12 h	24 h	48 h	72 h	96 h

DAC EX. 2040 IPR2022-01531 Page 1075 of 1299

Bioconjugate Chemistry

liver	7.30	6.65	10.15	14.91	19.60	18.83
	(0.25)	(1.94)	(1.90)	(6.27)	(7.19)	(3.32)
spleen	5.41	5.18	5.93	7.76	6.41	7.69
	(1.22)	(0.57)	(0.95)	(2.54)	(2.25)	(2.27)
kidney	6.36	5.62	4.36	3.46	2.82	2.63
	(1.43)	(0.46)	(0.56)	(1.08)	(0.46)	(0.43)
lung	14.01	8.59	5.50	2.99	1.87	0.90
	(3.27)	(1.26)	(0.72)	(1.36)	(0.88)	(0.59)
tumor	1.59	37.08	43.61	42.01	40.43	39.57
	(0.47)	(4.09)	(4.91)	(12.73)	(6.96)	(18.97)
carcass	1.57	2.58	2.15	1.47	1.05	0.96
	(0.15)	(0.10)	(0.29)	(0.48)	(0.26)	90.51)

[a] Five animals per group were injected with 4 μCi (4 μg) of VSC-DOTA coupled to chT84.66 via the hinge SH groups and radiolabeled with ^{111}In. The results are reported as mean %ID/g (±SD).

Table 3. Biodistribution of ^{111}In-Labeled VSC-DOTA-NH mAb in Nude Mice Bearing LS174T Xenografts[a]

	0 h	12 h	24 h	48 h	73 h	96 h
blood	47.61	17.98	17.50	8.98	5.84	3.08
	(2.97)	(6.29)	(6.74)	(3.18)	(4.14)	(4.50)
liver	9.16	12.38	13.93	16.27	19.64	18.42
	(0.97)	(3.77)	(5.75)	(4.25)	(5.36)	(4.79)

DAC EX. 2040 IPR2022-01531 Page 1076 of 1299

Bioconjugate Chemistry

kidney	7.29	4.24	5.03	3.44	2.60	2.15
	(1.36)	(1.14)	(1.77)	(0.87)	(0.79)	(0.76)
lung	13.07	5.63	6.58	3.44	2.58	1.45
	(1.18)	(1.79)	(2.58)	(1.30)	(1.57)	(1.63)
tumor	1.26	21.66	38.54	39.27	45.76	33.85
	(0.40)	(5.02)	(13.60)	(10.19)	(18.25)	(14.52)
carcass	1.76	2.20	2.64	1.72	1.43	0.89

[a] Five animals per group were injected with 4 μCi (3.4 μg) of VSC-DOTA coupled to chT84.66 via NH groups and radiolabeled with ^{111}In. The results are reported as mean %ID/g (± SD).

Discussion

In a search for site-specific BCA derivatives of DOTA we first synthesized a bis-maleimidohexane derivative of cysteineamido-DOTA (*32*). Maleimide is a commonly used reagent that undergoes sulfhydryl specific Michael additions that are thought to be chemically stable (*50*). Although this BCA allowed site-specific conjugation to the sulfhydryl groups of mildly reduced mAb, it proved to be chemically labile, undergoing pH-dependent hydrolysis at its resulting succinimidyl bonds (*32*). Surprisingly, this phenomenon did not prevent good tumor uptake in animal biodistribution studies (*33*). As a result, we proposed that further increasing the chemical lability of the linker may be beneficial, since this would result in lower blood levels. Indeed, oxidation of the thioether bond in the linker to a sulfone increased the chemical lability of the BCA (*32*), but the BCA decomposed too rapidly to allow good tumor uptake. On the basis of these studies, we decided to investigate other Michael addition linkers as candidates for site-specific conjugation to mAbs. We chose vinyl sulfone for its well-documented reaction with sufhydryl groups (*51*) However, we realized from the outset that vinyl sulfone can also react with amino groups (*52, 53*), and thus we were interested in seeing if this reaction could be controlled by manipulation of the reaction pH.

Vinyl sulfone is a viscous liquid with poor solubility in water, but when dissolved in DMF or acetonitrile reacts well with Michael acceptors in aqueous medium. In the synthesis of the title compound (**2**), we demonstrated a facile reaction between vinyl sulfone and cysteineamido-DOTA. Unlike the maleimido derivatives, the vinyl sulfone derivative of cysteineamido-DOTA is stable in PBS at pH 7. When **2** was reacted with chT84.66 at pH 7, no conjugate was formed unless the mAb was mildly reduced prior to reaction. In addition, we showed that the mAb conjugated with **2** at pH 9

DAC EX. 2040 IPR2022-01531 Page 1077 of 1299

Bioconjugate Chemistry

Since the biodistributions of radiolabeled mAbs is highly dependent on the mode of attachment of the radiolabel, it is always interesting to compare BCAs conjugated to the same mAb via different chemical linkages. In most cases, it is difficult to perform this type of comparative study. However, in this study, we have an almost ideal model. In one case, the same BCA is conjugated to sulfhydryl groups, and in the other case, amino groups, but the resulting BCA/mAb ratios are different. Even so, the resulting biodistributions are quite similar. When we compare these results to our previous studies in which DOTA was conjugated to chT84.66 by an active ester derivative of DOTA (*34, 35*), we find that the uptake curves are similar for both tumor and normal tissues. This suggests that linkage of DOTA based BCAs to mAbs via amides, amine, or sulfhydryl bonds results in similar tissue, including tumor, uptakes, and metabolism. Thus, if one wants to manipulate normal or tumor uptake and metabolism of DOTA-based BCAs, it is necessary to explore other modes of chemical linkage or to insert linkers which have built-in chemical or biological lability. Examples of such linkers have been described by Meares (*21*), Arano (*54*), and ourselves (*32*).

When we examined the comparative biodistributions of the SH and NH BCA-chT84.66 conjugates in more detail, we noticed some intriguing trends. They include the higher blood levels, higher tumor levels, and lower liver levels for the BCA chT84.66 SH conjugate at early time points 0–24 h. These three “organs” are interdependent in their biodistributions as follows: high tumor uptake is dependent on maintaining high blood levels, especially early in a biodistribution. If the blood is cleared by any mechanism, including rapid liver uptake, then blood and tumor levels will fall together. Thus, the lower liver uptake seen at early time points for the SH conjugate leads to higher blood levels and ultimately to higher tumor uptake which is sustained at later time points. While the biological reasons for these differences are unknown at this time, we can speculate that this mode of conjugation will lead to incremental improvements in the human, where most biodistributions are predicted from the animal model.

In summary, we have prepared a new BCA that allows site-specific conjugation to most mAbs either via sulfhydryl or amino groups by manipulating pH and use of reducing agents. The ^{111}In-radiolabeled versions of these conjugates give more or less equivalent animal biodistributions to previously described ^{111}In-radiolabeled BCA-mAbs, including are own version using the active ester of DOTA (*34, 35*). This approach should have utility, allowing the investigator to chose one type of chemistry over the other depending on the restrictions implied by a given antibody. Finally, the improvement in tumor to blood and tumor-to-liver ratios seen for the SH-specific conjugate may translate into improved performance in the clinic.

Author Information

Authors

Lin Li - *Division of Immunology, Beckman Research Institute of the City of Hope, Duarte, California 91010, Department of Radioimmunotherapy, City of Hope Medical Center, Duarte,*

DAC EX. 2040 IPR2022-01531 Page 1078 of 1299

Bioconjugate Chemistry

California 91010, and CURE Digestive Diseases Research Center, UCLA School of Medicine, Los Angeles, California 90095

Anne-Line Anderson - *Division of Immunology, Beckman Research Institute of the City of Hope, Duarte, California 91010, Department of Radioimmunotherapy, City of Hope Medical Center, Duarte, California 91010, and CURE Digestive Diseases Research Center, UCLA School of Medicine, Los Angeles, California 90095*

David A. Keire - *Division of Immunology, Beckman Research Institute of the City of Hope, Duarte, California 91010, Department of Radioimmunotherapy, City of Hope Medical Center, Duarte, California 91010, and CURE Digestive Diseases Research Center, UCLA School of Medicine, Los Angeles, California 90095*

Andrew A. Raubitschek - *Division of Immunology, Beckman Research Institute of the City of Hope, Duarte, California 91010, Department of Radioimmunotherapy, City of Hope Medical Center, Duarte, California 91010, and CURE Digestive Diseases Research Center, UCLA School of Medicine, Los Angeles, California 90095*

John E. Shively - *Division of Immunology, Beckman Research Institute of the City of Hope, Duarte, California 91010, Department of Radioimmunotherapy, City of Hope Medical Center, Duarte, California 91010, and CURE Digestive Diseases Research Center, UCLA School of Medicine, Los Angeles, California 90095*

Acknowledgment

The authors thank Stefanie Wright for the animal studies. This research was funded by NCI grant CA43904 (A.A.R. and J.E.S.) and the Department of the Army Grant DAMD 17-98-1-8031 (J.E.S.).

This article references 55 other publications.

1. Anderson, C. J., and Welch, M. J. (1999) Radiometal-labeled agents (non-technetium) for diagnostic imaging. *Chem. Rev.99*, 2219−2234.

| Google Scholar

2. Gansow, O. A. (1991) Newer Approaches to the Radiolabeling of Monoclonal Antibodies by Use of Metal Chelates. *Int. J. Radiat. Appl. Instrum. Part B Nucl. Med. Biol.18*, 369−381.

Google Scholar

3. Meares, C. F. (1986) Chelating Agents for the Binding of Metal Ions to Antibodies. *Int. J. Radiat. Appl. Instrum. Part B Nucl. Med. Biol.13*, 311−318.

DAC EX. 2040 IPR2022-01531 Page 1079 of 1299

Bioconjugate Chemistry

4. Liu, S., and Edwards, D. S. (2001) Bifunctional chelators for therapeutic lanthanide radiopharmaceuticals. *Bioconjugate Chem.12*, 7–34.

| Google Scholar

5. Meares, C. F., McCall, M. J., Reardan, D. T., Goodwin, D. A., Diamanti, C. I., and McTigue, M. (1984) Conjugation of Antibodies with Bifunctional Chelating Agents: Isothiocyanate and Bromoacetamide Reagents, Methods of Analysis, and Subsequent Addition of Metal Ions. *Anal. Biochem.142*, 68–78.

| Google Scholar

6. Brechbiel, M. W., Gansow, O. A., Atcher, R. W., Schlom, J., Esteban, J., Simpson, D. E., and Colcher, D. (1986) Synthesis of 1-(*p*-Isothiocyanatobenzyl) Derivatives of DTPA and EDTA. Antibody Labeling and Tumor-Imaging Studies. *Inorg. Chem.25*, 2772–2781.

Google Scholar

7. Brechbiel, M. W., and Gransow, O. A. (1991) Backbone-substituted DTPA ligands for ^{90}Y radioimmunotherapy. *Bioconjugate Chem.2*, 187–194.

Google Scholar

8. Cummins, C. H., Rutter, E. W., and Fordyce, W. A. (1991) A convenient synthesis of bifunctional chelating agents based on diethylenetriaminepentaacetic acid and their coordination chemistry with yttrium (III). *Bioconjugate Chem.2*, 180–186.

Google Scholar

9. Hnatowich, D. J., Virzi, F., and Doherty, P. W. (1985) DTPA-Coupled Antibodies Labeled with Yttrium-90. *J. Nucl. Med.26*, 503–509.

Google Scholar

10. Westerberg, D. A., Carney, P. L., Rogers, P. E., Kline, S. J., and Johnson, D. K. (1989) Synthesis of Novel Bifunctional Chelators and Their Use in Preparing Monoclonal Antibody Conjugates for Tumor Targeting. *J. Med. Chem.32*, 236–243.

DAC EX. 2040 IPR2022-01531 Page 1080 of 1299

Bioconjugate Chemistry

11. Corson, D. T., and Meares, C. F. (2000) Efficient multigram synthesis of the bifunctional chelating agent (S)-1-p-isothiocyanatobenzyl-diethylenetetraaminepentaacetic acid. *Bioconjugate Chem.11*, 292–299.

Google Scholar

12. Cox, J. P. L., Jankowski, K. J., Kataky, R., Parker, D., Beeley, N. R. A., Boyce, B. A., Eaton, M. A. W., Millar, K., Millican, A. T., Harrison, A., and Walker, C. (1989) Synthesis of a Kinetically Stable Yttrium-90 Labeled Macrocycle-Antibody Conjugate. *J. Chem. Soc., Chem. Commun.* 797–798.

| Google Scholar

13. Deshpande, S. V., DeNardo, S. J., Kukis, D. L., Moi, M. K., McCall, M. J., DeNardo, G. L., and Meares, C. F. (1990) Yttrium-90-labeled monoclonal antibody for therapy: labeling by a new macrocyclic bifunctional chelating agent. *J. Nucl. Med.31*, 473–479.

Google Scholar

14. Meares, C. F., Moi, M. K., Diril, H., Kukis, D. L., McCall, M. J., Deshpande, S. V., DeNardo, S. J., Snook, D., and Epenetos, A. A. (1990) Macrocyclic chelates of radiometals for diagnosis and therapy. *Br. J. Cancer62*, Suppl. X, 21–26.

Google Scholar

15. Smith-Jones, P. M., Fridrich, R., Kaden, T. A., Novak-Hofer, I., Siebold, K., Tschudin, D., and Maecke, H. R. (1991) Antibody Labeling with Copper-67 Using the Bifunctional Macrocycle 4-[(1,4,8,11-Tetraazacyclotetradec-1-yl)methyl]benzoic Acid. *Bioconjugate Chem.2*, 415–421.

Google Scholar

16. Kline, S. J., Betebenner, D. A., and Johnson, D. K. (1991) Carboxymethyl-Substituted Bifunctional Chelators: Preparation of Aryl Isothiocyanate Derivatives of 3-(Carboxymethyl)-3-azapentanedioic Acid, 3,12-Bis(carboxymethyl)-6,9-dioxa-3,12-diazatetradecanedioic Acid, and 1,4,7,10-Tetraazacyclododecane-*N*,*N*′,*N*″,*N*‴-tetraacetic Acid for Use as Protein Labels. *Bioconjugate Chem.2*, 26–31.

Google Scholar

17. Halpern, S. E., Hagan, P. L., Garver, P. R., Koziol, J. A., Chen, A. W. N., Frincke, J. M., Bartholomew, R. M., David, G. S., and Adams, T. H. (1983) Stability, Characterization, and Kinetics of ^{111}In-labeled Monoclonal Antitumor

DAC EX. 2040 IPR2022-01531 Page 1081 of 1299

Bioconjugate Chemistry

18. Jakowatz, J. G., Beatty, B. G., Vlahos, W. G., Porudominsky, D., Philben, V. J., Williams, L. E., Paxton, R. J., Shively, J. E., and Beatty, J. D. (1985) High-Specific-Activity ^{111}In-labeled Anticarcinoembryonic Antigen Monoclonal Antibody: Biodistribution and Imaging in Nude Mice Bearing Human Colon Cancer Xenografts. *Cancer Res.45*, 5700−5706.

Google Scholar

19. Larson, S. M., and Carrasquillo, J. A. (1988) Advatages of radioiodine over radioindium labeled monoclonal antibodies for imaging solid tumors. *Nucl. Med. Biol.15*, 231−233.

Google Scholar

20. Wong, J. Y. C., Thomas, G. E., Yamauchi, D. M., Williams, L. E., Odom-Maryon, T. L., E. J. M., Neumaier, M., Wu, A. M., Primus, F. J., Shively, J. E., and Raubitschek, A. A. (1997) Clinical evaluation of an ^{111}In labeled anti-CEA chimeric monoclonal antibody in patients with metastatic CEA producing malignancies. *J. Nucl. Med.38*, 1951−1959.

Google Scholar

21. Meares, C. F., McCall, M. J., Deshpande, S. V., DeNardo, S. J., and Goodwin, D. A. (1988) Chelate radiochemistry: cleavable linkers lead to altered levels of radioactivity in the liver. *Int. J. Cancer (suppl.)2*, 99−102.

Google Scholar

22. Bujis, W. C. A. M., Massuger, L. F. A. G., Claessens, R. A. M. J., Kenemans, P., and Corstens, F. H. M. (1992) Dosimetric evaluation of immunoscintigraphy using indium-11-labeled monoclonal antibody fragments in patients with ovarian cancer. *J. Nucl. Med.33*, 1113−1120.

Google Scholar

23. Govindan, S. V., Shih, L. B., Goldenberg, D. M., Sharkey, R. M., Karacay, H., Donnelly, J. E., Losman, M. J., Hansen, H. J., and Griffiths, G. L. (1998) 90-Yttrium-labeled complementarity-determining-region grafted monoclonal antibodies for radioimmunotherpay: radiolabeling and animal biodistribution studies. *Bioconjugate Chem.9*, 773−782.

Google Scholar

DAC EX. 2040 IPR2022-01531 Page 1082 of 1299

Bioconjugate Chemistry

Google Scholar

25. Yokota, T., Milenic, D. E., Whitlow, M., and Schlom, J. (1992) Rapid tumor penetration of a single-chain Fv and comparison with other immunoglobulin forms. *Cancer Res.52*, 3402–3408.

Google Scholar

26. Arano, Y. (1998) Strategies to reduce renal radioactivity levels of antibody fragments. *Quart. J. Nucl. Med.42*, 262–270.

Google Scholar

27. Duncan, J. R., and Welch, M. J. (1993) Intracellular metabolism of indium-111 DTPA labeled receptor targeted proteins. *J. Nucl. Med.34*, 1728–1738.

Google Scholar

28. Duncan, J. R., Stephenson, M. T., Wu, H. P., and Anderson, C. J. (1997) Indium-111-diethylenetriamine pentaacetic acid octreotide is delivered in vivo to pancreatic, tumor cell, renal, and hepatocyte lysosomes. *Cancer Res.57*, 659–671.

Google Scholar

29. Franano, F. N., Edwards, W. B., Welch, M. J., and Duncan, J. R. (1994) Metabolism of receptor targeted ^{111}In-DTPA-glycoporteins: identification of ^{111}In-DTPA-epsilon-lysine as the primary metabolic and excretory product. *Nucl. Med. Biol.21*, 1023–1034.

Google Scholar

30. Novak-Hofer, I., Amstutz, H. P., Macke, H. R., Schwartzbach, R., Zimmermann, K., Morgenthaler, J.-J., and Schubiger, P. A. (1995) Cellular processing of copper-67 labeled monoclonal antibody chCE7 by human neuroblastoma cells. *Cancer Res.55*, 46–50.

Google Scholar

31. Tsai, S. W., Li, L., Williams, L. E., Anderson, A.-L., Raubitschek, A. A., and Shively, J. E. (2001) Metabolism and renal clearance of ^{111}In-labeled DOTA conjugated antibody fragments. *Bioconjugate Chem.12*, 264–270.

DAC EX. 2040 IPR2022-01531 Page 1083 of 1299

Bioconjugate Chemistry

chelate conjugation to antibody sulfhydryl groups undergo pH-dependent clevage reactions. *Bioconjugate Chem.9*, 72–86.

| Google Scholar

33. Williams, L. E., Lewis, M. R., Bebb, G. G., Clarke, K. G., Odom-Maryon, T. L., Shively, J. E., and Raubitschek, A. A. (1998) Biodistribution of ^{111}In and ^{90}Y labeled DOTA and maleimidocysteineamido-DOTA conjugated to chimeric anti-carcinoembryonic antigen antibody in xenograft bearing nude mice: comparison of stable and chemically labile linker systems. *Bioconjugate Chem.9*, 87–93.

| Google Scholar

34. Lewis, M. R., Raubitschek, A. A., and Shively, J. E. (1994) A facile, water-soluble method for modification of proteins with DOTA. Use of elevated temperature and optimized pH to achieve high specific activity and high chelate stability in radiolabeled immunoconjugates. *Bioconjugate Chem.5*, 565–576.

Google Scholar

35. Williams, L. E., Primus, F. J., Wong, J. Y. C., Wu, A. M., Odom-Maryon, T. L., Johnson, D. K., Hefta, L. J. F., Shively, J. E., and Raubitschek, A. A. (1996) Biodistribution of an ^{111}In or ^{90}Y labeled chimeric anti-CEA monoclonal antibody (cT84.66) following its large scale production in a bioreactor. *Tumor Targeting2*, 116–124.

Google Scholar

36. Haseman, M. K., Goodwin, D. A., Meares, C. F., Kaminski, M. S., Wensel, T. G., McCall, M. J., and Levy, R. (1986) Metabolizable 111-In-chelate conjugated anti-iodiotype monoclonal antibody for radioimmunodetection of lymphoma in mice. *Eur. J. Nucl. Med.12*, 455–460.

| Google Scholar

37. Paik, C. H., Yokoyama, K., Reynolds, J. C., Quadri, S. M., Min, C. Y., Shin, Y., Maloney, P. J., Larson, S. M., and Reba, R. C. (1989) Reduction of background activities by introduction of a diester linkage between antibody and a chelate in radioimmunodetection of tumor. *J. Nucl. Med.30*, 1693–1701.

Google Scholar

DAC EX. 2040 IPR2022-01531 Page 1084 of 1299

Bioconjugate Chemistry

Google Scholar

39. Arano, Y., Mukai, T., Uezono, T., Wakisaka, K., Motonari, H., Akizawa, H., Taoka, Y., and Yokoyama, A. (1994) A biological method to evaluate bifunctional chelating agents to label antibodies with metallic radionuclides. *J. Nucl. Med.35*, 890−898.

Google Scholar

40. Arano, Y., Wakisaka, K., Ohmono, Y., Uezono, T., Akizawa, H., Nakayama, M., Sakahara, H., Tanaka, C., Konishi, J., and Yokoyama, A. (1996) Assessment of radiochemical design of antibodies using an ester bond as the metabolizable linkage: evaluation of maleimidoethyl 3-(tri-*n*-butylstannyl)hippurate as a radioiodination reagent of antibodies for diagnostic and therapeutic applications. *Bioconjugate Chem.7*, 628−637.

Google Scholar

41. Fujioka, Y., Arano, Y., Ono, M., Uehara, T., Ogawa, K., Namba, S., Saga, T., Nakamoto, Y., Mukai, T., Konishi, J., and Saji, H. (2001) Renal metabolism of 3′-iodohippuryl Nε-maleoyl-L-lysine (HML)-conjugated Fab fragments. *Bioconjugate Chem.12*, 178−185.

Google Scholar

42. Li, M., and Meares, C. F. (1993) Synthesis, metal chelate stability studies, and enzyme digestion of a peptide-linked DOTA derivative and its corresponding radiolabeled immunoconjugates. *Bioconjugate Chem.4*, 275−283.

Google Scholar

43. Peterson, J. J., Pak, R. H., and Meares, C. F. (1999) Total solid-phase synthesis of 1,4,7,10-tetraazacyclododecane-N,N′,N″,N‴-tertraacetic acid functionalized peptides for radioimmunotherpay. *Bioconjugate Chem.10*, 316−320.

Google Scholar

44. Peterson, J. J., and Meares, C. F. (1999) Enzymatic cleavage of peptide linked radiolabels from immunoconjugates. *Bioconjugate Chem.10*, 553−557.

Google Scholar

DAC EX. 2040 IPR2022-01531 Page 1085 of 1299

Bioconjugate Chemistry

Cancer Res.50, 2128−2134.

Google Scholar

46. Lewis, M. R., and Shively, J. E. (1998) Maleimidocysteineamido-DOTA Derivatives: New Reagents for Radiometal Chelate Conjugation to Antibody Hinge Region Sulfhydryl Groups Undergo pH-Dependent Cleavage Reactions. *Bioconjugate Chem.9*, 72−86.

| Google Scholar

47. Williams, L. E., Lewis, M. R., Bebb, G. G., Clarke, K. G., Odom-Maryon, T. L., Shively, J. E., and Raubitschek, A. A. (1998) Biodistribution of ^{111}In- and ^{90}Y-Labeled DOTA and Maleimidocysteineamido-DOTA Conjugated to Chimeric Anti-Carcinoembryonic Antigen Antibody in Xenograft-Bearing Nude Mice: Comparison of Stable and Chemically Labile Linker Systems. *Bioconjugate Chem.9*.

Google Scholar

48. Gunewardena, P., and Cook, K. B. (1966) 1,4-Dithiothreitol as a Reagent for Reductive Degradation of Human γG Globulin. *Biochem. J.99*, 8P.

Google Scholar

49. Willner, D., Trail, P. A., Hofstead, S. J., King, H. D., Lasch, S. J., Braslawsky, G. R., Greenfield, R. S., Kaneko, T., and Firestone, R. A. (1993) (6-Maleimidocaproyl)hydrazone of Doxorubicin- -A New Derivative for the Preparation of Immunoconjugates of Doxorubicin. *Bioconjugate Chem.4*, 521−527.

Google Scholar

50. Gregory, J. D. (1955) The Stability of *N*-Ethylmaleimide and its Reaction with Sulfhydryl Groups. *J. Am. Chem. Soc.77*, 3922−3923.

| Google Scholar

51. Houen, G., and Jensen, O. M. (1995) Conjugation to preactivated proteins using divinyl sulfone and iodoacetic acid. *J. Immunol. Methods181*, 187−200.

| Google Scholar

Bioconjugate Chemistry

53. Masri, M. S., and Friedman, M. (1988) Protein reactions with methyl and ethyl vinyl sulfones. *J. Protein Res.7*, 49−54.

Google Scholar

54. Arano, Y., Fujioka, Y., Akizawa, H., Ono, M., Uehara, T., Wakisaka, K., Nakayama, M., Sakahara, H. K. J., and Saji, H. (1999) Chemical design of radiolabeled antibody fragments for low renal radioactivity levels. *Cancer Res.59*, 128−134.

Google Scholar

1. Abbreviations: BCA, bifunctional chelating agent; CEA, carcinoembryonic antigen; DOTA, 1,4,7,10-tetraazacyclododecane-1,4,7,10-tetraacetic acid; EDC, 1-ethyl-3-[3-(dimethylamino)propyl]carbodiimide; DTPA, diethylenetriaminepentaacetic acid; HSA, human serum albumin; sulfo-NHS, *N*-hydroxysulfosuccinimide; TCEP, tris(carboxyethyl)phosphine; VSC-DOTA, vinyl sulfone-cysteineamido-DOTA.

Google Scholar

Cited By

This article is cited by 25 publications.

1. Li Wang, Hui Wang, Kun Shen, Hyejin Park, Tao Zhang, Xuedan Wu, Mei Hu, Hong Yuan, Yue Chen, Zhanhong Wu, Qiu Wang, Zibo Li. Development of Novel 18F-PET Agents for Tumor Hypoxia Imaging. *Journal of Medicinal Chemistry* **2021**, *64* (9) , 5593-5602. https://doi.org/10.1021/acs.jmedchem.0c01962

2. Brittney J. Mills, Qingxin Mu, Mary E. Krause, and Jennifer S. Laurence . claMP Tag: A Versatile Inline Metal-Binding Platform Based on the Metal Abstraction Peptide. *Bioconjugate Chemistry* **2014**, *25* (6) , 1103-1111. https://doi.org/10.1021/bc500115h

3. Subhadip Senapati, Saikat Manna, Stuart Lindsay, and Peiming Zhang . Application of Catalyst-Free Click Reactions in Attaching Affinity Molecules to Tips of Atomic Force Microscopy for Detection of Protein Biomarkers. *Langmuir* **2013**, *29* (47) , 14622-14630. https://doi.org/10.1021/la4039667

4. Zhanhong Wu, Ivan Todorov, Lin Li, James R. Bading, Zibo Li, Indu Nair, Kohei Ishiyama, David Colcher, Peter E. Conti, Scott E. Fraser, John E. Shively, and Fouad Kandeel . In Vivo Imaging of Transplanted Islets with 64Cu-

DAC EX. 2040 IPR2022-01531 Page 1087 of 1299

Bioconjugate Chemistry

5. Lin Li, Desiree Crow, Fabio Turatti, James R. Bading, Anne-Line Anderson, Erasmus Poku, Paul J. Yazaki, Jenny Carmichael, David Leong, Michael P. Wheatcroft, Andrew A. Raubitschek, Peter J. Hudson, David Colcher, and John E. Shively . Site-Specific Conjugation of Monodispersed DOTA-PEGn to a Thiolated Diabody Reveals the Effect of Increasing PEG Size on Kidney Clearance and Tumor Uptake with Improved 64-Copper PET Imaging. *Bioconjugate Chemistry* **2011**, *22* (4) , 709-716. https://doi.org/10.1021/bc100464e

6. Luis M. De León-Rodríguez and Zoltan Kovacs . The Synthesis and Chelation Chemistry of DOTA−Peptide Conjugates. *Bioconjugate Chemistry* **2008**, *19* (2) , 391-402. https://doi.org/10.1021/bc700328s

7. Lin Li, James Bading, Paul J. Yazaki, Amitkumar H. Ahuja, Desiree Crow, David Colcher, Lawrence E. Williams, Jeffrey Y. C. Wong, Andrew Raubitschek and John E. Shively . A Versatile Bifunctional Chelate for Radiolabeling Humanized Anti-CEA Antibody with In-111 and Cu-64 at Either Thiol or Amino Groups: PET Imaging Of CEA-Positive Tumors with Whole Antibodies. *Bioconjugate Chemistry* **2008**, *19* (1) , 89-96. https://doi.org/10.1021/bc700161p

8. Melford Chuka Egbujor, Brigitta Buttari, Elisabetta Profumo, Pelin Telkoparan-Akillilar, Luciano Saso. An Overview of NRF2-Activating Compounds Bearing α,β-Unsaturated Moiety and Their Antioxidant Effects. *International Journal of Molecular Sciences* **2022**, *23* (15) , 8466. https://doi.org/10.3390/ijms23158466

9. Megan Minnix, Lin Li, Paul Yazaki, Junie Chea, Erasmus Poku, David Colcher, John E. Shively. Improved targeting of an anti-TAG-72 antibody drug conjugate for the treatment of ovarian cancer. *Cancer Medicine* **2020**, *9* (13) , 4756-4767. https://doi.org/10.1002/cam4.3078

10. Oleksandr Koniev, Alain Wagner. Developments and recent advancements in the field of endogenous amino acid selective bond forming reactions for bioconjugation. *Chem. Soc. Rev.* **2015**, *44* (15) , 5495-5551. https://doi.org/10.1039/C5CS00048C

11. Bhumasamudram Jagadish, Tarik J. Ozumerzifon, Sue A. Roberts, Gabriel B. Hall, Eugene A. Mash, Natarajan Raghunand. Improved Synthesis of 10-(2-Alkylamino-2-oxoethyl)-1,4,7,10-tetraazacyclododecane-1,4,7-triacetic Acid Derivatives Bearing Acid-Sensitive Linkers. *Synthetic Communications* **2014**, *44* (3) , 441-449. https://doi.org/10.1080/00397911.2013.813547

12. Claire Bernhard, Mathieu Moreau, Damien Lhenry, Christine Goze, Frédéric Boschetti, Yoann Rousselin, François Brunotte, Franck Denat. DOTAGA−Anhydride: A Valuable Building Block for the Preparation of DOTA-Like Chelating Agents. *Chemistry – A European Journal* **2012**, *18* (25) , 7834-7841. https://doi.org/10.1002/chem.201200132

DAC EX. 2040 IPR2022-01531 Page 1088 of 1299

Bioconjugate Chemistry

2011, *40* (5) , 3019. https://doi.org/10.1039/c0cs00199f

14. Lin Li, Fabio Turatti, Desiree Crow, James R. Bading, Anne-Line Anderson, Erasmus Poku, Paul J. Yazaki, Lawrence E. Williams, Debra Tamvakis, Paul Sanders, David Leong, Andrew Raubitschek, Peter J. Hudson, David Colcher, John E. Shively. Monodispersed DOTA-PEG–Conjugated Anti-TAG-72 Diabody Has Low Kidney Uptake and High Tumor-to-Blood Ratios Resulting in Improved 64 Cu PET. *Journal of Nuclear Medicine* **2010**, *51* (7) , 1139-1146. https://doi.org/10.2967/jnumed.109.074153

15. Sara Lacerda, M. Paula Campello, Fernanda Marques, Lurdes Gano, Vojtěch Kubíček, Petra Fousková, Éva Tóth, Isabel Santos. A novel tetraazamacrocycle bearing a thiol pendant arm for labeling biomolecules with radiolanthanides. *Dalton Transactions* **2009**, *60* (23) , 4509. https://doi.org/10.1039/b820375j

16. Alessandro Barge, Enrico Cappelletti, Giancarlo Cravotto, Aurelia Ferrigato, Luciano Lattuada, Fabio Marinoni, Lorenzo Tei. Synthesis of functionalised HP-DO3A chelating agents for conjugation to biomolecules. *Organic & Biomolecular Chemistry* **2009**, *7* (18) , 3810. https://doi.org/10.1039/b905369g

17. Lorenzo Tei, Giuseppe Gugliotta, Stefano Avedano, Giovanni B. Giovenzana, Mauro Botta. Application of the Ugi four-component reaction to the synthesis of ditopic bifunctional chelating agents. *Organic & Biomolecular Chemistry* **2009**, *7* (21) , 4406. https://doi.org/10.1039/b907932g

18. Alessandro Barge, Lorenzo Tei, Dharita Upadhyaya, Franco Fedeli, Lorena Beltrami, Rachele Stefanìa, Silvio Aime, Giancarlo Cravotto. Bifunctional ligands based on the DOTA-monoamide cage. *Organic & Biomolecular Chemistry* **2008**, *6* (7) , 1176. https://doi.org/10.1039/b715844k

19. Lin Li, Paul J. Yazaki, Anne-Line Anderson, Desiree Crow, David Colcher, Anna M. Wu, Lawrence E. Williams, Jeffrey Y. C. Wong, Andrew Raubitschek, John E. Shively. Improved Biodistribution and Radioimmunoimaging with Poly(ethylene glycol)-DOTA-Conjugated Anti-CEA Diabody. *Bioconjugate Chemistry* **2006**, *17* (1) , 68-76. https://doi.org/10.1021/bc0502614

20. E Kleemann, M. Neu, N. Jekel, L. Fink, T. Schmehl, T. Gessler, W. Seeger, T. Kissel. Nano-carriers for DNA delivery to the lung based upon a TAT-derived peptide covalently coupled to PEG–PEI. *Journal of Controlled Release* **2005**, *109* (1-3) , 299-316. https://doi.org/10.1016/j.jconrel.2005.09.036

21. Bhupender S. Chhikara, Nitin Kumar, Vibha Tandon, Anil K. Mishra. Synthesis and evaluation of bifunctional chelating agents derived from bis(2-aminophenylthio)alkane for radioimaging with 99mTc. *Bioorganic &*

DAC EX. 2040 IPR2022-01531 Page 1089 of 1299

Bioconjugate Chemistry

22. Walter Mier, Johannes Hoffend, Susanne Krämer, Jochen Schuhmacher, William E. Hull, Michael Eisenhut, Uwe Haberkorn. Conjugation of DOTA Using Isolated Phenolic Active Esters: The Labeling and Biodistribution of Albumin as Blood Pool Marker. *Bioconjugate Chemistry* **2005**, *16* (1) , 237-240. https://doi.org/10.1021/bc034216c

23. Klaus Kunath, Thomas Merdan, Oliver Hegener, Hanns Häberlein, Thomas Kissel. Integrin targeting using RGD-PEI conjugates for in vitro gene transfer. *The Journal of Gene Medicine* **2003**, *5* (7) , 588-599. https://doi.org/10.1002/jgm.382

24. Lin Li, Tove Olafsen, Anne-Line Anderson, Anna Wu, Andrew A. Raubitschek, John E. Shively. Reduction of Kidney Uptake in Radiometal Labeled Peptide Linkers Conjugated to Recombinant Antibody Fragments. Site-Specific Conjugation of DOTA-Peptides to a Cys-Diabody. *Bioconjugate Chemistry* **2002**, *13* (5) , 985-995. https://doi.org/10.1021/bc025565u

25. Mark Woods, Zoltan Kovacs, A.Dean Sherry. Targeted Complexes of Lanthanide(III) Ions as Therapeutic and Diagnostic Pharmaceuticals. *Journal of Supramolecular Chemistry* **2002**, *2* (1-3) , 1-15. https://doi.org/10.1016/S1472-7862(02)00072-2

Download PDF

Partners

COUNTER

1155 Sixteenth Street N.W.
Washington, DC 20036

DAC EX. 2040 IPR2022-01531 Page 1090 of 1299

Bioconjugate Chemistry

About ACS Publications
ACS & Open Access
ACS Membership
ACS Publications Blog

Journals A-Z
Books and Reference
Advertising Media Kit
Institutional Sales
ACS Researcher Resources
Privacy Policy
Terms of Use

Help
Live Chat
FAQ

Connect with ACS Publications

Appendix LI02

Vinyl Sulfone Bifunctional Derivatives of DOTA Allow Sulfhydryl- or Amino-Directed Coupling to Antibodies. Conjugates Retain Immunoreactivity and Have Similar Biodistributions

Lin Li,[2] Shih-Wa Tsai,[2] Anne-Line Anderson,[3] David A. Keire,[§] Andrew A. Raubitschek,[3] and John E. Shively*,[2]

Division of Immunology, Beckman Research Institute of the City of Hope, Duarte, California 91010, Department of Radioimmunotherapy, City of Hope Medical Center, Duarte, California 91010, and CURE Digestive Diseases Research Center, UCLA School of Medicine, Los Angeles, California 90095.
Received July 24, 2001; Revised Manuscript Received October 25, 2001

We have synthesized a bifunctional vinyl sulfone–cysteineamido derivative of DOTA (1,4,7,10-tetraazacyclododecane-1,4,7,10-tetraacetic acid) that can be conjugated to the sulfhydryls of mildly reduced recombinant antibody (chimeric anti-CEA antibody cT84.66) at pH 7 or to the amino groups of lysine residues at pH 9. The conjugation is sulfhydryl specific at pH 7 (case 1), and amino specific at pH 9 (case 2) as long as the antibody has no free sulhydryl groups. At a molar ratio of 50 BCA (bifunctional chelating agent) to mAb, the number of chelates conjugated is 0.8 for case 1, and 4.6 for case 2. The resulting conjugates can be radiolabeled with ^{111}In to high specific activity (5 mCi/mg) with high efficiency (>95%) at 43 °C in 60 min. The radiolabeled conjugates retained >95% immunoreactivity and are stable in serum containing 1mM DTPA over 3 d. When the radiolabeled conjugates were injected into nude mice bearing LS174T human colon tumor xenografts, over 40% ID/g accumulated in tumors during the period 24–72h. Tumor-to-blood ratios were 4.5, 3.5, and 2.5 for the sulfhydryl coupled conjugate at 24, 48, and 72 h, respectively, and 2.7, 2.5, and 2.3 for the amino-coupled conjugate at the same time points. For other organs the biodistributions were nearly identical whether the conjugates were attached via sulfhydryl or amino groups. These novel BCAs are easy to synthesize, offer versatile conjugation options, and give equivalent biodistributions that result in high tumor uptake and good tumor-to-blood ratios.

Downloaded via PENNSYLVANIA STATE UNIV on December 2, 2024 at 17:52:08 (UTC).
See https://pubs.acs.org/sharingguidelines for options on how to legitimately share published articles.

INTRODUCTION

Bifunctional chelating agents (BCAs[1]) are routinely conjugated to recombinant antibodies for radiolabeling with radiometals such as ^{111}In for radioimmunoimaging and ^{90}Y for radioimmunotherapy (*1*–*4*). The main advantages of this approach is the ability to radiolabel the conjugate just prior to use and the exceptional stability of the chelated metal, preventing the release of the radionuclide from the conjugate. Starting with BCAs derived from EDTA (*5*, *6*), and then DTPA (*7*–*11*), and more recently DOTA (*12*–*16*), increasingly more stable radiometal–chelate–antibody conjugates have been crafted. Nonetheless, the approach has certain drawbacks inherent in the biodistribution of the antibody which in the case of intact antibody can be deposited in the liver (*17*–*21*), and in the case of antibody fragments, in the kidney (*22*–*25*). High uptake in normal tissues is due to the deposition of free antibody or antibody antigen conjugates in the liver for intact antibody (*21*) and to renal filtering and reabsorption for antibody fragments (*26*). In both cases, the exceptional stability of the radiometal–chelate and the lack of metabolizing enzymes prevents the excretion of these end-products from the lysosomal compartment. While it is assumed that the antibodies are completely degraded in the lysosome, releasing radiometal–chelate, it has only been proven in a few cases (*27*–*31*). In addition, the site of BCA conjugation to the antibody may play a key role in the fate of the radiolabel in both the tumor and normal organs. Furthermore, it is essential that the BCA be conjugated to the antibody without impairment of immunoreactivity. Since a major goal of the field is to reduce normal tissue uptake without decreasing the tumor uptake, we have investigated new BCA derivatives of DOTA that include the possibility of site-specific conjugation and linker specific cleavage. In previous work we showed that a maleimidocysteineamido derivative of DOTA coupled to sulfhydryl groups of mildly reduced intact antibody underwent pH dependent cleavage at the resulting succinimido groups (*32*), lowering blood levels while preserving high tumor uptake (*33*). However, the results were only a marginal improvement over our use of DOTA-active ester conjugated antibody (*34*, *35*). Oxidation of the thioether linker to a sulfone linker further increased the rate of linker bond cleavage, but the rate of blood clearance was too high, preventing good tumor uptake (*33*). Similar approaches utilizing ester linkers for reducing blood levels have been reported, but also suffer from lower blood levels to the point of reducing

* To whom correspondence should be addressed. e-mail: jshively@coh.org.
[2] Beckman Research Institute of the City of Hope.
[3] City of Hope Medical Center.
[§] UCLA School of Medicine.

[1] Abbreviations: BCA, bifunctional chelating agent; CEA, carcinoembryonic antigen; DOTA, 1,4,7,10-tetraazacyclododecane-1,4,7,10-tetraacetic acid; EDC, 1-ethyl-3-[3-(dimethylamino)propyl]carbodiimide; DTPA, diethylenetriaminepentaacetic acid; HSA, human serum albumin; sulfo-NHS, *N*-hydroxysulfosuccinimide; TCEP, tris(carboxyethyl)phosphine; VSC-DOTA, vinyl sulfone-cysteineamido-DOTA.

10.1021/bc015535b CCC: $22.00 © 2002 American Chemical Society
Published on Web 12/14/2001

DAC EX. 2040 IPR2022-01531 Page 1093 of 1299

tumor uptake (*21*, *36*−*38*). A similar problem is found in using antibody fragments, which clear the blood rapidly, but also give low tumor uptake (*25*). Thus, it is clear that the price of lowering blood levels is the concomitant lowering of tumor uptake, an unacceptable consequence in either radioimmunoimaging or radioimmunotherapy. A possible solution to the problem is the synthesis of BCAs with organ-specific cleavable linkers. Arano and co-workers (*26*, *39*−*41*) have synthesized C-terminal Lys linkers for a radioiodinated hippuric acid−Fab conjugatethat lowered kidney uptake by 50%. Meares and coworkers (*42*−*44*) have synthesized DOTA with cathepsin cleavable linkers for use in lowering liver levels. In the work reported here, we have made new derivatives of DOTA that incorporate a vinyl sulfone-based linker that shows versatility in terms of conjugation to either sulfhydryl or amino groups of antibodies. The BCA is easy to synthesize from readily available chemicals and gives high radiolabeling yields when conjugated to either sulfhydryl or amino groups. The biodistributions in tumor-bearing animals is nearly equivalent, suggesting that the site of conjugation has not affected either the tumor or normal organ uptake. The new BCA may be useful in preventing the impairment of immunoreactivity in cases where coupling through amino groups is problematic.

EXPERIMENTAL PROCEDURES

General. DOTA trisodium salt and the free acid were purchased from Parish Chemical Co. (Orem, UT) and Macrocyclics, Inc. (Richardson, TX), respectively. DTPA was obtained from Fluka (Milwaukee, WI), vinyl sulfone from Aldrich (Milwaukee, WI), Chelex 100 from BioRad (Hercules, CA), and L-cysteine from Sigma (St. Louis, MO). Ultrapure water (18 MΩ-cm) was used to make all buffers that were passed over Chelex 100 and pH adjusted if necessary. $^{111}InCl_3$ was obtained from NEN Life Science products, Inc. (Boston, MA). The anti-CEA chT84.66 has been previously described (*35*, *45*). HPLC and TLC were performed as previously described (*32*). Mass spectra were recorded on a Finnigan LCQ ion trap mass spectrometer using a custom nanospray interface. NMR spectra were recorded on a Varian Unity Plus 500 MHz spectrometer. Proton chemical shifts are reported relative to HOD (4.80 ppm). Antibody concentrations were calculated at 280 nm (A_{280}, 1 mg/mL = 1.42). UV spectrophometry was performed on a Shimadzu UV160 instrument using a 1 cm cell. Melting points were recorded on a Thomas-Hoover uni-melt apparatus and are uncorrected. SDS and IEF gel electrophoresis was performed on a Pharmacia PhastGel apparatus according to the manufacturer's instructions.

Vinyl Sulfone−Cysteineamido−DOTA (VSC-DOTA; 2). Cysteineamido-DOTA (**1**) was synthesized as previously reported (*46*). To a solution of 3.24 mg (6.1 μmol) of **1** in 0.6 mL of 50 mM, pH 7.5 potassium phosphate was added 0.06 mL of 0.1 M DTT (6 mmol) and stirred for 0.5 h at RT under Ar. Vinyl sulfone (6.6 μL (64 μmol) in 0.6 mL of DMF was added with continuous stirring for 5 h at RT. A second aliquot was added and the reaction continued for another 22 h (final vol = 1.2 mL, 5.3 mM **1**, 107 mM vinyl sulfone). The excess vinyl sulfone was extracted with ethyl acetate (2 mL, ×3). The aqueous layer was adjusted to pH 8.4, applied to a BioRad Ag1-X4 column (HCO_2^- form, 1 × 10 cm), washed with 30 mL of water, and eluted stepwise with 0.05−2 M HCO_2H (5 mL per step). The product (**2**) was found in fractions 8−13 by ESI/MS. The product was repeatedly lyophilyzed from water to remove excess HCO_2H (yield 3.4 mg). The product had the expected protonated mass by ESI/MS (626.71, expected; 626.73, observed), gave a single spot on TLC, and had a melting point of 140−142 °C. Proton NMR (H_2O): δ 2.92 (m, 2H, $SCH_2CH_2SO_2$), δ 3.10 (m, 2H, $SCH_2CH_2SO_2$), δ 3.10−3.45 [br, 16H, (CH_2-NCH_2) × 4], δ 3.53 (dd, 2H, CH_2SO_2), δ 3.45, 3.70, 3.84 (s, 6H, NCH_2CO_2H), δ 4.39 (m, 1H, $NHCHCO_2H$), δ 6.42 (dd, 2H, SO_2CHCH_2), δ 6.88 (dd, 1H, SO_2CHCH_2), δ 8.20 (d, 1H, CONH−CH).

Preparation of Amino-Conjnugated BCA Antibody (VSC-DOTA-NH-chT84.66). chT84.66 (FW= 150000, 1.0 mg, 6 nmol, at 10 mg/mL, 60 μM) was dialyzed vs 20 mM, pH 7.0 sodium phosphate buffer (three changes, × 1 L, 4 °C) and adjusted to pH 9.0 with 200 mM, pH 10 sodium phosphate (final volume, 0.1 mL). VSC-DOTA (0.1 mL of **2**, FW= 625, 0.7 mg, 1.12 μmol at 1.88 mg/mL, 3.1 mM in 50 mM, pH 9.0 sodium phosphate) was added and the solution rotated at 10 rpm for 4 h at 25 °C. The conjugate was dialyzed vs 250 mM NH_4 acetate (three changes, × 1 L, 4 °C).

Preparation of Sulfhydryl-Conjnugated BCA Antibody (VSC-DOTA-SH-chT84.66). chT84.66 was dialyzed as above and reduced with TCEP (20 μL of 10 mM in 50 mM sodium phosphate, pH 7.0) under argon for 2.5 h at 25 °C. TCEP was removed on a spin column (1 mL of Sephadex G25−50, 1200 rpm, 2 min) under argon. To 1.0 mg (60 nmol) of reduced chT84.66 in 0.1 mL of 50 mM sodium phosphate, pH 7, was added 0.1 mL of 3 mM (300 nmol) of VSC-DOTA (**2**) in the same buffer. The solution was rotated under argon overnight at 25 °C and dialyzed vs NH_4 acetate as described above. In parallel, 1 mg of TCEP reduced chT84.66 in 0.15 mL was reacted with 0.1 mL of 3 mM MC-DOTA and run as a control.

Radiolabeling of VSC-DOTA-chT84.66. The conjugates were radiolabeled with $^{111}InCl_3$ as previously described (*47*). For the animal studies, the conjugates (0.3 mL of 1 mg/mL in 250 mM NH_4 acetate, pH 5.7) were incubated with 0.3 mCi of ^{111}In (0.15 mL of 0.04 M HCl plus 0.03 mL of 250 mM NH_4 acetate, pH 5.7) for 60 min at 43 °C. Excess ^{111}In was chelated with 1 mM DTPA and the radiolabeled product purified on a TosoHaas TSK−Gel G2000SW column (0.75 × 30 cm in saline, 0.5 mL/min, 0.5 mL fractions). The protein peak was mixed with 1 drop of 25% (w/v) of HSA. In other test labelings, 1.0 mCi of ^{111}In was added to 0.2 mg of conjugate and the specific activity determined by ITLC (kit 151−770, Biodex, Medical, New York). Determination of the number of chelates per conjugate and the immunoreactivity was performed as previously described (*5*).

Stability Studies. Aliquots (0.5 mL) of the radiolabeled conjugates in 1% HSA were mixed with 0.05 mL of 10 mM DTPA, stored at 37 °C and injected at various time points onto a Pharmacia Superose 12HR column (as above) to determine the amount of radiolabel in the conjugate and DTPA.

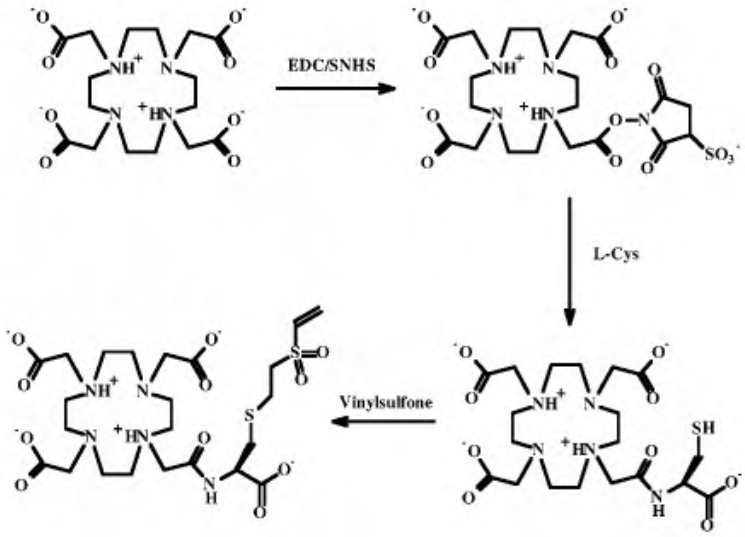
Animal Biodistributions. Groups of five nude mice (Charles River) bearing LS174T human colon tumor xenografts (ave size = 1.5 mg ± 0.5 at t = 0 h) were injected with 2 μCi (2 μg) of radiolabeled conjugate via tail vein. Animals were sacrificed at 0, 12, 24, 48, 72, and 96 h after injection. Major organs, tumor, and blood were weighed, radioactivity was measured, and the results were expressed as mean %ID/g ± SD.

RESULTS

Synthesis and Antibody Conjugation. The synthesis of VSC-DOTA (**2**) is shown in Scheme 1. The product gave the expected proton NMR spectrum and protonated

DAC EX. 2040 IPR2022-01531 Page 1094 of 1299

Scheme 1



mass by ESI/MS and was free of DOTA and the bis-derivative. The reactivity of **2** to free L-cysteine was confirmed by ESI/MS (data not shown). At pH 7, only the mono-derivative was formed, suggesting that the thiol and not the α-amino group of L-cysteine was reactive under these conditions. When VSC-DOTA was incubated for 1−7 d in pH 7 PBS and analyzed by RP-HPLC, there was no evidence of chemical instability (data not shown).

Since VSC-DOTA was expected to react with the ϵ-amino group on the lysines of proteins at pH 9−10, we investigated the reaction of VSC-DOTA with antibody over the pH range of 7−9. The degree of conjugation was determined by IEF gel electrophoresis, wherein conjugation of the acidic BCA to antibody results in a dramatic shift of the antibody to a more acidic pI. The results of the conjugation reaction at pH 7, 8, and 9 shown in Figure 1A, lanes 3−5, demonstrate that little or no reaction occurs at pH 7, while substantial amounts of conjugate are formed at pH 9. The results at pH 8 are intermediate, with <20% product formed. The results at 37 °C, pH 9 demonstrate the expected effect of temperature on the extent of reaction (Figure 1A, lane 6). The products show no change in mobility when run on SDS gel electrophoresis under nonreducing conditions (data not shown). On the basis of these results, we reasoned that sulfhydryl specific conjugation could be performed at pH 7 with little or no conjugation at amino groups, while amino group specific conjugation could be performed at pH 9, as long as no free sulfhydryl groups are present. Since the cysteine residues in most antibodies are engaged in disulfide bonds, this criterion is easily met. In addition, under mild reducing conditions (no denaturing agents), only the hinge disulfides of antibodies are reduced, allowing site-specific conjugation at just these sulfhydryl groups (*48*, *49*). The conjugation of VSC-DOTA to mildly reduced chT84.66 at pH 7 shown in Figure 1B, lane 4, demonstrates that >90% of the antibody is conjugated under these conditions. It should be noted that either DTT or TCEP were successfully used as reducing agents. We prefer TCEP because a lower molar excess is required and since removal of the reducing agent by spin columns is not quantitative, better conjugation yields are routinely obtained.

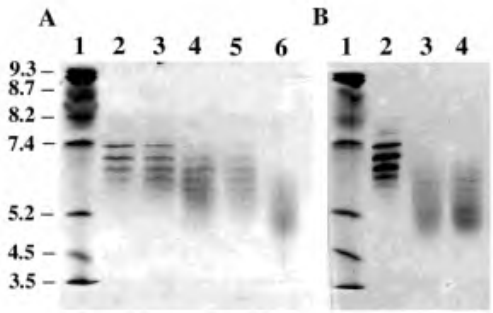


Figure 1. Analysis of VSC-DOTA-mAb conjugates by IEF gel electrophoresis. A: Lane 1: IEF standards; Lane 2: chT84.66 control; Lane 3: 30 μM chT84.66, 1.5 mM VSC-DOTA, pH 7.0, RT, 4h; Lane 4: 30 μM chT84.66, 1.5 mM VSC-DOTA, pH 8.0, RT, 4 h; Lane 5: 30 μM chT84.66, 1.5 mM VSC-DOTA, pH 9.0, RT, 4 h; Lane 6: 30 μM chT84.66, 1.5 mM VSC-DOTA, pH 9.0, 37 °C, 4 h. B: Lane 1: IEF standards; Lane 2: chT84.66 control; Lane 3: 30 μM chT84.66 reduced with 0.5 mM TCEP, the TCEP removed by spin column, and reacted with 1.5 mM MC-DOTA, pH 7.0, RT, 4 h; Lane 4: 30 μM chT84.66, reduced with 0.5 mM TCEP, the TCEP removed by spin column, and reacted with 1.5 mM VSC-DOTA, pH 7.0, RT, 4 h.

The number of chelates per antibody as determined by trace labeling with ^{111}In in a standard solution of $InCl_3$ is shown in Table 1. At pH 7 and with a 50:1 molar ratio of VSC-DOTA to mAb, mildly reduced antibody gave 0.8 chelates/mAb out of a theoretical of 8 for a human IgG1 hinge. At pH 9 with the same molar ratio of VSC-DOTA to mAb, unreduced mAb gave 4.6 chelates/mAb. Radiolabeling of these two conjugates with $^{111}InCl_3$ gave similar percent radiolabeling efficiencies, specific activities, and

Table 1. Radiometal Labeling and Immunoreactivity of VSC-DOTA-mAb[a]

sample	chelates/ mAb	labeling ratio (mCi/mg)	% efficiency	% immuno-reactivity
SH-mAb	0.8	1.0−5.0	>98	>98
NH-mAb	4.5	1.0−5.0	>98	>98

[a] VSC-DOTA was coupled to either SH or NH groups in the mAb as described in the text. The number of chelates per mAb was determined by trace labeling with ^{111}In in a standard solution of $InCl_3$. The labeling ratio was performed with 0.3 mCi of ^{111}In and 0.3 mg of conjugate in 0.3 mL of 0.25 mM ammonium acetate (pH 5.7), or 1.0 mCi of ^{111}In and 0.2 mg of conjugate in 0.2 mL of ammonium actetate (pH 5.7). Immunoreactivity was performed as described in Methods.

DAC EX. 2040 IPR2022-01531 Page 1095 of 1299

Table 2. Biodistribution of ^{111}In-Labeled VSC-DOTA-SH mAb in Nude Mice Bearing LS174T Xenografts[a]

	0 h	12 h	24 h	48 h	72 h	96 h
blood	47.97	23.83	15.00	7.33	3.98	2.49
	(2.58)	(2.43)	(2.07)	(3.78)	(2.51)	(3.02)
liver	7.30	6.65	10.15	14.91	19.60	18.83
	(0.25)	(1.94)	(1.90)	(6.27)	(7.19)	(3.32)
spleen	5.41	5.18	5.93	7.76	6.41	7.69
	(1.22)	(0.57)	(0.95)	(2.54)	(2.25)	(2.27)
kidney	6.36	5.62	4.36	3.46	2.82	2.63
	(1.43)	(0.46)	(0.56)	(1.08)	(0.46)	(0.43)
lung	14.01	8.59	5.50	2.99	1.87	0.90
	(3.27)	(1.26)	(0.72)	(1.36)	(0.88)	(0.59)
tumor	1.59	37.08	43.61	42.01	40.43	39.57
	(0.47)	(4.09)	(4.91)	(12.73)	(6.96)	(18.97)
carcass	1.57	2.58	2.15	1.47	1.05	0.96
	(0.15)	(0.10)	(0.29)	(0.48)	(0.26)	90.51)

[a] Five animals per group were injected with 4 μCi (4 μg) of VSC-DOTA coupled to chT84.66 via the hinge SH groups and radiolabeled with ^{111}In. The results are reported as mean %ID/g (±SD).

Table 3. Biodistribution of ^{111}In-Labeled VSC-DOTA-NH mAb in Nude Mice Bearing LS174T Xenografts[a]

	0 h	12 h	24 h	48 h	73 h	96 h
blood	47.61	17.98	17.50	8.98	5.84	3.08
	(2.97)	(6.29)	(6.74)	(3.18)	(4.14)	(4.50)
liver	9.16	12.38	13.93	16.27	19.64	18.42
	(0.97)	(3.77)	(5.75)	(4.25)	(5.36)	(4.79)
spleen	7.25	6.35	8.09	7.77	10.07	9.06
	(0.68)	(0.73)	(2.34)	(2.00)	(2.08)	(2.09)
kidney	7.29	4.24	5.03	3.44	2.60	2.15
	(1.36)	(1.14)	(1.77)	(0.87)	(0.79)	(0.76)
lung	13.07	5.63	6.58	3.44	2.58	1.45
	(1.18)	(1.79)	(2.58)	(1.30)	(1.57)	(1.63)
tumor	1.26	21.66	38.54	39.27	45.76	33.85
	(0.40)	(5.02)	(13.60)	(10.19)	(18.25)	(14.52)
carcass	1.76	2.20	2.64	1.72	1.43	0.89

[a] Five animals per group were injected with 4 μCi (3.4 μg) of VSC-DOTA coupled to chT84.66 via NH groups and radiolabeled with ^{111}In. The results are reported as mean %ID/g (± SD).

immunoreactivities (Table 1). When the radiolabeled conjugates were incubated in 1% HSA and 1 mM DTPA for 1−7d, negligible loss of radioactivity was seen to DTPA (Table 1). In addition, their immunoreactivities were >95% when radiolabeled, bound to excess CEA, and analyzed by gel filtration chromatography. Since their immunoreactivities were similar, we used these conjugates for a direct comparison in animal biodistribution studies.

Comparative Animal Biodistributions of [^{111}In]-VSC-DOTA-SH-chT84.66 and [^{111}In]VSC-DOTA-NH-chT84.66. The two ^{111}In-radiolabeled conjugates were injected into nude mice bearing human colon tumor xenografts and their biodistributions compared (Tables 2 and 3). The overall biodistributions are quite similar, resulting in maximal and sustained tumor uptake of 35−45% ID/g from 24 to 96 h. During the same time period the blood activity drops from about 45% ID/g to 2−3% ID/g. A comparison of tumor to blood curves over the time course suggests that the SH conjugate may be superior to the NH conjugate. Paradoxically, this difference may be due to a slightly slower blood clearance curve for the SH conjugate, resulting in higher uptake. A close analysis of the normal organs reveals nearly identical uptake levels and time courses for the spleen, kidney, and lung, but there are some interesting differences in the liver. The SH conjugate shows lower liver uptake at the earlier time points, suggesting that the NH conjugate accumulates more rapidly in the liver. This result would also account for their observed differences in blood clearance curves.

DISCUSSION

In a search for site-specific BCA derivatives of DOTA we first synthesized a bis-maleimidohexane derivative of cysteineamido-DOTA (*32*). Maleimide is a commonly used reagent that undergoes sulfhydryl specific Michael additions that are thought to be chemically stable (*50*). Although this BCA allowed site-specific conjugation to the sulfhydryl groups of mildly reduced mAb, it proved to be chemically labile, undergoing pH-dependent hydrolysis at its resulting succinimidyl bonds (*32*). Surprisingly, this phenomenon did not prevent good tumor uptake in animal biodistribution studies (*33*). As a result, we proposed that further increasing the chemical lability of the linker may be beneficial, since this would result in lower blood levels. Indeed, oxidation of the thioether bond in the linker to a sulfone increased the chemical lability of the BCA (*32*), but the BCA decomposed too rapidly to allow good tumor uptake. On the basis of these studies, we decided to investigate other Michael addition linkers as candidates for site-specific conjugation to mAbs. We chose vinyl sulfone for its well-documented reaction with sufhydryl groups (*51*). However, we realized from the outset that vinyl sulfone can also react with amino groups (*52*, *53*), and thus we were interested in seeing if this reaction could be controlled by manipulation of the reaction pH.

Vinyl sulfone is a viscous liquid with poor solubility in water, but when dissolved in DMF or acetonitrile reacts well with Michael acceptors in aqueous medium. In the synthesis of the title compound (**2**), we demonstrated a facile reaction between vinyl sulfone and cysteineamido-DOTA. Unlike the maleimido derivatives, the vinyl sulfone derivative of cysteineamido-DOTA is stable in PBS at pH 7. When **2** was reacted with chT84.66 at pH 7, no conjugate was formed unless the mAb was mildly reduced prior to reaction. In addition, we showed that the mAb conjugated with **2** at pH 9 to a greater extent (no. chelates/mAb) as it did to reduced mAb at pH 7 using the same molar ratio of **2** to mAb. Thus, we demonstrated that this BCA can be conjugated to the same mAb via different chemical linkages using pH and reducing agents to convey linkage specificity.

Since the biodistributions of radiolabeled mAbs is highly dependent on the mode of attachment of the radiolabel, it is always interesting to compare BCAs conjugated to the same mAb via different chemical linkages. In most cases, it is difficult to perform this type of comparative study. However, in this study, we have an almost ideal model. In one case, the same BCA is conjugated to sulfhydryl groups, and in the other case, amino groups, but the resulting BCA/mAb ratios are different. Even so, the resulting biodistributions are quite similar. When we compare these results to our previous studies in which DOTA was conjugated to chT84.66 by an active ester derivative of DOTA (*34*, *35*), we find that the uptake curves are similar for both tumor and normal tissues. This suggests that linkage of DOTA based BCAs to mAbs via amides, amine, or sulfhydryl bonds results in similar tissue, including tumor, uptakes, and metabolism. Thus, if one wants to manipulate normal or tumor uptake and metabolism of DOTA-based BCAs, it is necessary to explore other modes of chemical linkage or to insert linkers which have built-in chemical or biological lability. Examples of such linkers have been described by Meares (*21*), Arano (*54*), and ourselves (*32*).

When we examined the comparative biodistributions of the SH and NH BCA-chT84.66 conjugates in more detail, we noticed some intriguing trends. They include

DAC EX. 2040 IPR2022-01531 Page 1096 of 1299

the higher blood levels, higher tumor levels, and lower liver levels for the BCA chT84.66 SH conjugate at early time points 0−24 h. These three "organs" are interdependent in their biodistributions as follows: high tumor uptake is dependent on maintaining high blood levels, especially early in a biodistribution. If the blood is cleared by any mechanism, including rapid liver uptake, then blood and tumor levels will fall together. Thus, the lower liver uptake seen at early time points for the SH conjugate leads to higher blood levels and ultimately to higher tumor uptake which is sustained at later time points. While the biological reasons for these differences are unknown at this time, we can speculate that this mode of conjugation will lead to incremental improvements in the human, where most biodistributions are predicted from the animal model.

In summary, we have prepared a new BCA that allows site-specific conjugation to most mAbs either via sulfhydryl or amino groups by manipulating pH and use of reducing agents. The ^{111}In-radiolabeled versions of these conjugates give more or less equivalent animal biodistributions to previously described ^{111}In-radiolabeled BCA-mAbs, including are own version using the active ester of DOTA (*34*, *35*). This approach should have utility, allowing the investigator to chose one type of chemistry over the other depending on the restrictions implied by a given antibody. Finally, the improvement in tumor to blood and tumor-to-liver ratios seen for the SH-specific conjugate may translate into improved performance in the clinic.

ACKNOWLEDGMENT

The authors thank Stefanie Wright for the animal studies. This research was funded by NCI grant CA43904 (A.A.R. and J.E.S.) and the Department of the Army Grant DAMD 17-98-1-8031 (J.E.S.).

LITERATURE CITED

(1) Anderson, C. J., and Welch, M. J. (1999) Radiometal-labeled agents (non-technetium) for diagnostic imaging. *Chem. Rev. 99*, 2219−2234.

(2) Gansow, O. A. (1991) Newer Approaches to the Radiolabeling of Monoclonal Antibodies by Use of Metal Chelates. *Int. J. Radiat. Appl. Instrum. Part B Nucl. Med. Biol. 18*, 369−381.

(3) Meares, C. F. (1986) Chelating Agents for the Binding of Metal Ions to Antibodies. *Int. J. Radiat. Appl. Instrum. Part B Nucl. Med. Biol. 13*, 311−318.

(4) Liu, S., and Edwards, D. S. (2001) Bifunctional chelators for therapeutic lanthanide radiopharmaceuticals. *Bioconjugate Chem. 12*, 7−34.

(5) Meares, C. F., McCall, M. J., Reardan, D. T., Goodwin, D. A., Diamanti, C. I., and McTigue, M. (1984) Conjugation of Antibodies with Bifunctional Chelating Agents: Isothiocyanate and Bromoacetamide Reagents, Methods of Analysis, and Subsequent Addition of Metal Ions. *Anal. Biochem. 142*, 68−78.

(6) Brechbiel, M. W., Gansow, O. A., Atcher, R. W., Schlom, J., Esteban, J., Simpson, D. E., and Colcher, D. (1986) Synthesis of 1-(*p*-Isothiocyanatobenzyl) Derivatives of DTPA and EDTA. Antibody Labeling and Tumor-Imaging Studies. *Inorg. Chem. 25*, 2772−2781.

(7) Brechbiel, M. W., and Gransow, O. A. (1991) Backbone-substituted DTPA ligands for ^{90}Y radioimmunotherapy. *Bioconjugate Chem. 2*, 187−194.

(8) Cummins, C. H., Rutter, E. W., and Fordyce, W. A. (1991) A convenient synthesis of bifunctional chelating agents based on diethylenetriaminepentaacetic acid and their coordination chemistry with yttrium (III). *Bioconjugate Chem. 2*, 180−186.

(9) Hnatowich, D. J., Virzi, F., and Doherty, P. W. (1985) DTPA-Coupled Antibodies Labeled with Yttrium-90. *J. Nucl. Med. 26*, 503−509.

(10) Westerberg, D. A., Carney, P. L., Rogers, P. E., Kline, S. J., and Johnson, D. K. (1989) Synthesis of Novel Bifunctional Chelators and Their Use in Preparing Monoclonal Antibody Conjugates for Tumor Targeting. *J. Med. Chem. 32*, 236−243.

(11) Corson, D. T., and Meares, C. F. (2000) Efficient multigram synthesis of the bifunctional chelating agent (S)-1-p-isothiocyanatobenzyl-diethylenetetraaminepentaacetic acid. *Bioconjugate Chem. 11*, 292−299.

(12) Cox, J. P. L., Jankowski, K. J., Kataky, R., Parker, D., Beeley, N. R. A., Boyce, B. A., Eaton, M. A. W., Millar, K., Millican, A. T., Harrison, A., and Walker, C. (1989) Synthesis of a Kinetically Stable Yttrium-90 Labeled Macrocycle-Antibody Conjugate. *J. Chem. Soc., Chem. Commun.* 797−798.

(13) Deshpande, S. V., DeNardo, S. J., Kukis, D. L., Moi, M. K., McCall, M. J., DeNardo, G. L., and Meares, C. F. (1990) Yttrium-90-labeled monoclonal antibody for therapy: labeling by a new macrocyclic bifunctional chelating agent. *J. Nucl. Med. 31*, 473−479.

(14) Meares, C. F., Moi, M. K., Diril, H., Kukis, D. L., McCall, M. J., Deshpande, S. V., DeNardo, S. J., Snook, D., and Epenetos, A. A. (1990) Macrocyclic chelates of radiometals for diagnosis and therapy. *Br. J. Cancer 62*, Suppl. X, 21−26.

(15) Smith-Jones, P. M., Fridrich, R., Kaden, T. A., Novak-Hofer, I., Siebold, K., Tschudin, D., and Maecke, H. R. (1991) Antibody Labeling with Copper-67 Using the Bifunctional Macrocycle 4-[(1,4,8,11-Tetraazacyclotetradec-1-yl)methyl]-benzoic Acid. *Bioconjugate Chem. 2*, 415−421.

(16) Kline, S. J., Betebenner, D. A., and Johnson, D. K. (1991) Carboxymethyl-Substituted Bifunctional Chelators: Preparation of Aryl Isothiocyanate Derivatives of 3-(Carboxymethyl)-3-azapentanedioic Acid, 3,12-Bis(carboxymethyl)-6,9-dioxa-3,12-diazatetradecanedioic Acid, and 1,4,7,10-Tetraazacyclododecane-*N*,*N*′,*N*″,*N*‴-tetraacetic Acid for Use as Protein Labels. *Bioconjugate Chem. 2*, 26−31.

(17) Halpern, S. E., Hagan, P. L., Garver, P. R., Koziol, J. A., Chen, A. W. N., Frincke, J. M., Bartholomew, R. M., David, G. S., and Adams, T. H. (1983) Stability, Characterization, and Kinetics of ^{111}In-labeled Monoclonal Antitumor Antibodies in Normal Animals and Nude Mouse-Human Tumor Models. *Cancer Res. 43*, 5347−5355.

(18) Jakowatz, J. G., Beatty, B. G., Vlahos, W. G., Porudominsky, D., Philben, V. J., Williams, L. E., Paxton, R. J., Shively, J. E., and Beatty, J. D. (1985) High-Specific-Activity ^{111}In-labeled Anticarcinoembryonic Antigen Monoclonal Antibody: Biodistribution and Imaging in Nude Mice Bearing Human Colon Cancer Xenografts. *Cancer Res. 45*, 5700−5706.

(19) Larson, S. M., and Carrasquillo, J. A. (1988) Advatages of radioiodine over radioindium labeled monoclonal antibodies for imaging solid tumors. *Nucl. Med. Biol. 15*, 231−233.

(20) Wong, J. Y. C., Thomas, G. E., Yamauchi, D. M., Williams, L. E., Odom-Maryon, T. L., E. J. M., Neumaier, M., Wu, A. M., Primus, F. J., Shively, J. E., and Raubitschek, A. A. (1997) Clinical evaluation of an ^{111}In labeled anti-CEA chimeric monoclonal antibody in patients with metastatic CEA producing malignancies. *J. Nucl. Med. 38*, 1951−1959.

(21) Meares, C. F., McCall, M. J., Deshpande, S. V., DeNardo, S. J., and Goodwin, D. A. (1988) Chelate radiochemistry: cleavable linkers lead to altered levels of radioactivity in the liver. *Int. J. Cancer (suppl.) 2*, 99−102.

(22) Bujis, W. C. A. M., Massuger, L. F. A. G., Claessens, R. A. M. J., Kenemans, P., and Corstens, F. H. M. (1992) Dosimetric evaluation of immunoscintigraphy using indium-11-labeled monoclonal antibody fragments in patients with ovarian cancer. *J. Nucl. Med. 33*, 1113−1120.

(23) Govindan, S. V., Shih, L. B., Goldenberg, D. M., Sharkey, R. M., Karacay, H., Donnelly, J. E., Losman, M. J., Hansen, H. J., and Griffiths, G. L. (1998) 90-Yttrium-labeled complementarity-determining-region grafted monoclonal antibodies for radioimmunotherpay: radiolabeling and animal biodistribution studies. *Bioconjugate Chem. 9*, 773−782.

DAC EX. 2040 IPR2022-01531 Page 1097 of 1299

(24) Yemul, S., Leon, J. A., Pozniakoff, T., Esser, P. D., and Estabrook, A. (1993) Radioimmunoimaging of human breast carcinoma xenografts in nude mouse model with ^{111}In labeled new monoclonal antibody EBA-1 and F(ab')2 fragments. *Nucl. Med. Biol. 20*, 325−335.
(25) Yokota, T., Milenic, D. E., Whitlow, M., and Schlom, J. (1992) Rapid tumor penetration of a single-chain Fv and comparison with other immunoglobulin forms. *Cancer Res. 52*, 3402−3408.
(26) Arano, Y. (1998) Strategies to reduce renal radioactivity levels of antibody fragments. *Quart. J. Nucl. Med. 42*, 262−270.
(27) Duncan, J. R., and Welch, M. J. (1993) Intracellular metabolism of indium-111 DTPA labeled receptor targeted proteins. *J. Nucl. Med. 34*, 1728−1738.
(28) Duncan, J. R., Stephenson, M. T., Wu, H. P., and Anderson, C. J. (1997) Indium-111-diethylenetriamine pentaacetic acid octreotide is delivered in vivo to pancreatic, tumor cell, renal, and hepatocyte lysosomes. *Cancer Res. 57*, 659−671.
(29) Franano, F. N., Edwards, W. B., Welch, M. J., and Duncan, J. R. (1994) Metabolism of receptor targeted ^{111}In-DTPA-glycoporteins: identification of ^{111}In-DTPA-epsilon-lysine as the primary metabolic and excretory product. *Nucl. Med. Biol. 21*, 1023−1034.
(30) Novak-Hofer, I., Amstutz, H. P., Macke, H. R., Schwartzbach, R., Zimmermann, K., Morgenthaler, J.-J., and Schubiger, P. A. (1995) Cellular processing of copper-67 labeled monoclonal antibody chCE7 by human neuroblastoma cells. *Cancer Res. 55*, 46−50.
(31) Tsai, S. W., Li, L., Williams, L. E., Anderson, A.-L., Raubitschek, A. A., and Shively, J. E. (2001) Metabolism and renal clearance of ^{111}In-labeled DOTA conjugated antibody fragments. *Bioconjugate Chem. 12*, 264−270.
(32) Lewis, M. R., and Shively, J. E. (1998) Maleimidocysteine-amido-DOTA derivatives. New reagents for radiometal chelate conjugation to antibody sulfhydryl groups undergo pH-dependent clevage reactions. *Bioconjugate Chem. 9*, 72−86.
(33) Williams, L. E., Lewis, M. R., Bebb, G. G., Clarke, K. G., Odom-Maryon, T. L., Shively, J. E., and Raubitschek, A. A. (1998) Biodistribution of ^{111}In and ^{90}Y labeled DOTA and maleimidocysteineamido-DOTA conjugated to chimeric anti-carcinoembryonic antigen antibody in xenograft bearing nude mice: comparison of stable and chemically labile linker systems. *Bioconjugate Chem. 9*, 87−93.
(34) Lewis, M. R., Raubitschek, A. A., and Shively, J. E. (1994) A facile, water-soluble method for modification of proteins with DOTA. Use of elevated temperature and optimized pH to achieve high specific activity and high chelate stability in radiolabeled immunoconjugates. *Bioconjugate Chem. 5*, 565−576.
(35) Williams, L. E., Primus, F. J., Wong, J. Y. C., Wu, A. M., Odom-Maryon, T. L., Johnson, D. K., Hefta, L. J. F., Shively, J. E., and Raubitschek, A. A. (1996) Biodistribution of an ^{111}In or ^{90}Y labeled chimeric anti-CEA monoclonal antibody (cT84.66) following its large scale production in a bioreactor. *Tumor Targeting 2*, 116−124.
(36) Haseman, M. K., Goodwin, D. A., Meares, C. F., Kaminski, M. S., Wensel, T. G., McCall, M. J., and Levy, R. (1986) Metabolizable 111-In-chelate conjugated anti-iodiotype monoclonal antibody for radioimmunodetection of lymphoma in mice. *Eur. J. Nucl. Med. 12*, 455−460.
(37) Paik, C. H., Yokoyama, K., Reynolds, J. C., Quadri, S. M., Min, C. Y., Shin, Y., Maloney, P. J., Larson, S. M., and Reba, R. C. (1989) Reduction of background activities by introduction of a diester linkage between antibody and a chelate in radioimmunodetection of tumor. *J. Nucl. Med. 30*, 1693−1701.
(38) Deshpande, S. V., DeNardo, S. J., Meares, C. F., McCall, M. J., Adams, G. P., and DeNardo, G. L. (1989) Effect of different linkage between chelates and monoclonal antibodies on levels of radioactivity in the liver. *Nucl. Med. Biol. 16*, 587−597.
(39) Arano, Y., Mukai, T., Uezono, T., Wakisaka, K., Motonari, H., Akizawa, H., Taoka, Y., and Yokoyama, A. (1994) A biological method to evaluate bifunctional chelating agents to label antibodies with metallic radionuclides. *J. Nucl. Med. 35*, 890−898.
(40) Arano, Y., Wakisaka, K., Ohmono, Y., Uezono, T., Akizawa, H., Nakayama, M., Sakahara, H., Tanaka, C., Konishi, J., and Yokoyama, A. (1996) Assessment of radiochemical design of antibodies using an ester bond as the metabolizable linkage: evaluation of maleimidoethyl 3-(tri-*n*-butylstannyl)-hippurate as a radioiodination reagent of antibodies for diagnostic and therapeutic applications. *Bioconjugate Chem. 7*, 628−637.
(41) Fujioka, Y., Arano, Y., Ono, M., Uehara, T., Ogawa, K., Namba, S., Saga, T., Nakamoto, Y., Mukai, T., Konishi, J., and Saji, H. (2001) Renal metabolism of 3′-iodohippuryl Nϵ-maleoyl-L-lysine (HML)-conjugated Fab fragments. *Bioconjugate Chem. 12*, 178−185.
(42) Li, M., and Meares, C. F. (1993) Synthesis, metal chelate stability studies, and enzyme digestion of a peptide-linked DOTA derivative and its corresponding radiolabeled immunoconjugates. *Bioconjugate Chem. 4*, 275−283.
(43) Peterson, J. J., Pak, R. H., and Meares, C. F. (1999) Total solid-phase synthesis of 1,4,7,10-tetraazacyclododecane-N,N′,N″,N‴-tertraacetic acid functionalized peptides for radioimmunotherpay. *Bioconjugate Chem. 10*, 316−320.
(44) Peterson, J. J., and Meares, C. F. (1999) Enzymatic cleavage of peptide linked radiolabels from immunoconjugates. *Bioconjugate Chem. 10*, 553−557.
(45) Neumaier, M., Shively, L., Chen, F.-S., Gaida, F.-J., Ilgen, C., Paxton, R. J., Shively, J. E., and Riggs, A. D. (1990) Cloning of the Genes for T84.66, an Antibody That Has a High Specificity and Affinity for Carcinoembryonic Antigen, and Expression of Chimeric Human/Mouse T84.66 Genes in Myeloma and Chinese Hamster Ovary Cells. *Cancer Res. 50*, 2128−2134.
(46) Lewis, M. R., and Shively, J. E. (1998) Maleimidocysteineamido-DOTA Derivatives: New Reagents for Radiometal Chelate Conjugation to Antibody Hinge Region Sulfhydryl Groups Undergo pH-Dependent Cleavage Reactions. *Bioconjugate Chem. 9*, 72−86.
(47) Williams, L. E., Lewis, M. R., Bebb, G. G., Clarke, K. G., Odom-Maryon, T. L., Shively, J. E., and Raubitschek, A. A. (1998) Biodistribution of ^{111}In- and ^{90}Y-Labeled DOTA and Maleimidocysteineamido-DOTA Conjugated to Chimeric Anti-Carcinoembryonic Antigen Antibody in Xenograft-Bearing Nude Mice: Comparison of Stable and Chemically Labile Linker Systems. *Bioconjugate Chem. 9*.
(48) Gunewardena, P., and Cook, K. B. (1966) 1,4-Dithiothreitol as a Reagent for Reductive Degradation of Human γG Globulin. *Biochem. J. 99*, 8P.
(49) Willner, D., Trail, P. A., Hofstead, S. J., King, H. D., Lasch, S. J., Braslawsky, G. R., Greenfield, R. S., Kaneko, T., and Firestone, R. A. (1993) (6-Maleimidocaproyl)hydrazone of Doxorubicin- -A New Derivative for the Preparation of Immunoconjugates of Doxorubicin. *Bioconjugate Chem. 4*, 521−527.
(50) Gregory, J. D. (1955) The Stability of *N*-Ethylmaleimide and its Reaction with Sulfhydryl Groups. *J. Am. Chem. Soc. 77*, 3922−3923.
(51) Houen, G., and Jensen, O. M. (1995) Conjugation to preactivated proteins using divinyl sulfone and iodoacetic acid. *J. Immunol. Methods 181*, 187−200.
(52) Friedman, M., and Finley, J. W. (1975) Reactions of proteins with ethyl vinyl sulfone. *Int. J. Pept. Protein Res. 7*, 481−486.
(53) Masri, M. S., and Friedman, M. (1988) Protein reactions with methyl and ethyl vinyl sulfones. *J. Protein Res. 7*, 49−54.
(54) Arano, Y., Fujioka, Y., Akizawa, H., Ono, M., Uehara, T., Wakisaka, K., Nakayama, M., Sakahara, H. K. J., and Saji, H. (1999) Chemical design of radiolabeled antibody fragments for low renal radioactivity levels. *Cancer Res. 59*, 128−134.

BC015535B

DAC EX. 2040 IPR2022-01531 Page 1098 of 1299

Appendix BALLINI01

```
LEADER 00000cas  2200000I  4500
001    1553987
003    OCoLC
005    20150414133823.0
008    750817c19249999paubx p       0   a0eng d
010    25015032
016 7  C15600000|2DNLM
022 0  0009-2665
030    CHREAY
032    102020|bUSPS
035    200008|a100007|a203809|bUCU
040    MUL|cMUL|dOCL|dUCU|dCDO|dMUL|dNSD|dIUL|dHUL|dIUL|dSER|dRCS
       |dAIP|dNSD|dAIP|dNSD|dOCL|dWaOLN|dUtOrBLW
042    nsdp
069 1  C15600000
090    QD1|b.C45
210 0  Chem. rev.
222  0 Chemical reviews
245 00 Chemical reviews.
260    [Easton, Pa., etc.] :|bAmerican Chemical Society [etc.]
300    volumes :|bdiagrams ;|c26 cm
310    8 times a year
321    Bimonthly
336    text|btxt|2rdacontent
337    unmediated|bn|2rdamedia
338    volume|bnc|2rdacarrier
362 0  v. 1-    Apr. 1924-
510 1  Applied science & technology|x0003-6986
510 2  Abstract bulletin of the Institute of Paper Chemistry
       |x0020-3033
510 2  Chemical abstracts|x0009-2258
510 2  Coal abstracts|x0309-4979
510 2  Energy information abstracts|x0147-6521
510 2  Environment abstracts|x0093-3287
510 2  Excerpta medica
510 2  GeoRef|x0197-7482
510 2  International aerospace abstracts|x0020-5842
510 2  Life sciences collection
510 2  PESTDOC
510 2  RINGDOC
510 2  VETDOC
510 2  World surface coatings abstracts|x0043-9088
510 2  World textile abstracts|x0043-9118
550    Vols. for 19  -    "owned and controlled by the American
       Chemical Society;" for 19  -  published by the Society.
555    Vols. 1-10, Apr. 1924-June 1932, in vol. 10; vol. 11-20,
       Aug. 1932-June 1937, in v. 20; vol. 21-30, Aug. 1937-June
       1942, in v. 30; vol. 1-40, Apr. 1924-June 1947, in v. 40;
       vol. 1-60, Apr. 1924-Dec. 1960, in v. 60; vol. 61-70, Feb.
       1961-Dec. 1970, in v. 70.
580    Supplementary material published separately on microfiche.
650  0 Chemistry|vPeriodicals.
710 2  American Chemical Society.
770 1  |tChemical reviews. Supplementary material|w(OCoLC)8060381
776 1  |tChemical reviews (Dnline)|x1520-6890|w(DLC)sn 98004619
       |w(OCoLC)37459065
856 41 |uhttp://pubs.acs.org/journals/chreay/index.html|zaccess
       this title at Carnegie Library of Pittsburgh.
935    ADM-5470
936    INC|aDec. 1979 (surrogate)
997    xarxk
```

Location	Carnegie Library of Pittsburgh - Off Site Storage (Please ask for assistance)
Lib Has	Volume 1 (1924) to Volume 69 (1969).
Identity	ACS
Location	CLP Main (Oakland) - Internet
Location	CLP Main (Oakland) Second Floor - Magazines
Lib Has	Volume 70 (1970) to Volume 107 (2007).

Title	**Chemical reviews.**
Publisher	[Easton, Pa., etc.] : American Chemical Society [etc.]
Description	volumes : diagrams ; 26 cm
Frequency	8 times a year Bimonthly
Pub Date	v. 1- Apr. 1924-

Links:

access this title at Carnegie Library of Pittsburgh.

Location	Carnegie Library of Pittsburgh - Off Site Storage (Please ask for assistance)
Lib Has	Volume 1 (1924) to Volume 69 (1969).
Identity	ACS
Location	CLP Main (Oakland) - Internet
Location	CLP Main (Oakland) Second Floor - Magazines
Lib Has	Volume 70 (1970) to Volume 107 (2007).

Details

Indexed In:	Applied science & technology 0003-6986 Abstract bulletin of the Institute of Paper Chemistry 0020-3033 Chemical abstracts 0009-2258 Coal abstracts 0309-4979 Energy information abstracts 0147-6521 Environment abstracts 0093-3287 Excerpta medica GeoRef 0197-7482 International aerospace abstracts 0020-5842 Life sciences collection PESTDOC RINGDOC VETDOC World surface coatings abstracts 0043-9088 World textile abstracts 0043-9118
Issued By	Vols. for 19 - "owned and controlled by the American Chemical Society;" for 19 - published by the Society.
Indexes	Vols. 1-10, Apr. 1924-June 1932, in vol. 10; vol. 11-20, Aug. 1932-June 1937, in v. 20; vol. 21-30, Aug. 1937-June 1942, in v. 30; vol. 1-40, Apr. 1924-June 1947, in v. 40; vol. 1-60, Apr. 1924-Dec. 1960, in v. 60; vol. 61-70, Feb. 1961-Dec. 1970, in v. 70.
Note	Supplementary material published separately on microfiche.
Subject	Chemistry -- Periodicals.
Addt'l Author	American Chemical Society.
Key Title	Chem. rev. Chemical reviews
Related To	Chemical reviews. Supplementary material (OCoLC)8060381 Chemical reviews (Online) 1520-6890 (DLC)sn 98004619 (OCoLC)37459065 *Show similar items*
ISSN	0009-2665

Appendix BALLINI02


CHEMICAL
REVIEWS
105
JAN-APR
2005

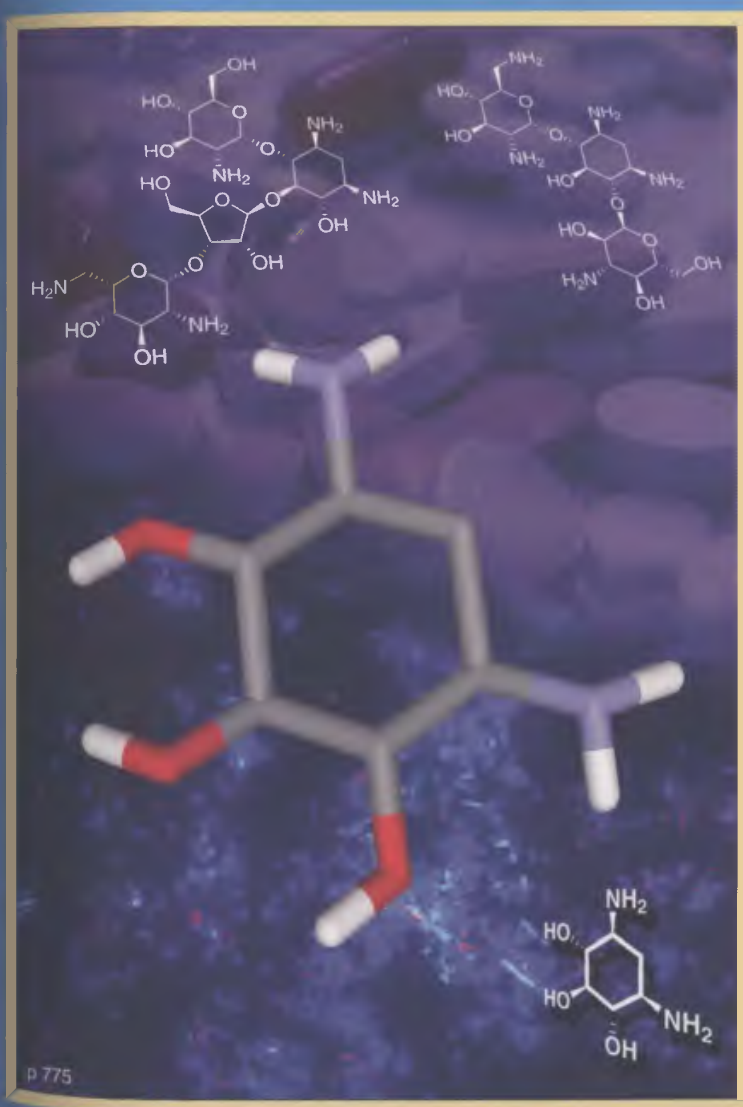

CARNEGIE LIBRARY of PITTSBURGH
3 1812 04048 3092

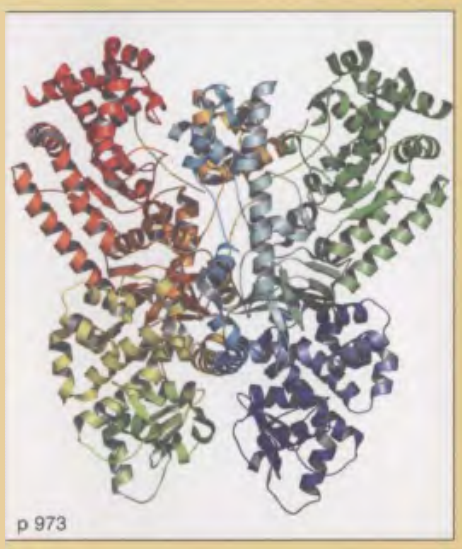

Carnegie
Library of
Pittsburgh
Main

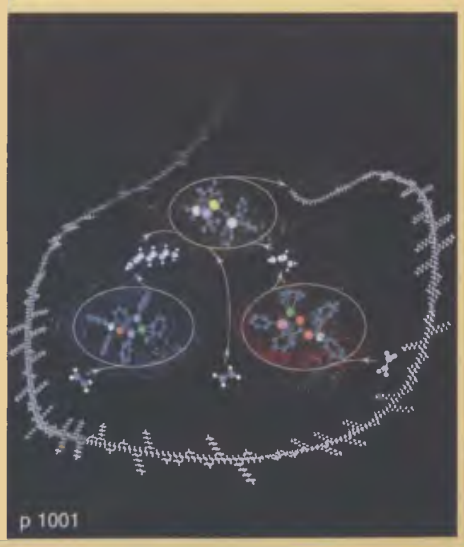
CHREAY

CHEMICAL REVIEWS

MARCH 2005
VOLUME 105
NUMBER 3







http://pubs.acs.org/CR

PUBLISHED BY THE
AMERICAN CHEMICAL SOCIETY

DAC EX. 2040 IPR2022-01531 Page 1108 of 1299

CHEMICAL REVIEWS®

AMERICAN CHEMICAL SOCIETY

Thematic Issue...
Antibiotic Resistance

Editors: **Christopher T. Walsh,** Harvard Medical School
Gerard D. Wright, McMaster University

Volume 105, No. 2



One of the central themes of success in human therapeutics in the 20th century was the discovery and development of antibiotics and antibacterial agents, for the treatment of bacterial infections. The introduction of antibiotics helped drop the death rates from infectious disease from 797 per hundred thousand in 1900 to 36 per hundred thousand in 1980, a 20-fold improvement. Two lines of chemical investigation proved fruitful: the isolation of natural products with antibiotic activity from microbial sources and the purposeful synthesis of antibacterial agents by medicinal chemists.

This comprehensive collection of reviews on the major classes of antibiotics in human clinical use should be a central resource for scientists to grapple with the questions of how antibiotics work, why they stop working, and how the molecular insights into molecules and their targets condition strategies for much needed new antibiotics.

Introduction – **Walsh** and Wright

Bacterial Cell Wall Inhibition

Bacterial Resistance to β-Lactam Antibiotics: Compelling Opportunism, Compelling Opportunity – **Fisher, Meroueh,** and **Mobashery**

Glycopeptide and Lipoglycopeptide Antibiotics – **Kahne, Leimkuhler, Lu,** and **Walsh**

Chemistry and Biology of Ramoplanin: A Lipoglycodepsipeptide with Potent Antibiotic Activity – **Walker, Chen, Hu, Rew, Shin,** and **Boger**

Bacterial Protein Biosynthesis Inhibition

Molecular Insights into Aminoglycoside Action and Resistance – **Magnet** and **Blanchard**

Translation and Protein Synthesis: Macrolides – **Katz** and **Ashley**

Streptogramins, Oxazolidinones, and Other Inhibitors of Bacterial Protein Synthesis – **Mukhtar** and **Wright**

Genetic Approaches to Polyketide Antibiotics – **McDaniel, Welch,** and **Hutchinson**

Inhibition of Bacterial DNA and RNA Metabolism

Bacterial Topoisomerase Inhibitors: Quinolone and Pyridone Antibacterial Agents – **Mitscher**

DNA and RNA Synthesis: Antifolates – **Kompis, Islam,** and **Then**

Rifamycin – Mode of Action, Resistance, and Biosynthesis – **Floss** and **Yu**

Peptide Antibiotics

Biosynthesis and Mode of Action of Lantibiotics – **Chatterjee, Paul, Xie,** and **van der Donk**

Thiopeptide Antibiotics – **Bagley, Dale, Merritt,** and **Xiong**

Molecular Mechanisms Underlying Nonribosomal Peptide Synthesis: Approaches to New Antibiotics – **Sieber** and **Marahiel**

Antitumor Antibiotics

Antitumor Antibiotics: Bleomycin, Enediynes, and Mitomycin – **Galm, Hager, Van Lanen, Ju, Thorson,** and **Shen**

New Targets and Screens

New Targets and Screening Approaches in Antimicrobial Drug Discovery – **Brown** and **Wright**

ORDER TODAY! Special ACS Member Rates:

Single Thematic Issue $35 (print) / Nonmembers $45

Call toll-free 1-800-227-5558
(ask for Publications Support Services, ext. 4554)

In Washington, D.C., and outside the U.S., call 202-872-4376.
Fax order to 202-872-6325. E-mail order requests to **pss@acs.org**
Visa / MasterCard / American Express accepted

Please include journal title, thematic issue title, volume, issue number and price; indicate credit card number and exp. date; add applicable sales tax (print only) in CA, D.C., MD, OH, IL, and 7% GST for all orders shipped to Canada.

For information about *Chemical Reviews*, go to http://pubs.acs.org/CR

Mail your order with payment to:
American Chemical Society, Sales & Marketing, Attn: W.S.
1155 Sixteenth Street, NW, Washington, D.C. 20036
Additional postage required for **air service** outside North America–$22.
Additional postage required for **surface mail** outside North America–$8.
Single issue price valid through 12/31/05.

Recommend *Chemical Reviews* to your library or institution for acquisition.

CHEMICAL REVIEWS

Chemical Reviews (ISSN 0009-2665) is published monthly by the American Chemical Society at 1155 16th St., N.W., Washington, DC 20036. Periodicals postage paid at Washington, DC, and additional mailing offices. POSTMASTER: Send address changes to *Chemical Reviews*, Member & Subscriber Services, P.O. Box 3337, Columbus, OH 43210.

American Chemical Society
1155 16th St., N.W.
Washington, DC 20036
(202) 872-4614
TDD (202) 872-6076
Fax (202) 776-8264

Journal Publications
American Chemical Society
2540 Olentangy River Road
P.O. Box 3330, Columbus, OH 43210
(614) 447-3665
Fax (614) 447-3745
E-mail acsproof@acs.org

Member & Subscriber Services
P.O. Box 3337
Columbus, OH 43210

Members & individuals contact:
(614) 447-3776; (800) 333-9511
Fax (614) 447-3671
E-mail: service@acs.org

Agencies & institutions contact:
(614) 447-3674; (888) 338-0012
Fax (614) 447-3671
E-mail: liblink@acs.org

Advertising Office
Centcom, Ltd.
676 East Swedesford Road
Suite 202, Wayne, PA 19087-1612
(610) 964-8061

Publications Division
Robert D. Bovenschulte, *President*
Brian D. Crawford, *Senior Vice President*

Journals Publishing Group

Journal Publications
Anne C. O'Melia, *Assistant Director*; Diane E. Needham, *Journals Editing Manager*; Ann M. McCarty, *Associate Editor*

Composition Services
Teresa K. Lewandowski, *Assistant Director*

Sales & Marketing/Publications
Dean J. Smith, *Vice President*
Matthew J. Price, *Director, Product Marketing*

Canadian GST Reg. No. 127571347
Printed in the USA

Copyright Permission: See copyright status form for certain rights (http://pubs.acs.org). Reprographic copying beyond that permitted by Section 107 or 108 of the U.S. Copyright Act is allowed, provided that the current per article fee is paid to the Copyright Clearance Center. Tel: (978) 750-8400. Republication or reproduction for sale of articles or abstracts in this journal is permitted only by written permission from the Copyright Office, ACS, Washington, DC. Tel: (202) 872-4368. Fax: (202) 776-8112. E-mail: copyright@acs.org.

Editorial Information

Instructions for Authors and Copyright Status Form: See the first issue of each volume or visit the Publications Division Web site (http://pubs.acs.org). Please conform to these instructions when submitting manuscripts.

Manuscript Submission: (1) Invited manuscripts should be submitted to the editorial office designated in the invitation. (2) Unsolicited manuscripts and proposals may be sent to either Josef Michl, Department of Chemistry and Biochemistry, University of Colorado at Boulder, Boulder, CO 80309-0215 (encouraged for North American authors) or John Gladysz, Institut für Organische Chemie, Henkestrasse 42, Universität Erlangen-Nürnberg, 91054 Erlangen, Germany (encouraged for authors outside of North America).

Accepted Papers and Proofs: Direct correspondence to Journal Publications, Columbus, OH. Tel: (614) 447-3665. Fax: (614) 447-3745. E-mail: acsproof@acs.org.

Journal Policies: The American Chemical Society and its Editors assume no responsibility for the statements and opinions advanced by contributors. Registered names and trademarks, etc., used in this publication, even without specific indication thereof, are not to be considered unprotected by law.

Document Number: At the end of each document is a 9-character code that serves as a link between the printed and electronic products and facilitates retrieval of the document in electronic form.

Digital Object Identifier (DOI): The DOI identification system for digital media has been designed to provide persistent and reliable identification of digital objects. Information on the DOI and its governing body, the International DOI Foundation, can be found at http://www.doi.org. In the Web editions of ACS journals, the DOI appears at the top of the HTML version of an article and at the bottom of the first page in its PDF version; in the printed editions, the DOI appears in the same location as in the PDF version.

2005 Subscription and Ordering Information

		North America	Outside North America
Printed Edition	Members	$108	$ 197
	Student Members	$ 81	$ 170
	Institutional	$970	$1059
Web Edition[†]	Members	$ 60	$ 60
Print/Web Combination[†]	Members	$168	$ 257
Printed Single Thematic Issues[§]	Members	$ 35	$ 57
	Nonmembers	$ 45	$ 67
	Institutional	$100	$ 122

[*] Air service included. [†] For Institutional rates, call M&SS Agency & Institutional Customer Service. [§] Single non-thematic issues are available at a cost of $100. Send requests to Publications Support Services, ACS, Washington, DC. Tel: (800) 227-5558 [in Washington, DC, and outside the United States, (202) 872-4376]. Fax: (202) 872-6325. E-mail: pss@acs.org.

Web Edition: This journal is available to subscribers via the Internet. Members may contact Customer Service. Tel: (614) 447-3776 or (800) 333-9511. E-mail: service@acs.org. Institutional subscribers may contact Agency & Institutional Customer Service. Tel: (614) 447-3674 or (888) 338-0012. Fax: (614) 447-3671. E-mail: liblink@acs.org. For additional details, visit the Publications Division Web site (http://pubs.acs.org).

New and Renewal Subscriptions: Send with payment to American Chemical Society, P.O. Box 182426, Columbus, OH 43218-2426.

Subscription Donations: Members may donate/share their personal subscriptions to/with libraries but only after 5 years from the date of publication.

Change of Address: Notify Member & Subscriber Services, ACS, Columbus, OH. Tel: (614) 447-3776 or (800) 333-9511. Fax: (614) 447-3671. E-mail: address@acs.org. Include both old and new addresses and a mailing label from a recent issue.

Microfilm, Microfiche, and Back Issue Orders: Send requests to Publications Support Services, ACS, Washington, DC. Tel: (202) 872-4376. Fax: (202) 872-6325. E-mail: pss@acs.org.

Bulk Reprint Orders: For quotes and information, contact Cadmus Reprints. Tel: (888) 257-2134 or (410) 819-3995. Fax: (410) 820-9765.

Claims for Issues Not Received: Claims will be honored only if submitted within 90 days of the issue date for subscribers in North America or within 180 days of the issue date for all other subscribers. Members and individuals may contact Customer Service. Tel: (614) 447-3776 or (800) 333-9511. E-mail: service@acs.org. Institutional subscribers may contact Agency & Institutional Customer Service. Tel: (614) 447-3674 or (888) 338-0012. Fax: (614) 447-3671. E-mail: liblink@acs.org.

Supporting Information (SI): SI from 1994 to present is available free of charge from the journal's home page (http://pubs.acs.org/cr). For information on electronic access, send E-mail to journalhelp@acs.org. SI prior to 1994 is available, for a fee, from Publications Support Services. Tel: (202) 872-4376. Fax: (202) 872-6325. E-mail: pss@acs.org.

© Copyright 2005 American Chemical Society

CHEMICAL REVIEWS

EDITOR

JOSEF MICHL

Department of Chemistry and Biochemistry
University of Colorado at Boulder
Boulder, Colorado 80309-0215

(303) 492-4064; Fax (303) 492-0799
E-mail chemrev@eefus.colorado.edu

ASSOCIATE EDITORS

John A. Gladysz
Universität Erlangen-Nürnberg

Robert D. Kuchta
University of Colorado at Boulder

EDITORIAL ADVISORY BOARD

Ruma Banerjee
University of Nebraska

Anthony G. M. Barrett
Imperial College of Science, Technology, and Medicine

James K. Bashkin
University of Missouri—St. Louis

Guy Bertrand
University of California, Riverside

Edwin A. Chandross
Bell Labs; Lucent Technologies

Carsten Bolm
Rheinisch-Westfälische Technische Hochschule Aachen

Peter Chen
Eidgenössische Technische Hochschule, Zürich

Robert H. Crabtree
Yale University

Ernest R. Davidson
University of Washington

Armin de Meijere
Georg-August-Universität, Göttingen

Marye Anne Fox
University of California, San Diego

Bernd Giese
Universität Basel

Lizbeth K. Hedstrom
Brandeis University

Donald Hilvert
Eidgenössische Technische Hochschule, Zürich

Pavel Hobza
Academy of Sciences of the Czech Republic, Prague

Richard H. Holm
Harvard University

István T. Horváth
Eötvös University

Kim D. Janda
The Scripps Research Institute

Nathan S. Lewis
California Institute of Technology

Shū Kobayashi
The University of Tokyo

David R. Liu
Harvard University

Robert D. Miller
IBM Almaden Research Center

Ryoji Noyori
Nagoya University

Mark A. Ratner
Northwestern University

Thomas B. Rauchfuss
University of Illinois at Urbana—Champaign

Edward I. Solomon
Stanford University

Joan S. Valentine
University of California, Los Angeles

John T. Yates, Jr.
University of Pittsburgh

Ahmed H. Zewail
California Institute of Technology

A New Publication from the American Chemical Society



"The ***Journal of Chemical Theory and Computation*** provides a focal point for publication of articles, letters, and reviews reporting new theories based on physical laws, advances in computational methods, and important applications to problems in chemistry. ...You are invited to participate in this undertaking to establish ***JCTC*** as the central source for the best work in the field."

—Editor,
William L. **Jorgensen**,
Whitehead Professor of
Chemistry, Yale University

Go to http://pubs.acs.org/JCTC for FREE access to the first issue. Submit your manuscripts online at http://paragon.acs.org

For more information,
call Member & Subscriber Services:
1-888-338-0012 in U.S. and Canada, or
(614) 447-3674 outside North America

ACS PUBLICATIONS
HIGH QUALITY. HIGH IMPACT.

March 2005

CHREAY 105(3) 775–1022 (2005)
ISSN 0009-2665

CHEMICAL REVIEWS®

2-Deoxystreptamine: Central Scaffold of Aminoglycoside Antibiotics 775
*Guuske F. Busscher, Floris P. J. T. Rutjes, and Floris L. van Delft**

Over One Hundred Peptide-Activated G Protein-Coupled Receptors Recognize Ligands with Turn Structure 793
*Joel D. A. Tyndall, Bernhard Pfeiffer, Giovanni Abbenante, and David P. Fairlie**

α-Fluorinated Ethers, Thioethers, and Amines: Anomerically Biased Species 827
*Frédéric Leroux, Peter Jeschke, and Manfred Schlosser**

BINOL: A Versatile Chiral Reagent 857
Jean Michel Brunel

Synthesis of β-Aminophosphonates and -Phosphinates 899
Francisco Palacios, Concepcion Alonso, and Jesús M. de los Santos*

Conjugate Additions of Nitroalkanes to Electron-Poor Alkenes: Recent Results 933
Roberto Ballini, Giovanna Bosica, Dennis Fiorini, Alessandro Palmieri, and Marino Petrini**

Proteases Universally Recognize Beta Strands In Their Active Sites 973
Joel D. A. Tyndall, Tessa Nall, and David P. Fairlie*

Concurrent Tandem Catalysis 1001
Julia-Christina Wasilke, Stephen J. Obrey, R. Tom Baker, and Guillermo C. Bazan**

ADDITIONS AND CORRECTIONS

What Are Batteries, Fuel Cells, and Supercapacitors? 1021
Martin Winter and Ralph J. Brodd

There is no Supporting Information for this issue.

* In papers with more than one author, the asterisk indicates the name of the author to whom inquiries about the paper should be addressed.

Digital Object Identifier (DOI): The DOI appears at the bottom of the first page of each article. We suggest that you include the DOI in all CCC reporting and document delivery requests. See the masthead of this journal or our Web site at http://pubs.acs.org for more details.

Conjugate Additions of Nitroalkanes to Electron-Poor Alkenes: Recent Results

Roberto Ballini,* Giovanna Bosica, Dennis Fiorini, Alessandro Palmieri, and Marino Petrini*

Dipartimento di Scienze Chimiche, Università di Camerino, via S. Agostino, 1, I-62032 Camerino, Italy

Received September 30, 2004

Contents

1. Introduction 933
2. General Aspects of the Conjugate Addition of Nitroalkanes 934
   2.1. Multiple Additions 934
   2.2. Basic Catalysts 935
3. New Basic Catalysts for the Conjugate Addition 936
4. Diastereoselective Conjugate Additions 936
   4.1. Intermolecular Additions 936
   4.2. Intramolecular Additions 948
5. Asymmetric Conjugate Additions Promoted by Chiral Catalysis 949
6. Conjugate Addition–Elimination Reactions 953
7. Synthetic Applications 957
   7.1. Pyrrolidines and Derivatives 957
   7.2. Lactones and Oxygenated Heterocycles 960
   7.3. Carbocycles 963
   7.4. Amino Acids and Derivatives 965
   7.5. Other Applications 965
8. Conclusion 968
9. Abbreviations 968
10. Acknowledgments 968
11. References 969

1. Introduction

Conjugate addition of carbon nucleophiles to electron-poor alkenes is of paramount importance among the large body of synthetic processes devoted to carbon−carbon bond formation.[1] The first nucleophilic systems used for this purpose, more than a century ago, were stabilized carbanions that can be prepared in polar solvents from malonates and β-dicarbonyl derivatives in relatively mild conditions using bases of moderate strength.[2] This process is usually referred to as Michael addition, and ever since the number of carbanionic species that have been used for conjugate additions has considerably increased to include various enolate systems and strong nucleophilic species such as organometallic reagents. The utilization of these carbon nucleophiles has allowed the accomplishment of many synthetic processes with an outstanding degree of selectivity even though the related experimental procedures are often elaborated and not amenable to scale-up at the industrial level.

* To whom correspondence should be addressed. Phone: +39 0737 402270. Fax: +39 0737 402297. E-mail: roberto.ballini@unicam.it; marino.petrini@unicam.it.

Conjugate additions using highly stabilized carbanions are still of interest since a growing number of these procedures can be carried out in environmentally benign solvents such as water and using catalytic amounts of the basic promoter. In addition, the achievement of diastereo- and enantioselective processes is no longer an exclusive domain of highly reactive carbanionic systems working in carefully controlled conditions[3] but can be nowadays conducted even at room temperature using easily available substrates and suitable base/solvent combinations.

Nitroalkanes are a valuable source of stabilized carbanions since the high electron-withdrawing power of the nitro group provides an outstanding enhancement of the hydrogen acidity at the α-position (cf. pk_a $MeNO_2$ = 10).[4−8] Nitronate anions **2** that can be generated from nitroalkanes **1** using a wide range of bases act as carbon nucleophiles with common electrophiles including haloalkanes,[9] aldehydes,[10,11] and Michael acceptors,[1] leading to carbon−carbon bond formation (Scheme 1).

The obtained adducts **3**−**5** still retain the nitro function, and therefore, a suitable transformation of the nitro group very often follows the main addition process. Reduction of the nitro group to a primary amine **7** can be easily carried out providing a modification of the oxidation state of the nitrogen atom (Scheme 2).

Alternatively, the nitro group can be removed from the molecule using two distinct synthetic strategies. Replacement of the nitro group with hydrogen gives the corresponding denitrated product **8** so that the whole process (nucleophilic addition−denitration) closely resembles the addition of an organometallic reagent to an electrophilic substrate.[5,12] The presence at the β-position of an electron-withdrawing group allows a base-assisted elimination of nitrous acid with consequent introduction of a double bond in the molecular framework **9**. A further option is represented by conversion of the nitro group into a carbonyl group **10**, a transformation widely known as the Nef reaction, which ultimately leads to a reversal in the polarity of the neighboring carbon atom from nucleophilic to electrophilic.[13,14] This review is focused on the utilization of nitroalkanes as nucleophiles in conjugate additions with electron-poor alkenes and covers the new procedures and related applications appearing in the literature after 1990. Emphasis will be given to asymmetric additions carried out using optically active alkenes or with the aid of chiral catalysts.

10.1021/cr040602r CCC: $53.50 © 2005 American Chemical Society
Published on Web 02/03/2005

DAC EX. 2040 IPR2022-01531 Page 1113 of 1299



Roberto Ballini obtained his Laurea degree in Chemistry from the University of Camerino-Italy. After experience at the ENI-ANIC (Petrolchemical Industry) in Ravenna, he began his academic career in 1975 as a Research Fellow at the University of Camerino. Then he became Assistant Professor in Organic Chemistry (1978), was promoted to Associate Professor (Organic Chemistry), and then was promoted to Full Professor of Organic Chemistry in 2000. His research interests include a huge area of the chemistry of aliphatic nitro compounds, with particular interest in a new generation of both carbon–carbon single bond and carbon–carbon double bond, cleavage of the carbon–carbon bond, and use of nitroalkanes as the key building blocks in the synthesis of important targets such as natural products featuring enhanced biologically activity. Other special fields of extensive interest also concern (i) different aspects of heterogeneous catalysis applied to fine chemicals and pharmaceuticals production, (ii) exploitation of solvent-free and multicomponent reactions, and (iii) use of aqueous medium in the organic reactions.



Giovanna Bosica was born in Atri, Italy, in 1967. She has been a researcher at the Department of Chemical Sciences of the University of Camerino, Faculty of Sciences and Technologies, since 1999. She received her Laurea in Chemistry *cum laude* in 1993 from the University of Camerino and 4 years later from the same institution her doctoral degree in Chemical Sciences working under the supervision of Professor R. Ballini. She spent a research period from April to September 1995 in the laboratories of Professor B. Zwanenburg (Department of Organic Chemistry, University of Nijmegen, The Netherlands) as an Erasmus Fellow. Her research interests concern the use of nitro compounds in new synthetic methodologies, synthesis of heterocycle compounds and biologically active natural products, heterogeneous catalysis, and green chemistry.

2. General Aspects of the Conjugate Addition of Nitroalkanes

Regioselectivity is an important feature that makes nitroalkanes particularly efficient in conjugate additions with α,β-unsaturated carbonyl derivatives. Indeed, while other activating groups such as phenylsulfonyl give variable amounts of 1,2-addition when



Dennis Fiorini was born in 1975 and received her degree in Chemistry from the University of Camerino, Italy, in 2000. During the same year she had a grant for research on the chemical reactivity of nitro compounds and worked under the supervision of Professor Roberto Ballini. She is currently a third-year Ph.D. student in the same research group and is involved in the study of nitroalkanes ability to form single and double carbon carbon bonds and their application in the synthesis of natural target products showing biological activity. Some aspects of her recent research concern heterogeneous catalysis, solventless reactions, and other procedures related to green chemistry.



Alessandro Palmieri, born in Jesi, Italy, began his studies in Chemistry in 1997 at the University of Camerino-Italy, where he received his Laurea degree *cum laude* in 2002 under the guidance of Professor E. Marcantoni. After a scholarship in the laboratory of Professor R. Ballini on the synthesis of natural products with important biological activities, in March 2004 he started his Ph.D. studies in the same lab. His research interests include natural products synthesis and application of aliphatic nitro compounds in the formation of new C–C and C=C bond.

reacted with enones or enals,[15] nitroalkanes afford exclusively 1,4-addition using α,β-unsaturated ketones and propenal as reactive acceptors.[16] Conversely, 3-substituted α,β-unsaturated aldehydes give predominantly 1,2-addition with secondary nitroalkanes and β-nitro alcohols.[17,18]

2.1. Multiple Additions

Undesired multiple additions on electron-poor alkenes are sometime possible on the initially formed products of conjugate addition. The amount of 1:2 adduct may be affected by the base/solvent combination used for the reaction (Scheme 3, Table 1).

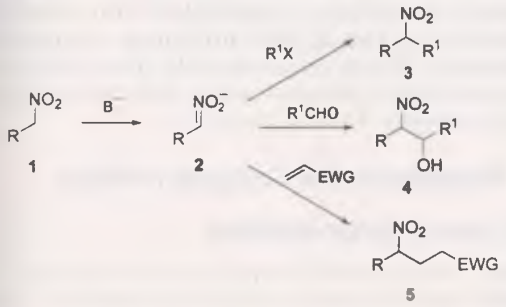
Reaction of nitro alcohol **1a** with phenylvinyl sulfone leads to an equimolar amount of mono and bis adducts, and this ratio is almost independent of the relative amounts of starting materials (Table 1,

DAC EX. 2040 IPR2022-01531 Page 1114 of 1299

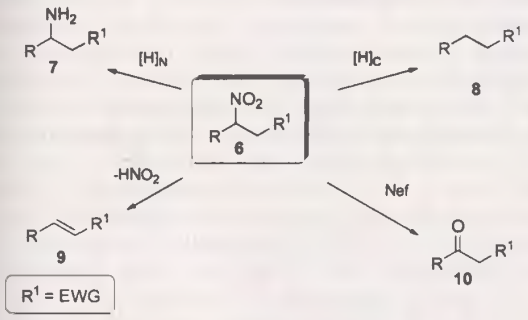


Marino Petrini received his Laurea degree in Chemistry in 1980 (University of Camerino). In 1983 he became Research Associate in organic chemistry at the University of Camerino, and during the period 1987–88 he was a visiting scientist at the University of Montreal (Professor S. Hanessian). In 1992 he was appointed Associate Professor and then (2004) Full Professor in Organic Chemistry at the University of Camerino. His research interests mainly deal with the following topics: synthesis and reactivity of aliphatic and aromatic nitro compounds; reactivity of organometallic reagents toward carbon and nitrogen electrophiles; synthesis of natural products featuring enhanced biological activity; synthesis and reactivity of imino derivatives.

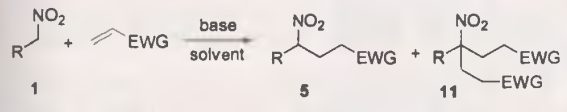
Scheme 1



Scheme 2



Scheme 3



entry 1).[19] The anion-solvating tendency exerted by the solvent and the electrophilicity of the alkene play a fundamental role in controlling the relative amounts of adducts obtained. Best results in the formation of 1:1 addition products are obtained exploiting moderate reaction rates, which for less reactive alkenes such as methylvinyl ketone (MVK)

Table 1. Multiple Additions in the Reaction of Nitroalkanes with Electron-Poor Alkenes

entry	1[a] R[1]	EWG	base/solvent	yield (%) 5:11	ref.
1	OH, 1a	SO_2Ph	TMG/CH_3CN	30:30	19
2	OR, 1b	$COCH_3$	TMG/THF	68:5	20
			TMG/CH_3CN	43:20	
3	OR, 1b	CN	TMG/THF	47:14	20
			TMG/CH_3CN	67:3	

[a] R^1 = *tert*-butyldimethylsilyl.

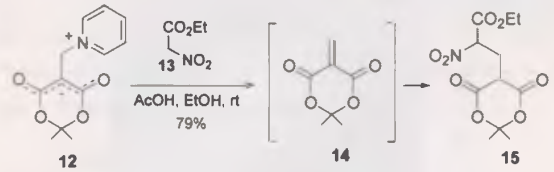
involve utilization of low-solvating media such as THF (Table 1, entry 2). With more reactive acceptors such as acrylonitrile it is advisable to use a good solvating agent such as acetonitrile in order to lower the reactivity of the carbanionic species involved in the process (Table 1, entry 3).[20] Highly polar solvents such as DMSO, methanol, and water are able to facilitate the addition of nitroalkanes to MVK in neutral conditions.[21] Of these solvents, water is the one that minimizes formation of the 1:2 adduct using nitromethane and avoids any 1:2 adduct with nitroethane as reagent. A consistent rate acceleration is experienced adding glucose or saccharose to water in order to enhance the relative hydrophobic effect. Ruthenium complex $[Ru(O_2CH)(CO)_2(PPh_3)_3]_2$ is an effective catalyst for the conjugate addition of active methylene derivatives to enones.[22] However, utilization of ethyl nitroacetate as nucleophile only allows isolation of multiple addition products in the reaction with butenone. Finally, multiple additions are often experienced using nitromethane as nucleophile since the primary nitroalkane formed in the monoaddition process is still sterically unhindered enough to give a second attack on the electron-poor alkene.[23]

2.2. Basic Catalysts

A suitable choice of base/solvent combination is mandatory for successful conjugate addition of a nitroalkane to an electron-poor alkene. Weak bases such as trialkylamines and triphenylphosphine are able to promote the conjugate addition using α-nitro ketones as nucleophiles or when very reactive electron-deficient alkenes are employed as electrophilic substrates.[24,25] Other basic systems such as fluoride salts,[26] ammonium hydroxides,[27] alkaline metal hydroxides, and alkoxides[28,29] have also found some utilization in these additions. When poorly electrophilic alkenes such as vinyl sulfoxides or β-substituted enones and enoates are used as substrates, stronger bases such as DBU and TMG are needed in order to ensure an efficient reaction.[30–32] On the other hand, some Michael acceptors are so reactive that they do not require basic catalysis for the conjugate addition of activated nitroalkanes. Methylene Meldrum's acid **14** is generated in situ from zwitterionic compound **12** in the presence of AcOH and reacts with nitroester **13** in the same conditions to give the corresponding adduct **15** (Scheme 4).[33]

DAC EX. 2040 IPR2022-01531 Page 1115 of 1299

Scheme 4



12 14 15

Besides the procedures that work in homogeneous conditions, a number of methods using basic catalysts that operate in heterogeneous systems can be profitably employed to carry out a conjugate addition. Basic alumina is a formidable promoter of such nucleophilic additions that can be accomplished even in solventless conditions.[34] Alternatively, basic alumina can be doped with potassium fluoride to enhance the catalytic properties of the solid support.[35] Amberlyst A-21, a macroreticular ion-exchange resin, assists the conjugate addition of functionalized nitroalkanes to α,β-unsaturated derivatives; a simple filtration of the resin allows easy work up of the reaction mixture and rapid recovery of the crude products.[36] Fluorinated nitroalkanes such as 2,2,2-trifluoronitroethane and 3,3,3-trifluoro-2-nitropropane can eliminate HF in the presence of basic systems. However, using KF in 2-propanol or basic alumina in solventless conditions makes possible the use of these nitro derivatives in conjugate additions with several electron-deficient alkenes.[37,38]

3. New Basic Catalysts for the Conjugate Addition

During the past decade a number of different basic systems has been introduced to carry out the conjugate addition of nitroalkanes to electron-poor alkenes. Some of them are just a slight modification of previously known catalysts that are currently used for such additions; others are conceptually new reagents that improve the selectivity and efficiency of the reaction (Table 2).

However, it should be pointed out that the choice of a suitable basic catalyst for such conjugate additions is often strongly conditioned by the ready availability of the reagent. In fact, nonionic bases such as $P(RNCH_2CH_2)_3N$ (Verkade's bases)[50] work quite efficiently in a number of examples but their widespread utilization has been hampered by the fact that some of these reagents have become commercially available only recently. Activating techniques such as microwave or ultrasound irradiation may improve the efficiency of known catalysts, especially those working in heterogeneous and solventless conditions.[41,45,53,54] In this context, it is interesting to observe that almost all the newly introduced catalysts belong to the class of solid supports that in many instances present consistent advantages over soluble bases. For particularly reactive nitro derivatives, such as α-nitro ketones or esters, mild bases can be used and cyclic α-nitro ketones react even in water without the need of any added base.[59] The utilization of $Yb(OTf)_3$, a mild Lewis acid catalyst, represents one of the first examples of a conjugate addition of α-nitro ester in acidic conditions carried out in water.[57] In a related procedure a number of solid acidic catalysts has been checked for the solventless addition of α-nitro ketones to enones, revealing that silica gel 60 is the most effective promoter for this reaction.[58] A common feature of these acid-promoted additions is the long reaction times required (1−7 days). In principle, cathodic reduction of a nitroalkane by electrolysis would afford the corresponding nitronate anion that is amenable to conjugate addition with electrophilic alkenes; practically, this procedure often leads to decomposition of the nitro derivative employed. However, when the reaction is carried out in air-saturated acetonitrile, oxygen is reduced at the cathode, producing a superoxide anion that acts as an electrogenerated base toward the nitroalkane.[60] This procedure was formerly set up using ethyl nitroacetate but has been extended to the reaction of other nitroalkanes with levoglucosenone **16** (Scheme 5).[60,61]

Dienoic acid ester reacts with nitroalkanes giving the corresponding 1,6-adducts as a regioisomeric mixture of α,β- and β,γ-unsaturated compounds.[62] The yield of the adducts and the relative amount of regioisomers strongly depend from the nature of the base employed, as illustrated for the reaction of methyl 1,3-butadiene-1-carboxylate with nitroethane (Scheme 6, Table 3). The utilization of microwave irradiation allows a considerable shortening in the reaction time and improvement of the chemical yield of the process (Table 3, entry 5).

4. Diastereoselective Conjugate Additions

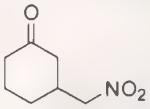
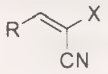
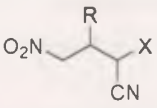
4.1. Intermolecular Additions

The newly formed carbon−carbon bond in a conjugate addition often involves the formation of stereogenic centers, and this has led to the development of stereoselective methods to prepare structurally defined compounds. The chiral information needed to obtain optically active derivatives can be contained in either the nucleophile or the alkene unit, but in any case, the best results in terms of diastereoselectivity are obtained using reagents bearing a chiral group in close proximity to the reaction center. In acyclic diastereoselection it is often advisable for cyclic frameworks containing heteroatoms linked to the alkene group to be present. The stereochemical bias offered by these heterocycles is extremely important for reactions that involve cyclic as well as open transition states. Enoate **21** bearing a chiral 1,3-dioxolane ring adds nitroalkanes in a diastereoselective fashion with enhanced preference for the *syn* stereoisomer **22** (Scheme 7, Table 4).[64,65]

The stereochemical outcome is little or not affected by the nature of the base employed (DBU or TBAF) but strongly depends on the stereochemistry of the double bond. Reaction of *Z*-**21** with most of nitroalkanes tested affords the corresponding adduct **22** with high diastereomeric excesses, while *E*-**21** gives poor results with the notable exception of nitromethane (Table 4, entry 1) and phenylnitromethane (Table 4, entries 11 and 12). Semiempirical calcula-

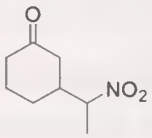
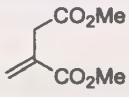
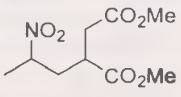
DAC EX. 2040 IPR2022-01531 Page 1116 of 1299

Table 2. Basic Catalysts for the Conjugate Addition of Nitroalkanes to Electron-Poor Alkenes

entry	nitro compound	alkene	conditions	product	yield %	ref
1	$MeNO_2$	CH_2=CHCOMe	HMS-R_3N, 4h, reflux	$O_2NCH_2CH_2CH_2COMe$	80	41
2			Al_2O_3-MW, 0.3h, 40°C		75	45
3			$P(RNCH_2CH_2)_3N$, Et(Me)CHCN, 0.15h, -63°C		78	50
4		Me_2C=CHCOMe	$P(RNCH_2CH_2)_3N$, Et(Me)CHCN, 0.5h, rt	$O_2NCH_2Me_2CCH_2COMe$	99	50
5		PhCH=CHCOMe	0.1% NaOH, CTAB, 12h, rt	O_2NCH_2(Ph)$CHCH_2COMe$	62	42
6			Al_2O_3-MW, 0.33h, 40°C		75	45
7			KF-natural phosphate, EtOH, 2h, rt		98	52
8		PhCH=CHCOPh	0.1% NaOH, CTAB, 8h, rt	O_2NCH_2(Ph)$CHCH_2COPh$	62	42
9			Mg-Al-O-*t*-Bu hydrotalcite MeOH, 0.16h, rt		93	44
10			Al_2O_3-MW, 0.3h, 40°C		90	45
11		MeCH=$CHCO_2Et$	$P(RNCH_2CH_2)_3N$, Et(Me)CHCN, 0.25h, -63°C	O_2NCH_2(Me)$CHCH_2CO_2Et$	99	50
12			0.5M NaOH, 5h, rt		65	43
13			HMS-R_3N, 4h, reflux		90	41
14			$P(RNCH_2CH_2)_3N$, THF, 0.5h, rt		89	50
15		CH_2=$CHCO_2Et$	Mg-Al-O-*t*-Bu hydrotalcite MeOH, 0.75h, rt	$O_2NCH_2CH_2CH_2CO_2Et$	96	44
16			KF-natural phosphate, EtOH, 2h, rt		51	52
			Al_2O_3, microwave, 0.1h, 90°C			53 54
17		X = CO_2Me R = Ph			70	
18		X = CO_2Me R = 4-ClC_6H_4			72	
19		X = CO_2Me R = 2-BrC_6H_4			83	
20		X = CO_2Me R = 2-FC_6H_4			100	
21		X = CO_2Me R = 3-FC_6H_4			72	
22		X = CO_2Et R = *i*-Bu			70	
23		X = CN R = Ph			100	
24		X = $CONH_2$ R = Ph			68	
25	$EtNO_2$	CH_2=CHCOMe	Al_2O_3-MW, 0.25h, 40°C	$MeCH(NO_2)CH_2CH_2COMe$	72	45
26			Al_2O_3, 2h, 0°C		60	46

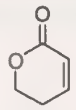
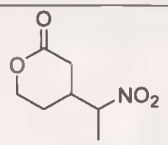
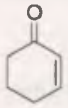
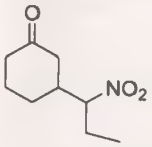
DAC EX. 2040 IPR2022-01531 Page 1117 of 1299

Table 2 (Continued)

entry	nitro compound	alkene	conditions	product	yield %	ref
27			0.025M NaOH, CTACl,1h, rt		85	39
28			$Zr(KPO_4)_2$, 3h, rt		69	47
29			HMS-R_3N, 12h, reflux		94	41
30			3%[$RuH_2(PPh_3)_4$], CH_3CN, 10h, rt		83	48
31			KF-natural phosphate, EtOH, 2h, rt		55	52
32			Amberlyst A-27, 4h, rt		76	55
33			KG-60-NEt_2, 3h, rt		75	40
34		CH_2=CHCOEt	0.025M NaOH, CTACl, 2h, rt	$MeCH(NO_2)CH_2CH_2COEt$	76	39
35		MeCH=CHCOEt	Amberlyst A-27, 25h, rt	$MeCH(NO_2)CH(Me)CH_2COEt$	75	55
36		CH_2=CHCO*n*-Pr	0.025M NaOH, CTACl, 2h, rt	$MeCH(NO_2)CH_2CH_2CO$*n*-Pr	68	39
37		CH_2=CHCHO	Al_2O_3, 2h, -10°C	$MeCH(NO_2)CH_2CH_2CHO$	60	46
38			Mg-Al-O-*t*-Bu hydrotalcite MeOH, 0.5h, rt		98	44
39			0.025M NaOH, CTACl,2h, rt		72	39
40			Amberlyst A-27, 20h, rt		93	55
41		CH_2=CHCO$_2$Me	CTAOH, 1h, rt	$MeCH(NO_2)CH_2CH_2CO_2Me$	78	63
42		CH_2=CHCO$_2$Et	KF-natural phosphate, EtOH, 2h, rt	$MeCH(NO_2)CH_2CH_2CO_2Et$	98	52
43			HMS-R_3N, 1.5h, reflux		88	41
44		MeCH=CHCO$_2$Me	K_2CO_3, Aliquat® 336, ultrasound, 2h, rt	$MeCH(NO_2)CH(Me)CH_2CO_2Me$	90	51
45			0.025M NaOH, CTACl,15h, rt		60	39
46		MeCH=CHCO$_2$Bn	K_2CO_3, Aliquat® 336, ultrasound, 0.5h, rt	$MeCH(NO_2)CH(Me)CH_2CO_2Bn$	94	51
47		PhCH=CHCO$_2$Me	K_2CO_3, Aliquat® 336, ultrasound, 0.5h, rt	$MeCH(NO_2)CH(Ph)CH_2CO_2Me$	93	51
48			K_2CO_3, Aliquat® 336, ultrasound, 0.5h, rt		73	51
49		CH_2=CHCH=CHCO$_2$Et	Amberlyst A-27, microwave, 0.1h, 70°C	$MeCH(NO_2)CH_2CH$=$CHCH_2CO_2Et$	70	62

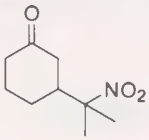
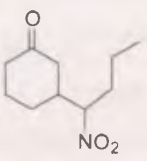
DAC EX. 2040 IPR2022-01531 Page 1118 of 1299

Table 2 (Continued)

entry	nitro compound	alkene	conditions	product	yield %	ref
50			Amberlyst A-27, 20h, rt		55	55
51		$MeO_2CCH=CHCO_2Me$	K_2CO_3, Aliquat® 336, ultrasound, 0.3h, rt	$MeCH(NO_2)CH(CO_2Me)CH_2CO_2Me$	80	51
52		$CH_2=CHSO_2Ph$	KG-60-NEt_2, 25h, rt	$MeCH(NO_2)CH_2CH_2SO_2Ph$	81	40
53	*n*-$PrNO_2$	$CH_2=CHCOMe$	HMS-R_3N, 1.5h, reflux	$CH_3CH_2CH(NO_2)CH_2CH_2COMe$	95	41
54			$P(RNCH_2CH_2)_3N$, Et(Me)CHCN, 0.15h, -63°C		81	50
55			0.025M NaOH, CTACl, 1h, rt		78	39
56			Amberlyst A-27, 7h, rt		90	55
57			KG-60-NEt_2, 25h, rt		80	40
58		$CH_2=CHCOEt$	0.025M NaOH, CTACl, 1h, rt	$CH_3CH_2CH(NO_2)CH_2CH_2COEt$	64	39
59			Amberlyst A-27, 5h, rt		77	55
60			CTAOH, 1h, rt		83	63
61		$CH_2=CHCO$*n*-Pr	0.025M NaOH, CTACl, 1h, rt	$CH_3CH_2CH(NO_2)CH_2CH_2CO$*n*-Pr	82	39
62			Amberlyst A-27, 4h, rt		85	55
63			CTAOH, 1h, rt		80	63
64		$CH_2=CHCO_2Me$	KG-60-NEt_2, 26h, rt	$CH_3CH_2CH(NO_2)CH_2CH_2CO_2Me$	61	40
65		$CH_2=CHCH=CHCO_2Et$	Amberlyst A-27, microwave, 0.1h, 70°C	$MeCH_2CH(NO_2)CH_2CH=CHCH_2CO_2Et$	62	62
66		$MeCH=CHCO_2Bn$	K_2CO_3, Aliquat® 336, ultrasound, 15h, rt	$CH_3CH_2CH(NO_2)CH(Me)CH_2CO_2Bn$	94	51
67			$P(RNCH_2CH_2)_3N$, Et(Me)CHCN, 0.25h, -63°C		71	50
68	9.5 equiv. nitro compound	$MeO_2CCH=CHCO_2Me$	K_2CO_3, Aliquat® 336, ultrasound, 0.05h, rt	$EtCH(NO_2)CH(CO_2Me)CH_2CO_2Me$	62	51
79	*i*-$PrNO_2$	$CH_2=CHCOMe$	$P(RNCH_2CH_2)_3N$, Et(Me)CHCN, 0.25h, rt	$Me_2C(NO_2)CH_2CH_2COMe$	99	50
70			0.025M NaOH, CTACl, 1h, rt		75	39
71			Amberlyst A-27, 25h, rt		75	55
72			KG-60-NEt_2, 5h, rt		82	40

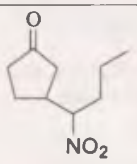
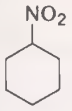
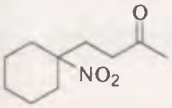
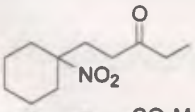
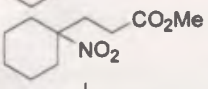
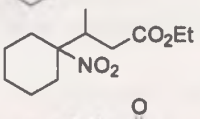
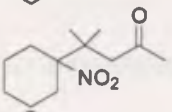
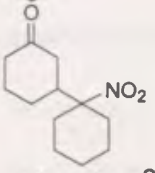
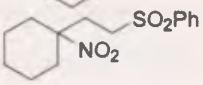
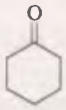
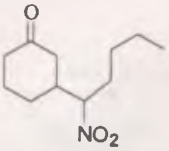
DAC EX. 2040 IPR2022-01531 Page 1119 of 1299

Table 2 (Continued)

entry	nitro compound	alkene	conditions	product	yield %	ref
73		CH_2=CHCOEt	0.025M NaOH, CTACl, 1h, rt	$Me_2C(NO_2)CH_2CH_2COEt$	71	39
74			Amberlyst A-27, 15h, rt		70	55
75		CH_2=CHCO*n*-Pr	0.025M NaOH, CTACl, 2h, rt	$Me_2C(NO_2)CH_2CH_2CO$*n*-Pr	77	39
76			Amberlyst A-27, 13h, rt		85	55
77		PhCH=CHCOPh	KF-natural phosphate, EtOH, 4h, rt	$Me_2C(NO_2)$ CH(Ph)CH_2COPh	98	52
78		Me_2C=CHCOMe	$P(RNCH_2CH_2)_3N$, Et(Me)CHCN, 0.33h, rt	$Me_2C(NO_2)CMe_2CH_2$COMe	99	50
79		CH_2=CHCO$_2$Me	Amberlyst A-27, 4h, rt	$Me_2C(NO_2)CH_2CH_2CO_2Me$	80	55
80		CH_2=CHCO$_2$Et	Ar_3P-polymer supported, heptane-MeOH, 24h, rt	$Me_2C(NO_2)CH_2CH_2CO_2Et$	71	49
81			KF-natural phosphate, EtOH, 4h, rt		91	52
82		MeO_2CCH=CHCO$_2$Me	K_2CO_3, Aliquat® 336, ultrasound, 0.3h, rt	$Me_2C(NO_2)CH(CO_2Me)CH_2CO_2Me$	80	51
83			$P(RNCH_2CH_2)_3N$, Et(Me)CHCN, 0.25h, rt		99	50
84		CH_2=CHSO$_2$Ph	Amberlyst A-27, 20h, rt	$Me_2C(NO_2)CH_2CH_2SO_2Ph$	80	55
85			KG-60-NEt_2, 25h, rt		90	40
86		CH_2=CHCN	Amberlyst A-27, 4h, rt	$Me_2C(NO_2)CH_2CH_2CN$	75	55
87	*n*-$BuNO_2$	CH_2=CHCOMe	0.025M NaOH, CTACl, 1h, rt	*n*-$PrCH(NO_2)CH_2CH_2$COMe	83	39
88			KG-60-NEt_2, 5h, rt		85	40
89		CH_2=CHCOEt	0.025M NaOH, CTACl, 1h, rt	*n*-$PrCH(NO_2)CH_2CH_2$COEt	70	39
90			CTAOH, 1h, rt		75	63
91			KG-60-NEt_2, 6h, rt		83	40
92		CH_2=CHCO*n*-Pr	0.025M NaOH, CTACl, 2h, rt	*n*-$PrCH(NO_2)CH_2CH_2CO$*n*-Pr	68	39
93			Amberlyst A-27, 7h, rt		86	55
94			0.025M NaOH, CTACl, 2h, rt		79	39

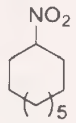
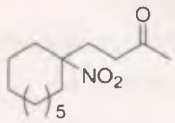
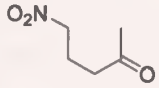
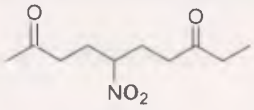
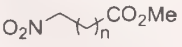
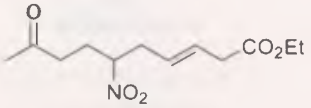
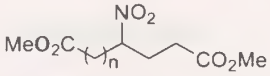
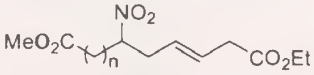
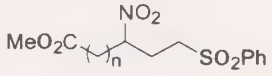
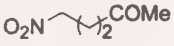
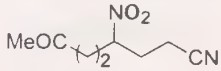
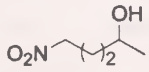
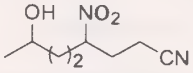
DAC EX. 2040 IPR2022-01531 Page 1120 of 1299

Table 2 (Continued)

entry	nitro compound	alkene	conditions	product	yield %	ref
95			0.025M NaOH, CTACl, 2h, rt		93	39
96		CH_2=$CHCO_2Me$	KG-60-NEt_2, 30h, rt	*n*-$PrCH(NO_2)CH_2CH_2CO_2Me$	62	40
97			CTAOH, 1h, rt		77	63
98		CH_2=$CHCH$=$CHCO_2Et$	Amberlyst A-27, microwave, 0.1h, 70°C	*n*-$PrCH(NO_2)CH_2CH$=$CHCH_2CO_2Et$	55	62
99		CH_2=$CHSO_2Ph$	KG-60-NEt_2, 28h, rt	*n*-$PrCH(NO_2)CH_2CH_2SO_2Ph$	65	40
100		CH_2=CHCN	KG-60-NEt_2, 15h, rt	*n*-$PrCH(NO_2)CH_2CH_2CN$	58	40
101		CH_2=$CHCOMe$	$P(RNCH_2CH_2)_3N$, Et(Me)CHCN, 0.25h, rt		93	50
102			0.025M NaOH, CTACl, 2h, rt		72	39
103		CH_2=$CHCOEt$	Amberlyst A-27, 8h, rt		65	55
104		CH_2=$CHCO_2Me$	$P(RNCH_2CH_2)_3N$, Et(Me)CHCN, 4h, rt		100	50
105		$MeCH$=$CHCO_2Et$	$P(RNCH_2CH_2)_3N$, Et(Me)CHCN, 4h, rt		100	50
106		Me_2C=$CHCOMe$	$P(RNCH_2CH_2)_3N$, Et(Me)CHCN, 1h, rt		95	50
107			$P(RNCH_2CH_2)_3N$, Et(Me)CHCN, 1h, rt		99	50
108		CH_2=$CHSO_2Ph$	Amberlyst A-27, 10h, rt		70	55
109	*n*-$C_5H_{11}NO_2$	CH_2=$CHCOMe$	CTAOH, 1h, rt	*n*-$C_4H_9CH(NO_2)CH_2CH_2COMe$	74	63
110		CH_2=$CHCOEt$	Amberlyst A-27, 5h, rt	*n*-$C_4H_9CH(NO_2)CH_2CH_2COEt$	84	55
111			CTAOH, 2h, rt		90	63
112		CH_2=$CHCO_2Me$	Amberlyst A-27, 9h, rt	*n*-$C_4H_9CH(NO_2)CH_2CH_2CO_2Me$	75	55
113		CH_2=$CHSO_2Ph$	Amberlyst A-27, 15h, rt	*n*-$C_4H_9CH(NO_2)CH_2CH_2SO_2Ph$	65	55

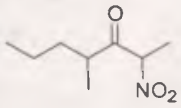
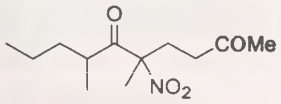
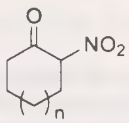
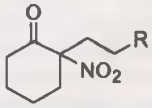
DAC EX. 2040 IPR2022-01531 Page 1121 of 1299

Table 2 (Continued)

entry	nitro compound	alkene	conditions	product	yield %	ref
114		CH_2=CHCN	Amberlyst A-27, 10h, rt	*n*-$C_4H_9CH(NO_2)CH_2CH_2CN$	60	55
115	*n*-$C_6H_{13}NO_2$	CH_2=CHCOMe	CTAOH, 1h, rt	*n*-$C_5H_{11}CH(NO_2)CH_2CH_2COMe$	77	63
116		CH_2=$CHCO_2Me$	CTAOH, 1h, rt	*n*-$C_5H_{11}CH(NO_2)CH_2CH_2CO_2Me$	87	63
117		CH_2=CHCN	KG-60-NEt_2, 16h, rt	*n*-$C_5H_{11}CH(NO_2)CH_2CH_2CN$	56	40
118			CTAOH, 1h, rt		70	63
119		CH_2=$CHSO_2Ph$	CTAOH, 1h, rt	*n*-$C_5H_{11}CH(NO_2)CH_2CH_2SO_2Ph$	70	63
120		CH_2=CHCH=$CHCO_2Et$	Amberlyst A-27, microwave, 0.1h, 70°C	*n*$C_5H_{11}CH(NO_2)CH_2CH$=$CHCH_2CO_2Et$	68	62
121		CH_2=CHCOMe	0.025M NaOH, CTACl, 2h, rt		74	39
122	$PhCH_2CH_2NO_2$	CH_2=CHCH=$CHCO_2Et$	Amberlyst A-27, microwave, 0.1h, 70°C	$PhCH_2CH(NO_2)CH_2CH$=$CHCH_2CO_2Et$	60	62
123		CH_2=CHCOEt	Amberlyst A-27, 4h, rt		75	55
124		CH_2=CHCH=$CHCO_2Et$	Amberlyst A-27, microwave, 0.1h, 70°C		55	62
125	n=2	CH_2=$CHCO_2Me$	Amberlyst A-27, 7h, rt		85	55
126		CH_2=CHCH=$CHCO_2Et$	Amberlyst A-27, microwave, 0.1h, 70°C		75	62
127	n=4	CH_2=$CHSO_2Ph$	CTAOH, 2h, rt		73	63
128		CH_2=CHCN	CTAOH, 1h, rt		65	63
129		CH_2=CHCN	CTAOH, 1h, rt		72	63
	$RCOCH(R^1)NO_2$					
130	R = Ph R^1 = H	CH_2=CHCOMe	Silica gel 60, 22h, rt	$PhCOCH(NO_2)CH_2CH_2COMe$	87	58
131		CH_2=CHCO*n*-Pr	Silica gel 60, 23h, rt	$PhCOCH(NO_2)CH_2CH_2CO$*n*-Pr	86	58
132	R = Me R^1 = Et	CH_2=CHCOMe	Silica gel 60, 100h, rt	$MeCOC(Et)(NO_2)CH_2CH_2COMe$	74	58

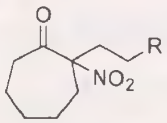
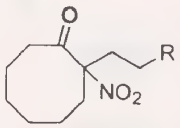
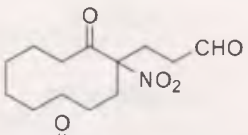
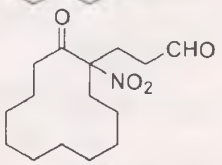
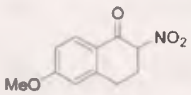
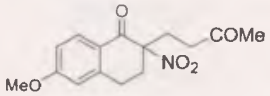
DAC EX. 2040 IPR2022-01531 Page 1122 of 1299

Table 2 (Continued)

entry	nitro compound	alkene	conditions	product	yield %	ref
133		CH_2=CHCO*n*-Pr	Silica gel 60, 23h, rt	MeCOC(Et)$(NO_2)CH_2CH_2$CO*n*-Pr	65	58
134	R = *i*-Pr R^1 = *n*-Pr	CH_2=CHCOEt	Silica gel 60, 20h, rt	*i*-PrCOC(*n*-Pr)$(NO_2)CH_2CH_2$COEt	72	58
135	R = *n*-C_5H_{11} R^1 = Me	CH_2=CHCOEt	Silica gel 60, 50h, rt	*n*-C_5H_{11}COC(Me)$(NO_2)CH_2CH_2$COEt	77	58
136	R = $Ph(CH_2)_2$ R^1 = Et	CH_2=CHCOEt	Silica gel 60, 120h, rt	$Ph(CH_2)_2$COC(Et)$(NO_2)CH_2CH_2$COEt	76	58
137	R = *c*-C_6H_{11} R^1 = *n*-Bu	CH_2=CHCOMe	Silica gel 60, 100h, rt	*c*-C_6H_{11}COC(*n*-Bu)$NO_2CH_2CH_2$COMe	86	58
138		CH_2=CHCOMe	Silica gel 60, 35h, rt		88	58
	$MeO_2CCH(R)NO_2$					
139	R = H	CH_2=CHCOMe	$Yb(OTf)_3$, H_2O, rt	$MeO_2CCH(NO_2)CH_2CH_2$COMe	98	57
140	R = CH_2=$CHCH_2$	CH_2=CHCOMe	$Yb(OTf)_3$, H_2O, rt	$MeO_2CC(R)(NO_2)CH_2CH_2$COMe	96	57
	$EtO_2CCH(R)NO_2$					
141	R = H	CH_2=$CHCO_2$Et	Bu_4NClO_4, THF, electrolysis, rt	$EtO_2CCH(NO_2)CH_2CH_2CO_2$Et	82	56
142		CH_2=CHCN	Bu_4NBr, MeCN, electrolysis, rt	$EtO_2CCH(NO_2)CH_2CH_2$CN	85	56
143	R = Me	CH_2=$CHCO_2$Et	Bu_4NBr, MeCN, electrolysis, rt	$EtO_2CC(Me)(NO_2)CH_2CH_2CO_2$Et	85	56
144		CH_2=CHCHO	$Yb(OTf)_3$, H_2O, 3d, rt	$EtO_2CC(Me)(NO_2)CH_2CH_2$CHO	98	57
145		CH_2=CHCOMe	$Yb(OTf)_3$, H_2O, 3d, rt	$EtO_2CC(Me)(NO_2)CH_2CH_2$COMe	99	57
146		CH_2=CHCOEt	$Yb(OTf)_3$, H_2O, 3d, rt	$EtO_2CC(Me)(NO_2)CH_2CH_2$COEt	98	57
147		CH_2=CHCOPh	$Yb(OTf)_3$, H_2O, 3d, rt	$EtO_2CC(Me)(NO_2)CH_2CH_2$COPh	98	57
148		CH_2=C(Me)CHO	$Yb(OTf)_3$, H_2O, 7d, rt	$EtO_2CC(Me)(NO_2)CH_2CH(Me)$CHO	72	57
149	R = Et	CH_2=CHCOMe	$Yb(OTf)_3$, H_2O, rt	$EtO_2CC(Et)(NO_2)CH_2CH_2$COMe	99	57
150	R = CH_2=$CHCH_2$	CH_2=CHCOMe	$Yb(OTf)_3$, H_2O, rt	$EtO_2CC(R)(NO_2)CH_2CH_2$COMe	99	57
151	R = $CH_2CH_2CO_2$Et	CH_2=$CHCO_2$Et	Bu_4NBr, MeCN, electrolysis, rt	$EtO_2CC(R)(NO_2)CH_2CH_2CO_2$Et	84	56
152	R = CH_2CH_2CN	CH_2=CHCN	Bu_4NBr, MeCN, electrolysis, rt	$EtO_2CC(R)(NO_2)CH_2CH_2$CN	82	56
	 n = 1					
153		CH_2=CHCOMe	Silica gel 60, 44h, rt	R = COMe	75	58

DAC EX. 2040 IPR2022-01531 Page 1123 of 1299

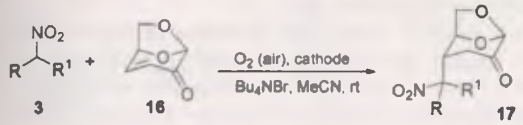
Table 2 (Continued)

entry	nitro compound	alkene	conditions	product	yield %	ref
154		CH_2=CHCHO	H_2O, 14h, rt	R = CHO	98	59
	n = 2					
155		CH_2=CHCOEt	Silica gel 60, 90h, rt	R =COEt	82	58
156		CH_2=CHCHO	H_2O, 8h, rt	R = CHO	85	59
157			0.07 M K_2CO_3, 0.5h, rt		55	59
158		CH_2=CHCOMe	H_2O, 4d, rt	R =COMe	93	59
159			0.07 M K_2CO_3, 0.5h, rt		92	59
160		CH_2=CHCOEt	H_2O, 4d, rt	R =COEt	85	59
161			0.07 M K_2CO_3, 1h, rt		80	59
162		CH_2=CHCO$_2$Me	0.07 M K_2CO_3, 0.75h, rt	R =CO$_2$Me	30	59
163		CH_2=CHCN	0.07 M K_2CO_3, CTAB (10%), 3h, rt	R =CN	60	59
164		CH_2=CHSO$_2$Ph	0.07 M K_2CO_3, 0.75h, rt	R =SO$_2$Ph	77	59
	n = 3					
165		CH_2=CHCHO	H_2O, 14h, rt	R = CHO	99	59
166		CH_2=CHCOMe	H_2O, 4d, rt	R =COMe	98	59
167	n = 5	CH_2=CHCHO	H_2O, 37h, rt		99	59
168	n = 7	CH_2=CHCHO	H_2O, CTAB (10%), 5d, rt		99	59
169		CH_2=CHCOMe	Silica gel 60, 70h, rt		88	58

tions (AM1) demonstrate that **RZ** is the most stable rotamer for enoate *Z*-**21**, but two nearly isoenergetic rotamers $\mathbf{RE_1}$ and $\mathbf{RE_2}$ are possible for compound *E*-**21** (Scheme 7). Thus, attack from the *re* side of *Z*-**21** through rotamer **RZ** produces *syn*-**22** with high diastereoselectivity, while the same reaction of *E*-**21** can occur on the *re* ($\mathbf{RE_1}$) or *si* ($\mathbf{RE_2}$) side without a great difference in the energy of the corresponding transition states. The stereoselectivity at the carbon atom bearing the nitro group is usually rather poor, and this result is probably due to the low enantiofacial discrimination exerted by the enoate on the nitronate anion. A *syn*-selective reaction is also observed in the reaction of nitromethane with 2-sub-

DAC EX. 2040 IPR2022-01531 Page 1124 of 1299

Scheme 5



3	R	R^1	yield 17 %
a	H	CO_2Et	85
b	Me	CO_2Et	89
c	CO_2Et	$CH_2CH_2CO_2Et$	82
d	Me	Me	93
e	$-(CH_2)_5-$		96
f	CO_2Et	$CH_2{=}CHCH_2$	89
g	H	NO_2	88

Scheme 6

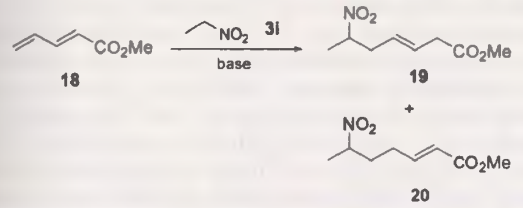
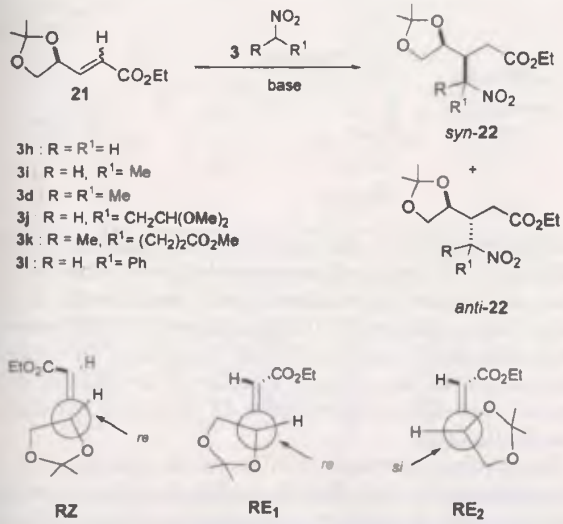


Table 3. Regioselective Addition of Nitroethane to Diene 18

entry	catalyst	solvent	reaction time	yield (%) 19:20
1	DBU	MeCN	2 days	6:40
2	NaOH 0.1M	H_2O	2 days	40:6
3	TMG	THF	12 h	35:7
4	Amberlyst A-27	neat	2 days	38:4
5	Amberlyst A-27 microwave 500W	neat	7 min	85:10

Scheme 7



stituted analogues of enoate **22** and other related systems.[66]

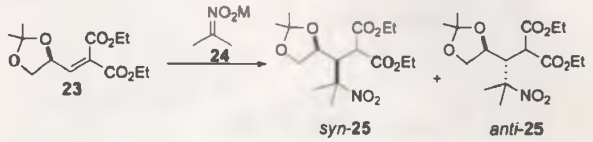
A diastereofacial preference for the *re* side of alkylidenemalonate **23** is also observed in the reaction with metal nitronate **24** (Scheme 8).[67] The addition is fully diastereoselective in THF at room temperature, but after 1 h in DMSO at room temperature the *syn/anti* ratio is much lower (77:23). After 48 h the diastereoselectivity in DMSO increases

Table 4. Diastereoselective Addidion of Nitro Compounds 3 to Chiral Enoate 21[a]

entry	21	3	base	product yield (%)	*syn:anti* d.e.(%)
1	Z/E	**3h**	TBAF	71	90
2	Z	**3h**	DBU	70	80
3	Z	**3i**	DBU	70	90
4	E	**3i**	DBU	65	50
5	Z	**3d**	TBAF	80	94
6	E	**3d**	DBU	68	0
7	Z	**3j**	TBAF	77	94
8	E	**3j**	TBAF	70	34
9	Z	**3k**	TBAF	80	100
10	E	**3k**	DBU	70	6
11	Z	**3l**	DBU	67	80
12	E	**3l**	DBU	65	80

[a] DBU/MeCN and TBAF/THF at room temperature are used.

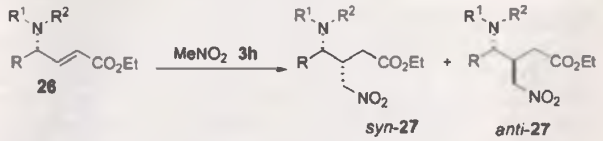
Scheme 8



M	solvent/T°C	time h	yield(%)	*syn:anti*
Li	THF, rt	0.5	71	100:0
Li	DMSO, rt	1	96	77:23
Li	DMSO, rt	48	-	98:2
K	DMSO, rt	1	77	90:10

to 98/2, and this definitely suggests thermodynamic control in the formation of the more stable *syn* diastereomer. This assumption is also corroborated by the diastereomeric ratio (*syn/anti* = 90:10) obtained using potassium nitronate **24** in DMSO at room temperature. Conjugate addition of nitromethane to optically active *N*-protected vinylogous amino esters affords the corresponding nitro derivatives in good yield and fair diastereoselectivity.[68] The *syn/anti* ratio of the resulting adducts is always around 80:20 regardless of the nature of the substituents at the nitrogen atom or in the alkenyl chain (Scheme 9). The basic system used to promote the

Scheme 9



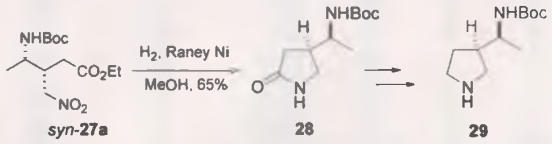
Entry	R	R^1	R^2	base	yield(%)	*syn:anti*
a	Me	H	Boc	DBN	95	84:16
b	Me	Bn	Bn	DBU	78	81:19
c	*i*-Pr	H	Boc	DBU	98	86:14
d	CH_2Ph	H	Boc	DBU	83	80:20

addition can affect the chemical yield of the process but has a narrow impact on the diastereoselection. Interestingly, the conjugate addition of cyanide ion on the same substrates occurs with no stereoselectivity under different reaction conditions.

DAC EX. 2040 IPR2022-01531 Page 1125 of 1299

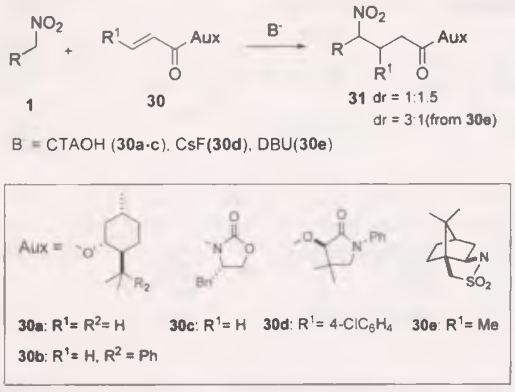
This study was originally designed as a synthetic approach to the preparation of chiral 3-aminoalkyl pyrrolidine residue in fluoroquinolone antibiotics (Scheme 10).

Scheme 10



The introduction of a chiral auxiliary in the acylic group of enoate systems does not usually produce a significant diastereoselection in the conjugate addition of nitroalkanes (Scheme 11). Nitromethane as

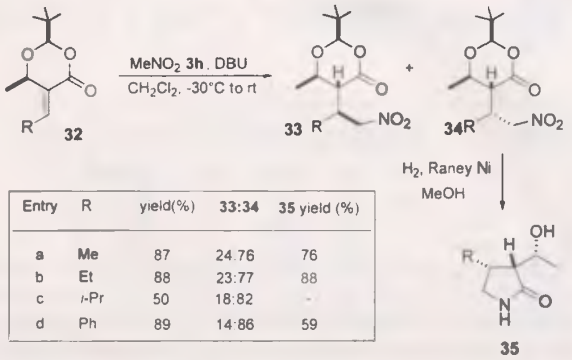
Scheme 11



well as functionalized secondary nitro derivatives add to enoates **30a−d** with a diastereomeric ratio of 1:1.5, a value that is not useful for whatever synthetic application.[69,70] Crotonylbornane sultam **30e** gives better results in the conjugate addition with nitromethane, affording a 3:1 diastereomeric couple of products in which stereoisomer 3*S* predominates.[195]

Chiral 5-alkenyl-1,3-dioxan-4-ones react with nitromethane at the exocyclic double bond in the presence of DBU with respectable diastereoselectivity. Attack of the nitronate anion occurs selectively at the *re* face, providing adduct **34** as the major stereoisomer (Scheme 12).[71]

Scheme 12

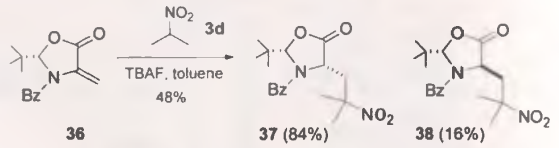


Entry	R	yield(%)	33:34	35 yield (%)
a	Me	87	24:76	76
b	Et	88	23:77	88
c	*i*-Pr	50	18:82	-
d	Ph	89	14:86	59

After chromatographic separation, compounds **34** are reduced and the resulting amino derivatives spontaneously cyclize to afford optically active hydroxypyrrolidinones **35.**

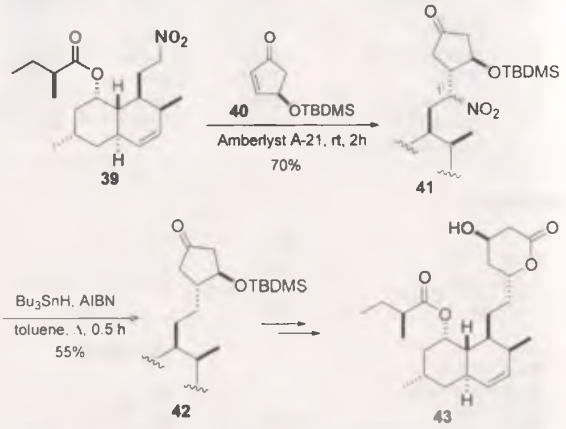
In a related procedure reaction of 2-nitropropane with chiral dehydroalanine **36** in the presence of TBAF gives a diastereomeric mixture of adducts with predominance of the *syn* isomer (Scheme 13).[72]

Scheme 13



As previously observed, stereocontrol at the carbon atom bearing the nitro group is hard to achieve, probably because of the consistent acidity of the related hydrogen that in basic conditions allows a thermodynamic equilibration between the epimers.[73] This drawback becomes ineffective when the nitro group needs to be eliminated from the molecular framework by means of a reductive denitration. A key step toward the total synthesis of the hypocholesterolemic agent dihydromevinolin **43** involves the conjugate addition of nitroalkane **39** to chiral cyclopentenone **40** (Scheme 14).[74] This addition is best effected

Scheme 14



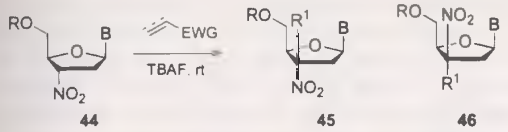
using Amberlyst A-21 in solventless conditions, and although it is highly diastereoselective in the formation of the carbon−carbon bond, product **41** is obtained as a mixture (3:2) of epimers at C-1′. However, radical-induced denitration of compound **41** affords derivative **42** as a single diastereomer that is converted into dihydromevinolin **43** after few synthetic manipulations.

Interesting stereoselectivities can be obtained when the nitro group is linked to a chiral cyclic structure that is able to produce consistent diastereofacial discrimination. Nitrothymidines **44** react with electron-poor alkenes from the less hindered α-face of the pentofuranose ring, giving compound **46** as major product (Scheme 15).[75]

Enantiomerically pure 5-glyco-4-nitrocyclohex-1-ene **47** reacts with various Michael acceptors with high diastereoselectivity, giving adducts **48** in which a *trans* relationship between the sugar chain and the added group is observed (Scheme 16).[76,77] The absence

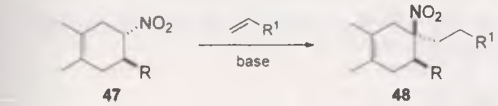
DAC EX. 2040 IPR2022-01531 Page 1126 of 1299

Scheme 15



R^1	45+46 yield(%)	45:46
CH_2CH_2CN	83	0:1
$CH=CHCO_2Et$	87	1:4
CH_2CH_2COMe	71	1:7

Scheme 16

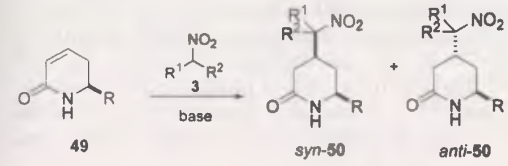


R^1	base	48 yield(%)
CO_2Me	DBU	60
COMe	TMG	82
CN	TMG	60
CHO	TMG	44

of enolizable hydrogen atoms near the nitro group probably avoids any epimerization of the addition products **48**.

Generally, because of the steric constraint present in rigid structures, chiral cycloalkenones are expected to react in conjugate additions with a consistent degree of diastereoselectivity. Chiral piperidinone **49** reacts with nitromethane with modest *syn* or no diastereoselectivity depending on the nature of the substituent present in the ring (Scheme 17).[78] Con-

Scheme 17

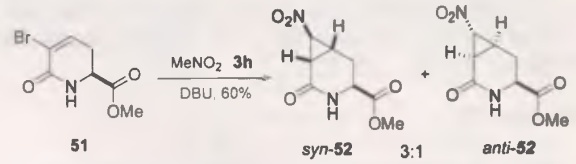


R	R^1	R^2	base	yield(%)	*syn:anti*
TBDPSO	H	H	DBU	85	1:1
TBDPSO	Me	Me	DBU	85	0:1
CO_2Me	H	H	DBU	85	3:1
CO_2Me	Me	Me	DBU	85	0:1
CO_2Me	$-(CH_2)_4-$		K_2CO_3	65	0:1
CO_2Me	$-(CH_2)_5-$		K_2CO_3	65	0:1

versely, secondary nitroalkanes add to piperidinone **49** with complete stereocontrol, giving exclusively the *anti* diastereomer.

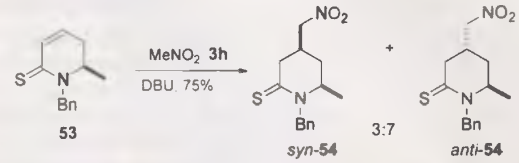
Reaction of 3-bromopiperidinone **51** with nitromethane takes place through a tandem conjugate addition−nucleophilic substitution by the corresponding nitronate anion, giving bicyclo derivatives **52**. Once again, the *syn/anti* ratio of the obtained compound **52** is 3:1 with a nitro group that adopts an *exo*-orientation with respect to the piperidinone ring (Scheme 18).

Scheme 18



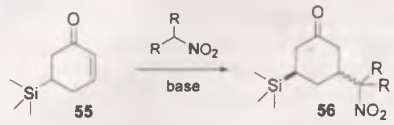
The *syn* diastereoselectivity observed in the conjugate addition of compounds **49** and **51** with nitromethane would be somewhat associated with the presence of a polar group in the 6-position that drives the nucleophilic attack from the same side of the substituent. Indeed, a structurally related thiolactam **53** bearing a 6-methyl group reacts with nitromethane in the presence of DBU with a *syn/anti* ratio of 3:7 (Scheme 19).[79]

Scheme 19



The steric hindrance of the incoming nitroalkane seems to have a deleterious effect on the diastereoselectivity displayed by 5-substituted cyclohexenones. Conjugate addition of 2-nitropropane on 5-trimethylsilyl cyclohexenone **55** occurs with high yield but unsatisfactory diastereoselectivity (Scheme 20).[80] On

Scheme 20

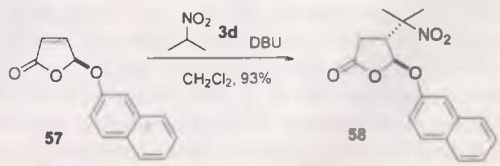


R	base	56 yield(%)	*syn anti*
Me, Me	DBU	80	2 3
Me, Me	KF/Al_2O_3	93	1 1
H, H	KF/Al_2O_3	80	1 20

the contrary, with the same substrate nitromethane gives excellent diastereoselectivity.

Chiral γ-aryloxybutenolide **57** prepared through dynamic kinetic asymmetric transformation of racemic acyloxybutenolides reacts with 2-nitropropane with high diastereoselectivity to give compound **58** as a single stereoisomer of *anti* configuration (Scheme 21).[81] In this context, butenolide **57** acts as a "chiral

Scheme 21

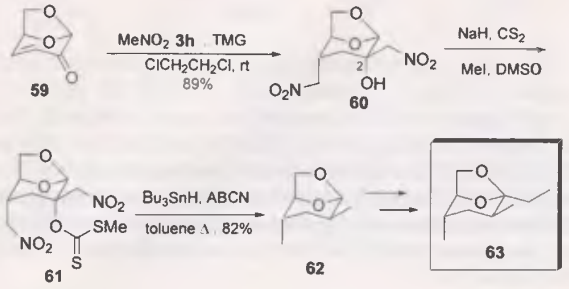


aldehyde" equivalent for a number of synthetic transformations including conjugate additions and cycloadditions.

DAC EX. 2040 IPR2022-01531 Page 1127 of 1299

Rigid bicyclic structures are very effective in diastereoselective reactions as demonstrated by the reaction of levoglucosenone **59** with nitromethane **3h** (Scheme 22).[82]

Scheme 22

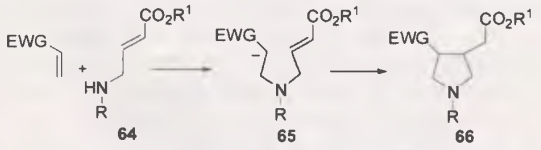


Using a large excess of nitromethane in the presence of TMG ensures a conjugate addition as well as a nitroaldol reaction on compound **59,** leading to adduct **60** in good yield and diastereoselectivity (10:1 at C-2). Deoxygenation and removal of the nitro functions can be made in a single step via thioxantate **61** using Bu_3SnH in a radical process. The obtained compound **62** is an advanced intermediate to the enantioselective synthesis of aggregation pheromone (−)-δ-multistriatin **63**.[83]

4.2. Intramolecular Additions

A viable strategy for the construction of pyrrolidine ring systems lies in the tandem conjugate additions of an amino derivative bearing a Michael acceptor **64** with an electron-poor olefin (Scheme 23). The

Scheme 23

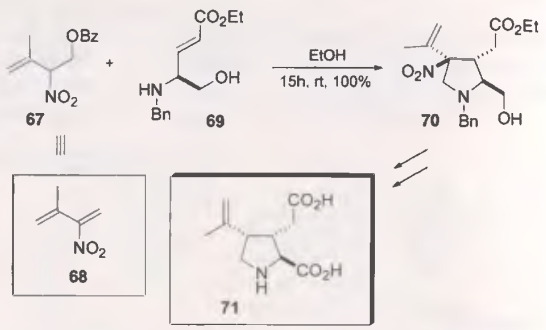


intermediate anion **65** undergoes to a further conjugate addition to give the final pyrrolidine **66**.

Nitroalkenes are ideal candidates as electrophilic olefins for this procedure, but sometimes their preparation and storage is made difficult by their instability and propensity to undergo polymerization processes. However, these reactive alkenes can be readily prepared *in situ* by an elimination reaction from a suitable β-acyloxy nitro derivative. This approach has been successfully applied to the enantioselective synthesis of neuroexcitatory amino acid (−)-α-kainic acid (Scheme 24).[84,85]

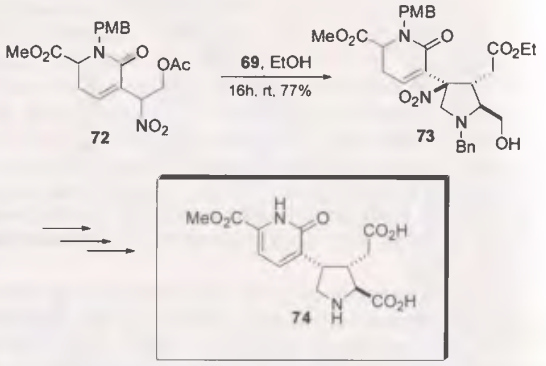
Benzyloxy nitroalkene **67** can be considered as a synthetic equivalent of nitrodiene **68** and by reaction with hydroxyester **69** in ethanol affords quantitatively pyrrolidine **70** as a sole diastereomer. The formation of nitrodiene **68** is presumably promoted by the amino group of **69**. Simple functional group transformations allow the total synthesis of (−)-α-kainic acid **71**. Using the same approach a structurally related compound, the neurotoxin acromelic acid A **74**, can be prepared using the nitroalkene pre-

Scheme 24



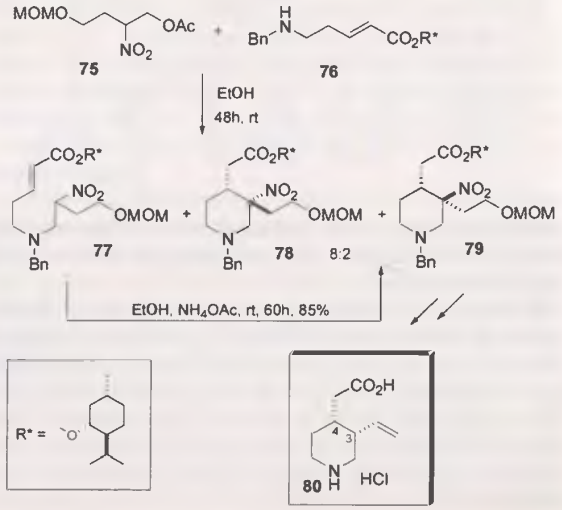
cursor **72** in the reaction with amino ester **69** (Scheme 25).[86]

Scheme 25



Ring closure to six-membered ring derivatives using the tandem conjugate addition previously described presents some remarkable differences compared to the assembling of five-membered rings. A synthetic plan to the enantioselective synthesis of (−)-meroquinene **80** requires the sequential inter- and intramolecular conjugate addition of chiral amino ester **76** to the nitroalkene precursor **75** (Scheme 26).[87] Surprisingly, only a partial cyclization of intermediate **77** is evidenced after 48 h at room temperature, and the diastereoselectivity of the obtained

Scheme 26

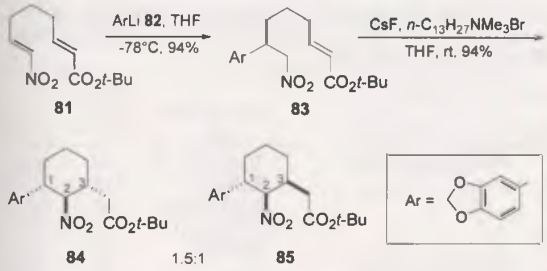


DAC EX. 2040 IPR2022-01531 Page 1128 of 1299

piperidine ester is 8:2 in favor of diastereomer **78**. Open-chain adduct **77** can be forced to cyclize in the presence of ammonium acetate to give compounds **78** and **79** with the same diastereomeric ratio (8:2) previously obtained. The modest level of diastereoselectivity observed does not affect the efficiency of the process since removal of the nitro group in a subsequent step provides the correct stereochemistry at C-3; anyways, the chiral induction exerted by the L-menthyl group at C-4 during the cyclization step is noteworthy.

The difficulties associated with intramolecular six-membered ring closures by conjugate additions are also evident in a related procedure devoted to the synthesis of lycorane alkaloids. Addition of aryllithium **82** to the nitroalkene portion of **81** is completely chemoselective, but the intermediate nitronate anion does not add to the enoate group in a tandem process, so that compound **83** is obtained in high yield (Scheme 27).[88] Cyclization of **83** realized

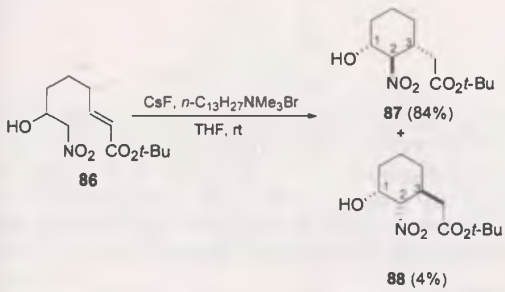
Scheme 27



using CsF is poorly diastereoselective at C-3 but displays a complete *trans* relationship between C-1 and C-2.

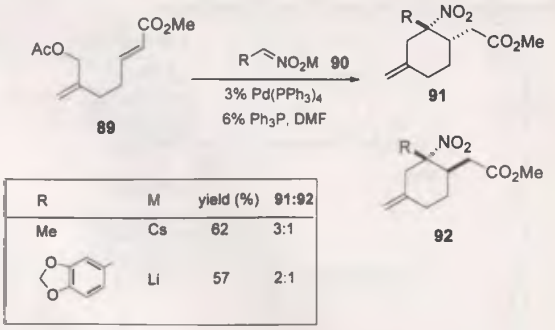
Better diastereoselections can be obtained starting from nitro alcohol **86** that in the same conditions (CsF, R_4NBr) produces a diastereomeric couple in which compound **87** strongly predominates (Scheme 28).[89]

Scheme 28



Allylic alkylation of nitro compounds catalyzed by Pd(0) can be associated with conjugate additions in order to prepare cyclohexane derivatives. Allyl acetate **89** reacts with metal nitronates **90** in the presence of $Pd(PPh_3)_4$ to give an open-chain homoallylic nitro derivative that as soon as it is formed cyclizes by means of a conjugate addition, leading to the diastereomeric couple of nitrocyclohexanes **91** and **92** (Scheme 29).[90-92] As for most of the six-membered ring cyclizations of this type, the diastereoselectivity

Scheme 29



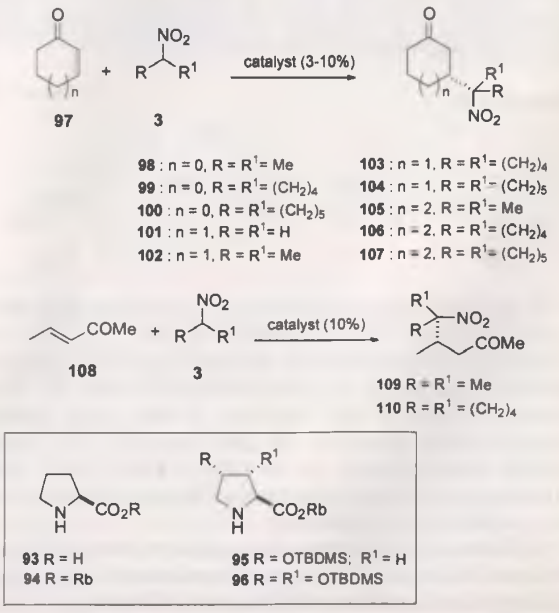
R	M	yield (%)	91:92
Me	Cs	82	3:1
	Li	57	2:1

observed is quite modest but the yields of the overall transformation are respectable.

5. Asymmetric Conjugate Additions Promoted by Chiral Catalysis

The utilization of chiral catalysts to produce enantiofacial discrimination in the conjugate addition of a nucleophile to electron-poor alkenes represents the optimum choice in terms of efficiency and stereoselectivity.[93-96] Conjugate additions of nitroalkanes to enones mediated by chiral catalysts have been known since at least the mid-1970s, but only in the past decade has their development provided important results in terms of efficiency and enantiomeric excess. Since these additions are prevalently base-promoted reactions, chiral amino derivatives have been among the first compounds to be used for this purpose. Ni(II) complexes of proline derivatives are able to catalyze the conjugate addition of nitromethane to chalcone, but the chemical yields are rather modest and the enantiomeric excesses (ee's) of the resulting adduct never exceed 61%.[97] Proline **93** and rubidium salt derivatives **94**–**96** are effective catalysts for the conjugate addition of various nitroalkanes **3** to enones **97** (Scheme 30).[98-100]

Scheme 30



DAC EX. 2040 IPR2022-01531 Page 1129 of 1299

Table 5. Enantioselective Conjugate Addition of Nitroalkanes to Enones 97 and 108 Mediated by Proline Derivatives 93–96 as Chiral Catalysts

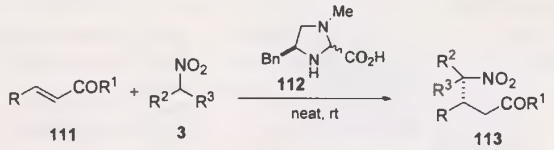
entry	enone	nitroalkane	catalyst[a]	product	yield (%)	ee % (config)	ref
1	2-cyclopentenone	*i*-$PrNO_2$	**93**	**98**	66	75(*R*)	101
2		*c*-$C_5H_9NO_2$	**93**	**99**	66	76(*R*)	101
3		*c*-$C_6H_{11}NO_2$	**93**	**100**	62	76(*R*)	101
4	2-cyclohexenone	$MeNO_2$	**93**	**101**	61	45(*R*)	101
5			**94**	**101**	55	45	98
6		*i*-$PrNO_2$	**93**	**102**	88	93*R*)	101
7			**94**	**102**	81	59(*R*)	98
8		*c*-$C_5H_9NO_2$	**93**	**103**	68	93(*R*)	101
9		*c*-$C_6H_{11}NO_2$	**93**	**104**	73	93(*R*)	101
10	2-cycloheptenone	*i*-$PrNO_2$	**93**	**105**	61	86(*R*)	101
11			**94**	**105**	79	73(*R*)	98
12			**95**	**105**	70	72(*R*)	98
13			**96**	**105**	73	76(*R*)	98
14		*c*-$C_5H_9NO_2$	**93**	**106**	71	87(*R*)	101
15			**94**	**106**	74	67	98
16		*c*-$C_6H_{11}NO_2$	**93**	**107**	49	89(*R*)	101
17			**94**	**107**	84	84	98
18	MeCH=CHCOMe	*i*-$PrNO_2$	**94**	**109**	74	68(*S*)	98
19		*c*-$C_5H_9NO_2$	**94**	**110**	64	59	98

[a] Proline **93** is used with 1 equiv of *trans*-2,5-dimethylpiperazine as an additive.

The ee's of the resulting adducts **98**–**107**, **109**, and **110** are quite modest (45–84%) and little affected by the substitution of the pyrrolidine ring (Table 5). (*S*)-Proline derivatives react efficiently with cycloalkenones, showing a marked preference for attack at the *si* face, leading to formation of the *R* enantiomer. A consistent improvement in these additions can be obtained using (*S*)-proline with a basic additive used in an equivalent amount.[101] Amino derivatives are particularly effective for this purpose, and *trans*-2,5-dimethylpiperazine is the most efficient catalyst.[102] Conjugate addition of primary nitroalkanes such as nitroethane or 1-nitro-4-butene to cycloalkenones occurs with poor diastereoselectivity and modest enantioselectivity of the obtained diastereomers.

Heterocyclic derivatives featured by the imidazolidine ring are also useful catalysts for conjugate addition of nitroalkanes to enones.[103] The level of enantioselection displayed by these catalysts is similar to that obtained with proline derivatives, and better results are usually obtained using secondary nitroalkanes (Scheme 31, Table 6).

Scheme 31



A possible explanation for the enantiofacial preference observed in this reaction would take into account the formation of an iminium ion intermediate between the enone and the catalyst (Scheme 32). The benzyl group in the catalyst in the more stable conformation assumed by the iminium ion would shield the *re* face of the reactive double bond, thus allowing a preferential attack of the nitroalkane from the *si* side of the molecule.

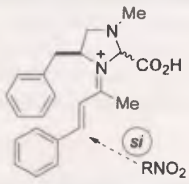
2-Nitrocycloalkanones **114** add to methyl vinyl ketone **115** in the presence of cinchonine **116,** which belongs to the class of *Cinchona* alkaloids.[104] The

Table 6. Enantioselective Conjugate Addition of Nitroalkanes to Enones Mediated by Imidazolidine 112 as Chiral Catalysts

entry	enone **111**	nitroalkane **3**	product **113** yield (%)	ee % (config)
1	PhCH=CHCOMe	$MeNO_2$	52	73(*S*)
2		$EtNO_2$	75	71/73[a]
3		*c*-$C_5H_9NO_2$	95	77(*S*)
4		*c*-$C_6H_{11}NO_2$	64	71(*S*)
5		*i*-$PrNO_2$	95	79(*S*)
6	PhCH=CHCOEt		69	83(*S*)
7	4-ClC_6H_4CH=CHCOMe		87	75(*S*)
8	4-OHC_6H_4CH=CHCOMe		86	75(*S*)
9	ArCH=CHCOMe[b]		69	70(*S*)
10	*n*-BuCH=CHCOMe		50	73(*S*)

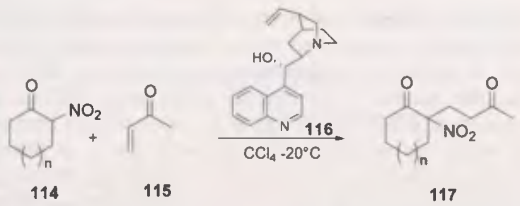
[a] Diastereomeric ratio 1:1. [b] Ar = 2-furyl.

Scheme 32



absolute configuration of the major enantiomer obtained of **117** is affected by the ring size of the 2-nitrocycloalkanone. Large rings ($n \geq 4$) give predominantly adducts with the *R* configuration, while the stereochemistry of medium rings does not follow a sharp trend (Scheme 33, Table 7).

Scheme 33



Chincona alkaloids can be easily transformed into quaternary ammonium salts that can be used for a

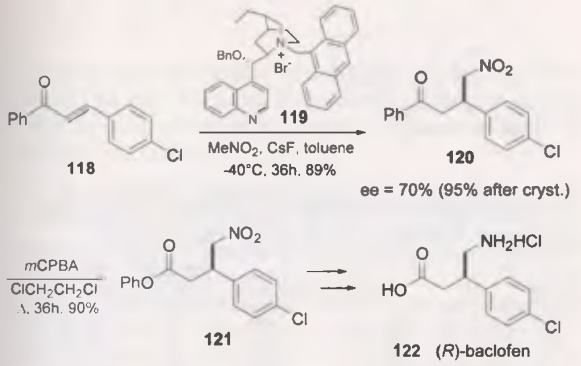
DAC EX. 2040 IPR2022-01531 Page 1130 of 1299

Table 7. Enantioselective Conjugate Addition of 2-Nitrocycloalkanones 114 to Methyl Vinyl Ketone 115 Mediated by Cinchonine 116 as Chiral Catalysts

entry	n	product yield (%)	ee % (config)
1	1	84	55(*S*)
2	2	95	45(*R*)
3	3	92	60(*S*)
4	4	95	25(*R*)
5	5	91	29(*R*)
6	7	87	25(*R*)
7	11	97	28(*R*)

variety of catalytic phase-transfer reactions. Conjugate addition of nitromethane to enone **118** in the presence of 10% chiral ammonium salt **119** produces nitro ketone **120** with modest enantioselectivity (Scheme 34).[105] The ee of **120** can be improved to 95%

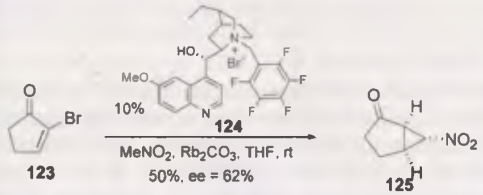
Scheme 34



after a single crystallization, and by means of a Baeyer–Villiger oxidation, ester **121** is obtained. This derivative can be easily transformed into (*R*)-baclofen hydrochloride, a γ-amino acid that acts as $GABA_B$ receptor agonist.

A tandem conjugate addition–nucleophilic substitution is experienced in the reaction of 2-bromo-2-cyclopentenone **123** with nitromethane (Scheme 35).

Scheme 35

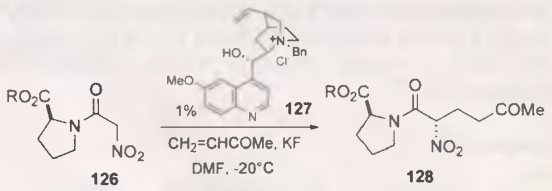


In the presence of 10% molar quinidine alkaloid **124** bicyclic nitro ketone **125** is formed in 50% yield and 62% ee.[106]

Conjugate addition of chiral nitroacetyl derivatives **126** to methyl vinyl ketone catalyzed by KF usually occurs with modest diastereoselectivity. However, addition of 1% *N*-benzylquinidinium chloride **127** slightly improves the diastereomeric excesses of the corresponding adducts **128** (Scheme 36).[107]

Amidine and guanidine bases are known to react with nitroalkanes in nonpolar solvents, giving tightly bound ion pairs whose structure has been determined by X-ray crystallography.[108,109] The utilization of complexes obtained using chiral amidines or guani-

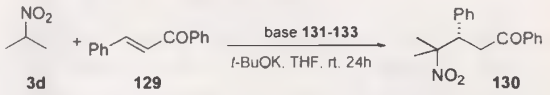
Scheme 36

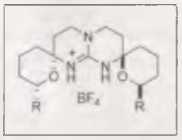


R	yield(%)	**128** d.e.(%)
Bn	92	51
Et	72	51
t-Bu	40	36
Ph_2CH	50	40

dines has been tested for the conjugate addition of simple nitroalkanes with enones, but the adducts obtained using 2,8-disubstituted bicyclic guanidines have low ee's (9–12%).[110] Better results can be obtained using spirocyclic guanidines **131**–**133** that catalyze the addition of 2-nitropropane to chalcone with fair enantioselectivity (Scheme 37).[111]

Scheme 37

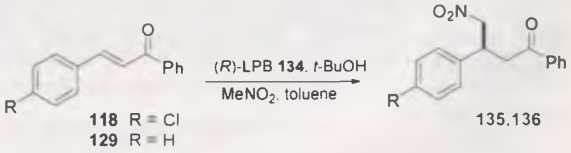


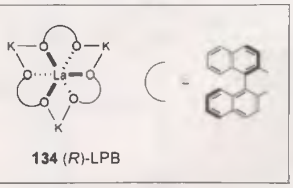


R	conversion %	ee 3 %
131 Me	97	86
132 $TBDMSOCH_2$	70	65
133 $TBDPSOCH_2$	80	74

Chiral heterobimetallic complexes of lanthanum have been extensively used as catalysts for nitroaldol reactions but have found only a limited application to the corresponding conjugate additions. Nitromethane adds to chalcone derivatives **118** and **129** in the presence of (*R*)-LaK_3trisbinaphthoxide **134** with satisfactory yield and enantioselectivity (Scheme 38).[112] However the efficiency of this reaction is highly

Scheme 38





	R	yield %	ee %
135	Cl	71	95
136	H	59	97

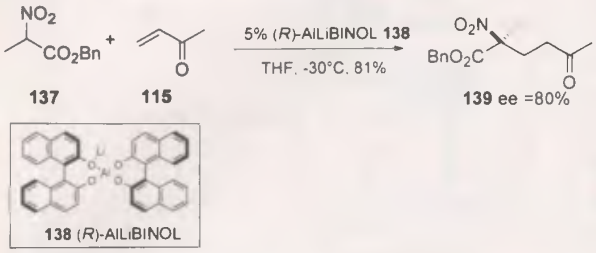
substrate dependent since other enones react with moderate ee's (40–45%) and yields (up to 40%)

Addition of α-nitro esters to enones using chiral lanthanum complexes is poorly or nonenantioselective, but the efficiency of the reaction can be some-

DAC EX. 2040 IPR2022-01531 Page 1131 of 1299

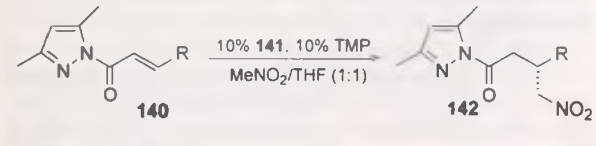
what improved moving to the Al–Li–BINOL complex **138** prepared in situ from $LiAlH_4$ and (*R*)-BINOL. The ee's of the resulting adducts lie in the range of 50% with a single example which reaches 80% (Scheme 39).[113]

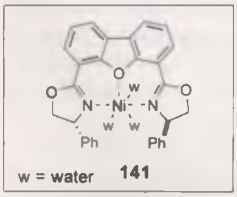
Scheme 39



The nickel complex of (*R,R*)-4,6-dibenzofurandiyl-2,2′-bis(4-phenyloxazoline) **141** is an effective catalyst for the enantioselective addition of nitromethane to alkenoylpyrazoles **140** (Scheme 40).[114] The complex

Scheme 40



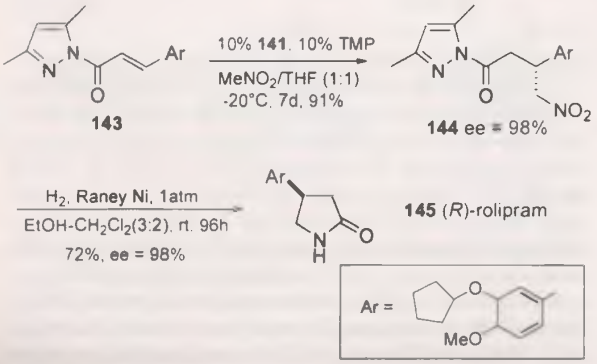


Entry	R	yield %	ee %
a	Me	85	94
b	*i*-Pr	74	97
c	*c*-C_5H_{11}	90	91
d	*t*-Bu	39	95
e	MeCH=CH	49	77
f	MeO_2C	91	83
g	Ph	90	93
h	2-furyl	75	97

alone is unable to catalyze the conjugate addition and requires a corresponding amount of TMP to be operative. Such a procedure is referred as a "catalytic double activation method" and usually works in a temperature range from −20 °C to room temperature with satisfactory yields and ee's.

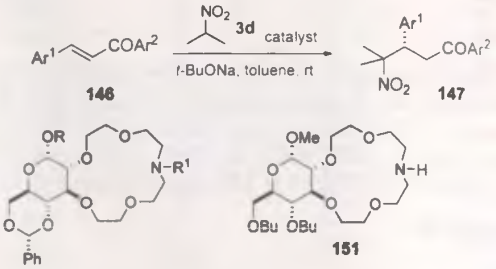
This approach has been successfully used for the total synthesis of the antidepressant agent (*R*)-rolipram **145** (Scheme 41).

Scheme 41



Azacrown ethers derived from D-glucose are able to catalyze the asymmetric conjugate addition of 2-nitropropane to chalcone derivatives **146**.[115–122] A consistent number of structural modifications have been introduced in the azacrown core as well as in the carbohydrate unit in order to obtain efficient results (Scheme 42, Table 8). Changing the ben-

Scheme 42



	R	R^1
148	Me	$(CH_2)_4P(O)Ph_2$
149	Me	$(CH_2)_3OH$
150	Ph	$(CH_2)_2Ph$

Table 8. Enantioselective Conjugate Addition of 2-Nitropropane 3d to Chalcones 129 Mediated by Azacrown Ethers 148–151 as Chiral Catalysts

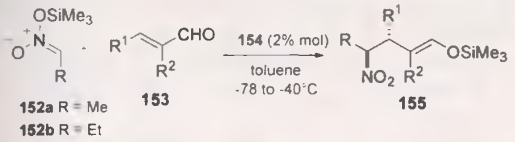
entry	Ar^1	Ar^2	catalyst	product yield (%)	ee % (config)	ref
1	Ph	Ph	**148**	43	94(*R*)	115
2	Ph	Ph	**149**	53	85(*R*)	119
3	Ph	Ph	**150**	78	82(*R*)	120
4	Ph	Ph	**151**	82	89(*S*)	117
5	4-ClPh	Ph	**148**	75	56(*R*)	115
6	Ph	4-NO_2Ph	**148**	67	78(*R*)	115
7	4-NO_2Ph	4-MeOPh	**148**	52	67(*R*)	115
8	2-furyl	Ph	**148**	56	80(*S*)	115

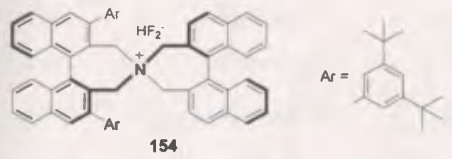
zylidene function in catalysts **148–150** with two butyl groups in **151** provides a reversal in the enantiofacial preference for the reaction of 2-nitropropane with chalcone (Table 8, entries 1–4). A similar inversion in enantioselectivity is observed when the phenyl group is substituted with a furan ring (Table 8, entry 8).

Chiral quaternary ammonium fluorides are able to promote a consistent number of reactions involving nitroalkanes as nucleophiles with an outstanding degree of asymmetric induction.[123] Silyl nitronates **152** react with enals **153** in the presence of chiral *N*-spiro ammonium bifluoride **154** to give silyl enol ethers **155** (Scheme 43).[124,125] The conjugate addition occurs with high *anti* diastereoselectivity, and the ee's of the major diastereomer are also noteworthy. This procedure represents one of the first examples in which a consistent diastereocontrol in the formation of the adduct can be observed using nitroalkanes as nucleophiles. The utilization of quaternary ammonium salt **154** also has a beneficial effect on the regioselectivity of the nucleophilic addition. Indeed, in the presence of TBAF as catalyst, reaction of **152a** with *trans*-cinnamaldehyde **153** (R^1 = Ph and R^2 = H) gives a mixture of 1,4- and 1,2-adducts in a ratio of 1.1:1 with an overall yield of 76%.

DAC EX. 2040 IPR2022-01531 Page 1132 of 1299

Scheme 43





154

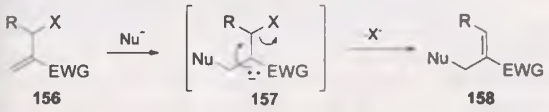
152	R^1	R^2	155 yield(%)	*syn:anti*	ee *anti*(%)
a	Ph	H	90	17:83	97
a	Ph	Me	90	5:95	95
a	-$(CH_2)_4$-		99	3:97	90
b	*n*-Pr	H	99	24:76	97

Ammonium bromides structurally related to compound **154** can be used as phase-transfer catalysts in the enantioselective conjugate addition of nitroalkanes to alkylidenemalonates.[126]

6. Conjugate Addition–Elimination Reactions

In conjugate additions the intermediate-stabilized anion that is produced by attack of the nucleophile to the electrophilic double bond is usually trapped with a proton or other electrophiles to give the final addition product. However, if a leaving group (X) is present in a suitable position of the substrate **156**, a subsequent elimination from the intermediate **157** can occur to produce a new unsaturation in molecule **158** (Scheme 44).

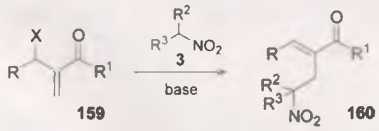
Scheme 44



X = leaving group EWG = electron-withdrawing group

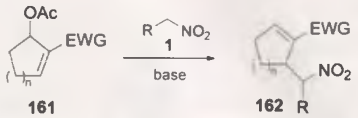
Derivatives of type **156** (X = acyloxy) are readily prepared by means of a base-catalyzed reaction of electron-poor olefins with aldehydes known as the Baylis–Hillman reaction.[127] Conjugate addition of nitroalkanes **3** with derivatives **159** leads to the expected products **160** with exclusive formation of the *E* stereoisomer (Scheme 45, Table 9).[128–132]

Scheme 45



The same procedure can be applied to cyclic derivatives **161** with formation of nitro derivatives **162** as a mixture of diastereomers and in fairy good yields (Scheme 46).[133]

Scheme 46



EWG	n	R	base	162 yield(%)
CO_2Et	1	Me	DBU	59
CO_2Et	2	Et	DBU	58
CN	1	Me	NaOH	58
CN	2	Et	DBU	80

Functionalization of the hydroxy group is mandatory for a successful addition–elimination mechanism since the corresponding alcohols **159** (X = OH) undergo a common conjugate addition with nitroalkanes.[134] The base used for this reaction may have a large influence on the related mechanistic route, so that the nature of the product obtained can be considerably different from that expected. Using DABCO as basic promoter involves a preliminary conjugate addition–elimination of the base to enoate **163,** giving salt **164** as an intermediate (Scheme 47).[130]

Compound **164** undergoes a conjugate addition by the nitroalkane followed by elimination of DABCO, leading to product **165** in a process that can be considered as a formal substitution of the acetoxy group by the nitroalkane. Enoates **166** bringing at least one halogen atom at C-2 of the aromatic ring react with nitroalkanes **1** in a tandem sequence that initially involves a conjugate addition–elimination leading to compound **167** (Scheme 48).[135] Nitro compound **167** reacts in an intramolecular aromatic nucleophilic substitution giving bicyclic derivative

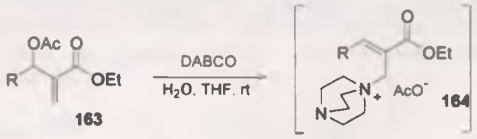
Table 9. Conjugate Addition–Elimination of Nitroalkanes 3 to Baylis–Hillman Adducts 159

entry	R	R^1	R^2	R^3	X	base[a]	product **160** yield (%)	ref
1	Et	Me	Me	H	OAc	A	78	129
2	*i*-Pr	Me	Me	H	OAc	A	77	129
3	Pr	Me	Et	H	OAc	A	68	129
4	*c*-C_6H_{11}	Et	Me	H	OAc	A	64	129
5	2-furyl	OMe	Me	H	OAc	B	90	128
6	Ph	OMe	Me	Me	OAc	B	70	128
7	Ph	OEt	Et	H	OAc	C	73	129
8	4-MePh	OEt	Et	H	OAc	C	71	129
9	H	OEt	$MeO_2C(CH_2)_4$	H	Br	A	72	131
10	H	OEt	$HO(CH_2)_5$	H	Br	A	71	131
11	H	OEt	$CH_2{=}CH(CH_2)_8$	H	Br	A	80	131
12	H	OEt	$PhCH_2$	H	Br	A	78	131

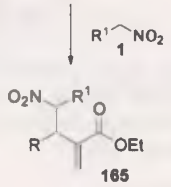
[a] A: 0.6 N NaOH, THF, room temperature. B: KF–Al_2O_3. C: K_2CO_3, DMF.

DAC EX. 2040 IPR2022-01531 Page 1133 of 1299

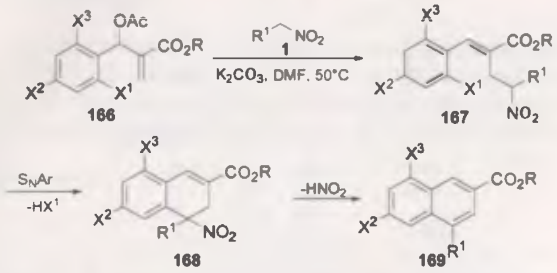
Scheme 47



R	R^1	165 yield(%)
Ph	Et	96
Ph	Pr	90
4-MePh	Et	92
4-ClPh	Et	97



Scheme 48



R	R^1	X^1	X^2	X^3	169 yield(%)
Et	Et	Cl	H	Cl	73
Et	Me	Cl	Cl	H	68
Et	CO_2Et	Cl	Cl	H	79
Me	Me	F	H	H	67

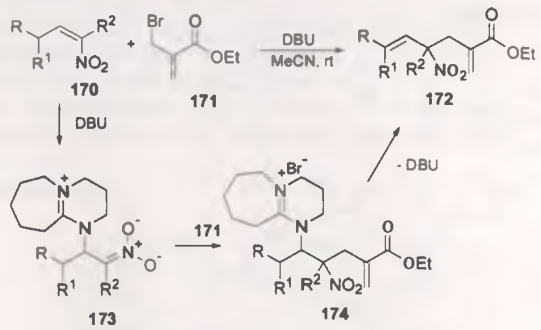
168 that quickly loses nitrous acid to afford functionalized naphthalene **169**. The final aromatization represents the key step of the whole process since its irreversibility ensures an efficient conversion of enoate **166** to naphthalene derivative **169**.

Nitroalkenes are widely known as reactive electrophilic substrates suitable for conjugate additions as well as cycloadditions reactions, but when involved in Baylis–Hillman processes, these compounds can act as allyl-type nucleophiles. Reaction of nitroalkenes **170** with bromomethyl acrylate **171** in the presence of DBU affords nitro dienes **172** (Scheme 49).[136] Conjugate addition of DBU to a nitroalkene gives a nitronate anion **173** that in the presence of acrylate **171** reacts as previously described, leading to ammonium salt **174** that upon elimination of DBU affords nitro diene **172**.

Electrophilic alkenes containing 1,2-electron-withdrawing substituents are particularly reactive toward conjugate additions. When alkenes **B** react with nucleophiles bearing a good leaving group **A** the intermediate adduct **C** undergoes a rapid base-catalyzed elimination to give an unsaturated derivative **D** (Scheme 50).

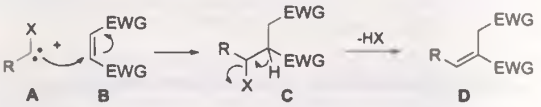
The nitro group in nitroalkanes is poorly reactive as a leaving group in nucleophilic substitutions but can be eliminated in basic conditions as nitrous acid. Enediones **175** react with nitro compounds **3** in the presence of DBU following this general mechanism to produce unsaturated carbonyl derivatives **176** (Scheme 51, Table 10).[137,138]

Scheme 49



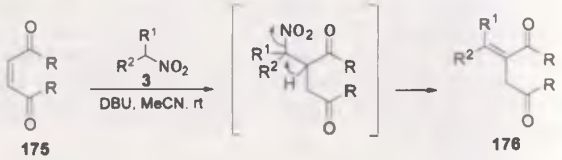
R	R^1	R^2	172 yield(%)
Et	H	Et	80
H	H	Pr	80
H		$-(CH_2)_3-$	82
Et	H	$MeCO(CH_2)_2$	84
Et	H	$MeO_2C(CH_2)_4$	84

Scheme 50



X = leaving group EWG = electron-withdrawing group

Scheme 51



The elimination step is highly diastereoselective since only the *E* stereoisomer of compound **176** is formed, regardless the configuration of the double bond in the starting dienoate **175**. Chemoselective reduction of the carbon–carbon double bond in derivatives **176** can be carried out by a simple catalytic hydrogenation in the presence of Pd/C to give saturated diesters or keto esters.[139] Maleimides **177** are also reactive substrates for the same procedure, giving the corresponding 3-alkylidene derivatives **178** with *E* configuration (Scheme 52, Table 11).[140,141]

Reduction of the exocyclic double bond and the imido group provides a rapid entry to 3-substituted pyrrolidines.[141] Trimethyl *trans*-aconitate **179** reacts similarly with nitroalkanes **1** giving the corresponding unsaturated derivatives **180**, after elimination of nitrous acid, with good *E* diastereoselectivity (Scheme 53).[142]

This procedure when applied to 1-alkyl dienoates such as dimethyl citraconate **181** provides unexpected results, leading to the formation of keto diesters **182** (Scheme 54).[143] As observed by ^1H NMR analysis, in the presence of DBU there is an equilibrium between **181** and its regioisomer **183** that is probably more reactive toward conjugate addition with nitroalkanes. The adducts **184** formed by the

DAC EX. 2040 IPR2022-01531 Page 1134 of 1299

Table 10. Conjugate Addition–Elimination of Nitroalkanes 3 to Enediones 175

entry	R	R^1	R^2	176 product yield (%)
1	OMe	H	Me	93
2	OMe	Me	Me	95
3	OMe	H	Me_2CHCH_2	89
4	OMe	H	$THPOCH_2$	80
5	OMe	H	$MeO_2C(CH_2)_3$	86
6	OMe	H		90
7	OMe	H	$MeCO(CH_2)_2$	90
8	OMe	H	$HO(CH_2)_4$	71
9	Me	H	n-C_4H_9	70
10	Me	H	$MeO_2C(CH_2)_3$	88
11	Me	Me	Me	65
12	Me	H	$MeCO(CH_2)_2$	95
13	Me	H	$HO(CH_2)_4$	85
14	Me	–$(CH_2)_5$–		85

Scheme 52

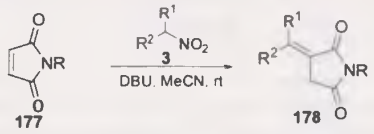


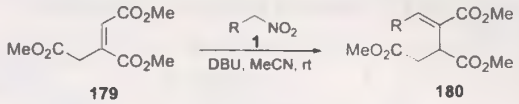
Table 11. Conjugate Addition–Elimination of Nitroalkanes 3 to *N*-Substituted Maleimides 177

entry	R	R^1	R^2	178 product yield (%)
1	Ph	Me	Me	70
2	Ph	H	n-C_4H_9	56
3	Ph	H	$MeO_2C(CH_2)_3$	80
4	Ph	H	$MeCO(CH_2)_2$	73
5	Et	H	n-C_4H_9	88
6	Et	H		88
7	Et	H	$HO(CH_2)_4$	87
8	Et	–$(CH_2)_5$–		80

usual conjugate addition are therefore subsequently transformed into the keto diesters **182** by a Nef reaction promoted by DBU.[144]

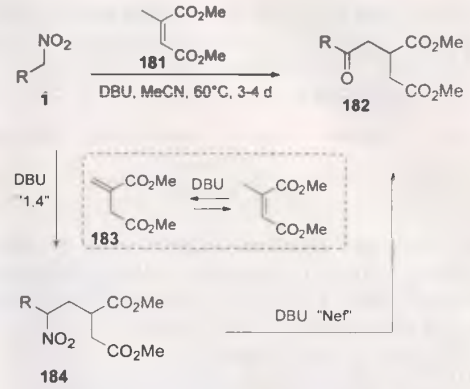
Conjugate addition of nitroalkanes to unsymmetrical 1,4-diketones usually leads to a regioisomeric mixture of products that endangers the efficiency of the synthetic procedure. However, (*Z*)-benzyl di-

Scheme 53



R	180 yield %	E/Z
Et	79	88:12
$MeCO(CH_2)_2$	81	88:12
$MeO_2C(CH_2)_2$	90	95:5
2-furylmethyl	76	99:1
$HO(CH_2)_4$	66	87:13

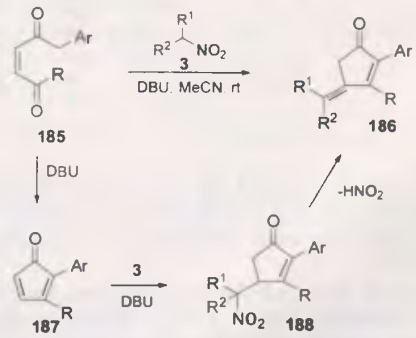
Scheme 54



R	182 yield(%)
n-C_5H_{11}	81
CH_2=$CH(CH_2)_8$	54
$HO(CH_2)_5$	54
$MeCO_2(CH_2)_2$	56

enones **185** react with nitroalkanes in the presence of DBU in acetonitrile, affording 4-alkylidene-cyclopent-2-en-1-ones **186** in good yield and high *E* diastereoselectivity (Scheme 55, Table 12).[145] The overall

Scheme 55



synthetic transformation probably starts with a chemoselective intramolecular aldol condensation of enediones **185**, promoted by the presence of the aromatic ring, that gives cyclopentadienones **187**. Under the same conditions intermediates **187** react with nitroalkanes **3** to afford the Michael adducts **188** that eliminate nitrous acid to the final cyclopentenones **186**.

Regiochemical troubles can be avoided or minimized using 1,2-disubstituted alkenes bearing com-

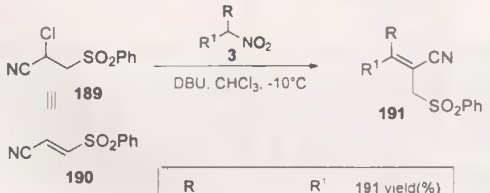
DAC EX. 2040 IPR2022-01531 Page 1135 of 1299

Table 12. Synthesis of Cyclopentenones 186 by Tandem Aldol–Conjugate Addition–Elimination Process

entry	R	Ar	R^1	R^2	**186** product yield (%)
1	Me	Ph	Me	Me	77
2	Me	Ph	H	*n*-C_9H_{19}	76
3	Me	Ph	H	CH_2=CH$(CH_2)_3$	68
4	Me	Ph	H	HO$(CH_2)_5$	78
5	Me	Ph	H		73
6	Me	Ph	H	MeCO$(CH_2)_2$	84
7	Et	Ph	H	$MeO_2C(CH_2)_2$	79
8	Me	3-MeOPh	H	*n*-C_5H_{11}	87
9	Et	4-FPh	H	$MeO_2C(CH_2)_4$	73
10	Me	3-ClPh	H	*n*-C_5H_{11}	93

pletely different electron-withdrawing groups that are able to drive the conjugate attack selectively at one carbon atom. 2-Chloro-3-phenylsulfonylpropanenitrile **189** generates, in the presence of DBU, alkene **190** that reacts regioselectively with nitroalkanes **3** at −10 °C to afford, by the usual conjugate addition–elimination mechanism, the corresponding conjugated nitriles **191** (Scheme 56).[146] The double-bond

Scheme 56



R	R^1	191 yield(%)
Me	Me	68
Et	H	61[a]
n-C_5H_{11}	H	71
$THPOCH_2$	H	51
$MeO_2C(CH_2)_4$ -$(CH_2)_5$-	H	66
		63

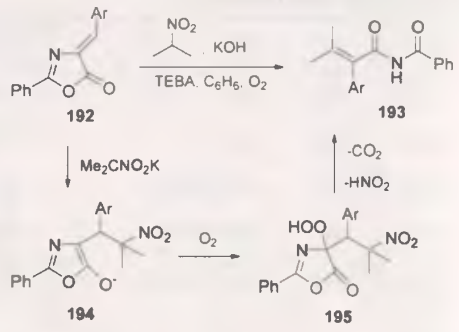
[a] *E*/*Z* = 7:3

configuration in most of the examples reported is ***E***, but depending on the nature of the nitroalkane used, a certain amount of *Z* stereoisomer can sometimes be formed.

Potassium salt of 2-nitropropane reacts with 4-arylideneoxazol-5-ones **192** in the presence of molecular oxygen to afford 2-arylbutenoic acid imides **193** (Scheme 57).[147] The addition product **194** initially formed is believed to react with oxygen, giving a hydroperoxide intermediate **195** that decomposes with loss of CO_2 and HNO_2 to the final product **193**. An endoperoxide arising from a cycloaddition reaction between **194** and oxygen is also a possible intermediate in this process.

In the conjugate addition of bromonitromethane **197** with electrophilic alkenes **196** the intramolecular nucleophilic substitution of the intermediate anion

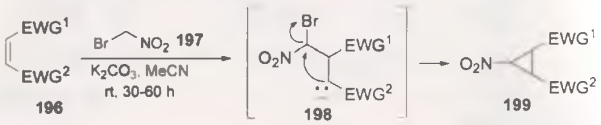
Scheme 57



Ar	yield **193** %
Ph	90
4-MeOPh	80
4-ClPh	80
4-NO_2Ph	60

198 is strongly favored over elimination of nitrous acid and ultimately leads to the synthesis of polyfunctionalized nitrocyclopropanes **199** as a mixture of diastereomers (Scheme 58).[148] Addition of bromoni-

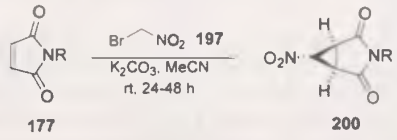
Scheme 58



EWG^1	EWG^2	**199** yield(%)
MeCO	MeCO	94
PhCO	MeCO	96
4-MePhCO	MeCO	96
PhCO	PhCO	75
CO_2Me	MeCO	86
CO_2Me	CO_2Me	88
CN	CN	78

tromethane in several portions is mandatory for the efficiency of the process. This cyclopropanation procedure can be extended to maleimido derivatives **177** that react with bromonitromethane in good yield and in a diastereoselective fashion giving *exo*-nitrocyclopropanes **200** as a single product (Scheme 59).

Scheme 59



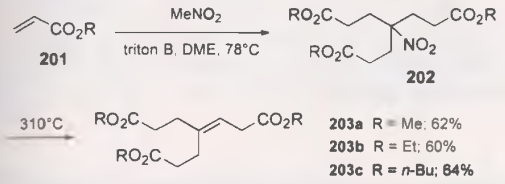
R	**200** yield(%)
Me	65
Et	70
t-Bu	82
Bn	70

Reduction of the nitro group to the corresponding amino derivative in compounds **200** provides an efficient entry to bicyclic intermediates employed for the synthesis of antibiotic trovafloxacin.[149] Elimina-

DAC EX. 2040 IPR2022-01531 Page 1136 of 1299

tion of nitrous acid can be obtained by thermolysis heating a quaternary nitro derivative **202** at 310 °C (Scheme 60).[150] The quaternary nitroalkane **202** can

Scheme 60



be obtained by triple conjugate addition of acrylate esters **201** to nitromethane in the presence of Triton B.[151,152]

Oxidation of the adducts between 3-nitropyrrolidines and Michael acceptors with NBS affords 3,4-substituted maleimides and involves elimination of HNO_2.[153]

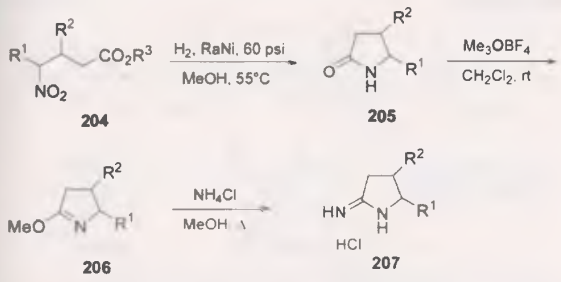
7. Synthetic Applications

As stated in the Introduction, the nitro group is amenable to many synthetic transformations once it has been inserted in a molecular framework. This feature has favored the utilization of functionalized nitro compounds in the preparation of various synthetic targets endowed of practical interest.

7.1. Pyrrolidines and Derivatives

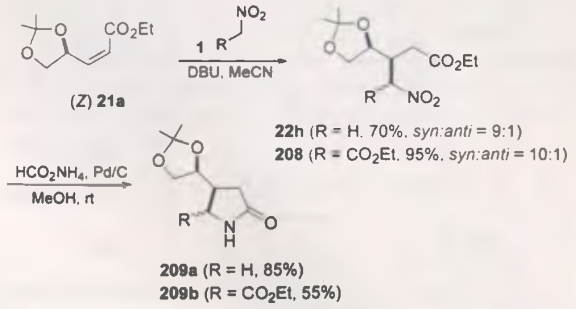
The most obvious transformation of the nitro group involves reduction of the nitrogen atom leading to an amino group. This process is often followed by a nucleophilic ring closure when a carbonyl or an ester function is present in the structure to afford directly pyrrolidinone derivatives.[154] A general method for the reduction of the nitro group in adducts **204** envisages the utilization of catalytic hydrogenation in the presence of Raney nickel (Scheme 61).[155] The ob-

Scheme 61



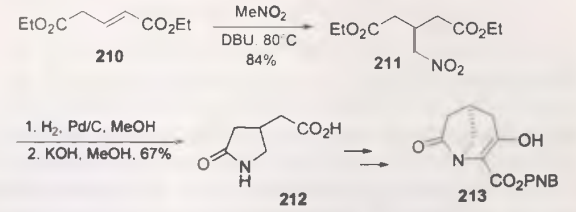
tained pyrrolidinones **205** can be transformed into 2-iminopyrrolidines **207** that act as potent and selective inhibitors of human inducible nitric oxide synthase. Diastereoselective conjugate addition of nitroalkanes **1** to chiral (*Z*)-enoate **21a** leads to the synthesis of compounds **22h** and **208** with predominance of the *syn* stereoisomer (Scheme 62).[156] Reduction of the nitro group and ring closure affords pyrrolidinones **209,** which can be used as synthetic intermediates in the preparation of several interesting compounds.

Scheme 62



Nitromethane addition to diester **210** affords product **211** that upon reduction of the nitro group and ester hydrolysis gives pyrrolidinone **212** (Scheme 63).[157] Acid **212** can be easily transformed in few

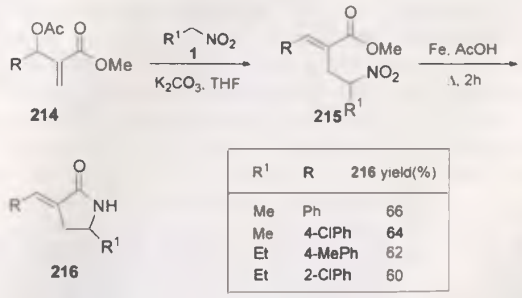
Scheme 63



steps into bicyclo-γ-lactam **213,** which acts as an inhibitor of penicillin-binding proteins. Disymmetric hydrolysis of racemic **211** using two enantiocomplementary enzymes allows the preparation of optically active **212** in both enantiomeric forms.[158]

Addition of nitroalkanes to Baylis–Hillman products **214** gives the corresponding unsaturated nitro esters **215** that are chemoselectively reduced by a 'one-pot' procedure to the corresponding pyrrolidinones **216** using Fe in boiling AcOH (Scheme 64).[159]

Scheme 64

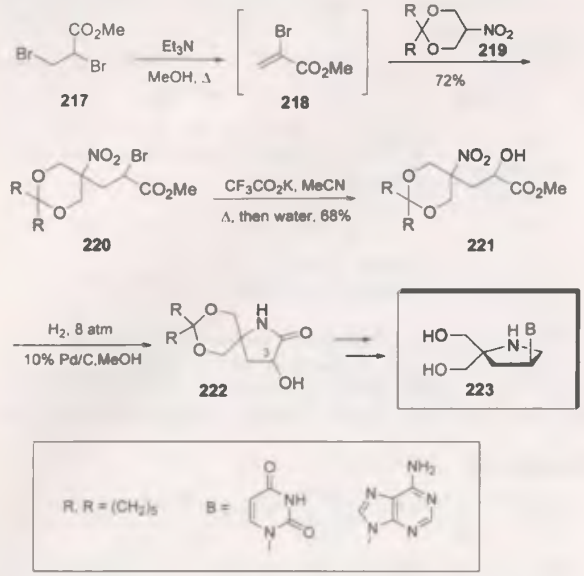


R¹	R	216 yield(%)
Me	Ph	66
Me	4-ClPh	64
Et	4-MePh	62
Et	2-ClPh	60

Methyl 2-bromoacrylate **218** can be generated in situ from the corresponding dibromo derivative **217** and then made to react with nitro compound **219** to give adduct **220** (Scheme 65).[160] Substitution of the halogen with a hydroxy group is followed by reduction of the nitro group using a catalytic hydrogenation to give pyrrolidinone **222**. This derivative can be converted into azaisonucleotide analogues **223** introducing the corresponding basic moiety using a Mitsunobu reaction and by further simple synthetic manipulations. 3,4-Dihydroxy pyrrolidinones structurally related to compound **223** can be obtained using the same strategy by conjugate addition of

DAC EX. 2040 IPR2022-01531 Page 1137 of 1299

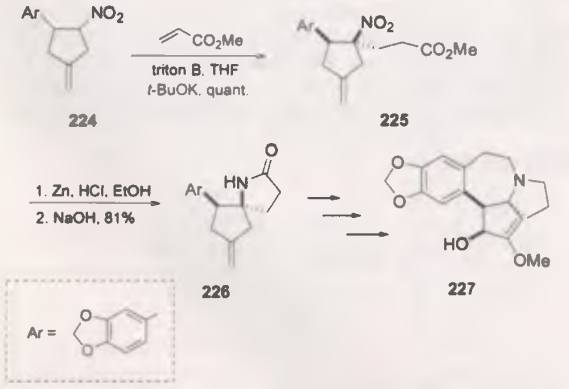
Scheme 65



nitroalkane **219** to ethyl propynoate followed by dihydroxylation of the resulting unsaturated derivative.[161]

Functionalized nitrocyclopentane **224** reacts with methyl acrylate in quantitative yield to give adduct **225** as a single diastereomer probably because of the stereodirecting effect of the vicinal phenyl group (Scheme 66).[162,163] Reduction of the nitro group using

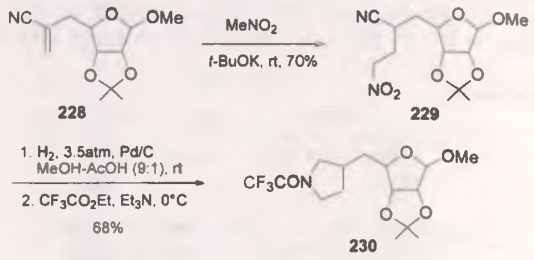
Scheme 66



zinc metal in ethanolic HCl affords spirolactam **226** without any migration of the exocyclic double bond. Lactam **226** is subsequently transformed into racemic alkaloid cephalotaxine **227**. A similar strategy can be adopted for the preparation of aza analogues of this natural alkaloid.[164,165]

Unsaturated nitrile **228** reacts with nitromethane giving the corresponding adduct **229** that upon catalytic hydrogenation with 10% Pd/C in MeOH/AcOH (9:1) and acylation furnishes *N*-trifluoroacetylpyrrolidine **230** (Scheme 67).[166] It is probable that the primary amine formed by reduction of the nitro group reacts with the intermediate imine formed by reduction of the nitrile to give the intermediate pyrrolidine. Compound **230** is an intermediate for the preparation of synthetic analogues of

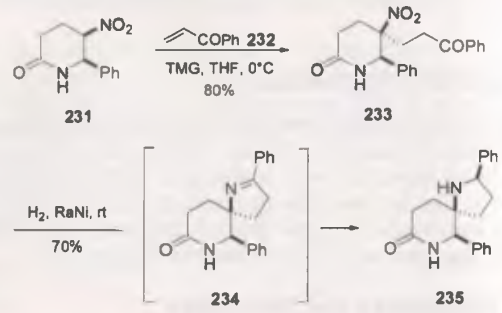
Scheme 67



sinefungin, a nucleoside active against viruses, fungi, and parasites.

Conjugate addition of nitrolactam **231** with acrylophenone **232** gives compound **233** with high diastereoselectivity (Scheme 68).[167] Catalytic hydrogena-

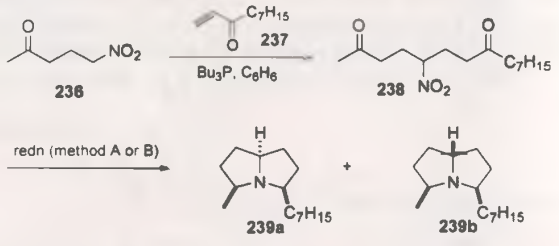
Scheme 68



tion of nitro ketone **233** occurs with concomitant formation of an intermediate imine **234** that is reduced in the same conditions to the spiropyrrolidine **235**. The presence of the phenyl group in the lactam ring hinders one face of the pyrroline ring in **234**, thus allowing complete diastereoselection in the imine reduction.

Nitro diketone **238** is readily obtained by addition of nitro ketone **236** to vinyl ketone **237** in the presence of Bu_3P (Scheme 69).[168] Reduction of compound

Scheme 69



method A: H_2 (8-10 atm), Pd/C, EtOH, **239a**:**239b** = 65:5

method B: NH_4OAc,KOH, MeOH, $NaBH_4CN$, then $NaBH_4$, **239a**:**239b** = 12:88

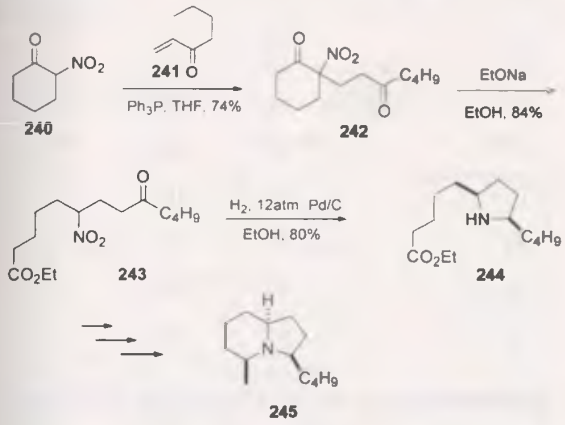
238 produces a mixture of pyrrolizidines **239** whose diastereomeric composition depends on the reducing system used. Catalytic hydrogenation (method A) provides the formation of compound **239a**, while utilization of complex hydrides (method B) favors isomer **239b**, an alkaloid known as xenovenine. It is highly probable that in the reduction with method B the nitro group in compound **238** is formerly trans-

DAC EX. 2040 IPR2022-01531 Page 1138 of 1299

formed by a Nef conversion into a carbonyl group and the nitrogen present in the final pyrrolizidine is provided by NH_4OAc.

2-Nitro ketones usually undergo conjugate additions in milder conditions with respect to simple nitroalkanes because of the enhanced acidity of the C-2 hydrogen atom.[169,170] 2-Nitrocyclohexanone **240** reacts with unsaturated ketone **241** in the presence of Ph_3P to give the corresponding adduct **242** (Scheme 70).[171]

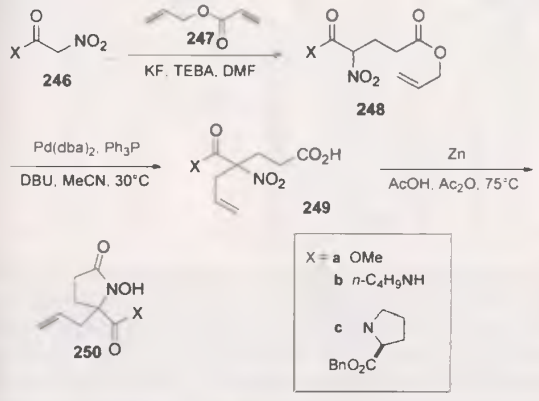
Scheme 70



The cyclohexanone moiety in **242** suffers a fast base-catalyzed retro-Claisen ring opening affording open-chain nitro derivative **243** that in reductive conditions chemoselectively furnishes *cis*-pyrrolidine **244**. This compound is a central intermediate for the synthesis of monomorine I **245**, a trail pheromone of the Pharao Ant and other similar biologically active substances.[172]

2-Nitro esters and 2-nitro amides **246** react with allyl acrylate **247** in the presence of KF to give adducts **248** (Scheme 71).[173,174] Intramolecular

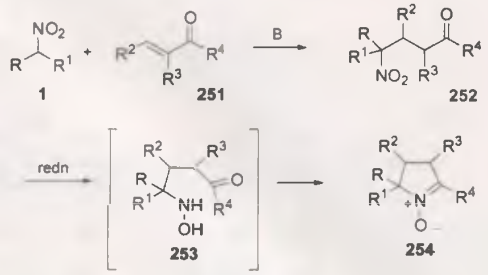
Scheme 71



Pd(0)-catalyzed allyl transfer converts esters **248** into acids **249** that, by carefully controlled reduction conditions, can be transformed into hydroxamic acids **250**.[175] The utilization of chiral nitro amides as **246c** does not produce significant levels of diastereoselection in the formation of acid **250c**.

Hydroxylamines are known intermediates in the reduction of nitro compounds to amines. Reduction of the adducts between nitroalkanes **1** and enones or enals **251** directly produces cyclic nitrones **254** by an intramolecular reaction of the intermediate hydroxylamine **253** and the carbonyl group (Scheme 72, Table 13).[176–183]

Scheme 72



A new entry for the 2-isoxazoline nucleus makes use of the conjugate addition of ethyl nitroacetate **256** with 2-bromoketones **255** (Scheme 72).[184] The intermediate adduct **257** undergoes an intramolecular nucleophilic substitution involving the oxygen of the nitronate anion and the bromine atom. The reaction can be realized in homogeneous (Et_3N, ether) as well as heterogeneous conditions (basic alumina), and the 2-isoxazolines **258** are formed predominantly as *trans* isomers (Scheme 73).

Alkylidene diesters and keto esters **260** obtained by the conjugate addition–elimination procedure can be suitably converted into 3-alkylidenepyrrolidines **262** by a simple synthetic procedure (Scheme 74).[185] Chemoselective reduction of the ester or keto functions leads to the corresponding diols that are subsequently converted into their mesylates **261**.[186] Ring closure is best realized using $TsNH_2$ in basic conditions to afford pyrrolidines **262**. Benzylamine can also be used for this purpose, but the process is less efficient and requires a large excess of the amine.

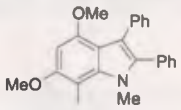
Reaction of nitroalkanes with dimethyl α-(bromomethyl)fumarate **263** follows the usual addition–elimination mechanism giving diene derivative **264** (Scheme 75).[187,188] Aliphatic amines react with diene **264** by means of a conjugate addition–cyclization process to afford alkylidene lactams **265**.

Oxidative cleavage of the furan **266** gives (*Z*)-enedione **267** that reacts with nitroalkanes **1** to afford the alkylidene derivatives **268** (Scheme 76). Double-bond reduction of these compounds provides diketones **269**, which are central intermediates for the synthesis of pyrroles **270** and furans **271** using a Paal–Knorr reaction.[189,190]

A three-component coupling among enones or enals **251**, nitroalkanes **1**, and primary amines **272** leads to the straightforward synthesis of *N*-alkylpyrroles **273** (Scheme 77, Table 14).[191] The reaction is carried out on solid support (SiO_2) without any solvent and is promoted by microwave irradiation. A Nef conversion of the nitro group in one of the possible intermediates of this process probably occurs, allowing the formation of the pyrrole ring through a Paal–Knorr-type reaction.[192] In a related procedure, 3-nitropyr-

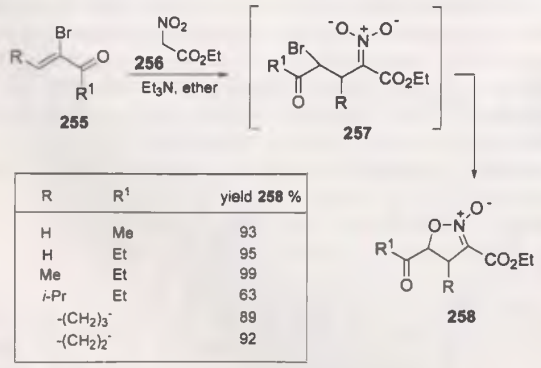
DAC EX. 2040 IPR2022-01531 Page 1139 of 1299

Table 13. Synthesis of Cyclic Nitrones 254

entry	R	R^1	R^2	R^3	R^4	**254** yield (%)[a]	ref.
1	Me	Me	H	$(CH_2)_2CO_2Me$	H	-	176
2	Me	Me	H	Me	H	64	177
3	Me	Me	Me	H	H	62	177
4	Me	Me	Ph	H		55[b]	178
5	Me	Me	H	MeOH	Me	72	179
6	H	H	H	H	Me	61	180
7	Me	Ph	H	H	H	28	180
8	Me	Me	H	H	H	51	181
9	H	CO_2Et	H	H	Ph	70	182
10	H	CO_2Et	H	H	Me	46	182
11	Me	$(EtO)_2(O)P$	H	Ph	H	52	183

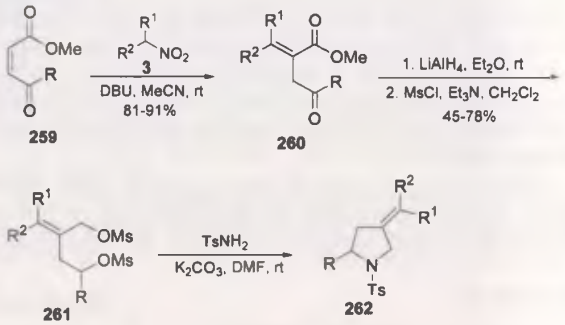
[a] Reductions are carried out using Zn metal in acidic conditions. [b] Reduction is carried out using Fe metal in acidic aqueous ethanol.

Scheme 73



R	R^1	yield **258** %
H	Me	93
H	Et	95
Me	Et	99
i-Pr	Et	63
$-(CH_2)_3-$		89
$-(CH_2)_2-$		92

Scheme 74



R	R^1	R^2	yield **262** %
Me	H	C_5H_{11}	84
Me	Me	Me	70
H	H	Et	78
H	H	Pr	81
H	H	C_5H_{11}	88
H	H	Ph	80
H	$-(CH_2)_5-$		94

roles are prepared by reaction of nitromethane with 1-isocyano-1-tosyl-1-alkenes in the presence of *t*-BuOK.[193]

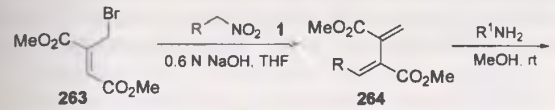
Conjugate addition of nitromethane to acrylate esters produces 4-nitrobutanoate derivatives that can be readily transformed into 5-nitro-2-oxopentanoate esters. These compounds can be enantioselectively reduced at the keto group using enzymes and then converted into optically active 3-hydroxypiperidin-2-ones.[194,195]

7.2. Lactones and Oxygenated Heterocycles

Lactones and cyclic derivatives bearing an oxygen atom in the ring are of considerable importance as both synthetic intermediates and compounds showing interesting biological properties. Preparation of lactone derivatives from Michael adducts of nitroalkanes generally involves a preliminary elimination of the nitro group to give an alkene derivative[196] or conversion of the nitro group into a carbonyl function by a Nef reaction. The former approach is especially useful for the preparation of small ring lactones, while the nitro to carbonyl conversion is mainly used for the synthesis of macrolactones and spirocyclic compounds. Unsaturated keto ester **274** obtained by a conjugate addition−elimination process is a central intermediate for the synthesis of various butyrolactone systems (Scheme 78). Reduction of the alkene and carbonyl groups in **274** allows the preparation of α-substituted-γ-methyl-γ-lactones **275** (Table

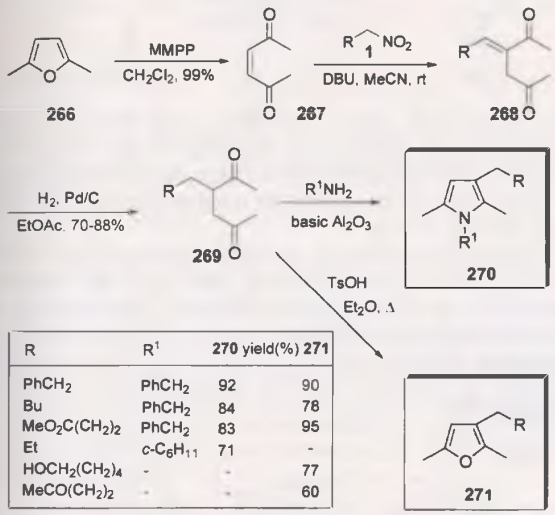
DAC EX. 2040 IPR2022-01531 Page 1140 of 1299

Scheme 75



R	R^1	265 yield (%)
Me	Bn	63
Me	Pr	80
Et	Bn	80
Et	Bu	64

Scheme 76



R	R^1	270 yield(%)	271
$PhCH_2$	$PhCH_2$	92	90
Bu	$PhCH_2$	84	78
$MeO_2C(CH_2)_2$	$PhCH_2$	83	95
Et	c-C_6H_{11}	71	-
$HOCH_2(CH_2)_4$	-	-	77
$MeCO(CH_2)_2$	-	-	60

Scheme 77

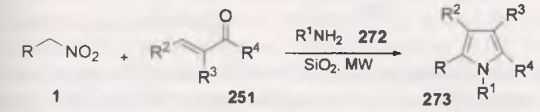


Table 14. Synthesis of *N*-Alkylpyrroles by Three-Component Coupling

entry	R	R^1	R^2	R^3	R^4	273 yield (%)
1	Me	Bn	Ph	H	H	60
2	Me	Bn	Ph	H	Me	64
3	Me	c-C_6H_{11}	H	H	Me	60
4	Me	(*S*)-PhCHMe	Ph	H	H	62
5	Me	*i*-Pr	Ph	H	H	64
6	Me	Bn	2-furyl	H	Me	72
7	Et	*n*-Bu	2-furyl	H	Me	68
8	Me	Bn	*n*-Pr	Et	H	60
9	Me	*n*-Bu	Ph	H	H	61

15).[197,198] Alternatively, the alkene function can be retained in the lactone moiety of **276** by a chemoselective reduction of the carbonyl function using the $NaBH_4/Na_2HPO_4 \cdot 12H_2O$ system.[199] Finally, nucleophilic attack of the carbonyl function can be selectively realized using a Grignard reagent in the presence of $CeCl_3$ with consequent formation of γ,γ-disubstituted lactones **277**.

Similarly, 2-alkylidene dimethyl succinates **278** can be hydrolyzed to the parent carboxylic acids and then converted into the corresponding anhydrides by reaction with acetyl chloride at reflux (Scheme 79).[200]

Scheme 78

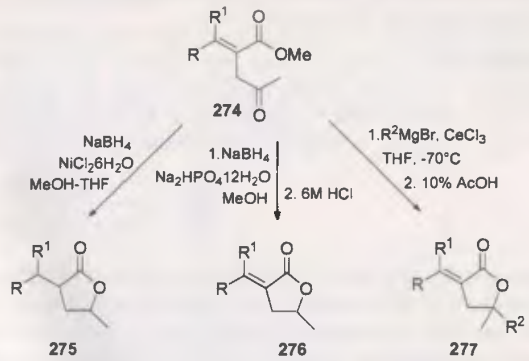
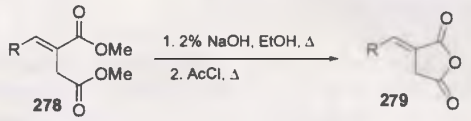


Table 15. Synthesis of Lactones 275–277 from Unsaturated Keto Ester 274

entry	R	R^1	R^2	275 yield (%)	276 yield (%)	277 yield (%)
1	Ph	H	*n*-Pr	70	70	53
2	*n*-Pr	H	Bn	85	67	65
3	$-(CH_2)_2-$		Me	66	85	75
4	$MeO_2C(CH_2)_2$	H		84	80	
5	$MeCH(OH)(CH_2)_2$	H		75	87	
6	Me	Me	Me		55	65
7	*n*-Bu	H	*n*-Pr			52

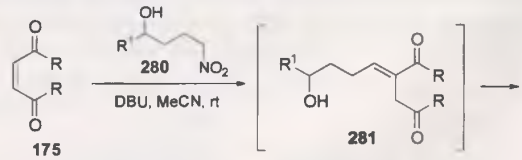
Scheme 79



R	yield 279 %
Et	71
$MeCO(CH_2)_2$	71
$HO(CH_2)_5$	72
i-Pr	64

Conjugate addition of δ-nitroalkanols **280** to dienones and dienoates **175** occurs with the usual mechanism giving an intermediate alkenol **281** that is not isolated since it undergoes to a rapid ring closure leading to tetrahydrofuran derivative **282** (Scheme 80).[201]

Scheme 80



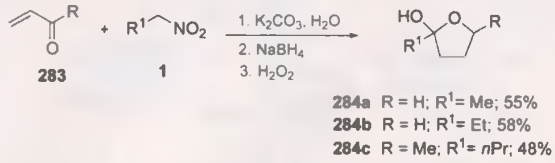
R	R^1	yield 282 %
Me	H	79
Me	Et	85
OMe	Me	70
-N(*t*Bu)-	Me	77
-N(Me)-	Et	82

Lactols **284** can be prepared by one-pot synthesis carried out in water as solvent involving a sequential conjugate addition of enones **283** with nitroalkanes **1**, reduction of the resulting γ-nitro ketone, and

DAC EX. 2040 IPR2022-01531 Page 1141 of 1299

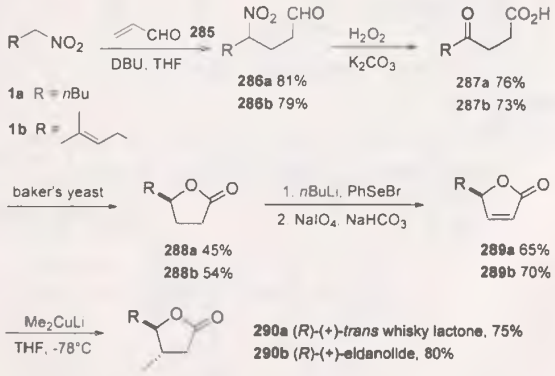
oxidative nitro to carbonyl conversion with concomitant cyclization (Scheme 81).[202]

Scheme 81



As previously stated, conjugate addition of nitroalkanes to α,β-unsaturated carbonyls coupled with the Nef reaction represents a rapid entry to a series of γ-keto derivatives that are useful intermediates for lactone syntheses. Structurally related compounds such as the flavor compound *trans* whisky lactone and the pheromone eldanolide can be prepared following the same synthetic strategy starting from the conjugate addition of nitroalkanes **1** to acrolein **285** (Scheme 82).[203] The addition products **286** are oxi-

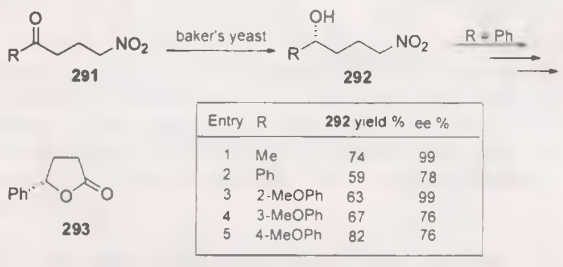
Scheme 82



dized with hydrogen peroxide in basic media that provides the Nef reaction and the aldehyde oxidation to give ketoacid **287**. Enantioselective reduction of the carbonyl group by Baker's yeast leads to lactone **288** that is easily converted into (*R*)-*trans* whisky lactone **290a** and (+)-eldanolide **290b**.

Baker's yeast reduction can also be applied to a series of γ-nitro ketones **291** with variable levels of enantioselectivity (Scheme 83).[204,205] Hydroxy alcohols

Scheme 83

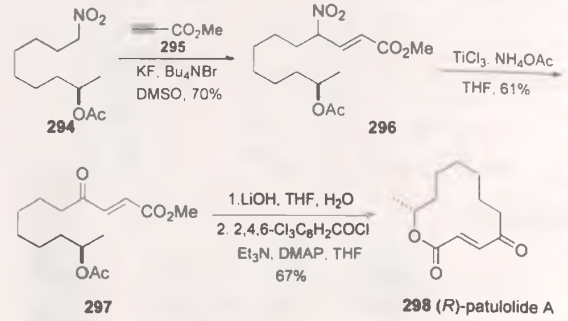


Entry	R	292 yield %	ee %
1	Me	74	99
2	Ph	59	78
3	2-MeOPh	63	99
4	3-MeOPh	67	76
5	4-MeOPh	82	76

292 (entry 2) can be transformed into lactones **293** by a simple sequence involving Nef reaction of the primary nitro group and lactonization in acidic conditions.

Optically active nitroacetate **294** can be readily prepared by enzymatic resolution from the corresponding nitro alcohol and reacts efficiently with methyl propiolate **295** giving the corresponding adduct (*E*)-**296** (Scheme 84).[206] The nitro group is then

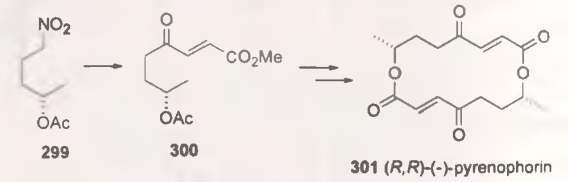
Scheme 84



converted into keto ester **297** using the McMurry method, and after ester hydrolysis the resulting hydroxy acid is lactonized to macrolide (*R*)-patulolide A. A similar strategy can be used to prepare (*Z*)-**296** and (*R*)-patulolide B.

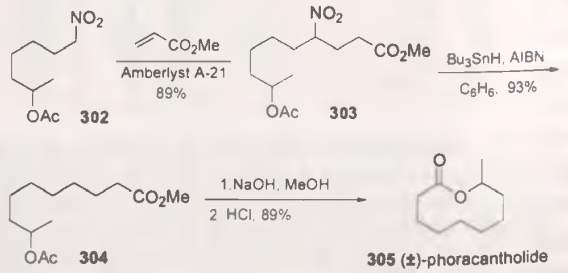
The enantioselective synthesis of macrolide dilactone (*R,R*)-(−)-pyrenophorin **301** can be realized using the usual conjugate addition−Nef reaction to produce keto ester **300** as a monomeric intermediate (Scheme 85).[207]

Scheme 85



Radical denitration allows a complete removal of the nitro group by its replacement with a hydrogen atom. Tertiary nitroalkanes and activated nitro compounds such as α-nitro ketones give the best results in this process.[208] This synthetic operation is particularly useful when simple macrolactones must be prepared using the chemistry of nitro compounds, as illustrated for the preparation of racemic phoracantholide (Scheme 86).[209] Conjugate addition of

Scheme 86



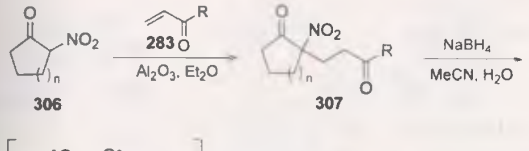
nitroalkane **302**[210] in solventless conditions using macroreticular resin Amberlyst A-21 affords adduct **303**, which is denitrated using Bu_3SnH to diester **304** and finally hydrolyzed to give phoracantholide **305**.

Spiroketalization of hydroxyketones is a spontaneous process that occurs in mild acidic conditions

DAC EX. 2040 IPR2022-01531 Page 1142 of 1299

because of the great stability of the resulting bicyclic system. This aptitude can be suitably used in a cascade reaction that involves some consecutive transformations. Conjugate addition of 2-nitrocycloalkanones **306** with enones **283** gives products **307** that are reduced with $NaBH_4$ in acetonitrile−water (Scheme 87).[211] This process also implies a retro-

Scheme 87

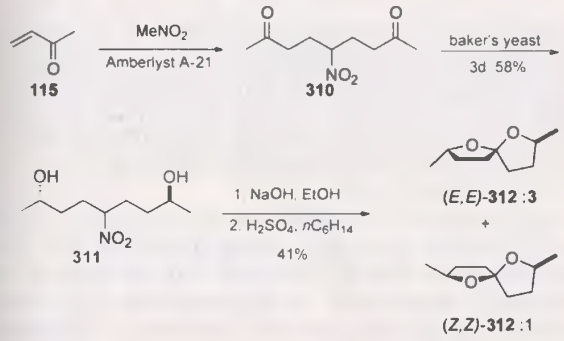


n	R	yield **309** %
1	Me	65
1	Et	70
2	Me	75
2	H	80

Claisen cleavage of the cycloalkanone ring giving hydroxynitronate **308** as an intermediate. Upon acidification of the reaction mixture a Nef reaction occurs, followed by a spontaneous cyclization to give spiroketals **309**.

Double conjugate addition of nitromethane to two equivalents of enones leads to the formation of symmetrical nitro diketones that upon reduction and Nef reaction afford the corresponding spiroketals.[212] Asymmetric reduction of the diketone **310** with Baker's yeast leads to the optically active alcohol **311** that after the nitro to carbonyl conversion gives the spiroketal system as a mixture of diastereomers (Scheme 88).[213] Reduction of symmetrical nitro dike-

Scheme 88



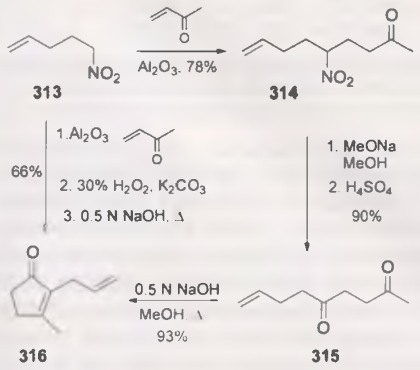
tones can also be realized using chiral reducing agents such as (+) or (−)-diisopinocampheylchloroborane with good results in terms of enantioselectivity of the obtained nitro alcohols.[214]

Asymmetric reduction using Baker's yeast can be successfully used with unsymmetrical nitro diketones to give optically active spiroketals featuring different ring sizes.[215]

7.3. Carbocycles

Allylrethrone **316** is an important component of an insecticidal pyrethroid, and its preparation can be realized in three distinct steps, starting from the nitroalkene **313** and methyl vinyl ketone (Scheme 89).[216] The obtained Michael adduct **314** is converted

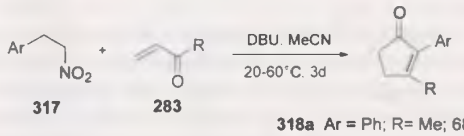
Scheme 89



into the diketone **315** by a hydrolytic Nef reaction and is then cyclized to allylrethrone **316** under basic conditions. Alternatively, the same process can be realized in a 'one-pot' reaction using hydrogen peroxide to carry out the nitro to carbonyl conversion.

The ability of DBU to promote a conjugate addition of nitroalkanes to enones as well as a Nef reaction on secondary nitroalkanes can be suitably used in a tandem process that allows the direct synthesis of cyclopentenone derivatives **318** (Scheme 90).[217]

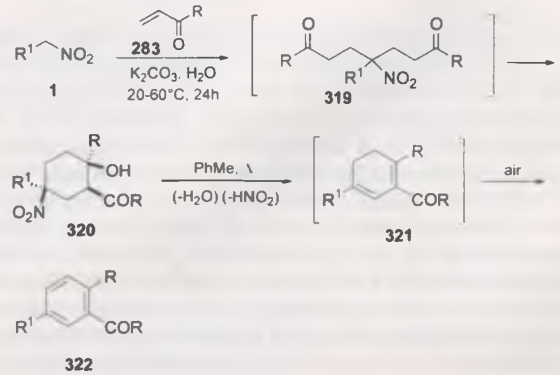
Scheme 90



318a Ar = Ph; R= Me; 68%
318b Ar = Ph; R= Et; 65%
318c Ar = 4-MePh; R= Me; 78%

Double conjugate addition of nitroalkanes **1** with enones **283** in the presence of K_2CO_3 initially gives nitro diketone **319,** which undergoes an intramolecular aldol condensation to produce 2-acyl-4-nitrocyclohexanol derivatives **320** in a diastereoselective fashion (Scheme 91, Table 16).[218,219] Heating com-

Scheme 91



DAC EX. 2040 IPR2022-01531 Page 1143 of 1299

Table 16. Synthesis of Nitrocyclohexanols 320 and Their Oxidation to Aromatic Compounds 322

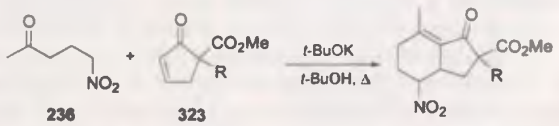
entry	R	R[1]	320 yield (%)	322 yield (%)[c]
1	Me	Me	90[a]	53
2	Et	Me	85[a]	55
3	*n*-Pr	Me	93[a]	65
4	*n*-Bu	Me	95[b]	72
5	*n*-C_5H_{11}	Me	95[b]	61
6	*i*-Pr	Me	75[b]	50
7	Ph	Me	70[b]	80[d]
8	Me	Et	77[b]	50

[a] Reaction performed at room temperature. [b] Reaction performed at 60 °C. [c] Reaction time 15 h. [d] Reaction time 3 h.

pounds **320** in toluene at reflux in the presence of bubbling air provides a double elimination of water and nitrous acid to diene **321** that is subsequently oxidized by oxygen to the aromatic derivative **322**.

A related process occurs upon reaction of 2-nitrocycloalkanones with acrolein, leading to the synthesis of nitrocyclohexene derivatives.[220] Reaction of γ-nitro ketone **236** with cyclic β-keto esters **323** directly affords bicyclic compounds **324** through a conjugate addition−aldol condensation reaction (Scheme 92).[221,222] These derivatives are important precursors

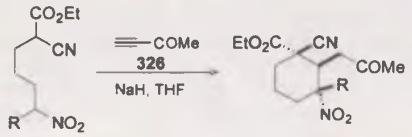
Scheme 92



of the germination stimulant strigol and its synthetic analogues.

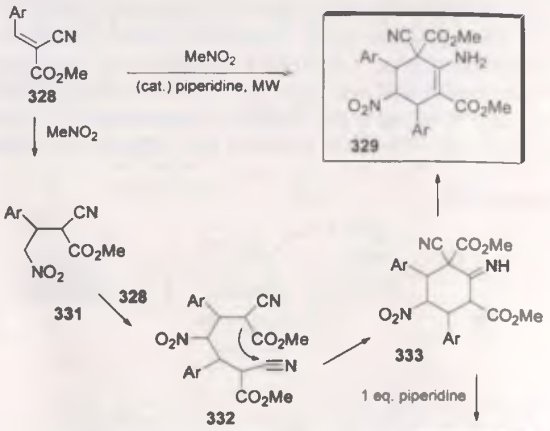
Nitro compounds **325** present two nucleophilic sites; therefore, by reaction with 3-butyn-2-one **326** a double conjugate addition occurs with formation of cyclohexyl derivative **327** as the main product (Scheme 93).[223] Compounds **327** are pivotal intermediates for the synthesis of *trans* decalines and hydrindanes.

Scheme 93



Functionalized cyclohexene derivatives **329** or **330** are obtained by reaction of arylidene cyanoacetate **328** with nitromethane in the presence of piperidine and under microwave irradiation (Scheme 94).[224,225] Double addition of alkene **328** to nitromethane affords compound **332,** which undergoes an intramolecular nucleophilic addition to give cyclic derivative **333**. If a catalytic amount of piperidine is used, tautomerization of imino derivative **333** occurs giving compound **329** as the main product. Alternatively, utilization of one equivalent of the basic promoter causes a decarboxylation of this intermediate, giving cyclohexene derivative **330** as the final product.

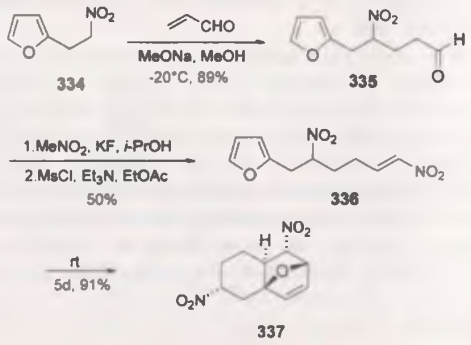
Scheme 94



Ar	329 yield (%)	330
Ph	70	75
4-ClPh	73	75
4-MeOPh	70	70
4-NO_2Ph	71	-
2-FPh	75	70
2-BrPh	75	75

Functionalized tricyclic derivative **337** is an intermediate for the synthesis of ergot alkaloids and valienamine analogues (Scheme 95).[226] Conjugate

Scheme 95

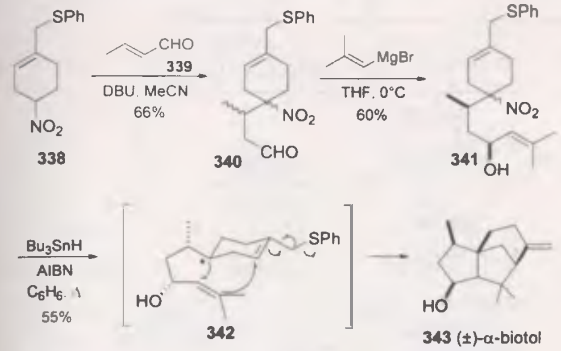


addition of 2-furylnitroethane **334** to acrolein is followed by a Henry (nitroaldol) reaction−elimination of the obtained aldehyde **335** to afford nitroalkene **336**. This compound on standing at room temperature for 5 days undergoes to an intramolecular Diels−Alder reaction giving derivative **337** in good yield as a single diastereomer.

Denitration of nitroalkanes can be easily carried out in radical conditions using Bu_3SnH/AIBN. The intermediate radical produced may be reduced by hydrogen abstraction or alternatively react with alkenes giving an addition reaction. A synthetic approach to cedranoid sesquiterpene α-biotol **343** starts with a conjugate addition of nitrocyclohexene **338** to crotonaldehyde **339** to give nitro aldehyde **340** that upon reaction with isobutenylmagnesium bromide affords nitro alcohol **341** (Scheme 96).[227−229] The radical intermediate **342** formed upon reaction with Bu_3SnH/AIBN reacts through a cascade cyclization giving α-biotol **343**. The stereochemistry of the obtained tricyclic compound **343** is totally controlled

DAC EX. 2040 IPR2022-01531 Page 1144 of 1299

Scheme 96

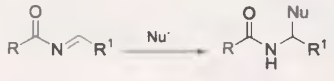


by the configuration of the carbon bearing the hydroxy group. Nitrocyclohexitols can be prepared from the adducts of nitroalkanes to acrolein using an enzymatic aldol reaction followed by a highly stereoselective intramolecular nitroaldol reaction.[230]

7.4. Amino Acids and Derivatives

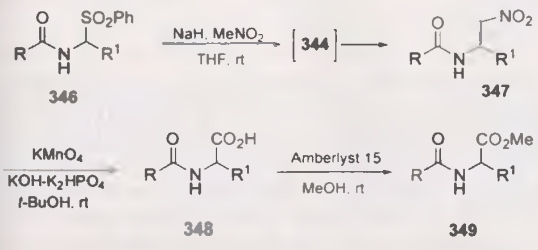
The synthesis of α-amino acid derivatives cannot be accomplished by usual conjugate addition of nitroalkanes to common Michael acceptors. However, keeping in mind that a primary nitro group can be easily converted into a carboxylic group using the Nef reaction, some alternative strategies can be devised to realize the synthesis of α-amino acids using a conjugate addition process. *N*-Acylimines **344** are powerful electrophilic substrates that upon reaction with nucleophilic reagents undergo to a conjugate addition giving the corresponding product **345** (Scheme 97).

Scheme 97



N-Acyl- and *N*-carbamoylimines **344** are too unstable to be stored when prepared from aliphatic aldehydes (R^1 = alkyl) since they rapidly decompose or tautomerize to the corresponding enecarbamate. However, imines **344** can be generated *in situ* starting from α-amidoalkylphenyl sulfones **346** by a base-induced elimination of benzenesulfinic acid (Scheme 98).[231] In the presence of a nucleophilic reagent as

Scheme 98



the nitromethane anion, a conjugate addition occurs giving the corresponding nitro derivative **347**. The nitro group of compound **347** can be readily converted into a carboxylic acid **348** using alkaline $KMnO_4$ solutions giving, after methylation, *N*-acyl-α-amino acid esters **349**. The utilization of α-carbamoylalkylphenyl sulfones (**346** R = OBn, O*t*-Bu) allows a rapid cleavage of the *N*-protecting group of the final acid **348** to give the free amino acid compound (Table 17).

This procedure can be extended to optically active α-amidoalkylphenyl sulfones that using the same synthetic approach lead to the preparation of interesting target molecules featured by the α-amino acid moiety. Chiral sulfones **350** react with the anion of nitromethane with high diastereoselectivity, preferentially giving the *anti* adducts **351** that upon Nef conversion produce β-hydroxy-α-amino acid esters **352** (Scheme 99).[232]

Similarly, sulfone **353** featuring a pyrrolidine ring can be transformed into nitro derivative **354** and α-amino acid ester **355,** which is a precursor of chiral piperazine-2-carboxylic acids **356** that are useful catalysts in asymmetric synthesis (Scheme 100).

Stable isotope-labeled L-glutamic acid can be prepared from ^{13}C-enriched compounds following a strategy involving the conjugate addition of ethyl nitroacetate **256** to ethyl acrylate (Scheme 101).[233] Oxidative Nef conversion of the 2-nitroglutarate **357** to diethyl 2-oxoglutarate and ester hydrolysis gives 2-oxoglutaric acid **358**. This diacid is trasformed into L-glutamic acid **359** using the commercially available enzyme glutamic dehydrogenase in the presence of ammonium ions.

Conjugate addition of nitroalkanes to dehydroalanine **360** affords γ-nitro-α-amino acids such as **361** in racemic form (Scheme 102).[234] This adduct is further elaborated by converting the nitro group into a carbonyl moiety that can be reduced *in situ* to a diastereomeric pair of γ-hydroxy-α-amino acids **362** in a 1:1 ratio. The acid-catalyzed cyclization of these hydroxy derivatives gives the 2-aminolactones **363**.

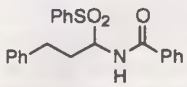
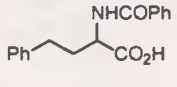
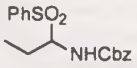
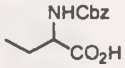
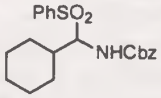
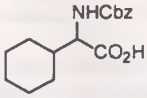
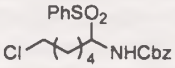
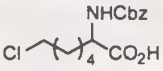
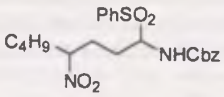
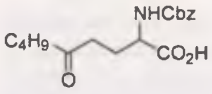
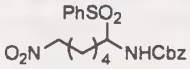
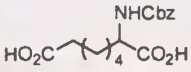
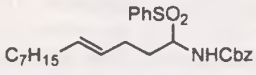
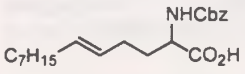
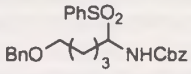
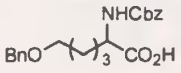
Conjugate addition of nitroalkanes to enoates results in the formation of γ-nitro ester derivatives that can be reduced at the nitro group to give the corresponding γ-amino esters. Enzymatic resolution of product **365** obtained by conjugate addition of nitromethane to benzyl 2-trifluoromethylpropenoate **364** provides acid **366** and ester **367** that after simple separation can be reduced at the nitro group to afford γ-amino acid **368** and γ-amino ester **369** in almost enantiomerically pure form (Scheme 103).[235]

7.5. Other Applications

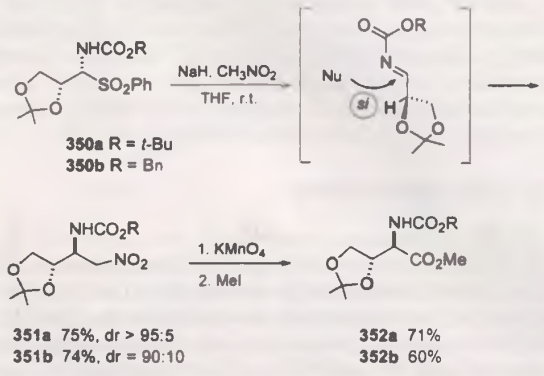
Polyfunctionalized compounds can be easily prepared combining the conjugate addition process with other transformations involving the nitro group in sequential reactions that can be often realized by a one-pot procedure, thus avoiding the isolation of any intermediate.[236] Addition of 2-nitrocycloalkanones **114** with enones **283** occurs in mild conditions to give 1,5-dicarbonyl derivatives **370** (Scheme 104).[237,238] A retro-Claisen cleavage of the 2-nitrocycloalkanones **370** can be realized by addition to the reaction mixture of a methanolic solution of KOH giving open-chain nitronates **371** that are oxidized to trioxo derivatives **372**–**374** simply adding aqueous permanganate solution.

DAC EX. 2040 IPR2022-01531 Page 1145 of 1299

Table 17. Base-Assisted Substitutions of Sulfones 346 into Nitro Derivatives 347 and Their Conversion to α-Amino Acids 348

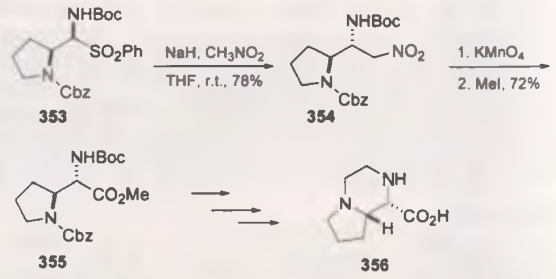
entry	sulfone **346**	nitro **347** yield (%)	amino acid **348**	yield (%) (methyl ester **349**)
a		87		90 (95)
b		78		81 (93)
c		90		88 (97)
d		77		85 (92)
e		80		83 (90)
f		83		78 (92)
g		85		72[a] (91)
h		79		70[a] (88)

Scheme 99



1,3-Dinitroalkanes **376** can be prepared heating at reflux an aldehyde **375** with an excess of nitromethane in the presence of basic alumina (Scheme 105).[239] Dinitro derivatives **376** are obtained by a tandem process involving a preliminary nitroaldol condensation followed by a dehydration to the corresponding nitroalkenes **378** that undergo a conjugate addition of the nitromethyl anion to the final compounds **376**.

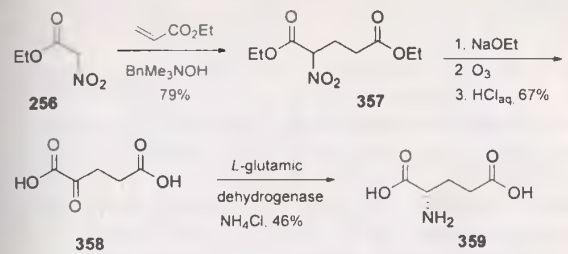
Scheme 100



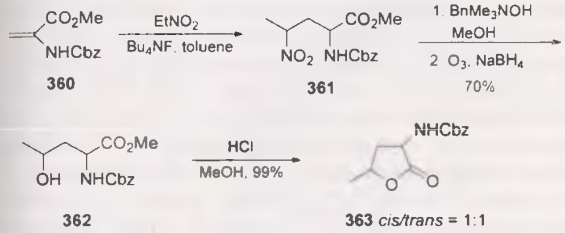
Diesters of (*E*)-2-alkylidenesuccinic acids **379** obtained by conjugate addition of nitroalkanes to dimethyl maleate can be selectively monohydrolyzed at the more reactive carboxyl group to the corresponding half-ester **380** (Scheme 106).[240] Alternatively, total hydrolysis to the diacid **381** allows a subsequent selective methyl esterification of the alkanoic carboxyl group to give the other regioisomeric half-ester **382**. 2-Alkylsuccinic monoesters can be also obtained by catalytic hydrogenation of the unsaturated derivatives **380**–**382**.

DAC EX. 2040 IPR2022-01531 Page 1146 of 1299

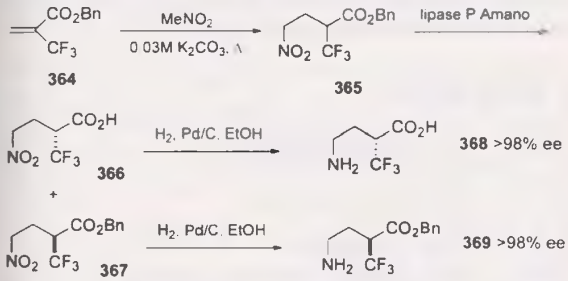
Scheme 101



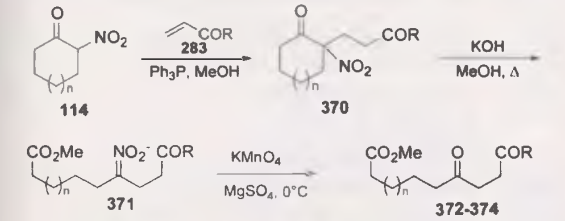
Scheme 102



Scheme 103



Scheme 104



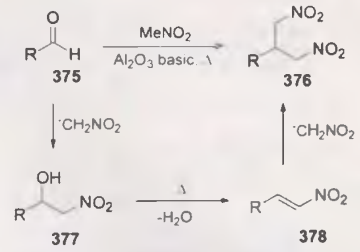
n	R	yield **372** %	R	yield **373** %	R	yield **374** %
1	Me	87	H	92	OMe	70
2	Me	75	H	75	OMe	67
7	Me	93	H	73	OMe	50
10	Me	80	H	70	OMe	50

The reactivity of nitroalkanes toward multiple addition can be profitably used for the preparation of nitro-substituted fatty acids, which are interesting derivatives resistant to β-oxidation in living systems.

Nitro derivatives **1** obtained from the corresponding fatty alcohols are made to react with a large excess of methyl acrylate in the presence of DBU giving bis adducts **383** that upon hydrolysis afford diacids **384** in good overall yield (Scheme 107).[241]

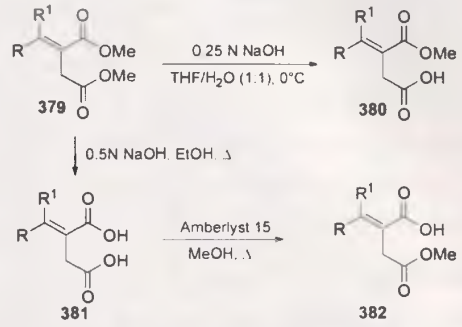
An interesting approach to the preparation of conjugated dienones involves as first step the Michael addition of nitroalkanes to 2-phenylsulfonyl-1,3-dienes **385** to give nitro sulfones **386** (Scheme 108).[242] Conversion of the nitro group into a ketone **387** is

Scheme 105



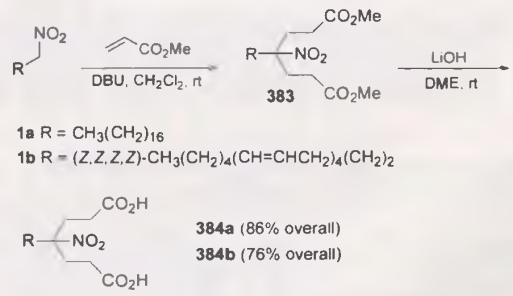
R	yield **376** %	R	yield **376** %
$Ph(CH_2)_2$	78	4-CF_3Ph	73
Me_2CH	62	4-MeOPh	74
$Me(CH_2)_2$	68	3-pyridyl	60
Ph	71	2-furyl	70

Scheme 106



R	R^1	**380** yield(%)	**381** yield(%)	**382** yield(%)
Et	H	95	98	86
$-(CH_2)_5-$		85	92	80
$HO(CH_2)_5$	H	74	89	76
$MeCO(CH_2)_2$	H	73	91	71

Scheme 107



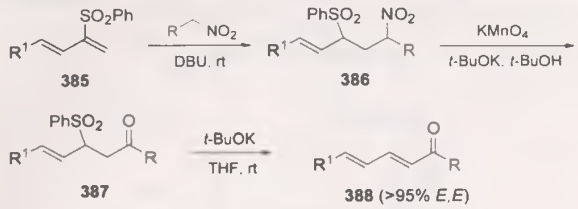
followed by a base-induced elimination of benzenesulfinic acid giving dienone **388** with high diastereoselectivity (>95% *E,E*).

Substituted allylnitro compounds **389** are regiochemically stable derivatives that undergo to a conjugate addition to methyl vinyl ketone giving nitroalkenes **390** (Scheme 109).[243] Despite the basic conditions the reaction occurs without any observed migration of the double bond.

Conjugated nitrosoalkenes **394** are typical electron-poor olefins that can be generated *in situ* by reaction of fluoride ions with *N,N*-bis(silyloxy)enamines **391** at low temperature (Scheme 110).[244] In the presence

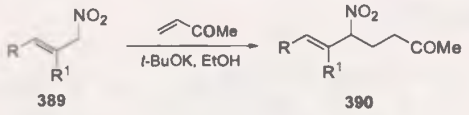
DAC EX. 2040 IPR2022-01531 Page 1147 of 1299

Scheme 108



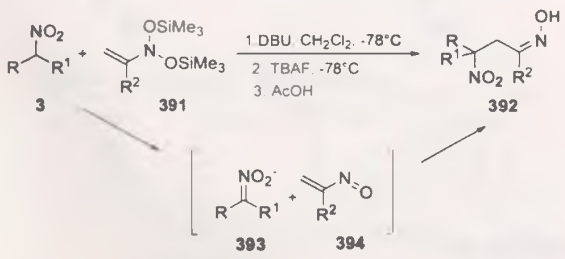
R	R^1	**386** yield(%)	**387** yield(%)	**388** yield(%)
Me	Me	92	81	76
H	Me	81	56	67
Me	n-C_5H_{11}	60	79	69
H	n-C_5H_{11}	43	77	64

Scheme 109



R	R^1	**390** yield (%)
Me	Me	83
Et	Me	61
n-C_5H_{11}	Me	64
Me	Et	70

Scheme 110



of nitronate anions **393** formed from the corresponding nitroalkanes **3** a conjugate reaction occurs leading, after acidic quenching, to β-nitro oximes **392** (Table 18).

Table 18. Synthesis of β-Nitro Oximes 392 from *N,N*-Bis(silyloxy)Enamines 391

entry	R	R^1	R^2	**392** yield (%)
1	Et	H	Me	78
2	$MeO_2C(CH_2)_2$	H	Me	90
3	MeO_2C	H	Me	64
4	MeO_2CCH_2	H	H	88
5	Et	H	$MeO_2C(CH_2)_2$	76
6	MeO_2C	H	$MeO_2C(CH_2)_2$	78
7	Me	Me	Me	72
8	MeO_2CCH_2	Me	Me	71
9	MeO_2CCH_2	Me	H	62
10	$MeO_2C(CH_2)_2$	Me	$MeO_2C(CH_2)_2$	70

8. Conclusion

Nitroalkanes are a convenient source of stabilized carbanions that react with electron-poor alkenes giving the corresponding 1,4-adducts with high regioselectivity. The addition process is usually realized in basic media that strongly affects the selectivity and efficiency achievable in carbon−carbon bond formation. The presence of chiral centers in the nitroalkane or in the α,β-unsaturated derivative allows a certain degree of stereocontrol in the formation of the corresponding adducts. Enantioselective processes can be realized with the aid of chiral catalysts, although only recently satisfactory results in terms of ee's have been obtained. Besides the formation of simple carbon−carbon bonds, the conjugate addition of nitroalkanes to dienones and dienoates permits the creation of new carbon−carbon double bonds by means of a tandem elimination of nitrous acid that occurs after the primary addition process. The nitro group, once it has been introduced in the molecular framework by the conjugate addition, really acts as a chemical chameleon since it can be reduced to the amino group, replaced by a hydrogen atom, or transformed into a carbonyl group. For these reasons an increasing number of synthetic procedures devoted to the preparation of important target molecules profitably include the conjugate addition of nitroalkanes to electron-deficient alkenes into some crucial step of the overall synthetic plan.

9. Abbreviations

ABCN	azobiscyclohexylnitrile
AIBN	azobisisobutyronitrile
Bn	benzyl
Boc	*tert*-butoxycarbamoyl
Bz	benzoyl
Cbz	benzylcarbamoyl
CTAB	cetyltrimethylammonium bromide
CTACl	cetyltrimethylammonium chloride
CTAOH	cetyltrimethylammonium hydroxide
DABCO	1,4-diazabicyclo[2.2.2]octane
DBN	1,5-diazabicyclo[4.3.0]non-5-ene
DBU	1,8-diazabicyclo[5.4.0]undec-7-ene
DME	1,2-dimethoxyethane
DMSO	dimethyl sulfoxide
ee	enantiomeric excess
EWG	electron-withdrawing group
HMS	hexagonal mesoporous silica
MMPP	magnesium monoperoxyphthalate
MOM	methoxymethyl
Ms	methanesulfonyl
MW	microwave
$Pd(dba)_2$	bis(dibenzylideneacetone)palladium
PMB	4-methoxybenzyl
PNB	4-nitrobenzyl
TBAF	tetrabutylammonium fluoride
TBDMS	*tert*-butyldimethylsilyl
TBDPS	*tert*-butyldiphenylsilyl
TEBA	triethylbenzylammonium chloride
THF	tetrahydrofuran
TMG	tetramethylguanidine
TMP	2,2,6,6-tetramethylpiperidine
Ts	4-toluenesulfonyl

10. Acknowledgments

The authors are greatly indebted to their coworkers whose names are cited in the references, for their enthusiasm and dedication. Financial support has been granted by M.I.U.R. and the University of Camerino. This review is dedicated to Professor

DAC EX. 2040 IPR2022-01531 Page 1148 of 1299

Goffredo Rosini (University of Bologna) on the occasion of his 65th birthday.

11. References

(1) Perlmutter, P. *Conjugate Addition Reactions in Organic Synthesis;* Pergamon: Oxford, 1992.
(2) Bergmann, E. D.; Ginsburg, D.; Pappo, R. *Org. React.* **1959**, *10*, 179.
(3) Rossiter, B. E.; Swingle, N. M. *Chem. Rev.* **1992**, *92*, 771.
(4) Rosini, G.; Ballini, R. *Synthesis* **1988**, 833.
(5) *Nitro Compounds Recent Advances in Synthesis and Chemistry*; Feuer, H., Nielsen, A. T., Eds.; VCH: Weinheim, 1990.
(6) Ono, N. *The Nitro Group in Organic Synthesis*; Wiley-VCH: New York, 2001.
(7) *The Chemistry of Amino, Nitroso, Nitro and Related Groups;* Patai, S., Ed.; Wiley: Chichester, 1996.
(8) Adams, J. P. *J. Chem. Soc., Perkin Trans.1* **2002**, 2586.
(9) Seebach, D.; Lehr, F. *Angew. Chem., Int. Ed. Engl.* **1976**, *15*, 505.
(10) Rosini, G. In *Comprehensive Organic Synthesis*; Trost, B. M. Ed.; Pergamon: Oxford, 1991; Vol. 2, p 321.
(11) Luzzio, F. A. *Tetrahedron* **2001**, *57*, 915.
(12) Rosini, G.; Ballini, R.; Zanotti, V. *Synthesis* **1983**, 137.
(13) Ballini, R.; Petrini, M. *Tetrahedron* **2004**, *60*, 1017.
(14) Pinnick, H. W. *Org. React.* **1990**, *38*, 655.
(15) Simpkins, N. S. *Sulphones in Organic Synthesis;* Pergamon: Oxford, 1993.
(16) Rosini, G.; Ballini, R.; Petrini, M.; Marotta, E. *Angew. Chem., Int. Ed. Engl.* **1986**, *25*, 941.
(17) Oshida, J.; Okamoto, M.; Azuma, S.; Tanaka, T. *Tetrahedron: Asymmetry* **1997**, *8*, 2579.
(18) Nakagawa, M.; Tsuruoka, A.; Yoshida, J.; Hino, T. *J. Chem. Soc., Chem. Commun.* **1990**, 603.
(19) Nakamura, K.; Kitayama, T.; Inoue, Y.; Ohno, A. *Bull. Chem. Soc. Jpn.* **1990**, *63*, 91.
(20) Kitayama, T. *Tetrahedron* **1996**, *52*, 6139.
(21) Lubineau, A.; Augé, J. *Tetrahedron Lett.* **1992**, *33*, 8073.
(22) Picquet, M.; Bruneau, C.; Dixneuf, P. H. *Tetrahedron* **1999**, *55*, 3937.
(23) Nan, F.; Bzdega, T.; Pshenichkin, S.; Wroblewski, J. T.; Wroblewska, B.; Neale, J. H.; Kozikowski, A. P. *J. Med. Chem.* **2000**, *43*, 772.
(24) Nakashita, N.; Hesse, M. *Helv. Chim. Acta* **1983**, *66*, 845.
(25) Derri Alcantara, M. P.; Escribano, F. C.; Gómez-Sánchez, A.; Diánez, M. J.; Estrada, M. D.; López-Castro, A.; Pérez-Garrido, S. *Synthesis* **1996**, 64.
(26) Clark, J. H. *Chem. Rev.* **1980**, *80*, 429.
(27) Grimm, E. L.; Zschiesche, R.; Reissig, H. U. *J. Org. Chem.* **1985**, *50*, 5543.
(28) Chasar, D. W. *Synthesis* **1982**, 841.
(29) Chetia, A.; Saikia, C. J.; Lekhok, K. C.; Boruah, R. C. *Tetrahedron Lett.* **2004**, *45*, 2649.
(30) Ono, N.; Kamimura, A.; Kaji, A. *Synthesis* **1984**, 226.
(31) Pollini, G. P.; Barco, A.; De Giuli, G. *Synthesis* **1972**, 44.
(32) Chavan, S. P.; Pasupathy, K.; Venkatraman, M. S.; Kale, R. R. *Tetrahedron Lett.* **2004**, *45*, 6879.
(33) Zia-Ebrahimi, M.; Huffman, G. W. *Synthesis* **1996**, 215.
(34) Rosini, G.; Marotta, E.; Ballini, R.; Petrini, M. *Synthesis* **1986**, 237.
(35) Bergbreiter, D. F.; Lalonde, J. J. *J. Org. Chem.* **1987**, *52*, 1601.
(36) Ballini, R.; Petrini, M.; Rosini, G. *Synthesis* **1987**, 711.
(37) Baasner, B.; Marhold, A.; Negele, M. *J. Fluorine Chem.* **1990**, *46*, 161.
(38) Beck, A. K.; Seebach, D. *Chem. Ber.* **1991**, *124*, 2897.
(39) Ballini, R.; Bosica, G.; *Tetrahedron Lett.* **1996**, *37*, 8027.
(40) Ballini, R.; Bosica, G.; Livi, D.; Palmieri, A.; Maggi, R.; Sartori, G. *Tetrahedron Lett.* **2003**, *44*, 2271.
(41) Mdoe, J. E. G.; Clark, J. H.; Macquarrie, D. J. *Synlett* **1998**, 625.
(42) Mudaliar, C. D.; Nivalkar, K. R.; Mashraqui, S. H. *Org. Prep. Proc. Int.* **1997**, *29*, 584.
(43) da Silva, F. M.; Gomes, A. K.; Jones, J. *Can. J. Chem.* **1999**, *77*, 624.
(44) Choudary, B. M.; Kantam, M. L.; Kavita, B.; Reddy, C. V.; Figueras, F. *Tetrahedron* **2000**, *56*, 9357.
(45) Boruah, A.; Baruah, M.; Prajapati, D.; Sandhu, J. S. *Chem. Lett.* **1996**, 965.
(46) Ranu, B. C.; Bhar, S. *Tetrahedron* **1992**, *48*, 1327.
(47) Costantino, U.; Marmottini, F.; Curini, M.; Rosati, O. *Catal. Lett.* **1993**, *22*, 333.
(48) Gómez-Bengoa, E.; Cuerva, J. M.; Mateo, C.; Echavarren, A. M. *J. Am. Chem. Soc.* **1996**, *118*, 8553.
(49) Bergbreiter, D. E.; Li, C. *Org. Lett.* **2003**, *5*, 2245.
(50) Kisanga, P. B.; Ilankumaran, P.; Fetterly, B. M.; Verkade, J. G. *J. Org. Chem.* **2002**, *67*, 3555.
(51) Jouglet, B.; Blanco, L.; Rousseau, G. *Synlett* **1991**, 907.
(52) Sebti, S.; Boukhal, H.; Hanafi, N.; Boulaajaj, S. *Tetrahedron Lett.* **1999**, *40*, 6207.
(53) Michaud, D.; Abdallah-El Ayoubi, S.; Dozias, M.-J.; Toupet, L.; Texier-Boullet, F.; Hamelin, J. *Chem. Commun.* **1997**, 1613.
(54) Michaud, D.; Texier-Boullet, F.; Hamelin, J. *Tetrahedron Lett.* **1997**, *38*, 7563.
(55) Ballini, R.; Marziali, P.; Mozzicafreddo, A. *J. Org. Chem.* **1996**, *61*, 3209.
(56) Niyazymbetov, M. E.; Evans, D. H. *J. Org. Chem.* **1993**, *58*, 779.
(57) Keller, E.; Feringa, B. L. *Synlett* **1997**, 842.
(58) Ballini, R.; Fiorini, D.; Gil, M. V.; Palmieri, A. *Green Chem.* **2003**, *5*, 475.
(59) Miranda, S.; López-Alvarado, P.; Giorgi, G.; Rodriguez, J.; Avedaño, C.; Menéndez, J. C. *Synlett* **2003**, 2159.
(60) Laikhter, A. L.; Niyazymbetov, M. E.; Evans, D. H.; Samet, A. V.; Semenov, V. V. *Tetrahedron Lett.* **1993**, *34*, 4465.
(61) Samet, A. V.; Niyazymbetov, M. E.; Semenov, V. V.; Laikhter, A. L.; Evans, D. H. *J. Org. Chem.* **1996**, *61*, 8786.
(62) Ballini, R.; Bosica, G.; Fiorini, D. *Tetrahedron Lett.* **2001**, *42*, 8471.
(63) Ballini, R.; Fiorini, D.; Gil, M. V.; Palmieri, A. *Tetrahedron* **2004**, *60*, 2799.
(64) Patrocinio, V.; Costa, P. R. R.; Correia, C. R. D. *Synthesis* **1994**, 474.
(65) Costa, J. S.; Dias, A. G.; Anholeto, A. L.; Monteiro, M. D.; Patrocinio, V. L.; Costa, P. R. R. *J. Org. Chem.* **1997**, *62*, 4002.
(66) Pinto, A. C.; Freitas, C. B. L.; Dias, A. G.; Pereira, V. L. P.; Tinant, B.; Declercq, J.-P.; Costa, P. R. R. *Tetrahedron: Asymmetry* **2002**, *13*, 1025.
(67) Krief, A.; Provins, L.; Froidbise, A. *Synlett* **1999**, 1936.
(68) Plummer, J. S.; Emery, L. A.; Stier, M. A.; Suto, M. J. *Tetrahedron Lett.* **1993**, *34*, 7529.
(69) Ballini, R.; Fiorini, D.; Palmieri, A.; Petrini, M. *Lett. Org. Chem.* **2004**, *1*, 335.
(70) Camps, P.; Muñoz-Torrero, D.; Sánchez, L. *Tetrahedron: Asymmetry* **2004**, *15*, 2039.
(71) Bartels, A.; Jones, P. G.; Liebscher, J. *Tetrahedron: Asymmetry* **1997**, *8*, 1545.
(72) Crossley, M. J.; Tansey, C. W. *Aust. J. Chem.* **1992**, *45*, 479.
(73) Versleijen, J. P. G.; van Leusen, A. M.; Feringa, B. L. *Tetrahedron Lett.* **1999**, *40*, 5803.
(74) Hanessian, S.; Roy, P. J.; Petrini, M.; Hodges, P. J.; Di Fabio, R.; Carganico, G. *J. Org. Chem.* **1990**, *55*, 5766.
(75) Garg, N.; Plavec, J.; Chattopadhyaya, J. *Tetrahedron* **1993**, *49*, 5189.
(76) Areces, P.; Gil, M. V.; Higes, F. J.; Román, E.; Serrano, J. A. *Tetrahedron Lett.* **1998**, *39*, 8557.
(77) Ballini, R.; Bosica, G.; Gil, M. V.; Román, E.; Serrano, J. A. *Tetrahedron: Asymmetry* **2002**, *13*, 1773.
(78) Hanessian, S.; Seid, M.; Nilsson, I. *Tetrahedron Lett.* **2002**, *43*, 1991.
(79) Sosnicki, J. G.; Liebscher, J. *Synlett* **1996**, 1117.
(80) Asaoka, M.; Sonoda, S.; Fujii, N.; Takei, H. *Tetrahedron* **1990**, *46*, 1541.
(81) Trost, B. M.; Crawley, M. L. *Chem. Eur. J.* **2004**, *10*, 2237.
(82) Forsyth, A. C.; Gould, R. O.; Paton, R. M.; Sadler, I. H.; Watt, I. *J. Chem. Soc., Perkin Trans. 1* **1993**, 2737.
(83) Witczak, Z. J.; Li, Y. *Tetrahedron Lett.* **1995**, *36*, 2595.
(84) Barco, A.; Benetti, S.; Pollini, G. P.; Spalluto, G.; Zanirato, V. *J. Chem. Soc., Chem. Commun.* **1991**, 390.
(85) Barco, A.; Benetti, S.; Spalluto, G.; Casolari, A.; Pollini, G. P.; Zanirato, V. *J. Org. Chem.* **1992**, *57*, 6279.
(86) Barco, A.; Benetti, S.; Pollini, G. P.; Spalluto, G.; Zanirato, V. *Gazz. Chim. Ital.* **1993**, *123*, 185.
(87) Barco, A.; Benetti, S.; De Risi, C.; Pollini, G. P.; Romagnoli, R.; Spalluto, G.; Zanirato, V. *Tetrahedron* **1994**, *50*, 2583.
(88) Yasuhara, T.; Nishimura, K.; Yamashita, M.; Fukuyama, N.; Yamada, K.; Muraoka, O.; Tomioka, K. *Org. Lett.* **2003**, *5*, 1123.
(89) Yasuhara, T.; Osafune, E.; Nishimura, K.; Yamashita, M.; Yamada, K.; Muraoka, O.; Tomioka, K. *Tetrahedron Lett.* **2004**, *45*, 3043.
(90) Jousse, C.; Mainguy, D.; Desmaële, D. *Tetrahedron Lett.* **1998**, *39*, 1349.
(91) Jousse, C.; Desmaële, D. *Eur. J. Org. Chem.* **1999**, 909.
(92) Jousse-Karinthi, C.; Zhouiri, F.; Mahuteau, J.; Desmaële, D. *Tetrahedron* **2003**, *59*, 2093.
(93) Cristoffers, J.; Baro, A. *Angew. Chem., Int. Ed.* **2003**, *42*, 1688.
(94) Krause, N.; Hoffmann-Röder, A. *Synthesis* **2001**, 171.
(95) Sibi, M. P.; Manyem, S. *Tetrahedron* **2000**, *56*, 8033.
(96) Leonard, J.; Díez-Barra, E.; Merino, S. *Eur. J. Org. Chem.* **1998**, 2051.
(97) Botteghi, C.; Paganelli, S.; Schionato, A.; Boga, C.; Fava, A. *J. Mol. Catal.* **1991**, *66*, 7.
(98) Yamaguchi, M.; Igarashi, Y.; Reddy, R. S.; Shiraishi, T.; Hirama, M. *Tetrahedron* **1997**, *53*, 11223.
(99) Yamaguchi, M.; Shiraishi, T.; Hirama, M. *J. Org. Chem.* **1996**, *61*, 3520.
(100) Yamaguchi, M.; Shiraishi, T.; Igarashi, Y.; Hirama, M. *Tetrahedron Lett.* **1994**, *35*, 8233.

DAC EX. 2040 IPR2022-01531 Page 1149 of 1299

(101) Hanessian, S.; Pham, V. *Org. Lett.* **2000**, *2*, 2975.
(102) Tsogoeva, S. B.; Jagtap, S. B.; Ardemasova, Z. A.; Kalikhevich, V. N. *Eur. J. Org. Chem.* **2004**, 4014.
(103) Halland, N.; Hazell, R. G.; Jørgensen, K. A. *J. Org. Chem.* **2002**, *67*, 8331.
(104) Latvala, A.; Stanchev, S.; Linden, A.; Hesse, M. *Tetrahedron: Asymmetry* **1993**, *4*, 173.
(105) Corey, E. J.; Zhang, F.-Y. *Org. Lett.* **2000**, *2*, 4257.
(106) Arai, S.; Nakayama, K.; Ishida, T.; Shioiri, T. *Tetrahedron Lett.* **1999**, *40*, 4215.
(107) Thomas, A.; Manjunatha, S. G.; Rajappa, S. *Helv. Chim. Acta* **1992**, *75*, 715.
(108) Boyle, P. H.; Convery, M. A.; Davis, A. P.; Hosken, G. D.; Murray, B. A. *J. Chem. Soc., Chem. Commun.* **1992**, 239.
(109) van Aken, E.; Wynberg, H.; van Bolhuis, F. *J. Chem. Soc., Chem. Commun.* **1992**, 629.
(110) Davis, A. P.; Dempsey, K. J. *Tetrahedron: Asymmetry* **1995**, *6*, 2829.
(111) Allingham, M. T.; Howard-Jones, A.; Murphy, P. J.; Thomas, D. A.; Caulkett, P. W. R. *Tetrahedron Lett.* **2003**, *44*, 8677.
(112) Funabashi, K.; Saida, Y.; Kanai, M.; Arai, T.; Sasai, H.; Shibasaki, M. *Tetrahedron Lett.* **1998**, *39*, 7557.
(113) Keller, E.; Veldman, N.; Spek, A. L.; Feringa, B. L. *Tetrahedron: Asymmetry* **1997**, *8*, 3403.
(114) Itoh, K.; Kanemasa, S. *J. Am. Chem. Soc.* **2002**, *124*, 13394.
(115) Bakó, T.; Bakó, P.; Szöllösy, M.; Czugler, M.; Keglevich, G.; Töke, L. *Tetrahedron: Asymmetry* **2002**, *13*, 203.
(116) Novák, T.; Tatai, J.; Bakó, P.; Czugler, M.; Keglevich, G.; Töke, L. *Synlett* **2001**, 424.
(117) Bakó, P.; Bajor, Z.; Töke, L. *J. Chem. Soc., Perkin Trans. 1* **1999**, 3651.
(118) Bakó, P.; Novák, T.; Ludányi, K.; Pete, B.; Töke, L.; Keglevich, G. *Tetrahedron: Asymmetry* **1999**, *10*, 2373.
(119) Bakó, P.; Czinege, E.; Bakó, T.; Czugler, M.; Töke, L. *Tetrahedron: Asymmetry* **1999**, *10*, 4539.
(120) Bakó, P.; Vizvárdi, K.; Bajor, Z.; Töke, L. *Chem. Commun.* **1998**, 1193.
(121) Bakó, P.; Szöllösy, M.; Bombicz, P.; Töke, L. *Synlett* **1997**, 291.
(122) Bakó, P.; Kiss, T.; Töke, L. *Tetrahedron Lett.* **1997**, *38*, 7259.
(123) Ooi, T.; Maruoka, K. *Acc. Chem. Res.* **2004**, *37*, 526.
(124) Ooi, T.; Doda, K.; Maruoka, K. *J. Am. Chem. Soc.* **2003**, *125*, 9022.
(125) Ooi, T.; Morimoto, K.; Doda, K.; Maruoka, K. *Chem. Lett.*. **2004**, *33*, 824.
(126) Ooi, T.; Fujioka, S.; Maruoka, K. *J. Am. Chem. Soc.* **2004**, *126*, 11790.
(127) Basavaiah, D.; Rao, A. J.; Satyanarayana, T. *Chem. Rev.* **2003**, *103*, 811.
(128) Bauchat, P.; Le Rouillé, E.; Foucaud, A. *Bull. Soc. Chim. Fr.* **1991**, *128*, 267.
(129) Chamakh, A.; M'hirsi, M.; Villiéras, J.; Lebreton, J.; Amri, H. *Synthesis* **2000**, 295.
(130) Kim, J. M.; Im, Y. J.; Kim, T. H.; Kim, J. N. *Bull. Kor. Chem. Soc.* **2002**, *23*, 657.
(131) Ballini, R.; Bosica, G.; Livi, D. *Synthesis* 2001, 1519.
(132) Ballini, R.; Bosica, G. *Eur. J. Org. Chem.* 1998, 355.
(133) Kraïem, H.; Turki, T.; Amri, H. *Synth. Commun.* **2003**, *33*, 3261.
(134) Wang, W.; Yu, M. *Tetrahedron Lett.* **2004**, *45*, 7141.
(135) Kim, J. N.; Im, Y. J.; Gong, J. H.; Lee, K. Y. *Tetrahedron Lett.* **2001**, *42*, 4195.
(136) Ballini, R.; Barboni, L.; Bosica, G.; Fiorini, D.; Mignini, E.; Palmieri, A. *Tetrahedron* **2004**, *60*, 4995.
(137) Ballini, R.; Rinaldi, A. *Tetrahedron Lett.* **1994**, *35*, 9247.
(138) Ballini, R.; Bosica, G. *Tetrahedron* **1995**, *51*, 4213.
(139) Ballini, R.; Bosica, G.; Petrelli, L.; Petrini, M. *Synthesis* **1999**, 1236.
(140) Kakiuchi, T.; Kato, H.; Jayasundera, K. P.; Higashi, T.; Watabe, K.; Sawamoto, D.; Kinoshita, H.; Inomata, K. *Chem. Lett* **1998**, 1001.
(141) Ballini, R.; Bosica, G.; Cioci, G.; Fiorini, D.; Petrini, M. *Tetrahedron* **2003**, *59*, 3603.
(142) Ballini, R.; Bosica, G.; Fiorini, D.; Gil, M. V.; Palmieri, A. *Synthesis* **2004**, 605.
(143) Ballini, R.; Barboni, L.; Bosica, G.; Fiorini, D.; Gil, M. V. *Synlett* **2002**, 1706.
(144) Ballini, R.; Bosica, G.; Fiorini, D.; Petrini, M. *Tetrahedron Lett.* **2002**, *43*, 5233.
(145) Ballini, R.; Bosica, G.; Fiorini, D.; Gil, M. V.; Petrini, M. *Org. Lett.* **2001**, *3*, 1265.
(146) Ballini, R.; Fiorini, D.; Gil, M. V.; Palmieri, A. *Tetrahedron Lett.* **2003**, *44*, 9033.
(147) Lalitha, N.; Bhalerao, U. T.; Iyengar, D. S. *J. Chem. Soc., Chem. Commun.* **1991**, 897.
(148) Ballini, R.; Fiorini, D.; Palmieri, A. *Synlett* **2003**, 1704.
(149) Braish, T. F.; Castaldi, M.; Chan, S.; Fox, D. A.; Keltonic, T.; McGarry, J.; Hawkins, J. M.; Norris, T.; Rose, P. R.; Sieser, J. E.; Sitter, B. J.; Watson, H., Jr. *Synlett* **1996**, 1100.
(150) Weis, C. D.; Newkome, G. R. *J. Org. Chem.* **1990**, *55*, 5801.
(151) Newkome, G. R.; Weis, C. D. *J. Org. Chem.* **1991**, *56*, 4798.
(152) Newkome, G. R.; Weis, C. D. *Org. Prep. Proc. Int.* **1996**, *28*, 495.
(153) Bajpal, L. K.; Bhanduri, A. P. *J. Chem. Res. (S)* **1996**, 522.
(154) Kan, T.; Fujimoto, T.; Ieda, S.; Asoh, Y.; Kitaoka, H.; Fukuyama, T. *Org. Lett.* **2004**, *6*, 2729.
(155) Hagen, T. J.; Bergmanis, A. A.; Kramer, S. W.; Fok, K. F.; Schmelzer, A. E.; Pitzele, B. S.; Swenton, L.; Jerome, G. M.; Kornmeier, C. M.; Moore, W. M.; Branson, L. F.; Connor, J. R.; Manning, P. T.; Currie, M. G.; Hallinan, E. A. *J. Med. Chem.* **1998**, *41*, 3675.
(156) Domingos, J. L. O.; Lima, E. C.; Dias, A. G.; Costa, P. R. R. *Tetrahedron: Asymmetry* **2004**, *15*, 2313.
(157) Aszodi, J.; Rowlands, D. A.; Mauvais, P.; Collette, P.; Bonnefoy, A.; Lampilas, M. *Bioorg. Med. Chem. Lett.* **2004**, *14*, 2489.
(158) Felluga, F.; Gombac, V.; Pitacco, G.; Valentin, E. *Tetrahedron: Asymmetry* **2004**, *15*, 3323.
(159) Basavaiah, D.; Rao, J. S. *Tetrahedron Lett.* **2004**, *45*, 1621.
(160) Mironiuk-Puchalska, E.; Kolaczkowska, E.; Sas, W. *Tetrahedron Lett.* **2002**, *43*, 8351.
(161) Kuciak, R.; Sas, W. *Tetrahedron Lett.* **1994**, *35*, 8647.
(162) Ishibashi, H.; Okano, M.; Tamaki, H.; Maruyama, K.; Yakura, T.; Ikeda, M. *J. Chem. Soc., Chem. Commun.* **1990**, 1436.
(163) Ikeda, M.; Okano, M.; Kosaka, K.; Kido, M.; Ishibashi, H. *Chem. Pharm. Bull.* **1993**, *41*, 276.
(164) Nyerges, M.; Bitter, I.; Kádas, I.; Tóth, G.; Töke, L. *Tetrahedron Lett.* **1994**, *35*, 4413.
(165) Nyerges, M.; Bitter, I.; Kádas, I.; Tóth, G.; Töke, L. *Tetrahedron* **1995**, *51*, 11489.
(166) Mouna, A. M.; Blanchard, P.; Fourrey, J.-L.; Robert-Gero, M. *Tetrahedron Lett.* **1990**, *31*, 7003.
(167) Desai, M. C.; Lefkowitz, S. L. *Bioorg. Med. Chem. Lett.* **1993**, *3*, 2083.
(168) Vavreka, M.; Janowitz, A.; Hesse, M. *Tetrahedron Lett.* **1991**, *32*, 5543.
(169) Rosini, G.; Ballini, R., Petrini, M.; Marotta, E.; Righi, P. *Org. Prep. Proc. Int.* **1990**, *22*, 707.
(170) Ballini, R. *Synlett.* **1999**, 1009.
(171) Vavreka, M.; Hesse, M. *Helv. Chim. Acta* **1991**, *74*, 438.
(172) Francke, W.; Schröder, F.; Walter, F.; Sinnwell, V.; Baumann, H.; Kaib, M. *Liebigs Ann.* **1995**, 965.
(173) Chittari, P.; Thomas, A.; Rajappa, S. *Tetrahedron Lett.* **1994**, *35*, 3793.
(174) Thomas, A.; Rajappa, S. *Tetrahedron* **1995**, *51*, 10571.
(175) Krawczyk, H.; Wolf, W. M.; Śliwiński, M. *J. Chem. Soc., Perkin Trans 1* **2002**, 2794.
(176) Zhang, Y.-K.; Xu, G.-Z. *J. Chem. Res.(S)* **1990**, 104.
(177) Zhang, Y.-K.; Lu, D.-H.; Xu, G.-Z. *J. Chem. Soc., Perkin Trans 2* **1991**, 1855
(178) Black, D. S. C.; Deb-Das, R. B.; Kumar, N. *Austr. J. Chem.* **1992** *45*, 1051.
(179) Gibson, N. J.; Forrester, A. R.; Brown, C. *J. Chem. Soc., Perkin Trans 1* **1995**, 507.
(180) Sankuratri, N.; Janzen, E. G.; West, M. S.; Poyer, J. L. *J. Org. Chem.* **1997**, *62*, 1176.
(181) Le, D. D.; Zhang, Y.; Nguyen, D.; Moravek, J. *J. Labelled Compd. Radiopharm.* **2000**, *43*, 1107.
(182) Black, D. S. C.; Edwards, G. L.; Evans, R. H.; Keller, P. A.; Laaman, S. M. *Tetrahedron* **2000**, *56*, 1889.
(183) Nsanzumuhire, C.; Clément, J.-L.; Ouari, O.; Karoui, H.; Finet, J.-P.; Tordo, P. *Tetrahedron Lett.* **2004**, *45*, 6785.
(184) Galli, C.; Marotta, E.; Righi, P.; Rosini, G. *J. Org. Chem.* **1995**, *60*, 6624.
(185) Ballini, R.; Bosica, G.; Masè, A.; Petrini, M. *Eur. J. Org. Chem.***2000**, 2927.
(186) Ballini, R.; Bosica, G.; Damiani, M.; Righi, P. *Tetrahedron* **1999**, *55*, 13451.
(187) Béji, F.; Lebreton, J.; Villiéras, J.; Amri, H. *Tetrahedron* **2001**, *57*, 9959.
(188) Béji, F.; Lebreton, J.; Villiéras, J.; Amri, H. *Synth. Commun.* **2002**, *32*, 3273.
(189) Ballini, R.; Barboni, L.; Bosica, G.; Petrini, M. *Synlett* **2000**, 391.
(190) Ballini, R.; Bosica, G.; Fiorini, D.; Giarlo, G. *Synthesis* **2001**, 2003.
(191) Ranu, B. C.; Hajra, A. *Tetrahedron* **2001**, *57*, 4767.
(192) Lui, K.-H.; Sammes, M. P. *J. Chem. Soc., Perkin Trans 1* **1990**, 457.
(193) van Leusen, D.; Flentge, E.; van Leusen, A. M. *Tetrahedron* **1991**, *47*, 4639.
(194) Gibbs, G.; Hateley, M. J.; McLaren, L.; Welham, M.; Willis, C. L. *Tetrahedron Lett.* **1999**, *40*, 1069.
(195) Crosby, S. R.; Hateley, M. J.; Willis, C. L. *Tetrahedron Lett.* **2000**, *41*, 397.
(196) Sil, D.; Sharon, A.; Maulik, P. R.; Ram. V. J. *Tetrahedron Lett.* **2004**, *45*, 6273.
(197) Ballini, R.; Bosica, G. *Synlett* **1996**, 1115.
(198) Ballini, R.; Bosica, G. *Liebigs Ann.* **1996**, 2087.
(199) Ballini, R.; Marcantoni, E.; Perella, S. *J. Org. Chem.* **1999**, *64*, 2954.
(200) Ballini, R.; Bosica, G.; Fiorini, D.; Righi, P. *Synthesis* **2002**, 681.

DAC EX. 2040 IPR2022-01531 Page 1150 of 1299

(201) Ballini, R.; Fiorini, D.; Gil, M. V.; Palmieri, A.; Román, E.; Serrano, J. A. *Tetrahedron Lett.* **2003**, *44*, 2795.
(202) Ballini, R.; Barboni, L.; Giarlo, G. *J. Org. Chem.* **2003**, *68*, 9173.
(203) Sarmah, B. K.; Barua, N. C. *Tetrahedron* **1993**, *49*, 2253.
(204) Guarna, A.; Occhiato, E. G.; Spinetti, L. M.; Vallecchi, M. E.; Scarpi, D. *Tetrahedron* **1995**, *51*, 1775.
(205) Fantin, G.; Fogagnolo, M.; Guerzoni, E. M.; Marotta, E.; Medici, A.; Pedrini, P. *Tetrahedron: Asymmetry* **1992**, *3*, 947.
(206) Kalita, D.; Khan, A. T.; Barua, N. C.; Bez, G. *Tetrahedron* **1999**, *55*, 5177.
(207) Kalita, D.; Khan, A. T.; Saikia, A. K.; Bez, G.; Barua, N. C. *Synthesis* **1998**, 975.
(208) Ballini, R.; Bosica, G. *J. Nat. Prod.* **1994**, *57*, 1462.
(209) Saikia, A. K.; Hazarika, M. J.; Barua, N. C.; Bezbarua, M. S.; Sharma, R. P.; Ghosh, A. C. *Synthesis* **1996**, 981.
(210) Bez, G.; Saikia, A. K.; Kalita, D.; Bezbarua, M. S.; Barua, N. C. *Indian J. Chem.* **1998**, *37B*, 325.
(211) Ballini, R.; Petrini, M.; Rosini, G. *Tetrahedron* **1990**, *46*, 7531.
(212) Ballini, R.; Bosica, G.; Uselli, A. *J. Heterocycl. Chem.* **1994**, *31*, 259.
(213) Occhiato, E. G.; Guarna, A.; De Sarlo, F.; Scarpi, D. *Tetrahedron: Asymmetry* **1995**, *6*, 2971.
(214) Occhiato, E. G.; Scarpi, D.; Menchi, G.; Guarna, A. *Tetrahedron: Asymmetry* **1996**, *7*, 1929.
(215) Bez, G.; Bezbarua, M. S.; Saikia, A. K.; Barua, N. C. *Synthesis* **2000**, 537.
(216) Ballini, R. *Synthesis* **1993**, 687.
(217) Ballini, R.; Barboni, L.; Bosica, G.; Fiorini, D. *Synthesis* **2002**, 2725.
(218) Ballini, R.; Barboni, L.; Bosica, G.; Filippone, P.; Peretti, S. *Tetrahedron* **2000**, *56*, 4095.
(219) Ballini, R.; Barboni, L.; Bosica, G. *J. Org. Chem.* **2000**, *65*, 6261.
(220) Ballini, R.; Barboni, L.; Bosica, G.; Fiorini, D.; Gil, M. V.; Petrini, M. *Tetrahedron* **2001**, *57*, 6079.
(221) Kádas, I.; Árvai, G.; Töke, L.; Tóth, G.; Szöllöszy, Á.; Bihari, M. *Tetrahedron* **1994**, *50*, 2895.
(222) Mikló, K.; Jaszberenyi, J. C.; Kádas, I.; Árvai, G.; Töke, L. *Tetrahedron Lett.* **1996**, *37*, 3491.
(223) Grossman, R. B.; Rasne, R. M.; Patrick, B. O. *J. Org. Chem.* **1999**, *64*, 7173.
(224) Michaud, D.; Hamelin, J.; Texier-Boullet, F.; Toupet, L. *Tetrahedron* **2002**, *58*, 5865.
(225) Correc, O.; Guillou, K.; Hamelin, J.; Paquin, L.; Texier-Boullet, F.; Toupet, L. *Tetrahedron Lett.* **2004**, *45*, 391.
(226) Sader-Bakaouni, L.; Charton, O.; Kunesch, N.; Tillequin, F. *Tetrahedron* **1998**, *54*, 1773.
(227) Chen, Y.-J.; Lin, W.-Y. *Tetrahedron Lett.* **1992**, *33*, 1749.
(228) Chen, Y.-J.; Chen, C. M.; Lin, W.-Y. *Tetrahedron Lett.* **1993**, *34*, 2961.
(229) Chen, Y.-J.; Chang, W.-H. *J. Org. Chem.* **1996**, *61*, 2536.
(230) El Blidi, L.; Crestia, D.; Gallienne, E.; Demuynck, C.; Bolte, J.; Lemaire, M. *Tetrahedron: Asymmetry.* **2004**, *15*, 2591.
(231) Ballini, R.; Petrini, M. *Tetrahedron Lett.* **1999**, *40*, 4449.
(232) Foresti, E.; Palmieri, G.; Petrini, M.; Profeta, R. *Org. Biomol. Chem.* **2003**, *1*, 4275.
(233) Cappon, J. J.; Baart, J.; van der Walle, G. A. M.; Raap, J.; Lugtenburg, J. *Recl. Trav. Chim. Pays-Bas* **1991**, *110*, 158.
(234) Crossley, M. J.; Fung, Y. M.; Kyriacopoulos, E.; Potter, J. J. *J. Chem. Soc., Perkin Trans. 1* **1998**, 1123.
(235) Yamazaki, T.; Ohnogi, T.; Kitazume, T. *Tetrahedron: Asymmetry* **1990**, *1*, 215.
(236) Ballini, R.; Bosica, G. *Org. Prepr. Proc. Int.* **1995**, *27*, 561.
(237) Ballini, R.; Petrini, M.; Polzonetti, V. *Synthesis* **1992**, 355.
(238) Ballini, R.; Bosica, G.; Gigli, F. *Tetrahedron* **1998**, *54*, 7573.
(239) Ballini, R.; Bosica, G.; Fiorini, D.; Palmieri, A. *Synthesis* **2004**, 1938.
(240) Ballini, R.; Bosica, G.; Palmieri, A.; Petrini, M.; Pierantozzi, C. *Tetrahedron* **2003**, *59*, 7283.
(241) Easton, C. J.; Xia, L.; Pitt, M. J.; Ferrante, A.; Poulos, A.; Rathjen, D. A. *Synthesis* **2001**, 451.
(242) Bäckvall, J.-E.; Ericsson, A. M.; Plobeck, N. A.; Juntunen, S. K. *Tetrahedron Lett.* **1992**, *33*, 131.
(243) Schneider, R.; Gerardin, P.; Loubinoux, B.; Rihs, G. *Tetrahedron* **1995**, *51*, 4997.
(244) Dilman, A. D.; Lyapkalo, I. M.; Ioffe, S. L.; Strelenko, Y. A.; Tartakovsky, V. A. *Synthesis* **1999**, 1767.

CR040602R

DAC EX. 2040 IPR2022-01531 Page 1151 of 1299

Appendix GALLAGHER01

```
leader  02561nas--2200553-a-4500
001     991000000000366564
005     20240208104926.0
006     m-----o--d--------
007     cr-cn|||||||||
008     011101c20012020nyuqr-pso-b---0---a2eng--
010     ##$a  2008215318
016     7#$a101287856 $2DNLM
022     ##$a1934-2616
035     ##$a(DE-599)ZDB2179048-6
035     ##$a(OCoLC)48253561
035     ##$a(CKB)1000000000366564
035     ##$a(CONSER)--2008215318
037     ##$bCurrent Protocols, John Wiley and Sons, Inc., 111 River St., Hoboken, New Jersey 07030-5774
042     ##$anlmcopyc $apcc $ansdp
050     10$aISSN RECORD
050     #4$aQH583.2
060     00$aQY 95 $bC975
070     0#$aQH583.2 $b.C87
082     04$a571.638
082     10$a571.638 $214
130     0#$aCurrent protocols in cell biology (Online)
210     ##$aCURR PROTOC CELL BIOL
210     0#$aCurr. protoc. cell biol. $b(Online)
222     #0$aCurrent protocols in cell biology $b(Online)
245     10$aCurrent protocols in cell biology / $ceditorial board, Juan S. Bonifacino [and others].
260     ##$aNew York : $bJohn Wiley, $c©2001-
310     ##$aUpdated quarterly
336     ##$atext $btxt $2rdacontent
337     ##$acomputer $bc $2rdamedia
338     ##$aonline resource $bcr $2rdacarrier
362     1#$aCeased with Volume 89, issue 1 (December 2020).
500     ##$aTitle from home page (viewed March 7, 2008).
516     ##$aText and images.
580     ##$aMerged with: Current protocols in bioinformatics; and: Current protocols in chemical biology; and: Current protocols in cytometry;
650     #0$aCytology.
650     12$aCytological Techniques
650     #7$aCytology. $2fast $0(OCoLC)fst00886282
655     #3$aInternet resource.
655     #7$aPeriodicals. $2fast $0(OCoLC)fst01411641
655     #7$aPeriodicals. $2lcgft
776     1#$x1934-2500
762     0#$tCurrent protocols in cell biology $w(CKB)111091830226014 $z0-471-14303-0
700     1#$aBonifacino, Juan S.
906     ##$aJOURNAL
```

JOURNAL

Current protocols in cell biology (Online) / editorial board, Juan S. Bonifacino [and others].

New York : John Wiley; Ceased with Volume 89, issue 1 (December 2020).

©2001-

Available Online >

TOP
SEND TO
SEARCH INSIDE
ONLINE ACCESS
LINKS
DETAILS

Send to

QR | PERMALINK | EMAIL | CITATION | EXPORT BIBTEX | ENDNOTE BASIC | EXPORT TO EXCEL | MENDELEY | REFWORKS | EXPORT RIS | PRINT

Search inside

Search for articles within this journal

Article title or keyword

Online access

Full availability (Access issues? Try using the VPN)

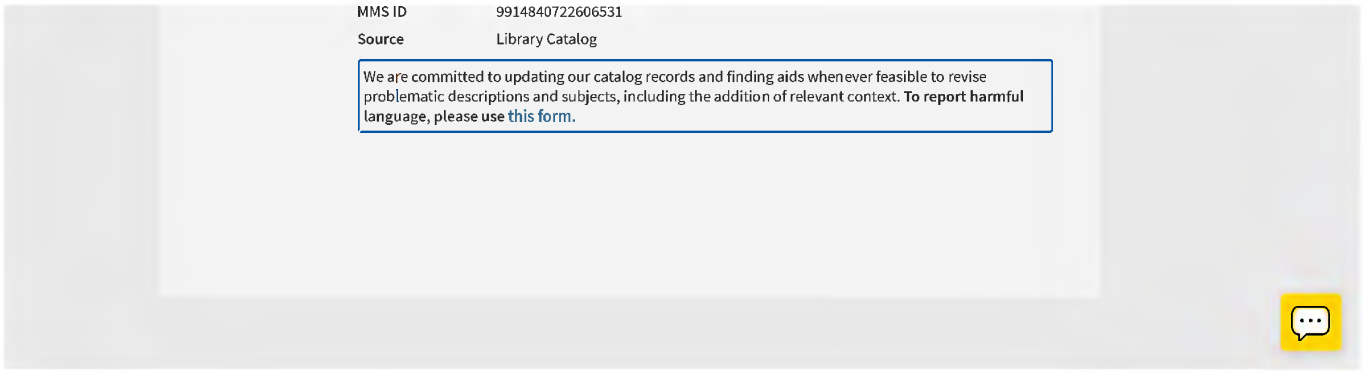
Wiley Online Library Current Protocols SHOW LICENSE

Links

MARC Record >

Details

Author / Contributor	Bonifacino, Juan S. >
Title	Current protocols in cell biology (Online) / editorial board, Juan S. Bonifacino [and others].
Uniform title	Current protocols in cell biology (Online)
Publication Information	New York : John Wiley, ©2001-
Related titles	Has sub-series : Current protocols in cell biology 0-471-14303-0 >
Type	Journal
Notes	Title from home page (viewed March 7, 2008). Text and images. Merged with: Current protocols in bioinformatics; and: Current protocols in chemical biology; and: Current protocols in cytometry; and: Current protocols essential laboratory techniques; and: Current protocols in human genetics; and: Current protocols in immunology; and: Current protocols in microbiology; and: Current protocols in molecular biology; and: Current protocols in mouse biology; and: Current protocols in neuroscience; and: Current protocols in nucleic acid chemistry; and: Current protocols in pharmacology; and: Current protocols in plant biology; and: Current protocols in protein science; and: Current protocols in stem cell biology; and: Current protocols in toxicology; to form: Current protocols.
Language	English
Subject	Cytology >
Genre	Internet resource. > Periodicals. >
MESH Subjects	Cytological Techniques >
Frequency	Updated quarterly
Identifier	LC : 2008215318 ISSN : 1934-2616 OCLC : (OCoLC)48253561 ISSN : 1934-2500


MMS ID 9914840722606531
Source Library Catalog
We are committed to updating our catalog records and finding aids whenever feasible to revise problematic descriptions and subjects, including the addition of relevant context. To report harmful language, please use this form.

Appendix GALLAGHER02

Immunoblotting and Immunodetection

Sean Gallagher,[1] Scott E. Winston (tank transfer systems),[2] Steven A. Fuller (tank transfer systems),[2] and John G.R. Hurrell (tank transfer systems; reversible staining of proteins)[3]

[1]UVP, Inc., Upland, California
[2]Nabi, Rockville, Maryland
[3]FluorRx, Carmel, Indiana

ABSTRACT

Immunoblotting (western blotting) is used to identify specific antigens recognized by polyclonal or monoclonal antibodies. This unit provides protocols for all steps, starting with solubilization of the protein samples, usually by means of SDS and reducing agents. Following solubilization, the material is separated by SDS-PAGE and the antigens are electrophoretically transferred to a membrane, a process that can be monitored by reversible staining with Ponceau S. The transferred proteins are bound to the surface of the membrane, providing access to immunodetection reagents. After nonspecific binding sites are blocked, the membrane is probed with the primary antibody and washed. The antibody-antigen complexes are tagged with horseradish peroxidase or alkaline phosphatase coupled to a secondary anti-IgG antibody, and detected using appropriate chromogenic or luminescent substrates. Finally, membranes may be stripped and reprobed. *Curr. Protoc. Cell Biol.* 52:6.2.1-6.2.28. © 2011 by John Wiley & Sons, Inc.

Keywords: immunoblot • western blot • horseradish peroxidase • alkaline phosphatase • antibodies

INTRODUCTION

Immunoblotting (often referred to as western blotting) is used to identify specific antigens recognized by polyclonal or monoclonal antibodies. Protein samples are solubilized, usually with sodium dodecyl sulfate (SDS) and reducing agents such as dithiothreitol (DTT) or 2-mercaptoethanol (2-ME). Following solubilization, the material is separated by SDS-PAGE (*UNITS 6.1 & 6.4*). The antigens are then electrophoretically transferred to a nitrocellulose, PVDF, or nylon membrane in a tank (see Basic Protocol 1) or semidry (see Alternate Protocol 1) transfer apparatus, or a dot or slot blotting apparatus (see Alternate Protocol 2). The transfer of proteins to the membrane can be monitored qualitatively or quantitatively by staining with Ponceau S (see Support Protocols 1 and 2). Proteins may also be transferred from previously stained gels (see Alternate Protocol 3).

The transferred proteins are bound to the surface of the membrane, providing access for reaction with immunodetection reagents. All remaining nonspecific binding sites are blocked by immersing the membrane in a solution containing a protein or detergent blocking agent. After probing with the primary antibody, the membrane is washed and the antibody-antigen complexes are identified with a secondary anti-IgG antibody coupled to a horseradish peroxidase (HRP) or alkaline phosphatase (AP) enzyme. The enzymes can be attached directly (see Basic Protocol 2) or via an avidin-biotin bridge (see Alternate Protocol 4) for increased sensitivity. Chromogenic or luminescent substrates (see Basic Protocol 3 and Alternate Protocols 5 and 6) are then used to visualize the enzyme activity. Finally, membranes may be stripped and reprobed (see Support Protocol 3).

NOTE: A video demonstration of this technique can be found at *http://www.jove.com/index/Details.stp?ID=759.*

Current Protocols in Cell Biology 6.2.1-6.2.28, September 2011
Published online September 2011 in Wiley Online Library (wileyonlinelibrary.com).
DOI: 10.1002/0471143030.cb0602s52
Copyright © 2011 John Wiley & Sons, Inc.

DAC EX. 2040 IPR2022-01531 Page 1157 of 1299

BASIC PROTOCOL 1

PROTEIN BLOTTING WITH TANK TRANSFER SYSTEMS

In this procedure, blotting is performed in a tank of buffer with the gel in a vertical orientation, completely submerged between two large electrode panels. In some systems up to four gels can be transferred at one time. For difficult-to-transfer proteins (>100 kDa or hydrophobic; e.g., myosin), tank blotting is preferable to semidry systems because prolonged transfers are possible without buffer depletion. However, transfers >1 hr at high power require cooling using a heat exchanger and a circulating water bath that can maintain a constant transfer temperature of 10° to 20°C.

Materials

Samples for analysis
Protein molecular weight standards (Table 6.2.1; *UNIT 6.1*): prestained (Sigma or Bio-Rad), biotinylated (Vector Labs or Sigma), fluorescent (e.g., BenchMark Fluorescent Protein Standards; Invitrogen), or compatible with other colorimetric and fluorescent detection method (e.g., MagicMark and MagicMark XP Western Protein Standards; Invitrogen)
Transfer buffer (see recipe)

Powder-free gloves
Scotch-Brite pads (3M) or equivalent sponge
Whatman 3MM filter paper or equivalent
Transfer membrane: 0.45-μm nitrocellulose (Millipore or Schleicher & Schuell), PVDF (Millipore Immobilon P), neutral nylon (Pall Biodyne A), *or* positively charged nylon (Pall Biodyne B; Bio-Rad Zetabind)
Electroblotting apparatus (Bio-Rad, Invitrogen, Amersham, or Hoefer; e.g., Figs. 6.2.1 and 6.2.2)
Indelible pen (e.g., Paper-Mate) or soft lead pencil

Additional reagents and equipment for one- and two-dimensional gel electrophoresis (*UNITS 6.1 & 6.4*) and staining proteins in gels (*UNIT 6.6*) and on membranes (see Support Protocol 1)

NOTE: Deionized, distilled water should be used throughout this protocol.

Electrophorese the protein sample

1. Prepare antigenic samples and separate proteins using small or standard-sized one- or two-dimensional gels (*UNITS 6.1 & 6.4*). Include prestained or biotinylated protein molecular weight standards in one or more gel lanes.

   The protein markers will transfer to the membrane and conveniently indicate membrane orientation and sizes of proteins after immunostaining.

Table 6.2.1 Protein Standards for Immunoblotting

Protein standard	Application
Unstained	Molecular weight calibration and transfer efficiency; can be visualized with total protein stains
Tagged	Molecular weight calibration and transfer efficiency; visualized during immunodetection steps; a variety of potential tags, including biotinylated and antibody-specific amino acid sequence engineered into standard proteins
Prestained	Excellent for checking transfer efficiency and visually inspecting the blot; typically does not produce as sharp a band as other standards, making precise molecular weight calculations difficult

DAC EX. 2040 IPR2022-01531 Page 1158 of 1299

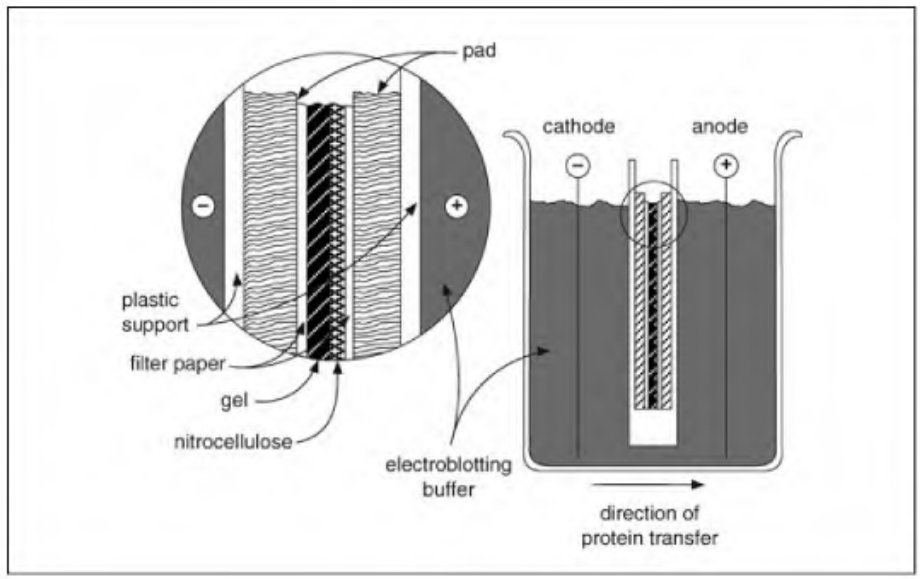


Figure 6.2.1 Immunoblotting with a tank blotting unit. The polyacrylamide gel containing the protein is laid on a sheet of filter paper. The uncovered side of the gel is overlaid with a sheet of membrane precut to the size of the gel plus 1 to 2 mm on each edge, then this membrane is overlaid with another sheet of filter paper. The filter paper containing the gel and membrane is sandwiched between Scotch-Brite pads. This sandwich is placed in a plastic support, and the entire assembly is placed in a tank containing transfer buffer. For transfer of negatively charged protein, the membrane is positioned on the anode side of the gel. For transfer of positively charged protein, the membrane is placed on the cathode side of the gel. Charged proteins are transferred electrophoretically from the gel onto the membrane. Transfer is achieved by applying a voltage of 100 V for 1 to 2 hr (with cooling) or 14 V overnight.



Figure 6.2.2 Minigel tank electrotransfer unit. Designed for smaller (8 × 10–cm) gels, these units will process four gels at a time. Note that the two outside panels hold the electrode grid.

DAC EX. 2040 IPR2022-01531 Page 1159 of 1299

MagicMark Western Protein Standards (Invitrogen) allow direct visualization of protein size standards on membrane blots without the need for protein modification or special detection reagents. The standard proteins are derived from E. coli cells containing a construct with repetitive units of a fusion protein forming the size variation and an IgG binding site. The proteins can be visualized with colorimetric, chemiluminescent, or fluorescent detection simply by probing the membrane for the specific protein. The IgG binding site will allow all the standards to react with the specific primary and secondary antibodies. The standards are in a ready-to-use format and do not have to be heated or reduced. Alternatively, BenchMark Fluorescent Protein Standards (Invitrogen) are visualized directly via UV transillumination on a UV transilluminator (UVP) when wet, or via overhead UV illumination (apparatus also available from UVP) when dry.

A variety of gel sizes and percentages of acrylamide can be used (UNIT 6.1). Most routinely used are either 14 cm × 14 cm × 0.75–mm gels or 8 cm × 10 cm × 0.75–mm minigels. Acrylamide concentrations vary from 5% to 20%, but are usually in the 10% to 15% range.

Assemble the immunoblot sandwich

2. When electrophoresis is complete, disassemble gel sandwich and remove stacking gel. Equilibrate gel 30 min at room temperature in transfer buffer.

   IMPORTANT NOTE: *Use gloves when manipulating filter papers, gels, and membranes. Oil from hands blocks the transfer.*

   Match the appropriate transfer buffer to the membrane (see Reagents and Solutions).

   Gel equilibration is required to prevent a change in the size of the gel during transfer. Any shift in gel dimension will result in a blurred transfer pattern.

3. Assemble transfer sandwich in a tray large enough to hold the plastic transfer cassette. Fill with transfer buffer so that cassette is covered.

   The transfer cassette should be assembled under buffer to minimize trapping of air bubbles. Use Figure 6.2.1 as a guide to assembly.

4. On bottom half of plastic transfer cassette, place Scotch-Brite pad or sponge, followed by a sheet of filter paper cut to same size as gel, and prewet with transfer buffer.

5. Place gel on top of filter paper; the side of the gel touching the paper arbitrarily becomes the cathode side of the gel (i.e., ultimately toward the negative electrode when positioned in the tank). Remove any air bubbles between gel and filter paper by gently rolling a test tube or glass rod over surface of gel.

   Any bubbles between the filter paper, gel, and membrane will block current flow and prevent protein transfer. This problem is indicated on the membrane by sharply defined white areas devoid of transferred protein.

   Proteins are usually negatively charged in transfer buffer and move toward the positive anode. However, some proteins may be positively charged. An additional membrane placed on the cathode side of the gel will bind these proteins.

6. Prepare transfer membrane. Cut membrane to same size as gel plus 1 to 2 mm on each edge. Place into distilled water slowly, with one edge at a 45° angle, so that the water wicks up into the membrane, wetting the entire surface. Equilibrate 10 to 15 min in transfer buffer.

   If the membrane is placed into the water too quickly, air will be trapped and will appear as white blotches in the membrane. Protein will not transfer onto these areas.

   This wetting procedure works for nitrocellulose and nylon membranes only. PVDF membranes are hydrophobic and will not wet simply from being placed into distilled water or transfer buffer. For these membranes, first immerse 1 to 2 sec in 100% methanol, then equilibrate 10 to 15 min with transfer buffer. Do not let membrane dry out at any time. If this occurs, wet once again with methanol and transfer buffer as described above.

DAC EX. 2040 IPR2022-01531 Page 1160 of 1299

7. Moisten surface of gel with transfer buffer. Place prewetted membrane directly on top side of gel (i.e., anode side). To avoid bubbles, start by placing one corner of the membrane on the gel and slowly lower the rest of the membrane onto the gel. Remove all air bubbles as in step 5.

   Poor contact between the gel and membrane will cause a swirled pattern of transferred proteins on the membrane. Some proteins will transfer as soon as the gel is placed on the membrane; repositioning the gel or membrane can result in a smeared or double image on the developed blot.

   The use of 0.2-μm membranes may improve retention of smaller-molecular-weight proteins.

8. Wet another piece of Whatman 3MM filter paper, place on anode side of membrane, and remove all air bubbles. Place another Scotch-Brite pad or sponge on top of this filter paper.

9. Complete assembly by locking the top half of the transfer cassette into place (Fig. 6.2.1).

   It is important to orient the sandwich so that the membrane faces the anode (positively charged) side of the tank.

Transfer proteins from gel to membrane

10. Fill tank with transfer buffer and place transfer cassette containing sandwich into electroblotting apparatus in correct orientation. Connect leads of power supply to corresponding anode and cathode sides of electroblotting apparatus.

    Transfer buffer should cover the electrode panels but should not touch the base of the banana plug.

11. Electrophoretically transfer proteins from gel to membrane for 30 min to 1 hr at 100 V with cooling or overnight at 14 V (constant voltage) in a cold room.

    Transfer time is dependent on the thickness and the percent acrylamide of the gel, as well as the size of the protein being transferred. In general, proteins are transferred within 1 to 6 hr, but high-molecular-weight molecules may take longer. Overnight transfer at low voltage is reliable and convenient. Cooling (at 10° to 20°C) is required for transfers >1 hr at high power. Heat exchanger cooling cores using a circulating water bath are placed into the transfer unit for cooling.

12. Turn off the power supply and disassemble the apparatus. Remove membrane from blotting apparatus and note orientation by cutting a corner or marking with a soft lead pencil or Paper-Mate pen.

    Many ballpoint inks come off, but Paper-Mate stays on the membrane.

    Membranes can be dried and stored in resealable plastic bags at 4°C for 1 year or longer at this point. Prior to further processing, dried PVDF membranes must be placed into a small amount of 100% methanol to wet the membrane, then in distilled water to remove the methanol.

13. Stain gel for total protein with Coomassie blue (*UNIT 6.6*) to verify transfer efficiency. If desired, visualize transferred proteins on nitrocellulose or PVDF membranes by staining reversibly with Ponceau S (see Support Protocol 1), or irreversibly with Coomassie blue, India ink, naphthol blue, or colloidal gold.

    These staining procedures are incompatible with nylon membranes.

    If membrane shows significant staining on the backside, either the gel was heavily overloaded or the membrane has poor protein-binding capacity (see Troubleshooting). In either case, protein-binding sites on the side facing the gel are saturated, allowing protein to migrate to the other side of the membrane. Nitrocellulose, in particular, will show diminished binding capacity with age or poor storage conditions (e.g., high temperature

DAC EX. 2040 IPR2022-01531 Page 1161 of 1299

and humidity). In addition, some proteins simply do not bind well to a particular matrix. By using several membrane sheets in place of one, the protein can be detected as it passes through each consecutive sheet. This will give an indication of how efficiently the membrane binds to a particular protein.

14. Proceed with immunoprobing and visual detection of proteins (see Basic Protocols 2 and 3 and Alternate Protocols 4 and 6).

ALTERNATE PROTOCOL 1

PROTEIN BLOTTING WITH SEMIDRY SYSTEMS

Even and efficient transfer of most proteins is also possible with semidry blotting, a convenient alternative to tank transfer systems. Instead of being placed vertically into a tank filled with transfer buffer, the gel is held horizontally between buffer-saturated blotting paper that is in contact with the electrodes (Fig. 6.2.3), greatly reducing the amount of buffer required. The electrodes are close together, giving high field strengths and rapid transfer with a standard electrophoresis power supply. Prolonged transfers (>1 hr) are not recommended; tank blotting (see Basic Protocol 1) should be used for proteins that require long blotting times for efficient transfer.

Additional Materials *(also see Basic Protocol 1)*

Six sheets of Whatman 3MM filter paper or equivalent, cut to size of gel and saturated with transfer buffer
Semidry transfer unit (Hoefer, Bio-Rad, or Invitrogen)

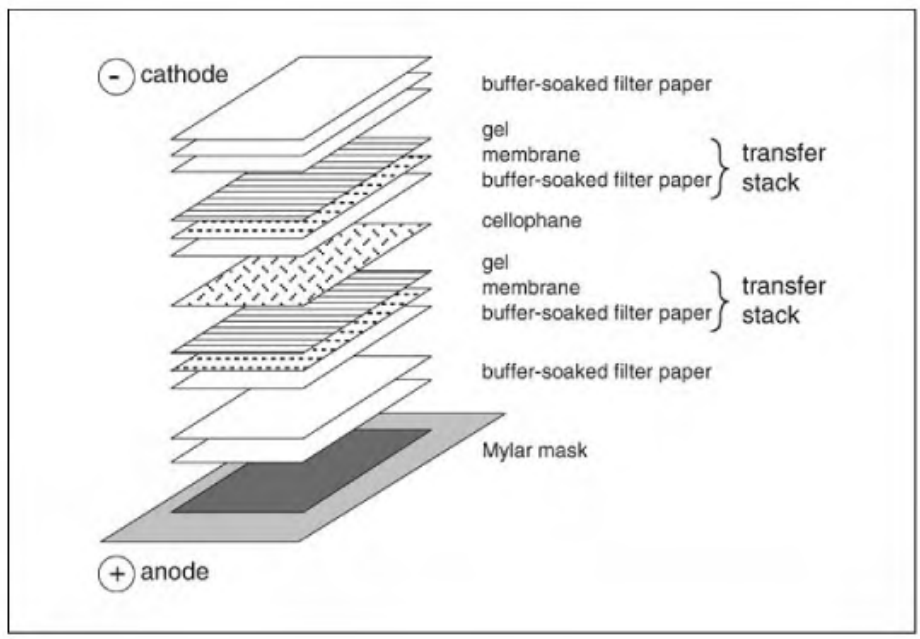


Figure 6.2.3 Immunoblotting with a semidry transfer unit. Generally, the lower electrode is the anode, and one gel is transferred at a time. A Mylar mask (optional in some units) is put in place on the anode. This is followed by three sheets of transfer buffer–soaked filter paper, the membrane, the gel, and finally, three more sheets of buffer-soaked filter paper. To transfer multiple gels, construct transfer stacks as illustrated, and separate with a sheet of porous cellophane. For transfer of negatively charged protein, the membrane is positioned on the anode side of the gel. For transfer of positively charged protein, the membrane is placed on the cathode side of the gel. Transfer is achieved by applying a maximum current of 0.8 mA/cm^2 of gel area. For a typical minigel (8 × 10 cm) and standard-sized gel (14 × 14 cm), this means 60 and 200 mA, respectively.

DAC EX. 2040 IPR2022-01531 Page 1162 of 1299

Assemble the immunoblot sandwich

1. Prepare samples and separate proteins using small or standard-sized one- or two-dimensional gels (*UNITS 6.1 & 6.4*).

   Because transfer efficiency depends on many factors (e.g., gel concentration and thickness, protein size, shape, and net charge) results may vary. Below is a guideline for 0.75–mm–thick SDS-PAGE gels transferred by semidry blotting.

Percent acrylamide (resolving gel)	Size range transferred (~100% efficiency)
5–7	29–150 kD
8–10	14–66 kD
13–15	<36 kD
18–20	<20 kD

2. Prepare transfer membrane (see Basic Protocol 1, step 6).

3. Disassemble gel sandwich. Remove and discard stacking gel.

   Equilibration of the separating gel with transfer buffer is not normally required for semidry blotting, but it may improve transfer in some cases.

4. Place three sheets of filter paper saturated with transfer buffer on the anode (Fig. 6.2.3).

   Most transfer units are designed so that negatively charged proteins move downward toward either a platinum or graphite positive electrode (anode).

   CAPS transfer buffer, pH 10.5 (see recipe for transfer buffer) can be used in place of the Tris/glycine/methanol transfer buffer of Basic Protocol 1. CAPS buffer should be used if the protein is to be sequenced right on the membrane (Moss, 2001), as glycine will interfere with this procedure.

   The filter paper should be cut to the exact size of the gel. This forces the current to flow only through the gel and not through overlapping filter paper. Some manufacturers (e.g., Hoefer) recommend placing a Mylar mask on the lower platinum anode. With an opening that is slightly less than the size of the gel, the mask forces the current to flow through the gel and not the surrounding electrode area during transfer.

5. Place equilibrated transfer membrane on top of filter paper stack. Remove all bubbles between membrane and filter paper by rolling a test tube over surface of membrane.

   Any bubbles in the filter paper stack or between the filter paper, membrane, and gel will block current flow and prevent protein transfer. This problem is indicated on the membrane by sharply defined white areas devoid of transferred protein.

6. Place gel on top of membrane. Gently roll a test tube over surface of gel to insure intimate contact between gel and membrane and to remove any interfering bubbles.

   Poor contact between the gel and membrane will cause a swirled pattern of transferred proteins on the membrane. Some proteins will transfer as soon as the gel is placed on the membrane; repositioning the gel or membrane can result in a smeared or double image on the developed blot.

7. Complete the transfer stack by putting the three remaining sheets of filter paper on top of gel. Roll out bubbles as described above.

   Multiple gels can be transferred at the same time by simply placing a sheet of porous cellophane (Hoefer) or dialysis membrane (Bio-Rad) equilibrated with transfer buffer between the transfer stacks (Fig. 6.2.3). Transfer efficiency is dependent on the position of the transfer stack in the blotting unit, with the most efficient transfer occurring in the stack closest to the anode. For critical applications, it is best to transfer one gel at a time.

DAC EX. 2040 IPR2022-01531 Page 1163 of 1299

Transfer proteins from gel to membrane

8. Place top electrode onto transfer stack.

   Most units have safety-interlock features and can only be assembled one way. Consult manufacturer's instructions for details.

   Once the transfer stack has been assembled with both electrodes, do not move the top electrode. This can shift the transfer stack and move the gel relative to the membrane, distorting the transfer pattern.

9. Carefully connect high-voltage leads to the power supply (see *UNIT 6.1* for safety precautions). Apply constant current to initiate protein transfer.

   Transfers of 1 hr are generally sufficient.

   In general, do not exceed 0.8 mA/cm^2 of gel area. For a typical minigel (8 × 10 cm) and standard-sized gel (14 × 14 cm) this means ~60 and 200 mA, respectively.

   Monitor the temperature of the transfer unit directly above the gel by touch. The unit should not exceed 45°C. If the outside of the unit is warm, too much current is being applied. Note that units with graphite electrodes are more prone to heating, because graphite has much more resistance to current flow than platinum or steel electrodes.

10. After transfer, turn off power supply and disassemble unit. Remove membrane from transfer stack, marking orientation as in step 12 of Basic Protocol 1. Proceed with staining and immunoprobing (see Basic Protocol 1, steps 13 and 14).

ALTERNATE PROTOCOL 2

SLOT AND DOT BLOTTING OF PROTEINS

Through use of a vacuum manifold or by simple hand spotting, up to 96 samples can be applied to a single nitrocellulose or PVDF membrane for immunoblotting analysis. In slot and dot blotting, proteins are not separated by electrophoresis. Instead, the entire sample is applied directly to the membrane. Although this approach cannot discriminate between the protein of interest and a cross-reactive antigen, it is a quick way to perform preliminary characterization and high-volume routine quantitation of samples.

Additional Materials *(also see Basic Protocol 1)*

<10 μg protein sample in <100 μl water or TBS (no detergent)
Tris-buffered saline (TBS; *APPENDIX 2A*)

Slot or dot blotting apparatus (e.g., Hoefer, Bio-Rad, or Whatman; Fig. 6.2.4)
Vacuum source

1. Prewet the membrane in distilled water or 100% methanol as described in Basic Protocol 1, steps 6 and 7.
2. Prepare the slot or dot blot manifold according to manufacturer's instructions.
3. Apply samples under a low house vacuum according to manufacturer's instructions.

   Typically, samples should contain <10 μg protein in <100 μl. Overloading the wells will prevent flow of liquid through the well.

   Typical systems use a low house vacuum to pull liquid through each slot, binding the proteins to the membrane.

4. Follow sample application with two equivalent volumes of water or TBS, depending on which was used to dissolved the sample, to rinse the wells of unbound protein.

DAC EX. 2040 IPR2022-01531 Page 1164 of 1299

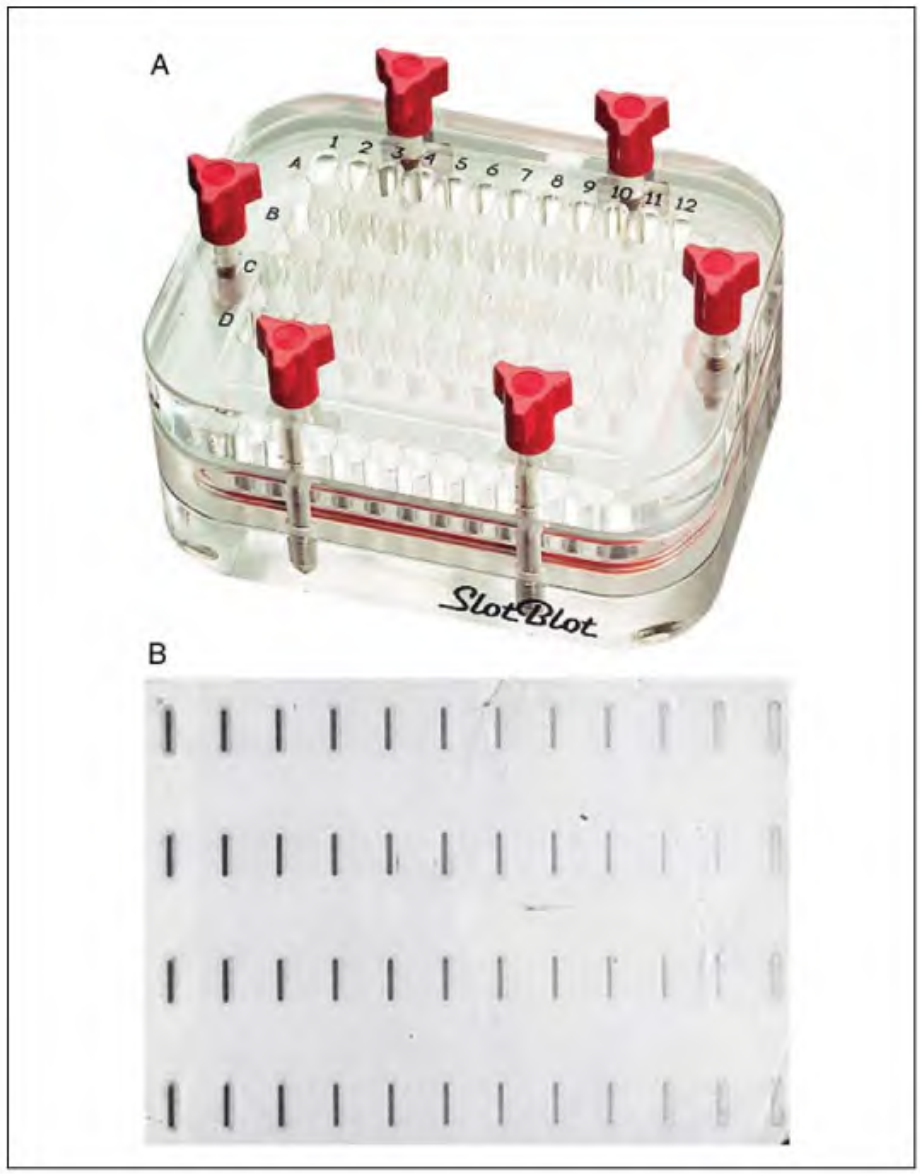


Figure 6.2.4 (**A**) Slot-blot unit. Through use of a vacuum manifold or by simple hand spotting, up to 96 samples can be applied to a single nitrocellulose or PVDF membrane for immunoblotting. Although this approach cannot discriminate between the protein of interest and a cross-reactive antigen, it is a quick way to perform preliminary characterization and high-volume, routine quantitation of samples. (**B**) Dilution series of immunoprobed BSA developed with peroxidase-tagged secondary antibody and DAB/$NiCl_2$.

BLOTTING OF STAINED GELS

ALTERNATE PROTOCOL 3

Gels stained with Coomassie blue R250 (*UNIT 6.6*) can be effectively immunoblotted by the following procedure, based on Perides et al. (1986) and Dionisi et al. (1995). Briefly, the stained gel is soaked in a series of solutions designed to increase the solubility of the proteins after staining and fixation. After transfer, the membranes are treated with 45% or 100% methanol to decrease the Coomassie blue bound to the membrane prior to processing for chromogenic development. For chemiluminescent development, removal of the Coomassie blue is generally not needed.

DAC EX. 2040 IPR2022-01531 Page 1165 of 1299

Materials

Destained gel containing proteins of interest (*UNIT 6.6*)
25 mM Tris base/192 mM glycine/1% SDS
25 mM Tris base/192 mM glycine/0.1% SDS
25 mM Tris base/192 mM glycine/0.1% SDS with 6 M urea (optional)

1. Soak destained gel containing proteins of interest in distilled water for 15 min.
2. Equilibrate gel with 25 mM Tris base/192 mM glycine/1% SDS for 1 hr with gentle agitation.
3. Transfer gel to 25 mM Tris base/192 mM glycine/0.1% SDS and equilibrate 30 min with gentle agitation.
4. *Optional:* To increase transfer efficiency of larger proteins >50 kDa, transfer gel to the above solution with 6 M urea for an additional 30 min.
5. Proceed with transfer (see Basic Protocol 1, steps 2 to 12).

   For the most efficient transfer and binding to the membrane, the transfer buffer should contain 0.1% (w/v) SDS.

6. After transfer, soak membranes for 10 to 30 min in 45% methanol (nitrocellulose) or 100% methanol (nylon or PVDF) to remove the bound Coomassie blue.

   This step is not needed if using chemiluminescent reactions or radiolabeled protein A for immunodevelopment. Destaining of the nitrocellulose membrane is enhanced by adding a small ball of laboratory tissue to the methanol to absorb the Coomassie blue.

7. Proceed with immunoprobing and visual detection of proteins (see Basic Protocols 2 and 3 and Alternate Protocols 4 and 6).

SUPPORT PROTOCOL 1

REVERSIBLE STAINING OF TRANSFERRED PROTEINS WITH PONCEAU S

To verify transfer efficiency, nitrocellulose and PVDF membranes can be reversibly stained. This method will not work on nylon membranes.

Additional Materials *(also see Basic Protocol 1)*

Ponceau S solution (see recipe)

Additional reagents and equipment for photographing membranes (*UNIT 6.6*)

1. Following protein transfer to nitrocellulose or PVDF (see Basic Protocol 1 or Alternate Protocol 1), place membrane in Ponceau S solution for 5 min at room temperature.
2. Destain 2 min in water. Photograph membrane if required (*UNIT 6.6*) and mark the molecular-weight-standard band locations with indelible ink.
3. Completely destain membrane by soaking an additional 10 min in water.

SUPPORT PROTOCOL 2

QUANTITATION OF TRANSFERRED PROTEINS WITH PONCEAU S

In addition to qualitatively visualizing proteins on membranes after blotting, Ponceau S provides a convenient method for quantitating the amount of protein in a given lane. By eluting the dye off a strip of membrane and reading in a spectrophotometer (OD_{525}), an internal control value of protein on a lane is obtained. This value is used to correct for any differences in protein loading from lane to lane. Comparison of the Ponceau S value to the chemiluminescent or chromogenic immunodetection value determined by densitometry provides a straightforward correction for lane-to-lane variation. This method works best for complex mixtures where the immunodetected protein represents a small proportion of the total protein (Klein et al., 1995).

DAC EX. 2040 IPR2022-01531 Page 1166 of 1299

1. Following protein transfer to nitrocellulose, PVDF, or nylon (see Basic Protocol 1 or Alternate Protocol 1), stain membrane, photograph, and destain (see Support Protocol 1).

   Membranes should be destained until the background becomes white.

2. Mark lanes with a soft pencil and cut lanes into strips.

3. Place each strip into 7 ml of distilled water for 7 min and remove the resulting solution. If any particulates are visible, centrifuge to remove them.

4. Read OD_{525} in a 2-ml cuvette.

   Any variation in gel-to-gel sample loading and blotting efficiency will be reflected in a change in OD of the sample lanes when compared to the control.

   The change in OD can be calibrated to a known amount of protein loaded on the control lane. This will be a relative value, however, since the efficiency of transfer out of the gel and binding to the membrane is rarely 100%.

IMMUNOPROBING WITH DIRECTLY CONJUGATED SECONDARY ANTIBODY

BASIC PROTOCOL 2

Immobilized proteins are probed with specific antibodies to identify and quantitate any antigens present. The membrane is immersed in blocking buffer to fill all protein-binding sites with a nonreactive protein or detergent. Next, it is placed in a solution containing the antibody directed against the antigen (primary antibody). The blot is washed and exposed to an enzyme-antibody conjugate directed against the primary antibody (secondary antibody; e.g., goat anti-rabbit IgG for a rabbit primary antibody). Antigens are identified by chromogenic or luminescent visualization (see Basic Protocol 3 and Alternate Protocol 5 or 6) of the enzyme bound to the membrane.

Materials

Membrane with transferred proteins (see Basic Protocol 1 or Alternate Protocols 1 to 3)
Blocking buffer appropriate for membrane and detection protocol (see recipes)
Primary antibody specific for protein of interest
TTBS (nitrocellulose or PVDF) or TBS (nylon; see *APPENDIX 2A* for recipes)
Secondary antibody conjugate: species-specific anti-Ig conjugated to horseradish peroxidase (HRP) or alkaline phosphatase (AP; e.g., Cappel, Vector Labs, Kirkegaard & Perry, or Sigma; dilute as indicated by manufacturer and store frozen in 25-μl aliquots until use)
Heat-sealable plastic bag
Powder-free gloves
Plastic box

1. Place membrane in heat-sealable plastic bag with 5 ml blocking buffer and seal bag. Incubate 30 min to 1 hr at room temperature with agitation on an orbital shaker or rocking platform.

   Usually 5 ml buffer is sufficient for two to three membranes (14 × 14–cm size). If membrane is to be stripped and reprobed (see Support Protocol 3), blocking buffer must contain casein (for AP systems) or nonfat dry milk.

   Plastic incubation trays are often used in place of heat-sealable bags, and can be especially useful when processing large numbers of strips in different primary antibody solutions.

DAC EX. 2040 IPR2022-01531 Page 1167 of 1299

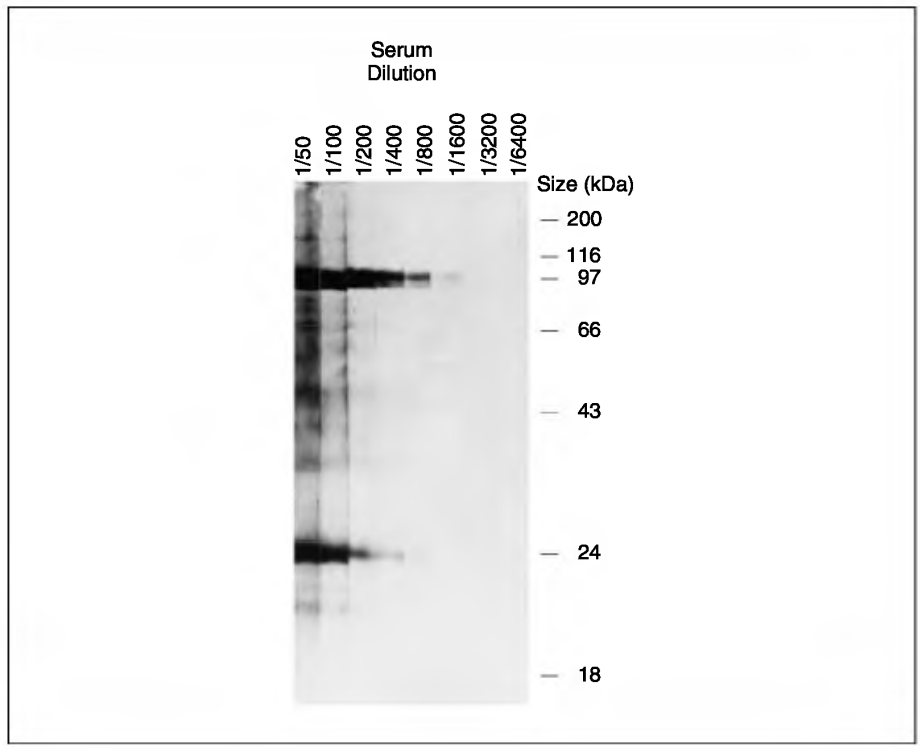


Figure 6.2.5 Serial dilution of primary antibody directed against the 97-kDa catalytic subunit of the plant plasma membrane ATPase. Blot was developed with HRPO-coupled avidin-biotin reagents according to Alternate Protocol 4 and visualized with 4-chloro-1-naphthol (4CN). Note how background improves with dilution.

2. Dilute primary antibody in blocking buffer.

   Primary antibody dilution is determined empirically, but is typically 1/100 to 1/1000 for a polyclonal antibody, 1/10 to 1/100 for hybridoma supernatants, and ≥1/1000 for murine ascites fluid. Ten- to one-hundred-fold higher dilutions can be used with AP- or luminescence-based detection systems. To determine the appropriate antibody concentration, a dilution series is easily performed with membrane strips. Separate antigens on a preparative gel (i.e., a single large sample well) and immunoblot the entire gel. Cut 2- to 4-mm strips by hand or with a membrane cutter (Inotech) and incubate individual strips in a set of serial dilutions of primary antibody. The correct dilution should give low background and high specificity (Fig. 6.2.5).

   Both primary and secondary antibody solutions can be used at least twice, but long-term storage (i.e., >2 days at 4°C) is not recommended.

3. Open bag and pour out blocking buffer. Replace with diluted primary antibody and incubate 30 min to 1 hr at room temperature with constant agitation.

   Usually 5 ml diluted primary antibody solution is sufficient for two to three membranes (14 × 14–cm size). Incubation time may vary depending on conjugate used.

   When using plastic trays, the primary and secondary antibody solution volume should be increased to 25 to 50 ml. For membrane strips, incubation trays with individual slots are recommended. Typically, 0.5 to 1 ml solution/slot is needed.

4. Remove membrane from plastic bag with gloved hand. Place in plastic box and wash four times by agitating with 200 ml TTBS (nitrocellulose or PVDF) or TBS (nylon), 10 to 15 min each time.

DAC EX. 2040 IPR2022-01531 Page 1168 of 1299

5. Dilute secondary antibody conjugate in blocking buffer.

   Commercially available enzyme–conjugated secondary antibody is usually diluted 1/200 to 1/2000 prior to use (Harlow and Lane, 1999).

6. Place membrane in new heat-sealable plastic bag, add diluted secondary antibody conjugate, and incubate 30 min to 1 hr at room temperature with constant agitation.

   When using plastic incubation trays, see step 3 annotation for proper antibody volumes.

7. Remove membrane from bag and wash as in step 4. Develop according to appropriate visualization protocol (see Basic Protocol 3 or Alternate Protocol 5 or 6).

IMMUNOPROBING WITH AVIDIN-BIOTIN COUPLING TO SECONDARY ANTIBODY

ALTERNATE PROTOCOL 4

The following procedure is based on the Vectastain ABC kit from Vector Labs. It uses an avidin-biotin complex to attach the enzyme to a biotinylated secondary antibody. Avidin-biotin systems are capable of extremely high sensitivity due to the multiple reporter enzymes bound to each secondary antibody.

Additional Materials *(also see Basic Protocol 2)*

Vectastain ABC (HRP) or ABC-AP (AP) kit (Vector Labs) containing the following: reagent A (avidin), reagent B (biotinylated HRP or AP), and biotinylated secondary antibody (request membrane immunodetection protocols when ordering)

1. Equilibrate membrane in appropriate blocking buffer in heat-sealed plastic bag with constant agitation using an orbital shaker or rocking platform. For nitrocellulose and PVDF, incubate 30 to 60 min at room temperature. For nylon, incubate $\geq$2 hr at 37°C.

   TTBS is well suited for avidin-biotin systems. For nylon, protein-binding agents are recommended. Because nonfat dry milk contains residual biotin, which will interfere with the immunoassay, it must be used in the blocking step only. If membrane is to be stripped and reprobed (see Support Protocol 3), blocking buffer must contain casein (for AP systems) or nonfat dry milk.

   Plastic incubation trays are often used in place of heat-sealable bags, and can be especially useful when processing large numbers of strips in different primary antibody solutions.

2. Prepare primary antibody solution in TTBS (nitrocellulose or PVDF) or TBS (nylon).

   Dilutions of sera containing primary antibody generally range from 1/100 to 1/100,000. This depends in large part on the sensitivity of the detection system. With high-sensitivity avidin-biotin systems, dilutions from 1/1000 to 1/100,000 are common. Higher dilutions can be used with AP- or luminescence-based detection systems. The correct dilution should give low background and high specificity (Fig. 6.2.5).

3. Open bag, remove blocking buffer, and add enough primary antibody solution to cover membrane. Incubate 30 min at room temperature with gentle rocking.

   Usually 5 ml diluted primary antibody solution is sufficient for two to three membranes (14 × 14–cm size). Incubation time may vary depending on conjugate used.

   When using plastic trays, the primary and secondary antibody solution volume should be increased to 25 to 50 ml. For membrane strips, incubation trays with individual slots are recommended. Typically, 0.5 to 1 ml solution/slot is needed.

4. Remove membrane from bag and place in plastic box. Wash membrane three times over a 15-min span in TTBS (nitrocellulose or PVDF) or TBS (nylon). Add enough

DAC EX. 2040 IPR2022-01531 Page 1169 of 1299

TTBS or TBS to fully cover the membrane (e.g., 5 to 10 ml/strip or 25 to 50 ml/whole membrane).

5. Prepare biotinylated secondary antibody solution by diluting two drops biotinylated antibody with 50 to 100 ml TTBS (nitrocellulose or PVDF) or TBS (nylon).

   This dilution gives both high sensitivity and enough volume to easily cover a large 14 × 14–cm membrane.

6. Transfer membrane to fresh plastic bag containing secondary antibody solution. Incubate 30 min at room temperature with slow rocking, then wash as in step 4.

   When using plastic incubation trays, see step 3 annotations for proper antibody volumes.

7. While membrane is being incubated with secondary antibody, prepare avidin-biotin-HRP or -AP complex. Mix two drops Vectastain reagent A and two drops reagent B into 10 ml TTBS (nitrocellulose or PVDF) or TBS (nylon). Incubate 30 min at room temperature, then further dilute to 50 ml with TTBS or TBS.

   Diluting the A and B reagents to 50 ml expands the amount of membrane that can be probed without greatly affecting sensitivity.

   Sodium azide is a peroxidase inhibitor and should not be used as a preservative. Casein, nonfat dry milk, serum, and some grades of BSA may interfere with the formation of the avidin-biotin complex and should not be used in the presence of avidin or biotin reagents (Gillespie and Hudspeth, 1991; Vector Labs).

8. Transfer membrane to avidin-biotin-enzyme solution. Incubate 30 min at room temperature with slow rocking, then wash over a 30-min span as in step 4.

9. Develop membrane according to the appropriate visualization protocol (see Basic Protocol 3 or Alternate Protocol 5 or 6).

BASIC PROTOCOL 3

VISUALIZATION WITH CHROMOGENIC SUBSTRATES

Bound antigens are typically visualized with chromogenic enzyme substrates. The substrates 4CN, DAB/$NiCl_2$, and TMB are commonly used with HRP, while BCIP/NBT is recommended for AP (see Table 6.2.2). After incubation with primary and secondary antibodies, the membrane is placed in the appropriate substrate solution. Protein bands usually appear within a few minutes.

Materials

Membrane with transferred proteins and probed with antibody-enzyme complex (see Basic Protocol 2 or Alternate Protocol 4)
TBS (*APPENDIX 2A*)
Chromogenic visualization solution (Table 6.2.2)

Additional reagents and equipment for gel photography (*UNIT 6.6*)

1. If final membrane wash was performed in TTBS, wash membrane 15 min at room temperature in 50 ml TBS.

   The Tween 20 in TTBS interferes with 4CN development (Bjerrum et al., 1988).

2. Place membrane into chromogenic visualization solution.

   Bands should appear in 10 to 30 min.

3. Terminate reaction by washing membrane in distilled water. Air dry and photograph (*UNIT 6.6*) for a permanent record.

DAC EX. 2040 IPR2022-01531 Page 1170 of 1299

Table 6.2.2 Chromogenic and Luminescent Visualization Systems[a]

System	Reagent[b]	Reaction/detection	Comments[c]
Chromogenic			
HRP-based	4CN	Oxidized products form purple precipitate	Not very sensitive (Tween 20 inhibits reaction); fades rapidly upon exposure to light
	DAB/$NiCl_2$[d]	Forms dark brown precipitate	More sensitive than 4CN but potentially carcinogenic; resulting membrane easily scanned
	TMB[e]	Forms dark purple stain	More stable, less toxic than DAB/$NiCl_2$; may be somewhat more sensitive[e]; can be used with all membrane types; kits available from Kirkegaard & Perry, Invitrogen, Sigma-Aldrich, and Vector Labs
AP-based	BCIP/NBT	BCIP hydrolysis produces indigo precipitate after oxidation with NBT; reduced NBT precipitates; dark blue-gray stain results	More sensitive and reliable than other AP-precipitating substrates; note that phosphate inhibits AP activity
Luminescent			
HRP-based	Luminol/H_2O_2/ *p*-iodophenol	Oxidized luminol substrate gives off blue light; *p*-iodophenol increases light output	Very convenient, sensitive system; reaction detected within a few seconds to 1 hr
AP-based	Substituted 1,2-dioxetane-phosphates (e.g., AMPPD, CSPD, Lumigen, Lumi-Phos 530[f])	Dephosphorylated substrate gives off light	Protocol described gives reasonable sensitivity on all membrane types; consult instructions of reagent manufacturer for maximum sensitivity and minimum background (see Troubleshooting); kits available from GE Life Sciences, ABI, Pierce, Vector Labs, Beckman Coulter, Perkin Elmer.

[a]Abbreviations: AMPPD or Lumigen, disodium 3-(4-methoxyspiro{1,2-dioxetane-3,2′-tricyclo[3.3.1.1^{3,7}] decan}-4-yl)phenyl phosphate; AP, alkaline phosphatase; BCIP, 5-bromo-4-chloro-3-indolyl phosphate; 4CN, 4-chloro-1-napthol; CSPD, AMPPD with substituted chlorine moiety on adamantine ring; DAB, 3,3′-diaminobenzidine; HRP, horseradish peroxidase; NBT, nitroblue tetrazolium; TMB, 3,3′,5,5′-tetramethylbenzidine.

[b]Recipes and suppliers are listed in Reagents and Solutions except for TMP, for which use of a kit is recommended.

[c]See Commentary for further details.

[d]DAB/$NiCl_2$ can be used without the nickel enhancement, but it is much less sensitive.

[e]McKimm-Breschkin (1990) reported that if nitrocellulose filters are first treated with 1% dextran sulfate for 10 min in 10 mM citrate-EDTA (pH 5.0), TMB precipitates onto the membrane with a sensitivity much greater than 4CN or DAB, and equal to or better than that of BCIP/NBT.

[f]Lumi-Phos 530 contains dioxetane phosphate, $MgCl_2$, CTAB, and fluorescent enhancer in a pH 9.6 buffer.

VISUALIZATION WITH LUMINESCENT SUBSTRATES

ALTERNATE PROTOCOL 5

Bound antigens can also be visualized with luminescent substrates. Detection with light offers both speed and enhanced sensitivity over chromogenic and radioisotopic procedures. After the final wash, the blot is immersed in a substrate solution containing luminol for HRP or dioxetane phosphate for AP (Table 6.2.2). Film contact exposure or CCD-based digital imaging is used to capture the chemiluminescent signal. Exposures range from a few seconds to several hours, although typically signals appear within a few seconds or minutes.

DAC EX. 2040 IPR2022-01531 Page 1171 of 1299

Additional Materials *(also see Basic Protocol 3)*

Luminescent substrate buffer: 50 mM Tris·Cl, pH 7.5 (for HRP; *APPENDIX 2A*) *or* dioxetane phosphate substrate buffer (for alkaline phosphatase; see recipe)
Nitro-Block solution (AP reactions only): 5% (v/v) Nitro-Block (Applied Biosystems) in dioxetane phosphate substrate buffer, prepared just before use
Luminescent visualization solution (Table 6.2.2)
Clear plastic wrap

Additional reagents and equipment for autoradiography

NOTE: See Troubleshooting section for suggestions concerning optimization of this protocol, particularly when employing AP-based systems.

1. Equilibrate membrane in two 15-min washes with 50 ml substrate buffer.

   For blots of whole gels, use 50 ml substrate buffer; for strips, use 5 to 10 ml/strip.

2. *For AP reactions using nitrocellulose or PVDF membranes:* Incubate 5 min in Nitro-Block solution, followed by 5 min in substrate buffer (volumes as in step 1).

   Nitro-Block enhances light output from the dioxetane substrate in reactions using AMPPD, CSPD, or Lumigen concentrate. It is required for nitrocellulose and recommended for PVDF membranes. It is not needed for Lumi-Phos 530, AP reactions on nylon membranes, or HRP reactions on any type of membrane. Lumi-Phos 530 is not recommended for nitrocellulose membranes.

3. Transfer membrane to visualization solution (volumes as in step 1). Soak 30 sec (HRP) to 5 min (AP).

   Alternatively, lay out a square of plastic wrap and pipet 1 to 2 ml visualization solution into the middle. Place membrane on the plastic so that the visualization solution spreads out evenly from edge to edge. Fold wrap back onto membrane, seal, and proceed to step .

4. Remove membrane, drain, and place face down on a sheet of clear plastic wrap. Fold wrap back onto membrane to form a liquid-tight enclosure and quickly place against film (step 5a) or in CCD imaging system (step 5b).

   To insure an optimal image, only one layer of plastic should be between the membrane and film. Sealable bags are an effective alternative. Moisture must not come in contact with the X-ray film.

5a. *For film:* In a darkroom, place membrane face down onto film and expose film for a few seconds to several hours.

   Do this quickly and do not reposition; a double image will be formed if the membrane is moved while in contact with the film. A blurred image is usually caused by poor contact between membrane and film; use a film cassette that insures a tight fit.

   Typically, immunoblots produce very strong signals within a few seconds or minutes. Weak signals may require several hours to overnight exposure (see Troubleshooting).

5b. *For CCD imaging:* Place the membrane in the imager, focus, and close the door. Preview the exposure with a high pixel binning (4 × 4 to 8 × 8). Once satisfied with the preview image, capture at 1 × 1 (highest resolution) to 4 × 4 (lower resolution, but faster more sensitive capture).

   Exposures with cooled CCD cameras fitted with low-light optics are rarely longer than 10 min. Once captured, archive the image for later analysis (Fig. 6.2.6; Medberry et al., 2004).

6. If desired, wash membrane in two 15-min washes of 50 ml TBS and process for chromogenic development (see Basic Protocol 3).

   Chemiluminescent and chromogenic immunoblotting can be easily combined on a single blot to provide a permanent visual marker of a known protein. First probe membrane

DAC EX. 2040 IPR2022-01531 Page 1172 of 1299



Figure 6.2.6 Chemiluminescent blot captured with a 5-min exposure using a 1-megapixel cooled (–100°C) CCD scientific camera. In this case the reaction had decayed to a point where film was not able to record an image, while the CCD camera shows the dilution series. The blot, a two-fold IgG dilution series from 500 to 2 ng, was probed using peroxidase-conjugated affinity-purified sheep anti-mouse IgG (H&L; Rockland Immunochemicals) and visualized with luminol.

with the chemiluminescent reactions to record on film. If stripping and reprobing are needed, process by wetting and NaOH treatment (see Support Protocol 3). For the last reaction, use chromogenic development to produce a permanent visual record of the blot. Alternatively, once the film record of the chemiluminescent blot is recorded, the blot can be rinsed briefly with distilled water and placed in the appropriate chromogenic solution for chromogenic development of the blot. This results in a permanent reference stain on the blot for comparison to the more easily scanned and quantitated film record.

SIGNAL AMPLIFICATION WITH AVIDIN-BIOTIN VISUALIZATION REAGENTS

ALTERNATE PROTOCOL 6

Specialized kits are available that provide significant signal amplification and can accommodate the chromogenic, chemiluminescent, or fluorescent development of a substrate. The Vectastain ABC-AmP Western Blotting Immunodetection Kit (Vector Labs) features a preformed complex between streptavidin and biotinylated alkaline phosphatase. The substrate is either the chromogenic substrate BCIP/NBT, which produces a blue-purple precipitate, or a chemiluminescent/fluorescent substrate, DuoLux, that provides very high sensitivity and has sustained light-emission characteristics. Blots can be exposed to film several times over an 8-hr period for the optimization of band intensities or resolution. In addition to providing an amplified signal, this approach produces a very low background on both nitrocellulose and PVDF membranes. These kits have been developed to produce maximum sensitivity with minimal background staining.

Materials

Membrane with transferred proteins (see Basic Protocol 1 or Alternate Protocols 1 to 3)

Primary antibody (from mouse or rabbit) specific for protein of interest

Vectastain ABC-AmP Chromogenic or Chemiluminescent Western Blotting Immunodetection Kit (Vector Labs) containing:

DAC EX. 2040 IPR2022-01531 Page 1173 of 1299

10× casein solution (250 ml)
Biotinylated secondary antibody (0.25 ml): anti-mouse IgG (for mouse primary antibodies) *or* anti-rabbit IgG (for rabbit primary antibodies)
Reagents A and B (0.5 ml each)
Substrate: chemiluminescent/fluorescent substrate (DuoLux; 100 ml) or BCIP/NBT chromogenic substrate kit (stock reagents for 200 ml)
PBS: 10 mM sodium phosphate buffer, pH 7.5 (*APPENDIX 2A*) containing 150 mM NaCl
0.1 M Tris·Cl, pH 9.5 (*APPENDIX 2A*)

Staining trays
X-ray film (e.g., Kodak BioMax)
UV transilluminator or UV imaging trans- and epi-CCD acquisition system (UVP, Inc.)

NOTE: The components supplied in each Vectastain ABC-AmP Western Blotting Immunodetection Kit provide sufficient reagents to develop approximately twenty 100-cm^2 blots. The volumes of the reagents in the protocol below are optimized for the development of a 100-cm^2 membrane. Volumes may be proportionally adjusted for blots of a different size. All kit reagents may be used immediately following dilution. For optimal results, it is recommended that all diluted reagents from the kit be used the same day that they are prepared. Vectastain ABC-AmP Kit stock reagents should be stored under refrigeration and kept in the box in which they are supplied.

Block membrane

1. For a 100-cm^2 (10 × 10–cm) blot, prepare 120 ml of 1× casein solution by adding 12 ml of 10× casein solution (provided with Vectastain kit) to 108 ml distilled water. Block membrane by incubating in 10 ml of 1× casein solution for 5 min at room temperature with gentle agitation. Save remaining 1× casein to be used in subsequent steps.

   In rare cases, some nonspecific bands may develop. This can usually be eliminated by increasing the concentration of NaCl to 0.3 to 0.5 M in the Vectastain ABC-AmP reagent (see step 5, below). Some enzymes isolated from tissues may have covalently attached biotin as a cofactor. If high salt does not prevent the Vectastain ABC-AmP reagent from binding to particular bands, use an avidin/biotin blocking step (Vector Laboratories, cat. No. SP-2001) between steps 1 and 2 in this protocol.

2. Incubate the membrane for 30 min (or for a time established to be optimal for the concentration of primary antibody used) with gentle agitation at room temperature in an appropriate concentration of primary antibody diluted in PBS.

3. Wash the membrane in 10 ml of 1× casein solution three times, each time for 4 min at room temperature with gentle agitation.

4. Prepare the biotinylated secondary antibody solution by adding 10 µl of biotinylated anti–mouse IgG or anti–rabbit IgG to 10 ml of 1× casein solution (final concentration 1.5 µg/ml). Incubate membrane 30 min at room temperature with gentle agitation in 10 ml of the biotinylated secondary antibody solution. At end of incubation, wash in 1× casein solution as in step 3.

5. Prepare the Vectastain ABC-AmP reagent by adding 20 µl reagent A and 20 µl reagent B to 10 ml of 1× casein solution. Incubate the membrane in 10 ml reagent for 10 min at room temperature with gentle agitation. At end of incubation, wash with 1× casein solution as in step 3.

Incubate membrane in substrate solution

It is recommended that the membrane be transferred to a different staining tray for the substrate development step.

DAC EX. 2040 IPR2022-01531 Page 1174 of 1299

To detect chemiluminescent and/or fluorescent signal

6a. Equilibrate membrane for 5 min in 0.1 M Tris·Cl, pH 9.5. Remove excess buffer by holding membrane vertically and touching edge of membrane to absorbent paper.

7a. Place membrane target-side-up on plastic wrap on a level surface. Pipet 5 ml of substrate on to membrane surface. Incubate 5 min under subdued light or in dark.

8a. Rinse membrane in 0.1 M Tris·Cl, pH 9.5, for a few seconds, then remove excess buffer by holding membrane vertically and touching edge of membrane to absorbent paper.

If necessary, background may be further reduced by washing membrane in 0.1 M Tris·Cl, pH 9.5, for 5 min at room temperature and removing excess buffer before exposure to film.

9a. Place membrane between two pieces of acetate, plastic wrap, or clear sheet protector. Expose membrane to X-ray film (e.g., KODAK BioMax film) for the appropriate time.

10a. *Optional:* To obtain fluorescent signal, following step 9a, wash membrane in 0.1 M Tris·Cl, pH 9.5, for 5 min at room temperature. Remove excess buffer. Place membrane target-side-up on a UV transilluminator (254 to 365 nm) or UV imaging trans- and epi-CCD acquisition system, and observe results.

To detect chromogenic signal

6b. Equilibrate membrane for 5 min in 0.1 M Tris·Cl, pH 9.5.

7b. Prepare chromogenic reagent by adding 4 drops of reagent from each of the three dropper bottles in the BCIP/NBT substrate kit into 10 ml of 0.1 M Tris·Cl, pH 9.5. Incubate membrane in the substrate solution at room temperature with gentle agitation until the appropriate density of colored bands develops.

Incubation times may vary from 30 min to several hours.

8b. Briefly rinse the membrane in PBS and air dry. Store blot protected from light.

STRIPPING AND REUSING MEMBRANES

SUPPORT PROTOCOL 3

This stripping procedure works with blotted membranes from one- and two-dimensional gels, including previously stained gels (Suck and Krupinska, 1996). Reprobing PVDF membranes that have been developed with chemiluminescent reagents is simple and straightforward. All residual antibodies are removed from the membrane by first rewetting it in water and then briefly treating it with NaOH. Although repeated reprobing can lead to loss of signal, up to five reprobings are generally feasible. The blot should have been blocked with 5% nonfat dry milk prior to treatment.

Chromogenic development leaves a permanent stain on the membrane that is difficult to remove, and should not be used when reprobing. The stain can interfere with subsequent analysis if reactive bands from sequential immunostainings are close together.

Materials

0.2 M NaOH

1. Wash blot 5 min in distilled water.

In order to effectively reprobe the membranes, casein (for AP systems) or nonfat dry milk must be used as the blocking agent.

2. Transfer to 0.2 M NaOH and wash 5 min.

DAC EX. 2040 IPR2022-01531 Page 1175 of 1299

3. Wash blot 5 min in distilled water.
4. Proceed with immunoprobing procedure (see Basic Protocol 2 and Alternate Protocol 4).

Casein or nonfat dry milk is recommended as blocking agent when reprobing membranes.

REAGENTS AND SOLUTIONS

Deionized, distilled water should be used to prepare all solutions. For common stock solutions, see ***APPENDIX 2A****; for suppliers, see* ***SUPPLIERS APPENDIX****. For selection of appropriate chromogenic or luminescent solutions, and for definition of abbreviations, see Table 6.2.2.*

Alkaline phosphate substrate buffer

100 mM Tris·Cl, pH 9.5 (*APPENDIX 2A*)
100 mM NaCl
5 mM $MgCl_2$

BCIP/NBT visualization solution

NBT stock: 50 mg/ml nitroblue tetrazolium in 70% *N,N*-dimethylformamide (DMF). Store <1 year at 4°C.
BCIP stock: 50 mg/ml 5-bromo-4-chloro-3-indolyl phosphate (BCIP) in 100% DMF. Store <1 year at 4°C.
Mix 33 µl NBT stock and 5 ml alkaline phosphate substrate buffer (see recipe). Add 17 µl BCIP stock and mix. Stable 1 hr at room temperature.

Recipe is from Harlow and Lane (1999). Alternatively, BCIP/NBT substrates may be purchased from Sigma, Kirkegaard & Perry, and Vector Labs.

Blocking buffer

For colorimetric detection:
For nitrocellulose and PVDF: 0.1% (v/v) Tween 20 in Tris-buffered saline (TTBS; *APPENDIX 2A*). Store up to 1 week at 4°C.

For neutral and positively charged nylon: Tris-buffered saline (TBS; *APPENDIX 2A*) containing 10% (w/v) nonfat dry milk. Prepare just before use.

For luminescent detection:
For nitrocellulose, PVDF, and neutral nylon (e.g., Pall Biodyne A): With constant mixing, add 0.2% casein (e.g., Hammarsten grade or I-Block; Applied Biosystems) to warm (65°C) TTBS (*APPENDIX 2A*). Stir for 5 min. Cool before use. Prepare just before use.

For positively charged nylon: With constant mixing, add 6% (w/v) casein and 1% (v/v) polyvinyl pyrrolidone (PVP) to warm (65°C) TTBS (*APPENDIX 2A*). Stir for 5 min. Cool before use. Prepare just before use.

4CN visualization solution

Mix 20 ml ice-cold methanol with 60 mg 4-chloro-1-naphthol (4CN). Separately, mix 60 µl of 30% H_2O_2 with 100 ml TBS (*APPENDIX 2A*) at room temperature. Rapidly mix the two solutions and use immediately.

DAB/$NiCl_2$ visualization solution

5 ml 100 mM Tris·Cl, pH 7.5 (*APPENDIX 2A*)
100 µl 3,3′-diaminobenzidine (DAB) stock (40 mg/ml in H_2O, stored in 100-µl aliquots at −20°C)
25 µl $NiCl_2$ stock (80 mg/ml in H_2O, stored in 100-µl aliquots at −20°C)

continued

DAC EX. 2040 IPR2022-01531 Page 1176 of 1299

15 µl 3% H_2O_2
Mix just before use

CAUTION: Handle DAB carefully, wearing gloves and mask, as it is a carcinogen.

Suppliers of peroxidase substrates are Sigma, Kirkegaard & Perry, Moss, and Vector Labs.

Dioxetane phosphate substrate buffer

1 mM $MgCl_2$
0.1 M diethanolamine
0.02% sodium azide (optional)
Adjust to pH 10 with HCl and use fresh

Traditionally, the AMPPD substrate buffer has been a solution containing 1 mM $MgCl_2$ and 50 mM sodium carbonate/bicarbonate, pH 9.6 (Gillespie and Hudspeth, 1991). The use of diethanolamine results in better light output (Applied Biosystems Western Light instructions).

Alternatively, 100 mM Tris·Cl (pH 9.5)/100 mM NaCl/5 mM $MgCl_2$ can be used (Sandhu et al., 1991).

Dioxetane phosphate visualization solution

Prepare 0.1 mg/ml AMPPD or CSPD (Applied Biosystems) *or* Lumigen (see Table 6.2.2) substrate in dioxetane phosphate substrate buffer (see recipe). Prepare just before use.

This concentration (240 µM) of AMPPD substrate is the minimum recommended by Applied Biosystems Western Light. Ten-fold lower concentrations can be used but require longer exposures.

Lumi-Phos 530 (Beckman Coulter, Lumigen, Perkin Elmer) is a ready-to-use solution and can be applied directly to the membrane.

Luminol visualization solution

0.5 ml 10× luminol stock [40 mg luminol (Sigma) in 10 ml DMSO]
0.5 ml 10× *p*-iodophenol stock [optional; 10 mg (Aldrich) in 10 ml DMSO]
2.5 ml 100 mM Tris·Cl, pH 7.5 (*APPENDIX 2A*)
25 µl 3% H_2O_2
H_2O to 5 ml
Prepare just before use

Recipe is from Schneppenheim et al. (1991). Alternative recipes are also available (Haan and Behrmann, 2007). Premixed luminol substrate mix (Amersham ECL; Perkin Elmer; Kirkegaard & Perry LumiGLO) may also be used. p-Iodophenol is an optional enhancing agent that increases light output. Luminol and p-iodophenol stocks can be stored for ≤6 months at −20°C.

Ponceau S solution

Dissolve 0.5 g Ponceau S in 1 ml glacial acetic acid. Bring to 100 ml with water. Prepare just before use.

Transfer buffer

Add 18.2 g Tris base and 86.5 g glycine to 4 liters of water. Add 1200 ml methanol and bring to 6 liters with water. The pH of the solution is ~8.3 to 8.4. For use with PVDF filters, decrease methanol concentration to 15%; for nylon filters, omit methanol altogether.

CAPS transfer buffer can also be used. Add 2.21 g cyclohexylaminopropane sulfonic acid (CAPS; free acid), 0.5 g DTT, 150 ml methanol, and water to 1 liter. Adjust to pH 10.5 with NaOH and chill to 4°C. For proteins >60 kDa, reduce methanol content to 1% (Moss, 2001).

DAC EX. 2040 IPR2022-01531 Page 1177 of 1299

COMMENTARY

Background Information

Immunoblotting

Immunoprecipitation has been widely used to visualize the antigens recognized by various antibodies, both polyclonal and monoclonal. However, there are several problems inherent in this method, including the requirement for radiolabeling of antigen, co-precipitation of tightly associated macromolecules, occasional difficulty in obtaining precipitating antibodies, and insolubility of various antigens (Talbot et al., 1984).

To circumvent these problems, electroblotting (Towbin et al., 1979; Kurien and Scofield, 2006)—subsequently popularized as western blotting or immunoblotting (Burnette, 1981)—was conceived. Immunoblotting is a rapid and sensitive assay for the detection and characterization of proteins that works by exploiting the specificity inherent in antigen-antibody recognition. It involves the solubilization and electrophoretic separation of proteins, glycoproteins, or lipopolysaccharides by SDS-PAGE (*UNIT 6.1*) or urea-PAGE, followed by quantitative transfer and irreversible binding to nitrocellulose, PVDF, or nylon.This technique has been useful in identifying specific antigens recognized by polyclonal or monoclonal antibodies and is highly sensitive (1 ng of antigen can be detected).

Protein blotting has many important research and clinical applications. For example, it is the confirmatory test for human immunodeficiency virus Type 1 (HIV-1). SDS-PAGE-separated virus proteins are blotted onto nitrocellulose and processed with patient sera. After washing and probing with an anti-human IgG coupled to HRP or alkaline phosphatase, the antigen-antibody complexes are identified by chromogenic development, indicating the presence of anti-HIV antibodies in the serum. For other selected applications, see Table 6.2.3.

Electroblotting of previously stained gels is a convenient way to visualize and document the gel prior to immunoblotting. Transfer efficiencies at all molecular weights will be lower with fixed and stained gels. This is particularly true of proteins >50 kDa (Perides et al., 1986). The additional incubation in 6 M urea will significantly increase transfer efficiency of all proteins and is required for proteins >50 kDa.

Ponceau S staining provides an easy method for calibrating and quantitating the amount of material on a nitrocellulose or PVDF blot. An alternative to this method is to use an internal protein control with a separate antibody probe, but these tend to be expensive and time-consuming to use. Other applications for Ponceau S calibration include monitoring transfer efficiency under varied conditions for optimization of tank and semidry blotting.

Desired antigens are probed using indirect immunochemistry with secondary antibodies conjugated to horseradish peroxidase (HRP) or alkaline phosphatase (AP). Signal amplification can be achieved by adding a biotin-avidin step using Vectastain ABC kits (Vector Labs). In Alternate Protocol 4, avidin acts as a bridge between biotinylated secondary antibody and biotinylated enzyme (HRP or AP). Sensitivity is improved because the multiple avidin-biotin binding sites increase the amount of enzyme per molecule of secondary antibody. Higher sensitivity is achieved using the Vectastain ABC-AmP kit (Alternate Protocol 6), which uses a preformed complex of streptavidin and biotinylated alkaline phosphatase.

Detection methods

Immunoblotted proteins can be detected using chromogenic or luminescent enzyme substrates (see Basic Protocol 3 and Alternate Protocol 5; see Table 6.2.2 for comparison). Luminescent detection methods offer several advantages over traditional chromogenic procedures. In general, luminescent substrates increase the sensitivity of both HRP and phosphatase systems without the need for radioisotopes (for alkaline phosphatase, see Gillespie and Hudspeth, 1991; Sandhu et al., 1991; Bronstein et al., 1992). Luminescent detection can be completed in as little as a few seconds; exposures rarely go more than 10 min. Depending on the system, the luminescence can last for several hours, permitting multiple exposures of the same blot.

AP-based luminescent protocols that achieve maximum sensitivity with minimum background can be complex, and the manufacturer's instructions should be consulted. The procedure described in Alternate Protocol 5 gives reasonable sensitivity on nitrocellulose, PVDF, and nylon membranes with a minimum of steps.

Alternate Protocol 6 describes an amplification protocol that can be used in chromogenic, chemiluminescent, or fluorescent detection schemes. Chemiluminescent and fluorescent detection are achieved using Vectastain's

DAC EX. 2040 IPR2022-01531 Page 1178 of 1299

Table 6.2.3 Applications of Immunoblotting

Application	Comment
Antibody development and characterization	Characterize antibody specificity
Subcellular localization of an expressed protein	Analyze isolated organelles (e.g., Golgi apparatus, plasma membrane, nucleus) for presence of specific proteins; probe intact cells and tissue for subcellular localization using visible light, fluorescence, and electron microscopy
Protein purification	Demonstrate enrichment of well-characterized antibody by sampling, electrophoresing, and blotting at various stages of purification
Diagnostics	Separate and blot a viral lysate to test serum for antibodies that bind key viral proteins, indicating presence of antibodies against an infection (e.g., HIV testing)
Gene expression	Detect presence or absence and amount of a specific protein during gene expression; track markers and reporter genes (e.g., luciferase) in transgenic organisms to get a complete picture of transcription and translation
Post-translational modifications	Phosphoproteomics: determine phosphorylation status of the protein complement in the cell or tissue using antibodies specific for phospho amino acids
Protein sequencing by mass spectrometry	Characterize the readily available proteins blotted onto membranes using sensitive methods, e.g., peptide sequencing by MALDI (Carr and Annan, 1996)

DuoLuX Chemiluminescent/Fluorescent Substrate, a novel acridan-based substrate that can be used not only in immunoblots, as described here, but also in nucleic acid detection methods (e.g., Southern and northern blotting, colony lifts, ELISAs). The substrate is available for either AP or HRP development. Generally, signal development is faster when using HRP. Thus, HRP may be preferred when digital imaging systems are used or when abundance of target reduces the need for a high signal-to-noise ratio. However, for applications where optimal sensitivity is required, AP is recommended, as it will provide a higher signal-to-noise ratio than HRP.

The DuoLuX Chemiluminescent/Fluorescent Substrate has very high sensitivity and prolonged light-emission characteristics. This enables image documentation with either film or digital imaging systems (see below). Unlike some chemiluminescent substrates, blots can be re-exposed to film as often as necessary over many hours. Because many digital imaging systems require a longer exposure time than film, the faster signal development of HRP relative to AP may be preferred when using these systems. PVDF, nitrocellulose, or nylon membranes can be used, although the chemiluminescent signal develops faster on nylon and PVDF.

In addition to its chemiluminescent properties, the reaction product is also fluorescent. Fluorescence can be recorded with a digital imaging system or a conventional camera months after chemiluminescence has faded. For fluorescence detection, nitrocellulose is recommended due to the intrinsic fluorescence of nylon. Acquisition of fluorescent signal requires a much shorter exposure time than chemiluminescence, often a fraction of a second.

Imaging methods

Film contact exposure or CCD-based digital imaging can be used to capture the signal from chemiluminescent blots. Film-based capture is inexpensive to get started and requires very little in the way of equipment: film, processing chemicals, and cassettes that hold the blot close to the film. Film produces a physical record that is robust, and the film can be scanned for quantitation. However, in spite of the high initial cost, CCD-based imaging hardware has a number of advantages over film, including speed, ease of use, and data quality. First, CCD cameras with appropriate optics, cooled to minimize thermal noise, are much more sensitive than film (Fig. 6.2.6). Second, CCD image capture requires many fewer steps. The camera's preview function gives an

DAC EX. 2040 IPR2022-01531 Page 1179 of 1299

accurate estimate of exposure time for capture of the image. Trial exposures and developing are not needed as with film. Finally, CCD capture yields higher-quality data with a wider linear range compared to film, and digital files can be automatically date stamped and archived on backup systems.

Scientific CCD cameras, cooled from ambient temperature to –20°C to –100°C, are needed for the range of exposures required for chemiluminescent imaging. Cooling lowers the dark noise on the CCD sensor, so that longer exposures (up to 60 min or more) are possible without a significant increase in background noise (Medberry et al., 2004).

In addition to cooling, CCD binning, where groups of pixels are imaged at one time, is important for high-sensitivity low-light imaging. By grouping pixels into a single large pixel, signal is collected much more quickly, giving a higher signal-to-noise ratio (Medberry et al., 2004). The disadvantage of this technique is that the output resolution is also reduced. By using a typical configuration of 4 × 4 binning, 16 pixels on the sensor become effectively one, lowering output resolution.

Successful digital imaging of chemiluminescent immunoblots depends not only on the camera sensor and cooling, but also on the optics, which determine how much light is collected and imaged onto the CCD sensor. The standard designation of light-gathering capacity in the lens is the *f* number or *f*-stop. Typical *f*-stops range from *f*/22, letting in the least light, to *f*/1.2 or lower, letting in the most light (aperture blades wide open). Lenses designed for low-light imaging typically have designations at or below *f*/1.2.

Image quantitation is accomplished with image analysis software. Internal standards can be added to the separation (a probe or protein of known amount) to serve as a relative reference. Luminescent blots can be easily erased and reprobed because the reaction products are soluble and do not deposit on the membrane. Compared to chromogenic development, the luminescent image is easier to photograph and to quantitate by densitometry.

Critical Parameters

First and foremost, the antibody being used should recognize denatured antigen. Nonspecific binding of antibodies can occur, so control antigens and antibodies should always be run in parallel. Time of transfer and primary antibody and conjugate dilutions should always be optimized.

A variety of agents are currently used to block binding sites on the membrane after blotting (Harlow and Lane, 1999). These include Tween 20, PVP, nonfat dry milk, casein, BSA, and serum. A 0.1% (v/v) solution of Tween 20 in TBS (TTBS), a convenient alternative to protein-based blocking agents, is recommended for chromogenic development of nitrocellulose and PVDF membranes (Blake et al., 1984). In contrast to dry milk/TBS blocking solution (BLOTTO), TTBS is stable and has a long shelf life at 4°C. Furthermore, TTBS generally produces a clean background and permits subsequent staining with India ink. However, even with the application of such standard blocking procedures as 5% to 10% milk protein or 0.05% to 0.1% Tween 20, background can still be a significant problem. If this happens, using a blocking protein (e.g., goat, horse, or rabbit normal serum) from the same species as the primary antibody can reduce the background, presumably by reducing cross-reactivity between the primary antibodies and the blocking agent. If a secondary antibody detection is used, the blocking protein (i.e., normal serum) should be from the same species as the secondary antibody. Combinations of blocking agents can also be effective. Thus, 0.1% human serum albumin (HSA) and 0.05% Tween 20 in TBS is recommended when probing Immobilon-P membranes with human serum (Craig et al., 1993). However, this can also lead to overall loss of antigen signal, requiring a ten-fold increase in the primary antibody (serum) concentration to achieve an adequate background-free antigen signal.

When using chemiluminescent detection for immunoblotting, high background frequently occurs, particularly for strong signals (Pampori et al., 1995). Several methods are available for reducing the background from chemiluminescent reactions. These include changing the type and concentration of blocking agents, optimizing antibody concentrations, letting the reaction proceed for several minutes before imaging, or simply limiting the exposure time of the blot. These procedures are not always successful, however, and can lead to inconsistent results. An alternative approach is to reduce the concentration of reagents tenfold. This effectively removes the background and has a number of advantages which include lower cost, increased signal-to-noise ratio, and reduced detection of cross-reacting species.

Currently, due to a combination of low background and ease of processing, PVDF and nitrocellulose membranes are the most

DAC EX. 2040 IPR2022-01531 Page 1180 of 1299

commonly used membranes for protein blotting. Nylon membranes, typically used for nucleic acid blotting applications, are robust and can be used for protein blotting as well. However, nylon requires more stringent blocking to minimize background, limiting its popularity for protein blotting applications. Two types of nylon membrane are used for protein transfer—neutral (e.g., Pall Biodyne A) and positively charged (e.g., Pall Biodyne B). Although the positively charged membranes have very good protein-binding characteristics, they tend to give a higher background. These membranes remain positively charged from pH 3 to pH 10. Neutral nylon membranes are also charged, having a mix of amino and carboxyl groups that give an isoelectric point of 6.5. Because of their high binding capacity, positively charged membranes have been popular for protein applications using luminescence.

Nylon membranes require more stringent blocking steps. Here 10% nonfat dry milk in TBS is recommended for chromogenic development. During luminescence development, however, background is a more significant problem. Compared to dry milk, purified casein has minimal endogenous alkaline phosphatase activity (AP activity leads to high background) and is therefore recommended as a blocking agent for nitrocellulose, PVDF, and nylon membranes. Positively charged nylon requires much more stringent blocking with 6% (w/v) casein and 1% (v/v) polyvinylpyrrolidone (PVP). Because nonfat dry milk and casein may contain biotin that will interfere with avidin-biotin reactions, subsequent steps are done without protein-blocking agents when using these systems. If background is a problem, highly purified casein (0.2% to 6%) added to the antibody incubation buffers may help.

If reprobing is desired, blots can be air dried and stored at 4°C for 3 months after chemiluminescence detection. After drying, store in a sealed freezer bag until use. Repeated probing will lead to a gradual loss of signal and increased background. However, this will depend in part on the properties of the sample.

If the primary procedure is problematic due to loss of sensitivity or an increase in background, two possible alternative procedures for stripping membranes are recommended. The first uses 2-mercaptoethanol and SDS (Kaufmann et al., 1987; Tesfaigzi et al., 1994). Briefly, the membranes are incubated in 2% SDS/100 mM Tris·Cl, pH 7.4/100 mM 2-mercaptoethanol for 30 min at 70°C, effectively removing primary and secondary antibodies. As with the primary procedure recommended above, repeated probing should be done with caution due to the potential loss of detection signal, and 5% nonfat dry milk is required as a blocking agent. The milk blocking agent facilitates antibody removal from the blot (Kaufmann et al., 1987). The second uses guanidine·HCl. For nylon and PVDF membranes (do *not* use with nitrocellulose), incubate the immunoblot in 7 M guanidine·HCl for 10 min at room temperature. (The short wash time is critical, as guanidine·HCl is a very strong denaturant, so do not leave the filter in this solution >15 min.) Pour off excess guanidine·HCl and then rinse the membrane several times in 1× TTBS. Reblock the membrane and proceed with the standard immunoblotting procedure. Membranes stripped using this procedure can generally be reused three or four times.

In Alternate Protocol 6, extensive washing will reduce signal strength, so the wash time should not be extended unless high background is observed. If background is excessive, use a wash time of 5 to 10 min in step 8a (may require optimization). The long emission lifetime of the substrate allows the blot to be re-exposed until an optimal signal-to-noise ratio is achieved. Blotting can be done onto either nylon or nitrocellulose. Nylon requires shorter exposure times, and is therefore preferred for chemiluminescent applications. However, because of nylon's intrinsic fluorescence, nitrocellulose is preferred for fluorescence detection.

Troubleshooting

There are several problems associated with immunoblotting. The antigen is solubilized and electrophoresed in the presence of denaturing agents (e.g., SDS or urea), and some antibodies may not recognize the denatured form of the antigen transferred to the membrane. The results observed may be entirely dependent on the denaturation and transfer system used. For example, zwitterionic detergents (e.g., Zwittergent 3-14 from EMD Chemicals, *http://www.emdbiosciences.com*) have been shown to restore the antigenicity of outer membrane proteins in immunoblotting (Mandrell and Zollinger, 1984). Gel electrophoresis under nondenaturing conditions can also be performed.

Other potential problems include high background, nonspecific or weak cross-reactivity of antibodies, poor protein transfer or membrane binding efficiency, and insufficient sensitivity. For an extensive survey and

DAC EX. 2040 IPR2022-01531 Page 1181 of 1299

discussion of immunoblotting problems and artifacts, see Bjerrum et al. (1988).

If no transfer of protein has occurred, check the power supply and electroblot apparatus to make sure that the proper electrical connections were made and that power was delivered during transfer. In addition, check that the correct orientation of filter and gel relative to the anode and cathode electrodes was used.

If the transfer efficiency using the tank system appears to be low, increase the transfer time or power. Cooling (using the unit's built-in cooling cores) is generally required for transfers >1 hr. At no time should the buffer temperature go above 45°C. Prolonged transfers (>1 hr) are not possible in semidry transfer units due to rapid buffer depletion.

Alternatively, the transfer buffer can be modified to increase efficiency. Adding SDS to the transfer buffer at a concentration of 0.1% improves the transfer of all proteins out of the gel, particularly those above 60 to 90 kDa in size. Lowering the concentration of methanol will also improve the recovery of proteins from the gel. These procedures are tradeoffs. Methanol improves the binding of proteins to PVDF and nitrocellulose, but at the same time hinders transfer. With SDS present, transfer efficiency is improved, but the SDS can interfere with protein binding to the membrane. Nylon and PVDF membranes are particularly sensitive to SDS interference. If needed, 0.01% to 0.02% SDS may be used in PVDF membrane transfer buffers (Pluskal et al., 1986). SDS and methanol should not be used in the transfer buffer for nylon (Peluso and Rosenberg, 1987).

Gel cross-linking and thickness also have a profound effect on the transfer efficiency. In general, 0.5- to 0.75-mm-thick gels will transfer much more efficiently than thicker gels (e.g., 1.5 mm thick). Gels with a higher acrylamide percentage will also transfer less efficiently. Proteins can be particularly difficult to transfer from gradient gels, and a combination of longer transfer times, thin gels, and the addition of SDS to the transfer buffer may be needed.

If the protein bands are diffuse, check the transfer cassette. The gel must be held firmly against the membrane during transfer. If the transfer sandwich is loose in the cassette, add another thin sponge or more blotter paper to both sides.

Occasionally, a grid pattern will be apparent on the membrane after tank transfer. This is caused by having either the gel or the membrane too close to the sides of the cassette. Correct this by adding more layers of filter paper to diffuse the current flowing through the gel and membrane. Use a thinner sponge and more filter paper if necessary.

If air bubbles are trapped between the filter and the gel, they will appear as clear white areas on the filter after blotting and staining. Take extra care to make sure that all bubbles are removed.

Insufficient blocking or nonspecific binding of the primary or secondary antibody will cause a high background stain. A control using preimmune serum or only the secondary antibody will determine if these problems are due to the primary antibody. Try switching to another blocking agent; protein blocking agents may weakly cross-react. Lowering the concentration of primary antibody should decrease background and improve specificity (Fig. 6.2.5).

Due to the nature of light and the method of detection, certain precautions are warranted when using luminescent visualization (e.g., Harper and Murphy, 1991). Very strong signals can overshadow nearby weaker signals on the membrane. Because light will pipe through the membrane and the surrounding plastic wrap, overexposure will produce a broad diffuse image on the film. The signal can also saturate the film, exposing the film to a point whereby increased exposure will not cause a linear increase in the density of the image on the film.

With the alkaline phosphatase substrate AMPPD, nitrocellulose, PVDF, and nylon membranes require 2, 4, and 8 to 12 hr, respectively, to reach maximum light emission. In addition, PVDF is reported to give a stronger signal than nitrocellulose (Applied Biosystems Western Light instructions). Positively charged nylon requires special blocking procedures to minimize background (Gillespie and Hudspeth, 1991). These procedures include using a blocking and primary antibody solution containing 6% casein, 1% polyvinylpyrrolidone-40 (PVP-40), 3 mM NaN_3, 10 mM EDTA, and PBS, pH 6.8. Prior to use, the casein must be heated to 65°C to reduce alkaline phosphatase activity in the casein itself. In addition, maximum sensitivity has been observed when free biotin or biotinylated proteins are removed by pretreating the casein with avidin-agarose (Sigma).

Anticipated Results

Immunoblotting should result in the detection of one or more bands. Although antibodies directed against a single protein should produce a single band, degradation of the

DAC EX. 2040 IPR2022-01531 Page 1182 of 1299

sample (e.g., via endogenous proteolytic activity) may cause visualization of multiple bands of slightly different size. Multimers will also form spontaneously, causing higher-molecular-weight bands on the blot. If simultaneously testing multiple antibodies directed against a complex protein mixture (e.g., using patient sera against viral proteins in AIDS western blot test), multiple bands will be visualized.

For immunoblot or protein dot blot chemiluminescent applications, the sensitivity using HRP is ~1 pg of target protein. For chemiluminescent blots, DuoLuX Chemiluminescent/Fluorescent Substrate (see Alternate Protocol 6) can be used on either nitrocellulose or PVDF membranes.

Time Considerations

The entire immunoblotting procedure can be completed in 1 to 2 days, depending on transfer time and type of gel. Gel electrophoresis requires 4 to 6 hr on a regular gel and 1 hr on a minigel. Transfer time can be 1 hr (high-power transfer) to overnight. Blocking, antibody probing, conjugate incubation, and washing each take 30 min to 1 hr. Finally, substrate incubation requires 10 to 30 min (chromogen) and a few seconds to several hours (luminescence).

For the DuoLuX Chemiluminescent/Fluorescent Substrate (see Alternate Protocol 6), optimal exposure times can vary from 5 sec to 15 min. It is recommended that initial exposures be taken between 1 and 5 min. Band intensities or resolution can then be optimized by lengthening or shortening exposure times based on the initial results.

Literature Cited

Bjerrum, O.J., Larsen, K.P., and Heegaard, N.H.H. 1988. Nonspecific binding and artifacts-specificity problems and troubleshooting with an atlas of immunoblotting artifacts. *In* CRC Handbook of Immunoblotting of Proteins, Vol. I: Technical Descriptions (O.J. Bjerrum and N.H.H. Heegaard, eds.) pp. 227-254. CRC Press, Boca Raton, Fla.

Blake, M.S., Johnston, K.H., Russell-Jones, G.J., and Gotschlich, E.C. 1984. A rapid, sensitive method for detection of alkaline phosphatase–conjugated anti-antibody on Western blots. *Anal. Biochem.* 136:175-179.

Bronstein, I., Voyta, J.C., Murphy, O.J., Bresnick, L., and Kricka, L.J. 1992. Improved chemiluminescent Western blotting procedure. *BioTechniques* 12:748-753.

Burnette, W.N. 1981. Western blotting: Electrophoretic transfer of proteins from sodium dodecyl sulfate-polyacrylamide gels to unmodified nitrocellulose and radiographic detection with antibody and radioiodinated protein A. *Anal. Biochem.* 112:195-203.

Carr, S.A. and Annan, R.S. 1996. Overview of peptide and protein analysis by mass spectrometry. *Curr. Protoc. Prot. Sci.* 4:16.1.1-16.1.27.

Craig, W.Y., Poulin, S.E., Collins, M.F., Ledue, T.B., and Ritchie, R.F. 1993. Background staining in immunoblot assays. Reduction of signal caused by cross-reactivity with blocking agents. *J. Immunol. Methods* 158:67-76.

Dionisi, H.M., Checa, S.K., and Viale, A.M. 1995. Protein immunoblotting of stained gels. *BioTechniques* 19:348-350.

Gillespie, P.G. and Hudspeth, A.J. 1991. Chemiluminescence detection of proteins from single cells. *Proc. Natl. Acad. Sci. U.S.A.* 88:2563-2567.

Haan, C. and Behrmann, I. 2007. A cost effective noncommercial ECL-solution for Western blot detections yielding strong signals and low background. *J. Immunol. Methods* 318:11-19.

Harlow, E. and Lane, D. 1999. Using Antibodies: A Laboratory Manual. Cold Spring Harbor Laboratory Press, Cold Spring Harbor, N.Y.

Harper, D.R. and Murphy, G. 1991. Nonuniform variation in band pattern with luminol/horseradish peroxidase Western blotting. *Anal. Biochem.* 192:59-63.

Kaufmann, S.H., Ewing, C.M., and Shaper, J.H. 1987. The erasable Western blot. *Anal. Biochem.* 161:89-95.

Klein, D., Kern, R.M., and Sokol, R.Z. 1995. A method for quantification and correction of proteins after transfer to immobilization membranes. *Biochem. Mol. Biol. Int.* 36:59-66.

Kurien, B.T. and Scofield, R.H. 2006. Western blotting. *Methods* 38:283-293.

Mandrell, R.E. and Zollinger, W.D. 1984. Use of zwitterionic detergent for the restoration of antibody-binding capacity of electroblotted meningococcal outer membrane proteins. *J. Immunol. Methods* 67:1-11.

McKimm-Breschkin, J.L. 1990. The use of tetramethylbenzidine for solid phase immunoassays. *J. Immunol. Methods* 135:277-280.

Medberry, S., Gallagher, S., and Moomaw, B. 2004. Overview of digital electrophoresis analysis. *Curr. Protoc. Moe. Biol.* 66:10.5.1-10.5.25.

Moss, M. 2001. Isolation of proteins for microsequence analysis. *Curr. Protoc. Mol. Biol.* 21:10.19.1-10.19.12.

Pampori, N.A., Pampori, M.K., and Shapiro, B.H. 1995. Dilution of the chemiluminescence reagents reduces the background noise on Western blots. *BioTechniques* 18:588-590.

Peluso, R.W. and Rosenberg, G.H. 1987. Quantitative electrotransfer of proteins from sodium dodecyl sulfate polyacrylamide gels onto positively charged nylon membranes. *Anal. Biochem.* 162:389-398.

DAC EX. 2040 IPR2022-01531 Page 1183 of 1299

Perides, G., Plagens, U., and Traub, P. 1986. Protein transfer from fixed, stained, and dried polyacrylamide gels and immunoblot with protein A–gold. *Anal. Biochem.* 152:94-99.

Pluskal, M.G., Przekop, M.B., Kavonian, M.R., Vecoli, C., and Hicks, D.A. 1986. A new membrane substrate for western blotting of proteins. *BioTechniques*. 4:272.

Sandhu, G.S., Eckloff, B.W., and Kline, B.C. 1991. Chemiluminescent substrates increase sensitivity of antigen detection in Western blots. *BioTechniques* 11:14-16.

Schneppenheim, R., Budde, U., Dahlmann, N., and Rautenberg, P. 1991. Luminography—a new, highly sensitive visualization method for electrophoresis. *Electrophoresis* 12:367-372.

Suck, R.W.L. and Krupinska, K. 1996. Repeated probing of Western blots obtained from Coomassie Brilliant Blue–stained or unstained polyacrylamide gels. *BioTechniques* 21:418-422.

Talbot, P.V., Knobler, R.L., and Buchmeier, M. 1984. Western and dot immunoblotting analysis of viral antigens and antibodies: Application to murine hepatitis virus. *J. Immunol. Methods* 73:177-188.

Tesfaigzi, J., Smith-Harrison, W., and Carlson, D.M. 1994. A simple method for reusing western blots on PVDF membranes. *BioTechniques* 17:268-269.

Towbin, H., Staehelin, T., and Gordon, J. 1979. Electrophoretic transfer of proteins from polyacrylamide gels to nitrocellulose sheets: Procedure and some applications. *Proc. Natl. Acad. Sci. U.S.A.* 76:4350-4354.

Key References

Bjerrum, O.J. and Schafer-Nielsen, C. 1986. Buffer systems and transfer parameters for semidry electroblotting with a horizontal apparatus. *In* Electrophoresis '86 (M.J. Dunn, ed.) pp. 315-327. VCH Publishers, Deerfield Beach, Fla.

Describes the semidry blotting system.

Gillespie and Hudspeth, 1991. See above.

Describes alkaline phosphatase–luminescent detection methods.

Harlow and Lane, 1999. See above.

Details alternative detection methods.

Salinovich, O. and Montelaro, R.C. 1986. Reversible staining and peptide mapping of proteins transferred to nitrocellulose after separation by sodium dodecyl sulfate-polyacrylamide gel electrophoresis. *Anal. Biochem.* 156:341-347.

Describes the use of Ponceau S staining for immunoblotting.

Schneppenheim et al., 1991. See above.

Details peroxidase-based luminescent detection methods.

DAC EX. 2040 IPR2022-01531 Page 1184 of 1299

Appendix WIDDISON01

MARC View

LEADER 02264nas a2200493 a 4500				
001 46009249				
003 SIRSI				
005 20241114090046.0				
006 m o d				
007 cr n				
008 980714c19639999dcuer pss 0 a0eng c				
010				a| sn 98004585
016	7			a| 1491411 6 2| DE-600
019				a| DO NOT EDIT this 360 MARC RECORD
022				a| 1520-4804 l| 0022-2623 y| 0022-2623
035				a| (WaSeSS)ssj0003123
037				b| Journal of Medicinal Chemistry, Member & Subscriber Services, Dept. L-0011, Columbus OH 43210 c| Members: $89.00-$113.00 c| Non-Members: $246.00-$313.00 c| Institutional: $1,132.00-$2,037.00
040				a| NSD b| eng e| pn c| NSD d| UMC d| IUL d| RBN d| OCLCQ d| MUQ d| OCLCQ d| OCL d| NSD d| CIT d| OCLCQ d| OCLCF d| OCLCO d| EUW d| OCLCO d| OCLCQ d| EZC d| GILDS d| AU@ d| OCLCO d| OCLCA d| DCHUA d| TKN d| U3W d| VT2 d| OCLCO d| DLC d| OCLCQ d| UAB d| WaSeSS
042				a| nsdp a| pcc
050	0	0	a| RS402	
050	1	4	a| RS400 b| .J65	
082	1	0	a| 616 2| 13	
130	0			a| Journal of medicinal chemistry (Online)
210	0			a| J. med. chem. b| (Online)
222		0	a| Journal of medicinal chemistry b| (Online)	
245	1	0	a| Journal of medicinal chemistry h| [electronic resource].	
260				a| Washington DC : b| ACS Publications
310				a| Biweekly
362	1			a| Print began with vol. 6, no. 1 (Jan. 1963).
500				a| Title from issue contents display (viewed Oct. 29, 1998).
530				a| Also issued in print.
538				a| Mode of access: World Wide Web.
588				a| Latest issue consulted: Vol. 64, Issue 18 (Sept. 23, 2021) (ACS Publications website, viewed Sept. 24, 2021).
650		0	a| Pharmaceutical chemistry v| Periodicals.	
650		0	a| Clinical chemistry v| Periodicals.	
650		2	a| Chemistry, Pharmaceutical.	
655		0	a| Electronic journals.	
710	2			a| American Chemical Society.
776	1			t| Journal of medicinal chemistry x| 0022-2623 w| (DLC)a 63000643 w| (OCoLC)1754668
780	0	0	t| Journal of medicinal and pharmaceutical chemistry x| 1943-2992 w| (DLC) 2008213191 w| (OCoLC)51314022	
856	4	0	u| http://SK8ES4MC2L.search.serialssolutions.com/?V=1.0&L=SK8ES4MC2L&S=JCs&C=JOUROFMEDCH&T=marc	
910				a| CONSER online
850				a| DLC
949				a| Electronic resource w| ASIS c| 1 i| 46009249-1001 l| ONLINE m| ONLINE r| Y s| Y t| ONLINE u| 11/16/2024 o| .STAFF. 360 MARC

ASK A LIBRARIAN

PennState

Copyright ©2019 The Pennsylvania State University. All rights reserved. Except where otherwise noted, this work is subject to a Creative Commons Attribution 4.0 license. Details and exceptions.

Legal Statements | PSU Hotlines

PENN STATE UNIVERSITY LIBRARIES

Libraries Home (814) 865-6368
Libraries Intranet (Staff Only)
Accessibility Help
Website Feedback
Policies and Guidelines
Staff Directory

CONNECT WITH PENN STATE UNIVERSITY LIBRARIES

Facebook
Twitter
Instagram

Journal of medicinal chemistry [electronic resource].

Uniform Title	Journal of medicinal chemistry (Online)
Additional Titles	J. med. chem. (Online)
Published	Washington DC : ACS Publications
Additional Creators	American Chemical Society

ASK A LIBRARIAN

Access Online
serialssolutions.com

Continues
Journal of medicinal and pharmaceutical chemistry

Dates of Publication and/or Sequential Designation
Print began with vol. 6, no. 1 (Jan. 1963).

Subject(s)
Pharmaceutical chemistry—Periodicals
Clinical chemistry—Periodicals
Chemistry, Pharmaceutical

Genre(s)
Electronic journals

ISSN
1520-4804

Publication Frequency
Biweekly

Note
Title from issue contents display (viewed Oct. 29, 1998).

Other Forms
Also issued in print.

Technical Details
Mode of access: World Wide Web.

View MARC record | catkey: 46009249

PennState

Copyright @2019 The Pennsylvania State University. All rights reserved. Except where otherwise noted, this work is subject to a Creative Commons Attribution 4.0 license. Details and exceptions.

Legal Statements | PSU Hotlines

PENN STATE UNIVERSITY LIBRARIES
Libraries Home (814) 865-6368
Libraries Intranet (Staff Only)
Accessibility Help
Website Feedback
Policies and Guidelines
Staff Directory

CONNECT WITH PENN STATE UNIVERSITY LIBRARIES
Facebook
Twitter
Instagram

○ All ● Journals Only ○ Books Only ○ Videos Only

Title begins with | Search

Show more search options ▼

Showing results 1 through 1 of 1

for the search: "JOUROFMEDCH"

Refine Results: All | Journals Only | Books Only | Videos Only

Limit by: Peer Reviewed | Open Access



Journal of medicinal chemistry

ISSN: 0022-2623

Peer Reviewed

01/01/1963 to 12/31/1995 in American Chemical Society Legacy Archives

01/01/1963 to Present in American Chemical Society Publications

Search inside this journal | Search

Back to Top

Last Updated on 12-02-2024 © Ex Libris, a ProQuest Company, 2000-2024

Privacy Policy

Journal of Medicinal Chemistry

ADVERTISEMENT

Get e-Alerts

Subscribed

Cite Share Jump to

ARTICLE | June 10, 2006

Semisynthetic Maytansine Analogues for the Targeted Treatment of Cancer

Wayne C. Widdison, Sharon D. Wilhelm, Emily E. Cavanagh, Kathleen R. Whiteman, Barbara A. Leece, Yelena Kovtun, Victor S. Goldmacher, Hongsheng Xie, Rita M. Steeves, Robert J. Lutz, Robert Zhao, Lintao Wang, Walter A. Blättler, and Ravi V. J. Chari

View Author Information

Open PDF | Supporting Information (1)

Journal of Medicinal Chemistry

Cite this: *J. Med. Chem.* 2006, 49, 14, 4392–4408

https://doi.org/10.1021/jm060319f

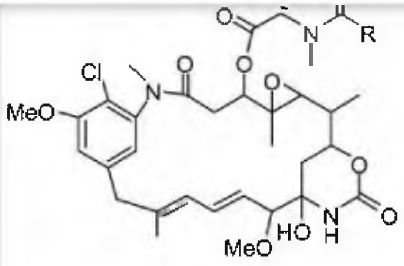
Published June 10, 2006

Copyright © 2006 American Chemical Society

Request reuse permissions

DAC EX. 2040 IPR2022-01531 Page 1189 of 1299

Journal of
Medicinal Chemistry



R = CH_2CH_2SSR', $CH_2CH_2CH(CH_3)SSR'$, $CH_2CH_2C(CH_3)_2SSR'$

R' = CH_3 or a monoclonal antibody

Maytansine, a highly cytotoxic natural product, failed as an anticancer agent in human clinical trials because of unacceptable systemic toxicity. The potent cell killing ability of maytansine can be used in a targeted delivery approach for the selective destruction of cancer cells. A series of new maytansinoids, bearing a disulfide or thiol substituent were synthesized. The chain length of the ester side chain and the degree of steric hindrance on the carbon atom bearing the thiol substituent were varied. Several of these maytansinoids were found to be even more potent in vitro than maytansine. The targeted delivery of these maytansinoids, using monoclonal antibodies, resulted in a high, specific killing of the targeted cells in vitro and remarkable antitumor activity in vivo.

This publication is licensed under the terms of your institutional subscription. Request reuse permissions.

Copyright © 2006 American Chemical Society

Subjects

Biopolymers Conjugate Acid-Base Pairs Disulfides Immunology Peptides And Proteins

* Corresponding author. Tel: (617) 995-2500. Fax: (617) 995-2510. E-mail: ravi.chari@immunogen.com.

Abbreviations: DMA, dimethylacetamide; SPP, *N*-succinimidyl 4-(2-pyridyldithio)pentanoate; SPDB, *N*-succinimidyl 4-(2-pyridyldithio)butanoate.

Introduction

Maytansine (**1**) was originally isolated from the bark of the African shrub *Maytenus ovatus* by Kupchan and colleagues [1] and is the first compound of a class of benzoansamacrolide antibiotics named maytansinoids. [2] Maytansinoids are antimitotic agents that bind to tubulin and inhibit microtubule assembly. [3] They bind to the same site on tubulin as the *Vinca* alkaloids do, and similar inhibitory constants were measured for both drug classes. [4] However, many maytansinoids are 100

DAC EX. 2040 IPR2022-01531 Page 1190 of 1299

Journal of
Medicinal Chemistry

Further development stopped, and maytansine became one of the many cytotoxic agents that were discontinued for the lack of a sufficiently large therapeutic window.

Although, maytansine was not effective in human clinical trials, the unusually high cytotoxic activity of the maytansinoids makes them attractive candidates for tissue-specific delivery. Tumor-reactive monoclonal antibodies are large proteins that bind with high affinity to receptors that are selectively expressed on the surface of cancer cells. Although these antibodies display high specificity for the tumor, a majority of them are not potent enough to be therapeutically useful. Imaging studies with radiolabeled antibodies have demonstrated the localization of antibodies at the tumor site in cancer patients; however, the concentration of antibodies achieved at the tumor was quite low.[7] The in vitro cytotoxic inhibitory concentrations (IC_{50} values) of maytansinoids are even lower than the antibody concentrations achieved at the tumor, making them suitable candidates for targeted delivery using antibodies. The selective delivery to tumor tissue has the effect of changing the in vivo distribution and pharmacokinetics of the cytotoxic agent. Humanized monoclonal antibodies typically have a circulation half-life of about two weeks in humans and are largely found in the vascular and extravascular plasma space. Thus, linking a small drug molecule to the antibody will prevent penetration into healthy tissue and can extend the in vivo half-life of the drug (typically, minutes to a few hours for the unconjugated drug) to as long as two weeks, thereby accumulating a proportionally larger amount at the malignant tissue than at the healthy tissues.[8] Thus, this method of delivery should effectively contribute to a wider therapeutic window for the maytansinoids and make them effective anticancer agents. Preclinical evaluations of the first set of antibody−maytansinoid conjugates have demonstrated that this targeted delivery approach greatly improves the tumor specificity and the antitumor activity of the maytansinoid.[9,10] On the basis of this promising preclinical data, the first antibody−maytansinoid conjugate has undergone a phase I clinical evaluation in patients with colorectal and pancreatic cancers.[11,12]

Delivery of the maytansinoid by a monoclonal antibody requires that the maytansinoid is stably linked to the antibody. However, once the antibody has bound to the antigen on the cancer cells and the antibody−antigen complex is internalized into the cell, the cytotoxic agent needs to be released inside the cell to enable it to efficiently arrive at the target and inactivate it. If one considers that the cytoplasm of cells contains millimolar concentrations of the thiol-containing tripeptide, glutathione, whereas the concentration of glutathione in human blood is about 1000-fold lower (generally in the micromolar range), then a disulfide bond appears to have ideal chemical characteristics.[13] It is thermodynamically very stable (bond energy of about 65 kcal/mol) but kinetically labile in the presence of sulfhydryl groups. The strength of the disulfide bond can be manipulated to achieve maximal stability during circulation in the blood stream, while allowing for efficient cleavage inside the target cell. This is achieved by the introduction of methyl substituents on the carbon atoms geminal to the disulfide link, conferring varying degrees of steric hindrance. We, therefore, set out to synthesize maytansinoid analogues that contained sulfhydryl groups and showed equal or enhanced cytotoxic activity relative to that of the parent compound, maytansine. Some of these

DAC EX. 2040 IPR2022-01531 Page 1191 of 1299

Journal of
Medicinal Chemistry

side chain, the C4-C5 epoxide moiety, the C9 carbinol function, and the position of the conjugated C11 and C13 double bonds as critical elements for activity. [14] This left the phenyl ring and the *N*-acyl group as chemically modifiable entities. Although the *N*-acyl group is required for biological activity, studies by Kupchan et al [15] have shown that the nature of the acyl group can be varied without a significant loss in activity. Thus, we initially replaced the *N*-acetyl group in maytansine (**1**) with a 3-methyldithiopropionyl group, thus producing disulfide-containing maytansinoid **2b** (DM1SMe), (Figure 1). On the basis of the promising in vitro potency data of this compound, we then synthesized a variety of disulfide and thiol-containing maytansinoids bearing different *N*-acyl-*N*-methyl-L-alanyl ester moieties at the C3 position. A representative set of these maytansinoids were then conjugated to monoclonal antibodies to provide conjugates with varying disulfide bond strengths. The synthesis of these new maytansinoids and the results from their biological testing in free form or as conjugates of monoclonal antibodies is reported herein.

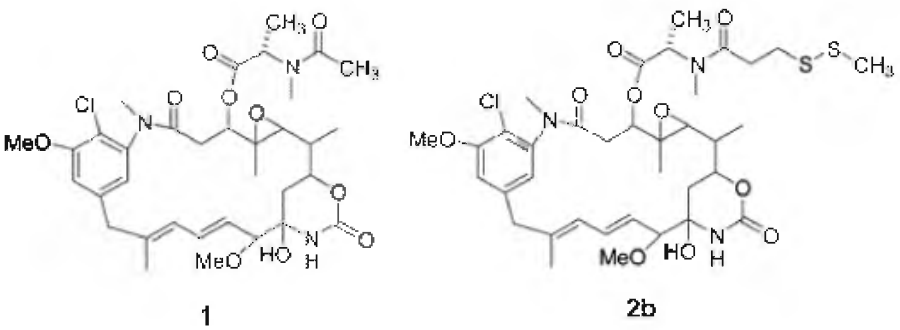


Figure 1 Structures of maytansine and disulfide-containing maytansinoid.

Biosynthetically, maytansinoids are complex polyketides. Consequently, soon after the initial isolation from plants, a bacterial actinomycetes strain *Actinosynnema pretiosum* was isolated, which produces ansamycin antibiotics called ansamitocins that are maytansinoids with C3 alkanoic acid esters. [16,17] Because ansamitocins lack the C3 *N*-acyl-*N*-methyl-L-alanyl side chain, they have diminished cytotoxicity; however, they constitute a ready starting material for the preparation of maytansinoid analogues with novel C3 side chains.

Results and Discussion

Chemistry. The chemistry followed the scheme originally designed by Kupchan at al.,[5,15] who first reported the chemical conversion of maytansine to the C3 hydroxy compound, maytansinol, and its subsequent conversion to different C3 esters. Esterification of maytansinol with alkanoic acids gave the bacterial ansamitocins. Kawai et al., [18] have described the esterification of maytansinol with a variety of *N*-acyl- *N*-methyl-L-alanyl compounds to produce highly active C3 ester analogues of maytansine.

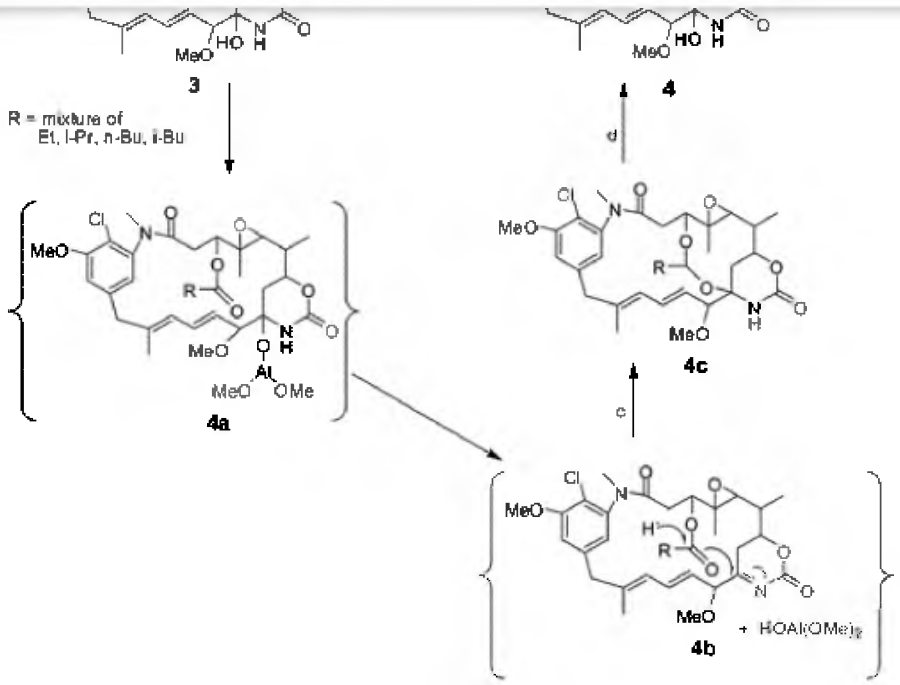
DAC EX. 2040 IPR2022-01531 Page 1192 of 1299

Journal of
Medicinal Chemistry

and pentanoate esters. The predominant species (~80%) was the C3 isobutyrate ansamitocin P-3. Because the C3 ester group in maytansinoids is susceptible to elimination under mild basic conditions (pH >9) to give the α,β-unsaturated maytansinoid maysine,[19] ester hydrolysis was achieved through a reductive cleavage process. The previously described method[15] for the reductive cleavage of the C3 ester used lithium aluminum hydride and gave low yields of maytansinol with several side products. Several other reducing agents, including DIBAL, $NaBH_4$, Red-Al, or Red-Al + 1 eq methanol, gave poor yields and multiple side products. Attempted enzymatic cleavage of the ester using a wide panel of commercially available esterases and lipases was also unsuccessful, with no detectable hydrolysis. However, the ester group in the ansamitocins was efficiently cleaved using the mild reducing agent lithium trimethoxyaluminum hydride, under controlled temperature (−30 to −40 °C), to give maytansinol in good yields. Higher reaction temperatures led to epoxide opening, whereas colder reaction temperatures resulted in a high proportion of unreacted starting material. Maytansinol was obtained after quenching the reaction mixture at −40 °C with water, which resulted in a pH of about 12, and holding at this pH for 30 min, followed by subsequent neutralization with formic acid. Interestingly, when the reaction mixture was neutralized with acid to a pH between 6 and 7, the very stable acetal intermediate **4c** (presumably formed via **4a**, **4b**) was obtained. This intermediate could be isolated and stored. It was converted to maytansinol (**4**) either by acidification and holding at pH 2 for 2 h or by adding a base and holding at basic pH (~11) for 30 min (Scheme 1).

DAC EX. 2040 IPR2022-01531 Page 1193 of 1299

Journal of
Medicinal Chemistry

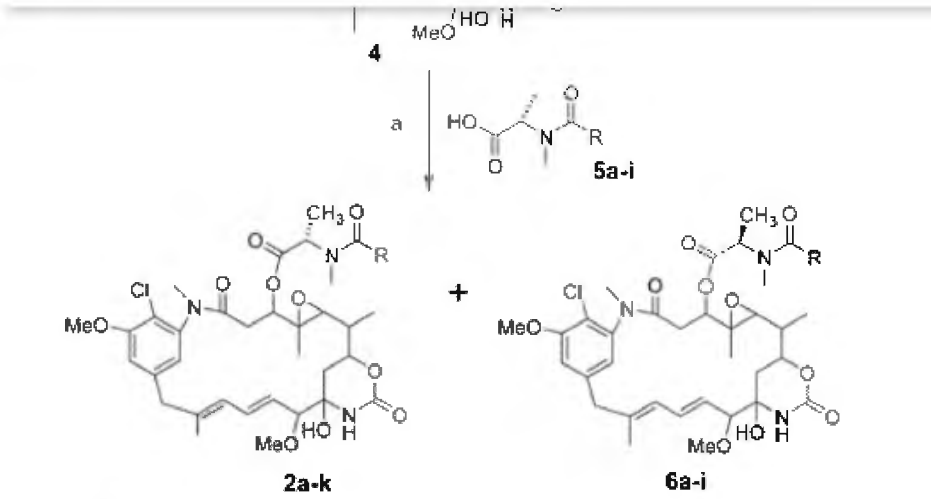


Scheme 1. Synthesis of Maytansinol[a]

[a] (a) $LiAlH(OMe)_3$, THF, −30 to −40 °C; (b) pH 12, 30 min (c) pH 6–7, (d) pH 2, 2 h or pH 12, 30 min.

DAC EX. 2040 IPR2022-01531 Page 1194 of 1299

Journal of
Medicinal Chemistry



Compound	R	Compound	R
2a (DM0SMe), 5a, 6a	SSMe	2j (DM1-TPA)	
2b (DM1SMe), 5b. 6b	SSMe		
2c (DM1SPh), 5c, 6c	SSPh	2k (DM4-TBA)	
2d (DM2'SMe), 5d, 6d	SSMe		
2e (DM2SMe), 5e, 6e	SSMe		
2f (DM3SMe, *RS*), 5f, 6f	SSMe		
2g (DM3SMe, *S*), 5g, 6g	SSMe		
2h (DM3SMe, *R*), 5h 6h	SSMe		
2i (DM4SMe), 5i, 6i	SSMe		

Scheme 2. Synthesis of Disulfide-Containing Maytansinoids[a]

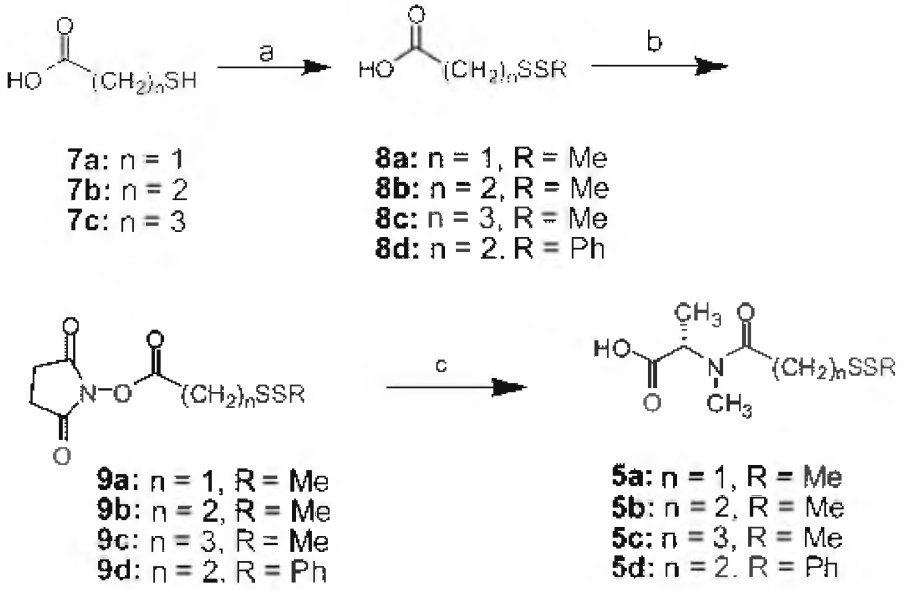
[a] Reaction conditions: (a) DCC/$ZnCl_2$/CH_2Cl_2, rt.

Mercaptocarboxylic acids of varying linear chain lengths were converted into methyldithio or aryldithio carboxylic acids by reacting with methyl methanethiolsulfonate or aryl disulfides, respectively (Scheme 3). The dithio-carboxylic acids were converted into their *N*-hydroxysuccinimide esters, followed by reaction with *N*-methyl-L-alanine to form the desired C3 *N*-acyl-*N*-methyl-L-alanine side chains for reaction with maytansinol (**4**). The two enantiomeric 4-(methydithio)pentanoic acids (compounds **13** and **18**) were prepared from the corresponding optically pure 1,3-dihdroxybutanes as shown in Schemes 4 and 5. The conversion of the 1,3-dihdroxybutanes to the ditosylates,

DAC EX. 2040 IPR2022-01531 Page 1195 of 1299

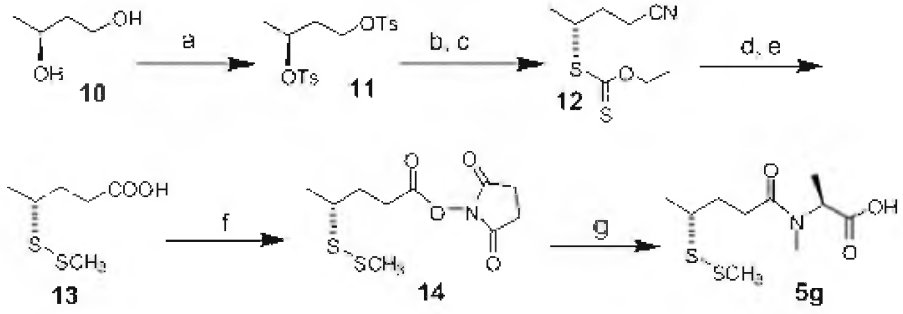
Journal of
Medicinal Chemistry

N-methyl-L-alanine with the *N*-hydroxysuccinimde ester of *S*- and *R*-4-(methyldithio)pentanoic acids gave the two diastereomeric acyl *N*-methyl-L-alanyl side chains **5g** and **5h** for condensation with maytansinol. To synthesize a maytansinoid ester bearing a sterically hindered thiol substituent, the *N*-acyl-*N*-methyl-L-alanine compound **5i**, bearing two methyl substituents on the carbon bearing the disulfide bond, was synthesized from isobutylene sulfide using the steps shown in Scheme 6. Ring opening of episulfide **20** with lithiated acetonitrile gave nitrile **21**. The hydrolysis of the nitrile, followed by disulfide exchange with methylmethanethiolsulfonate gave carboxylic acid **23**. The condensation of **23** with *N*-hydroxysuccinimide in the presence of EDC gave hydroxysuccinimide ester **24**, followed by the reaction with *N*-methyl-L-alanine to give **5i**.



Scheme 3. Synthesis of *N*-Acyl-*N*-methyl-L-alanines[a]

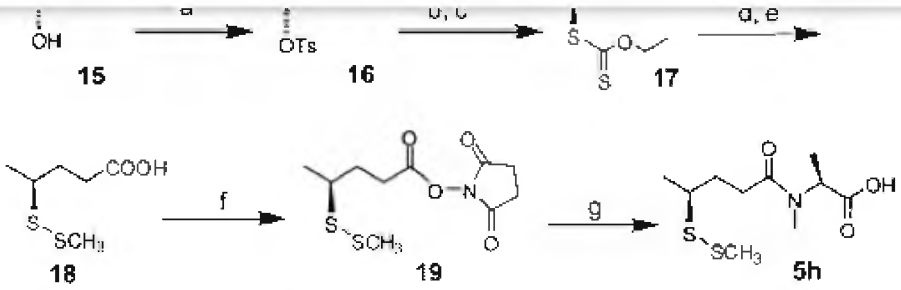
[a] Reaction conditions: (a) $CH_3SSO_2CH_3$, (PhSSPh for **8d**); (b) *N*-hydroxysuccinimide, EDC; (c) *N*-methyl-L-alanine, triethylamine.



Scheme 4. Synthesis of *N*-Methyl-*N*-[(4-*(S)*-methyldithio)-1-oxopentyl]-*S*-alanine[a]

DAC EX. 2040 IPR2022-01531 Page 1196 of 1299

Journal of
Medicinal Chemistry



Scheme 5. Synthesis of *N*-Methyl-*N*-[(4-*(R)*-methyldithio)-1-oxopentyl]-*S*-alanine[a]

[a] Reaction conditions: (a) TsCl. Py; (b) NaCN; (c) KSSCOEt; (d) NaOH; (e) $CH_3SSO_2CH_3$; (f) *N*-hydroxysuccinimide, EDC; (g) *N*-methyl-L-alanine, triethylamine.

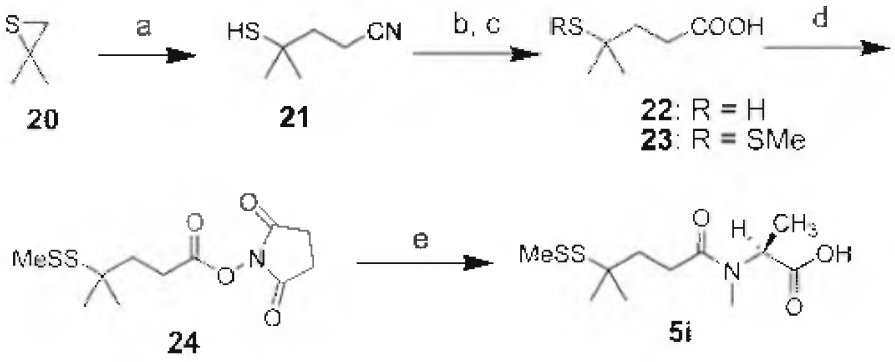
Disulfide-containing maytansinoid esters (**2a–i**), in which both the chain length and degree of branching in the acyl group were varied, were prepared by condensing maytansinol (**4**) with the *N*-acyl-*N*-methyl-L-alanyl derivatives described above in the presence of the coupling reagent 1,3-dicyclohexylcarbodiimide (DCC) along with catalytic amounts of zinc chloride (Scheme 2). In all cases, two diastereomeric products (**2a–i** and **6a–i**) containing the L- and D-aminoacyl side chain, respectively, were obtained, despite the fact that enantiomerically pure acylamino acids were used in the reaction. This indicates that epimerization at the α-carbon of the *N*-methyl-L-alanine moiety takes place during the reaction. In addition, unreacted maytansinol (typically 10–20%) was also recovered. The addition of another aliquot of the carboxylic acid, DCC, and $ZnCl_2$ did not result in any further reaction. Several other coupling agents, solvents, and reaction conditions were tried but generally gave poorer yields. Of the Lewis acids investigated, zinc chloride gave the best yields. The substitution of zinc chloride with acyl transfer catalysts such as (dimethylamino)pyridine or hydroxybenzotriazole gave little or no product. The diastereomeric maytansinoid esters were readily separated by normal phase HPLC, using a cyano-bonded silica column. On this column, the two diastereomers had retention times that were about 10 min apart, enabling a facile separation. In some cases, the diastereomers could also be separated by preparative TLC on silica gel. In one case, the maytansinoid ester could not be isolated in a reasonable yield. In this case, the maytansinoid DM2SMe (**2e**) was found to be unstable under the reaction conditions and underwent rapid decomposition, presumably because of facile β-elimination of the methydithio substituent to give the substituted alkene, which is the thermodynamically favored product.

Because maytansinoids are sensitive to bases, nucleophiles, and strong reducing agents, the reduction of disulfide-containing maytansinoids to the thiol compounds had to be achieved using very mild and disulfide-specific reagents. The reduction of the disulfide-containing maytansinoids (**2b,c,e,f,i**) proceeded smoothly upon treatment, in neutral buffered aqueous solution, with a small excess (2–3 equiv) of dithiothreitol (DTT), a reducing agent commonly used by biochemists for the scission of disulfide bonds in proteins (Scheme 7). Initial attempts to obtain pure thiol-containing drugs by reverse phase HPLC using a water–acetonitrile mobile phase resulted in a considerable

DAC EX. 2040 IPR2022-01531 Page 1197 of 1299

Journal of
Medicinal Chemistry

reduction of the disulfide-containing-D-aminoacyl maytansinoids (**6b,c,f,i**) gave the thiol-containing maytansinoids **26a–c**. The water soluble reducing agent tris-(2-carboxyethyl)phosphine (TCEP) could also be used instead of DTT with similar results. Once purified, using nonaqueous solvents, the thiol-containing drugs were stable upon extended storage in dry form. For a subsequent reaction with antibodies, the thiol-containing maytansinoids had to be reconstituted in a water-miscible solvent that would keep the drug in solution in the predominantly aqueous milieu (<5% organic solvent) and also compatible with proteins. Dimethylacetamide (DMA[a]) was found to be the ideal solvent, once it was re-purified and freed of metal ions. This was achieved by the careful glass-distillation of high-grade commercial DMA.

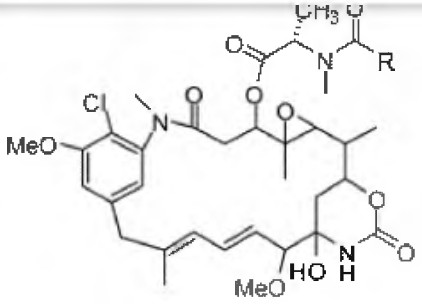


Scheme 6. Synthesis of *N*-Methyl-*N*-[4-methyl-(4-methyldithio)-1-oxopentyl)-*S*-alanine[a]

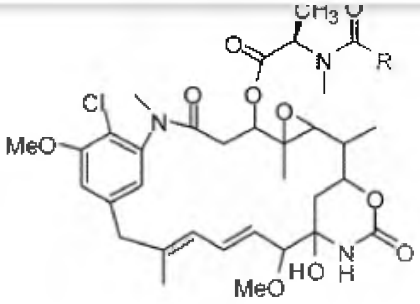
[a] Reaction conditions: (a) CH_3CN, ^nBu-Li; (b) NaOH; (c) $CH_3SSO_2CH_3$; (d) *N*-hydroxysuccinimide, EDC; (e) *N*-methyl-L-alanine.

DAC EX. 2040 IPR2022-01531 Page 1198 of 1299

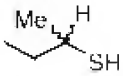
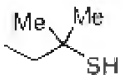
Journal of
Medicinal Chemistry



25a-c



26a-c

Compound	R
25a, 26a	
25b ,26b	
25c, 26c	

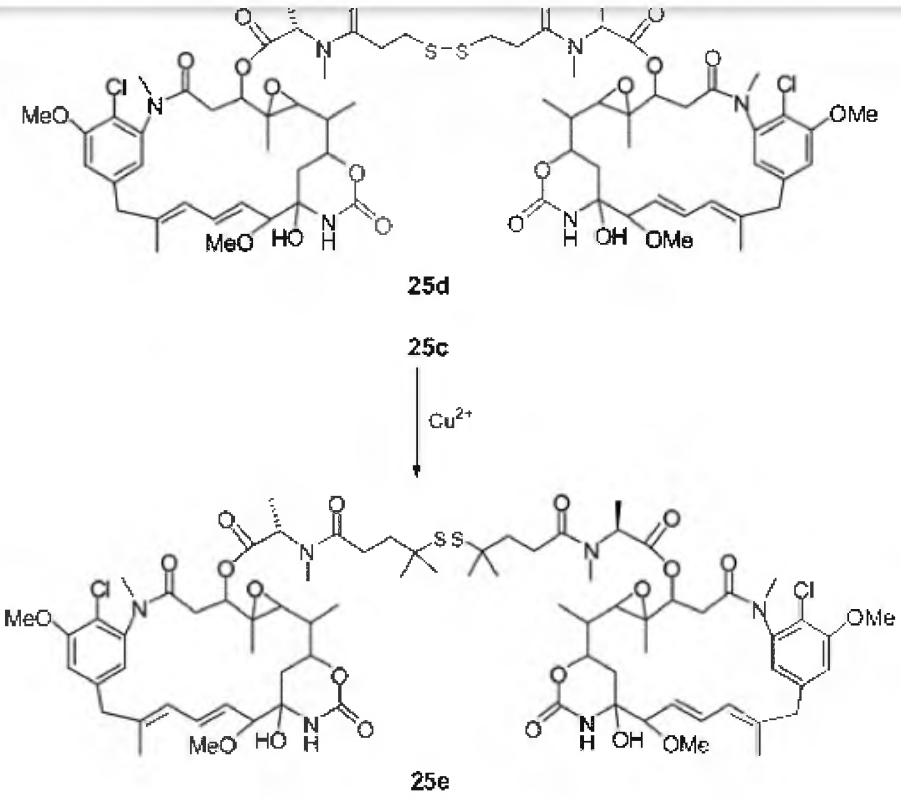
Scheme 7. Synthesis of Thiol-Containing Maytansinoids[a]

[a] Reaction conditions: (a) dithiothreitol/RT.

Maytansinoids **2j** (DM1-TPA) and **2k** (DM4-TBA) were sometimes obtained as byproducts of the conjugation reaction of thiol-containing maytansinoids with antibodies. To determine the potency of these compounds, they were independently synthesized from the corresponding thiol-containing maytansinoids **25a** and **25c**, respectively, by a disulfide exchange with the appropriate pyridyldithioalkanoic acids. The disulfide dimers **25d** and **25e** of DM1 and DM4, respectively, were also sometimes obtained as byproducts of the conjugation reaction. These two dimers were synthesized either by disulfide exchange or by metal-ion-catalyzed oxidation of the parent thiol-containing maytansinoids **25a** and **25c**, respectively (Scheme 8).

DAC EX. 2040 IPR2022-01531 Page 1199 of 1299

Journal of
Medicinal Chemistry



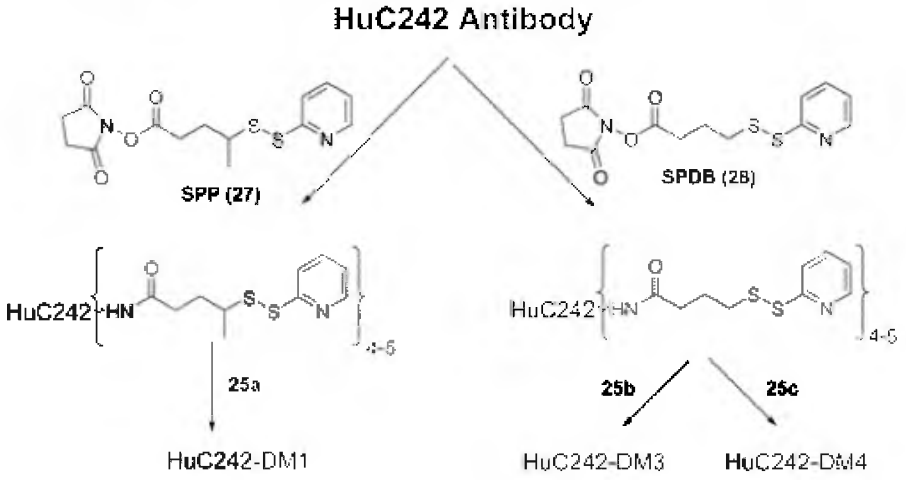
Scheme 8. Synthesis of Maytansinoid Dimers[a]

Antibody Conjugates. The antibody used in this study was huC242, a humanized version of the murine monoclonal antibody C242 [20] that binds to the CanAg antigen that is highly expressed on the surface of several human solid tumors, including colon, pancreatic, gastric, and some lung tumors. This antibody displayed limited cross-reactivity with human normal tissues. The conjugation of the maytansinoid to the monoclonal antibodies was accomplished in two steps (Scheme 9). First, the monoclonal antibody was modified either with *N*-succinimidyl 4-(2-pyridyldithio)pentanoate (SPP, **27**) or with *N*-succinimidyl 4-(2-pyridyldithio)butanoate (SPDB, **28**) to introduce an active disulfide-containing group. The treatment with these bifunctional cross-linking agents resulted in the formation of stable amide bonds with the ε-amino group of lysine residues to generate a modified antibody bearing, on an average, four to five linked pyridyldithio groups per antibody molecule. Modification with SPP results in the introduction of a sterically hindered center on the carbon atom bearing the disulfide moiety, whereas the treatment with SPDB results in the introduction of a nonhindered disulfide. In the second step, the treatment with a thiol-containing maytansinoid led to disulfide exchange with the pyridyldithio group to give antibody conjugates containing, on the average, three to four maytansinoid drugs linked via the newly formed disulfide bonds. The strength of the disulfide bond was varied by using maytansinoids **25b** and **25c** that bear sterically hindered thiols or by utilizing the SPP cross-linker, which would introduce a methyl substituent on the antibody side of the disulfide link. For example, the huC242−DM1 conjugate cantuzumab

DAC EX. 2040 IPR2022-01531 Page 1200 of 1299

Journal of
Medicinal Chemistry

soluble in neutral buffered aqueous solution, and stable for up to two years upon storage at 4 °C.



Scheme 9. Preparation of Antibody−Maytansinoid Conjugates[a]

DAC EX. 2040 IPR2022-01531 Page 1201 of 1299

Journal of
Medicinal Chemistry

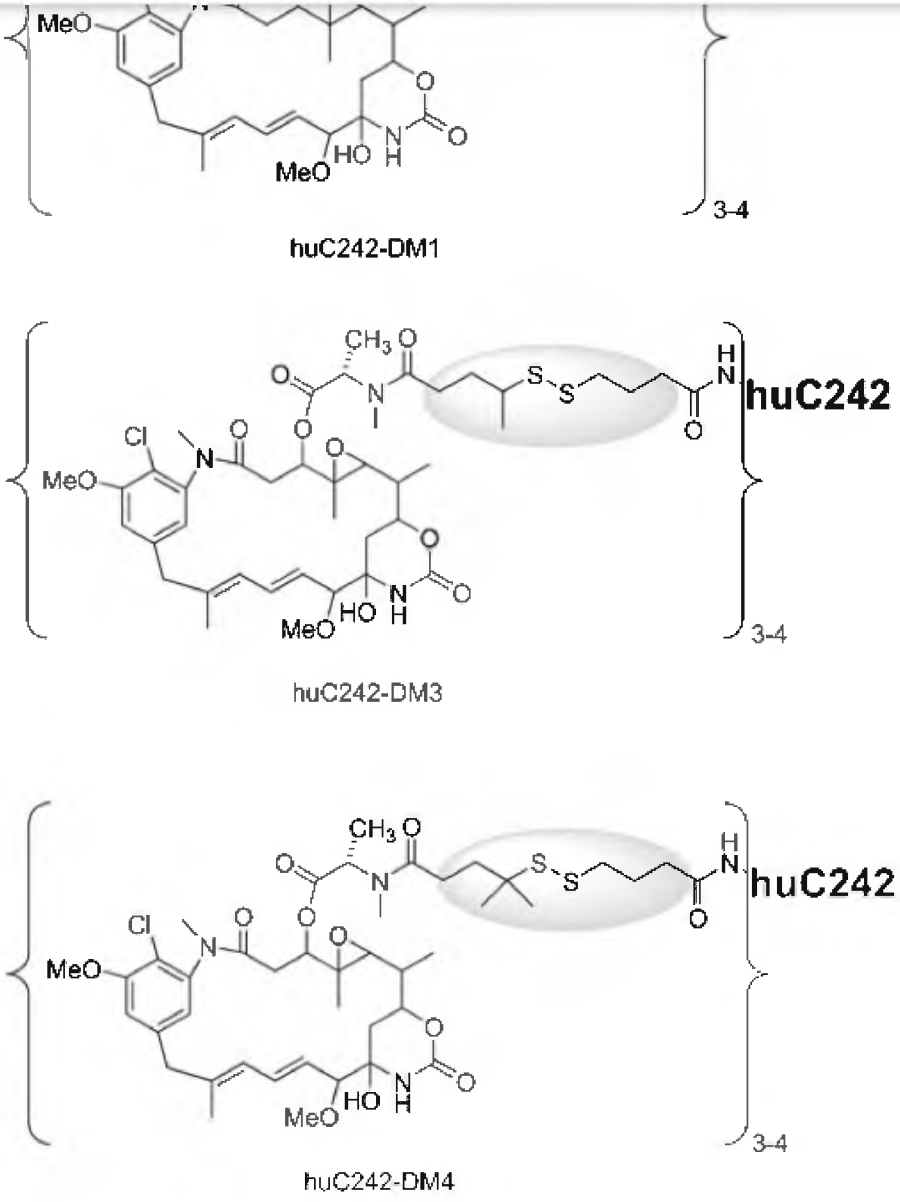


Figure 2 Structural representation of maytansinoid conjugates with the huC242 antibody. The differences in the linker region are shadowed.

Biological Studies. Free Drugs. The disulfide-containing maytansinoid drugs and thiol-containing maytansinoid drugs were evaluated for their ability to suppress the proliferation of human tumor cell lines in vitro. KB (human epidermoid carcinoma) and SK-BR-3 (human breast tumor) cells were exposed to the compounds for 24 or 72 h, and the surviving fractions of cells were measured using a clonogenic plating efficiency assay. The IC_{50} values were then calculated from these data. The L-aminoacyl maytansinoid **2b** (DM1SMe), bearing a methyldithio-propanoyl substituent in the C3 ester

DAC EX. 2040 IPR2022-01531 Page 1202 of 1299

Journal of
Medicinal Chemistry

wider panel of human tumor cell lines (see Table 1). Compound **2b** was potent toward SW-620 (colon adenocarcinoma) with an IC_{50} value of 0.040 nM, about 3-fold more potent than maytansine. Both **2b** and maytansine were less potent toward HCT-15 (colon carcinoma) cells with IC_{50} values of 0.13 and 0.75 nM, respectively. The lower potency of these drugs toward HCT-15 cells line can be explained by the reported expression of the multidrug resistance gene (mdr1/P-glycoprotein) in this cell line.[21] Compound **2b** was about twice as cytotoxic (IC_{50} = 0.05 nM) as maytansine against the ovarian cancer line OVCAR3. Thus, the replacement of the acetyl group in the C3 side chain of maytansine with a methyldithiopropanoyl group not only preserved the cytotoxic activity of maytansine but, in some cases, even enhanced its potency toward cancer cell lines.

Table 1. Comparison of the in Vitro Potency of Maytansine (1) and Disulfide-Containing Maytansinoid, DM1SMe (2b) after 72 h of Exposure to the Drugs

	IC_{50} (nM)	
cell line	maytansine (**1**)	maytansinoid **2b**
KB	0.034 ± 0.005	0.029 ± 0.003
Sk-Br-3	0.030 ± 0.005	0.014 ± 0.006
A-431	0.040	<0.030
A-549	0.160 ± 0.040	0.120
SW-620[a]	>0.100	0.040 ± 0.004
Ovcar-3[a]	0.100 ± 0.020	0.050 ± 0.010
HCT-15	0.750	0.130
MCF-7	0.044 ± 0.002	<0.03
A-375	0.037	0.030 ± 0.015

[a] 24 h exposure.

We then examined the effect of the chain length of the acyl group on potency (Table 2). Maytansinoid **2d**, bearing the methyldithiobutanoyl side chain (one methylene longer than **2b**), displayed similar potency to that of **2b**. In contrast, the methyldithioacetyl maytansinoid **2a** (one methylene unit shorter than **2b**) was about 10-fold less cytotoxic than **2b**, suggesting that a

DAC EX. 2040 IPR2022-01531 Page 1203 of 1299

Journal of
Medicinal Chemistry

the carbon atom bearing the methydithio substituent, were highly potent, with IC_{50} values ranging from 0.0042 to 0.011 nM for **2f** and 0.011 to 0.0032 nM for **2i**. Maytansinoid **2f** bears a new chiral center in the acyl side chain. Maytansinoids **2g** and **2h** bearing the *R* and *S* configurations in the acyl side chains, respectively, were found to display potencies similar to that of **2f**, which bears the racemic acyl side chain. Although the stereochemistry in the acyl side chain was not important for activity, the stereochemistry of the *N*-methylalanyl moiety had a dramatic influence on potency. Thus, the maytansinoids **6b,d,f,g,h,i** bearing the unnatural *N*-methyl-D-alanyl moiety were about 100-fold less cytotoxic than their corresponding L-epimers toward both cell lines.

Table 2. Cytotoxicity of Various Maytansinoids in Vitro toward Tumor Cell Lines (72 h of Exposure)

	IC_{50} (nM)	
compd	KB cells	SK-Br-3 cells
4	>3	1.2
1	0.034	0.030
2a	0.190	nd
2b	0.029	0.014
2c	0.100	nd
2d	0.0085	0.038
2f	0.011	0.0042
2g	0.040	0.032
2h	0.042	0.027
2i	0.0011	0.0032
2j	1.80	3.40
2k	23.0	7.10
6b	3.0	6.0

DAC EX. 2040 IPR2022-01531 Page 1204 of 1299

Journal of
Medicinal Chemistry

6g	>3.0	>3.0
6h	2.40	2.20
6i	>0.30	>0.30
25a	1.10	1.10
25b	0.077	0.031
25c	0.290	0.120
25d	0.140	0.100
25e	0.0016	0.0012
26a	>3.0	>3.0
26c	>1.0	3.3

In all cases, the mercapto-containing maytansinoids were less potent than their corresponding methydisulfide analogues. Thus, maytansinoid **25a** (DM1), bearing the mercaptopropanoyl side chain, had an IC_{50} value of 1.1 nM toward KB and SK-BR-3 cells, rendering it about 30- and 100-fold less potent than **2b** toward these cell lines. This decrease in potency may be attributed to the instability of thiol-containing maytansinoids such as **25a** under cell culture conditions wherein the oxidation of **25a** to its disulfide dimer **25d** was observed. However, dimer **25d** was independently synthesized and found to be only about 3- to 10-fold less potent than **2b**, suggesting that **25a** might be inactivated additionally by some other mechanism. For example, the thiol group could react with a cell culture component such as cystine to provide a charged maytansinoid carboxylate, which is incapable of internalization into the cell, resulting in diminished potency. Maytansinoids **25b**,**c** bearing sterically hindered thiols were 3- to 12-fold more potent than **25a**, which is consistent with the predicted lower reactivity and consequently, the greater stability of these compounds in the cell culture milieu. The dimer (**25e**) of DM4 was the most potent maytansinoid tested, with IC_{50} values of 0.0012 and 0.0016 nM toward the two cell lines tested. Maytansinoids **2j** and **2k** bear a terminal carboxyl group that renders them at least 100-fold less potent than the parent compounds **2b** and **2i**, suggesting that the charged carboxylate residue might interfere with the internalization into cells, resulting in diminished potency.

Antibody−Drug Conjugates.Cytotoxicity in Vitro. The conjugation of the huC242 antibody, via disulfide bonds, with thiol-containing maytansinoids DM1 (**25a**), DM3 (**25b**), and DM4 (**25c**) gave the

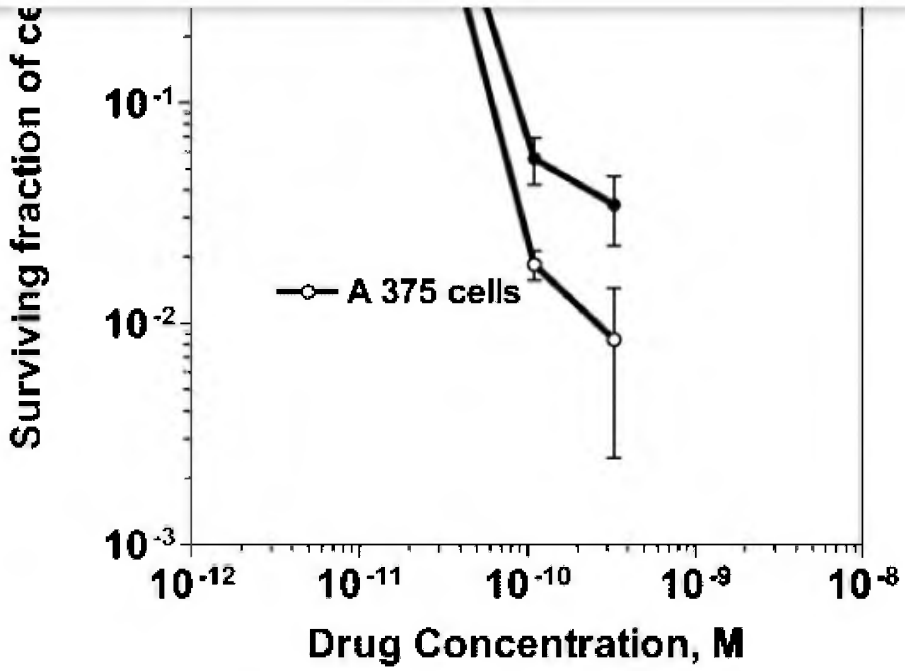
DAC EX. 2040 IPR2022-01531 Page 1205 of 1299

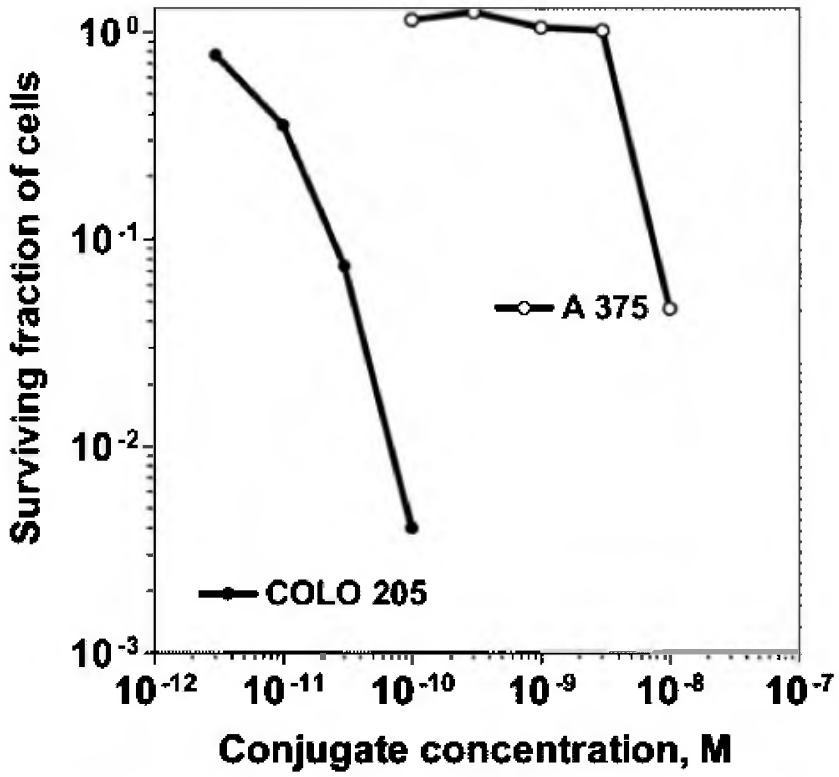
Journal of
Medicinal Chemistry

of 1.1×10^{-11}, 1.3×10^{-11}, and 3.8×10^{-11} M for huC242−DM4, huC242−DM3, and huC242−DM1, respectively. Thus, the disulfide bond strength does not appear to play an important role in determining the magnitude of in vitro potency toward target cells. Importantly, all three conjugates were about 200-fold less cytotoxic toward antigen-negative A-375 cells, demonstrating the specificity of the cytotoxic effect. Figure 3 shows an example of how an antibody can confer target specificity to an otherwise nonspecifically cytotoxic drug. Both the COLO 205 and A-375 cell lines were killed equally well by the nonconjugated maytansinoid **2i** (DM4SMe). In contrast, the conjugated maytansinoid huC242−DM4 kills the target COLO 205 cells at a 1000-fold lower concentration than the nontarget A-375 cell, establishing that the linkage to antibodies confers tumor specificity to the otherwise indiscriminately toxic maytansinoid drugs.

DAC EX. 2040 IPR2022-01531 Page 1206 of 1299

Journal of
Medicinal Chemistry





DAC EX. 2040 IPR2022-01531 Page 1207 of 1299

Journal of
Medicinal Chemistry

Antitumor Activity in Vivo. The antitumor activity of the three huC242−maytansinoid conjugates, huC242−DM1, huC242−DM3, and huC242−DM4, were compared in human colon tumor xenograft models established with COLO 205 cells. We have previously shown[10] that C242−DM1 is curative in this model and that the free DM1 and the unconjugated C242 antibody show little or no antitumor effect. To compare the relative efficacy of the three conjugates, we selected a treatment regimen that used a low dose of the conjugate (~20% of the maximum tolerated dose) that would result in a delay in tumor growth but would not be curative. The results are shown in Figure 4. The tumors in the control group of mice grew to a size of nearly 900 mm^3 in 24 days. The treatment with huC242−DM1 (linked maytansinoid dose of 75 μg/kg, qd × 5) resulted in a tumor growth delay of 20 days, whereas the treatment with huC242−DM3, at an equivalent dose, resulted in a greater therapeutic effect and caused complete tumor regressions lasting 45 days. Treatment at an equivalent dose of the huC242−DM4 conjugate was even more efficacious, resulting in cures of all of the treated animals. Interestingly, the antitumor activity of huC242−DM3 is superior to that of huC242−DM1, although both conjugates would have been predicted to display similar stability in vivo. The huC242−DM3 conjugate bears one methyl group on the carbon atom bearing the disulfide bond on the drug side of the conjugate, whereas huC242−DM1 bears one methyl substituent at the carbon atom on the antibody side of the disulfide link. However, cleavage of the disulfide bond in huC242−DM3 releases the thiol-containing maytansinoid DM3, which is about 10-fold more potent than DM1, the active component released from huC242−DM1, which could explain the greater efficacy observed with the DM3 conjugate.

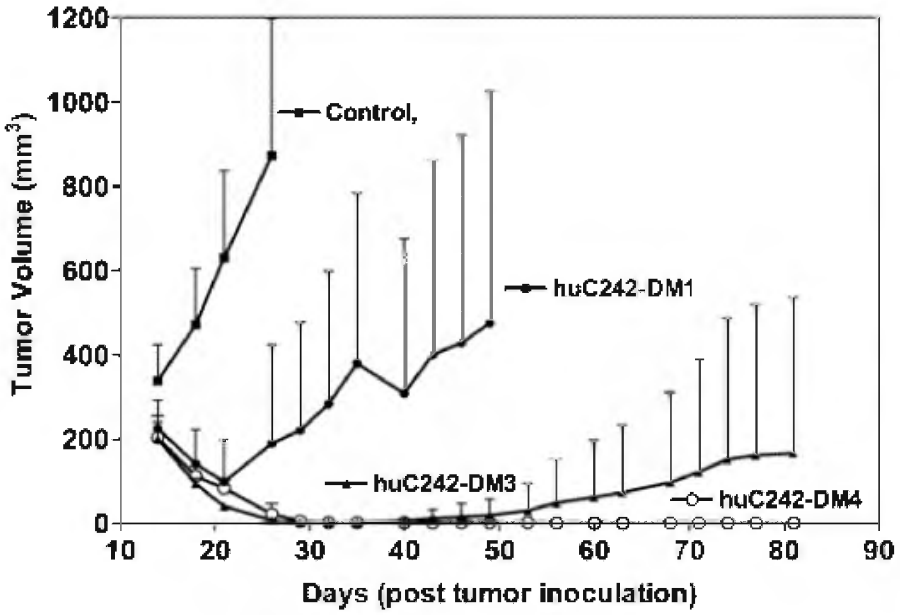


Figure 4 Comparison of the antitumor activity of huC242−maytansinoid conjugates in a human colon tumor xenograft model established subcutaneously with COLO 205 cells.

DAC EX. 2040 IPR2022-01531 Page 1208 of 1299

Journal of
Medicinal Chemistry

drug, which bears a thiol substituent at a tertiary carbon center. Studies to determine the parameters contributing to the different in vivo activities of the conjugates are ongoing.

Conclusions

To harness the potent cytotoxic activity of maytansinoids for the treatment of cancer, we prepared analogues of maytansine that can be covalently linked to monoclonal antitumor antibodies for targeted treatment. Such analogues not only have to maintain the activity of maytansine but also have to be able to readily form a stable chemical bond with a protein in aqueous solution. For manufacturing reasons, bond formation must be efficient and occur in high yield. Sulfhydryl groups or their respective thiolate anions react readily in aqueous solutions with maleimido moieties in a Michael-type addition reaction to form thioethers and with disulfide groups in a disulfide exchange reaction to form new disulfide bonds. We, therefore, prepared and tested maytansinoid compounds with reactive sulfhydryl groups, which during synthesis and for some biological testing were protected in the form of simple disulfide compounds.

Thus, we have synthesized a series of new maytansinoids bearing a disulfide or thiol substituent. The series was chosen so as to evaluate the influence of the chain length of the ester side chain and the degree of steric hindrance on the carbon atom bearing the thiol substituent on in vitro cytotoxicity. Several of these maytansinoids were found to be even more potent than the parent drug maytansine in killing human tumor cells in vitro. Antibody conjugates bearing varying degrees of steric hindrance around the disulfide link between the maytansinoid and antibody were shown to be highly active in selectively killing target cells to which the antibody was capable of binding. Nontarget cells were not affected even at a 100-fold higher concentration, demonstrating that the high potency of the maytansinoids could be directed toward the specific killing of target cells. Remarkable antitumor efficacy was observed in a xenograft model. These studies, in part, have led to the development of huC242−DM4 for evaluation as an antitumor agent in human clinical trials in patients expressing the antigen for C242.

Experimental Section

All reagents were obtained from the Aldrich Chemical Co., unless otherwise stated. Maytansine (NCI 158358/26/0) was obtained from the National Cancer Institute. Ansamitocin P-3 was produced by fermentation of an *Actinosynnema pretiosum* strain derived from several rounds of mutagenesis of the parent ATCC 31565 strain. Human tumor cell lines used in biological assays were obtained from the American Type Culture Collection (ATCC). Melting points were determined on an electrothermal melting point apparatus. Proton magnetic resonance (^{1}H NMR) spectra were obtained on a Bruker Avance spectrometer operating at 400 MHz. The chemical shifts are reported in δ values relative to that of an internal tetramethylsilane (Me_4Si) standard. UV spectra were recorded on a Beckman DU-640 spectrophotometer. The optical rotations were determined using a Rudolph AUTOPOL IV

DAC EX. 2040 IPR2022-01531 Page 1209 of 1299

Journal of
Medicinal Chemistry

Synthesis of Maytansinol (4). To a 200 mL flask was added a 1 M solution of lithium aluminum hydride (45 mmol, 45 mL) in THF. The solution was placed under an argon atmosphere and cooled to −40 °C. A mixture of anhydrous methanol (5.4 mL, 135 mmol) in THF (25 mL) was added dropwise. The temperature was maintained between −30 and −40 °C. After the addition was complete, the reaction mixture was stirred at this temperature for an additional period of 10 min to give lithium trimethoxyaluminum hydride ($LiAlH(OMe)_3$). In a separate 250 mL flask, ansamitocin (3.2 g, 5.0 mmol) was dissolved in anhydrous THF (30 mL), and the solution was placed under an argon atmosphere and cooled in a dry ice−acetone bath to −40 °C. The solution of $LiAlH(OMe)_3$ was transferred via a cannula over 10 min into the chilled solution of ansamitocins. The reaction temperature was maintained between −30 and −35 °C under argon and stirred for 2 h. Deionized water (22 mL) was added dropwise while the reaction mixture was maintained at −30 and −35 °C. After 30 min, 88% formic acid (1.8 mL) and ethyl acetate (50 mL) were added. The mixture was allowed to warm up to room temperature. The precipitate was removed by vacuum filtration, and the filtrate was concentrated under vacuum. The residue was dissolved in a minimum volume of dichloromethane and loaded onto a silica gel column packed in dichloromethane. The column was eluted with dichloromethane/methanol (95:5, v/v). The fractions containing the desired product were pooled and evaporated under reduced pressure to give 2.3 g of maytansinol (81% yield) as a white solid: mp 205−207 °C; ^{1}H NMR ($CDCl_3$) δ 0.82 (3H, s), 1.28 (3H, d, J = 6 Hz), 1.52−1.54 (1H, m), 1.67 (3H, s), 1.80 (br s s), 2.07−2.29 (4H, m), 2.56 (1H, d, J = 11 Hz), 2.95 (br s), 3.10 (1H, d, J = 12 Hz), 3.19 (3H, s), 3.41 (3H, s), 3.44−3.51 (3H, m), 3.97 (3H, s), 4.34 (1H, t, J = 11 Hz), 5.50 (1H, dd, J = 9 and 15 Hz), 6.13 (1H, d, J = 11 Hz), 6.37 (1H, s), 6.42 (1H, dd, J = 11 and 15 Hz), 6.79 (1H, d, J = 1.5 Hz), 7.02 (1H, d, J = 1.5 Hz); HRMS calcd for $C_{28}H_{33}ClN_2O_8$ $(M + H)^+ m/z$ = 565.2317; found, 565.2329. HPLC analysis was performed on a Kromasil analytical C-8 column (length: 100 mm, i.d.: 4.6 mm), at a flow rate of 1 mL/min, eluting with a gradient of water and acetonitrile (30% to 45% CH_3CN over 30 min). Under these conditions, maytansinol eluted as a sharp peak with a retention time of 11.15 min.

Acetal 4c. A solution of ansamitocins (3.0 g, 4.72 mmol) in THF (15 mL) was cooled to −35 °C, and a solution of 0.67 M $LiAl(OMe)_3H$ (56 mL, 37.7 mmol) in THF was added dropwise by syringe using a syringe pump. The temperature of the reaction was maintained between −30 and −40 °C throughout the addition. After addition was complete, the reaction was stirred for 2 h at between −34 and −37 °C. A solution of 88% formic acid (1.85 mL, 2.16 g, 41.5 mmol) in deionized water (23 mL) was added dropwise to the flask at a rate that did not produce excessive frothing, followed by the addition of ethyl acetate (60 mL). The cooling bath was removed, and the mixture was allowed to warm up to room temperature. The pH of the mixture was checked with pH paper and found to be approximately 6. Precipitated aluminum-based byproducts were removed by vacuum filtration, and the solvent was removed from the filtrate by rotary evaporation under vacuum. Butyl acetate (10 mL) was added to the residue, and the solvent was then evaporated to remove the residual water. The residue was purified by silica chromatography using dichloromethane/methanol 95:5 (v:v), giving a later eluting band (maytansinol) and an early eluting band. The maytansinol band was

DAC EX. 2040 IPR2022-01531 Page 1210 of 1299

Journal of
Medicinal Chemistry

($CDCl_3$) δ 0.78 (s, 3H), 0.97 (d, 3H, *J* = 6.9), 1.04 (d, 3H, *J* = 6.7), 1.23 (m, 1H), 1.28 (d, 3H, *J* = 6.4), 1.54 (m, 1H), 1.66 (s, 3H), *1.72 (m, 2H)*, 2.03 (dd, 1H, *J* = 14, 3.6 Hz), 2.3 (d, 1H, *J* = 14), 2.49 (dd, 1H, *J* = 11.7, 14), 2.92 (d, 1H, *J* = 9.5 Hz), 3.14 (s, 3H), 3.12 (m, 1H), 3.37, (s, 3H), 3.52 (m, 3H), 3.65 (m, 1H), 3.75 (m, 1H), 3.97 (s, 1H), 4.31 (m, 2H), 5.52 (dd, 1H, *J* = 16, 8.7 Hz), 6.13(d, 1H, *J* = 11 Hz), 6.34 (s, 1H), 6.45 (dd, 1H, *J* = 16, 11 Hz), 6.80 (d, 1H, *J* = 1.5 Hz), 6.92 (d, 1H, *J* = 1.5 Hz); MS *m/z* 619.3 (M +H)+.

3-(Methyldithio)propanoic Acid (8b). To a stirred solution of 3-mercaptopropanoic acid (**7b**) (5.00 g, 0.047 mol) in water (150 mL) cooled in an ice bath was added methyl methanethiolsulfonate (6.54 g, 0.052 mol) in absolute ethanol (75 mL). The reaction mixture was stirred overnight at room temperature. The mixture was then diluted with saturated aqueous NaCl (400 mL) and extracted with ether (3 × 150 mL), and the combined ether extracts were then washed with saturated NaCl. The solution was dried over Na_2SO_4, concentrated, and then distilled to afford a colorless liquid (6.47 g, 90%); bp (1 mm) = 105 °C; ^{1}H NMR ($CDCl_3$) δ 2.32 (3H, s), 2.80 (4H, m), 11.20 (1H, s).

4-(Methyldithio)butanoic Acid (8c). To a stirred solution of bis-(3-carboxypropyl)disulfide (1.00 g, 4.20 mmol) in methanol (20 mL) was added a solution of dithiothreitol (0.647 g, 4.20 mmol) in H_2O (20 mL). A solution of 10 M NaOH (0.842 mL, 8.42 mmol) was then added and the mixture was allowed to stir overnight at room temperature to effect complete reduction. Methyl methanethiolsulfonate (1.17 g, 9.24 mmol) was added, and the reaction mixture was stirred for another 3 h. The mixture was then diluted with saturated aqueous NaCl (150 mL), acidified (aqueous HCl), and extracted with ethyl ether (3 × 100 mL). The combined organic layers were washed with saturated NaCl, dried (Na_2SO_4), concentrated, and chromatographed on silica gel, eluting with dichloromethane/ethyl acetate to give 0.867 g (56%) of a colorless liquid; ^{1}H NMR ($CDCl_3$) δ 2.12 (2H, m), 2.40 (3H, s), 2.74 (2H, m), 11.18 (1H, s).

3-(Phenyldithio)propanoic Acid (8d). To a stirred solution of diphenyl disulfide (3.0 g, 13.8 mmol) in a mixture of ether (10 mL) and methanol (20 mL) under a nitrogen atmosphere at room temperature was added a solution of 3-mercaptopropanoic acid (**7b**) (0.49 g, 4.6 mmol) in ether (5 mL), followed by a solution of 10 M NaOH (0.46 mL, 4.6 mmol). The reaction mixture was stirred at room temperature for 20 h and then stripped of the solvents under reduced pressure. The product was purified by column chromatography on silica gel, eluting with ethyl acetate/hexane. The product was obtained as a white solid (0.56 g, 56.6%); mp 57−59 °C; ^{1}H NMR ($CDCl_3$, TMS) δ 2.6−3.0 (4H, m), 7.12−7.60 (5H, m), 10.6 (1H, s).

***R*-1,3-Di-*O*-(*para*-toluenesulfonyl)butane (11).** A solution of *R*-(−)-1,3-butanediol (**10**, 2.00 g, 22.22 mmol) in a mixture of dry pyridine (40 mL) and dry toluene (60 mL) was treated with *p*-toluenesulfonyl chloride (12.70 g, 66.84 mmol) under argon at 0 °C. After stirring at 0 °C for 5 min followed by stirring at room temperature for 2 h, the mixture was evaporated under vacuum, redissolved in ethyl acetate, and washed with 0.1 M aqueous $NaHCO_3$, followed by saturated aqueous NaCl. The organic layer was dried over $MgSO_4$ and filtered, and the solvent was

DAC EX. 2040 IPR2022-01531 Page 1211 of 1299

Journal of
Medicinal Chemistry

133.00, 130.11, 128.12, 127.91, 76.28, 66.21, 36.08, 21.86, 21.06; MS: *m*/*z* 420.99 $(M + Na)^+$.

***S*-4-(*O*-Ethylxanthic)pentanenitrile (12).** A solution of *R*-1,3-di-*O*-*p*-toluenesulfonyl-butane (**11**, 4.80 g, 12.06 mmol) in dry DMSO (50 mL) was treated with NaCN (0.65 g, 13.26 mmol). After stirring at room temperature under argon for 18 h, the reaction mixture was diluted with ethyl acetate, washed successively with cold 1.0 M NaH_2PO_4 at pH 7.5, water, and 1.0 M aqueous NaH_2PO_4 at pH 4.0. The organic layer was separated and dried over $MgSO_4$, filtered, and then evaporated to give 2.63 g of crude *R*-3-*O*-*p*-toluenesulfonyl-pentanenitrile. MS: *m*/*z* 275.80 $(M + Na)^+$. The product was used directly without further purification. To the solution of crude of *R*-3-*O*-*p*-toluenesulfonyl-pentanenitrile (2.63 g) in ethanol (15 mL) was added potassium *O*-ethylxanthate (4.55 g) in ethanol (50 mL). After stirring overnight under argon, the mixture was concentrated, diluted with ethyl acetate, and filtered through a short silica column. The eluant was concentrated and purified by chromatography on silica gel, eluting with 1:4 (v/v) EtOAc/hexane, to give 1.54 g (63%, 2 steps) of the title compound (R_f = 0.40 (1:4 EtOAc/hexane)) as a colorless oil. ^1H NMR ($CDCl_3$) δ 4.67 (dd, 2H, *J* = 7.1, 14.2 Hz), 3.86 (ddd, 1H, *J* = 7.0, 14.0, 21.9 Hz), 2.50 (t, 2H *J* = 7.3 + 7.6 Hz), 2.06 (m, 2H), 1.44 (m, 6H); ^{13}C NMR 213.04, 119.16, 70.28, 44.57, 32.10, 20.20, 15.21, 13.93; MS: *m*/*z* 226.51 $(M + Na)^+$, 242.51 $(M + K)^+$.

***S*-(+)-4-(Methyldithio)pentanoic Acid (13).** To a solution of *S*-4-*O*-Ethylxanthic-pentanenitrile (**12**, 1.95 g, 9.61 mmol) in a mixture of ethanol (10 mL) and water (150 mL) was added NaOH (5 g). The reaction mixture was refluxed overnight under argon. The mixture was cooled to room temperature and diluted with water (150 mL) and extracted with 1:1 EtOAc/hexane (2 × 100 mL). The aqueous layer was acidified with H_3PO_4 to pH 2.5–3.0 and extracted with EtOAc (6 × 75 mL). The organic layers were combined, dried over $MgSO_4$, filtered, and evaporated to dryness to give the crude *S*-4-mercaptopentanoic acid. This crude product was used directly in the next step without further purification. To a solution of crude *S*-4-mercaptopentanoic acid (1.2 g) in a mixture of ethanol (50 mL) and 0.5 M NaH_2PO_3 buffer (75 mL) at pH 7.0 was added dropwise methyl methanethiolsulfonate (1.47 g, 11.65 mmol) in dry THF (5 mL) over 45 min at 0 °C. After stirring under argon at 0 °C for 30 min followed by stirring at room temperature for 2 h, the mixture was concentrated and extracted with dichloromethane (2 × 50 mL). The aqueous layer was acidified with H_3PO_4 to pH 2.5–3.0 and extracted with EtOAc (4 × 100 mL). The organic layers were combined, dried over $MgSO_4$, filtered, and evaporated. The residue was purified by chromatography over silica gel, eluting with 1:100:400 HOAc/EtOAc/hexane to give 1.43 g (83%) of the desired product (R_f = 0.32, 1:100:400 HOAc/EtOAc/hexane) as a white solid; mp 290–293 °C (dec); ^1H NMR ($CDCl_3$) δ 2.91 (ddd, 1H, *J* = 6.8, 13.7, 20.5 Hz), 2.53 (t, 2H, *J* = 7.7 + 7.4 Hz), 2.42 (s, 3H), 1.94 (m, 2H), 1.36 (d, 3H, *J* = 6.8 Hz); ^{13}C NMR 179.18, 45.35, 31.58, 30.73, 24.70, 21.05; MS: (*m*/*z*) 202.92 $(M + Na)^+$; $[\alpha]^{25}_D$ = +41.35 (*c* = 2, CH_3OH).

***S*-1,3-Di-*O*-(*para*-toluenesulfonyl)butane (16).** A solution of *S*-(−)-1,3-butanediol (**15**, 2.00 g, 22.22 mmol) in a mixture of dry pyridine (40 mL) and dry toluene (60 mL) was treated with *p*-toluenesulfonyl chloride (12.70 g, 66.84 mmol) under argon at 0 °C. After stirring at 0 °C for 5 min

DAC EX. 2040 IPR2022-01531 Page 1212 of 1299

Journal of
Medicinal Chemistry

of the title compound (R_f = 0.40 (1:1 EtOAc/hexane)). Recrystallization from ether/hexane afforded a white solid; mp 56–58 °C; ^{1}H NMR ($CDCl_3$) δ 7.76 (dd, 4H, *J* = 1.0, 8.0 Hz), 7.35 (dt, 4H, *J* = 0.4, 8.0 +8.0 Hz), 4.70 (m, 1H), 4.03 (m, 1H), 3.94 (m, 1H), 2.46 (s, 6H), 1.92 (m, 2H), 1.26 (d, 3H, *J* = 6.3 Hz); ^{13}C NMR 145.17, 133.00, 130.11, 128.12, 127.91, 76.28, 66.21, 36.08, 21.86, 21.06; MS: *m*/*z* 420.99 $(M + Na)^+$.

***R*-4-*O*-(Ethylxanthic)pentanenitrile (17).** A solution of *S*-1,3-di-*O*-(*p*-toluenesulfonyl)butane (**16**, 6.25 g, 15.70 mmol) in 60 dry DMSO (50 mL) was treated with NaCN (0.85 g). The reaction mixture was stirred under argon for 18 h at room temperature. The reaction mixture was then diluted with ethyl acetate, washed sequentially with cold 1.0 M NaH_2PO_4 buffer at pH 7.5, water, and 1.0 M NaH_2PO_4 buffer at pH 4.0. The organic layer was dried over $MgSO_4$, filtered, and evaporated to give 3.62 g of crude *S*-3-*O*-(*p*-toluenesulfonyl)pentanenitrile. The product was used directly without further purification. To a solution of crude *S*-3-O-*p*-toluenesulfonyl-pentanenitrile (3.62 g) in ethanol (50 mL) was added potassium *O*-ethylxanthate (5.72 g) in ethanol (100 mL). After stirring overnight under argon, the mixture was concentrated, diluted with ethyl acetate, and filtered through a short column of silica gel. The eluant was concentrated, and the residue was purified by chromatography over silica gel, eluting with 1:4 EtOAc/hexane to give 2.0 g (62%, 2 steps) of the title compound (R_f = 0.40 (1:4 EtOAc/hexane)) as a colorless liquid. ^{1}H NMR ($CDCl_3$) δ 4.67 (dd, 2H, *J* = 7.1, 14.2 Hz), 3.86 (ddd, 1H, *J* = 7.0, 14.0, 21.9 Hz), 2.50 (t, 2H *J* = 7.3 + 7.6 Hz), 2.06 (m, 2H), 1.44 (m, 6H); ^{13}C NMR 213.04, 119.16, 70.28, 44.57, 32.10, 20.20, 15.21, 13.93; MS: *m*/*z* 226.51 $(M + Na)^+$, 242.51 $(M + K)^+$.

***R*-(−)-4-(Methyldithio)pentanoic Acid (18).** A solution of *R*-4-*O*-(ethylxanthic)pentanenitrile (**17**, 2.0 g, 9.85 mmol) in a mixture of ethanol (10 mL) and water (200 mL) was treated with NaOH (6.0 g). The reaction mixture was refluxed overnight under argon. The mixture was diluted with water (150 mL) and extracted with 1:1 EtOAc/hexane (2 × 100 mL). The aqueous layer was acidified with H_3PO_4 to pH 2.5–3.0 and extracted with EtOAc (6 × 75 mL). The organic layers were combined, dried over $MgSO_4$, filtered, and evaporated to dryness to give crude *R*-4-mercaptopentanoic acid. This crude product was used directly in the next step without further purification. To a solution of 1.60 g of the crude *R*-4-mercaptopentanoic acid in a mixture of ethanol (50 mL) and 0.5 M NaH_2PO_4 buffer at pH 7.0 (75 mL) was added dropwise a solution of methyl methanethiolsulfonate (1.96 g, 15.53 mmol) in dry THF (7 mL) over 45 min at 0 °C. The reaction mixture was stirred under argon at 0 °C for 30 min and then at room temperature for 2 h. The mixture was concentrated and extracted with dichloromethane (2 × 50 mL). The aqueous layer was acidified with H_3PO_4 to pH 2.5–3.0 and extracted with EtOAc (4 × 100 mL). The organic layers were combined, dried over $MgSO_4$, filtered, and evaporated. The residue was purified by chromatography over silica gel, eluting with HOAc/EtOAc/hexane (1:100:400) to give 1.65 g (93%) of the title compound (R_f = 0.32 (HOAc/EtOAc/hexane, 1:100:400). Recrystallization from ether/hexanes afforded a white solid; mp 157–160 °C; ^{1}H NMR ($CDCl_3$) δ 2.91 (ddd, 1H, *J* = 6.8, 13.7, 20.4 Hz), 2.53 (t, 2H, *J* = 7.7 + 7.4 Hz), 2.42 (s, 3H), 1.96 (m, 2H), 1.36 (d, 3H, *J* = 6.8 Hz); ^{13}C NMR 179.46, 45.67, 31.91, 31.07, 25.02, 21.36; MS: 202.9 $(M + Na)^+$, 203.9; $[\alpha]^{25}_D$ = −39.16 (*c* = 2, CH_3OH).

DAC EX. 2040 IPR2022-01531 Page 1213 of 1299

Journal of
Medicinal Chemistry

ice/acetone bath. Acetonitrile (9.4 mL, 18 mmol) was added dropwise via a syringe over approximately 5 min. The reaction mixture was stirred for 30 min, while a white precipitate of lithiated acetonitrile was formed. Isobutylene sulfide (15.0 g, 17 mmol) was dissolved in anhydrous THF (100 mL) and added dropwise over approximately 30 min via the addition funnel. The cooling bath was removed, and the reaction was allowed to stir at room temperature for 3 h. The flask was cooled in an ice/water bath as 0.5 M HCl (38 mL) was added dropwise. The THF layer was retained, and the aqueous layer was washed twice with 75 mL of ethyl acetate. The THF and ethyl acetate layers were combined, dried over approximately 20 g of anhydrous sodium sulfate, and transferred to a 250 mL flask. The solvent was removed by rotary evaporation under reduced pressure to give crude **21**. Ethanol (30 mL) was added, and the contents were stirred. A solution of NaOH (8 g) in water (30 mL) was slowly added. The flask was equipped with a reflux condenser and placed under an argon atmosphere. The reaction was refluxed overnight and then cooled to room temperature. Water (60 mL) was added, and the mixture was extracted twice with 25 mL portions of a 2:1 mixture of ethyl acetate and hexane. The aqueous layer was acidified to pH 2 with concentrated HCl and then extracted with ethyl acetate (3 × 75 mL). The organic layers were dried over anhydrous Na_2SO_4, and the solvent was removed by rotary evaporation under vacuum to give 10 g of product **22** (39% yield). The material was used without further purification. ^{1}H NMR ($CDCl_3$) δ 1.38 (6H, s), 1.87–1.93 (2H, m), 2.08 (1H, s), 2.51–2.57 (2H, m).

4-Methyl-4-(methyldithio)pentanoic Acid (23). A solution of 4-mercapto-4-methylpentanoic acid (**22**) (6.0 mL, 40 mmol) was dissolved in deionized water (50 mL) in a 250 mL flask. The solution was magnetically stirred as sodium carbonate (6.4 g, 60 mmol) was added to the acid at a rate that would not cause excessive frothing. The flask was equipped with a 100 mL addition funnel, which was charged with a solution of methyl methanethiolsulfonate (7.5 g, 60 mmol) dissolved in absolute ethanol (30 mL). The flask was cooled in an ice/water bath, and the system was maintained under an argon atmosphere. The methyl methanethiolsulfonate solution was added dropwise to the flask as rapidly as possible but without causing excessive frothing. The cooling bath was removed, and the reaction mixture was allowed to stir at room temperature for an additional 3 h. The solvent was removed by rotary evaporation under vacuum, until approximately 20 mL remained. Then, saturated sodium bicarbonate (10 mL) and deionized water (30 mL) were added. The mixture was washed with ethyl acetate (3 × 25 mL), and the aqueous layer was separated and adjusted to approximately pH 2 with 5 M HCl and then extracted with ethyl acetate (2 × 120 mL). The organic layers were combined and washed with a solution composed of saturated NaCl (16 mL) and 1 M HCl (4 mL). The organic layer was then dried over 14 g of anhydrous sodium sulfate and filtered, and the solvent was removed by rotary evaporation under vacuum to give 5.4 g of product **23** (70% yield) as a white solid. ^{1}H NMR ($CDCl_3$) δ 1.54 (6H, s), 2.15–2.21 (2H, m), 2.64 (3H, s), 2.69–2.72 (2H, m); MS: *m/z* 217.1 $(M + Na)^+$.

General Method for the Synthesis of *N*-Hydroxysuccinimide Esters 9a–d, 14, 19, and 24. (Methyldithio)-alkanoic acid (15 mmol) was dissolved in dichloromethane (20 mL) and stirred magnetically as *N*-hydroxysuccinimide (2.65 g, 23 mmol) was added followed by 1-[3-

DAC EX. 2040 IPR2022-01531 Page 1214 of 1299

Journal of
Medicinal Chemistry

organic layer was dried over anhydrous Na_2SO_4, and the solvent was removed by rotary evaporation under vacuum to give the desired product, which was used without further purification.

General Method for the Synthesis of *N*-Acyl-*N*-methyl-L-alanines (5a–i). *N*-Methyl-L-alanine (18.0 mmol) was dissolved in a mixture of dimethoxyethane (25 mL) and deionized water (25 mL) in a 125 mL flask equipped with a magnetic stir bar. Triethylamine (6.9 g, 36 mmol) was added, and the solution was vigorously stirred as the *N*-hydroxysuccinimidyl ester (**9a–d**, **14**, **19**, **24**) (18 mmol) dissolved in 40 mL of the same solvent mixture was added dropwise over approximately 5 min. After 2 h, the reaction mixture was concentrated to approximately 40 mL by rotary evaporation under vacuum. Deionized water (10 mL) and 1 M HCl were added to give a pH of approximately 2. The mixture was poured into a separatory funnel and extracted with ethyl acetate (2 × 50 mL). The organic layers were combined and washed with saturated sodium chloride solution (10 mL). The organic layer was dried over 8.0 g of anhydrous Na_2SO_4, and the solvent was removed by rotary evaporation under vacuum. The residue was taken up in a minimum volume of ethyl acetate and purified by chromatography on silica (silica: 40 micron flash grade, silica bed: 24 × 3.0 cm, mobile phase: hexanes/ethyl acetate/acetic acid, 50:48:2). The fractions containing the desired product were combined, and the solvent was removed under vacuum. Residual acetic acid was removed by dissolving the residue in a minimum volume of ethyl acetate and precipitating the product by the rapid but dropwise addition of hexane with stirring. Hexane was added until the product was no longer detected in the supernatant by TLC analysis. The precipitate was vacuum-dried for 4 h to give the desired products **5a–i**.

***N*-Methyl-*N*-[(2-methyldithio)-1-oxoethyl]-L-alanine (5a).** Pale yellow solid (19% yield); ^{1}H NMR ($CDCl_3$) δ 1.458 (3H, d, J = 7.6), 2.446 (3H, s), 3.069 (3H, s), 3.666 (2H, s), 5.185 (1H, m); MS: m/z 246.0 $(M + Na)^+$.

***N*-Methyl-*N*-[(3-methyldithio)-1-oxopropyl]-L-alanine (5b).** White solid (60% yield); mp 103–104 °C; ^{1}H NMR ($CDCl_3$) δ 1.449 (3H, d, J = 7.6), 2.422 (3H, s), 2.821 (2H, m), 2.989 (2H,m), 3.017 (3H, s), 5.194 (1H, m). Anal. ($C_8H_{15}NO_3S_2$) C, H, N. MS: m/z 259.9 $(M + Na)^+$.

***N*-Methyl-*N*-[(3-phenyldithio)-1-oxopropyl]-L-alanine (5c).** White solid (60% yield); mp 96–97 °C; ^{1}H NMR ($CDCl_3$) δ 1.42 (2H, d), 2.7–3.0 (7H, m), 5.24 (1H, q), 7.24–7.60 (5H, m).

***N*-Methyl-*N*-[(4-methyldithio-1-oxobutyl]-L-alanine (5d).** White crystals (44% yield); mp 92–93 °C; ^{1}H NMR ($CDCl_3$) δ 1.439 (3H, d, J = 7.2), 2.089 (2H, t, J = 7.2), 2.405 (3H, s), 2.517 (2H, t, J = 7.2), 2.779 (2H, m), 2.989 (3H, s), 5.123 (1H, m); MS: m/z 290.0 $(M + K)^+$.

***N*-Methyl-*N*-[(4-*(R,S)*-methyldithio-1-oxopentyl)] -L-alanine (5f).** White solid (60% yield). ^{1}H NMR δ 1.35 (3H, d, J = 7), 1.41 (3H, d, J = 7), 1.94–2.03 (2H, m), 2.43(3H, s), 2.50–2.55 (2H, m), 2.83–2.93 (1H, m), 2.98 (3H, s), 5.14 (1H, q, J = 7). MS: m/z 288.1 $(M + Na)^+$.

DAC EX. 2040 IPR2022-01531 Page 1215 of 1299

Journal of
Medicinal Chemistry

***N*-Methyl-*N*-[(4-(*R*)-methyldithio)-1-oxopentyl]-*S*-alanine (5h).** White solid (60% yield); ^{1}H NMR δ 1.35 (3H, d, *J* = 7), 1.42 (3H, d, *J* = 7), 1.93–2.00 (2H, m), 2.43 (3H, s), 2.50–2.55 (2H, m), 2.88–2.95 (1H, m), 3.00 (3H, s), 5.14 (1H, q, *J* = 7), MS: *m/z* 288.1 $(M + Na)^+$.

***N*-Methyl-*N*-[4-methyl-(4-methyldithio)-1-oxopentyl]-L-alanine (5i).** White solid (51% yield) mp 77–79 °C; ^{1}H NMR ($CDCl_3$) δ 1.32 (6H, s), 1.42 (3H, d, *J* = 7 Hz), 1.90–97 (2H, m), 2.40 (3H, s), 2.42–2.49 (2H, m), 2.9 (3H, s), 5.15 (1H, q, *J* = 7 Hz). MS: *m/z* 302.0. $(M + Na)^+$.

General Procedure for the Esterification of Maytansinol to Give Maytansinoids 2a–i and 6a–i. In a typical experiment, maytansinol (**4**, 25 mg, 0.044 mmol) and carboxylic acids **5a–i** (0.264 mmol) were dissolved in dichloromethane (3 mL) and stirred under an argon atmosphere. A solution of dicyclohexylcarbodiimide (DCC, 57.2 mg, 0.277 mmol) in dichloromethane (0.7 mL) was added. After 1 min, a solution of 1 M $ZnCl_2$ in diethyl ether (0.055 mL, 0.055 mmol) was added. The mixture was stirred at room temperature for 2 h, then ethyl acetate (5 mL) was added, and the mixture was vacuum filtered through course filter paper. The filtrate was washed with a solution of saturated aqueous sodium bicarbonate (2 mL) followed by a saturated sodium chloride solution (1 mL). The organic layer was separated, dried over anhydrous sodium sulfate, and filtered, and the solvent was removed under reduced pressure. The residue was purified by silica chromatography using a mixture of dichloromethane and methanol to remove the unreacted maytansinol. The fractions containing the desired product were combined, and the solvent was removed under vacuum to give a mixture of diastereomeric maytansinoids bearing the *N*-methyl-*N*-acyl-L- and D-alanine eaters. The residue was taken up in a minimum volume of ethyl acetate and purified by one of three ways: (1) preparative TLC on silica, (2) HPLC on an analytical Kromasil cyano-bonded silica column (4.6 mm × 250 mm), using an isocratic elution at a flow rate of 1 mL/min, with hexane/ethyl acetate/2-propanol (68:24:8, v/v/v), or (3) HPLC using a preparative (50 cm × 250 cm, 10 micron) Kromasil or Diazem cyano-bonded silica column using as mobile phase a 68:8:24 mixture of hexane, 2-propanol, and ethyl acetate. The flow rate was 118 mL/min. Under either HPLC condition, typically, the desired product L-aminoacyl maytansinoid (**2a**–**i**) eluted about 8–10 min before the corresponding D-aminoacyl isomer (**6a**–**i**).

***N*$^{2'}$-Deacetyl-*N*$^{2'}$-[2-(methyldithio)-1-oxoethyl]maytansine (DM0SMe, 2a).** Maytansinol (**4**) was reacted with *N*-methyl-*N*-[(2-methyldithio)-1-oxoethyl]-L-alanine (**5a**) as described above. The desired maytansinoid **2a**, and the corresponding D-aminoacyl isomer **6a** were isolated by purification using preparative TLC, eluting with 5% methanol in ethyl acetate to give a white solid. **6a** ^{1}H NMR δ 0.796 (3H, s), 1.252 (1H, m), 1.306 (3H, d, *J* = 6.4 Hz), 1.322 (3H, d, *J* = 6.8 Hz), 1.344 (3H, d, *J* = 10.8 Hz), 1.414 (2H, m), 1.553 (1H, d, *J* = 14.4 Hz), 1.640 (3H, s), 2.182 (1H, dd, *J* = 12.4, 2.8 Hz), 2.416 (3H, s), 2.624 (1H, dd, *J* = 12, 2.4 Hz), 2.914 (3H, s), 3.022 (1H, d, *J* = 9.6 Hz), 3.099 (1H, d, *J* = 12.4 Hz), 3.210 (3H, s), 3.357 (3H, s), 3.499 (1H, d, *J* = 9.2 Hz), 3.571 (1H, d, *J* = 14 Hz), 3.980 (3H, s), 4.266 (1H, dt, *J* = 12, 1.6 Hz), 4.787 (1H, dd, *J* = 9.2, 2.8 Hz), 5.379 (1H, m), 5.674 (1H, dd, *J* = 9.2, 6 Hz), 6.287 (1H, s), 6.422 (1H, dd, *J* = 11.2, 4 Hz), 6.678 (1H, d, *J* = 1.6 Hz), 6.691 (1H, d, *J* = 8.8 Hz) and

DAC EX. 2040 IPR2022-01531 Page 1216 of 1299

Journal of
Medicinal Chemistry

d, J = 7.6 Hz), 1.689 (3H, s), 1.765 (1H, d, J = 13.6 Hz), 2.214 (1H, dd, J = 11.2, 3.2 Hz), 2.487 (3H, s), 2.667 (1H, dd, J = 12, 2.4 Hz), 2.856 (1H, d, J = 9.6 Hz), 3.114 (3H, s), 3.168 (3H, s), 3.203 (1H, d, J = 13.2 Hz), 3.340 (3H, s), 3.458 (1H, d, J = 9.2 Hz), 3.508 (1H, d, J = 12.8 Hz), 3.636 (2H, J = 6 Hz), 3.995 (3H, s), 4.293 (1H, t), 4.888 (1H, dd, J = 8.8, 3.2 Hz), 5.126 (1H, m), 5.869 (1H, dd, J = 9.6, 6 Hz), 6.230 (1H, d, J = 10.8 Hz), 6.331 (1H, s), 6.423 (1H, dd, J = 11.2, 4 Hz), 6.801 (1H, d, J = 1.2 Hz) and 6.852 (1H, d, J = 1.6 Hz). HRMS calcd for $C_{35}H_{48}ClN_3O_{10}S_2Na$ $(M + Na)^+$, 792.2367; found, 792.2350.

***N*$^{2'}$-Deacetyl-*N*$^{2'}$-(3-methyldithio-1-oxopropyl)-maytansine (DM1SMe, 2b) and Its D-Alanyl Isomer D-DM1SMe (6b).** Maytansinol (**4**) was reacted with *N*-methyl-*N*-[(2-methyldithio)-1-oxopropyl]-L-alanine (**5b**) as described above. Purification by column chromatography over silica gel, eluting with a mixture of dichloromethane/ethyl acetate/methanol to give a mixture of DM1SMe (**2b**) and the D-aminoacyl isomer D-DM1SMe (**6b**). The two diastereomers were separated by HPLC on a Kromasil cyano preparative HPLC column (250 mm × 50 mm, 10 micron particle size). The column was equilibrated in a mixture of hexanes/2-propanol/ethyl acetate (17:2:6, v/v/v) at a flow rate of 150 mL/min. Under these conditions, the desired L-DM1SMe (**2b**) had a retention time of 42 min, whereas the D-DM1SMe isomer (**6b**) elutes at 56 min. Optically pure products were obtained by this method (ee >99.9%). HPLC analysis using a Vydac analytical C-18 column (length: 100 mm, i.d.: 4.6 mm, particle size: 3 microns) at a flow rate of 1 mL/min, eluting with a gradient of water and acetonitrile (0–3 min, 35% CH_3CN; 3–13 min, 35–65% CH_3CN). Under these conditions L-DM1SMe (**2b**) eluted with a retention time of 10.76 min.

DM1SMe (2b). White solid (32% yield); ^{1}H NMR ($CDCl_3$) δ 0.84 (3H, s), 1.11–1.23 (1H, m), 1.31 (3H, d, J = 6 Hz), 1.35 (3H, d, J = 7 Hz), 1.46–1.52 (1H, m), 1.68 (3H, s), 1.97 (1H, d, J = 9 Hz), 2.24 (1H, dd, J = 12, 15 Hz), 2.30 (3H, s), 2.65 (1H, dd, J = 12, 15 Hz), 2.73–2.86 (2H, m), 2.90 (3H, s), 2.92–3.03 (2H, m), 3.08 (1H, d, J = 9 Hz), 3.14 (1H, d, J = 12 Hz), 3.28 (3H, s), 3.39 (3H, s), 3.54 (1H, d, J = 9 Hz), 3.72 (1H, d, J = 13 Hz), 4.02 (3H, s), 4.31 (1H, t, J = 11 Hz), 4.82 (1H, dd, J = 3, 12 Hz), 5.45 (1H, q, J = 7 Hz), 5.69 (1H, dd, J = 9, 15 Hz), 6.25 (1H, s), 6.47 (1H, dd, J = 11, 15 Hz), 6.67 (1H, d, J = 1.5 Hz), 6.77 (1H, d, J = 11 Hz), 6.85 (1H, d, J = 1.5 Hz). HRMS calcd for $C_{36}H_{51}ClN_3O_{10}S_2$ $(M + H)^+$, 784.2704; found, 784.2693; extinction coefficient $\varepsilon_{280\ nm}$ (ethanol) = 5545 M^{-1} cm^{-1}, $\varepsilon_{252\ nm}$ = 25 700 M^{-1} cm^{-1}.

D-DM1SMe (6b). White solid (30% yield); mp 170–171 °C; ^{1}H NMR ($CDCl_3$) δ 0.85 (3H, s), 1.11–1.20 (1H, m 1.22–1.29 (3H, m), 1.49 (3H, d, J = 7.5 Hz), 1.69 (3H, s), 2.20 (1H, dd, J = 3, 14 Hz), 2.40 (3H, s), 2.65 (1H, dd, J = 12, 14 Hz), 2.79–2.84 (3H, m), 2.92–2.96 (2H, m), 3.04 (3H, s), 3.15 (3H, s), 3.33 (3H, s), 3.43 (1H, d, J = 9 Hz), 3.50 (1H, d, J = 12 Hz), 3.98 (3H, s), 4.28 (1H, m), 4.90 (1H, dd, J = 3, 12 Hz), 5.17 (1H, q, J = 7 Hz), 5.88 (1H, dd, J = 9 Hz), 6.22–6.26 (2H, m), 6.41 (1H, dd, J = 11, 15 Hz), 6.78 (1H, d, J = 1.6 Hz), 6.84 (1H, d, J = 1.6 Hz). HRMS calcd for $C_{36}H_{51}ClN_3O_{10}S_2$ $(M + Na)^+$, 806.2524; found, 806.2518.

DAC EX. 2040 IPR2022-01531 Page 1217 of 1299

Journal of
Medicinal Chemistry

0.6. The two products were isolated by extraction with ethyl acetate. The higher R_f band was found to be the D-aminoacyl ester **6c** of maytansinol, and the lower band was the L-aminoacyl ester **2c**. The products were separated and further purified by HPLC on a Waters Radialpak C-18 column, eluting at a flow rate of 1.5 mL/min with a linear gradient of acetonitrile/water (70–90% acetonitrile/10 min). Under these conditions, both isomers had an identical retention time of 6.0 min.

DM1SPh (2c). ^{1}H NMR ($CDCl_3$) δ 0.82 (3H, s), 1.11–1.25 (1H, m), 1.33 (3H, d, J = 3 Hz), 1.61 (3H, s), 1.63 (3H, d, J = 14 Hz), 2.19 (1H, dd, J = 3, 15 Hz), 2.61 (1H, dd, J = 12, 15 Hz), 2.78 (3H, s), 2.68–3.03 (2H, m), 3.07 (1H, d, J = 9 Hz), 3.20 (3H, s), 3.38 (3H, s), 3.53 (1H, d, J = 9 Hz), 3.63 (1H, d, J = 13 Hz), 3.68 (3H, s), 4.01 (3H, s), 4.30 (1H, t, J = 11 Hz), 4.79 (1H, dd, J = 3, 8 Hz), 5.43 (1H, q, J = 7 Hz), 5.68 (1H, dd, J = 9, 15 Hz), 6.23 (1H, s), 6.45 (1H, dd, J = 12, 15 Hz), 6.60 (1H, d, J = 1.5 Hz), 6.75 (1H, d, J = 12 Hz), 6.77 (1H, d, J = 1.5 Hz), 7.22–7.40 (5H, m). HRMS cacld for $C_{41}H_{52}ClN_3O_{10}S_2Na$ $(M+Na)^+$, 868.2680; found, 868.2670.

D-DM1SPh (6c). ^{1}H NMR ($CDCl_3$) δ 0.89 (3H, s), 1.31 (3H, d, J = 6.4 Hz), 1.48–1.53 (m, 1H), 1.51 (3H, d), 1.72 (3H, s), 2.10 (1 H, d, J = 6 Hz), 2.15 (1H, dd, J = 3, 15 Hz), 2.69 (1H, dd, J = 12, 15 Hz), 2.81–2.89 (2H, m), 2.96 (3H, s), 3.02 (1H, d, J = 7 Hz), 3.20 (3H, s), 3.36 (3H, s), 3.47 (1H, d, J = 9 Hz), 3.55 (1H, d, J = 13 Hz), 3.68 (3H, s), 4.04 (3H, s), 4.31 (1H, t, J = 11 Hz), 4.93 (1H, dd, J = 3, 12 Hz), 5.20 (1H, q, J = 7 Hz), 5.90 (1H, dd, J = 9, 15 Hz), 6.25 (1H, s), 6.27 (1H, d, J = 12 Hz), 6.45 (1H, dd, J = 12, 15 Hz), 6.83 (1H, d, J = 1.5 Hz, 6.89 (1H, d, J = 1.5 Hz), 7.27–7.49 (5H, m). HRMS cacld for $C_{41}H_{52}ClN_3O_{10}S_2Na$ $(M+Na)^+$, 868.2680; found, 868.2672.

***N*$^{2'}$-Deacetyl-*N*$^{2'}$-[3-(methyldithio)-1-oxobutyl]maytansine (DM2'SMe, 2d).** Maytansinol (**4**) was reacted with *N*-methyl-*N*-3-(methyldithio)-1-oxobutyl]-L-alanine (**5d**) as described above. The reaction mixture was purified by preparative TLC on silica gel, eluting twice with 7% MeOH in $CHCl_3$. Two new UV absorbing bands (R_f = 0.65, 0.75) were obtained. The products were isolated by extraction with ethyl acetate. The higher R_f band was determined to be the D-aminoacyl ester **6d** (31%), whereas the lower R_f band was the desired L-aminoacyl ester **2d** (44%). Both isomers were further purified by HPLC using a Waters Radialpak C-18 column, eluting at a flow rate of 2 mL/min with a linear gradient of acetonitrile/water (50–80% acetonitrile/10 min). Under these conditions, the D-aminoacyl ester had a retention time of 7.4 min, whereas the L-aminoacyl isomer had a retention time of 7.6 min. The diastereomeric purity of **2d** and **6d** were determined by HPLC analysis using a Kromasil cyano column (250 mm × 4.6 mm, 10 micron particle size) at a flow rate of 1.50 mL/min, eluting with an isocratic mixture of ethyl acetate/hexane/2-propanol (24:66:10/v/v). Under these conditions, **2d** eluted with a retention time of 11.96 min, and its D-alanyl **6d** isomer eluted with a retention time of 17.30 min.

2d. ^{1}H NMR ($CDCl_3$) δ 0.803 (3H, s), 1.265 (2H, m), 1.280 (3H, d, J = 2.4 Hz), 1.309 (3H, d, J = 2.4 Hz), 1.638 (1H, d, J = 13.6 Hz), 1.643 (3H, s), 1.760 (1H, m), 2.051 (2H, m), 2.179 (1H, dd, J = 11.2, 2.8 Hz), 2.318 (3H, s), 2.365–2.536 (2H, m), 2.611 (1H, dd, J = 12.4, 2 Hz), 2.719 (2H, m), 2.852 (3H, s), 3.033 (1H, d, J = 9.6 Hz), 3.110 (1H, d, J = 12.4 Hz), 3.219 (3H, s), 3.355 (3H, s), 3.498 (1H, d, J = 10.8

DAC EX. 2040 IPR2022-01531 Page 1218 of 1299

Journal of
Medicinal Chemistry

6d. ^{1}H NMR ($CDCl_3$) δ 0.874 (3H, s), 1.193−1.429 (3H, m), 1.290 (3H, d, *J* = 6.4 Hz), 1.314 (3H, d, *J* = 6.8 Hz), 1.696 (3H, s), 1.777 (1H, d, *J* = 13.6 Hz), 2.058 (2H, m), 2.209 (1H, dd, *J* = 11.2, 3.2 Hz), 2.420 (3H, s), 2.529 (2H, m), 2.662 (1H, dd, *J* = 12, 3.6 Hz), 2.727−2.801 (2H, m), 2.826 (1H, d, *J* = 9.6 Hz), 3.044 (3H, s), 3.167 (3H, s), 3.204 (1H, d, *J* = 11.2 Hz), 3.342 (3H, s), 3.439 (1H, d, *J* = 9.2 Hz), 3.514 (1H, d, *J* = 7.6 Hz), 3.999 (3H, s), 4.351 (1H, t), 4.933 (1H, dd, *J* = 8.8, 3.2 Hz), 5.082 (1H, m), 5.844 (1H, dd, *J* = 9.6, 5.6 Hz), 6.231 (1H, d, *J* = 8.8 Hz), 6.242 (1H, s), 6.434 (1H, dd, *J* = 11.2, 4.4 Hz), 6.799 (1H, d, *J* = 2 Hz) and 6.851 (1H, d, *J* = 2 Hz). HRMS calcd for $C_{37}H_{52}ClN_3O_{10}S_2Na$ $(M + Na)^+$, 820.2680; found, 820.2658.

***N*$^{2'}$-Deacetyl-*N*$^{2'}$-[4-(*R,S*)-(methyldithio)-1-oxopentyl]maytansine (DM3-SMe, 2f).** Maytansinol (**4**) was reacted with *N*-methyl-*N*-[(4-*(R,S)*-methyldithio-1-oxopentyl)]-*S*-alanine (**5f**) as described above. The reaction mixture was purified by silica chromatography using a mixture of dichloromethane and methanol to remove unreacted maytansinol. The fractions containing the desired product were combined, and the solvent was removed under vacuum to give a mixture of the diastereomers **2f** and **6f.** The residue was purified on a 50 cm × 250 cm, 10 micron Diazem CN column using as mobile phase a 68:8:24 mixture of hexane, 2-propanol, and ethyl acetate. The flow rate was 118 mL/min. The desired product **2f** eluted with a retention time of 11 min, and the undesired diastereomer **6f** had a retention time of 19 min.

2f. White solid (36% yield). ^{1}H NMR ($CDCl_3$) δ 0.80 (3H, s), 1.19−1.23(1H,m), 1.28−1.36 (9H, m), 1.42−1.46(1H, m), 1.53−1.63 (2H, m), 1.64 (3H, s), 1.80−1.89 (1H, m), 1.90−2.09 (1H, m), 2.18 (1H, dd, *J* = 3 and 14 Hz), 2.32 (3H, s), 2.33−2.42 (1H, m), 2.49−2.62 (2H, m), 2.88 (3H, s), 3.04 (1H, d, *J* = 9 Hz), 3.11 (1H,d,*J* = 11 Hz), 3.23 (3H,s), 3.35 (3H,s), 3.49 (1H, d, *J* = 9 Hz), 3.63 (1H, d, *J* = 12 Hz), 3.98 (3H, s), 4.27 (1H, t, *J* = 10 Hz), 4.79 (1H, dd, *J* = 3 and 12 Hz), 5.41 (1H, q, *J* = 7 Hz), 5.66 (1H, dd *J* = 9 and 15 Hz), 6.21 (1H, s), 6.42 (1H, dd, *J* = 11 and 15 Hz), 6.65 (1H, d, *J* = 1.5 Hz), 6.73 (1H, d, *J* = 11 Hz), 6.81 (1H, d, *J* = 1.5 Hz). HRMS calcd for $C_{38}H_{54}ClN_3O_{10}S_2Na$ $(M + Na)^+$, 834.2837; found, 834.2819.

6f. White solid (30% yield) ^{1}H NMR δ 0.869 (3H, s), 1.200−1.315 (2H, m), 1.283 (3H, d, *J* = 6.8 Hz), 1.373 (3H, dd, *J* = 5.6, 1.2 Hz), 1.498 (3H, d, *J* = 7.6 Hz), 1.600 (1H, d, *J* = 14.4 Hz), 1.691 (3H, s), 1.772 (1H, m), 1.929 (2H, m), 2.203 (1H, dd, *J* = 11.6, 3.2 Hz), 2.421 (3H, s), 2.518 (2H, m), 2.654 (1H, t), 2.814 (1H, dd, *J* = 8, 1.6 Hz), 2.902 (1H, m), 3.038 (3H, d, *J* = 3.2 Hz), 3.164 (3H, s), 3.200 (1H, d, *J* = 13.2 Hz), 3.339 (3H, s), 3.436 (1H, d, *J* = 8 Hz), 3.507 (1H, d, *J* = 12.8 Hz), 3.996 (3H, s), 4.309 (1H, t), 4.936 (1H, dd, *J* = 4.8, 4 Hz), 5.093 (1H, m), 5.851 (1H, m), 6.233 (1H, d, *J* = 11.2 Hz), 6.269 (1H, s), 6.429 (1H, dd, *J* = 10.8, 4.4 Hz), 6.792 (1H, s) and 6.848 (1H, s). HRMS calcd for $C_{38}H_{54}ClN_3O_{10}S_2Na$ $(M + Na)^+$, 834.2837; found, 834.2830.

***N*$^{2'}$-Deacetyl-*N*$^{2'}$-[4-(*S*)-(methyldithio)-1-oxopentyl]maytansine (2g).** Maytansinol (**4**) was coupled with *N*-methyl-*N*-[(4-*(S)*-methyldithio)-1-oxopentyl]-*S*-alanine (**5g**) using DCC and zinc chloride in dichloromethane as described above for the synthesis of **2f**. A mixture of 2 diastereomers bearing

DAC EX. 2040 IPR2022-01531 Page 1219 of 1299

Journal of
Medicinal Chemistry

(*R,S*) was well separated and eluted at 34.6 min.

2g. ^{1}H NMR ($CDCl_3$) δ 0.798 (3H, s), 1.197–1.267 (2H, m), 1.292 (3H, d, *J* = 7.2 Hz), 1.283 (3H, d, *J* = 2 Hz), 1.300 (3H, d, *J* = 1.2 Hz), 1.462 (1H, m), 1.536 (1H, d, *J* = 8 Hz), 1.640 (3H, s), 1.834–2.020 (2H, m), 2.176 (1H, dd, *J* = 11.6, 2.8 Hz), 2.326 (3H, s), 2.373–2.522 (2H, m), 2.603 (1H, dd, *J* = 12.4, 2 Hz), 2.847 (3H, s), 2.871–2.903 (1H, m), 3.028 (1H, d, *J* = 9.6 Hz), 3.108 (1H, d, *J* = 12.4 Hz), 3.223 (3H, s), 3.351 (3H, s), 3.499 (1H, d, *J* = 9.2 Hz), 3.639 (1H, d, *J* = 12.8 Hz), 3.983 (3H, s), 4.279 (1H, t), 4.627 (1H, dd, *J* = 8.8, 3.2 Hz), 5.388 (1H, m), 5.658 (1H, dd, *J* = 8.8, 6.4 Hz), 6.207 (1H, s), 6.426 (1H, dd, *J* = 11.2, 4.4 Hz), 6.639 (1H, d, *J* = 1.6 Hz), 6.737 (1H, d, *J* = 11.2 Hz) and 6.818 (1H, d, *J* = 2 Hz). MS: *m/z* 834.2 $(M + Na)^+$.

6g. ^{1}H NMR ($CDCl_3$) δ 0.867 (3H, s), 1.251–1.383 (3H, m), 1.284 (3H, d, *J* = 6 Hz), 1.374 (3H, d, *J* = 6.8 Hz), 1.498 (3H, d, *J* = 7.6 Hz), 1.691 (3H, s), 1.763 (1H, d, *J* = 14 Hz), 1.932 (2H, m), 2.206 (1H, dd, *J* = 11.2, 3.2 Hz), 2.421 (3H, s), 2.518 (2H, m), 2.653 (1H, dd, *J* = 12.4, 2.4 Hz), 2.817 (1H, d, *J* = 9.6 Hz), 2.911 (1H, m), 3.034 (3H, s), 3.165 (3H, s), 3.200 (1H, d, *J* = 13.2 Hz), 3.339 (3H, s), 3.438 (1H, d, *J* = 9.2 Hz), 3.508 (1H, d, *J* = 12.8 Hz), 3.996 (3H, s), 4.311 (1H, t), 4.929 (1H, dd, *J* = 8.8, 3.2 Hz), 5.095 (1H, m), 5.856 (1H, dd, *J* = 9.2, 6 Hz), 6.236 (1H, d, *J* = 13.2 Hz), 6.253 (1H, s), 6.428 (1H, dd, *J* = 11.2, 4 Hz), 6.794 (1H, d, *J* = 1.6 Hz) and 6.849 (1H, d, *J* = 1.2 Hz). MS: *m/z* 834.2 $(M + Na)^+$.

***N*$^{2'}$-Deacetyl-*N*$^{2'}$-(4-*(R)*-methyldithio-1-oxopentyl)maytansine (2h).** Maytansinol (**4**) was coupled with *N*-methyl-*N*-[(4-*(R)*-methyldithio)-1-oxopentyl]-*S*-alanine (**5h**) using DCC and zinc chloride in dichloromethane as described above. A mixture of 2 diastereomers bearing the *N*-methyl-*S*-alanyl moiety (**2h**, *S,R*) and the *N*-methyl-*R*-alanyl moiety (**6h**, *R,R*) were obtained. The diastereomers were separated by HPLC on a Kromasil cyano column (4.6 mm × 250 mm), using an isocratic elution at a flow rate of 1 mL/min, with hexane/ethyl acetate/2-propanol (68:24:8, v/v/v). Under these conditions, isomer **2h** (*S.R)* eluted at 23.9 min. The peak for the other isomer **6h** (*R,R*) was well separated and eluted at 33.7 min.

2h. ^{1}H NMR ($CDCl_3$) δ 0.796 (3H, s), 1.230 (2H, m), 1.290 (3H, d, *J* = 5.6 Hz), 1.297 (3H, d, *J* = 1.2 Hz), 1.305 (3H, d, *J* = 6.4 Hz), 1.447 (1H, m), 1.575 (1H, d, *J* = 13.6 Hz), 1.637 (3H, s), 1.815–2.002 (2H, m), 2.170 (1H, dd, *J* = 11.2, 3.2 Hz), 2.303 (3H, s), 2.357–2.547 (2H, m), 2.606 (1H, dd, *J* = 12, 2.4 Hz), 2.846 (3H, s), 3.027 (1H, d, *J* = 9.6 Hz), 3.108 (1H, d, *J* = 12.8 Hz), 3.215 (3H, s), 3.350 (3H, s), 3.494 (1H, d, *J* = 9.6 Hz), 3.648 (1H, d, *J* = 12.8 Hz), 3.978 (3H, s), 4.273 (1H, t), 4.775 (1H, dd, *J* = 9.2, 2.8 Hz), 5.384 (1H, m), 5.665 (1H, m), 6.227 (1H, s), 6.634 (1H, d, *J* = 1.6 Hz), 6.734 (1H, d, *J* = 11.2 Hz) and 6.816 (1H, d, *J* = 1.6 Hz). MS: *m/z* 834.2 $(M + Na)^+$.

6h. ^{1}H NMR ($CDCl_3$) δ 0.867 (3H, s), 1.280 (3H, d, *J* = 6.4 Hz), 1.359 (2H, m), 1.384 (3H, d, *J* = 6.4 Hz), 1.446 (1H, m), 1.495 (3H, d, *J* = 7.2 Hz), 1.689 (3H, s), 1.780 (1H, d, *J* = 13.4 Hz), 1.886–1.964 (2H, m), 2.200 (1H, dd, *J* = 11.6, 2.8 Hz), 2.419 (3H, s), 2.470–2.564 (2H, m), 2.651 (1H, dd, *J* = 12, 2.4 Hz), 2.808 (1H, d, *J* = 9.6 Hz), 2.893 (1H, m), 3.040 (3H, s), 3.161 (3H, s), 3.196 (1H, d, *J* = 13.2 Hz), 3.338 (3H, s), 3.432 (1H, d, *J* = 9.2 Hz), 3.504 (1H, d, *J* = 12.8 Hz), 3.993 (3H, s), 4.303 (1H, t), 4.938 (1H, dd,

DAC EX. 2040 IPR2022-01531 Page 1220 of 1299

Journal of
Medicinal Chemistry

Alanyl Isomer D-DM4SMe. Maytansinol (**4**) was reacted with *N*-methyl-*N*-[4-methyl-4-(methyldithio)-1-oxopentyl]-L-alanine (**5i**), as described above. The reaction mixture was purified by silica chromatography using a mixture of dichloromethane and methanol to remove the unreacted maytansinol. The fractions containing the desired product were combined, and the solvent was removed under vacuum to give a mixture of diastereomers **2i** and **6i**. The residue was taken up in a minimum volume of ethyl acetate and purified on a 50 cm × 250 cm, 10 micron Diazem CN column using as mobile phase a mixture of hexane, 2-propanol, and ethyl acetate at a ratio of 68:8:24. The flow rate was 118 mL/min. Under these conditions, the desired product **2i** eluted with a retention time of 11 min, and the undesired diastereomer **6i** had a retention time of 19 min.

2i (DM4SMe). White solid (36% yield); ^{1}H NMR ($CDCl_3$) δ 0.80 (3H, s), 1.28–1.36 (13H, m), 1.42–1.46(2H, m), 1.53–1.63 (2H, m), 1.64 (3H, s), 1.75–1.85 (1H, m), 1.90–2.10 (1H, m), 2.18 (1H, dd, *J* = 3 and 14 Hz), 2.31 (3H,s), 2.40–2.49 (1H, m), 2.50–2.65 (1H, m), 2.85 (3H, s), 3.04 (1H, d, *J* = 9 Hz), 3.11 (1H,d,*J* = 11 Hz), 3.23 (3H,s), 3.35 (3H,s), 3.49 (1H, d, *J* = 9 Hz), 3.63 (1H, d, *J* = 12 Hz), 3.98 (3H, s), 4.27 (1H, t, *J* = 10 Hz), 4.79 (1H, dd, *J* = 3 and 12 Hz), 5.41 (1H, q, *J* = 7 Hz), 5.66 (1H, dd *J* = 9 and 15 Hz), 6.21 (1H, s), 6.42 (1H, dd, *J* = 11 and 15 Hz), 6.65 (1H, d, *J* = 1.5 Hz), 6.73 (1H, d, *J* = 11 Hz), 6.81 (1H, d, *J* = 1.5 Hz). HRMS $(M + H)^+$ calcd for $C_{39}H_{57}ClN_3O_{10}S_2$. $(M + H)^+$, 826.3174; found, 826.3150; extinction coefficient (ethanol) $\varepsilon_{280\ nm}$ = 5140 M^{-1} cm^{-1}, $\varepsilon_{252\ nm}$ = 24 700 M^{-1} cm^{-1}.

6i (D-DM4SMe). White solid; mp 165–167 °C; ^{1}H NMR ($CDCl_3$) δ 0.869 (3H, s), 1.265 (3H, d, *J* = 7.2 Hz), 1.327 (6H, s), 1.495 (3H, d, *J* = 7.6 Hz), 1.590 (2H, m), 1.690 (3H, s), 1.785 (1H, m), 1.915 (2H, m), 2.201 (1H, dd, *J* = 17.6 and 11.6 Hz), 2.422 (3H, s), 2.452 (2H, m), 2.646 (1H, d, *J* = 26.8 and 2.4 Hz), 2.800 (1H, d, *J* = 9.6 Hz), 3.041 (3H, s) 3.165 (3H, s), 3.195 (1H, d, *J* = 13.2 Hz), 3.340 (3H, s), 3.431 (1H, d, *J* = 9.2 Hz), 3.508 (1H, d, *J* = 12.8 Hz), 3.995 (3H, s), 4.313 (1H, t), 4.960 (1H, dd, *J* = 15.2 and 8.8 Hz), 5.117 (1H, q, *J* = 7.6 Hz), 5.838 (1H, dd, *J* = 24.4 and 6 Hz), 6.233 (1H, d, *J* = 10 Hz), 6.246 (1H, s), 6.428 (1H, dd, *J* = 26 and 4 Hz), 6.785 (1H, d, *J* = 1.6) and 6.847 (1H, d, *J* = 1.6 Hz). HRMS calcd $C_{39}H_{56}ClN_3O_{10}S_2Na$ $(M + Na)^+$, 848.2993; found, 848.2975.

***N*$^{2'}$-Deacetyl-*N*$^{2'}$-(3-mercapto-1-oxopropyl)-maytansine (DM1, 25a).** A solution of *N*$^{2'}$-deacetyl-*N*$^{2'}$-(3-methyldithio-1-oxopropyl)-maytansine (**2b**) (1.95 g, 2.5 mmol) in a mixture of ethyl acetate (140 mL) and methanol (210 mL) was stirred at room temperature under an argon atmosphere and treated with a solution of dithiothreitol (0.95 g, 6.2 mmol) in 0.05 M potassium phosphate buffer (140 mL) at pH 7.5 containing 2 mM ethylenediaminetetraacetic acid (EDTA). The progress of the reaction was monitored by HPLC and was complete in three hours. The reaction mixture was treated with a solution of 0.2 M potassium phosphate buffer (250 mL) at pH 6.0 containing 2 mM EDTA and then extracted with ethyl acetate (3 × 600 mL). The organic layers were combined, washed with brine (100 mL), and then dried over sodium sulfate. Evaporation of the solvent gave a residue of crude thiol-containing maytansinoid **25a**. The crude residue was purified by HPLC using a preparative Diazem cyano HPLC column (250 mm × 50 mm, 10 micron particle size) that was equilibrated in a mixture of hexanes/2-propanol/ethyl acetate (78.0:5.5:16.5, v/v/v) and run at a flow rate of 150 mL/min. The desired product **25a** eluted as a peak centered at 16 min. The fractions

DAC EX. 2040 IPR2022-01531 Page 1221 of 1299

Journal of
Medicinal Chemistry

(1H, dd, J = 3 and 12 Hz), 5.45 (1H, q, J = 7 Hz), 5.67 (1H, dd J = 9 and 15 Hz), 6.25 (1H, s), 6.47 (1H, dd, J = 11 and 15 Hz), 6.70 (1H, d, J = 1.5 Hz), 6.75 (1H, d, J = 11 Hz), 6.86 (1H, d, J = 1.5 Hz). HRMS calcd for $C_{35}H_{49}ClN_3O_{10}S$ $(M + H)^+$ 738.2827; found, 738.2820; $[\alpha]^{25}_D$ = −113.2, (c = 0.306, $CHCl_3$); extinction coefficient (methanol): $\varepsilon_{280\ nm}$ = 5422 M^{-1} cm^{-1}, $\varepsilon_{252\ nm}$ = 25 800 M^{-1} cm^{-1}.

HPLC Analysis. HPLC analysis was performed using a Waters symmetry shield analytical C-8 column (length: 150 mm, i.d.: 3.9 mm, particle size: 5 microns) operating at 40 °C and at a flow rate of 1 mL/min, eluting with a linear gradient of water (containing 0.05% TFA) and acetonitrile (containing 0.05% TFA) from 35% to 45% acetonitrile over 30 min. Under these conditions, DM1 (**25a**) eluted with a retention time of 12.13 min. The diastereomeric purity of **25a** was determined by HPLC analysis using a Diazem cyano column (length: 250 mm, i.d.: 4.6 mm, particle size: 5 microns) at a flow rate of 1 mL/min, eluting with a isocratic mixture of ethyl acetate/hexane/2-propanol (24:68:8 v/v respectively). Under these conditions, **25a** eluted with a retention time of 13.70 min. There was no detectable signal for the D-isomer **26a**, which elutes at 17.3 min.

D-DM1 (26a). A solution of D-DM1SMe (**6b**) (20 mg, 0.027 mmol) in a mixture of ethyl acetate (0.5 mL) and methanol (1.0 mL) was stirred at room temperature under an argon atmosphere and treated with a solution of dithiothreitol (6.1 mg, 0.039 mmol) in 0.05 M potassium phosphate buffer (0.5 mL) at pH 7.5 containing 2 mM ethylenediamine-tetraacetic acid (EDTA). The progress of the reaction was monitored by HPLC and was complete in 2 h. The reaction mixture was then extracted with ethyl acetate (3 × 1 mL). The organic layers were combined and dried over sodium sulfate. Evaporation of the solvent gave a residue of crude thiol-containing maytansinoid **26a**. The crude residue was purified by HPLC using a semipreparative Diazem cyano HPLC column (250 mm × 10 mm, 10 micron particle size) that was equilibrated in a mixture of hexanes/2-propanol/ethyl acetate (65:10:25, v/v/v) and run at an initial flow rate of 2 mL/min. After 2 min, the flow rate was increased to 4.5 mL/min for the remainder of the run. The desired product eluted as a peak centered at 15 min. The fractions containing the product were evaporated to give **26a** as a white solid; mp 187−192 °C (dec); ^{1}H NMR ($CDCl_3$) δ 0.85 (3H, s), 1.26−1.29 (4H, m), 1.50 (3H, d, J = 7.6 Hz), 1.69 (3H, s), 2.21 (1H, dd, J = 3 and 14 Hz), 2.65 (1H, dd, J = 12 Hz and 14 Hz), 2.79−2.84 (3H, m), 2.92−2.96 (6H, m), 3.03 (3H, s), 3.16 (3H, s), 3.34 (3H, s), 3.45 (1H, d, J = 9 Hz), 3.51 (1H, d, J = 12 Hz), 4.00 (3H, s), 4.04 91H, m), 4.29 (1H, m), 4.88 (1H, dd, J = 3 and 12 Hz), 5.20 (1H, q, J = 7 Hz), 5.90 (1H, dd, J = 9 and 15 Hz), 6.23−6.27 (2H, m), 6.43 (1H, dd, J = 11 and 15 Hz), 6.80 (1H, d, J = 1.6 Hz), 6.85 (1H, d, J = 1.6 Hz). HRMS calcd for $C_{35}H_{48}ClN_3O_{10}SNa$ m/z: 760.2647 $(M + H)^+$; found, 760.2637; $[\alpha]^{25}_D$ = −135.0, (c = 0.294, $CHCl_3$). HPLC analysis: The diastereomeric purity of **26a** was determined as described above for **26a**. The isomer **26a** eluted with a retention time of 17.25 min. There was no detectable signal for the L-isomer, which elutes at 13.7 min,

***N*$^{2'}$-Deacetyl-*N*$^{2'}$-(4-mercapto-1-oxopentyl)maytansine (DM3, 25b).** DM3-SMe (**2f**, 12 mg, 0.015 mmol) was dissolved in 1.0 mL of a 1:1 mixture of ethyl acetate and methanol. A solution of dithiothreitol (18 mg, 0.117 mmol) in 0.50 mL of 50 mM phosphate buffer at pH 7.5 was then added. The reaction solution was magnetically stirred under an argon atmosphere for 3 h, then 1 mL of 200

DAC EX. 2040 IPR2022-01531 Page 1222 of 1299

Journal of
Medicinal Chemistry

a 50 cm × 250 cm, 10 micron Diazem CN column using as mobile phase a 70:8:22 mixture of hexane, 2-propanol, and ethyl acetate. The flow rate was 22 mL/min. The desired product eluted with a retention time of 10 min. The fractions containing the pure product were combined, and the solvent was removed under vacuum to give 11 mg of product **25b** (97% yield). ^{1}H NMR ($CDCl_3$) δ 0.80 (3H, s), 1.19–1.23(1H,m), 1.28–1.36 (9H, m), 1.42–1.46(1H, m), 1.53–1.63 (2H, m), 1.64 (3H, s), 1.80–1.89 (1H, m), 1.90–2.09 (1H, m), 2.18 (1H, dd, *J* = 3 and 14 Hz), 2.33–2.42 (1H, m), 2.49- -2.62 (2H, m), 2.88 (3H, s), 3.04 (1H, d, *J* = 9 Hz), 3.11 (1H,d,*J* = 11 Hz), 3.23 (3H,s), 3.35 (3H,s), 3.49 (1H, d, *J* = 9 Hz), 3.63 (1H, d, *J* = 12 Hz), 3.98 (3H, s), 4.27 (1H, t, *J* = 10 Hz), 4.79 (1H, dd, *J* = 3 and 12 Hz), 5.41 (1H, q, *J* = 7 Hz), 5.66 (1H, dd *J* = 9 and 15 Hz), 6.21 (1H, s), 6.42 (1H, dd, *J* = 11 and 15 Hz), 6.65 (1H, d, *J* = 1.5 Hz), 6.73 (1H, d, *J* = 11 Hz), 6.81 (1H, d, *J* = 1.5 Hz). HRMS calcd for $C_{37}H_{52}ClN_3O_{10}SNa$ $(M + Na)^+$, 788.2960; found, 788.2957.

***N*$^{2'}$-Deacetyl-*N*$^{2'}$-(4-mercapto-4-methyl-1-oxopentyl)maytansine (DM4, 25c).** DM4SMe (**2i**) (12 mg, 0.015 mmol) was dissolved in 1.0 mL of 1:1 ethyl acetate/methanol. A solution of dithiothreitol (18 mg, 0.117 mmol) in 0.50 mL of 50 mM phosphate buffer at pH 7.5 was then added. The solution was magnetically stirred under an argon atmosphere for 3 h, then 1 mL of 200 mM phosphate buffer at pH 6.0 was added, and the mixture was extracted three times with 2 mL portions of ethyl acetate. The organic layers were combined and washed with 1 mL of saturated sodium chloride solution and then dried over 1 g of anhydrous sodium sulfate. The solvent was removed under vacuum, and the residue was taken up in a minimum of ethyl acetate and purified on a 50 cm × 250 cm, 10 micron Diazem CN column using as mobile phase a mixture of hexane, 2-propanol, and ethyl acetate at a ratio of 70:8:22. The flow rate was 22 mL/min. The desired product eluted with a retention time of 10 min. The fractions containing product were combined, and the solvent was removed under vacuum to give 11 mg of **25c** (97% yield) as a white solid; mp 185–187 °C (dec); ^{1}H NMR ($CDCl_3$) δ 0.80 (3H, s), 1.19–1.23(1H,m), 1.28–1.36 (12H, m), 1.42–1.46(2H, m), 1.53–1.63 (2H, m), 1.64 (3H, s), 1.75–1.85 (1H, m), 1.90–2.10 (1H, m), 2.18 (1H, dd, *J* = 3 and 14 Hz), 2.40–2.49 (1H, m), 2.50–2.65 (2H, m), 2.88 (3H, s), 3.04 (1H, d, *J* = 9 Hz), 3.11 (1H,d,*J* = 11 Hz), 3.23 (3H,s), 3.35 (3H,s), 3.49 (1H, d, *J* = 9 Hz), 3.63 (1H, d, *J* = 12 Hz), 3.98 (3H, s), 4.27 (1H, t, *J* = 10 Hz), 4.79 (1H, dd, *J* = 3 and 12 Hz), 5.41 (1H, q, *J* = 7 Hz), 5.66 (1H, dd *J* = 9 and 15 Hz), 6.21 (1H, s), 6.42 (1H, dd, *J* = 11 and 15 Hz), 6.65 (1H, d, *J* = 1.5 Hz), 6.73 (1H, d, *J* = 11 Hz), 6.81 (1H, d, *J* = 1.5 Hz). HRMS calcd for $C_{38}H_{54}ClN_3O_{10}SNa$ $(M + Na)^+$, 802.3101; found, 802.3116. $[\alpha]^{25}_D$ = −106.7, (*c* = 0.057, $CHCl_3$), extinction coefficient (ethanol): $\varepsilon_{280\ nm}$ = 5180 M^{-1} cm^{-1}, $\varepsilon_{252\ nm}$ = 26 200 M^{-1} cm^{-1}. HPLC analysis: purity was determined by HPLC analysis using a Vydac analytical C-18 column (250 mm × 4.6 mm, 3 micron particle size) at a flow rate of 1.00 mL/min in a gradient of water and acetonitrile, eluting with 37–58% acetonitrile over 25 min. Under these conditions L-DM4 (**25c**) eluted with a retention time of 11.8 min. The purity of L-DM4 was 98.8%. The diastereomeric purity of **25c** was determined by HPLC analysis using a Diazem cyano column (50 mm × 4.6 mm, 5 micron particle size) at a flow rate of 1.00 mL/min, eluting with a isocratic mixture of ethyl acetate/hexane/2-propanol (20:75:5 v/v/v). Under these conditions, **25c** eluted with a retention time of 4.52 min. There was no

DAC EX. 2040 IPR2022-01531 Page 1223 of 1299

Journal of
Medicinal Chemistry

mL) and methanol (0.5 mL) was stirred at room temperature under an argon atmosphere and treated with a 0.50 mL solution containing dithiothreitol (59.7 mg, 0.387 mmol) in 0.050 M potassium phosphate buffer (0.5 mL) at pH 7.5 and 2 mM ethylenediamine-tetraacetic acid (EDTA). The progress of the reaction was monitored by HPLC and was complete after stirring overnight. The reaction mixture was treated 0.05 M potassium phosphate buffer (1.0 mL) at pH 6.0 containing 2 mM EDTA, and the product was extracted with ethyl acetate (3 × 1 mL). The organic layers were combined and dried over sodium sulfate. Evaporation of the solvent gave a residue of crude thiol-containing maytansinoid **26c**. The crude residue was purified by HPLC using a preparative Diazem cyano HPLC column (250 mm × 10 mm, 10 micron particle size) that was equilibrated in a mixture of hexanes/2-propanol/ethyl acetate (65:10:25, v/v/v) and run at an initial flow rate of 118 mL/min. The desired product **26c** eluted as a peak centered at 12.0 min. The fractions containing the product were evaporated to give **26c** as a white solid.

^{1}H NMR ($CDCl_3$) δ 0.866 (3H, s), 1.282 (3H, d, J = 6.4 Hz), 1.409 (6H, s), 1.500 (3H, d, J = 6.4 Hz), 1.625 (2H, m), 1.689 (3H, s), 1.766 (1H, m), 1.875 (2H, m), 2.205 (1H, dd, J = 17.6 and 11.2 Hz), 2.578 (2H, m), 2.646 (1H, dd, J = 26.8 and 2.8 Hz), 2.811 (1H, d, J = 9.6 Hz), 3.168 (3H, s), 3.196 (1H, d, J = 12.4 Hz), 3.341 (3H, s), 3.431 (1H, d, J = 9.2 Hz), 3.511 (1H, d, J = 13.2 Hz), 3.995 (3H, s), 4.300 (1H, t), 4.946 (1H, dd, J = 15.2 and 8.8 Hz), 5.156 (1H, q, J = 7.6 Hz), 5.836 (1H, dd, J = 24.4 and 6 Hz), 6.243 (1H, d, J = 10.4 Hz), 6.246 (1H, s),6.426 (1H, dd, J = 26.4 and 4 Hz), 6.790 (1H, d, J = 1.6 Hz) and 6.848 (1H, d, J = 1.6 Hz). HRMS calcd for $C_{38}H_{54}ClN_3O_{10}SNa$ $(M + Na)^+$, 802.3101; found, 802.3099; $[\alpha]^{25}_D$ = −90.4, (c = 0.052, $CHCl_3$). HPLC analysis: purity was determined by HPLC analysis using a Vydac analytical C-18 column (250 mm × 4.6 mm, 3 micron particle size) at a flow rate of 1.00 mL/min with a gradient of water and acetonitrile, eluting with 20–50% acetonitrile over 30 min. Under these conditions, D-DM4 (**26c**) eluted with a retention time of 17.85 min. The purity of **26c** was 97.8%. The diastereomeric purity of **26c** was determined as described above for DM4 (**25c**). The isomer eluted with a retention time of 5.42 min. There was no detectable signal for the **25c** isomer, which elutes at 4.52 min, indicating that **26c** was a diastereomerically pure compound.

Synthesis of $N^{2'}$-Deacetyl-$N^{2'}$-[3-(3-carboxy-1-methyl-propyldithio)-1-oxopropyl]-maytansine (DM1-TPA, 2j). A solution of 4-(2-pyridyldithio)pentanoic acid (24 mg, 0.10 mmol) and DM1 (**25a**, 30 mg, 0.041 mmol) in glass distilled methanol (5 mL) was vigorously stirred, and 3 mL of an aqueous buffer (200 mM KH_2PO_4, 2 mM EDTA at pH 7.6) was added dropwise. The reaction was strirred overnight, and the product was purified by HPLC using a Vydac C-18 column (10 × 250 mm) operating at 30 °C and a flow rate of 4.75 mL/min, eluting with a linear gradient of acetonitrile (15% to 85% over 30 min) in 40 mM ammonium acetate buffer at pH 7.2. DM1-TPA (**2j**) eluted with a retention time of 12 min. The product was collected as the ammonium salt was taken up in ethyl acetate (15 mL). The solution was washed with 1 M HCl (4 mL) followed by saturated sodium chloride (3 mL). The organic layer was dried over anhydrous sodium sulfate, and the solvent was removed under vacuum to give 15 mg (37% yield) of product **2j**. ^{1}H NMR (400 MHz, $CDCl_3$) δ 0.81 (3H, s), 1.21–1.37 (11H, m), 1.44–1.48 (1H, m), 1.61 (1H, m), 1.65 (3H, s), 1.77–1.93 (3H, m), 2.20 (1H, d, J = 12 Hz), 2.39–2.49 (2H, m), 2.60 (1H, d, J = 12 Hz), 2.70 (1H, t, J = 9 Hz), 2.78–3.00 (7H,

DAC EX. 2040 IPR2022-01531 Page 1224 of 1299

Journal of
Medicinal Chemistry

Vydac analytical C-18 column (length: 100 mm, i.d.: 4.6 mm, particle size: 3 microns) at a flow rate of 1 mL/min, eluting with a gradient of water and acetonitrile as follows: 0 min: 5% CH_3CN, 5 min: 5% CH_3CN, 5–65 min: 5–95% CH_3CN. Under these conditions DM1-TPA eluted with a retention time of 23.75 min.

Synthesis of $N^{2'}$-Deacetyl-$N^{2'}$-[4-methyl-4-(3-carboxy-propyldithio)-1-oxopentyl]-maytansine (DM4-TBA, 2k). A solution of 4-(2-pyridyldithio)butanoic acid (41.1 mg, 0.179 mmol) and DM4 (**25c**, 70.0 mg, 0.09 mmol) in glass distilled methanol (7 mL) was vigorously stirred, and 5 mL of an aqueous buffer (50 mM KH_2PO_4, 2 mM EDTA at pH 7.5) was added dropwise. The reaction was monitored by HPLC and was complete after 3 h. The solvent was evaporated, and the residue was purified by column chromatography over silica gel, eluting with a mixture of dichloromethane/methanol (97:3, v/v containing 0.1% glacial acetic acid) to give 45 mg (57% yield) of the purified product DM4-TBA (**2k**). ^{1}H NMR ($CDCl_3$) 0.800 (3H, s), 1.239 (6H, s), 1.302 (3H, d, J = 2 Hz), 1.303 (3H, d, J = 15.6 Hz), 1.414–1.513 (1H, m), 1.601 (2H, m), 1.642 (3H, s), 1.813–1.991 (2H, m), 1.932 (2H, t), 2.188 (1H, dd, J = 17.2 and 11.2 Hz), 2.346–2.530 (2H, m), 2.415 (2H, t), 2.636 (1H, dd, J = 18 and 12 Hz), 2.667 (2H, t), 2.875 (3H, s), 3.001 (1H, d, J = 9.6 Hz), 3.121 (1H, d, J = 12.4 Hz), 3.219 (3H, s), 3.356 (3H, s), 3.492 (1H, d, J = 8.8 Hz), 3.641 (1H, d, J = 12.8 Hz), 3.981 (3H, s), 4.293 (1H, t), 4.791 (1H, dd, J = 15.2 and 8.8 Hz), 5.324 (1H, q, J = 6.8 Hz), 5.667 (1H, dd, J = 24.4 and 6.4 Hz), 6.399 (1H, s), 6.421 (1H, dd, J = 26.4 and 4 Hz), 6.500 (1H, d, J = 1.6 Hz), 6.674 (1H, d, J = 11.2 Hz) and 6.826 (1H, d, J = 1.6 Hz). HRMS calcd for $C_{42}H_{60}ClN_3O_{12}S_2Na$ $(M + Na)^+$, 920.3186; found, 920.3192. HPLC analysis was performed using a Vydac analytical C-18 column (length: 100 mm, i.d.: 4.6 mm, particle size: 3 microns) at a flow rate of 1 mL/min, eluting with a linear gradient of 40 mM ammonium acetate buffer at pH 7.2 and acetonitrile as follows: 0 min: 5% CH_3CN, 5 min: 5% CH_3CN, 5–35 min: 5–35% CH_3CN, Under these conditions DM4-TBA eluted with a retention time of 18.40 min.

Synthesis of $N^{2'}$-Deacetyl-$N^{2'}$-(3-mercapto-1-oxopropyl)-maytansine dimer (DM1 dimer, 25d). A solution of **25a** (26.4 mg, 0.035 mmol) in a 1:1 (v/v) mixture of ethanol and 0.05 M potassium phosphate buffer at pH 7.5 (5 mL) was treated with a solution of 2,2′-dithiodipyridine (3.9 mg, 0.017 mmol) in ethanol (1 mL). The reaction mixture was stirred at room temperature for 2 h. Most of the ethanol in the reaction mixture was removed by evaporation under reduced pressure. The resulting aqueous layer was extracted with ethyl acetate (3 × 5 mL), and the combined organic layer was washed with saturated sodium chloride solution (1 × 5 mL) and then dried over sodium sulfate and filtered. The solvent was evaporated under reduced pressure, and the residue was purified by HPLC using a Metachem Inertsil ODS column, eluting with a gradient of water and acetonitrile to provide dimer **25d** as a white solid (13.7 mg, 52% yield). ^{1}H NMR ($CDCl_3$) δ 0.75 (3H, s), 1.23–1.26 (1H, m), 1.28 (3H, d, J = 6 Hz), 1.30 (3H, d, J = 7 Hz), 1.42–1.52 (1H, m), 1.66 (3H, s), 2.15 (1H, m), 2.59 (1H, dd, J = 6 and 14 Hz), 2.71–2.82 (2H, m), 2.84 (3H, s), 3.00 (1H, d, J = 9 Hz), 3.09 (1H, d, J = 12 Hz), 3.18 (3H, s), 3.35 (3H, s), 3.48 (1H, d, J = 9 Hz), 3.61 (1H, d, J = 13 Hz), 3.97 (3H, s), 4.26 (1H, t, J = 11 Hz), 4.76 (1H, dd, J = 3 and 12 Hz), 5.33 (1H, q, J = 7 Hz), 5.61 (1H, dd, J = 9 and 15 Hz), 6.28 (1H, s), 6.41 (1H, dd, J = 11 and 15 Hz), 6.61 (1H, d, J = 1.6 Hz), 6.65 (1H, d, J = 11 Hz), 6.81 (1H, d, J =

DAC EX. 2040 IPR2022-01531 Page 1225 of 1299

Journal of
Medicinal Chemistry

min 40% CH_3CN, 5 min 40% CH_3CN, 5–30 min 40–60% CH_3CN. Under these conditions, DM1 dimer eluted with a retention time of 13.69 min.

Synthesis of $N^{2'}$-Deacetyl-$N^{2'}$-(4-mercapto-4-methyl-1-oxopentyl)-maytansine Dimer (DM4 Dimer, 25e). A solution of **25c** (100.0 mg, 0.128 mmol) in a 1:1 (v/v) mixture of dichloromethane and ethyl acetate (4 mL) was treated with a solution of $CuCl_2$ (85.76 mg, 0.640 mmol) in 0.50 M HCl (3 mL). The reaction mixture was stirred at room temperature for 2 h. The product was extracted with ethyl acetate (5 mL), and the aqueous phase was separated. An additional extraction of the aqueous phase with ethyl acetate (3 mL) was combined with the original mixture and washed with brine (2 mL) and dried over anhydrous Na_2SO_4 and filtered. The solvent was evaporated under reduced pressure to give the L-DM4-dimer **25e** (11.7 mg, 12% yield). ^{1}H NMR ($CDCl_3$) δ 0.796 (6H, s), 1.136 (6H, d, J = 4 Hz), 1.227 (2H, m), 1.298 (12H, s), 1.299 (6H, d, J = 12 Hz), 1.463 (2H, m), 1.633 (6H, s), 1.670–1.842 (4H, m), 2.171 (2H, dd, J = 17.2 and 11.2 Hz), 2.262–2.456 (4H, m), 2.596 (2H, dd, J = 26.4 and 2 Hz), 2.842 (6H, s), 3.028 (2H, d, J = 9.6 Hz), 3.105 (2H, d, J = 12.4 Hz), 3.209 (6H, s), 3.353 (6H, s), 3.489 (2H, d, J = 8.8 Hz), 3.634 (2H, d, J = 12.8 Hz), 3.966 (6H, s), 4.277 (2H, t), 4.766 (2H, dd, J = 14.8 and 9.2 Hz), 5.366 (2H, q, J = 6.8 Hz), 5.644 (2H, dd, J = 24.4 and 6.4 Hz), 6.346 (2H, s), 6.417 (2H, dd, J = 26.4 and 4 Hz), 6.623 (2H, d, J = 1.6 Hz), 6.708 (2H, d, J = 11.2 Hz) and 6.816 (2H, d, J = 1.6 Hz). HRMS calcd for $C_{76}H_{106}Cl_2N_6O_{20}S_2Na$ $(M + Na)^+$, 1579.6178; *m/z*: found, 1579.6180. HPLC analysis was performed using a Vydac analytical C-18 column (length: 100 mm, i.d.: 4.6 mm, particle size: 3 microns) at a flow rate of 1 mL/min, eluting with a gradient of water and acetonitrile (0 min: 5% CH_3CN, 5 min: 5% CH_3CN, 5–65 min: 5–95% CH_3CN. HPLC analysis was performed using a Vydac analytical C-18 column (length: 100 mm, i.d.: 4.6 mm, particle size: 3 microns) at a flow rate of 1 mL/min, eluting with a gradient of water and acetonitrile (37–58% CH_3CN over 25 min). Under these conditions, the DM4 dimer eluted with a retention time of 22.48 min.

***N*-Succinimidyl 4-(2-pyridyldithio)pentanoate(SPP, 27).** A solution of 2.2′-dithiodipyridine (300 g, 1.36 mol) in a mixture of ethanol (1 L) and glacial acetic acid (42 mL) was placed in a flask and stirred under an argon atmosphere. A solution of 4-mercaptopentanoic acid (101.8 g, 0.76 mol) in ethyl acetate (400 mL) was added dropwise over 15 min, and the reaction was stirred for an additional 2 h. The solvent was removed by rotary evaporation, and the residue was purified by column chromatography over silica gel, eluting with a mixture of hexanes/ethyl acetate/acetic acid (4:1:0.1) to give 4-(2-pyridyldithio)pentanoic acid (40 g, 21.4% yield). ^{1}H NMR in $CDCl_3$ δ 1.34 (3H, d, J = 7.0 Hz), 1.72–1.95 (2H, m), 2.52–2.63 (2H, m), 2.91–3.02 (1H, m), 7.08–7.13 (1H, m), 7.62–7.77 (2H, m), 8.46–8.49 (1H, m), 11.5 (1H, br s).

A solution of 4-(2-pyridyldithio)pentanoic acid (30 g, 123 mmol) in dichloromethane (525 mL) was treated with *N*-hydroxysuccinimide (14.3 g, 124 mmol) and 1-[3-(dimethylamino)propyl]-3-ethylcarbodiimide (EDC, 31.8 g, 165 mmol). The contents were stirred at room temperature for 2 h after which ethyl acetate (750 mL) was added. The solution was washed with 0.5% aqueous acetic acid (3 × 300 mL) and then with saturated aqueous NaCl (150 mL). The organic layer was separated

DAC EX. 2040 IPR2022-01531 Page 1226 of 1299

Journal of
Medicinal Chemistry

as ethyl ether (350 mL) was added, followed by hexanes (100 mL). The resulting precipitate was collected by vacuum filtration and dried in a vacuum oven at 30 °C for 12 h, to give SPP (**27**) as a white solid (18.7 g, 45% yield); mp 48–9 °C; ^{1}H NMR ($CDCl_3$) δ 1.36(3H, d, J = 7.0 Hz), 1.97–2.8 (2H, m), 2.73–2.86 (2H, m), 2.84 (4H, br s), 3.02–3.11 (1H, m), 7.08–7.13 (1H, m), 7.62–7.77 (2H, m), 8.46–8.49 (1H, m); Anal. ($C_{14}H_{16}N_2O_4S_2$) C, H, N, S.

***N*-Succinimidyl 4-(2-pyridyldithio)butanoate(SPDB, 28).** A solution of 2,2′-dithiopyridine (3.8 g, 17.3 mmol) in a mixture of acetic acid (0.5 mL) and ethyl alcohol (20 mL) was stirred under an argon atmosphere. A solution of 4-mercaptobutyric acid (**7c**, 1.39 g, 11.6 mmol) in ethyl acetate (10 mL) was added dropwise over approximately 2 min. The contents were stirred for 2 h, and the solvent was evaporated under reduced pressure. The residue was taken up in a minimum volume of ethyl acetate and purified by column chromatography on silica gel, eluting with a mixture of hexanes/ethyl acetate/acetic acid (65:33:2). The fractions containing the pure product were combined, and the solvent was removed under vacuum to give 1.5 g (6.55 mmol, 56% yield) of 4-(2-pyridyldithio)butanoic acid. ^{1}H NMR ($CDCl_3$) δ 2.0–2.1(2H, m), 2.505(1H, t, J = 7 Hz), 2.508 (1H, t, J = 7), 2.74 (1H, t, J = 7 Hz), 2.86 (1H, t, J = Hz), 7.10–7.13 (1H, m), 7.67 (1H, dt, J = 1, J = 5), 7.73 (1H, d, J = 8 Hz), 8.49 (1H, dd, J = 0.7, J = 5 Hz), 11.81 (1H, br s).

A flask containing a stir bar was charged with 4-(2-pyridyldithio)butanoic acid (1.1 g, 4.8 mmol) in dichloromethane (20 mL). *N*-Hydroxysuccinimide (0.64 g, 5.6 mmol) and 1-[3-(dimethylamino)propyl]-3-ethylcarbodiimide (EDC, 1.1 g, 5.6 mmol) were then added. The contents were stirred at room temperature for 2 h after which ethyl acetate (35 mL) was added. The reaction mixture was washed with 0.5 M HCl (3 × 10 mL) and then with saturated aqueous NaCl (1 × 10 mL). The organic layer was separated and dried over anhydrous sodium sulfate and filtered. The solvent was evaporated, and the residue was purified by column chromatography on silica gel, eluting with a mixture of hexanes/ethyl acetate/acetic acid (71:28.8:0.2). The fractions containing the pure product were combined, and the solvent was removed under vacuum. The resulting oil was taken up in a minimum volume of warm reagent-grade ethanol and stirred while ethyl ether (30 mL) was added, followed by hexanes (9.0 mL). The resulting precipitate was collected by filtration and dried in a vacuum oven at 30 °C for 12 h to give 0.50 g of SPDB (**28**) as a white solid (~31% yield); mp 47–48 °C; ^{1}H NMR in $CDCl_3$ δ 2.16 (2H, tt, J = 7, J = 15 Hz), 2.795 (2H, t, J = 7 Hz), 2.83(4H, br s), 2.91(1H, t, J = 7 Hz), 7.09 (1H, m), 7.65–7.67 (2H, m), 8.48 (1H, d, J = 5 Hz); Anal. ($C_{13}H_{14}N_2O_4S_2$) C, H, N, S.

Preparation of Antibody Conjugates with Maytansinoids 25a, 25b, and 25c. A solution of huC242 antibody (8 mg/mL) in aqueous buffer (50 mM potassium phosphate, 50 mM sodium chloride, 2 mM ethylenediaminetetraacetic acid disodium salt) at pH 6.5 was incubated for 2 h with a 7- to 10-fold molar excess of either *N*-succinimidyl 4-(2-pyridyldithio)pentanoate (SPP, **27**, or *N*-succinimidyl-4-(2-pyridyldithio)butanoate (SPDB, **28**). The reaction mixture was purified by passage through a Sephadex G25 gel filtration column to remove low molecular weight material. The concentration of the antibody was determined spectrophotometrically using the known extinction coefficients for the

DAC EX. 2040 IPR2022-01531 Page 1227 of 1299

Journal of
Medicinal Chemistry

determined using the literature extinction coefficients of $\varepsilon_{343\ nm}$ [illegible] and $\varepsilon_{280\ nm}$ [illegible] ^{1} cm^{-1} for pyridine-2-thione.

The modified antibody was diluted to 2.5 mg/mL in aqueous buffer (50 mM potassium phosphate, 50 mM sodium chloride, 2 mM ethylenediaminetetraacetic acid disodium salt) at pH 6.5. The SPP-modified antibody was treated with 1.7 equiv of DM1 (**25a**), whereas the SPDB-modified antibody was treated with a 1.7 equiv of either DM3 (**25b**) or DM4 (**25c**) dissolved in glass-distilled DMA (final concentration of DMA was 3% v/v). The reaction mixture was incubated for 18 h at room temperature. The reaction mixture was purified by passage through a Sephadex G25 gel filtration column to remove the unconjugated drug and other low molecular weight species. The concentration of the conjugate was determined spectrophotometrically using the known extinction coefficients for the antibody ($\varepsilon_{280\ nm}$ = 217 560 M^{-1} cm^{-1} and $\varepsilon_{252\ nm}$ = 80 062 M^{-1} cm^{-1}) and the drugs. The resulting conjugate was monomeric and contained, on the average, 3.2–3.5 maytansinoid molecules linked per antibody molecule.

Cytotoxicity Assays in Vitro. The cell lines used in cytotoxicity assays were (1) KB (ATCC CCl-17), a cell line of human epithelial origin, (2) SK-BR-3 (ATCC HTB-30), a cell line established from a human breast adenocarcinoma, (3) COLO 205 (ATCC CCL-222), a human colon tumor cell line, and (4) A-375 (ATCC CRL 1619), a human melanoma cell line. The cell lines were grown in Dulbecco's modified Eagles Medium (DMEM, Biowhittaker, Walkersville, MD) with L-glutamine supplemented with 10% fetal bovine serum (Hyclone, Logan, UT) and 50 μg/mL of gentamycin sulfate (Life Technologies, Rockville, MD). The cells were maintained at 36–37.5 °C in a humidified atmosphere that contained 6% CO_2.

The cytotoxicity study was performed using a clonogenic assay as previously described.[23,24] The test cell lines were plated into 6-well culture dishes at a constant number of 1000 cells per well. The cells were incubated with varying concentrations (0 to 3 nM) of the various maytansinoids (free or conjugated to antibodies) for 72 h. The medium was then aspirated from the plates and replaced with fresh medium. The cultures were allowed to grow and form colonies for a total of 7–10 days after plating. The cultures were then fixed and stained with 0.2% crystal violet in 10% formalin/PBS, and the colonies were counted. Plating efficiency of nontreated cells (medium alone) was determined by dividing the number of colonies counted by the number of cells plated. The surviving fraction of cells exposed to the drugs was determined by dividing the number of colonies in wells that were exposed to the drug by the number of colonies in the control wells.

Antitumor Activity in Vivo. The in vivo efficacy of conjugates of maytansinoids DM1 (**25a**), DM3 (**25b**), and DM4 (**25c**) with the huC242 antibody was evaluated in a human colon tumor zenograft model established with COLO 205 cells. Five-week-old female SCID mice (20 animals) were inoculated subcutaneously in the right flank with COLO 205 human colon carcinoma cells (1.5×10^6 cells/mouse) in 0.1 mL of serum-free medium. The tumors were grown for 11 days to an average size of 100 mm^3. The animals were then randomly divided into four groups (5 animals per group). The first group of mice served as the control group and were treated with the phosphate-buffered

DAC EX. 2040 IPR2022-01531 Page 1228 of 1299

Journal of
Medicinal Chemistry

weight of the animals was also measured twice per week.

Supporting Information Available

Analytical data (elemental analysis and HRMS and HPLC purity data) for target compounds. This material is available free of charge via the Internet at http://pubs.acs.org.

» jm060319fsi20060505_033029.pdf (26.39 kb)

Semisynthetic Maytansine Analogues for the Targeted Treatment of Cancer

41 views 138 shares 0 downloads



Supporting Information

Semisynthetic Maytansine Analogs for Targeted Treatment of Cancer

*Wayne C. Widdison, Sharon D. Wilhelm, Emily E. Cavanagh, Kathleen R. White Barbara A. Leece, Yelena Kovtun, Victor S. Goldmacher, Hongsheng Xie, Rita M Steeves, Robert J. Lutz, Robert Zhao, Lintao Wang, Walter A. Blättler and Ravi. Chari**

ImmunoGen, Inc., 128 Sidney Street, Cambridge, MA 02139

*Corresponding_Author: Tel. (617) 995-2500. Fax. (617) 995-2510, ravi.chari@immunogen.com

Contents: HPLC purity data for target compounds, including the methods used, data and elemental analysis results.

figshare Share Download

Terms & Conditions

Journal of
Medicinal Chemistry

http://pubs.acs.org/page/copyright/permissions.html.

Author Information

Authors

Wayne C. Widdison - *ImmunoGen, Inc., 128 Sidney Street, Cambridge, Massachusetts 02139*
Sharon D. Wilhelm - *ImmunoGen, Inc., 128 Sidney Street, Cambridge, Massachusetts 02139*
Emily E. Cavanagh - *ImmunoGen, Inc., 128 Sidney Street, Cambridge, Massachusetts 02139*
Kathleen R. Whiteman - *ImmunoGen, Inc., 128 Sidney Street, Cambridge, Massachusetts 02139*
Barbara A. Leece - *ImmunoGen, Inc., 128 Sidney Street, Cambridge, Massachusetts 02139*
Yelena Kovtun - *ImmunoGen, Inc., 128 Sidney Street, Cambridge, Massachusetts 02139*
Victor S. Goldmacher - *ImmunoGen, Inc., 128 Sidney Street, Cambridge, Massachusetts 02139*
Hongsheng Xie - *ImmunoGen, Inc., 128 Sidney Street, Cambridge, Massachusetts 02139*
Rita M. Steeves - *ImmunoGen, Inc., 128 Sidney Street, Cambridge, Massachusetts 02139*
Robert J. Lutz - *ImmunoGen, Inc., 128 Sidney Street, Cambridge, Massachusetts 02139*
Robert Zhao - *ImmunoGen, Inc., 128 Sidney Street, Cambridge, Massachusetts 02139*
Lintao Wang - *ImmunoGen, Inc., 128 Sidney Street, Cambridge, Massachusetts 02139*
Walter A. Blättler - *ImmunoGen, Inc., 128 Sidney Street, Cambridge, Massachusetts 02139*
Ravi V. J. Chari - *ImmunoGen, Inc., 128 Sidney Street, Cambridge, Massachusetts 02139*

References

This article references 24 other publications.

1. Kupchan, S. M.; Komoda, Y.; Court, W. A.; Thomas, G. J.; Smith, R. M.; Karim, A.; Gilmore, C. J.; Haltiwanger, R. C.; Bryan, R. F. Maytansine, a novel antileukemic ansa macrolide from *Maytenus ovatus*. *J. Am. Chem. Soc.* **1972**, *94*, 1354−1356.

| Google Scholar

2. Kupchan, S. M.; Branfman, A. R.; Sneden, A. T.; Verma, A. K.; Dailey, R. G., Jr.; Komoda, Y.; Nagao, Y. Novel maytansinoids. Naturally occurring and synthetic antileukemic esters of maytansinol. *J. Am. Chem. Soc.* **1975**, *97*, 5294−5295.

| Google Scholar

3. Remillard, S.; Rebhun, L. I.; Howie, G. A.; Kupchan, S. M. Antimitotic activity of the potent tumor inhibitor maytansine. *Science***1975**, *189*, 1002−1005.

DAC EX. 2040 IPR2022-01531 Page 1230 of 1299

Journal of
Medicinal Chemistry

4. Huang, A. B.; Lin, C. M.; Hamel, E. Maytansine inhibits nucleotide binding at the exchangeable site of tubulin. *Biochem. Biophys. Res. Commun.* **1985**, *128*, 1239−1246.

| Google Scholar

5. Kupchan, S. M.; Komoda, Y.; Branfman, A. R.; Sneden, A.T.; Court, W. A.; Thomas, G. J.; Hintz, H. P.; Smith, R. M.; Karim, A.; Howie, G. A.; Verma, A. K.; Nagao, Y.; Dailey, R. G., Jr.; Zimmerly, V. A.; Sumner, W. C., Jr.; The maytansinoids. Isolation, structural elucidation, and chemical interrelation of novel ansa macrolides. *J. Org. Chem.* **1977**, *42*, 2349−2357.

| Google Scholar

6. Issell, B. F.; Crooke, S. T. Maytansine. *Cancer Treat. Rev.***1978**, *5*, 199−207.

| Google Scholar

7. Sedlacek, H.-H.; Seemann, G.; Hoffmann, D.; Czech, J.; Lorenz, P.; Kolar, C.; Bosslet, K.; Antibodies as carriers of cytotoxicity. In *Contributions to Oncolology;* Sedlacek, H.-H., et al., Eds.; Basel: New York, 1992; pp 1−145.

Google Scholar

8. Xie, H.; Audette, C.; Hoffee, M.; Lambert, J. M.; Blättler, W. A. Pharmacokinetics and biodistribution of the antitumor immunoconjugate, cantuzumab mertansine (huC242-DM1), and its two components in mice. *J. Pharmacol. Exp. Ther.* **2004**, *310*, 1073−1082.

Google Scholar

9. Chari, R. V. J.; Martell, B. A.; Gross, J. L.; Cook, S. B.; Shah, S. A.; Blättler, W. A.; McKenzie, S. J.; Goldmacher, V. S. Immunoconjugates containing novel maytansinoids: promising anticancer drugs. *Cancer Res.* **1992**, *52*, 127−131.

Google Scholar

10. Liu, C.; Tadayoni, B. M.; Bourret, L. A.; Mattocks, K. M.; Derr, S. M.; Widdison, W. C.; Kedersha, N. L.; Ariniello, P. D.; Goldmacher, V. S.; Lambert, J. M.; Blättler, W. A.; Chari, R. V. J. Eradication of large colon tumor xenografts by targeted delivery of maytansinoids. *Proc. Natl. Acad. Sci. U.S.A.* **1996**, *93*, 8618−8623.

DAC EX. 2040 IPR2022-01531 Page 1231 of 1299

Journal of
Medicinal Chemistry

11. Tolcher, A. W.; Ochoa, L.; Hammond, L. A.; Patnaik, A.; Edwards, T.; Takimoto, C.; Smith, L.; de Bono, J.; Schwartz, G.; Mays, T.; Jonak, Z.L.; Johnson, R.; DeWitte, M.; Martino, H.; Audette, C.; Maes, K.; Chari, R. V. J.; Lambert, J. M.; Rowinsky, E. K. Cantuzumab mertansine, a maytansinoid immunoconjugate directed to the CanAg antigen: a phase I, pharmacokinetic, and biologic correlative study. *J. Clin. Oncol.* **2003**, *21*, 211−222

| Google Scholar

12. Helft, P. R.; Schilsky, R. L.; Hoke, F. J.; Williams, D.; Kindler, H. L.; Sprague, E.; DeWitte, M.; Martino, H. K.; Erickson, J.; Pandite, L.; Russo, M.; Lambert, J. M.; Howard, M.; Ratain, M. J. A phase I study of cantuzumab mertansine administered as a single intravenous infusion once weekly in patients with advanced solid tumors. *Clin. Cancer Res.* **2004**, *10*, 4363−4468.

| Google Scholar

13. Meister, A.; Anderson, M. E. *Annu. Rev. Biochem.* **1983**, *52*, 711−760.

| Google Scholar

14. Cassady, J. M.; Chan, K. K.; Floss, H. G.; Leistner, E. Recent developments in the maytansinoid antitumor agents. *Chem Pharm Bull (Tokyo)***2004**, *52*, 1−26.

| Google Scholar

15. Kupchan, S. M.; Sneden, A, T.; Branfman, A. R.; Howie, G. A.; Rebhun, L. I.; McIvor, W. E.; Wang, R. W.; Schnaitman, T. C. Structural requirements for antileukemic activity among the naturally occurring and semisynthetic maytansinoids. *J. Med. Chem.* **1978**, *21*, 31−37.

| Google Scholar

16. Higashide, E.; Asai, M.; Ootsu, K.; Tanida, S.; Kozai, Y.; Hasegawa, T.; Kishi, T.; Sugino, Y.; Yoneda, M. Ansamitocin, a group of novel maytansinoid antibiotics with antitumour properties from Nocardia. *Nature***1977**, *29*, 721−722.

Google Scholar

17. Asai, M.; Mizuta, E.; Izawa, M.; Haibaba, K.; Kishi, T. Isolation, chemical characterization and structure of ansamitocin, a new antitumor antibiotic. *Tetrahedron***1978**, *35*, 1079−1085.

DAC EX. 2040 IPR2022-01531 Page 1232 of 1299

Journal of
Medicinal Chemistry

ansamitocins. III. Synthesis and biological effects of 3-acyl esters of maytansinol. *Chem. Pharm. Bull. (Tokyo)***1984**, *32*, 3341−3351.

| Google Scholar

19. Kupchan, S. M.; Komoda, Y.; Branfman, A. R.; Dailey, R. G.; Zimmerly, V. A. Novel maytansinoids. Structural interrelations and requirements for antileukemic activity. *J. Am. Chem. Soc.***1974**, *96*, 3706−3708.

| Google Scholar

20. Lindholm, L.; Holmgren, J.; Svennerholm, L.; Fredman, P.; Nilsson, O.; Persson, B.; Myrvold, H.; Lagergard, T. Monoclonal antibodies against gastrointestinal tumour-associated antigens isolated as monosialogangliosides. *Int. Arch. Allergy Appl. Immunol.* **1983**, *71*, 178−181.

| Google Scholar

21. Mickley, L. A.; Bates, S. E.; Richert, N. D.; Currier, S.; Tanaka, S.; Foss, F.; Rosen, N.; Fojo, A. T. Modulation of the expression of a multidrug resistance gene (mdr1/P-glycoprotein) by differentiating agents. *J. Biol. Chem.* **1989**, *264*, 18031−18040.

| Google Scholar

22. Goff, D. A.; Carroll, S. F. Substituted 2-iminothiolanes: Reagents for the preparation of disulfide cross-linked conjugates with increased stability. *Bioconjugate Chem.* **1990**, *1*, 381−386.

| Google Scholar

23. Goldmacher, V. S.; Tinnel, N. L.; Nelson, B. C. Evidence that pinocytosis in lymphoid cells has a low capacity. *J. Cell Biol.***1986**, *102*, 1312−1319.

| Google Scholar

24. Goldmacher, V. S.; Anderson, J.; Blättler, W. A.; Lambert, J. M.; Senter, P. D. Antibody-complement-mediated cytotoxicity is enhanced by ribosome-inactivating proteins. *J. Immunol.***1985**, *135*, 3648−3651.

Google Scholar

DAC EX. 2040 IPR2022-01531 Page 1233 of 1299

Journal of
Medicinal Chemistry

1. Zhongyue Li, Zhongnang Zhu, Guangsen Xu, Lin Wei, Jiang Liu, Haoxin Wang, Chunhua Lu, Yaoyao Li, Deyu Zhu, Yuemao Shen. Functional Application of the Single-Module NRPS-like d-Alanyltransferase in Maytansinol Biosynthesis. *ACS Catalysis* **2024**, *14* (10) , 8062-8072. https://doi.org/10.1021/acscatal.4c00082

2. Xiao Zhang, Bowen Zhao, Shiwei Fu, Ronald S. Seruya, John F. Madey, III, Eva Bukhryakova, Fuwu Zhang. Rapid and Versatile Synthesis of Glutathione-Responsive Polycarbonates from Activated Cyclic Carbonates. *Macromolecules* **2024**, *57* (6) , 2858-2867. https://doi.org/10.1021/acs.macromol.3c02633

3. Qingqing Liu, Yu Wang, Xin Xia, Zhongyue Li, Yaoyao Li, Yuemao Shen, Haoxin Wang. Combinatorial Biosynthesis of 3-O-Carbamoylmaytansinol by Rational Engineering of the Tailoring Steps of Ansamitocins. *ACS Synthetic Biology* **2024**, *13* (3) , 721-727. https://doi.org/10.1021/acssynbio.3c00575

4. William R. F. Goundry, Jeremy S. Parker. Payloads for Antibody–Drug Conjugates. *Organic Process Research & Development* **2022**, *26* (8) , 2121-2123. https://doi.org/10.1021/acs.oprd.2c00227

5. Syed Muhammad Usama, Sierra C. Marker, Donald R. Caldwell, Nimit L. Patel, Yang Feng, Joseph D. Kalen, Brad St. Croix, Martin J. Schnermann. Targeted Fluorogenic Cyanine Carbamates Enable In Vivo Analysis of Antibody–Drug Conjugate Linker Chemistry. *Journal of the American Chemical Society* **2021**, *143* (51) , 21667-21675. https://doi.org/10.1021/jacs.1c10482

6. Heng Cheng, Qiang Cong, Dan Dervin, Alice Stevens, Kavitha Vemuri, Mary Huber, Jennifer Juliano, Severino Cuison, Janette Sung, David Passmore, Colin Chong, Meghan Greenbaum, Eilene Kwok, Jerry Jiang, Chin Pan, Chetana Rao-Naik, Vangipuram Rangan, Tom Kempe, Andrea Tatum, Shrikant Deshpande, Pina Cardarelli, Gregory Vite, Sanjeev Gangwar. Synthesis and Biological Evaluation of a Carbamate-Containing Tubulysin Antibody–Drug Conjugate. *Bioconjugate Chemistry* **2020**, *31* (10) , 2350-2361. https://doi.org/10.1021/acs.bioconjchem.0c00429

7. Mine Canakci, Khushboo Singh, Oyuntuya Munkhbat, Sudarvili Shanthalingam, Ankita Mitra, Mallory Gordon, Barbara A. Osborne, S. Thayumanavan. Targeting CD4+ Cells with Anti-CD4 Conjugated Mertansine-Loaded Nanogels. *Biomacromolecules* **2020**, *21* (6) , 2473-2481. https://doi.org/10.1021/acs.biomac.0c00442

8. Sudath Hapuarachchige, Colin T. Huang, Madeline C. Donnelly, Cyril Bařinka, Shawn E. Lupold, Martin G. Pomper, Dmitri Artemov. Cellular Delivery of Bioorthogonal Pretargeting Therapeutics in PSMA-Positive Prostate Cancer. *Molecular Pharmaceutics* **2020**, *17* (1) , 98-108. https://doi.org/10.1021/acs.molpharmaceut.9b00788

DAC EX. 2040 IPR2022-01531 Page 1234 of 1299

Journal of
Medicinal Chemistry

10. Kelsey E. Knewtson, Chamani Perera, David Hymel, Zhe Gao, Molly M. Lee, Blake R. Peterson. Antibody–Drug Conjugate that Exhibits Synergistic Cytotoxicity with an Endosome–Disruptive Peptide. *ACS Omega* **2019**, *4* (7) , 12955-12968. https://doi.org/10.1021/acsomega.9b01585

11. Brian H. White, Kerry Whalen, Kristina Kriksciukaite, Rossitza Alargova, Tsun Au Yeung, Patrick Bazinet, Adam Brockman, Michelle DuPont, Haley Oller, Charles-Andre Lemelin, Patrick Lim Soo, Benoît Moreau, Samantha Perino, James M. Quinn, Gitanjali Sharma, Rajesh Shinde, Beata Sweryda-Krawiec, Richard Wooster, Mark T. Bilodeau. Discovery of an SSTR2-Targeting Maytansinoid Conjugate (PEN-221) with Potent Activity in Vitro and in Vivo. *Journal of Medicinal Chemistry* **2019**, *62* (5) , 2708-2719. https://doi.org/10.1021/acs.jmedchem.8b02036

12. Yang Ni, Honghua Zuo, Huaibin Yu, Yuzhou Wu, Fangrui Zhong. Synergistic Catalysis-Enabled Thia-Aza-Prins Cyclization with DMSO and Disulfides: Entry to Sulfenylated 1,3-Oxazinanes and Oxazolidines. *Organic Letters* **2018**, *20* (18) , 5899-5904. https://doi.org/10.1021/acs.orglett.8b02551

13. Zhengyang Jiang, Zhen Yang, Feng Li, Zheng Li, Nathan Fishkin, Kevin Burgess. Targeted Maytansinoid Conjugate Improves Therapeutic Index for Metastatic Breast Cancer Cells. *Bioconjugate Chemistry* **2018**, *29* (9) , 2920-2926. https://doi.org/10.1021/acs.bioconjchem.8b00340

14. Sean W. Smith, Vasu Jammalamadaka, Dmitry Borkin, Jianyu Zhu, Sylvia J. Degrado, Jennifer Lu, Jianqing Huang, Ying-Ping Jiang, Nareshkumar Jain, and Jagath R. Junutula . Design and Synthesis of Isoquinolidinobenzodiazepine Dimers, a Novel Class of Antibody–Drug Conjugate Payload. *ACS Medicinal Chemistry Letters* **2018**, *9* (1) , 56-60. https://doi.org/10.1021/acsmedchemlett.7b00436

15. Leanna R. Staben, Shang-Fan Yu, Jinhua Chen, Gang Yan, Zijin Xu, Geoffrey Del Rosario, Jeffrey T. Lau, Luna Liu, Jun Guo, Bing Zheng, Josefa dela Cruz-Chuh, Byoung-Chul Lee, Rachana Ohri, Wenwen Cai, Hongxiang Zhou, Katherine R. Kozak, Keyang Xu, Gail D. Lewis Phillips, Jiawei Lu, John Wai, Andrew G. Polson, Thomas H. Pillow. Stabilizing a Tubulysin Antibody–Drug Conjugate To Enable Activity Against Multidrug-Resistant Tumors. *ACS Medicinal Chemistry Letters* **2017**, *8* (10) , 1037-1041. https://doi.org/10.1021/acsmedchemlett.7b00243

16. Ping Zhong, Jian Zhang, Chao Deng, Ru Cheng, Fenghua Meng, and Zhiyuan Zhong . Glutathione-Sensitive Hyaluronic Acid-SS-Mertansine Prodrug with a High Drug Content: Facile Synthesis and Targeted Breast Tumor Therapy. *Biomacromolecules* **2016**, *17* (11) , 3602-3608. https://doi.org/10.1021/acs.biomac.6b01094

DAC EX. 2040 IPR2022-01531 Page 1235 of 1299

Journal of
Medicinal Chemistry

Megan Bogalhas, Lintao Wang, Sharon Wilhelm, Wayne Widdison, Jan Pinkas, Thomas A. Keating, Ravi Chari, Hans K. Erickson, and John M. Lambert . Understanding How the Stability of the Thiol-Maleimide Linkage Impacts the Pharmacokinetics of Lysine-Linked Antibody–Maytansinoid Conjugates. *Bioconjugate Chemistry* **2016**, *27* (7) , 1588-1598. https://doi.org/10.1021/acs.bioconjchem.6b00117

18. Kevin J. Hamblett, Tiep Le, Brooke M. Rock, Dan A. Rock, Sophia Siu, Justin N. Huard, Kip P. Conner, Robert R. Milburn, Jason W. O'Neill, Mark E. Tometsko, and William C. Fanslow . Altering Antibody–Drug Conjugate Binding to the Neonatal Fc Receptor Impacts Efficacy and Tolerability. *Molecular Pharmaceutics* **2016**, *13* (7) , 2387-2396. https://doi.org/10.1021/acs.molpharmaceut.6b00153

19. Nils Griebenow, Alicia M. Dilmaç, Simone Greven, and Stefan Bräse . Site-Specific Conjugation of Peptides and Proteins via Rebridging of Disulfide Bonds Using the Thiol–Yne Coupling Reaction. *Bioconjugate Chemistry* **2016**, *27* (4) , 911-917. https://doi.org/10.1021/acs.bioconjchem.5b00682

20. Christoph Meyer, Sandra Liebscher, and Frank Bordusa . Selective Coupling of Click Anchors to Proteins via Trypsiligase. *Bioconjugate Chemistry* **2016**, *27* (1) , 47-53. https://doi.org/10.1021/acs.bioconjchem.5b00618

21. Mallory R. Gordon, Mine Canakci, Longyu Li, Jiaming Zhuang, Barbara Osborne, and S. Thayumanavan . Field Guide to Challenges and Opportunities in Antibody–Drug Conjugates for Chemists. *Bioconjugate Chemistry* **2015**, *26* (11) , 2198-2215. https://doi.org/10.1021/acs.bioconjchem.5b00399

22. Wayne C. Widdison, Jose F. Ponte, Jennifer A. Coccia, Leanne Lanieri, Yulius Setiady, Ling Dong, Anna Skaletskaya, E. Erica Hong, Rui Wu, Qifeng Qiu, Rajeeva Singh, Paulin Salomon, Nathan Fishkin, Luke Harris, Erin K. Maloney, Yelena Kovtun, Karen Veale, Sharon D. Wilhelm, Charlene A. Audette, Juliet A. Costoplus, and Ravi V. J. Chari . Development of Anilino-Maytansinoid ADCs that Efficiently Release Cytotoxic Metabolites in Cancer Cells and Induce High Levels of Bystander Killing. *Bioconjugate Chemistry* **2015**, *26* (11) , 2261-2278. https://doi.org/10.1021/acs.bioconjchem.5b00430

23. Paulin L. Salomon and Rajeeva Singh . Sensitive ELISA Method for the Measurement of Catabolites of Antibody–Drug Conjugates (ADCs) in Target Cancer Cells. *Molecular Pharmaceutics* **2015**, *12* (6) , 1752-1761. https://doi.org/10.1021/acs.molpharmaceut.5b00028

24. E. Erica Hong, Hans Erickson, Robert J. Lutz, Kathleen R. Whiteman, Gregory Jones, Yelena Kovtun, Veronique Blanc, and John M. Lambert . Design of Coltuximab Ravtansine, a CD19-Targeting Antibody–Drug Conjugate (ADC) for the Treatment of B-Cell Malignancies: Structure–Activity Relationships and Preclinical Evaluation. *Molecular Pharmaceutics* **2015**, *12* (6) , 1703-1716. https://doi.org/10.1021/acs.molpharmaceut.5b00175

DAC EX. 2040 IPR2022-01531 Page 1236 of 1299

Journal of
Medicinal Chemistry

Characteristics and in Vitro Potencies. *Molecular Pharmaceutics* **2015**, *12* (6) , 1762-1773. https://doi.org/10.1021/mp5007757

26. Nathan Fishkin . Maytansinoid–BODIPY Conjugates: Application to Microscale Determination of Drug Extinction Coefficients and for Quantification of Maytansinoid Analytes. *Molecular Pharmaceutics* **2015**, *12* (6) , 1745-1751. https://doi.org/10.1021/mp500843r

27. Pamela T. Wong and Seok Ki Choi . Mechanisms of Drug Release in Nanotherapeutic Delivery Systems. *Chemical Reviews* **2015**, *115* (9) , 3388-3432. https://doi.org/10.1021/cr5004634

28. Thomas H. Pillow, Janet Tien, Kathryn L. Parsons-Reponte, Sunil Bhakta, Hao Li, Leanna R. Staben, Guangmin Li, Josefa Chuh, Aimee Fourie-O'Donohue, Martine Darwish, Victor Yip, Luna Liu, Douglas D. Leipold, Dian Su, Elmer Wu, Susan D. Spencer, Ben-Quan Shen, Keyang Xu, Katherine R. Kozak, Helga Raab, Richard Vandlen, Gail D. Lewis Phillips, Richard H. Scheller, Paul Polakis, Mark X. Sliwkowski, John A. Flygare, and Jagath R. Junutula . Site-Specific Trastuzumab Maytansinoid Antibody–Drug Conjugates with Improved Therapeutic Activity through Linker and Antibody Engineering. *Journal of Medicinal Chemistry* **2014**, *57* (19) , 7890-7899. https://doi.org/10.1021/jm500552c

29. John M. Lambert and Ravi V. J. Chari . Ado-trastuzumab Emtansine (T-DM1): An Antibody–Drug Conjugate (ADC) for HER2-Positive Breast Cancer. *Journal of Medicinal Chemistry* **2014**, *57* (16) , 6949-6964. https://doi.org/10.1021/jm500766w

30. Jacob G. Vineberg, Edison S. Zuniga, Anushree Kamath, Ying-Jen Chen, Joshua D. Seitz, and Iwao Ojima . Design, Synthesis, and Biological Evaluations of Tumor-Targeting Dual-Warhead Conjugates for a Taxoid–Camptothecin Combination Chemotherapy. *Journal of Medicinal Chemistry* **2014**, *57* (13) , 5777-5791. https://doi.org/10.1021/jm500631u

31. Robert Yongxin Zhao, Hans K. Erickson, Barbara A. Leece, Emily E. Reid, Victor S. Goldmacher, John M. Lambert, and Ravi V. J. Chari . Synthesis and Biological Evaluation of Antibody Conjugates of Phosphate Prodrugs of Cytotoxic DNA Alkylators for the Targeted Treatment of Cancer. *Journal of Medicinal Chemistry* **2012**, *55* (2) , 766-782. https://doi.org/10.1021/jm201284m

32. Robert Y. Zhao, Sharon D. Wilhelm, Charlene Audette, Gregory Jones, Barbara A. Leece, Alexandru C. Lazar, Victor S. Goldmacher, Rajeeva Singh, Yelena Kovtun, Wayne C. Widdison, John M. Lambert, and Ravi V. J. Chari . Synthesis and Evaluation of Hydrophilic Linkers for Antibody–Maytansinoid Conjugates. *Journal of Medicinal Chemistry* **2011**, *54* (10) , 3606-3623. https://doi.org/10.1021/jm2002958

DAC EX. 2040 IPR2022-01531 Page 1237 of 1299

Journal of
Medicinal Chemistry

Lambert, and Robert J. Lutz . Disulfide-Linked Antibody–Maytansinoid Conjugates: Optimization of In Vivo Activity by Varying the Steric Hindrance at Carbon Atoms Adjacent to the Disulfide Linkage. *Bioconjugate Chemistry* **2011**, *22* (4) , 717-727. https://doi.org/10.1021/bc100480a

34. Xiuxia Sun, Wayne Widdison, Michele Mayo, Sharon Wilhelm, Barbara Leece, Ravi Chari, Rajeeva Singh, and Hans Erickson . Design of Antibody–Maytansinoid Conjugates Allows for Efficient Detoxification via Liver Metabolism. *Bioconjugate Chemistry* **2011**, *22* (4) , 728-735. https://doi.org/10.1021/bc100498q

35. Laurent Ducry and Bernhard Stump. Antibody–Drug Conjugates: Linking Cytotoxic Payloads to Monoclonal Antibodies. *Bioconjugate Chemistry* **2010**, *21* (1) , 5-13. https://doi.org/10.1021/bc9002019

36. Hans K. Erickson, Wayne C. Widdison, Michele F. Mayo, Kathleen Whiteman, Charlene Audette, Sharon D. Wilhelm and Rajeeva Singh. Tumor Delivery and In Vivo Processing of Disulfide-Linked and Thioether-Linked Antibody–Maytansinoid Conjugates. *Bioconjugate Chemistry* **2010**, *21* (1) , 84-92. https://doi.org/10.1021/bc900315y

37. P Holland Alday and John J. Correia. Macromolecular Interaction of Halichondrin B Analogues Eribulin (E7389) and ER-076349 with Tubulin by Analytical Ultracentrifugation. *Biochemistry* **2009**, *48* (33) , 7927-7938. https://doi.org/10.1021/bi900776u

38. Matthias D'hooghe, Stijn Dekeukeleire, Karen Mollet, Carmen Lategan, Peter J. Smith, Kelly Chibale and Norbert De Kimpe . Synthesis of Novel 2-Alkoxy-3-amino-3-arylpropan-1-ols and 5-Alkoxy-4-aryl-1,3-oxazinanes with Antimalarial Activity. *Journal of Medicinal Chemistry* **2009**, *52* (13) , 4058-4062. https://doi.org/10.1021/jm9002632

39. Stephen C. Alley, Dennis R. Benjamin, Scott C. Jeffrey, Nicole M. Okeley, Damon L. Meyer, Russell J. Sanderson and Peter D. Senter. Contribution of Linker Stability to the Activities of Anticancer Immunoconjugates. *Bioconjugate Chemistry* **2008**, *19* (3) , 759-765. https://doi.org/10.1021/bc7004329

40. Ravi V. J. Chari. Targeted Cancer Therapy: Conferring Specificity to Cytotoxic Drugs. *Accounts of Chemical Research* **2008**, *41* (1) , 98-107. https://doi.org/10.1021/ar700108g

41. Sahani Sandalima Uthumange, Angie Jun Hui Liew, Xavier Wezen Chee, Keng Yoon Yeong. Ringing medicinal chemistry: The importance of 3-membered rings in drug discovery. *Bioorganic & Medicinal Chemistry* **2024**, *116* , 117980. https://doi.org/10.1016/j.bmc.2024.117980

DAC EX. 2040 IPR2022-01531 Page 1238 of 1299

Journal of
Medicinal Chemistry

024-04377-1

43. Meiyang Xi, Jingjing Zhu, Fengxia Zhang, Hualiang Shen, Jianhui Chen, Ziyan Xiao, Yanping Huangfu, Chunlei Wu, Haopeng Sun, Gang Xia. Antibody-drug conjugates for targeted cancer therapy: Recent advances in potential payloads. *European Journal of Medicinal Chemistry* **2024**, *276* , 116709. https://doi.org/10.1016/j.ejmech.2024.116709

44. Tingting Yuan, Xiang-Yu Chen, Tengfei Ji, Huifeng Yue, Kathiravan Murugesan, Magnus Rueping. Nickel-catalyzed selective disulfide formation by reductive cross-coupling of thiosulfonates. *Chemical Science* **2024**, *15* (37) , 15474-15479. https://doi.org/10.1039/D4SC02969K

45. Jong Chul Park, Donghoon Shin. Current Landscape of Antibody-Drug Conjugate Development in Head and Neck Cancer. *JCO Precision Oncology* **2024**, *7* (8) https://doi.org/10.1200/PO.24.00179

46. Cuiping Li, Kourong Shi, Siyuan Zhao, Juan Liu, Qiaoli Zhai, Xiaoli Hou, Jie Xu, Xinyu Wang, Jiahui Liu, Xin Wu, Wei Fan. Natural-source Payloads used in the conjugated drugs architecture for cancer therapy: Recent advances and future directions. *Pharmacological Research* **2024**, *127* , 107341. https://doi.org/10.1016/j.phrs.2024.107341

47. Chukwunonso K. Nwabufo. Mirvetuximab soravtansine in ovarian cancer therapy: expert opinion on pharmacological considerations. *Cancer Chemotherapy and Pharmacology* **2024**, *93* (2) , 89-105. https://doi.org/10.1007/s00280-023-04575-y

48. Natalya I. Vasilevich, Huangyu Jiang, Haihua Xiao, Kunxian Feng, Chengfang Jian, Changfeng Chen, Min Li, Zhenhua Chen, Li Pang, Xiang Li, Alexander V. Chestkov, Andre H. Sun, Wang Xu, Joseph A. Fuselier, David H. Coy, Lichun Sun. Biological evaluation of 9-thioansamitocin P3. *Biochemical and Biophysical Research Communications* **2024**, *696* , 149483. https://doi.org/10.1016/j.bbrc.2024.149483

49. Shivangi Kumari, Sonam Raj, M. Arockia Babu, Gurjit Kaur Bhatti, Jasvinder Singh Bhatti. Antibody-drug conjugates in cancer therapy: innovations, challenges, and future directions. *Archives of Pharmacal Research* **2024**, *47* (1) , 40-65. https://doi.org/10.1007/s12272-023-01479-6

50. Maryam Ahani, Maryam Salarian, Malihe Salehi, Neda Jalili, Soodabeh Shafiee, Amir Taheri, Leila Farahmand. Synthesis of Succinimidyl 4-(N-maleimidomethyl)-Cyclohexane-1-Carboxylate (SMCC) as a Linker

DAC EX. 2040 IPR2022-01531 Page 1239 of 1299

Journal of
Medicinal Chemistry

51. Toan D. Nguyen, Brandon M. Bordeau, Joseph P. Balthasar. Use of Payload Binding Selectivity Enhancers to Improve Therapeutic Index of Maytansinoid–Antibody–Drug Conjugates. *Molecular Cancer Therapeutics* **2023**, *22* (11) , 1332-1342. https://doi.org/10.1158/1535-7163.MCT-22-0804

52. Zhijia Wang, Hanxuan Li, Lantu Gou, Wei Li, Yuxi Wang. Antibody–drug conjugates: Recent advances in payloads. *Acta Pharmaceutica Sinica B* **2023**, *13* (10) , 4025-4059. https://doi.org/10.1016/j.apsb.2023.06.015

53. Anne-Marie Lefebvre, Julien Adam, Céline Nicolazzi, Christelle Larois, Florence Attenot, François Falda-Buscaiot, Colette Dib, Nina Masson, Nils Ternès, Anne-Laure Bauchet, Brigitte Demers, Mustapha Chadjaa, Sukhvinder Sidhu, Cécile Combeau, Jean-Charles Soria, Jean-Yves Scoazec, Souad Naimi, Eric Angevin, Marielle Chiron, Christophe Henry. The search for therapeutic targets in lung cancer: Preclinical and human studies of carcinoembryonic antigen-related cell adhesion molecule 5 expression and its associated molecular landscape. *Lung Cancer* **2023**, *184* , 107356. https://doi.org/10.1016/j.lungcan.2023.107356

54. Sameen Zafar, Muhammad Armaghan, Khushbukhat Khan, Nazia Hassan, Javad Sharifi-Rad, Solomon Habtemariam, Marek Kieliszek, Monica Butnariu, Iulia-Cristina Bagiu, Radu Vasile Bagiu, William C. Cho. New insights into the anticancer therapeutic potential of maytansine and its derivatives. *Biomedicine & Pharmacotherapy* **2023**, *165* , 115039. https://doi.org/10.1016/j.biopha.2023.115039

55. Devesh Aggarwal, Jie Yang, Md. Abdus Salam, Sagnik Sengupta, Md. Yusuf Al-Amin, Saad Mustafa, Mohammad Aasif Khan, Xun Huang, Jogendra Singh Pawar. Antibody-drug conjugates: the paradigm shifts in the targeted cancer therapy. *Frontiers in Immunology* **2023**, *14* https://doi.org/10.3389/fimmu.2023.1203073

56. Logan Salamone, Martin Lepeintre, Vincent L. Revil-Baudard, Fabien Serpier, Laurent Petit. A Simple and Modular Access to 4-Mercapto-4-methylpentanoic Acid: A Useful Building Block in Antibody-Drug Conjugates Research. *Synthesis* **2023**, *55* (14) , 2177-2185. https://doi.org/10.1055/s-0042-1751436

57. Jiangling Huang, Shanshan Song, Min Wang, Hangxiang Wang. Transforming a highly toxic agent DM1 into injectable safe nanomedicines via prodrug self-assembly for the treatment of taxane-resistant cancer. *Nanoscale* **2023**, *15* (23) , 10110-10124. https://doi.org/10.1039/D3NR00680H

58. Katja E. Grier, Anders H. Hansen, Christina S. Haxvig, Xin Li, Oliver Krigslund, Niels Behrendt, Lars H. Engelholm, Fabio Rossi, Bebiana C. Sousa, Grant J. Harradence, Nicolas Camper, Katrine M. Qvortrup. Targeted delivery of alcohol-containing payloads with antibody-drug conjugates. *Chemical Communications* **2023**, *59* (47) , 7240-7242. https://doi.org/10.1039/D3CC01596C

DAC EX. 2040 IPR2022-01531 Page 1240 of 1299

Journal of
Medicinal Chemistry

Disulfides**. *Angewandte Chemie* **2023**, *135* (18) https://doi.org/10.1002/ange.202219156

60. Hayato Asanuma, Kazuya Kanemoto, Tokiharu Watanabe, Shin-ichi Fukuzawa. N -(Morpholine-4-dithio)phthalimide: A Shelf-Stable, Bilateral Platform Molecule Enabling Access to Diverse Unsymmetrical Disulfides**. *Angewandte Chemie International Edition* **2023**, *62* (18) https://doi.org/10.1002/anie.202219156

61. Qiu-Yan Zhang, Qing-Long Yu, Wei-Jing Luan, Tong-Fang Li, Ya-Ni Xiao, Li Zhang, Yi Li, Rong Rong, Chun-Guang Ren. LWJ-M30, a conjugate of DM1 and B6, for the targeted therapy of colorectal cancer with improved therapeutic effects. *RSC Advances* **2023**, *13* (16) , 10840-10846. https://doi.org/10.1039/D2RA07758B

62. Dipankar Pramanik. Development of Antibody-Drug Conjugates: Future Perspective Towards Solid Tumor Treatment. *Anti-Cancer Agents in Medicinal Chemistry* **2023**, *23* (6) , 642-657. https://doi.org/10.2174/1871520623666221031105432

63. Jindra Valentová, Lucia Lintnerová, Natalia Miklášová, Bianka Oboňová, Ladislav Habala. Analogues of Anticancer Natural Products: Chiral Aspects. *International Journal of Molecular Sciences* **2023**, *24* (6) , 5679. https://doi.org/10.3390/ijms24065679

64. Yangping Wu, Wenting Li, Xiangzheng Chen, Haichuan Wang, Siyuan Su, Ying Xu, Xiangbing Deng, Tinghan Yang, Mingtian Wei, Li Li, Yixin Liu, Jinliang Yang, Weimin Li. DOG1 as a novel antibody-drug conjugate target for the treatment of multiple gastrointestinal tumors and liver metastasis. *Frontiers in Immunology* **2023**, *14* https://doi.org/10.3389/fimmu.2023.1051506

65. Manisha Pandey, Bapi Gorain, Shom Prakash Kushwaha, Neha Gulati, Jayashree Mayuren, Adeel Masood Butt. Antibody–drug conjugate: Emerging trend for targeted treatment. **2023**, 347-387. https://doi.org/10.1016/B978-0-323-91663-9.00013-8

66. Chaowei Hao, Peng Chen, Hui Zhang, Sarra Setrerrahmane, Hanmei Xu, . 'Renovation of old drugs' – can peptide drug conjugates lead the post-ADC era?. *Australian Journal of Chemistry* **2023**, *76* (8) , 318-336. https://doi.org/10.1071/CH22252

67. Aaron T. Jacobs, Diana Martinez Castaneda-Cruz, Mark M. Rose, Linda Connelly. Targeted therapy for breast cancer: An overview of drug classes and outcomes. *Biochemical Pharmacology* **2022**, *204* , 115209. https://doi.org/10.1016/j.bcp.2022.115209

DAC EX. 2040 IPR2022-01531 Page 1241 of 1299

Journal of
Medicinal Chemistry

enhance therapeutic response. *Pharmacology & Therapeutics* **2022**, *236* , 108108. https://doi.org/10.1016/j.pharmthera.2022.108108

69. Jamileh Kadkhoda, Ali Tarighatnia, Mohammad Reza Tohidkia, Nader D. Nader, Ayuob Aghanejad. Photothermal therapy-mediated autophagy in breast cancer treatment: Progress and trends. *Life Sciences* **2022**, *298* , 120499. https://doi.org/10.1016/j.lfs.2022.120499

70. Utsab Debnath, Saroj Verma, Jeevan Patra, Sudip Kumar Mandal. A review on recent synthetic routes and computational approaches for antibody drug conjugation developments used in anti-cancer therapy. *Journal of Molecular Structure* **2022**, *1256* , 132524. https://doi.org/10.1016/j.molstruc.2022.132524

71. Matteo Duca, Darren Wan-Teck Lim, Vivek Subbiah, Shunji Takahashi, John Sarantopoulos, Andrea Varga, Joseph A. D'Alessio, Tinya Abrams, Qing Sheng, Eugene Youchin Tan, Maria Santos Rosa, Juan Gonzalez-Maffe, Janna Sand-Dejmek, Claire Fabre, Miguel Martin. A First-in-Human, Phase I, Multicenter, Open-Label, Dose-Escalation Study of PCA062: An Antibody–Drug Conjugate Targeting P-Cadherin, in Patients With Solid Tumors. *Molecular Cancer Therapeutics* **2022**, *21* (4) , 625-634. https://doi.org/10.1158/1535-7163.MCT-21-0652

72. Jin-Ock Kim, Kwang-Hyeok Kim, Eun Ji Baek, Bomi Park, Min Kyung So, Byoung Joon Ko, Han-Jik Ko, Sang Gyu Park. A novel anti-c-Kit antibody–drug conjugate to treat wild-type and activating-mutant c-Kit-positive tumors. *Molecular Oncology* **2022**, *16* (6) , 1290-1308. https://doi.org/10.1002/1878-0261.13084

73. Jian Xu, Xiang Li, Yue Du. Antibody–Pattern Recognition Receptor Agonist Conjugates: A Promising Therapeutic Strategy for Cancer. *Advanced Biology* **2022**, *6* (3) https://doi.org/10.1002/adbi.202101065

74. Paola Marzullo, Zlata Boiarska, Helena Pérez-Peña, Anne-Catherine Abel, Beatriz Álvarez-Bernad, Daniel Lucena-Agell, Francesca Vasile, Maurizio Sironi, Karl-Heinz Altmann, Andrea E. Prota, J. Fernando Díaz, Stefano Pieraccini, Daniele Passarella. Maytansinol Derivatives: Side Reactions as a Chance for New Tubulin Binders. *Chemistry – A European Journal* **2022**, *28* (2) https://doi.org/10.1002/chem.202103520

75. Xintuo Yang, Pinhong Chen, Guosheng Liu. Asymmetric Palladium-Catalyzed Aza-Wacker Reaction of Alkenes: Efficient Synthesis of Chiral 1,3-Oxazinan-2-ones. *Chinese Journal of Organic Chemistry* **2022**, *42* (10) , 3382. https://doi.org/10.6023/cjoc202208021

76. Kinga Panuciak, Mikołaj Margas, Karolina Makowska, Monika Lejman. Insights into Modern Therapeutic Approaches in Pediatric Acute Leukemias. *Cells* **2022**, *11* (1) , 139. https://doi.org/10.3390/cells11010139

DAC EX. 2040 IPR2022-01531 Page 1242 of 1299

Journal of
Medicinal Chemistry

78. Kai Gong, Yilin Zhou, Xuefeng Jiang. From symmetrical tetrasulfides to trisulfide dioxides via photocatalysis. *Green Chemistry* **2021**, *23* (24) , 9865-9869. https://doi.org/10.1039/D1GC03242A

79. Davinder Singh, Divya Dheer, Abhilash Samykutty, Ravi Shankar. Antibody drug conjugates in gastrointestinal cancer: From lab to clinical development. *Journal of Controlled Release* **2021**, *340* , 1-34. https://doi.org/10.1016/j.jconrel.2021.10.006

80. Jing Zhang, Arvind Jain, Sabine Milhas, Daniel J. Williamson, Justyna Mysliwy, Adam Lodge, Jenny Thirlway, Majid Al Nakeeb, Ami Miller, Terry H. Rabbitts. An antibody-drug conjugate with intracellular drug release properties showing specific cytotoxicity against CD7-positive cells. *Leukemia Research* **2021**, *108* , 106626. https://doi.org/10.1016/j.leukres.2021.106626

81. Chiu Ling Ong, Salam Titinchi, Joon Ching Juan, Nader Ghaffari Khaligh. An Overview of Recent Advances in the Synthesis of Organic Unsymmetrical Disulfides. *Helvetica Chimica Acta* **2021**, *104* (8) https://doi.org/10.1002/hlca.202100053

82. Wenting Li, Minhao Huang, Yuyan Li, Anjie Xia, Lun Tan, Zhixiong Zhang, Yuxi Wang, Jinliang Yang. C3 ester side chain plays a pivotal role in the antitumor activity of Maytansinoids. *Biochemical and Biophysical Research Communications* **2021**, *566* , 197-203. https://doi.org/10.1016/j.bbrc.2021.05.071

83. Saima Rafique, Farukh Kiyani, Sumbal Jawaid, Rubina Nasir, Mahmoosh Ahmad, Shazia Bashir, Muhammad Idress, Jan Sher Khan, Rizwan Akram, . Reusable, Noninvasive, and Sensitive Fluorescence Enhanced ZnO-Nanorod-Based Microarrays for Quantitative Detection of AFP in Human Serum. *BioMed Research International* **2021**, *2021* , 1-11. https://doi.org/10.1155/2021/9916909

84. Jeffrey L. Wong, Jonathan E. Rosenberg. Targeting nectin-4 by antibody-drug conjugates for the treatment of urothelial carcinoma. *Expert Opinion on Biological Therapy* **2021**, *21* (7) , 863-873. https://doi.org/10.1080/14712598.2021.1929168

85. Miganoosh Simonian, , Mozhan Haji Ghaffari, , Babak Negahdari, . Immunotherapy for Breast Cancer Treatment. *Iranian Biomedical Journal* **2021**, *25* (3) , 140-156. https://doi.org/10.52547/ibj.25.3.140

DAC EX. 2040 IPR2022-01531 Page 1243 of 1299

Journal of
Medicinal Chemistry

and microparticles: synthesis, fabrication, and therapeutic applications. *Chemical Communications* **2021**, *57* (35) , 4212-4229. https://doi.org/10.1039/D1CC00811K

87. Yufei Xue, Hua Bai, Bo Peng, Bin Fang, Jonathan Baell, Lin Li, Wei Huang, Nicolas Hans Voelcker. Stimulus-cleavable chemistry in the field of controlled drug delivery. *Chemical Society Reviews* **2021**, *50* (8) , 4872-4931. https://doi.org/10.1039/D0CS01061H

88. Rajeshwari Tiwari, Prashant S. Shinde, Sreejesh Sreedharan, Anik Kumar Dey, Katherine A. Vallis, Santosh B. Mhaske, Sumit Kumar Pramanik, Amitava Das. Photoactivatable prodrug for simultaneous release of mertansine and CO along with a BODIPY derivative as a luminescent marker in mitochondria: a proof of concept for NIR image-guided cancer therapy. *Chemical Science* **2021**, *12* (7) , 2667-2673. https://doi.org/10.1039/D0SC06270G

89. Trevor S. Anderson, Amanda L. Wooster, Ninh M. La-Beck, Dipongkor Saha, Devin B. Lowe. Antibody-drug conjugates: an evolving approach for melanoma treatment. *Melanoma Research* **2021**, *31* (1) , 1-17. https://doi.org/10.1097/CMR.0000000000000702

90. Stephan Dickgiesser, Marcel Rieker, Nicolas Rasche. Antibody–Drug Conjugates. **2021**, 189-214. https://doi.org/10.1007/978-3-030-54630-4_8

91. John Porter, Yao Ding, Sarah J.M. Hale, Richard D. Perrins, Angela Robinson, Michael P. Mazanetz, Yubo Wu, Yinping Ma, Kelly Conlon, Tom Coulter. A highly potent maytansinoid analogue and its use as a cytotoxic therapeutic agent in gold nanoparticles for the treatment of hepatocellular carcinoma. *Bioorganic & Medicinal Chemistry Letters* **2020**, *30* (24) , 127634. https://doi.org/10.1016/j.bmcl.2020.127634

92. Pengxuan Zhao, Yuebao Zhang, Wenqing Li, Christopher Jeanty, Guangya Xiang, Yizhou Dong. Recent advances of antibody drug conjugates for clinical applications. *Acta Pharmaceutica Sinica B* **2020**, *10* (9) , 1589-1600. https://doi.org/10.1016/j.apsb.2020.04.012

93. Shuo Cao, Yue-Hui Dong, De-Feng Wang, Zhao-Peng Liu. Tubulin Maytansine Site Binding Ligands and their Applications as MTAs and ADCs for Cancer Therapy. *Current Medicinal Chemistry* **2020**, *27* (27) , 4567-4576. https://doi.org/10.2174/0929867327666200316144610

94. Céline Nicolazzi, Anne Caron, Alexia Tellier, Marc Trombe, Jan Pinkas, Gillian Payne, Chantal Carrez, Stéphane Guérif, Marie Maguin, Raffaele Baffa, Matteo Fassan, Julien Adam, Lydie Mangatal-Wade, Véronique

DAC EX. 2040 IPR2022-01531 Page 1244 of 1299

Journal of
Medicinal Chemistry

95. Dangquan Zhang, Arun Kanakkanthara. Beyond the Paclitaxel and Vinca Alkaloids: Next Generation of Plant-Derived Microtubule-Targeting Agents with Potential Anticancer Activity. *Cancers* **2020**, *12* (7) , 1721. https://doi.org/10.3390/cancers12071721

96. Hendrik Schneider, Lukas Deweid, Olga Avrutina, Harald Kolmar. Recent progress in transglutaminase-mediated assembly of antibody-drug conjugates. *Analytical Biochemistry* **2020**, *595* , 113615. https://doi.org/10.1016/j.ab.2020.113615

97. Hyunbo Shim. Bispecific Antibodies and Antibody–Drug Conjugates for Cancer Therapy: Technological Considerations. *Biomolecules* **2020**, *10* (3) , 360. https://doi.org/10.3390/biom10030360

98. Won-Gu Choi, Ria Park, Dong Kyun Kim, Yongho Shin, Yong-Yeon Cho, Hye Suk Lee. Mertansine Inhibits mRNA Expression and Enzyme Activities of Cytochrome P450s and Uridine 5'-Diphospho-Glucuronosyltransferases in Human Hepatocytes and Liver Microsomes. *Pharmaceutics* **2020**, *12* (3) , 220. https://doi.org/10.3390/pharmaceutics12030220

99. Garima Agarwal, Peter J. Blanco Carcache, Ermias Mekuria Addo, A. Douglas Kinghorn. Current status and contemporary approaches to the discovery of antitumor agents from higher plants. *Biotechnology Advances* **2020**, *38* , 107337. https://doi.org/10.1016/j.biotechadv.2019.01.004

100. Puregmaa Khongorzul, Cai Jia Ling, Farhan Ullah Khan, Awais Ullah Ihsan, Juan Zhang. Antibody–Drug Conjugates: A Comprehensive Review. *Molecular Cancer Research* **2020**, *18* (1) , 3-19. https://doi.org/10.1158/1541-7786.MCR-19-0582

Load more citations

Download PDF

Partners

DAC EX. 2040 IPR2022-01531 Page 1245 of 1299

Journal of
Medicinal Chemistry



1155 Sixteenth Street N.W.
Washington, DC 20036
Copyright © 2024
American Chemical Society

About

About ACS Publications
ACS & Open Access
ACS Membership
ACS Publications Blog

Resources and Information

Journals A-Z
Books and Reference
Advertising Media Kit
Institutional Sales
ACS Researcher Resources
Privacy Policy
Terms of Use

Support & Contact

Help
Live Chat
FAQ

Connect with ACS Publications



DAC EX. 2040 IPR2022-01531 Page 1246 of 1299

Appendix WIDDISON02

Semisynthetic Maytansine Analogues for the Targeted Treatment of Cancer

Wayne C. Widdison, Sharon D. Wilhelm, Emily E. Cavanagh, Kathleen R. Whiteman, Barbara A. Leece, Yelena Kovtun, Victor S. Goldmacher, Hongsheng Xie, Rita M. Steeves, Robert J. Lutz, Robert Zhao, Lintao Wang, Walter A. Blättler, and Ravi V. J. Chari*

ImmunoGen, Inc., 128 Sidney Street, Cambridge, Massachusetts 02139

Received March 20, 2006

Maytansine, a highly cytotoxic natural product, failed as an anticancer agent in human clinical trials because of unacceptable systemic toxicity. The potent cell killing ability of maytansine can be used in a targeted delivery approach for the selective destruction of cancer cells. A series of new maytansinoids, bearing a disulfide or thiol substituent were synthesized. The chain length of the ester side chain and the degree of steric hindrance on the carbon atom bearing the thiol substituent were varied. Several of these maytansinoids were found to be even more potent in vitro than maytansine. The targeted delivery of these maytansinoids, using monoclonal antibodies, resulted in a high, specific killing of the targeted cells in vitro and remarkable antitumor activity in vivo.

Downloaded via PENNSYLVANIA STATE UNIV on December 2, 2024 at 17:54:00 (UTC).
See https://pubs.acs.org/sharingguidelines for options on how to legitimately share published articles.

Introduction

Maytansine (**1**) was originally isolated from the bark of the African shrub *Maytenus ovatus* by Kupchan and colleagues[1] and is the first compound of a class of benzoansamacrolide antibiotics named maytansinoids.[2] Maytansinoids are antimitotic agents that bind to tubulin and inhibit microtubule assembly.[3] They bind to the same site on tubulin as the *Vinca* alkaloids do, and similar inhibitory constants were measured for both drug classes.[4] However, many maytansinoids are 100 to 1000-times more cytotoxic than vincristine and vinblastine toward cancer cell lines in vitro.[5] Maytansine was extensively tested in preclinical and clinical settings.[6] Several phase I and phase II clinical trials that were performed with patients suffering from diverse types of cancers established the toxicity profile in humans, but failed to demonstrate therapeutic benefits at tolerable doses. Further development stopped, and maytansine became one of the many cytotoxic agents that were discontinued for the lack of a sufficiently large therapeutic window.

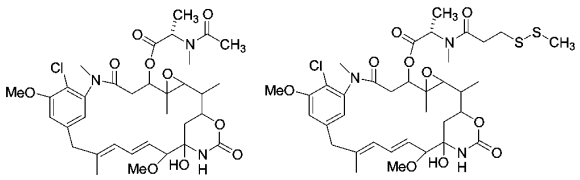
Although, maytansine was not effective in human clinical trials, the unusually high cytotoxic activity of the maytansinoids makes them attractive candidates for tissue-specific delivery. Tumor-reactive monoclonal antibodies are large proteins that bind with high affinity to receptors that are selectively expressed on the surface of cancer cells. Although these antibodies display high specificity for the tumor, a majority of them are not potent enough to be therapeutically useful. Imaging studies with radiolabeled antibodies have demonstrated the localization of antibodies at the tumor site in cancer patients; however, the concentration of antibodies achieved at the tumor was quite low.[7] The in vitro cytotoxic inhibitory concentrations (IC_{50} values) of maytansinoids are even lower than the antibody concentrations achieved at the tumor, making them suitable candidates for targeted delivery using antibodies. The selective delivery to tumor tissue has the effect of changing the in vivo distribution and pharmacokinetics of the cytotoxic agent. Humanized monoclonal antibodies typically have a circulation half-life of about two weeks in humans and are largely found in the vascular and extravascular plasma space. Thus, linking a small drug molecule to the antibody will prevent penetration into healthy tissue and can extend the in vivo half-life of the drug (typically, minutes to a few hours for the unconjugated drug) to as long as two weeks, thereby accumulating a proportionally larger amount at the malignant tissue than at the healthy tissues.[8] Thus, this method of delivery should effectively contribute to a wider therapeutic window for the maytansinoids and make them effective anticancer agents. Preclinical evaluations of the first set of antibody−maytansinoid conjugates have demonstrated that this targeted delivery approach greatly improves the tumor specificity and the antitumor activity of the maytansinoid.[9,10] On the basis of this promising preclinical data, the first antibody−maytansinoid conjugate has undergone a phase I clinical evaluation in patients with colorectal and pancreatic cancers.[11,12]

Delivery of the maytansinoid by a monoclonal antibody requires that the maytansinoid is stably linked to the antibody. However, once the antibody has bound to the antigen on the cancer cells and the antibody−antigen complex is internalized into the cell, the cytotoxic agent needs to be released inside the cell to enable it to efficiently arrive at the target and inactivate it. If one considers that the cytoplasm of cells contains millimolar concentrations of the thiol-containing tripeptide, glutathione, whereas the concentration of glutathione in human blood is about 1000-fold lower (generally in the micromolar range), then a disulfide bond appears to have ideal chemical characteristics.[13] It is thermodynamically very stable (bond energy of about 65 kcal/mol) but kinetically labile in the presence of sulfhydryl groups. The strength of the disulfide bond can be manipulated to achieve maximal stability during circulation in the blood stream, while allowing for efficient cleavage inside the target cell. This is achieved by the introduction of methyl substituents on the carbon atoms geminal to the disulfide link, conferring varying degrees of steric hindrance. We, therefore, set out to synthesize maytansinoid analogues that contained sulfhydryl groups and showed equal or enhanced cytotoxic activity relative to that of the parent compound, maytansine. Some of these maytansinoids were linked to a monoclonal antibody, and the effect of disulfide bond strength correlated with antitumor activity.

Structure−activity studies with maytansinoids had identified the C3 *N*-acyl-*N*-methyl-L-alanyl ester side chain, the C4-C5 epoxide moiety, the C9 carbinol function, and the position of

* Corresponding author. Tel: (617) 995-2500. Fax: (617) 995-2510. E-mail: ravi.chari@immunogen.com.

10.1021/jm060319f CCC: $33.50 © 2006 American Chemical Society
Published on Web 06/10/2006



1 **2b**

Figure 1. Structures of maytansine and disulfide-containing maytansinoid.

the conjugated C11 and C13 double bonds as critical elements for activity.[14] This left the phenyl ring and the *N*′-acyl group as chemically modifiable entities. Although the *N*′-acyl group is required for biological activity, studies by Kupchan et al.[15] have shown that the nature of the acyl group can be varied without a significant loss in activity. Thus, we initially replaced the *N*-acetyl group in maytansine (**1**) with a 3-methyldithiopropionyl group, thus producing disulfide-containing maytansinoid **2b** (DM1SMe), (Figure 1). On the basis of the promising in vitro potency data of this compound, we then synthesized a variety of disulfide and thiol-containing maytansinoids bearing different *N*-acyl-*N*-methyl-L-alanyl ester moieties at the C3 position. A representative set of these maytansinoids were then conjugated to monoclonal antibodies to provide conjugates with varying disulfide bond strengths. The synthesis of these new maytansinoids and the results from their biological testing in free form or as conjugates of monoclonal antibodies is reported herein.

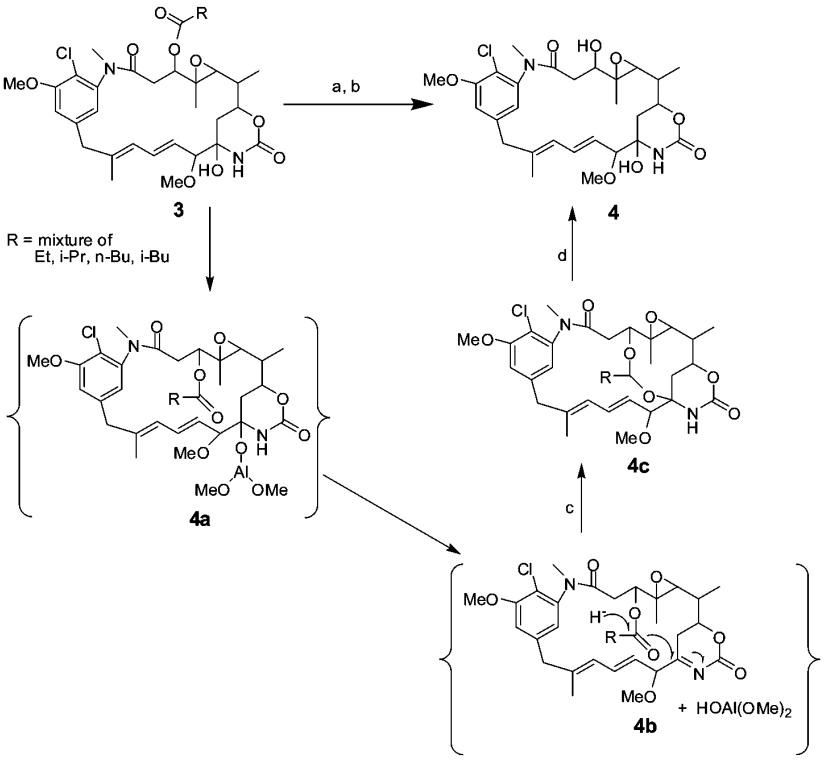
Biosynthetically, maytansinoids are complex polyketides. Consequently, soon after the initial isolation from plants, a bacterial actinomycetes strain *Actinosynnema pretiosum* was isolated, which produces ansamycin antibiotics called ansamitocins that are maytansinoids with C3 alkanoic acid esters.[16,17] Because ansamitocins lack the C3 *N*-acyl-*N*-methyl-L-alanyl side chain, they have diminished cytotoxicity; however, they constitute a ready starting material for the preparation of maytansinoid analogues with novel C3 side chains.

Results and Discussion

Chemistry. The chemistry followed the scheme originally designed by Kupchan at al.,[5,15] who first reported the chemical conversion of maytansine to the C3 hydroxy compound, maytansinol, and its subsequent conversion to different C3 esters. Esterification of maytansinol with alkanoic acids gave the bacterial ansamitocins. Kawai et al.,[18] have described the esterification of maytansinol with a variety of *N*-acyl- *N*-methyl-L-alanyl compounds to produce highly active C3 ester analogues of maytansine.

The synthetic route for the preparation of disulfide-containing maytansinoid esters is shown in Schemes 1 and 2. Maytansinol (**4**) was synthesized from ansamitocins (**3**), which in turn were obtained from the fermentation of the microorganism *Actinosynnema pretiosum*. Ansamitocins were isolated as a mixture of C3 esters of maytansinol, including propanoate, butyrate, isobutyrate, and pentanoate esters. The predominant species (~80%) was the C3 isobutyrate ansamitocin P-3. Because the C3 ester group in maytansinoids is susceptible to elimination under mild basic conditions (pH >9) to give the α,β-unsaturated maytansinoid maysine,[19] ester hydrolysis was achieved through a reductive cleavage process. The previously described method[15] for the reductive cleavage of the C3 ester used lithium aluminum hydride and gave low yields of maytansinol with several side products. Several other reducing agents, including DIBAL, $NaBH_4$, Red-Al, or Red-Al + 1 eq methanol, gave poor yields

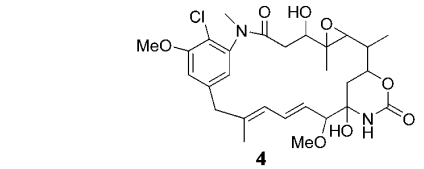
Scheme 1. Synthesis of Maytansinol[a]



[a] (a) $LiAlH(OMe)_3$, THF, −30 to −40 °C; (b) pH 12, 30 min (c) pH 6−7, (d) pH 2, 2 h or pH 12, 30 min.

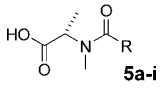
DAC EX. 2040 IPR2022-01531 Page 1249 of 1299

Scheme 2. Synthesis of Disulfide-Containing Maytansinoids[a]

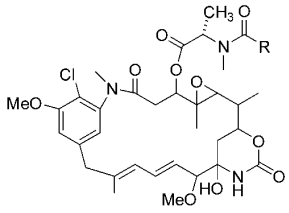


4

a

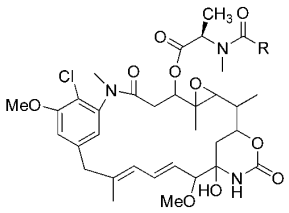


5a-i



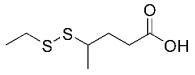
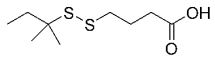
2a-k

+



6a-i

Compound	R
2a (DM0SMe), 5a, 6a	
2b (DM1SMe), 5b. 6b	
2c (DM1SPh), 5c, 6c	
2d (DM2'SMe), 5d, 6d	
2e (DM2SMe), 5e, 6e	
2f (DM3SMe, *RS*), 5f, 6f	
2g (DM3SMe, *S*), 5g, 6g	
2h (DM3SMe, *R*), 5h 6h	
2i (DM4SMe), 5i, 6i	

Compound	R
2j (DM1-TPA)	
2k (DM4-TBA)	

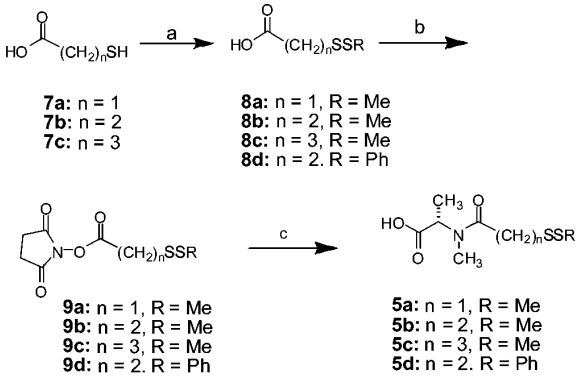
[a] Reaction conditions: (a) DCC/$ZnCl_2$/CH_2Cl_2, rt.

and multiple side products. Attempted enzymatic cleavage of the ester using a wide panel of commercially available esterases and lipases was also unsuccessful, with no detectable hydrolysis. However, the ester group in the ansamitocins was efficiently cleaved using the mild reducing agent lithium trimethoxyaluminum hydride, under controlled temperature (−30 to −40 °C), to give maytansinol in good yields. Higher reaction temperatures led to epoxide opening, whereas colder reaction temperatures resulted in a high proportion of unreacted starting material. Maytansinol was obtained after quenching the reaction mixture at −40 °C with water, which resulted in a pH of about 12, and holding at this pH for 30 min, followed by subsequent neutralization with formic acid. Interestingly, when the reaction mixture was neutralized with acid to a pH between 6 and 7, the very stable acetal intermediate **4c** (presumably formed via **4a**, **4b**) was obtained. This intermediate could be isolated and stored. It was converted to maytansinol (**4**) either by acidification and holding at pH 2 for 2 h or by adding a base and holding at basic pH (~11) for 30 min (Scheme 1).

Mercaptocarboxylic acids of varying linear chain lengths were converted into methyldithio or aryldithio carboxylic acids by reacting with methyl methanethiolsulfonate or aryl disulfides, respectively (Scheme 3). The dithio-carboxylic acids were converted into their *N*-hydroxysuccinimide esters, followed by reaction with *N*-methyl-L-alanine to form the desired C3 *N*-acyl-*N*-methyl-L-alanine side chains for reaction with maytansinol (**4**). The two enantiomeric 4-(methydithio)pentanoic acids (compounds **13** and **18**) were prepared from the corresponding optically pure 1,3-dihdroxybutanes as shown in Schemes 4 and 5. The conversion of the 1,3-dihdroxybutanes to the ditosylates, followed by the displacement of the primary tosyl group by cyanide, and the substitution of the secondary tosyl group with a xanthate moiety gave compounds **12** and **17**. Base hydrolysis, followed by disulfide exchange with methyl methanethiolsulfonate gave compounds **13** and **18**, which were then converted to their respective *N*-hydroxysuccinimide esters **14** and **19**. Acylation of *N*-methyl-L-alanine with the *N*-hydroxysuccinimde ester of *S*- and *R*-4-(methyldithio)pentanoic acids gave the two diastereomeric acyl *N*-methyl-L-alanyl side chains **5g** and **5h** for condensation with maytansinol. To synthesize a maytansinoid ester bearing a sterically hindered thiol substituent, the *N*-acyl-*N*-methyl-L-alanine compound **5i**, bearing two methyl

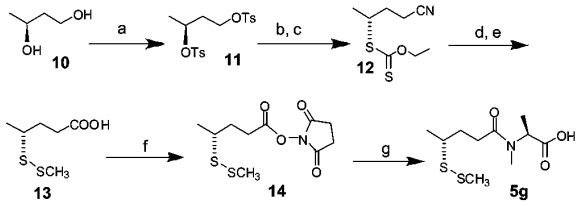
DAC EX. 2040 IPR2022-01531 Page 1250 of 1299

Scheme 3. Synthesis of *N*-Acyl-*N*-methyl-L-alanines[a]



[a] Reaction conditions: (a) $CH_3SSO_2CH_3$, (PhSSPh for **8d**); (b) *N*-hydroxysuccinimide, EDC; (c) *N*-methyl-L-alanine, triethylamine.

Scheme 4. Synthesis of *N*-Methyl-*N*-[(4-*(S)*-methyldithio)-1-oxopentyl]-*S*-alanine[a]



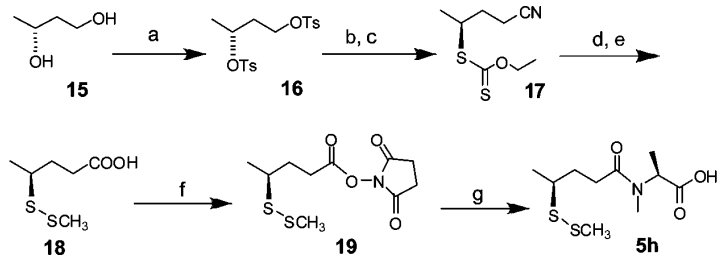
[a] Reaction conditions: (a) TsCl. Py; (b) NaCN; (c) KSSCOEt; (d) NaOH; (e) $CH_3SSO_2CH_3$; (f) *N*-hydroxysuccinimide, EDC; (g) *N*-methyl-L-alanine, triethylamine.

substituents on the carbon bearing the disulfide bond, was synthesized from isobutylene sulfide using the steps shown in Scheme 6. Ring opening of episulfide **20** with lithiated acetonitrile gave nitrile **21**. The hydrolysis of the nitrile, followed by disulfide exchange with methylmethanethiolsulfonate gave carboxylic acid **23**. The condensation of **23** with *N*-hydroxysuccinimide in the presence of EDC gave hydroxysuccinimide ester **24**, followed by the reaction with *N*-methyl-L-alanine to give **5i**.

Disulfide-containing maytansinoid esters (**2a**–**i**), in which both the chain length and degree of branching in the acyl group were varied, were prepared by condensing maytansinol (**4**) with the *N*-acyl-*N*-methyl-L-alanyl derivatives described above in the presence of the coupling reagent 1,3-dicyclohexylcarbodiimide (DCC) along with catalytic amounts of zinc chloride (Scheme 2). In all cases, two diastereomeric products (**2a**–**i** and **6a**–**i**) containing the L- and D-aminoacyl side chain, respectively, were obtained, despite the fact that enantiomerically pure acylamino acids were used in the reaction. This indicates that epimerization at the α-carbon of the *N*-methyl-L-alanine moiety takes place during the reaction. In addition, unreacted maytansinol (typically 10–20%) was also recovered. The addition of another aliquot of the carboxylic acid, DCC, and $ZnCl_2$ did not result in any further reaction. Several other coupling agents, solvents, and reaction conditions were tried but generally gave poorer yields. Of the Lewis acids investigated, zinc chloride gave the best yields. The substitution of zinc chloride with acyl transfer catalysts such as (dimethylamino)pyridine or hydroxybenzotriazole gave little or no product. The diastereomeric maytansinoid esters were readily separated by normal phase HPLC, using a cyano-bonded silica column. On this column, the two diastereomers had retention times that were about 10 min apart, enabling a facile separation. In some cases, the diastereomers could also be separated by preparative TLC on silica gel. In one case, the maytansinoid ester could not be isolated in a reasonable yield. In this case, the maytansinoid DM2SMe (**2e**) was found to be unstable under the reaction conditions and underwent rapid decomposition, presumably because of facile β-elimination of the methydithio substituent to give the substituted alkene, which is the thermodynamically favored product.

Because maytansinoids are sensitive to bases, nucleophiles, and strong reducing agents, the reduction of disulfide-containing maytansinoids to the thiol compounds had to be achieved using very mild and disulfide-specific reagents. The reduction of the disulfide-containing maytansinoids (**2b,c,e,f,i**) proceeded smoothly upon treatment, in neutral buffered aqueous solution, with a small excess (2–3 equiv) of dithiothreitol (DTT), a reducing agent commonly used by biochemists for the scission of disulfide bonds in proteins (Scheme 7). Initial attempts to obtain pure thiol-containing drugs by reverse phase HPLC using a water–acetonitrile mobile phase resulted in a considerable loss of product because of the rapid oxidation of the thiols to dimeric maytansinoids that had low solubility in aqueous solutions. The thiol-containing maytansinoids could be efficiently purified using nonaqueous solvents on a normal phase cyano-bonded HPLC column to provide mercapto-L-aminoacyl-maytansinoids **25a** (DM1), **25b** (DM3), and **25c** (DM4) (Scheme 7). Similarly, the reduction of the disulfide-containing-D-aminoacyl maytansinoids (**6b,c,f,i**) gave the thiol-containing maytansinoids **26a**–**c**. The water soluble reducing agent tris-(2-carboxyethyl)-phosphine (TCEP) could also be used instead of DTT with similar results. Once purified, using nonaqueous solvents, the thiol-containing drugs were stable upon extended storage in dry form. For a subsequent reaction with antibodies, the thiol-containing maytansinoids had to be reconstituted in a water-miscible solvent that would keep the drug in solution in the predominantly aqueous milieu (<5% organic solvent) and also compatible with proteins. Dimethylacetamide (DMA[a]) was found to be the ideal solvent, once it was re-purified and freed

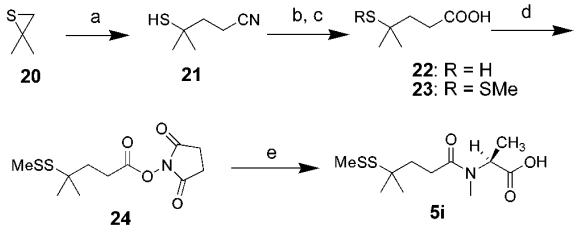
Scheme 5. Synthesis of *N*-Methyl-*N*-[(4-*(R)*-methyldithio)-1-oxopentyl]-*S*-alanine[a]



[a] Reaction conditions: (a) TsCl. Py; (b) NaCN; (c) KSSCOEt; (d) NaOH; (e) $CH_3SSO_2CH_3$; (f) *N*-hydroxysuccinimide, EDC; (g) *N*-methyl-L-alanine, triethylamine.

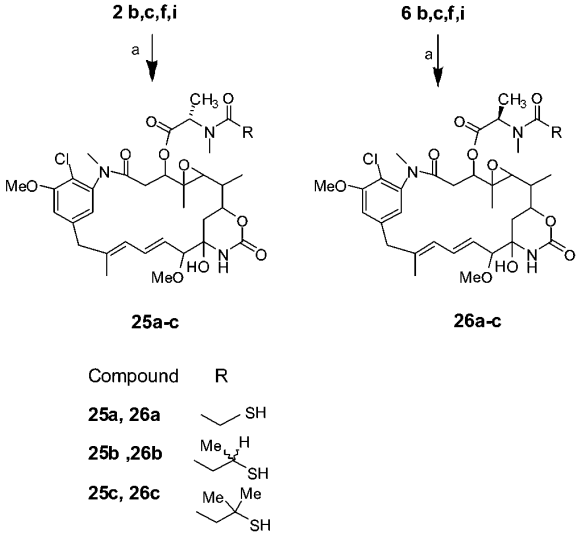
DAC EX. 2040 IPR2022-01531 Page 1251 of 1299

Scheme 6. Synthesis of *N*-Methyl-*N*-[4-methyl-(4-methyldithio)-1-oxopentyl)-*S*-alanine[a]



[a] Reaction conditions: (a) CH_3CN, ^nBu-Li; (b) NaOH; (c) $CH_3SSO_2CH_3$; (d) *N*-hydroxysuccinimide, EDC; (e) *N*-methyl-L-alanine.

Scheme 7. Synthesis of Thiol-Containing Maytansinoids[a]



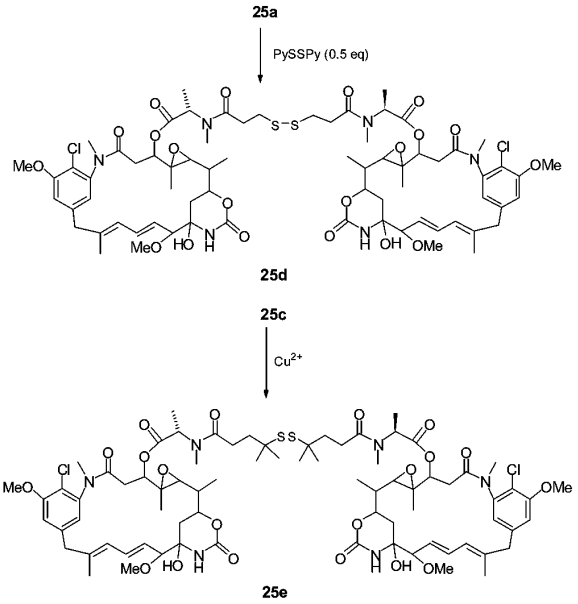
[a] Reaction conditions: (a) dithiothreitol/RT.

of metal ions. This was achieved by the careful glass-distillation of high-grade commercial DMA.

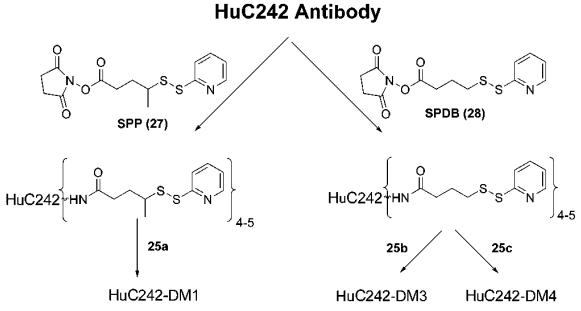
Maytansinoids **2j** (DM1-TPA) and **2k** (DM4-TBA) were sometimes obtained as byproducts of the conjugation reaction of thiol-containing maytansinoids with antibodies. To determine the potency of these compounds, they were independently synthesized from the corresponding thiol-containing maytansinoids **25a** and **25c**, respectively, by a disulfide exchange with the appropriate pyridyldithioalkanoic acids. The disulfide dimers **25d** and **25e** of DM1 and DM4, respectively, were also sometimes obtained as byproducts of the conjugation reaction. These two dimers were synthesized either by disulfide exchange or by metal-ion-catalyzed oxidation of the parent thiol-containing maytansinoids **25a** and **25c**, respectively (Scheme 8).

Antibody Conjugates. The antibody used in this study was huC242, a humanized version of the murine monoclonal antibody C242[20] that binds to the CanAg antigen that is highly expressed on the surface of several human solid tumors, including colon, pancreatic, gastric, and some lung tumors. This antibody displayed limited cross-reactivity with human normal tissues. The conjugation of the maytansinoid to the monoclonal antibodies was accomplished in two steps (Scheme 9). First, the monoclonal antibody was modified either with *N*-succinimidyl 4-(2-pyridyldithio)pentanoate (SPP, **27**) or with *N*-succinimidyl 4-(2-pyridyldithio)butanoate (SPDB, **28**) to introduce an active disulfide-containing group. The treatment with these bifunctional cross-linking agents resulted in the formation of stable amide bonds with the ϵ-amino group of lysine residues to generate a modified antibody bearing, on an average, four to five linked pyridyldithio groups per antibody molecule. Modification with SPP results in the introduction of a sterically hindered center on the carbon atom bearing the disulfide moiety, whereas the treatment with SPDB results in the introduction of a nonhindered disulfide. In the second step, the treatment with a thiol-containing maytansinoid led to disulfide exchange with the pyridyldithio group to give antibody conjugates containing, on the average, three to four maytansinoid drugs linked via the newly formed disulfide bonds. The strength of the disulfide bond was varied by using maytansinoids **25b** and **25c** that bear sterically hindered thiols or by utilizing the SPP cross-linker, which would introduce a methyl substituent on the antibody side of the disulfide link. For example, the huC242−DM1 conjugate cantuzumab mertansine contains one methyl substituent on the antibody side of the disulfide link. The huC242−DM3 conjugate bears one methyl substituent on the drug side of the disulfide link, whereas the huC242−DM4 conjugate bears two methyl substituents on the drug side of the disulfide link. A structural representation of these conjugates is shown in Figure 2. The conjugates were monomeric, soluble in neutral

Scheme 8. Synthesis of Maytansinoid Dimers[a]



Scheme 9. Preparation of Antibody−Maytansinoid Conjugates[a]



[a] Abbreviations: DMA, dimethylacetamide; SPP, *N*-succinimidyl 4-(2-pyridyldithio)pentanoate; SPDB, *N*-succinimidyl 4-(2-pyridyldithio)butanoate.

DAC EX. 2040 IPR2022-01531 Page 1252 of 1299

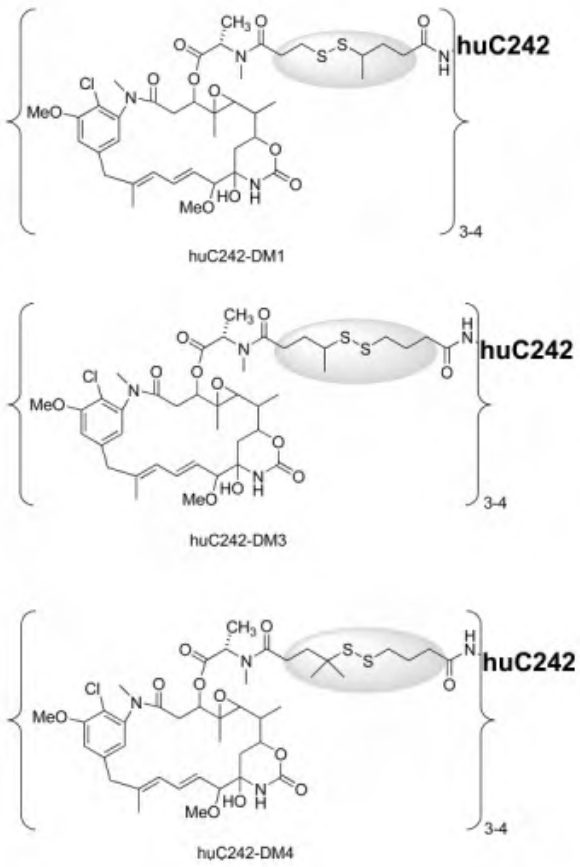


Figure 2. Structural representation of maytansinoid conjugates with the huC242 antibody. The differences in the linker region are shadowed.

buffered aqueous solution, and stable for up to two years upon storage at 4 °C.

Biological Studies. Free Drugs. The disulfide-containing maytansinoid drugs and thiol-containing maytansinoid drugs were evaluated for their ability to suppress the proliferation of human tumor cell lines in vitro. KB (human epidermoid carcinoma) and SK-BR-3 (human breast tumor) cells were exposed to the compounds for 24 or 72 h, and the surviving fractions of cells were measured using a clonogenic plating efficiency assay. The IC_{50} values were then calculated from these data. The L-aminoacyl maytansinoid **2b** (DM1SMe), bearing a methyldithio-propanoyl substituent in the C3 ester side chain, was found to be highly potent with IC_{50} values of 0.029 and 0.014 nM toward KB and SK-BR-3 cells, respectively (Table 1). This methyldithio-maytansinoid displayed cytotoxicity similar to that of the parent drug maytansine toward KB cells and increased potency compared to that of maytansine toward SK-BR-3 cells. The potency of **2b** was then compared to that of maytansine on a wider panel of human tumor cell lines (see Table 1). Compound **2b** was potent toward SW-620 (colon adenocarcinoma) with an IC_{50} value of 0.040 nM, about 3-fold more potent than maytansine. Both **2b** and maytansine were less potent toward HCT-15 (colon carcinoma) cells with IC_{50} values of 0.13 and 0.75 nM, respectively. The lower potency of these drugs toward HCT-15 cells line can be explained by the reported expression of the multidrug resistance gene (mdr1/P-glycoprotein) in this cell line.[21] Compound **2b** was about twice as cytotoxic (IC_{50} = 0.05 nM) as maytansine against the ovarian cancer line OVCAR3. Thus, the replacement of the acetyl group

Table 1. Comparison of the in Vitro Potency of Maytansine (**1**) and Disulfide-Containing Maytansinoid, DM1SMe (**2b**) after 72 h of Exposure to the Drugs

	IC_{50} (nM)	
cell line	maytansine (**1**)	maytansinoid **2b**
KB	0.034 ± 0.005	0.029 ± 0.003
Sk-Br-3	0.030 ± 0.005	0.014 ± 0.006
A-431	0.040	<0.030
A-549	0.160 ± 0.040	0.120
SW-620[a]	>0.100	0.040 ± 0.004
Ovcar-3[a]	0.100 ± 0.020	0.050 ± 0.010
HCT-15	0.750	0.130
MCF-7	0.044 ± 0.002	<0.03
A-375	0.037	0.030 ± 0.015

[a] 24 h exposure.

Table 2. Cytotoxicity of Various Maytansinoids in Vitro toward Tumor Cell Lines (72 h of Exposure)

	IC_{50} (nM)	
compd	KB cells	SK-Br-3 cells
4	>3	1.2
1	0.034	0.030
2a	0.190	nd
2b	0.029	0.014
2c	0.100	nd
2d	0.0085	0.038
2f	0.011	0.0042
2g	0.040	0.032
2h	0.042	0.027
2i	0.0011	0.0032
2j	1.80	3.40
2k	23.0	7.10
6b	3.0	6.0
6d	2.0	nd
6f	1.20	0.22
6g	>3.0	>3.0
6h	2.40	2.20
6i	>0.30	>0.30
25a	1.10	1.10
25b	0.077	0.031
25c	0.290	0.120
25d	0.140	0.100
25e	0.0016	0.0012
26a	>3.0	>3.0
26c	>1.0	3.3

in the C3 side chain of maytansine with a methyldithiopropanoyl group not only preserved the cytotoxic activity of maytansine but, in some cases, even enhanced its potency toward cancer cell lines.

We then examined the effect of the chain length of the acyl group on potency (Table 2). Maytansinoid **2d**, bearing the methyldithiobutanoyl side chain (one methylene longer than **2b**), displayed similar potency to that of **2b**. In contrast, the methyldithioacetyl maytansinoid **2a** (one methylene unit shorter than **2b**) was about 10-fold less cytotoxic than **2b**, suggesting that a minimum of two methylene groups are required in the *N*-acyl side chain to achieve high potency. The phenyldithio analogue **2c** was also about 10-fold less potent than the corresponding methydithio-maytansinoid **2b**. Maytansinoids bearing a branched L-aminoacyl side chain, incorporating one methyl substituent (DM3SMe, **2f**,**g**,**h**) or two methyl substituents (DM4SMe, **2i**) on the carbon atom bearing the methydithio substituent, were highly potent, with IC_{50} values ranging from 0.0042 to 0.011 nM for **2f** and 0.011 to 0.0032 nM for **2i**. Maytansinoid **2f** bears a new chiral center in the acyl side chain. Maytansinoids **2g** and **2h** bearing the *R* and *S* configurations in the acyl side chains, respectively, were found to display potencies similar to that of **2f**, which bears the racemic acyl side chain. Although the stereochemistry in the acyl side chain

DAC EX. 2040 IPR2022-01531 Page 1253 of 1299

was not important for activity, the stereochemistry of the *N*-methylalanyl moiety had a dramatic influence on potency. Thus, the maytansinoids **6b,d,f,g,h,i** bearing the unnatural *N*-methyl-D-alanyl moiety were about 100-fold less cytotoxic than their corresponding L-epimers toward both cell lines.

In all cases, the mercapto-containing maytansinoids were less potent than their corresponding methydisulfide analogues. Thus, maytansinoid **25a** (DM1), bearing the mercaptopropanoyl side chain, had an IC_{50} value of 1.1 nM toward KB and SK-BR-3 cells, rendering it about 30- and 100-fold less potent than **2b** toward these cell lines. This decrease in potency may be attributed to the instability of thiol-containing maytansinoids such as **25a** under cell culture conditions wherein the oxidation of **25a** to its disulfide dimer **25d** was observed. However, dimer **25d** was independently synthesized and found to be only about 3- to 10-fold less potent than **2b**, suggesting that **25a** might be inactivated additionally by some other mechanism. For example, the thiol group could react with a cell culture component such as cystine to provide a charged maytansinoid carboxylate, which is incapable of internalization into the cell, resulting in diminished potency. Maytansinoids **25b,c** bearing sterically hindered thiols were 3- to 12-fold more potent than **25a**, which is consistent with the predicted lower reactivity and consequently, the greater stability of these compounds in the cell culture milieu. The dimer (**25e**) of DM4 was the most potent maytansinoid tested, with IC_{50} values of 0.0012 and 0.0016 nM toward the two cell lines tested. Maytansinoids **2j** and **2k** bear a terminal carboxyl group that renders them at least 100-fold less potent than the parent compounds **2b** and **2i**, suggesting that the charged carboxylate residue might interfere with the internalization into cells, resulting in diminished potency.

Antibody−Drug Conjugates. Cytotoxicity in Vitro. The conjugation of the huC242 antibody, via disulfide bonds, with thiol-containing maytansinoids DM1 (**25a**), DM3 (**25b**), and DM4 (**25c**) gave the conjugates labeled huC242−DM1, huC242−DM3, and huC242−DM4, respectively (Figure 2). In these conjugates, the antibody modifying agent and the maytansinoids were chosen with the goal of producing conjugates of varying disulfide bond stability. All three conjugates displayed high potency in vitro toward the antigen-expressing COLO 205 cell line, with IC_{50} values (in protein concentration) of 1.1×10^{-11}, 1.3×10^{-11}, and 3.8×10^{-11} M for huC242−DM4, huC242−DM3, and huC242−DM1, respectively. Thus, the disulfide bond strength does not appear to play an important role in determining the magnitude of in vitro potency toward target cells. Importantly, all three conjugates were about 200-fold less cytotoxic toward antigen-negative A-375 cells, demonstrating the specificity of the cytotoxic effect. Figure 3 shows an example of how an antibody can confer target specificity to an otherwise nonspecifically cytotoxic drug. Both the COLO 205 and A-375 cell lines were killed equally well by the nonconjugated maytansinoid **2i** (DM4SMe). In contrast, the conjugated maytansinoid huC242−DM4 kills the target COLO 205 cells at a 1000-fold lower concentration than the nontarget A-375 cell, establishing that the linkage to antibodies confers tumor specificity to the otherwise indiscriminately toxic maytansinoid drugs.

Antitumor Activity in Vivo. The antitumor activity of the three huC242−maytansinoid conjugates, huC242−DM1, huC242−DM3, and huC242−DM4, were compared in human colon tumor xenograft models established with COLO 205 cells. We have previously shown[10] that C242−DM1 is curative in this model and that the free DM1 and the unconjugated C242 antibody show little or no antitumor effect. To compare the

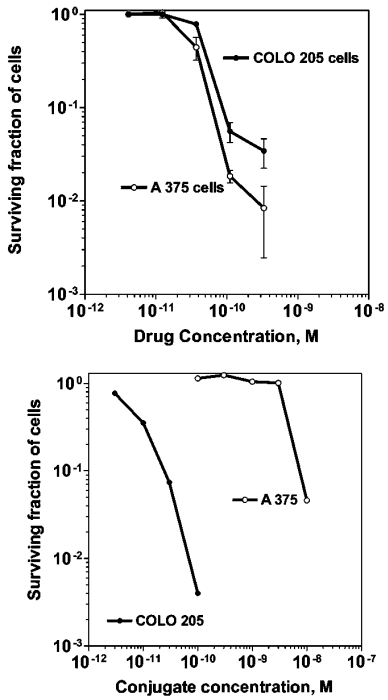


Figure 3. Top panel: in vitro potency of unconjugated drug DM4SMe (**2i**) toward COLO 205 and A-375 cells. Bottom panel: in vitro potency of huC242−DM4 conjugate toward target COLO 205 cells and no-target A-375 cells.

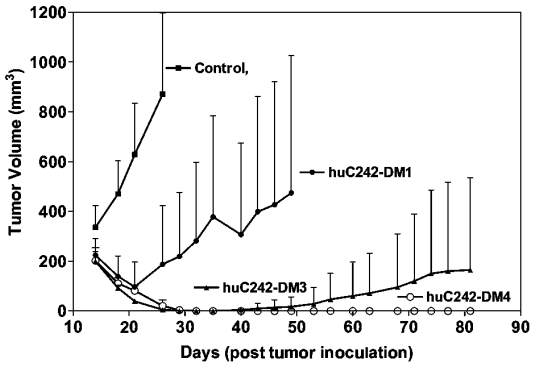


Figure 4. Comparison of the antitumor activity of huC242−maytansinoid conjugates in a human colon tumor xenograft model established subcutaneously with COLO 205 cells.

relative efficacy of the three conjugates, we selected a treatment regimen that used a low dose of the conjugate (~20% of the maximum tolerated dose) that would result in a delay in tumor growth but would not be curative. The results are shown in Figure 4. The tumors in the control group of mice grew to a size of nearly 900 mm^3 in 24 days. The treatment with huC242−DM1 (linked maytansinoid dose of 75 μg/kg, qd × 5) resulted in a tumor growth delay of 20 days, whereas the treatment with huC242−DM3, at an equivalent dose, resulted in a greater therapeutic effect and caused complete tumor regressions lasting 45 days. Treatment at an equivalent dose of the huC242−DM4 conjugate was even more efficacious, resulting in cures of all of the treated animals. Interestingly, the antitumor activity of huC242−DM3 is superior to that of huC242−DM1, although both conjugates would have been predicted to display similar stability in vivo. The huC242−DM3 conjugate bears one methyl

DAC EX. 2040 IPR2022-01531 Page 1254 of 1299

group on the carbon atom bearing the disulfide bond on the drug side of the conjugate, whereas huC242−DM1 bears one methyl substituent at the carbon atom on the antibody side of the disulfide link. However, cleavage of the disulfide bond in huC242−DM3 releases the thiol-containing maytansinoid DM3, which is about 10-fold more potent than DM1, the active component released from huC242−DM1, which could explain the greater efficacy observed with the DM3 conjugate.

The greater antitumor activity of huC242−DM4 compared to that of huC242−DM1 can be attributed to at least two factors: (a) the greater stability of the disulfide bond between the antibody and the drug in huC242−DM4, which results in a longer circulation time of the intact conjugate and thus potentially greater accumulation at the tumor site, and (b) the greater stability of the released DM4 drug, which bears a thiol substituent at a tertiary carbon center. Studies to determine the parameters contributing to the different in vivo activities of the conjugates are ongoing.

Conclusions

To harness the potent cytotoxic activity of maytansinoids for the treatment of cancer, we prepared analogues of maytansine that can be covalently linked to monoclonal antitumor antibodies for targeted treatment. Such analogues not only have to maintain the activity of maytansine but also have to be able to readily form a stable chemical bond with a protein in aqueous solution. For manufacturing reasons, bond formation must be efficient and occur in high yield. Sulfhydryl groups or their respective thiolate anions react readily in aqueous solutions with maleimido moieties in a Michael-type addition reaction to form thioethers and with disulfide groups in a disulfide exchange reaction to form new disulfide bonds. We, therefore, prepared and tested maytansinoid compounds with reactive sulfhydryl groups, which during synthesis and for some biological testing were protected in the form of simple disulfide compounds.

Thus, we have synthesized a series of new maytansinoids bearing a disulfide or thiol substituent. The series was chosen so as to evaluate the influence of the chain length of the ester side chain and the degree of steric hindrance on the carbon atom bearing the thiol substituent on in vitro cytotoxicity. Several of these maytansinoids were found to be even more potent than the parent drug maytansine in killing human tumor cells in vitro. Antibody conjugates bearing varying degrees of steric hindrance around the disulfide link between the maytansinoid and antibody were shown to be highly active in selectively killing target cells to which the antibody was capable of binding. Nontarget cells were not affected even at a 100-fold higher concentration, demonstrating that the high potency of the maytansinoids could be directed toward the specific killing of target cells. Remarkable antitumor efficacy was observed in a xenograft model. These studies, in part, have led to the development of huC242−DM4 for evaluation as an antitumor agent in human clinical trials in patients expressing the antigen for C242.

Experimental Section

All reagents were obtained from the Aldrich Chemical Co., unless otherwise stated. Maytansine (NCI 158358/26/0) was obtained from the National Cancer Institute. Ansamitocin P-3 was produced by fermentation of an *Actinosynnema pretiosum* strain derived from several rounds of mutagenesis of the parent ATCC 31565 strain. Human tumor cell lines used in biological assays were obtained from the American Type Culture Collection (ATCC). Melting points were determined on an electrothermal melting point apparatus. Proton magnetic resonance (^{1}H NMR) spectra were obtained on a Bruker Avance spectrometer operating at 400 MHz. The chemical shifts are reported in δ values relative to that of an internal tetramethylsilane (Me_4Si) standard. UV spectra were recorded on a Beckman DU-640 spectrophotometer. The optical rotations were determined using a Rudolph AUTOPOL IV polarimeter. Mass spectra were obtained on a Bruker Daltonics spectrometer or a Waters QTOF-API-US spectrometer. Elemental analyses were performed by Atlantic Microlabs, Atlanta, GA. High performance liquid chromatography (HPLC) was performed on a Beckman or Varian instrument (analytical or preparative scale) equipped with a diode array detector.

Synthesis of Maytansinol (4). To a 200 mL flask was added a 1 M solution of lithium aluminum hydride (45 mmol, 45 mL) in THF. The solution was placed under an argon atmosphere and cooled to −40 °C. A mixture of anhydrous methanol (5.4 mL, 135 mmol) in THF (25 mL) was added dropwise. The temperature was maintained between −30 and −40 °C. After the addition was complete, the reaction mixture was stirred at this temperature for an additional period of 10 min to give lithium trimethoxyaluminum hydride ($LiAlH(OMe)_3$). In a separate 250 mL flask, ansamitocin (3.2 g, 5.0 mmol) was dissolved in anhydrous THF (30 mL), and the solution was placed under an argon atmosphere and cooled in a dry ice−acetone bath to −40 °C. The solution of $LiAlH(OMe)_3$ was transferred via a cannula over 10 min into the chilled solution of ansamitocins. The reaction temperature was maintained between −30 and −35 °C under argon and stirred for 2 h. Deionized water (22 mL) was added dropwise while the reaction mixture was maintained at −30 and −35 °C. After 30 min, 88% formic acid (1.8 mL) and ethyl acetate (50 mL) were added. The mixture was allowed to warm up to room temperature. The precipitate was removed by vacuum filtration, and the filtrate was concentrated under vacuum. The residue was dissolved in a minimum volume of dichloromethane and loaded onto a silica gel column packed in dichloromethane. The column was eluted with dichloromethane/methanol (95:5, v/v). The fractions containing the desired product were pooled and evaporated under reduced pressure to give 2.3 g of maytansinol (81% yield) as a white solid: mp 205−207 °C; ^{1}H NMR ($CDCl_3$) δ 0.82 (3H, s), 1.28 (3H, d, J = 6 Hz), 1.52−1.54 (1H, m), 1.67 (3H, s), 1.80 (br s s), 2.07−2.29 (4H, m), 2.56 (1H, d, J = 11 Hz), 2.95 (br s), 3.10 (1H, d, J = 12 Hz), 3.19 (3H, s), 3.41 (3H, s), 3.44−3.51 (3H, m), 3.97 (3H, s), 4.34 (1H, t, J = 11 Hz), 5.50 (1H, dd, J = 9 and 15 Hz), 6.13 (1H, d, J = 11 Hz), 6.37 (1H, s), 6.42 (1H, dd, J = 11 and 15 Hz), 6.79 (1H, d, J = 1.5 Hz), 7.02 (1H, d, J = 1.5 Hz); HRMS calcd for $C_{28}H_{33}ClN_2O_8$ $(M + H)^+$ m/z = 565.2317; found, 565.2329. HPLC analysis was performed on a Kromasil analytical C-8 column (length: 100 mm, i.d.: 4.6 mm), at a flow rate of 1 mL/min, eluting with a gradient of water and acetonitrile (30% to 45% CH_3CN over 30 min). Under these conditions, maytansinol eluted as a sharp peak with a retention time of 11.15 min.

Acetal 4c. A solution of ansamitocins (3.0 g, 4.72 mmol) in THF (15 mL) was cooled to −35 °C, and a solution of 0.67 M $LiAl(OMe)_3H$ (56 mL, 37.7 mmol) in THF was added dropwise by syringe using a syringe pump. The temperature of the reaction was maintained between −30 and −40 °C throughout the addition. After addition was complete, the reaction was stirred for 2 h at between −34 and −37 °C. A solution of 88% formic acid (1.85 mL, 2.16 g, 41.5 mmol) in deionized water (23 mL) was added dropwise to the flask at a rate that did not produce excessive frothing, followed by the addition of ethyl acetate (60 mL). The cooling bath was removed, and the mixture was allowed to warm up to room temperature. The pH of the mixture was checked with pH paper and found to be approximately 6. Precipitated aluminum-based byproducts were removed by vacuum filtration, and the solvent was removed from the filtrate by rotary evaporation under vacuum. Butyl acetate (10 mL) was added to the residue, and the solvent was then evaporated to remove the residual water. The residue was purified by silica chromatography using dichloromethane/methanol 95:5 (v:v), giving a later eluting band (maytansinol) and an early eluting band. The maytansinol band was collected, and the solvent was removed by rotary evaporation to give 1.55 g of maytansinol (58%). The solvent was removed from the earlier eluting band,

DAC EX. 2040 IPR2022-01531 Page 1255 of 1299

and the material was dissolved in a minimum volume of acetonitrile and then purified by preparative reverse-phase HPLC. The solvent was removed by rotary evaporation to give 440 mg (15% yield) of **4c**, R = $-CH(CH_3)_2$; ^1H NMR ($CDCl_3$) δ 0.78 (s, 3H), 0.97 (d, 3H, J = 6.9), 1.04 (d, 3H, J = 6.7), 1.23 (m, 1H), 1.28 (d, 3H, J = 6.4), 1.54 (m, 1H), 1.66 (s, 3H), *1.72 (m, 2H)*, 2.03 (dd, 1H, J = 14, 3.6 Hz), 2.3 (d, 1H, J = 14), 2.49 (dd, 1H, J = 11.7, 14), 2.92 (d, 1H, J = 9.5 Hz), 3.14 (s, 3H), 3.12 (m, 1H), 3.37, (s, 3H), 3.52 (m, 3H), 3.65 (m, 1H), 3.75 (m, 1H), 3.97 (s, 1H), 4.31 (m, 2H), 5.52 (dd, 1H, J = 16, 8.7 Hz), 6.13(d, 1H, J = 11 Hz), 6.34 (s, 1H), 6.45 (dd, 1H, J = 16, 11 Hz), 6.80 (d, 1H, J = 1.5 Hz), 6.92 (d, 1H, J = 1.5 Hz); MS *m/z* 619.3 (M +H)+.

3-(Methyldithio)propanoic Acid (8b). To a stirred solution of 3-mercaptopropanoic acid (**7b**) (5.00 g, 0.047 mol) in water (150 mL) cooled in an ice bath was added methyl methanethiolsulfonate (6.54 g, 0.052 mol) in absolute ethanol (75 mL). The reaction mixture was stirred overnight at room temperature. The mixture was then diluted with saturated aqueous NaCl (400 mL) and extracted with ether (3 × 150 mL), and the combined ether extracts were then washed with saturated NaCl. The solution was dried over Na_2SO_4, concentrated, and then distilled to afford a colorless liquid (6.47 g, 90%); bp (1 mm) = 105 °C; ^1H NMR ($CDCl_3$) δ 2.32 (3H, s), 2.80 (4H, m), 11.20 (1H, s).

4-(Methyldithio)butanoic Acid (8c). To a stirred solution of bis-(3-carboxypropyl)disulfide (1.00 g, 4.20 mmol) in methanol (20 mL) was added a solution of dithiothreitol (0.647 g, 4.20 mmol) in H_2O (20 mL). A solution of 10 M NaOH (0.842 mL, 8.42 mmol) was then added and the mixture was allowed to stir overnight at room temperature to effect complete reduction. Methyl methanethiolsulfonate (1.17 g, 9.24 mmol) was added, and the reaction mixture was stirred for another 3 h. The mixture was then diluted with saturated aqueous NaCl (150 mL), acidified (aqueous HCl), and extracted with ethyl ether (3 × 100 mL). The combined organic layers were washed with saturated NaCl, dried (Na_2SO_4), concentrated, and chromatographed on silica gel, eluting with dichloromethane/ethyl acetate to give 0.867 g (56%) of a colorless liquid; ^1H NMR ($CDCl_3$) δ 2.12 (2H, m), 2.40 (3H, s), 2.74 (2H, m), 11.18 (1H, s).

3-(Phenyldithio)propanoic Acid (8d). To a stirred solution of diphenyl disulfide (3.0 g, 13.8 mmol) in a mixture of ether (10 mL) and methanol (20 mL) under a nitrogen atmosphere at room temperature was added a solution of 3-mercaptopropanoic acid (**7b**) (0.49 g, 4.6 mmol) in ether (5 mL), followed by a solution of 10 M NaOH (0.46 mL, 4.6 mmol). The reaction mixture was stirred at room temperature for 20 h and then stripped of the solvents under reduced pressure. The product was purified by column chromatography on silica gel, eluting with ethyl acetate/hexane. The product was obtained as a white solid (0.56 g, 56.6%); mp 57−59 °C; ^1H NMR ($CDCl_3$, TMS) δ 2.6−3.0 (4H, m), 7.12−7.60 (5H, m), 10.6 (1H, s).

***R*-1,3-Di-*O*-(*para*-toluenesulfonyl)butane (11).** A solution of *R*-(−)-1,3-butanediol (**10**, 2.00 g, 22.22 mmol) in a mixture of dry pyridine (40 mL) and dry toluene (60 mL) was treated with *p*-toluenesulfonyl chloride (12.70 g, 66.84 mmol) under argon at 0 °C. After stirring at 0 °C for 5 min followed by stirring at room temperature for 2 h, the mixture was evaporated under vacuum, redissolved in ethyl acetate, and washed with 0.1 M aqueous $NaHCO_3$, followed by saturated aqueous NaCl. The organic layer was dried over $MgSO_4$ and filtered, and the solvent was evaporated. Purification by chromatography on silica gel, eluting with 1:2 (v/v) ethyl acetate/hexane gave 6.51 g (74%) of the title compound (R_f = 0.40, 1:1 EtOAc/hexane) as a white solid; mp 56−58 °C; ^1H NMR ($CDCl_3$) δ 7.76 (dd, 4H, J = 1.0, 8.0 Hz), 7.35 (dt, 4H, J = 0.4, 8.0 +8.0 Hz), 4.70 (m, 1H), 4.03 (m, 1H), 3.94 (m, 1H), 2.46 (s, 6H), 1.92 (m, 2H), 1.26 (d, 3H, J = 6.3 Hz); ^{13}C NMR 145.17, 133.00, 130.11, 128.12, 127.91, 76.28, 66.21, 36.08, 21.86, 21.06; MS: *m/z* 420.99 $(M + Na)^+$.

***S*-4-(*O*-Ethylxanthic)pentanenitrile (12).** A solution of *R*-1,3-di-*O*-*p*-toluenesulfonyl-butane (**11**, 4.80 g, 12.06 mmol) in dry DMSO (50 mL) was treated with NaCN (0.65 g, 13.26 mmol). After stirring at room temperature under argon for 18 h, the reaction mixture was diluted with ethyl acetate, washed successively with cold 1.0 M NaH_2PO_4 at pH 7.5, water, and 1.0 M aqueous NaH_2PO_4 at pH 4.0. The organic layer was separated and dried over $MgSO_4$, filtered, and then evaporated to give 2.63 g of crude *R*-3-*O*-*p*-toluenesulfonyl-pentanenitrile. MS: *m/z* 275.80 $(M + Na)^+$. The product was used directly without further purification. To the solution of crude of *R*-3-*O*-*p*-toluenesulfonyl-pentanenitrile (2.63 g) in ethanol (15 mL) was added potassium *O*-ethylxanthate (4.55 g) in ethanol (50 mL). After stirring overnight under argon, the mixture was concentrated, diluted with ethyl acetate, and filtered through a short silica column. The eluant was concentrated and purified by chromatography on silica gel, eluting with 1:4 (v/v) EtOAc/hexane, to give 1.54 g (63%, 2 steps) of the title compound (R_f = 0.40 (1:4 EtOAc/hexane)) as a colorless oil. ^1H NMR ($CDCl_3$) δ 4.67 (dd, 2H, J = 7.1, 14.2 Hz), 3.86 (ddd, 1H, J = 7.0, 14.0, 21.9 Hz), 2.50 (t, 2H J = 7.3 + 7.6 Hz), 2.06 (m, 2H), 1.44 (m, 6H); ^{13}C NMR 213.04, 119.16, 70.28, 44.57, 32.10, 20.20, 15.21, 13.93; MS: *m/z* 226.51 $(M + Na)^+$, 242.51 $(M + K)^+$.

***S*-(+)-4-(Methyldithio)pentanoic Acid (13).** To a solution of *S*-4-*O*-Ethylxanthic-pentanenitrile (**12**, 1.95 g, 9.61 mmol) in a mixture of ethanol (10 mL) and water (150 mL) was added NaOH (5 g). The reaction mixture was refluxed overnight under argon. The mixture was cooled to room temperature and diluted with water (150 mL) and extracted with 1:1 EtOAc/hexane (2 × 100 mL). The aqueous layer was acidified with H_3PO_4 to pH 2.5−3.0 and extracted with EtOAc (6 × 75 mL). The organic layers were combined, dried over $MgSO_4$, filtered, and evaporated to dryness to give the crude *S*-4-mercaptopentanoic acid. This crude product was used directly in the next step without further purification. To a solution of crude *S*-4-mercaptopentanoic acid (1.2 g) in a mixture of ethanol (50 mL) and 0.5 M NaH_2PO_3 buffer (75 mL) at pH 7.0 was added dropwise methyl methanethiolsulfonate (1.47 g, 11.65 mmol) in dry THF (5 mL) over 45 min at 0 °C. After stirring under argon at 0 °C for 30 min followed by stirring at room temperature for 2 h, the mixture was concentrated and extracted with dichloromethane (2 × 50 mL). The aqueous layer was acidified with H_3PO_4 to pH 2.5−3.0 and extracted with EtOAc (4 × 100 mL). The organic layers were combined, dried over $MgSO_4$, filtered, and evaporated. The residue was purified by chromatography over silica gel, eluting with 1:100:400 HOAc/EtOAc/hexane to give 1.43 g (83%) of the desired product (R_f = 0.32, 1:100:400 HOAc/EtOAc/hexane) as a white solid; mp 290−293 °C (dec); ^1H NMR ($CDCl_3$) δ 2.91 (ddd, 1H, J = 6.8, 13.7, 20.5 Hz), 2.53 (t, 2H, J = 7.7 + 7.4 Hz), 2.42 (s, 3H), 1.94 (m, 2H), 1.36 (d, 3H, J = 6.8 Hz); ^{13}C NMR 179.18, 45.35, 31.58, 30.73, 24.70, 21.05; MS: (*m/z*) 202.92 $(M + Na)^+$; $[\alpha]^{25}_D$ = +41.35 (c = 2, CH_3OH).

***S*-1,3-Di-*O*-(*para*-toluenesulfonyl)butane (16).** A solution of *S*-(−)-1,3-butanediol (**15**, 2.00 g, 22.22 mmol) in a mixture of dry pyridine (40 mL) and dry toluene (60 mL) was treated with *p*-toluenesulfonyl chloride (12.70 g, 66.84 mmol) under argon at 0 °C. After stirring at 0 °C for 5 min followed by stirring at room temperature for 2 h, the mixture was evaporated under vacuum. The residue was redissolved in ethyl acetate and washed with 0.1 M aqueous $NaHCO_3$ and saturated NaCl. The organic layer was separated, dried over $MgSO_4$, filtered, and evaporated. The residue was purified by chromatography over silica gel, eluting with 1:2 ethyl acetate/hexane to give 6.25 g (71%) of the title compound (R_f = 0.40 (1:1 EtOAc/hexane)). Recrystallization from ether/hexane afforded a white solid; mp 56−58 °C; ^1H NMR ($CDCl_3$) δ 7.76 (dd, 4H, J = 1.0, 8.0 Hz), 7.35 (dt, 4H, J = 0.4, 8.0 +8.0 Hz), 4.70 (m, 1H), 4.03 (m, 1H), 3.94 (m, 1H), 2.46 (s, 6H), 1.92 (m, 2H), 1.26 (d, 3H, J = 6.3 Hz); ^{13}C NMR 145.17, 133.00, 130.11, 128.12, 127.91, 76.28, 66.21, 36.08, 21.86, 21.06; MS: *m/z* 420.99 $(M + Na)^+$.

***R*-4-*O*-(Ethylxanthic)pentanenitrile (17).** A solution of *S*-1,3-di-*O*-(*p*-toluenesulfonyl)butane (**16**, 6.25 g, 15.70 mmol) in 60 dry DMSO (50 mL) was treated with NaCN (0.85 g). The reaction mixture was stirred under argon for 18 h at room temperature. The reaction mixture was then diluted with ethyl acetate, washed sequentially with cold 1.0 M NaH_2PO_4 buffer at pH 7.5, water, and 1.0 M NaH_2PO_4 buffer at pH 4.0. The organic layer was dried

DAC EX. 2040 IPR2022-01531 Page 1256 of 1299

over $MgSO_4$, filtered, and evaporated to give 3.62 g of crude *S*-3-*O*-(*p*-toluenesulfonyl)pentanenitrile. The product was used directly without further purification. To a solution of crude *S*-3-O-*p*-toluenesulfonyl-pentanenitrile (3.62 g) in ethanol (50 mL) was added potassium *O*-ethylxanthate (5.72 g) in ethanol (100 mL). After stirring overnight under argon, the mixture was concentrated, diluted with ethyl acetate, and filtered through a short column of silica gel. The eluant was concentrated, and the residue was purified by chromatography over silica gel, eluting with 1:4 EtOAc/hexane to give 2.0 g (62%, 2 steps) of the title compound (R_f = 0.40 (1:4 EtOAc/hexane)) as a colorless liquid. ^{1}H NMR ($CDCl_3$) δ 4.67 (dd, 2H, J = 7.1, 14.2 Hz), 3.86 (ddd, 1H, J = 7.0, 14.0, 21.9 Hz), 2.50 (t, 2H J = 7.3 + 7.6 Hz), 2.06 (m, 2H), 1.44 (m, 6H); ^{13}C NMR 213.04, 119.16, 70.28, 44.57, 32.10, 20.20, 15.21, 13.93; MS: *m/z* 226.51 (M + Na) $^+$, 242.51 (M + K) $^+$.

***R*-(−)-4-(Methyldithio)pentanoic Acid (18).** A solution of *R*-4-*O*-(ethylxanthic)pentanenitrile (**17**, 2.0 g, 9.85 mmol) in a mixture of ethanol (10 mL) and water (200 mL) was treated with NaOH (6.0 g). The reaction mixture was refluxed overnight under argon. The mixture was diluted with water (150 mL) and extracted with 1:1 EtOAc/hexane (2 × 100 mL). The aqueous layer was acidified with H_3PO_4 to pH 2.5−3.0 and extracted with EtOAc (6 × 75 mL). The organic layers were combined, dried over $MgSO_4$, filtered, and evaporated to dryness to give crude *R*-4-mercaptopentanoic acid. This crude product was used directly in the next step without further purification. To a solution of 1.60 g of the crude *R*-4-mercapto-pentanoic acid in a mixture of ethanol (50 mL) and 0.5 M NaH_2PO_4 buffer at pH 7.0 (75 mL) was added dropwise a solution of methyl methanethiolsulfonate (1.96 g, 15.53 mmol) in dry THF (7 mL) over 45 min at 0 °C. The reaction mixture was stirred under argon at 0 °C for 30 min and then at room temperature for 2 h. The mixture was concentrated and extracted with dichloromethane (2 × 50 mL). The aqueous layer was acidified with H_3PO_4 to pH 2.5−3.0 and extracted with EtOAc (4 × 100 mL). The organic layers were combined, dried over $MgSO_4$, filtered, and evaporated. The residue was purified by chromatography over silica gel, eluting with HOAc/EtOAc/hexane (1:100:400) to give 1.65 g (93%) of the title compound (R_f = 0.32 (HOAc/EtOAc/hexane, 1:100:400). Recrystallization from ether/hexanes afforded a white solid; mp 157−160 °C; ^{1}H NMR ($CDCl_3$) δ 2.91 (ddd, 1H, J = 6.8, 13.7, 20.4 Hz), 2.53 (t, 2H, J = 7.7 + 7.4 Hz), 2.42 (s, 3H), 1.96 (m, 2H), 1.36 (d, 3H, J = 6.8 Hz); ^{13}C NMR 179.46, 45.67, 31.91, 31.07, 25.02, 21.36; MS: 202.9 (M + Na)$^+$, 203.9; $[\alpha]^{25}_D$ = −39.16 (c = 2, CH_3OH).

4-Mercapto-4-methylpentanoic Acid (22). Compound **21** was prepared by the method previously described.[22] A 500 mL flask was equipped with a stir bar and a 150 mL addition funnel. The system was placed under an argon atmosphere, and anhydrous THF (150 mL) and *n*-BuLi (2.5 M, 75 mL, 18.7 mmol) in hexanes were added via a cannula, and the solution was cooled in a −78 °C dry ice/acetone bath. Acetonitrile (9.4 mL, 18 mmol) was added dropwise via a syringe over approximately 5 min. The reaction mixture was stirred for 30 min, while a white precipitate of lithiated acetonitrile was formed. Isobutylene sulfide (15.0 g, 17 mmol) was dissolved in anhydrous THF (100 mL) and added dropwise over approximately 30 min via the addition funnel. The cooling bath was removed, and the reaction was allowed to stir at room temperature for 3 h. The flask was cooled in an ice/water bath as 0.5 M HCl (38 mL) was added dropwise. The THF layer was retained, and the aqueous layer was washed twice with 75 mL of ethyl acetate. The THF and ethyl acetate layers were combined, dried over approximately 20 g of anhydrous sodium sulfate, and transferred to a 250 mL flask. The solvent was removed by rotary evaporation under reduced pressure to give crude **21**. Ethanol (30 mL) was added, and the contents were stirred. A solution of NaOH (8 g) in water (30 mL) was slowly added. The flask was equipped with a reflux condenser and placed under an argon atmosphere. The reaction was refluxed overnight and then cooled to room temperature. Water (60 mL) was added, and the mixture was extracted twice with 25 mL portions of a 2:1 mixture of ethyl acetate and hexane. The aqueous layer was acidified to pH 2 with concentrated HCl and then extracted with ethyl acetate (3 × 75 mL). The organic layers were dried over anhydrous Na_2SO_4, and the solvent was removed by rotary evaporation under vacuum to give 10 g of product **22** (39% yield). The material was used without further purification.^{1}H NMR ($CDCl_3$) δ 1.38 (6H, s), 1.87−1.93 (2H, m), 2.08 (1H, s), 2.51−2.57 (2H, m).

4-Methyl-4-(methyldithio)pentanoic Acid (23). A solution of 4-mercapto-4-methylpentanoic acid (**22**) (6.0 mL, 40 mmol) was dissolved in deionized water (50 mL) in a 250 mL flask. The solution was magnetically stirred as sodium carbonate (6.4 g, 60 mmol) was added to the acid at a rate that would not cause excessive frothing. The flask was equipped with a 100 mL addition funnel, which was charged with a solution of methyl methanethiolsulfonate (7.5 g, 60 mmol) dissolved in absolute ethanol (30 mL). The flask was cooled in an ice/water bath, and the system was maintained under an argon atmosphere. The methyl methanethiolsulfonate solution was added dropwise to the flask as rapidly as possible but without causing excessive frothing. The cooling bath was removed, and the reaction mixture was allowed to stir at room temperature for an additional 3 h. The solvent was removed by rotary evaporation under vacuum, until approximately 20 mL remained. Then, saturated sodium bicarbonate (10 mL) and deionized water (30 mL) were added. The mixture was washed with ethyl acetate (3 × 25 mL), and the aqueous layer was separated and adjusted to approximately pH 2 with 5 M HCl and then extracted with ethyl acetate (2 × 120 mL). The organic layers were combined and washed with a solution composed of saturated NaCl (16 mL) and 1 M HCl (4 mL). The organic layer was then dried over 14 g of anhydrous sodium sulfate and filtered, and the solvent was removed by rotary evaporation under vacuum to give 5.4 g of product **23** (70% yield) as a white solid. ^{1}H NMR ($CDCl_3$) δ 1.54 (6H, s), 2.15−2.21 (2H, m), 2.64 (3H, s), 2.69−2.72 (2H, m); MS: *m/z* 217.1 (M + Na) $^+$.

General Method for the Synthesis of *N*-Hydroxysuccinimide Esters 9a−d, 14, 19, and 24. (Methyldithio)-alkanoic acid (15 mmol) was dissolved in dichloromethane (20 mL) and stirred magnetically as *N*-hydroxysuccinimide (2.65 g, 23 mmol) was added followed by 1-[3-(dimethylamino)propyl]-3-ethylcarbodiimide hydrochloride (EDC, 4.4 g, 23 mmol). The mixture was stirred under an argon atmosphere for 2 h. The reaction mixture was poured into a 125 mL separatory funnel, 40 mL of ethyl acetate was added, and the solution was washed with 50 mM potassium phosphate buffer at pH 6.0 (2 × 20 mL) and saturated sodium chloride (20 mL). The organic layer was dried over anhydrous Na_2SO_4, and the solvent was removed by rotary evaporation under vacuum to give the desired product, which was used without further purification.

General Method for the Synthesis of *N*-Acyl-*N*-methyl-L-alanines (5a−i). *N*-Methyl-L-alanine (18.0 mmol) was dissolved in a mixture of dimethoxyethane (25 mL) and deionized water (25 mL) in a 125 mL flask equipped with a magnetic stir bar. Triethylamine (6.9 g, 36 mmol) was added, and the solution was vigorously stirred as the *N*-hydroxysuccinimidyl ester (**9a−d, 14, 19, 24**) (18 mmol) dissolved in 40 mL of the same solvent mixture was added dropwise over approximately 5 min. After 2 h, the reaction mixture was concentrated to approximately 40 mL by rotary evaporation under vacuum. Deionized water (10 mL) and 1 M HCl were added to give a pH of approximately 2. The mixture was poured into a separatory funnel and extracted with ethyl acetate (2 × 50 mL). The organic layers were combined and washed with saturated sodium chloride solution (10 mL). The organic layer was dried over 8.0 g of anhydrous Na_2SO_4, and the solvent was removed by rotary evaporation under vacuum. The residue was taken up in a minimum volume of ethyl acetate and purified by chromatography on silica (silica: 40 micron flash grade, silica bed: 24 × 3.0 cm, mobile phase: hexanes/ethyl acetate/acetic acid, 50:48:2). The fractions containing the desired product were combined, and the solvent was removed under vacuum. Residual acetic acid was removed by dissolving the residue in a minimum volume of ethyl acetate and precipitating the product by the rapid but dropwise addition of hexane with stirring. Hexane was added until the product

DAC EX. 2040 IPR2022-01531 Page 1257 of 1299

was no longer detected in the supernatant by TLC analysis. The precipitate was vacuum-dried for 4 h to give the desired products **5a**−**i**.

***N*-Methyl-*N*-[(2-methyldithio)-1-oxoethyl]-L-alanine (5a).** Pale yellow solid (19% yield); ^{1}H NMR ($CDCl_3$) δ 1.458 (3H, d, J = 7.6), 2.446 (3H, s), 3.069 (3H, s), 3.666 (2H, s), 5.185 (1H, m); MS: m/z 246.0 $(M + Na)^+$.

***N*-Methyl-*N*-[(3-methyldithio)-1-oxopropyl]-L-alanine (5b).** White solid (60% yield); mp 103−104 °C; ^{1}H NMR ($CDCl_3$) δ 1.449 (3H, d, J = 7.6), 2.422 (3H, s), 2.821 (2H, m), 2.989 (2H,m), 3.017 (3H, s), 5.194 (1H, m). Anal. ($C_8H_{15}NO_3S_2$) C, H, N. MS: m/z 259.9 $(M + Na)^+$.

***N*-Methyl-*N*-[(3-phenyldithio)-1-oxopropyl]-L-alanine (5c).** White solid (60% yield); mp 96−97 °C; ^{1}H NMR ($CDCl_3$) δ 1.42 (2H, d), 2.7−3.0 (7H, m), 5.24 (1H, q), 7.24−7.60 (5H, m).

***N*-Methyl-*N*-[(4-methyldithio-1-oxobutyl]-L-alanine (5d).** White crystals (44% yield); mp 92−93 °C; ^{1}H NMR ($CDCl_3$) δ 1.439 (3H, d, J = 7.2), 2.089 (2H, t, J = 7.2), 2.405 (3H, s), 2.517 (2H, t, J = 7.2), 2.779 (2H, m), 2.989 (3H, s), 5.123 (1H, m); MS: m/z 290.0 $(M + K)^+$.

***N*-Methyl-*N*-[(4-*(R,S)*-methyldithio-1-oxopentyl)] -L-alanine (5f).** White solid (60% yield). ^{1}H NMR δ 1.35 (3H, d, J = 7), 1.41 (3H, d, J = 7), 1.94−2.03 (2H, m), 2.43(3H, s), 2.50−2.55 (2H, m), 2.83−2.93 (1H, m), 2.98 (3H, s), 5.14 (1H, q, J = 7). MS: m/z 288.1 $(M + Na)^+$.

***N*-Methyl-*N*-[(4-*(S)*-methyldithio)-1-oxopentyl]-*S*-alanine (5g).** White solid (62% yield); ^{1}H NMR δ 1.36 (3H, d, J = 7), 1.42 (3H, d, J = 7), 1.93−1.98 (2H, m), 2.40 (3H, s), 2.50−2.53 (2H, m), 2.90−2.95 (1H, m), 2.99 (3H, s), 5.14 (1H, q, J = 7), MS: m/z 288.1 $(M + Na)^+$

***N*-Methyl-*N*-[(4-*(R)*-methyldithio)-1-oxopentyl]-*S*-alanine (5h).** White solid (60% yield); ^{1}H NMR δ 1.35 (3H, d, J = 7), 1.42 (3H, d, J = 7), 1.93−2.00 (2H, m), 2.43 (3H, s), 2.50−2.55 (2H, m), 2.88−2.95 (1H, m), 3.00 (3H, s), 5.14 (1H, q, J = 7), MS: m/z 288.1 $(M + Na)^+$.

***N*-Methyl-*N*-[4-methyl-(4-methyldithio)-1-oxopentyl)-L-alanine (5i).** White solid (51% yield) mp 77−79 °C; ^{1}H NMR ($CDCl_3$) δ 1.32 (6H, s), 1.42 (3H, d, J = 7 Hz), 1.90−97 (2H, m), 2.40 (3H, s), 2.42−2.49 (2H, m), 2.9 (3H, s), 5.15 (1H, q, J = 7 Hz). MS: m/z 302.0. $(M + Na)^+$.

General Procedure for the Esterification of Maytansinol to Give Maytansinoids 2a−i and 6a−i. In a typical experiment, maytansinol (**4**, 25 mg, 0.044 mmol) and carboxylic acids **5a**−**i** (0.264 mmol) were dissolved in dichloromethane (3 mL) and stirred under an argon atmosphere. A solution of dicyclohexylcarbodiimide (DCC, 57.2 mg, 0.277 mmol) in dichloromethane (0.7 mL) was added. After 1 min, a solution of 1 M $ZnCl_2$ in diethyl ether (0.055 mL, 0.055 mmol) was added. The mixture was stirred at room temperature for 2 h, then ethyl acetate (5 mL) was added, and the mixture was vacuum filtered through course filter paper. The filtrate was washed with a solution of saturated aqueous sodium bicarbonate (2 mL) followed by a saturated sodium chloride solution (1 mL). The organic layer was separated, dried over anhydrous sodium sulfate, and filtered, and the solvent was removed under reduced pressure. The residue was purified by silica chromatography using a mixture of dichloromethane and methanol to remove the unreacted maytansinol. The fractions containing the desired product were combined, and the solvent was removed under vacuum to give a mixture of diastereomeric maytansinoids bearing the *N*-methyl-*N*-acyl-L- and D-alanine eaters. The residue was taken up in a minimum volume of ethyl acetate and purified by one of three ways: (1) preparative TLC on silica, (2) HPLC on an analytical Kromasil cyano-bonded silica column (4.6 mm × 250 mm), using an isocratic elution at a flow rate of 1 mL/min, with hexane/ethyl acetate/2-propanol (68:24:8, v/v/v), or (3) HPLC using a preparative (50 cm × 250 cm, 10 micron) Kromasil or Diazem cyano-bonded silica column using as mobile phase a 68:8:24 mixture of hexane, 2-propanol, and ethyl acetate. The flow rate was 118 mL/min. Under either HPLC condition, typically, the desired product L-aminoacyl maytansinoid (**2a**−**i**) eluted about 8−10 min before the corresponding D-aminoacyl isomer (**6a**−**i**).

***N*^{2}-Deacetyl-*N*^{2}-[2-(methyldithio)-1-oxoethyl]maytansine (D-M0SMe, 2a).** Maytansinol (**4**) was reacted with *N*-methyl-*N*-[(2-methyldithio)-1-oxoethyl]-L-alanine (**5a**) as described above. The desired maytansinoid **2a**, and the corresponding D-aminoacyl isomer **6a** were isolated by purification using preparative TLC, eluting with 5% methanol in ethyl acetate to give a white solid. **6a** ^{1}H NMR δ 0.796 (3H, s), 1.252 (1H, m), 1.306 (3H, d, J = 6.4 Hz), 1.322 (3H, d, J = 6.8 Hz), 1.344 (3H, d, J = 10.8 Hz), 1.414 (2H, m), 1.553 (1H, d, J = 14.4 Hz), 1.640 (3H, s), 2.182 (1H, dd, J = 12.4, 2.8 Hz), 2.416 (3H, s), 2.624 (1H, dd, J = 12, 2.4 Hz), 2.914 (3H, s), 3.022 (1H, d, J = 9.6 Hz), 3.099 (1H, d, J = 12.4 Hz), 3.210 (3H, s), 3.357 (3H, s), 3.499 (1H, d, J = 9.2 Hz), 3.571 (1H, d, J = 14 Hz), 3.980 (3H, s), 4.266 (1H, dt, J = 12, 1.6 Hz), 4.787 (1H, dd, J = 9.2, 2.8 Hz), 5.379 (1H, m), 5.674 (1H, dd, J = 9.2, 6 Hz), 6.287 (1H, s), 6.422 (1H, dd, J = 11.2, 4 Hz), 6.678 (1H, d, J = 1.6 Hz), 6.691 (1H, d, J = 8.8 Hz) and 6.822 (1H, d, J = 1.6 Hz). HRMS calcd for $C_{35}H_{48}ClN_3O_{10}S_2Na$ $(M + Na)^+$, 792.2367; found, 792.2350.

6a. ^{1}H NMR δ 0.861 (3H, s), 1.273 (1H, m), 1.275 (3H, d, J = 6.4 Hz), 1.428−1.478 (2H, m), 1.519 (3H, d, J = 7.6 Hz), 1.689 (3H, s), 1.765 (1H, d, J = 13.6 Hz), 2.214 (1H, dd, J = 11.2, 3.2 Hz), 2.487 (3H, s), 2.667 (1H, dd, J = 12, 2.4 Hz), 2.856 (1H, d, J = 9.6 Hz), 3.114 (3H, s), 3.168 (3H, s), 3.203 (1H, d, J = 13.2 Hz), 3.340 (3H, s), 3.458 (1H, d, J = 9.2 Hz), 3.508 (1H, d, J = 12.8 Hz), 3.636 (2H, J = 6 Hz), 3.995 (3H, s), 4.293 (1H, t), 4.888 (1H, dd, J = 8.8, 3.2 Hz), 5.126 (1H, m), 5.869 (1H, dd, J = 9.6, 6 Hz), 6.230 (1H, d, J = 10.8 Hz), 6.331 (1H, s), 6.423 (1H, dd, J = 11.2, 4 Hz), 6.801 (1H, d, J = 1.2 Hz) and 6.852 (1H, d, J = 1.6 Hz). HRMS calcd for $C_{35}H_{48}ClN_3O_{10}S_2Na$ $(M + Na)^+$, 792.2367; found, 792.2350.

***N*$^{2'}$-Deacetyl-*N*$^{2'}$-(3-methyldithio-1-oxopropyl)-maytansine (DM1SMe, 2b) and Its D-Alanyl Isomer D-DM1SMe (6b).** Maytansinol (**4**) was reacted with *N*-methyl-*N*-[(2-methyldithio)-1-oxopropyl]-L-alanine (**5b**) as described above. Purification by column chromatography over silica gel, eluting with a mixture of dichloromethane/ethyl acetate/methanol to give a mixture of DM1SMe (**2b**) and the D-aminoacyl isomer D-DM1SMe (**6b**). The two diastereomers were separated by HPLC on a Kromasil cyano preparative HPLC column (250 mm × 50 mm, 10 micron particle size). The column was equilibrated in a mixture of hexanes/2-propanol/ethyl acetate (17:2:6, v/v/v) at a flow rate of 150 mL/min. Under these conditions, the desired L-DM1SMe (**2b**) had a retention time of 42 min, whereas the D-DM1SMe isomer (**6b**) elutes at 56 min. Optically pure products were obtained by this method (ee >99.9%). HPLC analysis using a Vydac analytical C-18 column (length: 100 mm, i.d.: 4.6 mm, particle size: 3 microns) at a flow rate of 1 mL/min, eluting with a gradient of water and acetonitrile (0−3 min, 35% CH_3CN; 3−13 min, 35−65% CH_3CN). Under these conditions L-DM1SMe (**2b**) eluted with a retention time of 10.76 min.

DM1SMe (2b). White solid (32% yield); ^{1}H NMR ($CDCl_3$) δ 0.84 (3H, s), 1.11−1.23 (1H, m), 1.31 (3H, d, J = 6 Hz), 1.35 (3H, d, J = 7 Hz), 1.46−1.52 (1H, m), 1.68 (3H, s), 1.97 (1H, d, J = 9 Hz), 2.24 (1H, dd, J = 12, 15 Hz), 2.30 (3H, s), 2.65 (1H, dd, J = 12, 15 Hz), 2.73−2.86 (2H, m), 2.90 (3H, s), 2.92−3.03 (2H, m), 3.08 (1H, d, J = 9 Hz), 3.14 (1H, d, J = 12 Hz), 3.28 (3H, s), 3.39 (3H, s), 3.54 (1H, d, J = 9 Hz), 3.72 (1H, d, J = 13 Hz), 4.02 (3H, s), 4.31 (1H, t, J = 11 Hz), 4.82 (1H, dd, J = 3, 12 Hz), 5.45 (1H, q, J = 7 Hz), 5.69 (1H, dd, J = 9, 15 Hz), 6.25 (1H, s), 6.47 (1H, dd, J = 11, 15 Hz), 6.67 (1H, d, J = 1.5 Hz), 6.77 (1H, d, J = 11 Hz), 6.85 (1H, d, J = 1.5 Hz). HRMS calcd for $C_{36}H_{51}ClN_3O_{10}S_2$ $(M + H)^+$, 784.2704; found, 784.2693; extinction coefficient $\epsilon_{280\ nm}$ (ethanol) = 5545 M^{-1} cm^{-1}, $\epsilon_{252\ nm}$ = 25 700 M^{-1} cm^{-1}.

D-DM1SMe (6b). White solid (30% yield); mp 170−171 °C; ^{1}H NMR ($CDCl_3$) δ 0.85 (3H, s), 1.11−1.20 (1H, m 1.22−1.29 (3H, m), 1.49 (3H, d, J = 7.5 Hz), 1.69 (3H, s), 2.20 (1H, dd, J = 3, 14 Hz), 2.40 (3H, s), 2.65 (1H, dd, J = 12, 14 Hz), 2.79−2.84 (3H, m), 2.92−2.96 (2H, m), 3.04 (3H, s), 3.15 (3H, s), 3.33 (3H, s), 3.43 (1H, d, J = 9 Hz), 3.50 (1H, d, J = 12 Hz), 3.98 (3H, s), 4.28 (1H, m), 4.90 (1H, dd, J = 3, 12 Hz), 5.17 (1H, q, J = 7 Hz),

DAC EX. 2040 IPR2022-01531 Page 1258 of 1299

5.88 (1H, dd, J = 9 Hz), 6.22−6.26 (2H, m), 6.41 (1H, dd, J = 11, 15 Hz), 6.78 (1H, d, J = 1.6 Hz), 6.84 (1H, d, J = 1.6 Hz). HRMS calcd for $C_{36}H_{51}ClN_3O_{10}S_2$ $(M + Na)^+$, 806.2524; found, 806.2518.

N^2-Deacetyl-$N^{2'}$-[2-(phenydithio)-1-oxopropyl]maytansine (DMISPh, 2c) and Its D-Alanyl Isomer D-DM1SPh (6c). Maytansinol (**4**) was reacted with *N*-methyl-*N*-[(2-phenyldithio)-1-oxoproyl]-L-alanine (**5c**) as described above. The product was purified by preparative TLC of the residue on silica gel, and eluting twice with 5% MeOH/$CHCL_3$ gave two strongly UV absorbing bands with R_f = 0.5 and 0.6. The two products were isolated by extraction with ethyl acetate. The higher R_f band was found to be the D-aminoacyl ester **6c** of maytansinol, and the lower band was the L-aminoacyl ester **2c**. The products were separated and further purified by HPLC on a Waters Radialpak C-18 column, eluting at a flow rate of 1.5 mL/min with a linear gradient of acetonitrile/water (70−90% acetonitrile/10 min). Under these conditions, both isomers had an identical retention time of 6.0 min.

DM1SPh (2c). ^{1}H NMR ($CDCl_3$) δ 0.82 (3H, s), 1.11−1.25 (1H, m), 1.33 (3H, d, J = 3 Hz), 1.61 (3H, s), 1.63 (3H, d, J = 14 Hz), 2.19 (1H, dd, J = 3, 15 Hz), 2.61 (1H, dd, J = 12, 15 Hz), 2.78 (3H, s), 2.68−3.03 (2H, m), 3.07 (1H, d, J = 9 Hz), 3.20 (3H, s), 3.38 (3H, s), 3.53 (1H, d, J = 9 Hz), 3.63 (1H, d, J = 13 Hz), 3.68 (3H, s), 4.01 (3H, s), 4.30 (1H, t, J = 11 Hz), 4.79 (1H, dd, J = 3, 8 Hz), 5.43 (1H, q, J = 7 Hz), 5.68 (1H, dd, J = 9, 15 Hz), 6.23 (1H, s), 6.45 (1H, dd, J = 12, 15 Hz), 6.60 (1H, d, J = 1.5 Hz), 6.75 (1H, d, J = 12 Hz), 6.77 (1H, d, J = 1.5 Hz), 7.22−7.40 (5H, m). HRMS cacld for $C_{41}H_{52}ClN_3O_{10}S_2Na$ $(M + Na)^+$, 868.2680; found, 868.2670.

D-DM1SPh (6c). ^{1}H NMR ($CDCl_3$) δ 0.89 (3H, s), 1.31 (3H, d, J = 6.4 Hz), 1.48−1.53 (m, 1H), 1.51 (3H, d), 1.72 (3H, s), 2.10 (1 H, d, J = 6 Hz), 2.15 (1H, dd, J = 3, 15 Hz), 2.69 (1H, dd, J = 12, 15 Hz), 2.81−2.89 (2H, m), 2.96 (3H, s), 3.02 (1H, d, J = 7 Hz), 3.20 (3H, s), 3.36 (3H, s), 3.47 (1H, d, J = 9 Hz), 3.55 (1H, d, J = 13 Hz), 3.68 (3H, s), 4.04 (3H, s), 4.31 (1H, t, J = 11 Hz), 4.93 (1H, dd, J = 3, 12 Hz), 5.20 (1H, q, J = 7 Hz), 5.90 (1H, dd, J = 9, 15 Hz), 6.25 (1H, s), 6.27 (1H, d, J = 12 Hz), 6.45 (1H, dd, J = 12, 15 Hz), 6.83 (1H, d, J = 1.5 Hz, 6.89 (1H, d, J = 1.5 Hz), 7.27−7.49 (5H, m). HRMS cacld for $C_{41}H_{52}ClN_3O_{10}S_2Na$ $(M + Na)^+$, 868.2680; found, 868.2672.

N^2-Deacetyl-N^2-[3-(methyldithio)-1-oxobutyl]maytansine (D-M2′SMe, 2d). Maytansinol (**4**) was reacted with *N*-methyl-*N*-3-(methyldithio)-1-oxobutyl]-L-alanine (**5d**) as described above. The reaction mixture was purified by preparative TLC on silica gel, eluting twice with 7% MeOH in $CHCl_3$. Two new UV absorbing bands (R_f = 0.65, 0.75) were obtained. The products were isolated by extraction with ethyl acetate. The higher R_f band was determined to be the D-aminoacyl ester **6d** (31%), whereas the lower R_f band was the desired L-aminoacyl ester **2d** (44%). Both isomers were further purified by HPLC using a Waters Radialpak C-18 column, eluting at a flow rate of 2 mL/min with a linear gradient of acetonitrile/water (50−80% acetonitrile/10 min). Under these conditions, the D-aminoacyl ester had a retention time of 7.4 min, whereas the L-aminoacyl isomer had a retention time of 7.6 min. The diastereomeric purity of **2d** and **6d** were determined by HPLC analysis using a Kromasil cyano column (250 mm × 4.6 mm, 10 micron particle size) at a flow rate of 1.50 mL/min, eluting with an isocratic mixture of ethyl acetate/hexane/2-propanol (24:66:10/v/v). Under these conditions, **2d** eluted with a retention time of 11.96 min, and its D-alanyl **6d** isomer eluted with a retention time of 17.30 min.

2d. ^{1}H NMR ($CDCl_3$) δ 0.803 (3H, s), 1.265 (2H, m), 1.280 (3H, d, J = 2.4 Hz), 1.309 (3H, d, J = 2.4 Hz), 1.638 (1H, d, J = 13.6 Hz), 1.643 (3H, s), 1.760 (1H, m), 2.051 (2H, m), 2.179 (1H, dd, J = 11.2, 2.8 Hz), 2.318 (3H, s), 2.365−2.536 (2H, m), 2.611 (1H, dd, J = 12.4, 2 Hz), 2.719 (2H, m), 2.852 (3H, s), 3.033 (1H, d, J = 9.6 Hz), 3.110 (1H, d, J = 12.4 Hz), 3.219 (3H, s), 3.355 (3H, s), 3.498 (1H, d, J = 10.8 Hz), 3.657 (1H, d, J = 12.4 Hz), 3.983 (3H, s), 4.284 (1H, t), 4.872 (1H, dd, J = 8.8, 2.8 Hz), 5.660 (1H, dd, J = 8.8, 5.6 Hz), 6.197 (1H, s), 6.430 (1H, dd, J = 11.2, 4 Hz), 6.648 (1H, d, J = 2 Hz), 6.740 (1H, d, J = 11.6 Hz) and 6.820 (1H, d, J = 2 Hz). HRMS calcd for $C_{37}H_{52}ClN_3O_{10}S_2Na$ $(M + Na)^+$, 820.2680; found, 820.2667.

6d. ^{1}H NMR ($CDCl_3$) δ 0.874 (3H, s), 1.193−1.429 (3H, m), 1.290 (3H, d, J = 6.4 Hz), 1.314 (3H, d, J = 6.8 Hz), 1.696 (3H, s), 1.777 (1H, d, J = 13.6 Hz), 2.058 (2H, m), 2.209 (1H, dd, J = 11.2, 3.2 Hz), 2.420 (3H, s), 2.529 (2H, m), 2.662 (1H, dd, J = 12, 3.6 Hz), 2.727−2.801 (2H, m), 2.826 (1H, d, J = 9.6 Hz), 3.044 (3H, s), 3.167 (3H, s), 3.204 (1H, d, J = 11.2 Hz), 3.342 (3H, s), 3.439 (1H, d, J = 9.2 Hz), 3.514 (1H, d, J = 7.6 Hz), 3.999 (3H, s), 4.351 (1H, t), 4.933 (1H, dd, J = 8.8, 3.2 Hz), 5.082 (1H, m), 5.844 (1H, dd, J = 9.6, 5.6 Hz), 6.231 (1H, d, J = 8.8 Hz), 6.242 (1H, s), 6.434 (1H, dd, J = 11.2, 4.4 Hz), 6.799 (1H, d, J = 2 Hz) and 6.851 (1H, d, J = 2 Hz). HRMS calcd for $C_{37}H_{52}ClN_3O_{10}S_2Na$ $(M + Na)^+$, 820.2680; found, 820.2658.

$N^{2'}$-Deacetyl-$N^{2'}$-[4-(*R,S*)-(methyldithio)-1-oxopentyl]maytansine (DM3-SMe, 2f). Maytansinol (**4**) was reacted with *N*-methyl-*N*-[(4-*(R,S)*-methyldithio-1-oxopentyl)]-*S*-alanine (**5f**) as described above. The reaction mixture was purified by silica chromatography using a mixture of dichloromethane and methanol to remove unreacted maytansinol. The fractions containing the desired product were combined, and the solvent was removed under vacuum to give a mixture of the diastereomers **2f** and **6f.** The residue was purified on a 50 cm × 250 cm, 10 micron Diazem CN column using as mobile phase a 68:8:24 mixture of hexane, 2-propanol, and ethyl acetate. The flow rate was 118 mL/min. The desired product **2f** eluted with a retention time of 11 min, and the undesired diastereomer **6f** had a retention time of 19 min.

2f. White solid (36% yield). ^{1}H NMR ($CDCl_3$) δ 0.80 (3H, s), 1.19−1.23(1H,m), 1.28−1.36 (9H, m), 1.42−1.46(1H, m), 1.53−1.63 (2H, m), 1.64 (3H, s), 1.80−1.89 (1H, m), 1.90−2.09 (1H, m), 2.18 (1H, dd, J = 3 and 14 Hz), 2.32 (3H, s), 2.33−2.42 (1H, m), 2.49−2.62 (2H, m), 2.88 (3H, s), 3.04 (1H, d, J = 9 Hz), 3.11 (1H,d,J = 11 Hz), 3.23 (3H,s), 3.35 (3H,s), 3.49 (1H, d, J = 9 Hz), 3.63 (1H, d, J = 12 Hz), 3.98 (3H, s), 4.27 (1H, t, J = 10 Hz), 4.79 (1H, dd, J = 3 and 12 Hz), 5.41 (1H, q, J = 7 Hz), 5.66 (1H, dd J = 9 and 15 Hz), 6.21 (1H, s), 6.42 (1H, dd, J = 11 and 15 Hz), 6.65 (1H, d, J = 1.5 Hz), 6.73 (1H, d, J = 11 Hz), 6.81 (1H, d, J = 1.5 Hz). HRMS calcd for $C_{38}H_{54}ClN_3O_{10}S_2Na$ $(M + Na)^+$, 834.2837; found, 834.2819.

6f. White solid (30% yield) ^{1}H NMR δ 0.869 (3H, s), 1.200−1.315 (2H, m), 1.283 (3H, d, J = 6.8 Hz), 1.373 (3H, dd, J = 5.6, 1.2 Hz), 1.498 (3H, d, J = 7.6 Hz), 1.600 (1H, d, J = 14.4 Hz), 1.691 (3H, s), 1.772 (1H, m), 1.929 (2H, m), 2.203 (1H, dd, J = 11.6, 3.2 Hz), 2.421 (3H, s), 2.518 (2H, m), 2.654 (1H, t), 2.814 (1H, dd, J = 8, 1.6 Hz), 2.902 (1H, m), 3.038 (3H, d, J = 3.2 Hz), 3.164 (3H, s), 3.200 (1H, d, J = 13.2 Hz), 3.339 (3H, s), 3.436 (1H, d, J = 8 Hz), 3.507 (1H, d, J = 12.8 Hz), 3.996 (3H, s), 4.309 (1H, t), 4.936 (1H, dd, J = 4.8, 4 Hz), 5.093 (1H, m), 5.851 (1H, m), 6.233 (1H, d, J = 11.2 Hz), 6.269 (1H, s), 6.429 (1H, dd, J = 10.8, 4.4 Hz), 6.792 (1H, s) and 6.848 (1H, s). HRMS calcd for $C_{38}H_{54}ClN_3O_{10}S_2Na$ $(M + Na)^+$, 834.2837; found, 834.2830.

$N^{2'}$-Deacetyl-$N^{2'}$-[4-(*S*)-(methyldithio)-1-oxopentyl]maytansine (2g). Maytansinol (**4**) was coupled with *N*-methyl-*N*-[(4-*(S)*-methyldithio)-1-oxopentyl]-*S*-alanine (**5g**) using DCC and zinc chloride in dichloromethane as described above for the synthesis of **2f.** A mixture of 2 diastereomers bearing the *N*-methyl-L-alanyl moiety (**2g**, *S,S*) and the *N*-methyl-D-alanyl moiety (**6g**, *R,S*) were obtained. The diastereomers were separated by HPLC on a Kromasil cyano column (4.6 mm × 250 mm), using an isocratic elution at a flow arte of 1 mL/min with hexane/ethyl acetate/2-propanol (68:24:8, v/v/v). Under these conditions, the isomer **2g** (*S,S*) eluted at 24.5 min. The peak for the other isomer **6g** (*R,S*) was well separated and eluted at 34.6 min.

2g. ^{1}H NMR ($CDCl_3$) δ 0.798 (3H, s), 1.197−1.267 (2H, m), 1.292 (3H, d, J = 7.2 Hz), 1.283 (3H, d, J = 2 Hz), 1.300 (3H, d, J = 1.2 Hz), 1.462 (1H, m), 1.536 (1H, d, J = 8 Hz), 1.640 (3H, s), 1.834−2.020 (2H, m), 2.176 (1H, dd, J = 11.6, 2.8 Hz), 2.326 (3H, s), 2.373−2.522 (2H, m), 2.603 (1H, dd, J = 12.4, 2 Hz), 2.847 (3H, s), 2.871−2.903 (1H, m), 3.028 (1H, d, J = 9.6 Hz), 3.108 (1H, d, J = 12.4 Hz), 3.223 (3H, s), 3.351 (3H, s), 3.499 (1H, d, J = 9.2 Hz), 3.639 (1H, d, J = 12.8 Hz), 3.983 (3H, s),

DAC EX. 2040 IPR2022-01531 Page 1259 of 1299

4.279 (1H, t), 4.627 (1H, dd, J = 8.8, 3.2 Hz), 5.388 (1H, m), 5.658 (1H, dd, J = 8.8, 6.4 Hz), 6.207 (1H, s), 6.426 (1H, dd, J = 11.2, 4.4 Hz), 6.639 (1H, d, J = 1.6 Hz), 6.737 (1H, d, J = 11.2 Hz) and 6.818 (1H, d, J = 2 Hz). MS: m/z 834.2 $(M + Na)^+$.

6g. ^{1}H NMR ($CDCl_3$) δ 0.867 (3H, s), 1.251−1.383 (3H, m), 1.284 (3H, d, J = 6 Hz), 1.374 (3H, d, J = 6.8 Hz), 1.498 (3H, d, J = 7.6 Hz), 1.691 (3H, s), 1.763 (1H, d, J = 14 Hz), 1.932 (2H, m), 2.206 (1H, dd, J = 11.2, 3.2 Hz), 2.421 (3H, s), 2.518 (2H, m), 2.653 (1H, dd, J = 12.4, 2.4 Hz), 2.817 (1H, d, J = 9.6 Hz), 2.911 (1H, m), 3.034 (3H, s), 3.165 (3H, s), 3.200 (1H, d, J = 13.2 Hz), 3.339 (3H, s), 3.438 (1H, d, J = 9.2 Hz), 3.508 (1H, d, J = 12.8 Hz), 3.996 (3H, s), 4.311 (1H, t), 4.929 (1H, dd, J = 8.8, 3.2 Hz), 5.095 (1H, m), 5.856 (1H, dd, J = 9.2, 6 Hz), 6.236 (1H, d, J = 13.2 Hz), 6.253 (1H, s), 6.428 (1H, dd, J = 11.2, 4 Hz), 6.794 (1H, d, J = 1.6 Hz) and 6.849 (1H, d, J = 1.2 Hz). MS: m/z 834.2 $(M + Na)^+$.

***N*$^{2'}$-Deacetyl-*N*$^{2'}$-(4-*(R)*-methyldithio-1-oxopentyl)maytansine (2h).** Maytansinol (**4**) was coupled with *N*-methyl-*N*-[(4-*(R)*-methyldithio)-1-oxopentyl]-*S*-alanine (**5h**) using DCC and zinc chloride in dichloromethane as described above. A mixture of 2 diastereomers bearing the *N*-methyl-*S*-alanyl moiety (**2h**, *S,R*) and the *N*-methyl-*R*-alanyl moiety (**6h**, *R,R*) were obtained. The diastereomers were separated by HPLC on a Kromasil cyano column (4.6 mm × 250 mm), using an isocratic elution at a flow rate of 1 mL/min, with hexane/ethyl acetate/2-propanol (68:24:8, v/v/v). Under these conditions, isomer **2h** (*S.R)* eluted at 23.9 min. The peak for the other isomer **6h** (*R,R*) was well separated and eluted at 33.7 min.

2h. ^{1}H NMR ($CDCl_3$) δ 0.796 (3H, s), 1.230 (2H, m), 1.290 (3H, d, J = 5.6 Hz), 1.297 (3H, d, J = 1.2 Hz), 1.305 (3H, d, J = 6.4 Hz), 1.447 (1H, m), 1.575 (1H, d, J = 13.6 Hz), 1.637 (3H, s), 1.815−2.002 (2H, m), 2.170 (1H, dd, J = 11.2, 3.2 Hz), 2.303 (3H, s), 2.357−2.547 (2H, m), 2.606 (1H, dd, J = 12, 2.4 Hz), 2.846 (3H, s), 3.027 (1H, d, J = 9.6 Hz), 3.108 (1H, d, J = 12.8 Hz), 3.215 (3H, s), 3.350 (3H, s), 3.494 (1H, d, J = 9.6 Hz), 3.648 (1H, d, J = 12.8 Hz), 3.978 (3H, s), 4.273 (1H, t), 4.775 (1H, dd, J = 9.2, 2.8 Hz), 5.384 (1H, m), 5.665 (1H, m), 6.227 (1H, s), 6.634 (1H, d, J = 1.6 Hz), 6.734 (1H, d, J = 11.2 Hz) and 6.816 (1H, d, J = 1.6 Hz). MS: m/z 834.2 $(M + Na)^+$.

6h. ^{1}H NMR ($CDCl_3$) δ 0.867 (3H, s), 1.280 (3H, d, J = 6.4 Hz), 1.359 (2H, m), 1.384 (3H, d, J = 6.4 Hz), 1.446 (1H, m), 1.495 (3H, d, J = 7.2 Hz), 1.689 (3H, s), 1.780 (1H, d, J = 13.4 Hz), 1.886−1.964 (2H, m), 2.200 (1H, dd, J = 11.6, 2.8 Hz), 2.419 (3H, s), 2.470−2.564 (2H, m), 2.651 (1H, dd, J = 12, 2.4 Hz), 2.808 (1H, d, J = 9.6 Hz), 2.893 (1H, m), 3.040 (3H, s), 3.161 (3H, s), 3.196 (1H, d, J = 13.2 Hz), 3.338 (3H, s), 3.432 (1H, d, J = 9.2 Hz), 3.504 (1H, d, J = 12.8 Hz), 3.993 (3H, s), 4.303 (1H, t), 4.938 (1H, dd, J = 8.8, 3.2 Hz), 5.091 (1H, m), 5.842 (1H, m), 6.234 (1H, d, J = 12.8 Hz), 6.250 (1H, s), 6.428 (1H, dd, J = 10.8, 4.4 Hz), 6.788 (1H, d, J = 1.6 Hz) and 6.847 (1H, d, J = 1.6 Hz). MS: m/z 834.2 $(M + Na)^+$.

***N*$^{2'}$-Deacetyl-*N*$^{2'}$-(4-methyl-4-(methyldithio)-1-oxopentyl)maytansine (DM4-SMe, 2i) and Its D-Alanyl Isomer D-DM4SMe.** Maytansinol (**4**) was reacted with *N*-methyl-*N*-[4-methyl-4-(methyldithio)-1-oxopentyl]-L-alanine (**5i**), as described above. The reaction mixture was purified by silica chromatography using a mixture of dichloromethane and methanol to remove the unreacted maytansinol. The fractions containing the desired product were combined, and the solvent was removed under vacuum to give a mixture of diastereomers **2i** and **6i**. The residue was taken up in a minimum volume of ethyl acetate and purified on a 50 cm × 250 cm, 10 micron Diazem CN column using as mobile phase a mixture of hexane, 2-propanol, and ethyl acetate at a ratio of 68:8:24. The flow rate was 118 mL/min. Under these conditions, the desired product **2i** eluted with a retention time of 11 min, and the undesired diastereomer **6i** had a retention time of 19 min.

2i (DM4SMe). White solid (36% yield); ^{1}H NMR ($CDCl_3$) δ 0.80 (3H, s), 1.28−1.36 (13H, m), 1.42−1.46(2H, m), 1.53−1.63 (2H, m), 1.64 (3H, s), 1.75−1.85 (1H, m), 1.90−2.10 (1H, m), 2.18 (1H, dd, J = 3 and 14 Hz), 2.31 (3H,s), 2.40−2.49 (1H, m), 2.50−2.65 (1H, m), 2.85 (3H, s), 3.04 (1H, d, J = 9 Hz), 3.11 (1H,d,J = 11 Hz), 3.23 (3H,s), 3.35 (3H,s), 3.49 (1H, d, J = 9 Hz), 3.63 (1H, d, J = 12 Hz), 3.98 (3H, s), 4.27 (1H, t, J = 10 Hz), 4.79 (1H, dd, J = 3 and 12 Hz), 5.41 (1H, q, J = 7 Hz), 5.66 (1H, dd J = 9 and 15 Hz), 6.21 (1H, s), 6.42 (1H, dd, J = 11 and 15 Hz), 6.65 (1H, d, J = 1.5 Hz), 6.73 (1H, d, J = 11 Hz), 6.81 (1H, d, J = 1.5 Hz). HRMS $(M + H)^+$ calcd for $C_{39}H_{57}ClN_3O_{10}S_2$. $(M + H)^+$, 826.3174; found, 826.3150; extinction coefficient (ethanol) $\epsilon_{280\ nm}$ = 5140 M^{-1} cm^{-1}, $\epsilon_{252\ nm}$ = 24 700 M^{-1} cm^{-1}.

6i (D-DM4SMe). White solid; mp 165−167 °C; ^{1}H NMR ($CDCl_3$) δ 0.869 (3H, s), 1.265 (3H, d, J = 7.2 Hz), 1.327 (6H, s), 1.495 (3H, d, J = 7.6 Hz), 1.590 (2H, m), 1.690 (3H, s), 1.785 (1H, m), 1.915 (2H, m), 2.201 (1H, dd, J = 17.6 and 11.6 Hz), 2.422 (3H, s), 2.452 (2H, m), 2.646 (1H, d, J = 26.8 and 2.4 Hz), 2.800 (1H, d, J = 9.6 Hz), 3.041 (3H, s) 3.165 (3H, s), 3.195 (1H, d, J = 13.2 Hz), 3.340 (3H, s), 3.431 (1H, d, J = 9.2 Hz), 3.508 (1H, d, J = 12.8 Hz), 3.995 (3H, s), 4.313 (1H, t), 4.960 (1H, dd, J = 15.2 and 8.8 Hz), 5.117 (1H, q, J = 7.6 Hz), 5.838 (1H, dd, J = 24.4 and 6 Hz), 6.233 (1H, d, J = 10 Hz), 6.246 (1H, s), 6.428 (1H, dd, J = 26 and 4 Hz), 6.785 (1H, d, J = 1.6) and 6.847 (1H, d, J = 1.6 Hz). HRMS calcd $C_{39}H_{56}ClN_3O_{10}S_2Na$ $(M + Na)^+$, 848.2993; found, 848.2975.

***N*$^{2'}$-Deacetyl-*N*^{2}-(3-mercapto-1-oxopropyl)-maytansine (DM1, 25a).** A solution of *N*$^{2'}$-deacetyl-*N*$^{2'}$-(3-methyldithio-1-oxopropyl)-maytansine (**2b**) (1.95 g, 2.5 mmol) in a mixture of ethyl acetate (140 mL) and methanol (210 mL) was stirred at room temperature under an argon atmosphere and treated with a solution of dithiothreitol (0.95 g, 6.2 mmol) in 0.05 M potassium phosphate buffer (140 mL) at pH 7.5 containing 2 mM ethylenediaminetetraacetic acid (EDTA). The progress of the reaction was monitored by HPLC and was complete in three hours. The reaction mixture was treated with a solution of 0.2 M potassium phosphate buffer (250 mL) at pH 6.0 containing 2 mM EDTA and then extracted with ethyl acetate (3 × 600 mL). The organic layers were combined, washed with brine (100 mL), and then dried over sodium sulfate. Evaporation of the solvent gave a residue of crude thiol-containing maytansinoid **25a**. The crude residue was purified by HPLC using a preparative Diazem cyano HPLC column (250 mm × 50 mm, 10 micron particle size) that was equilibrated in a mixture of hexanes/2-propanol/ethyl acetate (78.0:5.5:16.5, v/v/v) and run at a flow rate of 150 mL/min. The desired product **25a** eluted as a peak centered at 16 min. The fractions containing the product were evaporated to give **25a** as a white solid (76% yield); mp 190−192 °C (dec); ^{1}H NMR ($CDCl_3$) δ 0.84 (3H, s), 1.33 (3H, d, J = 5 Hz), 1.35 (3H, d, J = 5 Hz), 1.60 (3H, s), 1.68 (3H, s), 2.22 (1H, dd, J = 3 and 14 Hz, 2.60−2.82 (2H, m), 2.88 (3H, s), 3.08−3.20 (2H, m), 3.25 (3H, s), 3.39 (3H, s), 3.55 (1H, d, J = 9 Hz), 3.71 (1H, d, J = 12 Hz), 4.02 (3H, s), 4.32 (1H, t, J = 10 Hz), 4.81 (1H, dd, J = 3 and 12 Hz), 5.45 (1H, q, J = 7 Hz), 5.67 (1H, dd J = 9 and 15 Hz), 6.25 (1H, s), 6.47 (1H, dd, J = 11 and 15 Hz), 6.70 (1H, d, J = 1.5 Hz), 6.75 (1H, d, J = 11 Hz), 6.86 (1H, d, J = 1.5 Hz). HRMS calcd for $C_{35}H_{49}ClN_3O_{10}S$ $(M + H)^+$ 738.2827; found, 738.2820; $[\alpha]^{25}_D$ = −113.2, (c = 0.306, $CHCl_3$); extinction coefficient (methanol): $\epsilon_{280\ nm}$ = 5422 M^{-1} cm^{-1}, $\epsilon_{252\ nm}$ = 25 800 M^{-1} cm^{-1}.

HPLC Analysis. HPLC analysis was performed using a Waters symmetry shield analytical C-8 column (length: 150 mm, i.d.: 3.9 mm, particle size: 5 microns) operating at 40 °C and at a flow rate of 1 mL/min, eluting with a linear gradient of water (containing 0.05% TFA) and acetonitrile (containing 0.05% TFA) from 35% to 45% acetonitrile over 30 min. Under these conditions, DM1 (**25a**) eluted with a retention time of 12.13 min. The diastereomeric purity of **25a** was determined by HPLC analysis using a Diazem cyano column (length: 250 mm, i.d.: 4.6 mm, particle size: 5 microns) at a flow rate of 1 mL/min, eluting with a isocratic mixture of ethyl acetate/hexane/2-propanol (24:68:8 v/v respectively). Under these conditions, **25a** eluted with a retention time of 13.70 min. There was no detectable signal for the D-isomer **26a**, which elutes at 17.3 min.

D-DM1 (26a). A solution of D-DM1SMe (**6b**) (20 mg, 0.027 mmol) in a mixture of ethyl acetate (0.5 mL) and methanol (1.0 mL) was stirred at room temperature under an argon atmosphere

DAC EX. 2040 IPR2022-01531 Page 1260 of 1299

and treated with a solution of dithiothreitol (6.1 mg, 0.039 mmol) in 0.05 M potassium phosphate buffer (0.5 mL) at pH 7.5 containing 2 mM ethylenediamine-tetraacetic acid (EDTA). The progress of the reaction was monitored by HPLC and was complete in 2 h. The reaction mixture was then extracted with ethyl acetate (3 × 1 mL). The organic layers were combined and dried over sodium sulfate. Evaporation of the solvent gave a residue of crude thiol-containing maytansinoid **26a**. The crude residue was purified by HPLC using a semipreparative Diazem cyano HPLC column (250 mm × 10 mm, 10 micron particle size) that was equilibrated in a mixture of hexanes/2-propanol/ethyl acetate (65:10:25, v/v/v) and run at an initial flow rate of 2 mL/min. After 2 min, the flow rate was increased to 4.5 mL/min for the remainder of the run. The desired product eluted as a peak centered at 15 min. The fractions containing the product were evaporated to give **26a** as a white solid; mp 187−192 °C (dec); ^{1}H NMR ($CDCl_3$) δ 0.85 (3H, s), 1.26−1.29 (4H, m), 1.50 (3H, d, J = 7.6 Hz), 1.69 (3H, s), 2.21 (1H, dd, J = 3 and 14 Hz), 2.65 (1H, dd, J = 12 Hz and 14 Hz), 2.79−2.84 (3H, m), 2.92−2.96 (6H, m), 3.03 (3H, s), 3.16 (3H, s), 3.34 (3H, s), 3.45 (1H, d, J = 9 Hz), 3.51 (1H, d, J = 12 Hz), 4.00 (3H, s), 4.04 91H, m), 4.29 (1H, m), 4.88 (1H, dd, J = 3 and 12 Hz), 5.20 (1H, q, J = 7 Hz), 5.90 (1H, dd, J = 9 and 15 Hz), 6.23−6.27 (2H, m), 6.43 (1H, dd, J = 11 and 15 Hz), 6.80 (1H, d, J = 1.6 Hz), 6.85 (1H, d, J = 1.6 Hz). HRMS calcd for $C_{35}H_{48}ClN_3O_{10}$SNa *m/z*: 760.2647 (M + H)$^+$; found, 760.2637; $[\alpha]^{25}_D$ = −135.0, (c = 0.294, $CHCl_3$). HPLC analysis: The diastereomeric purity of **26a** was determined as described above for **26a**. The isomer **26a** eluted with a retention time of 17.25 min. There was no detectable signal for the L-isomer, which elutes at 13.7 min,

***N*$^{2'}$-Deacetyl-*N*$^{2'}$-(4-mercapto-1-oxopentyl)maytansine (DM3, 25b).** DM3-SMe (**2f**, 12 mg, 0.015 mmol) was dissolved in 1.0 mL of a 1:1 mixture of ethyl acetate and methanol. A solution of dithiothreitol (18 mg, 0.117 mmol) in 0.50 mL of 50 mM phosphate buffer at pH 7.5 was then added. The reaction solution was magnetically stirred under an argon atmosphere for 3 h, then 1 mL of 200 mM phosphate buffer at pH 6.0 was added, and the mixture was extracted three times with 2 mL portions of ethyl acetate. The organic layers were combined and washed with 1 mL of saturated sodium chloride solution and then dried over 1 g of anhydrous sodium sulfate. The solvent was removed under vacuum, and the residue was taken up in a minimum of ethyl acetate and purified on a 50 cm × 250 cm, 10 micron Diazem CN column using as mobile phase a 70:8:22 mixture of hexane, 2-propanol, and ethyl acetate. The flow rate was 22 mL/min. The desired product eluted with a retention time of 10 min. The fractions containing the pure product were combined, and the solvent was removed under vacuum to give 11 mg of product **25b** (97% yield). ^{1}H NMR ($CDCl_3$) δ 0.80 (3H, s), 1.19−1.23(1H,m), 1.28−1.36 (9H, m), 1.42−1.46-(1H, m), 1.53−1.63 (2H, m), 1.64 (3H, s), 1.80−1.89 (1H, m), 1.90−2.09 (1H, m), 2.18 (1H, dd, J = 3 and 14 Hz), 2.33−2.42 (1H, m), 2.49- -2.62 (2H, m), 2.88 (3H, s), 3.04 (1H, d, J = 9 Hz), 3.11 (1H,d,J = 11 Hz), 3.23 (3H,s), 3.35 (3H,s), 3.49 (1H, d, J = 9 Hz), 3.63 (1H, d, J = 12 Hz), 3.98 (3H, s), 4.27 (1H, t, J = 10 Hz), 4.79 (1H, dd, J = 3 and 12 Hz), 5.41 (1H, q, J = 7 Hz), 5.66 (1H, dd J = 9 and 15 Hz), 6.21 (1H, s), 6.42 (1H, dd, J = 11 and 15 Hz), 6.65 (1H, d, J = 1.5 Hz), 6.73 (1H, d, J = 11 Hz), 6.81 (1H, d, J = 1.5 Hz). HRMS calcd for $C_{37}H_{52}ClN_3O_{10}$SNa (M + Na)$^+$, 788.2960; found, 788.2957.

***N*$^{2'}$-Deacetyl-*N*$^{2'}$-(4-mercapto-4-methyl-1-oxopentyl)maytansine (DM4, 25c).** DM4SMe (**2i**) (12 mg, 0.015 mmol) was dissolved in 1.0 mL of 1:1 ethyl acetate/methanol. A solution of dithiothreitol (18 mg, 0.117 mmol) in 0.50 mL of 50 mM phosphate buffer at pH 7.5 was then added. The solution was magnetically stirred under an argon atmosphere for 3 h, then 1 mL of 200 mM phosphate buffer at pH 6.0 was added, and the mixture was extracted three times with 2 mL portions of ethyl acetate. The organic layers were combined and washed with 1 mL of saturated sodium chloride solution and then dried over 1 g of anhydrous sodium sulfate. The solvent was removed under vacuum, and the residue was taken up in a minimum of ethyl acetate and purified on a 50 cm × 250 cm, 10 micron Diazem CN column using as mobile phase a mixture of hexane, 2-propanol, and ethyl acetate at a ratio of 70:8:22. The flow rate was 22 mL/min. The desired product eluted with a retention time of 10 min. The fractions containing product were combined, and the solvent was removed under vacuum to give 11 mg of **25c** (97% yield) as a white solid; mp 185−187 °C (dec); ^{1}H NMR ($CDCl_3$) δ 0.80 (3H, s), 1.19−1.23(1H,m), 1.28−1.36 (12H, m), 1.42−1.46(2H, m), 1.53−1.63 (2H, m), 1.64 (3H, s), 1.75−1.85 (1H, m), 1.90−2.10 (1H, m), 2.18 (1H, dd, J = 3 and 14 Hz), 2.40−2.49 (1H, m), 2.50−2.65 (2H, m), 2.88 (3H, s), 3.04 (1H, d, J = 9 Hz), 3.11 (1H,d,J = 11 Hz), 3.23 (3H,s), 3.35 (3H,s), 3.49 (1H, d, J = 9 Hz), 3.63 (1H, d, J = 12 Hz), 3.98 (3H, s), 4.27 (1H, t, J = 10 Hz), 4.79 (1H, dd, J = 3 and 12 Hz), 5.41 (1H, q, J = 7 Hz), 5.66 (1H, dd J = 9 and 15 Hz), 6.21 (1H, s), 6.42 (1H, dd, J = 11 and 15 Hz), 6.65 (1H, d, J = 1.5 Hz), 6.73 (1H, d, J = 11 Hz), 6.81 (1H, d, J = 1.5 Hz). HRMS calcd for $C_{38}H_{54}ClN_3O_{10}$SNa (M + Na)$^+$, 802.3101; found, 802.3116. $[\alpha]^{25}_D$ = −106.7, (c = 0.057, $CHCl_3$), extinction coefficient (ethanol): $\epsilon_{280\ nm}$ = 5180 M^{-1} cm^{-1}, $\epsilon_{252\ nm}$ = 26 200 M^{-1} cm^{-1}. HPLC analysis: purity was determined by HPLC analysis using a Vydac analytical C-18 column (250 mm × 4.6 mm, 3 micron particle size) at a flow rate of 1.00 mL/min in a gradient of water and acetonitrile, eluting with 37−58% acetonitrile over 25 min. Under these conditions L-DM4 (**25c**) eluted with a retention time of 11.8 min. The purity of L-DM4 was 98.8%. The diastereomeric purity of **25c** was determined by HPLC analysis using a Diazem cyano column (50 mm × 4.6 mm, 5 micron particle size) at a flow rate of 1.00 mL/min, eluting with a isocratic mixture of ethyl acetate/hexane/2-propanol (20:75:5 v/v/v). Under these conditions, **25c** eluted with a retention time of 4.52 min. There was no detectable signal for the D-alanyl isomer, which elutes at 5.42 min, indicating that **25c** was a diastereomerically pure compound.

D-DM4 (26c). A solution of D-DM4SMe (**6i**) (40.0 mg, 0.048 mmol) in a mixture of ethyl acetate (0.2 mL) and methanol (0.5 mL) was stirred at room temperature under an argon atmosphere and treated with a 0.50 mL solution containing dithiothreitol (59.7 mg, 0.387 mmol) in 0.050 M potassium phosphate buffer (0.5 mL) at pH 7.5 and 2 mM ethylenediamine-tetraacetic acid (EDTA). The progress of the reaction was monitored by HPLC and was complete after stirring overnight. The reaction mixture was treated 0.05 M potassium phosphate buffer (1.0 mL) at pH 6.0 containing 2 mM EDTA, and the product was extracted with ethyl acetate (3 × 1 mL). The organic layers were combined and dried over sodium sulfate. Evaporation of the solvent gave a residue of crude thiol-containing maytansinoid **26c**. The crude residue was purified by HPLC using a preparative Diazem cyano HPLC column (250 mm × 10 mm, 10 micron particle size) that was equilibrated in a mixture of hexanes/2-propanol/ethyl acetate (65:10:25, v/v/v) and run at an initial flow rate of 118 mL/min. The desired product **26c** eluted as a peak centered at 12.0 min. The fractions containing the product were evaporated to give **26c** as a white solid.

^{1}H NMR ($CDCl_3$) δ 0.866 (3H, s), 1.282 (3H, d, J = 6.4 Hz), 1.409 (6H, s), 1.500 (3H, d, J = 6.4 Hz), 1.625 (2H, m), 1.689 (3H, s), 1.766 (1H, m), 1.875 (2H, m), 2.205 (1H, dd, J = 17.6 and 11.2 Hz), 2.578 (2H, m), 2.646 (1H, dd, J = 26.8 and 2.8 Hz), 2.811 (1H, d, J = 9.6 Hz), 3.168 (3H, s), 3.196 (1H, d, J = 12.4 Hz), 3.341 (3H, s), 3.431 (1H, d, J = 9.2 Hz), 3.511 (1H, d, J = 13.2 Hz), 3.995 (3H, s), 4.300 (1H, t), 4.946 (1H, dd, J = 15.2 and 8.8 Hz), 5.156 (1H, q, J = 7.6 Hz), 5.836 (1H, dd, J = 24.4 and 6 Hz), 6.243 (1H, d, J = 10.4 Hz), 6.246 (1H, s),6.426 (1H, dd, J = 26.4 and 4 Hz), 6.790 (1H, d, J = 1.6 Hz) and 6.848 (1H, d, J = 1.6 Hz). HRMS calcd for $C_{38}H_{54}ClN_3O_{10}$SNa (M + Na)$^+$, 802.3101; found, 802.3099; $[\alpha]^{25}_D$ = −90.4, (c = 0.052, $CHCl_3$). HPLC analysis: purity was determined by HPLC analysis using a Vydac analytical C-18 column (250 mm × 4.6 mm, 3 micron particle size) at a flow rate of 1.00 mL/min with a gradient of water and acetonitrile, eluting with 20−50% acetonitrile over 30 min. Under these conditions, D-DM4 (**26c**) eluted with a retention time of 17.85 min. The purity of **26c** was 97.8%. The diastereomeric purity of **26c** was determined as described above for DM4 (**25c**). The isomer eluted with a retention time of 5.42 min. There was no

DAC EX. 2040 IPR2022-01531 Page 1261 of 1299

detectable signal for the **25c** isomer, which elutes at 4.52 min, indicating that **26c** was a diastereomerically pure compound.

Synthesis of $N^{2'}$-Deacetyl-$N^{2'}$-[3-(3-carboxy-1-methyl-propyldithio)-1-oxopropyl]-maytansine (DM1-TPA, 2j). A solution of 4-(2-pyridyldithio)pentanoic acid (24 mg, 0.10 mmol) and DM1 (**25a**, 30 mg, 0.041 mmol) in glass distilled methanol (5 mL) was vigorously stirred, and 3 mL of an aqueous buffer (200 mM KH_2PO_4, 2 mM EDTA at pH 7.6) was added dropwise. The reaction was stirred overnight, and the product was purified by HPLC using a Vydac C-18 column (10 × 250 mm) operating at 30 °C and a flow rate of 4.75 mL/min, eluting with a linear gradient of acetonitrile (15% to 85% over 30 min) in 40 mM ammonium acetate buffer at pH 7.2. DM1-TPA (**2j**) eluted with a retention time of 12 min. The product was collected as the ammonium salt was taken up in ethyl acetate (15 mL). The solution was washed with 1 M HCl (4 mL) followed by saturated sodium chloride (3 mL). The organic layer was dried over anhydrous sodium sulfate, and the solvent was removed under vacuum to give 15 mg (37% yield) of product **2j**. ^{1}H NMR (400 MHz, $CDCl_3$) δ 0.81 (3H, s), 1.21−1.37 (11H, m), 1.44−1.48 (1H, m), 1.61 (1H, m), 1.65 (3H, s), 1.77−1.93 (3H, m), 2.20 (1H, d, J = 12 Hz), 2.39−2.49 (2H, m), 2.60 (1H, d, J = 12 Hz), 2.70 (1H, t, J = 9 Hz), 2.78−3.00 (7H, m), 3.12 (1H, d, J = 14 Hz), 3.22 (3H, s), 3.36 (3H, s), 3.48 (1H, d, J = 9 Hz), 3.64 (1H, d, J = 12 Hz), 3.98 (3H, s), 4.31 (1H, t, J = 10 Hz), 4.82 (1H, d, J = 12 Hz), 5.15−5.20 (1H, m), 5.63 (1H, dd J = 9 and 15 Hz), 6.39−6.45 (2H, m), 6.59 (1H, t, J = 12 Hz), 6.67 (1H, d, J = 9 Hz), 6.82 (1H, s). HRMS calcd for $C_{40}H_{56}ClN_3O_{12}S_2Na$ $(M + Na)^+$, 892.2891; found, 892.2955. HPLC analysis was performed using a Vydac analytical C-18 column (length: 100 mm, i.d.: 4.6 mm, particle size: 3 microns) at a flow rate of 1 mL/min, eluting with a gradient of water and acetonitrile as follows: 0 min: 5% CH_3CN, 5 min: 5% CH_3CN, 5−65 min: 5−95% CH_3CN. Under these conditions DM1-TPA eluted with a retention time of 23.75 min.

Synthesis of $N^{2'}$-Deacetyl-$N^{2'}$-[4-methyl-4-(3-carboxy-propyldithio)-1-oxopentyl]-maytansine (DM4-TBA, 2k). A solution of 4-(2-pyridyldithio)butanoic acid (41.1 mg, 0.179 mmol) and DM4 (**25c**, 70.0 mg, 0.09 mmol) in glass distilled methanol (7 mL) was vigorously stirred, and 5 mL of an aqueous buffer (50 mM KH_2PO_4, 2 mM EDTA at pH 7.5) was added dropwise. The reaction was monitored by HPLC and was complete after 3 h. The solvent was evaporated, and the residue was purified by column chromatography over silica gel, eluting with a mixture of dichloromethane/methanol (97:3, v/v containing 0.1% glacial acetic acid) to give 45 mg (57% yield) of the purified product DM4-TBA (**2k**). ^{1}H NMR ($CDCl_3$) 0.800 (3H, s), 1.239 (6H, s), 1.302 (3H, d, J = 2 Hz), 1.303 (3H, d, J = 15.6 Hz), 1.414−1.513 (1H, m), 1.601 (2H, m), 1.642 (3H, s), 1.813−1.991 (2H, m), 1.932 (2H, t), 2.188 (1H, dd, J = 17.2 and 11.2 Hz), 2.346−2.530 (2H, m), 2.415 (2H, t), 2.636 (1H, dd, J = 18 and 12 Hz), 2.667 (2H, t), 2.875 (3H, s), 3.001 (1H, d, J = 9.6 Hz), 3.121 (1H, d, J = 12.4 Hz), 3.219 (3H, s), 3.356 (3H, s), 3.492 (1H, d, J = 8.8 Hz), 3.641 (1H, d, J = 12.8 Hz), 3.981 (3H, s), 4.293 (1H, t), 4.791 (1H, dd, J = 15.2 and 8.8 Hz), 5.324 (1H, q, J = 6.8 Hz), 5.667 (1H, dd, J = 24.4 and 6.4 Hz), 6.399 (1H, s), 6.421 (1H, dd, J = 26.4 and 4 Hz), 6.500 (1H, d, J = 1.6 Hz), 6.674 (1H, d, J = 11.2 Hz) and 6.826 (1H, d, J = 1.6 Hz). HRMS calcd for $C_{42}H_{60}ClN_3O_{12}S_2Na$ $(M + Na)^+$, 920.3186; found, 920.3192. HPLC analysis was performed using a Vydac analytical C-18 column (length: 100 mm, i.d.: 4.6 mm, particle size: 3 microns) at a flow rate of 1 mL/min, eluting with a linear gradient of 40 mM ammonium acetate buffer at pH 7.2 and acetonitrile as follows: 0 min: 5% CH_3CN, 5 min: 5% CH_3CN, 5−35 min: 5−35% CH_3CN, Under these conditions DM4-TBA eluted with a retention time of 18.40 min.

Synthesis of $N^{2'}$-Deacetyl-$N^{2'}$-(3-mercapto-1-oxopropyl)-maytansine dimer (DM1 dimer, 25d). A solution of **25a** (26.4 mg, 0.035 mmol) in a 1:1 (v/v) mixture of ethanol and 0.05 M potassium phosphate buffer at pH 7.5 (5 mL) was treated with a solution of 2,2′-dithiodipyridine (3.9 mg, 0.017 mmol) in ethanol (1 mL). The reaction mixture was stirred at room temperature for 2 h. Most of the ethanol in the reaction mixture was removed by evaporation under reduced pressure. The resulting aqueous layer was extracted with ethyl acetate (3 × 5 mL), and the combined organic layer was washed with saturated sodium chloride solution (1 × 5 mL) and then dried over sodium sulfate and filtered. The solvent was evaporated under reduced pressure, and the residue was purified by HPLC using a Metachem Inertsil ODS column, eluting with a gradient of water and acetonitrile to provide dimer **25d** as a white solid (13.7 mg, 52% yield). ^{1}H NMR ($CDCl_3$) δ 0.75 (3H, s), 1.23−1.26 (1H, m), 1.28 (3H, d, J = 6 Hz), 1.30 (3H, d, J = 7 Hz), 1.42−1.52 (1H, m), 1.66 (3H, s), 2.15 (1H, m), 2.59 (1H, dd, J = 6 and 14 Hz), 2.71−2.82 (2H, m), 2.84 (3H, s), 3.00 (1H, d, J = 9 Hz), 3.09 (1H, d, J = 12 Hz), 3.18 (3H, s), 3.35 (3H, s), 3.48 (1H, d, J = 9 Hz), 3.61 (1H, d, J = 13 Hz), 3.97 (3H, s), 4.26 (1H, t, J = 11 Hz), 4.76 (1H, dd, J = 3 and 12 Hz), 5.33 (1H, q, J = 7 Hz), 5.61 (1H, dd, J = 9 and 15 Hz), 6.28 (1H, s), 6.41 (1H, dd, J = 11 and 15 Hz), 6.61 (1H, d, J = 1.6 Hz), 6.65 (1H, d, J = 11 Hz), 6.81 (1H, d, J = 1.5 Hz). HRMS: calcd for $C_{70}H_{94}Cl_2N_6O_{20}S_2Na$ $(M + Na)^+$, 1495.5239, found 1495.5242; extinction coefficients (methanol): $\epsilon_{280\ nm}$ = 11 195 M^{-1} cm^{-1}, $\epsilon_{252\ nm}$ = 68 035 M^{-1} cm^{-1}. HPLC analysis was performed using a Vydac analytical C-18 column (length: 100 mm, i.d.: 4.6 mm, particle size: 3 microns) at a flow rate of 1 mL/min, eluting with a gradient of water and acetonitrile as follows: 0 min 40% CH_3CN, 5 min 40% CH_3CN, 5−30 min 40−60% CH_3CN. Under these conditions, DM1 dimer eluted with a retention time of 13.69 min.

Synthesis of $N^{2'}$-Deacetyl-$N^{2'}$-(4-mercapto-4-methyl-1-oxopentyl)-maytansine Dimer (DM4 Dimer, 25e). A solution of **25c** (100.0 mg, 0.128 mmol) in a 1:1 (v/v) mixture of dichloromethane and ethyl acetate (4 mL) was treated with a solution of $CuCl_2$ (85.76 mg, 0.640 mmol) in 0.50 M HCl (3 mL). The reaction mixture was stirred at room temperature for 2 h. The product was extracted with ethyl acetate (5 mL), and the aqueous phase was separated. An additional extraction of the aqueous phase with ethyl acetate (3 mL) was combined with the original mixture and washed with brine (2 mL) and dried over anhydrous Na_2SO_4 and filtered. The solvent was evaporated under reduced pressure to give the L-DM4-dimer **25e** (11.7 mg, 12% yield). ^{1}H NMR ($CDCl_3$) δ 0.796 (6H, s), 1.136 (6H, d, J = 4 Hz), 1.227 (2H, m), 1.298 (12H, s), 1.299 (6H, d, J = 12 Hz), 1.463 (2H, m), 1.633 (6H, s), 1.670−1.842 (4H, m), 2.171 (2H, dd, J = 17.2 and 11.2 Hz), 2.262−2.456 (4H, m), 2.596 (2H, dd, J = 26.4 and 2 Hz), 2.842 (6H, s), 3.028 (2H, d, J = 9.6 Hz), 3.105 (2H, d, J = 12.4 Hz), 3.209 (6H, s), 3.353 (6H, s), 3.489 (2H, d, J = 8.8 Hz), 3.634 (2H, d, J = 12.8 Hz), 3.966 (6H, s), 4.277 (2H, t), 4.766 (2H, dd, J = 14.8 and 9.2 Hz), 5.366 (2H, q, J = 6.8 Hz), 5.644 (2H, dd, J = 24.4 and 6.4 Hz), 6.346 (2H, s), 6.417 (2H, dd, J = 26.4 and 4 Hz), 6.623 (2H, d, J = 1.6 Hz), 6.708 (2H, d, J = 11.2 Hz) and 6.816 (2H, d, J = 1.6 Hz). HRMS calcd for $C_{76}H_{106}Cl_2N_6O_{20}S_2Na$ $(M + Na)^+$, 1579.6178; *m/z*: found, 1579.6180. HPLC analysis was performed using a Vydac analytical C-18 column (length: 100 mm, i.d.: 4.6 mm, particle size: 3 microns) at a flow rate of 1 mL/min, eluting with a gradient of water and acetonitrile (0 min: 5% CH_3CN, 5 min: 5% CH_3CN, 5−65 min: 5−95% CH_3CN. HPLC analysis was performed using a Vydac analytical C-18 column (length: 100 mm, i.d.: 4.6 mm, particle size: 3 microns) at a flow rate of 1 mL/min, eluting with a gradient of water and acetonitrile (37−58% CH_3CN over 25 min). Under these conditions, the DM4 dimer eluted with a retention time of 22.48 min.

***N*-Succinimidyl 4-(2-pyridyldithio)pentanoate (SPP, 27).** A solution of 2.2′-dithiodipyridine (300 g, 1.36 mol) in a mixture of ethanol (1 L) and glacial acetic acid (42 mL) was placed in a flask and stirred under an argon atmosphere. A solution of 4-mercaptopentanoic acid (101.8 g, 0.76 mol) in ethyl acetate (400 mL) was added dropwise over 15 min, and the reaction was stirred for an additional 2 h. The solvent was removed by rotary evaporation, and the residue was purified by column chromatography over silica gel, eluting with a mixture of hexanes/ethyl acetate/acetic acid (4:1:0.1) to give 4-(2-pyridyldithio)pentanoic acid (40 g, 21.4% yield). ^{1}H NMR in $CDCl_3$ δ 1.34 (3H, d, J = 7.0 Hz), 1.72−1.95 (2H, m), 2.52−2.63 (2H, m), 2.91−3.02 (1H, m), 7.08−7.13 (1H, m), 7.62−7.77 (2H, m), 8.46−8.49 (1H, m), 11.5 (1H, br s).

DAC EX. 2040 IPR2022-01531 Page 1262 of 1299

A solution of 4-(2-pyridyldithio)pentanoic acid (30 g, 123 mmol) in dichloromethane (525 mL) was treated with *N*-hydroxysuccinimide (14.3 g, 124 mmol) and 1-[3-(dimethylamino)propyl]-3-ethylcarbodiimide (EDC, 31.8 g, 165 mmol). The contents were stirred at room temperature for 2 h after which ethyl acetate (750 mL) was added. The solution was washed with 0.5% aqueous acetic acid (3 × 300 mL) and then with saturated aqueous NaCl (150 mL). The organic layer was separated and dried over anhydrous sodium sulfate and filtered, and the solvent was evaporated. The residue was purified by column chromatography over silica gel, eluting with hexanes/ethyl acetate (1:1). The fractions containing the pure product were combined, and the solvent was removed by rotary evaporation. The resulting oil (31 g) was taken up in a minimum volume of warm ethanol and stirred as ethyl ether (350 mL) was added, followed by hexanes (100 mL). The resulting precipitate was collected by vacuum filtration and dried in a vacuum oven at 30 °C for 12 h, to give SPP (**27**) as a white solid (18.7 g, 45% yield); mp 48−9 °C; ^{1}H NMR ($CDCl_3$) δ 1.36(3H, d, $J = 7.0$ Hz), 1.97−2.8 (2H, m), 2.73−2.86 (2H, m), 2.84 (4H, br s), 3.02−3.11 (1H, m), 7.08−7.13 (1H, m), 7.62−7.77 (2H, m), 8.46−8.49 (1H, m); Anal. ($C_{14}H_{16}N_2O_4S_2$) C, H, N, S.

***N*-Succinimidyl 4-(2-pyridyldithio)butanoate (SPDB, 28).** A solution of 2,2′-dithiopyridine (3.8 g, 17.3 mmol) in a mixture of acetic acid (0.5 mL) and ethyl alcohol (20 mL) was stirred under an argon atmosphere. A solution of 4-mercaptobutyric acid (**7c**, 1.39 g, 11.6 mmol) in ethyl acetate (10 mL) was added dropwise over approximately 2 min. The contents were stirred for 2 h, and the solvent was evaporated under reduced pressure. The residue was taken up in a minimum volume of ethyl acetate and purified by column chromatography on silica gel, eluting with a mixture of hexanes/ethyl acetate/acetic acid (65:33:2). The fractions containing the pure product were combined, and the solvent was removed under vacuum to give 1.5 g (6.55 mmol, 56% yield) of 4-(2-pyridyldithio)-butanoic acid. ^{1}H NMR ($CDCl_3$) δ 2.0−2.1(2H, m), 2.505(1H, t, $J = 7$ Hz), 2.508 (1H, t, $J = 7$), 2.74 (1H, t, $J = 7$ Hz), 2.86 (1H, t, $J =$ Hz), 7.10−7.13 (1H, m), 7.67 (1H, dt, $J = 1$, $J = 5$), 7.73 (1H, d, $J = 8$ Hz), 8.49 (1H, dd, $J = 0.7$, $J = 5$ Hz), 11.81 (1H, br s).

A flask containing a stir bar was charged with 4-(2-pyridyldithio)-butanoic acid (1.1 g, 4.8 mmol) in dichloromethane (20 mL). *N*-Hydroxysuccinimide (0.64 g, 5.6 mmol) and 1-[3-(dimethylamino)propyl]-3-ethylcarbodiimide (EDC, 1.1 g, 5.6 mmol) were then added. The contents were stirred at room temperature for 2 h after which ethyl acetate (35 mL) was added. The reaction mixture was washed with 0.5 M HCl (3 × 10 mL) and then with saturated aqueous NaCl (1 × 10 mL). The organic layer was separated and dried over anhydrous sodium sulfate and filtered. The solvent was evaporated, and the residue was purified by column chromatography on silica gel, eluting with a mixture of hexanes/ethyl acetate/acetic acid (71:28.8:0.2). The fractions containing the pure product were combined, and the solvent was removed under vacuum. The resulting oil was taken up in a minimum volume of warm reagent-grade ethanol and stirred while ethyl ether (30 mL) was added, followed by hexanes (9.0 mL). The resulting precipitate was collected by filtration and dried in a vacuum oven at 30 °C for 12 h to give 0.50 g of SPDB (**28**) as a white solid (~31% yield); mp 47−48 °C; ^{1}H NMR in $CDCl_3$ δ 2.16 (2H, tt, $J = 7$, $J = 15$ Hz), 2.795 (2H, t, $J = 7$ Hz), 2.83(4H, br s), 2.91(1H, t, $J = 7$ Hz), 7.09 (1H, m), 7.65−7.67 (2H, m), 8.48 (1H, d, $J = 5$ Hz); Anal. ($C_{13}H_{14}N_2O_4S_2$) C, H, N, S.

Preparation of Antibody Conjugates with Maytansinoids 25a, 25b, and 25c. A solution of huC242 antibody (8 mg/mL) in aqueous buffer (50 mM potassium phosphate, 50 mM sodium chloride, 2 mM ethylenediaminetetraacetic acid disodium salt) at pH 6.5 was incubated for 2 h with a 7- to 10-fold molar excess of either *N*-succinimidyl 4-(2-pyridyldithio)pentanoate (SPP, **27**, or *N*-succinimidyl-4-(2-pyridyldithio)butanoate (SPDB, **28**). The reaction mixture was purified by passage through a Sephadex G25 gel filtration column to remove low molecular weight material. The concentration of the antibody was determined spectrophotometrically using the known extinction coefficients for the antibody $\epsilon_{280\ nm} = 217\ 560\ M^{-1}\ cm^{-1}$. The number of pyridylthio groups introduced per antibody molecule was determined using a spectrophotometric assay. An aliquot of the modified antibody was treated with an excess (>20 equiv) of dithiothreitol and the release of pyridine-2-thione determined using the known extinction coefficients of $\epsilon_{343\ nm} = 8080\ M^{-1}\ cm^{-1}$ and $\epsilon_{280\ nm} = 5100\ M^{-1}\ cm^{-1}$ for pyridine-2-thione.

The modified antibody was diluted to 2.5 mg/mL in aqueous buffer (50 mM potassium phosphate, 50 mM sodium chloride, 2 mM ethylenediaminetetraacetic acid disodium salt) at pH 6.5. The SPP-modified antibody was treated with 1.7 equiv of DM1 (**25a**), whereas the SPDB-modified antibody was treated with a 1.7 equiv of either DM3 (**25b**) or DM4 (**25c**) dissolved in glass-distilled DMA (final concentration of DMA was 3% v/v). The reaction mixture was incubated for 18 h at room temperature. The reaction mixture was purified by passage through a Sephadex G25 gel filtration column to remove the unconjugated drug and other low molecular weight species. The concentration of the conjugate was determined spectrophotometrically using the known extinction coefficients for the antibody ($\epsilon_{280\ nm} = 217\ 560\ M^{-1}\ cm^{-1}$ and $\epsilon_{252\ nm} = 80\ 062\ M^{-1}\ cm^{-1}$) and the drugs. The resulting conjugate was monomeric and contained, on the average, 3.2−3.5 maytansinoid molecules linked per antibody molecule.

Cytotoxicity Assays in Vitro. The cell lines used in cytotoxicity assays were (1) KB (ATCC CCl-17), a cell line of human epithelial origin, (2) SK-BR-3 (ATCC HTB-30), a cell line established from a human breast adenocarcinoma, (3) COLO 205 (ATCC CCL-222), a human colon tumor cell line, and (4) A-375 (ATCC CRL 1619), a human melanoma cell line. The cell lines were grown in Dulbecco's modified Eagles Medium (DMEM, Biowhittaker, Walkersville, MD) with L-glutamine supplemented with 10% fetal bovine serum (Hyclone, Logan, UT) and 50 μg/mL of gentamycin sulfate (Life Technologies, Rockville, MD). The cells were maintained at 36−37.5 °C in a humidified atmosphere that contained 6% CO_2.

The cytotoxicity study was performed using a clonogenic assay as previously described.[23,24] The test cell lines were plated into 6-well culture dishes at a constant number of 1000 cells per well. The cells were incubated with varying concentrations (0 to 3 nM) of the various maytansinoids (free or conjugated to antibodies) for 72 h. The medium was then aspirated from the plates and replaced with fresh medium. The cultures were allowed to grow and form colonies for a total of 7−10 days after plating. The cultures were then fixed and stained with 0.2% crystal violet in 10% formalin/PBS, and the colonies were counted. Plating efficiency of nontreated cells (medium alone) was determined by dividing the number of colonies counted by the number of cells plated. The surviving fraction of cells exposed to the drugs was determined by dividing the number of colonies in wells that were exposed to the drug by the number of colonies in the control wells.

Antitumor Activity in Vivo. The in vivo efficacy of conjugates of maytansinoids DM1 (**25a**), DM3 (**25b**), and DM4 (**25c**) with the huC242 antibody was evaluated in a human colon tumor zenograft model established with COLO 205 cells. Five-week-old female SCID mice (20 animals) were inoculated subcutaneously in the right flank with COLO 205 human colon carcinoma cells (1.5×10^6 cells/mouse) in 0.1 mL of serum-free medium. The tumors were grown for 11 days to an average size of 100 mm^3. The animals were then randomly divided into four groups (5 animals per group). The first group of mice served as the control group and were treated with the phosphate-buffered saline vehicle. The remaining three groups were treated with either huC242−DM1 (DM1 dose of 75 μg/kg, qd × 5), huC242−DM3 (DM3 dose of 75 μg/kg, qd × 5), or huC242−DM4 conjugate (DM4 dose of 75 μg/kg, qd × 5), administered intravenously. Tumor sizes were measured twice weekly, and the tumor volumes were calculated using the formula tumor volume = 1/2(length × width × height). The weight of the animals was also measured twice per week.

DAC EX. 2040 IPR2022-01531 Page 1263 of 1299

Supporting Information Available: Analytical data (elemental analysis and HRMS and HPLC purity data) for target compounds. This material is available free of charge via the Internet at http://pubs.acs.org.

References

(1) Kupchan, S. M.; Komoda, Y.; Court, W. A.; Thomas, G. J.; Smith, R. M.; Karim, A.; Gilmore, C. J.; Haltiwanger, R. C.; Bryan, R. F. Maytansine, a novel antileukemic ansa macrolide from *Maytenus ovatus*. *J. Am. Chem. Soc.* **1972**, *94*, 1354−1356.

(2) Kupchan, S. M.; Branfman, A. R.; Sneden, A. T.; Verma, A. K.; Dailey, R. G., Jr.; Komoda, Y.; Nagao, Y. Novel maytansinoids. Naturally occurring and synthetic antileukemic esters of maytansinol. *J. Am. Chem. Soc.* **1975**, *97*, 5294−5295.

(3) Remillard, S.; Rebhun, L. I.; Howie, G. A.; Kupchan, S. M. Antimitotic activity of the potent tumor inhibitor maytansine. *Science* **1975**, *189*, 1002−1005.

(4) Huang, A. B.; Lin, C. M.; Hamel, E. Maytansine inhibits nucleotide binding at the exchangeable site of tubulin. *Biochem. Biophys. Res. Commun.* **1985**, *128*, 1239−1246.

(5) Kupchan, S. M.; Komoda, Y.; Branfman, A. R.; Sneden, A.T.; Court, W. A.; Thomas, G. J.; Hintz, H. P.; Smith, R. M.; Karim, A.; Howie, G. A.; Verma, A. K.; Nagao, Y.; Dailey, R. G., Jr.; Zimmerly, V. A.; Sumner, W. C., Jr.; The maytansinoids. Isolation, structural elucidation, and chemical interrelation of novel ansa macrolides. *J. Org. Chem.* **1977**, *42*, 2349−2357.

(6) Issell, B. F.; Crooke, S. T. Maytansine. *Cancer Treat. Rev.* **1978**, *5*, 199−207.

(7) Sedlacek, H.-H.; Seemann, G.; Hoffmann, D.; Czech, J.; Lorenz, P.; Kolar, C.; Bosslet, K.; Antibodies as carriers of cytotoxicity. In *Contributions to Oncolology;* Sedlacek, H.-H., et al., Eds.; Basel: New York, 1992; pp 1−145.

(8) Xie, H.; Audette, C.; Hoffee, M.; Lambert, J. M.; Blättler, W. A. Pharmacokinetics and biodistribution of the antitumor immunoconjugate, cantuzumab mertansine (huC242-DM1), and its two components in mice. *J. Pharmacol. Exp. Ther.* **2004**, *310*, 1073−1082.

(9) Chari, R. V. J.; Martell, B. A.; Gross, J. L.; Cook, S. B.; Shah, S. A.; Blättler, W. A.; McKenzie, S. J.; Goldmacher, V. S. Immunoconjugates containing novel maytansinoids: promising anticancer drugs. *Cancer Res.* **1992**, *52*, 127−131.

(10) Liu, C.; Tadayoni, B. M.; Bourret, L. A.; Mattocks, K. M.; Derr, S. M.; Widdison, W. C.; Kedersha, N. L.; Ariniello, P. D.; Goldmacher, V. S.; Lambert, J. M.; Blättler, W. A.; Chari, R. V. J. Eradication of large colon tumor xenografts by targeted delivery of maytansinoids. *Proc. Natl. Acad. Sci. U.S.A.* **1996**, *93*, 8618−8623.

(11) Tolcher, A. W.; Ochoa, L.; Hammond, L. A.; Patnaik, A.; Edwards, T.; Takimoto, C.; Smith, L.; de Bono, J.; Schwartz, G.; Mays, T.; Jonak, Z.L.; Johnson, R.; DeWitte, M.; Martino, H.; Audette, C.; Maes, K.; Chari, R. V. J.; Lambert, J. M.; Rowinsky, E. K. Cantuzumab mertansine, a maytansinoid immunoconjugate directed to the CanAg antigen: a phase I, pharmacokinetic, and biologic correlative study. *J. Clin. Oncol.* **2003**, *21*, 211−222

(12) Helft, P. R.; Schilsky, R. L.; Hoke, F. J.; Williams, D.; Kindler, H. L.; Sprague, E.; DeWitte, M.; Martino, H. K.; Erickson, J.; Pandite, L.; Russo, M.; Lambert, J. M.; Howard, M.; Ratain, M. J. A phase I study of cantuzumab mertansine administered as a single intravenous infusion once weekly in patients with advanced solid tumors. *Clin. Cancer Res.* **2004**, *10*, 4363−4468.

(13) Meister, A.; Anderson, M. E. *Annu. Rev. Biochem.* **1983**, *52*, 711−760.

(14) Cassady, J. M.; Chan, K. K.; Floss, H. G.; Leistner, E. Recent developments in the maytansinoid antitumor agents. *Chem Pharm Bull (Tokyo)* **2004**, *52*, 1−26.

(15) Kupchan, S. M.; Sneden, A, T.; Branfman, A. R.; Howie, G. A.; Rebhun, L. I.; McIvor, W. E.; Wang, R. W.; Schnaitman, T. C. Structural requirements for antileukemic activity among the naturally occurring and semisynthetic maytansinoids. *J. Med. Chem.* **1978**, *21*, 31−37.

(16) Higashide, E.; Asai, M.; Ootsu, K.; Tanida, S.; Kozai, Y.; Hasegawa, T.; Kishi, T.; Sugino, Y.; Yoneda, M. Ansamitocin, a group of novel maytansinoid antibiotics with antitumour properties from Nocardia. *Nature* **1977**, *29*, 721−722.

(17) Asai, M.; Mizuta, E.; Izawa, M.; Haibaba, K.; Kishi, T. Isolation, chemical characterization and structure of ansamitocin, a new antitumor antibiotic. *Tetrahedron* **1978**, *35*, 1079−1085.

(18) Kawai, A.; Akimoto, H.; Kozai, Y.; Ootsu, K.; Tanida, S.; Hashimoto, N.; Nomura, H. Chemical modification of ansamitocins. III. Synthesis and biological effects of 3-acyl esters of maytansinol. *Chem. Pharm. Bull. (Tokyo)* **1984**, *32*, 3341−3351.

(19) Kupchan, S. M.; Komoda, Y.; Branfman, A. R.; Dailey, R. G.; Zimmerly, V. A. Novel maytansinoids. Structural interrelations and requirements for antileukemic activity. *J. Am. Chem. Soc.* **1974**, *96*, 3706−3708.

(20) Lindholm, L.; Holmgren, J.; Svennerholm, L.; Fredman, P.; Nilsson, O.; Persson, B.; Myrvold, H.; Lagergard, T. Monoclonal antibodies against gastrointestinal tumour-associated antigens isolated as monosialogangliosides. *Int. Arch. Allergy Appl. Immunol.* **1983**, *71*, 178−181.

(21) Mickley, L. A.; Bates, S. E.; Richert, N. D.; Currier, S.; Tanaka, S.; Foss, F.; Rosen, N.; Fojo, A. T. Modulation of the expression of a multidrug resistance gene (mdr1/P-glycoprotein) by differentiating agents. *J. Biol. Chem.* **1989**, *264*, 18031−18040.

(22) Goff, D. A.; Carroll, S. F. Substituted 2-iminothiolanes: Reagents for the preparation of disulfide cross-linked conjugates with increased stability. *Bioconjugate Chem.* **1990**, *1*, 381−386.

(23) Goldmacher, V. S.; Tinnel, N. L.; Nelson, B. C. Evidence that pinocytosis in lymphoid cells has a low capacity. *J. Cell Biol.* **1986**, *102*, 1312−1319.

(24) Goldmacher, V. S.; Anderson, J.; Blättler, W. A.; Lambert, J. M.; Senter, P. D. Antibody-complement-mediated cytotoxicity is enhanced by ribosome-inactivating proteins. *J. Immunol.* **1985**, *135*, 3648−3651.

JM060319F

Appendix STRAUS01

SpringerLink Nature.com SpringerNature APIs SpringerMaterials

SPRINGER NATURE

Citations

HOME | ABOUT

GO

Citation Details



Article

Unusual binding sites for horseradish peroxidase on the surface of cultured and isolated mammalian cells

Histochemistry, 1986, Volume 85, Number 4, Page 277
W. Straus, J. M. Keller

Read Online

14 ITEMS CITE THIS ARTICLE Crossref

Page: 1 | 2 | > | >>

Article

73 CITATIONS

Detection and functions of mammalian lectins — with emphasis on membrane lectins

Hans-Joachin Gabius
Journal: Biochimica et Biophysica Acta (BBA) - Reviews on Biomembranes, 1991, Volume 1071, Number 1, Page 1
DOI: 10.1016/0304-4157(91)90010-T

Read Online

Article

24 CITATIONS

Concanavalin A binding sites on the surface of Drosophila melanogaster sperm: A fluorescence and ultrastructural study

Maria Elisa Perotti and Antonella Riva
Journal: Journal of Ultrastructure and Molecular Structure Research, 1988, Volume 100, Number 2, Page 173
DOI: 10.1016/0889-1605(88)90024-9

Read Online

Article

20 CITATIONS

Introduction to glycopathology: the concept, the tools and the perspectives

Hans-Joachim Gabius and Klaus Kayser
Journal: Diagnostic Pathology, 2014, Volume 9, Number 1
DOI: 10.1186/1746-1596-9-4

Read Online

Article

16 CITATIONS

Spatial differences of endogenous lectin expression within the cellular organization of the human heart: A glycohistochemical, immunohistochemical, and glycobiochemical study

A. Bardosi, L. Bardosi, M. Hendrys, B. Wosgien and H-J. Gabius
Journal: American Journal of Anatomy, 1990, Volume 188, Number 4, Page 409
DOI: 10.1002/aja.1001880409

Read Online

Chapter

0 CITATIONS

Neoglycoconjugates

HANS-JOACHIM GABIUS, ULRICH BRINCK, KLAUS KAYSER, ALFRED SCHAUER, DANKWART STILLER and SIGRUN GABIUS
Year: 1994, Page 403
DOI: 10.1016/B978-0-12-440585-1.50015-2

Read Online

Article

0 CITATIONS

Competition between ligands of glycosyltransferases and horseradish peroxidase for binding sites on intracellular and plasma membranes of HeLa cells

W. Straus and J. M. Keller
Journal: Histochemistry, 1990, Volume 94, Number 5, Page 509
DOI: 10.1007/BF00272615

Read Online

Crossref
14 ITEMS CITE THIS ARTICLE

WEB OF SCIENCE
24 ITEMS CITE THIS ARTICLE

Scopus logo
14 ITEMS CITE THIS ARTICLE

CITATION RANK

83rd PERCENTILE

CITATIONS PER YEAR

CITING JOURNALS

Histochemistry	
American Journal of Anatomy	1
Biochimica et Biophysica Acta (BBA) - R ...	1
Diagnostic Pathology	1
European Journal of Cell Biology	1
Journal of Ultrastructure and Molecular ...	1

CITING BOOKS

Neoglycoconjugates

Article

6 CITATIONS

Estrous cycle-related alterations in the expression of glycoconjugates and lectins in the mouse endometrium shown histochemically

F. Akif H J. Gabius and A. Danguy
Journal: Tissue and Cell, 1995, Volume 27, Number 2, Page 197
DOI: 10.1016/S0040-8166(95)80022-0

Read Online

Article

2 CITATIONS

Binding sites for horseradish peroxidase on the cell surface

W. Straus and J. M. Keller
Journal: Histochemistry 1987, Volume 86, Number 5, Page 453
DOI: 10.1007/BF00500616

Read Online

Article

35 CITATIONS

Neoglycoproteins as Tools in Glycohistochemistry

H.-J. Gabius and A. Bardosi
Journal: Progress in Histochemistry and Cytochemistry, 1991, Volume 22, Number 3, Page iii
DOI: 10.1016/S0079-6336(11)80019 7

Read Online

Article

3 CITATIONS

Identification of endogenous sugar-binding proteins in the accessory sex glands of NMRI mice. A histochemical and biochemical study

F. Sinowatz, H. -J. Gabius, Ch. Hauke, W. Breipohl and W. Amselgruber
Journal: Histochemistry 1991, Volume 95, Number 4, Page 357
DOI: 10.1007/BF00266963

Read Online

SPRINGER NATURE
© 2024 Springer. Part of Springer Nature.
Manage Cookies

SpringerLink Nature.com SpringerNature APIs SpringerMaterials

SPRINGER NATURE

Citations

HOME ABOUT GO

Citation Details



Article

Unusual binding sites for horseradish peroxidase on the surface of cultured and isolated mammalian cells

Histochemistry, 1986, Volume 85, Number 4, Page 277
W. Straus, J. M. Keller

Read Online

14 ITEMS CITE THIS ARTICLE Crossref

Page: << | < | 1 | 2

Article

0 CITATIONS

MAPPING OF RECEPTORS FOR CARBOHYDRATE CONSTITUENTS OF GLYCOCONJUGATES IN WELL–DIFFERENTIATED AND MALIGNANT EPENDYMOMAS: A GLYCOHISTOCHEMICAL STUDY

T. DIMITRI, A. BARDOSI and H. J. GABIUS
Journal: Neuropathology and Applied Neurobiology, 1989, Volume 15, Number 2, Page 121
DOI: 10.1111/j.1365-2990.1989.tb01215.x

Read Online

Article

26 CITATIONS

Azithromycin, a lysosomotropic antibiotic, impairs fluid-phase pinocytosis in cultured fibroblasts

Donatienne Tyteca, Patrick Van Der Smissen, Françoise Van Bambeke, Karin Leys, Paul M. Tulkens, Pierre J. Courtoy and Marie-Paule Mingeot-Leclercq
Journal: European Journal of Cell Biology, 2001, Volume 80, Number 7, Page 466
DOI: 10.1078/0171-9335-00180

Read Online

Article

14 CITATIONS

(Neo)glycoproteins as tools in neuropathology: Histochemical patterns of the extent of expression of endogenous carbohydrate-binding receptors, like lectins, in meningiomas

Attila Bardosi, Thomas Dimitri and Hans-Joachim Gabius
Journal: Virchows Archiv B Cell Pathology Including Molecular Pathology, 1988, Volume 56, Number 1, Page 35
DOI: 10.1007/BF02889999

Read Online

Article

10 CITATIONS

Malignant and normally developing trophoblastic cells of human placenta display different characteristics defined by histochemical and biochemical mapping of endogenous lectins

H. -J. Gabius, P. L. Debbage, N. Lang and W. Lange
Journal: Histochemistry, 1989, Volume 92, Number 4, Page 283
DOI: 10.1007/BF00500542

Read Online

Page << | < | 1 | 2

Crossref
14 ITEMS CITE THIS ARTICLE

WEB OF SCIENCE
24 ITEMS CITE THIS ARTICLE

Scopus logo
14 ITEMS CITE THIS ARTICLE

CITATION RANK

83rd PERCENTILE

CITATIONS PER YEAR

CITING JOURNALS

Histochemistry	
American Journal of Anatomy	1
Biochimica et Biophysica Acta (BBA) - R ...	1
Diagnostic Pathology	1
European Journal of Cell Biology	1
Journal of Ultrastructure and Molecular ...	1

CITING BOOKS

Neoglycoconjugates 1

SPRINGER NATURE
© 2024 Springer. Part of Springer Nature.
Manage Cookies

Appendix COLLIN01

MARC View

LEADER 01448cam a2200397 a 4500				
001 4437958				
003 SIRSI				
005 20151215082045.0				
008 070809s2007 enk d 000 0 eng				
015			a| GBA763943 2| bnb	
016	7		a| 013817962 2| Uk	
019			a| MARS	
020			a| 9780713686517 q| (pbk.)	
020			a| 0713686510 q| (pbk.)	
035			a| BD100477799	
035			a| (OCoLC)154704184	
040			a| UKM c| UKM d| BTCTA d| YDXCP d| BAKER d| MOF d| CUI d| XQJ d| UtOrBLW	
042			a| ukscp	
049			a| UPMM	
050		4	a| Q123 b| C63 2007	
082	0	4	a| 503 2| 22	
100	1		a| Collin, S. M. H., d| 1966-	
245	1	0	a| Dictionary of science and technology / c| Simon Collin.	
250			a| 2nd ed.	
264		1	a| London : b| A. & C. Black, c| 2007.	
300			a| 658 pages, 7 unnumbered pages ; c| 20 cm	
336			a| text b| txt 2| rdacontent	
337			a| unmediated b| n 2| rdamedia	
338			a| volume b| nc 2| rdacarrier	
500			a| Previous ed.: London: Bloomsbury, 2003.	
541			3| Life Sciences copy: c| Purchased with funds from the a| Paterno Libraries Endowment; d| 20078. 5| PSt.	
650		0	a| Science v| Dictionaries.	
650		0	a| Technology v| Dictionaries.	
993			a| 700000010274 n| Paterno Libraries Endowment	
949			a| Q123.C482 2007 w| LC c| 1 i| 000060850157 d| 12/23/2013 f| 12/23/2013 g| 1 l| REF-LS m| UP-LIFESCI r| Y s| Y t| BOOK u| 6/10/2008	
949			a| Q123C63 2007 w| LC c| 1 i| 000061403536 d| 4/19/2011 e| 3/17/2011 l| STACKS-BD m| BEHREND r| Y s| Y t| BOOKFLOAT u| 1/20/2011 o| .STAFF. GOBI	

ASK A LIBRARIAN

PennState

Copyright @2019 The Pennsylvania State University. All rights reserved. Except where otherwise noted, this work is subject to a Creative Commons Attribution 4.0 license. Details and exceptions.

Legal Statements | PSU Hotlines

PENN STATE UNIVERSITY LIBRARIES

Libraries Home (814) 865-6368
Libraries Intranet (Staff Only)
Accessibility Help
Website Feedback
Policies and Guidelines
Staff Directory

CONNECT WITH PENN STATE UNIVERSITY LIBRARIES

Facebook
Twitter
Instagram



Dictionary of science and technology / Simon Collin

Author	Collin, S. M. H., 1966-
Published	London : A. & C. Black, 2007.
Edition	2nd ed.
Physical Description	658 pages, 7 unnumbered pages ; 20 cm

ASK A LIBRARIAN

Availability

Browse Nearby on Shelf I Want It

Penn State Behrend (1 item)

Call number	Material	Location
Q123C63 2007	Book	Stacks - General Collection

Life Sciences Library (Paterno) (1 item)

Call number	Material	Location
Q123.C482 2007	Book	Life Sciences, 4th Paterno - Reference Area - In-Library Use

Subject(s)
Science—Dictionaries
Technology—Dictionaries

ISBN
9780713686517 (pbk.)
0713686510 (pbk.)

Note
Previous ed.: London: Bloomsbury, 2003.

Source of Acquisition
Life Sciences copy: Purchased with funds from the Paterno Libraries Endowment; 20078.

Endowment Note
Paterno Libraries Endowment

View MARC record | catkey: 4437958

PennState

Copyright ©2019 The Pennsylvania State University. All rights reserved. Except where otherwise noted, this work is subject to a Creative Commons Attribution 4.0 license. Details and exceptions.

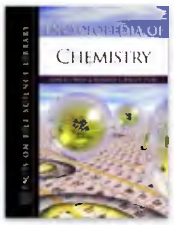
Legal Statements | PSU Hotlines

PENN STATE UNIVERSITY LIBRARIES
Libraries Home (814) 865-6368
Libraries Intranet (Staff Only)
Accessibility Help
Website Feedback
Policies and Guidelines
Staff Directory

CONNECT WITH PENN STATE UNIVERSITY LIBRARIES
Facebook
Twitter
Instagram

Appendix RITTNER01

Field Description	Field #	I1	I2	Field Data
Leader	LDR			01299pam a22003854a 4500
Control #	001			ocm55149372
Control # Id	003			OCoLC
Date	005			20190407191313.0
Fixed Data	008			040512t20052005nyua be 001 0 eng
LC Card	010			‡a 2004011242
ISBN	020			‡a0816048940
Cat. Source	040			‡aDLC‡cDLC‡dYDX‡dUKM‡dBAKER‡dLPU‡dUtOrBLW
Authen. Ctr.	042			‡apcc
Non-MARC	049			‡aLPUA
LC Call	050	0	0	‡aQD4‡b.R57 2005
Dewey Class	082	0	0	‡a540/.3‡222
Local Call #	099			‡a540.3 R615‡eich vn
ME:Pers Name	100	1		‡aRittner, Don
Title	245	1	0	‡aEncyclopedia of chemistry /‡cDon Rittner and Ronald A. Bailey.
Pub. Data	264		1	‡aNew York, NY :‡bFacts On File,‡c[2005]
Pub. Data	264		4	‡c©2005
Phys Descrpt	300			‡ax, 342 pages :‡billustrations ;‡c29 cm.
Content Type	336			‡atext‡btxt‡2rdacontent
Media Type	337			‡aunmediated‡bn‡2rdamedia
Carrier Type	338			‡avolume‡bnc‡2rdacarrier
Series:Diff	490	1		‡aFacts on File science library
Note:Bibliog	504			‡aIncludes bibliographical references (pages 289-312) and index.
Subj:Topical	650		0	‡aChemistry‡vEncyclopedias
AE:Pers Name	700	1		‡aBailey, R. A.‡q(Ronald Albert),‡d1933-
SE:Ufm Title	830		0	‡aFacts on File science library
Non-MARC	898			‡aqBook Book
Non-MARC	898			‡aqEnglish English
Local Option	910			‡aCARL0001958442
Local Option	994			‡aC0‡bLPU
Local Option	998	1	2	‡aITS181 ITS 20050818143720.0 ILDR LAPL ‡bLDR0905 20191020155110 BKSG ‡bLDR75.0 20101024181626 LTI ‡bLDR73.3 20091002212215 LAP1



Book

Details
Copy Locations
Reviews, Ratings & Related Titles
More Info

MARC Record

Encyclopedia of chemistry

by Rittner, Don

Place Hold | Add To List | Share

Summary

With a structure that reflects the way chemistry is currently studied, the Encyclopedia of Chemistry has hundreds of chemistry-related entries, thought-provoking essays, leading discoveries, and biographies of notable chemists throughout history. It is written for high school and early college students.

Call #
540.3 R615

Author(s)
Rittner, Don

Title(s)
Encyclopedia of chemistry / Don Rittner and Ronald A. Bailey.

Publisher
New York, NY : Facts On File, [2005]
©2005

Description
x, 342 pages : illustrations ; 29 cm.

Series
Facts on File science library
Facts on File science library

Notes
Includes bibliographical references (pages 289-312) and index.

Subject(s)
Chemistry Encyclopedias

Other Entries
Bailey, R. A.

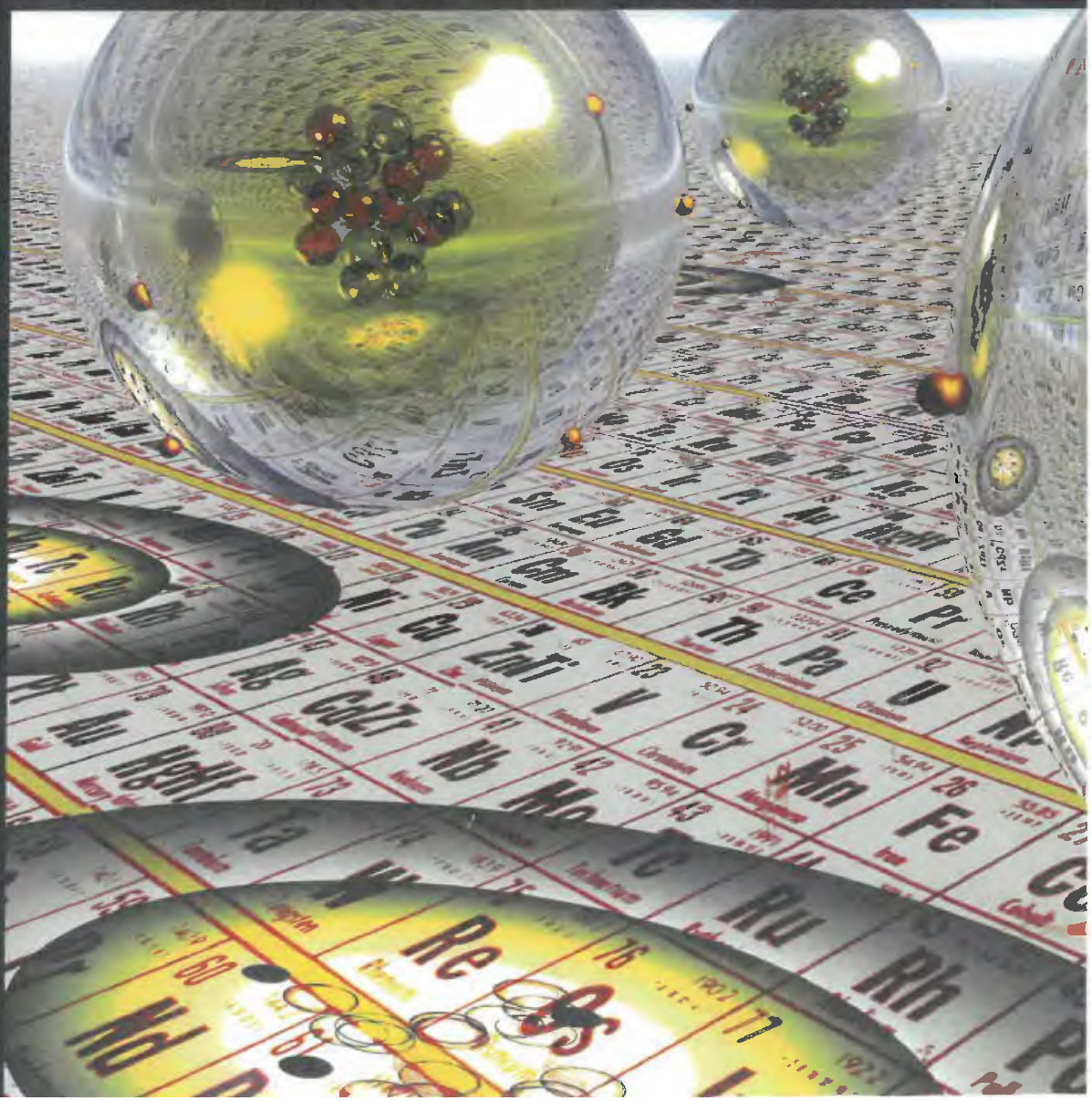
Share | Post | Send

Appendix RITTNER02

FACTS ON FILE SCIENCE LIBRARY

ENCYCLOPEDIA OF CHEMISTRY

DON RITTNER & RONALD A. BAILEY, PH.D.




ENCYCLOPEDIA OF CHEMISTRY
Rittner & Bailey
540.3
R615

ENCYCLOPEDIA OF
CHEMISTRY

DON RITTNER
AND
RONALD A. BAILEY, PH.D.

LOS ANGELES PUBLIC LIBRARY
CENTRAL LIBRARY
DEPT. OF SCIENCE, TECHNOLOGY & PATENTS
630 W. 5TH ST
LOS ANGELES, CA 90071

540.3
R615

Facts On File, Inc.

OCT 2 4 2006

To Nancy, Christopher, Kevin, Jackson, Jennifer, and Jason

Encyclopedia of Chemistry

Copyright © 2005 by Don Rittner

All rights reserved. No part of this book may be reproduced or utilized in any form or by any means, electronic or mechanical, including photocopying, recording, or by any information storage or retrieval systems, without permission in writing from the publisher.
For information contact:

Facts On File, Inc.
132 West 31st Street
New York NY 10001

Library of Congress Cataloging-in-Publication Data
Rittner, Don.
Encyclopedia of chemistry / Don Rittner and Ronald A. Bailey.
p. cm.
Includes bibliographical references and index.
ISBN 0-8160-4894-0
1. Chemistry—Encyclopedias. I. Bailey, R. A. (Ronald Albert), 1933 –
II. Title.
QD4.R57 2005
540'.3—dc22 2004011242

Facts On File books are available at special discounts when purchased in bulk quantities for businesses, associations, institutions, or sales promotions. Please call our Special Sales Department in New York at (212) 967-8800 or (800) 322-8755.

You can find Facts On File on the World Wide Web at http://www.factsonfile.com.

Text design by Joan M. Toro
Cover design by Cathy Rincon
Illustrations by Richard Garratt

Printed in the United States of America

VB Hermitage 10 9 8 7 6 5 4 3 2 1

This book is printed on acid-free paper.

Los Angeles Public Library
Science/Technology/Patents Dept.
630 W. Fifth Street
Los Angeles, CA 90071

SEP 3 0 2006

CONTENTS

Acknowledgments
v

Preface
vii

Introduction
ix

A-to-Z Entries
1

Feature Essays:

"The Power of Chemistry: Natural versus Synthetic Compounds"
by Theresa Beaty, Ph.D.
57

"What a Crime Lab Does, It Does with Chemistry"
by Harry K. Garber
81

"Molecular Modeling"
by Karl F. Moschner, Ph.D.
183

"The Role of Chemistry"
by Karl F. Moschner, Ph.D.
248

Appendixes:

Appendix I
Bibliography
289

Appendix II
Chemistry-Related Web Sites
311

Appendix III
Chemistry Software Sources
313

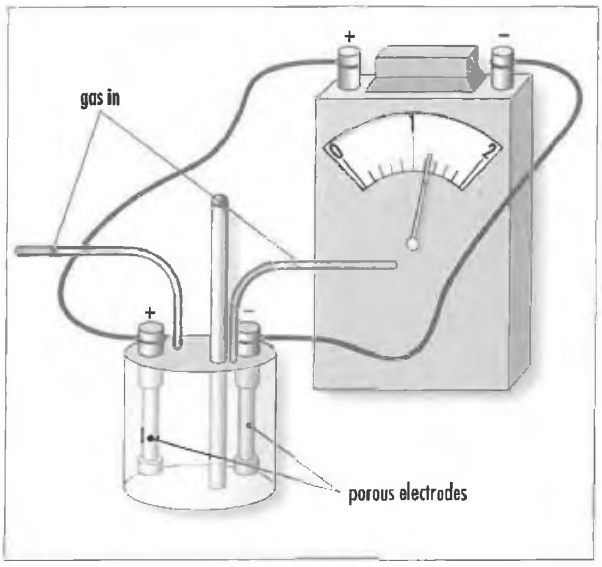
Appendix IV
Nobel Laureates Relating to Chemistry
315

Appendix V
Periodic Table of Elements
321

Appendix VI
Chemical Reaction Types
323

Appendix VII
Metals and Alloys
325

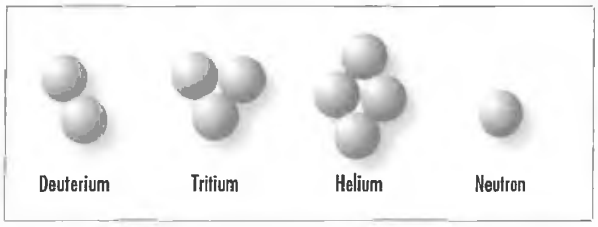
Index
326



Fuel cell. A voltaic cell where reactants are continually supplied to convert chemical energy to electrical energy

fullerene An ALLOTROPE of carbon containing five- and six-membered rings, whose structure is based on that of C_{60}, BUCKMINSTERFULLERENE.

functional group Organic compounds are thought of as consisting of a relatively unreactive backbone—for example, a chain of sp^3 hybridized carbon atoms—and one or several functional groups. The functional group is an atom (or a group of atoms) that has similar chemical properties whenever it occurs in different



Fusion. A nuclear reaction in which light atomic nuclei combine to form heavier nuclei, typically accompanied by the release of energy

compounds. It defines the characteristic physical and chemical properties of families of organic compounds.

fur The iron-uptake-regulating protein present in PROKARYOTES that binds simultaneously Fe and DNA, thereby preventing the biosynthesis of ENZYMES for the production of SCAVENGER chelates (SIDEROPHORES).

See also CHELATION.

fused-ring compound A fused ring is two rings joined together through one or more atoms. Examples include *trans*-decalin, *cis*-decalin, bicyclo [2.2.2] octane, bicyclo [2.2.1] heptane (norbornane), and adamantane.

fusion A nuclear reaction in which light atomic nuclei combine to form heavier nuclei, typically accompanied by the release of energy. Also used to describe chemical reactions in which rings are formed.

DAC EX. 2040 IPR2022-01531 Page 1283 of 1299

Appendix MCGRAW01

MARC View

LEADER 01789cam a2200433 a 4500				
001 2299423				
003 SIRSI				
005 20160707135725.0				
008 020619t20032003nyua d 000 0 eng				
010			a	2002026436
015			a	GBA2-Y8700
019			a	48977232
019			a	MARS
020			a	007042313X q | (alk. paper)
035			a	(OCoLC)50143897
040			a	DLC c | DLC d | UKM d | C#P d | VET d | UtOrBLW
050	0	0	a	Q123 b | M15 2003
082	0	0	a	503 2 | 21
245	0	0	a	McGraw-Hill dictionary of scientific and technical terms.
246	3	0	a	Dictionary of scientific and technical terms
250			a	6th ed.
264		1	a	New York : b | McGraw-Hill, c | [2003]
264		4	c	©2003
300			a	xvii, 2,380 pages : b | illustrations ; c | 28 cm
336			a	text b | txt 2 | rdacontent
337			a	unmediated b | n 2 | rdamedia
338			a	volume b | nc 2 | rdacarrier
541			3 | Engineering copy: c | Purchased with funds from the a | J. Harvey Fahnestock Endowment for Scientific, Engineering and Rare Books; d | 2002. 5 | PSt.	
650		0	a	Science v | Dictionaries.
650		0	a	Technology v | Dictionaries.
650		2	a	Science.
650		2	a	Technology.
655		2	a	Dictionary.
993			a	700000010275 n | Paterno Libraries Endowment (Campus College Libraries)
993			a	700000010421 n | J. Harvey Fahnestock Endowment for Scientific, Engineering and Rare Books
949			a	Q123.M15 2003 w | LC c | 1 i | 000049064902 d | 9/6/2023 e | 8/29/2023 f | 5/21/2018 g | 1 l | STACKS-BK m | BERKS n | 1 r | Y s | Y t | BOOK u | 11/1/2002
949			a	Q123.M15 2003 w | LC c | 1 i | 000053433350 l | REF-MA m | MONTALTO r | Y s | Y t | REF-ITEM u | 1/27/2004
949			a	Q123.M15 2003 w | LC c | 1 i | 000056295948 l | STACKS-SV m | SHENANGO r | Y s | Y t | BOOKFLOAT u | 11/22/2004
949			a	Q123.M15 2003 w | LC c | 1 i | 000057257402 d | 3/14/2022 e | 2/16/2022 l | REF-FE m | FAYETTE n | 1 r | Y s | Y t | REF-ITEM u | 11/30/2005

ASK A LIBRARIAN

PennState

Copyright ©2019 The Pennsylvania State University. All rights reserved. Except where otherwise noted, this work is subject to a Creative Commons Attribution 4.0 license. Details and exceptions.

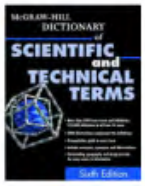
Legal Statements | PSU Hotlines

PENN STATE UNIVERSITY LIBRARIES

Libraries Home (814) 865-6368
Libraries Intranet (Staff Only)
Accessibility Help
Website Feedback
Policies and Guidelines
Staff Directory

CONNECT WITH PENN STATE UNIVERSITY LIBRARIES

Facebook
Twitter
Instagram



McGraw-Hill dictionary of scientific and technical terms

Additional Titles	Dictionary of scientific and technical terms
Published	New York : McGraw-Hill, [2003]
Copyright Date	©2003
Edition	6th ed.
Physical Description	xvii, 2,380 pages : illustrations ; 28 cm

ASK A LIBRARIAN

Availability

Browse Nearby on Shelf I Want It

Penn State Berks (1 item)

Call number	Material	Location
Q123.M15 2003	Book	Being transferred between libraries

Penn State Fayette (1 item)

Call number	Material	Location
Q123.M15 2003	Book, Reference	Fayette - Reference Collection - In-Library Use

Penn State Mont Alto (1 item)

Call number	Material	Location
Q123.M15 2003	Book, Reference	Mont Alto - Reference Collection - In-Library Use

Penn State Shenango (1 item)

Call number	Material	Location
Q123.M15 2003	Book	Stacks - General Collection

Subject(s)

Science—Dictionaries
Technology—Dictionaries
Science
Technology

ISBN

007042313X (alk. paper)

Source of Acquisition

Engineering copy: Purchased with funds from the J. Harvey Fahnestock Endowment for Scientific, Engineering and Rare Books; 2002.

Endowment Note

Paterno Libraries Endowment (Campus College Libraries)
J. Harvey Fahnestock Endowment for Scientific, Engineering and Rare Books

PennState

Copyright ©2019 The Pennsylvania State University. All rights reserved. Except where otherwise noted, this work is subject to a Creative Commons Attribution 4.0 license. Details and

PENN STATE UNIVERSITY LIBRARIES
Libraries Home (814) 865-6368

CONNECT WITH PENN STATE UNIVERSITY LIBRARIES


exceptions.
Legal Statements | PSU Hotlines
Libraries Intranet (Staff Only)
Accessibility Help
Website Feedback
Policies and Guidelines
Staff Directory
Twitter
Instagram

Appendix OXFORD01

```
LEADER 00000cam  2200000 a 4500
001    444383696
003    OCoLC
005    20150415233224.0
008    100501s2010    enka     d    000 0 eng
010    2010287468
020    9780199561469 (pbk.)
020    019956146X (pbk.)
035    (OCoLC)444383696
040    DLC|cDLC|dUKM|dYDXCP|dIEB|dC#P|dBWX|dCDX|dSZR|dSGB|dCPL
       |dUtOrBLW
049    CPLL
050 00 Q123|b.C68 2010
082 04 503|222
245 02 A dictionary of science.
246 14 Oxford dictionary of science
250    6th ed. / edited by John Daintith and Elizabeth Martin.
260    Oxford ;|aNew York :|bOxford University Press,|c2010.
300    900 pages :|billustrations ;|c20 cm.
336    text|btxt|2rdacontent
337    unmediated|bn|2rdamedia
338    volume|bnc|2rdacarrier
490 0  Oxford paperback reference
650  0 Science|vDictionaries.
700 1  Daintith, John.
700 1  Martin, E. A.|q(Elizabeth A.)
994    C0|bCPL
997    xajrc
997    xagap
```

LOCATION	CALL #	STATUS
CLP Main (Oakland) Second Floor - Non-fiction	Q123.C68 2010	AVAILABLE

The CATALOG
Connecting Public Libraries in Allegheny County, PA

Title	**A dictionary of science.**
Publisher	Oxford ; New York : Oxford University Press, 2010.
Edition	6th ed. / edited by John Daintith and Elizabeth Martin.
Description	900 pages : illustrations ; 20 cm.



LOCATION	CALL #	STATUS
CLP Main (Oakland) Second Floor - Non-fiction	Q123.C68 2010	AVAILABLE

Details

Series	Oxford paperback reference
Subject	Science -- Dictionaries.
Addt'l Author	Daintith, John. Martin, E. A. (Elizabeth A.)
Cover Ti	Oxford dictionary of science
ISBN	9780199561469 (pbk.) 019956146X (pbk.)

Appendix OXFORD02

BEST-SELLING DICTIONARY WITH OVER 9,200
CLEAR AND CONCISE ENTRIES

Web Linked

Oxford



DICTIONARY OF Science

CLP Main



Q
123
.C68
2010

Science

CARNEGIE LIBRARY of PITTSBURGH
3 1812 04558 9976

This best-selling dictionary covers chem physics, biology (including human b earth sciences, and astronomy. It includes short biographies of leading scientists, full page illustrated features on key topics, and chronologies of major scientific subjects. An essential reference work for students and an ideal introduction for non-scientists.

Oxford Paperback Reference

THE WORLD'S MOST TRUSTED REFERENCE BOOKS



- Over 9,200 clear and concise entries and more than 200 diagrams
- Useful appendices include SI units and unit conversion, fundamental constants, the solar system, geological time scale, and the periodic table

Sixth Edition

'The book will appeal not just to scientists and science students but also to the interested lay person... it is well worth browsing.' *New Scientist*

'All entries are clear and brief, written in no-nonsense prose. . . A handy reference work.' *Times Educational Supplement*

Recommended web links updated via the *Dictionary of Science* companion website: www.oup.com/uk/reference/resources/science

Cover illustrations (main) © Punchstock, (inset) © iStockphoto

Many books in the Oxford Paperback Reference series are available as e-books. Visit www.askoxford.com/shoponline/ebooks/ for details

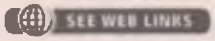
ISBN 978-0-19-956146-9

OXFORD UNIVERSITY PRESS

OXFORD PAPERBACK REFERENCE

A Dictionary of

Science



Many entries in this dictionary have recommended web links. When you see the above symbol at the end of an entry go to the dictionary's web page at http://www.oup.com/uk/reference/resources/science, click on **Web links** in the Resources section and locate the entry in the alphabetical list, then click straight through to the relevant websites.

A Dictionary of

Science

SIXTH EDITION

Q123.C68 2010
A dictionary of science.
Oxford ; New York : Oxford
University Press, 2010.

OXFORD
UNIVERSITY PRESS

OXFORD
UNIVERSITY PRESS
Great Clarendon Street, Oxford OX2 6DP
Oxford University Press is a department of the University of Oxford.
It furthers the University's objective of excellence in research, scholarship,
and education by publishing worldwide in
Oxford New York
Auckland Cape Town Dar es Salaam Hong Kong Karachi
Kuala Lumpur Madrid Melbourne Mexico City Nairobi
New Delhi Shanghai Taipei Toronto
With offices in
Argentina Austria Brazil Chile Czech Republic France Greece
Guatemala Hungary Italy Japan Poland Portugal Singapore
South Korea Switzerland Thailand Turkey Ukraine Vietnam
Oxford is a registered trade mark of Oxford University Press
in the UK and in certain other countries
Published in the United States
by Oxford University Press Inc., New York

© Market House Books Ltd, 1984, 1991, 1996, 1999, 2005, 2010

The moral rights of the author have been asserted
Database right Oxford University Press (maker)

First published 1984 as *Concise Science Dictionary*
Second edition 1991
Third edition 1996
Fourth edition 1999
Fifth edition 2005
Sixth edition 2010

All rights reserved. No part of this publication may be reproduced,
stored in a retrieval system, or transmitted in any form or by any means,
without the prior permission in writing of Oxford University Press,
or as expressly permitted by law, or under terms agreed with the appropriate
reprographics rights organization. Enquiries concerning reproduction
outside the scope of the above should be sent to the Rights Department,
Oxford University Press, at the address above

You must not circulate this book in any other binding or cover
and you must impose this same condition on any acquirer

British Library Cataloguing in Publication Data
Data available

Library of Congress Cataloging in Publication Data
Data available

Typeset by Market House Books Ltd.
Printed in Great Britain by
Clays Ltd, St Ives plc

ISBN 978–0–19–956146–9

10 9 8 7 6 5 4 3 2 1

Contents

Preface	vii
Credits	viii
A Dictionary of Science	1
Atomic Theory Chronology	63
The Big-Bang Theory (Feature)	86
Biochemistry Chronology	90
Cell Biology Chronology	144
Cosmology Chronology	200
Crystal Defects (Feature)	210
Electronics Chronology	275
El Niño (Feature)	284
Explosives Chronology	308
Genetically Modified Organisms (Feature)	352
Learning in Animals (Feature)	470
Microscopy Chronology	528
Moon Exploration Chronology	541
Magnetic Resonance Imaging (Feature)	569
Plastics Chronology	638
Polymers (Feature)	648
Refrigeration (Feature)	702
Solar System (Feature)	766
Optical Astronomical Telescopes (Feature)	809
Vitamins Chronology	863
Appendices	
SI units	893
Fundamental constants	895
The solar system	895
Geological time scale	896
Simplified classification of land plants	897
Simplified classification of the animal kingdom	898
The periodic table	899
Useful websites	900

relates one variable to one or more other variables. If y is a function of x, written $y = f(x)$, a change in x produces a change in y, and if x is known, y can be determined. x is the **independent variable** and y is the **dependent variable**.

functional A function of a function. Functionals are used very extensively in the quantum-mechanical many-body problem, statistical mechanics, and quantum field theory.

functional group The group of atoms responsible for the characteristic reactions of a compound. The functional group is –OH for alcohols, –CHO for aldehydes, –COOH for carboxylic acids, etc.

fundamental *See* HARMONIC.

fundamental constants (universal constants) Those parameters that do not change throughout the universe. The charge on an electron, the speed of light in free space, the Planck constant, the gravitational constant, the electric constant, and the magnetic constant are all thought to be examples. It has been suggested that some fundamental constants might change with time, although there is no conclusive evidence that this occurs.

SEE WEB LINKS

- Values of fundamental physical constants from NIST

fundamental interactions The four different types of interaction that can occur between bodies. These interactions can take place even when the bodies are not in physical contact and together they account for all the observed forces that occur in the universe. While the unification of these four types of interaction into a single theory has long been the aim of physicists, this has not yet been fully achieved. *See also* ELEMENTARY PARTICLES; GAUGE THEORY; UNIFIED-FIELD THEORY.

The **gravitational interaction**, some 10^{40} times weaker than the electromagnetic interaction, is the weakest of all. The force that it generates acts between all bodies that have mass and the force is always attractive. The interaction can be visualized in terms of a classical *field of force in which the strength of the force falls off with the square of the distance between the interacting bodies (*see* NEWTON'S LAW OF GRAVITATION). The hypothetical gravitational quantum, the **graviton**, is also a useful concept in some contexts. On the atomic scale the gravitational force is negligibly weak, but on the cosmological scale, where masses are enormous, it is immensely important in holding the components of the universe together. Because gravitational interactions are long-ranged, there is a well-defined macroscopic theory in general relativity. At present, there is no satisfactory quantum theory of gravitational interaction.

The **weak interaction**, some 10^{10} times weaker than the electromagnetic interaction, occurs between *leptons and in the decay of hadrons. It is responsible for the *beta decay of particles and nuclei. In the current model, the weak interaction is visualized as a force mediated by the exchange of virtual particles, called intermediate vector bosons. The weak interactions are described by *electroweak theory, which unifies them with the electromagnetic interactions.

The **electromagnetic interaction** is responsible for the forces that control atomic structure, chemical reactions, and all electromagnetic phenomena. It accounts for the forces between charged particles, but unlike the gravitational interaction, can be either attractive or repulsive. Some neutral particles decay by electromagnetic interaction. The interaction is either visualized as a classical field of force (*see* COULOMB'S LAW) or as an exchange of virtual *photons. As with gravitational interactions, the fact that electromagnetic interactions are long-ranged means that they have a well-defined classical theory given by *Maxwell's equations. The quantum theory of electromagnetic interactions is described by *quantum electrodynamics.

The **strong interaction**, some 10^2 times stronger than the electromagnetic interaction, functions only between *hadrons and is responsible for the force between nucleons that gives the atomic nucleus its great stability. It operates at very short range inside the nucleus (10^{-15} metre) and is visualized as an exchange of virtual mesons. The strong interactions are described by *quantum chromodynamics.

fundamental units A set of independently defined *units of measurement that forms the basis of a system of units. Such a set requires three mechanical units (usually of length, mass, and time) and, in some systems, one electrical unit; it has also been found convenient to treat certain other quantities as fundamental, even though they

DAC EX. 2040 IPR2022-01531 Page 1299 of 1299